Vinko V. Dolenc
Larry Rogers
Editors

Cavernous Sinus

Developments and Future Perspectives

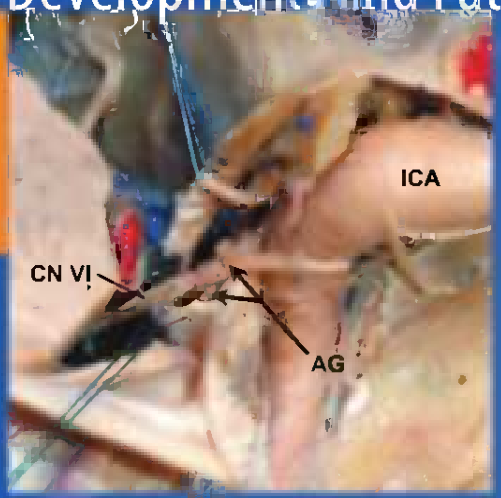

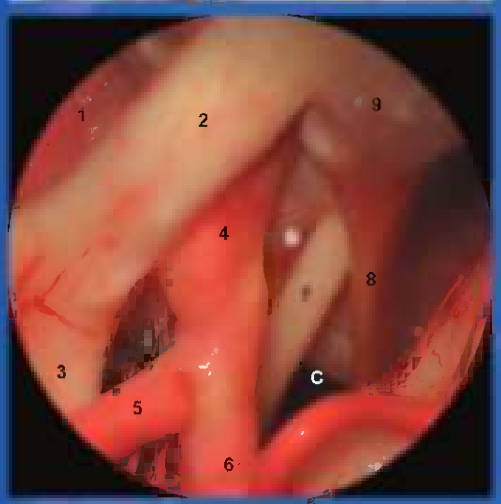

SpringerWienNewYork

SpringerWienNewYork

Vinko V. Dolenc
Larry Rogers (eds.)

Cavernous Sinus

Developments and Future Perspectives

SpringerWienNewYork

Prof. Dr. Vinko V. Dolenc
University Ljubljana
Medical Center
Department of Neurosurgery
Ljubljana
Slovenia

Dr. Larry Rogers
Charlotte, NC, U.S.A.

Printed in Austria

SpringerWienNewYork is part of Springer Science + Business Media
springer.at

Typesetting: Thomson Press (India) Ltd., Chennai
Printing: Holzhausen Druck & Medien, 1140 Wien

Printed on acid-free and chlorine-free bleached paper

SPIN: 11817734

With 88 partly coloured Figures

Library of Congress Control Number: 2008930119

ISBN 978-3-211-72137-7 SpringerWienNewYork

Preface

Treatment of cavernous sinus (CS) pathologies is still the subject of many discussions. The enthusiasm which was brought into the field of surgical treatment of vascular and tumorous pathologies of the region more than two decades ago has not faded away. On the contrary, the number of neurosurgeons who devoted enough time to the anatomy of the region are convinced that surgery will remain to be the most important modality of treatment for CS tumorous pathologies also in the future.

The introduction of radiosurgery into the field has not replaced neurosurgical treatment of tumors of the region; however, this is a very important adjunct treatment modality to surgery. The endovascular treatment of the ICA aneurysms in the CS becomes an important modality and has a great future because it is believed that the balloon(s), coils, and glue should be combined with the stenting of the ICA at the skull base aneurysms. However, even the most sophisticated and advanced endovascular treatment will not be able to rule out surgery, in particular in those fusiform aneurysms in which a long segment of the ICA has to be repaired in order to provide the patency of the ICA. And if endovascular treatment of this kind of lesions will not provide an acceptable solution, and direct neurosurgery will not be in the position to reconstruct the diseased ICA, then either a short high-flow by-pass or another kind of by-passing of the blood flow will be needed, and will only be possible by surgical techniques. The alternative answer in this kind of treatment will be found in a combination of different procedures of different modalities in order to provide this end result.

The advancement in treatment of vascular and tumorous pathologies in the central skull base during the last two decades has been great in understanding of the normal and pathological anatomy as well as in eradicating the pathologies. In the surgical domain of treatment of tumorous pathologies of the central skull base, the major advancement has been in refining the approaches from above, that is transcranial, as well as from below, that is splanchnocranial.

The initial enthusiasm for each of the transcranial and splanchnocranial approaches has reached already the zenith and is now on the level which does allow co-existence of the other approaches as well. And again, in the future, a combination of the transcranial and splanchnocranial approaches will be used more frequently for the same pathology. It is evident that when surgery will not be successful in total eradicating the tumorous lesion, radiosurgery – Gamma Knife, Proton Beam treatment, etc. – will be included accordingly.

Vinko V. Dolenc
October 2008

Contents

List of contributors

K. M. **Abdel Aziz**, Department of Neurosurgery, Allegheny General Hospital, Pittsburgh, PA, USA

O. **Al-Mefty**, Department of Neurosurgery, University of Arkansas for Medical Sciences, Little Rock, AR, USA

G. W. **Britz**, Department of Neurological Surgery, University of Washington, Seattle, WA, USA

P. **Cappabianca**, Department of Neurological Sciences, Division of Neurosurgery, Università degli Studi di Napoli Federico II, Naples, Italy

L. M. **Cavallo**, Department of Neurological Sciences, Division of Neurosurgery, Università degli Studi di Napoli Federico II, Naples, Italy

E. **de Divitiis**, Department of Neurological Sciences, Division of Neurosurgery, Università degli Studi di Napoli Federico II, Naples, Italy

O. **de Divitiis**, Department of Neurological Sciences, Division of Neurosurgery, Università degli Studi di Napoli Federico II, Naples, Italy

V. V. **Dolenc**, International Institute for Neurosurgery and Neuroresearch (IINN), Ljubljana, Slovenia

W. **Eisner**, Neurosurgical Department, Medical University Innsbruck, Innsbruck, Austria

F. **Esposito**, Department of Neurological Sciences, Division of Neurosurgery, Università degli Studi di Napoli Federico II, Naples, Italy

T. **Fiegele**, Neurosurgical Department, Medical University Innsbruck, Innsbruck, Austria

E. G. **Figueiredo**, Department of Neurological Surgery, University of Sao Paulo School of Medicine, Sao Paulo, Brazil

S. **Froelich**, Department of Neurosurgery, Strasbourg University, CHU de Hautepierre, Strasbourg, France

R. J. **Galzio**, Department of Neurosurgery, University of L'Aquila, L'Aquila, Italy

V. M. **Gerganov**, International Neuroscience Institute-Hannover, Hannover, Germany

B. **Ghodke**, Department of Neurological Surgery, University of Washington, Seattle, WA, USA

A. **Goel**, Department of Neurosurgery, King Edward Memorial Hospital, Seth G.S. Medical College, Parel, Mumbai, India

J. A. **Heth**, Department of Neurosurgery, University of Michigan Health System, Ann Arbor, MI, USA

J. T. **Keller**, Department of Neurosurgery, University of Cincinnati College of Medicine, Cincinnati, OH, USA

I. **Kocijančič**, International Institute for Neurosurgery and Neuroresearch (IINN), Ljubljana, Slovenia

J. L. **Leach**, The Neuroscience Institute, Department of Radiology, University of Cincinnati College of Medicine, Cincinnati, OH, USA

C. **Lindquist**, Gamma Knife Centre, The Cromwell Hospital, London, UK

H. R. van **Loveren**, Department of Neurosurgery, University of South Florida, Tampa, FL, USA

D. **Muzumdar**, Department of Neurosurgery, King Edward VII Memorial Hospital and Seth G.S. Medical College, Parel, Mumbai, India

T. D. **Nadkarni**, Department of Neurosurgery, King Edward Memorial Hospital, Seth G.S. Medical College, Parel, Mumbai, India

S. K. **Natarajan**, Department of Neurological Surgery, University of Washington, Seattle, WA, USA

E. **de Oliveira**, Instituto de Ciências Neurológicas, Sao Paulo, Brazil

R. **Pregelj**, International Institute for Neurosurgery and Neuroresearch (IINN), Ljubljana, Slovenia

A. L. **Rhoton**, Jr., Department of Neurosurgery, University of Florida, Gainesville, FL, USA

M. **Samii**, International Neuroscience Institute-Hannover, Hannover, Germany

L. N. **Sekhar**, Department of Neurological Surgery, University of Washington, Seattle, WA, USA

W. M. **Tavares**, Department of Neurological Surgery, University of Sao Paulo School of Medicine, Sao Paulo, Brazil

M. **Tschabitscher**, Microsurgical & Endoscopic Anatomy, University of Vienna, Vienna, Austria

Chapter 1. Anatomy of the cavernous sinus

The middle cranial base and cavernous sinus

A. L. Rhoton, Jr.

Department of Neurosurgery, University of Florida, Gainesville, FL, USA

Introduction

The middle cranial base can be divided into a medial portion, the sellar and the parasellar region, where the pituitary gland and cavernous sinus are located and a lateral portion, containing the middle cranial fossa and the upper surface of the temporal bone (Fig. 1). The focus of this paper is the cavernous sinus and adjacent parts of the middle cranial fossa [22, 23].

The cavernous sinus

Although the anatomy of the cavernous sinus has been well described, the sinus remains a challenging and unfamiliar place for many neurosurgeons [23, 35]. Browder [3] and Parkinson [16] performed the first cavernous sinus approaches for the treatment of carotid–cavernous fistula, and Taptas [31], Dolenc [4–8], and Umansky [32, 33] were pioneers in studying this region. The paired cavernous sinuses are located near the center of the head on each side of the sella, pituitary gland, and sphenoid sinus (Fig. 2). Each sinus has dural walls that surround a venous plexus and space through which a segment of the internal carotid artery courses. The dural envelope contains not only the cavernous carotid artery, but is also the site of a venous confluence that receives the terminal end of multiple veins draining the cerebrum, cerebellum, brainstem, face, eye, orbit, nasopharynx, mastoid, and middle ear [10, 11] and has free communication with the basilar, superior and inferior petrosal, and intercavernous sinuses. The oculomotor, trochlear, and ophthalmic nerves course in the lateral wall. The abducens nerve courses on the medial side of the ophthalmic nerve between it and the internal carotid artery.

Overall, the sinus is shaped like a boat with its narrow keel located at the superior orbital fissure and its broader bow (posterior wall) located lateral to the dorsum sellae above the petrous apex (Fig. 3). The sinus has four walls: a roof and lateral, medial, and posterior walls. The wide deck or roof of the sinus faces upward and the narrow lower edge, at the junction of the medial and lateral walls, gives the sinus a triangular shape in cross-section. The roof is formed by the dura lining the lower margin of the anterior clinoid process anteriorly and the patch of dura, called the oculomotor triangle, through which the oculomotor nerve penetrates the sinus roof posteriorly.

The cavernous sinus has a wide posterior dural wall that it shares with the lateral part of the basilar sinus, which extends across the back of the upper clivus and dorsum sellae. The cavernous sinus opens into and communicates widely at its posterior end with the basilar sinus. The part of the posterior wall of the cavernous sinus shared with the basilar sinus is located lateral to the dorsum sellae, where the cavernous sinus opens into the basilar sinus and communicates with the superior and inferior petrosal sinuses. The lower margin of the posterior wall of the

cavernous sinus is located above the petrous apex at the upper margin of the petroclival fissure. The abducens nerve passes through the lower margin of the posterior wall and under the petrosphenoid ligament to enter the sinus. The upper edge of the posterior wall is located at the level of the posterior petroclinoid dural fold, which extends from the petrous apex to the posterior clinoid process. The lateral edge of the posterior wall is located just medial to the ostium of Meckel's cave, and the medial edge is located at the lateral margin of the dorsum sellae.

The lateral wall extends from the medial edge of Meckel's cave posteriorly to the lateral margin of the superior orbital fissure anteriorly, and from the anterior petroclinoid dural fold above to the lower edge of the carotid sulcus below (Fig. 2). The carotid sulcus is the groove on the lateral aspect of the body of the sphenoid along which the internal carotid artery courses. The dura forming the posterior part of

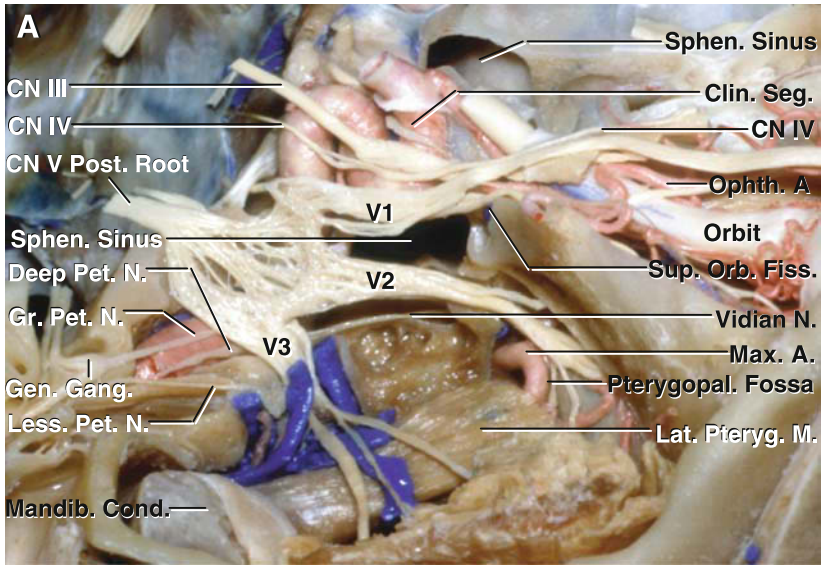

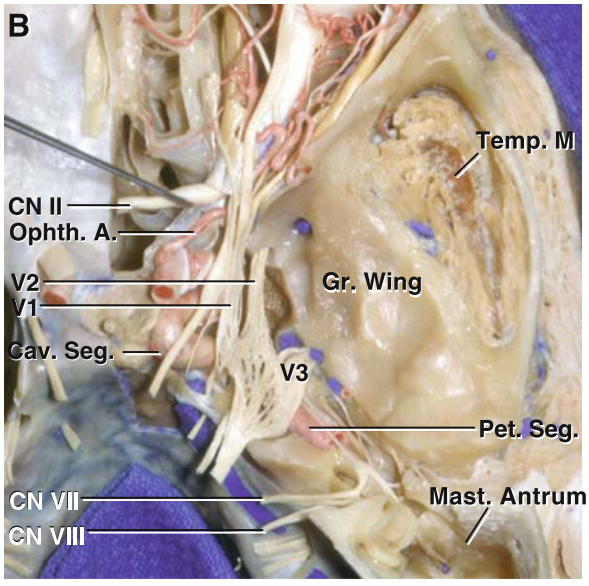

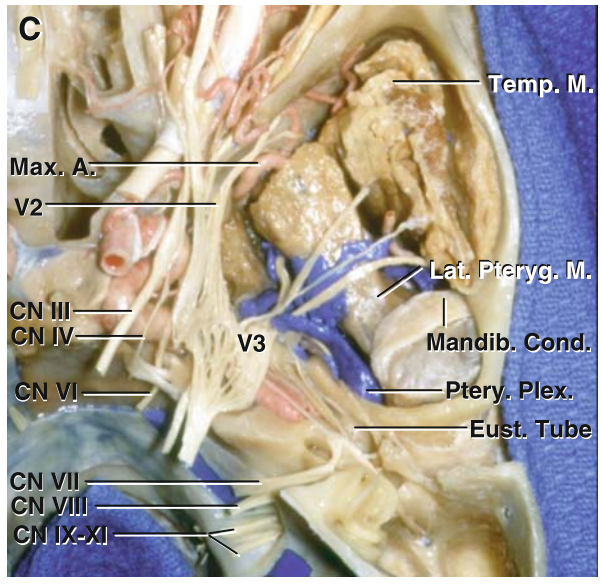

the lateral wall of the sinus also forms the upper third of the medial wall of Meckel's cave.

The medial wall is formed by the dura that constitutes the lateral wall of the sella turcica and covers the lateral surface of the body of the sphenoid bone [36]. The medial wall extends from the lateral edge of the dorsum sellae posteriorly to the medial edge of the superior orbital fissure anteriorly, and from the interclinoid dural fold above to the lower edge of the carotid sulcus below. Anteriorly, the lower edge of the sinus, where the medial and lateral walls meet, is located just below where the ophthalmic nerve courses in the lateral sinus wall, and posteriorly, it is located medial to the junction of the upper and middle third of the gasserian ganglion and Meckel's cave. Only the upper part of the medial wall of Meckel's cave and the upper part of the gasserian ganglion are located directly lateral to the cavernous sinus; thus almost all of Meckel's cave is located below and lateral to the posterior part of the cavernous sinus.

The terminal part of the petrous carotid exits the carotid canal and passes under the trigeminal nerve and the petrolingual ligament, where it turns upward to enter the posterior part of the cavernous sinus. The artery becomes enclosed in the dural envelope of the cavernous sinus after traveling below the petrolingual ligament to reach the carotid sulcus on the lateral surface of the sphenoid body (Fig. 2).

Numerous venous channels course along the lateral margin of the sella, the medial part of the middle fossa, the superior and inferior orbital fissures, the foramina ovale, rotundum, and spinosum and surrounding the pituitary gland. However, they course outside the dural envelope containing the internal carotid artery and open into the sinus through discrete ostia. The part of these veins outside the dural envelope form the pericavernous venous plexus. They become part of the cavernous venous plexus where they pass through the ostia in the dural wall of the sinus (Figs. 2 and 3).

Osseous relationships

The cavernous sinus sits on the lateral aspect of the body of the sphenoid bone and adjacent part of the petrous apex (Fig. 4) [24]. The lower edge of the posterior part of the lower edge of the sinus is positioned above the junction of the petrous apex and body of the sphenoid bone at the upper end of

Fig. 1. Lateral view of the right middle fossa. **A** The dura has been peeled away from the middle fossa and cavernous sinus and the floor of the middle fossa removed. The oculomotor and trochlear nerves enter the roof of the cavernous sinus and pass forward through the superior orbital fissure with the first trigeminal division. The cavernous sinus, located medial to the upper third of the gasserian ganglion, extends from the superior orbital fissure to the petrous apex. The carotid artery exits the cavernous sinus on the medial side of the anterior clinoid process, which has been removed. The bone between the first and second and the second and third trigeminal divisions has been drilled to expose the lateral wing of the sphenoid sinus. The vidian nerve, formed by the union of the greater and deep petrosal nerves, courses forward in the vidian canal to reach the pterygopalatine fossa. The posterior wall of the cavernous sinus extends laterally from the dorsum sellae to the medial edge of the ostium of Meckel's cave. Removal of the floor of the middle fossa exposes the infratemporal fossa, which contains the branches of the maxillary artery and the mandibular nerve, the pterygoid venous plexus, and the pterygoid muscles. The maxillary nerve courses just below the cavernous sinus and passes through the foramen rotundum to enter the pterygopalatine. **B** Superior view of middle cranial base. The floor of the middle fossa, except in the area above the temporalis muscle, has been preserved. The anterior part of the floor of the middle fossa is formed by the greater sphenoid wing, which roofs the infratemporal fossa, and the posterior part of the floor is formed by the upper surface of the temporal bone. The internal acoustic meatus, mastoid antrum, and tympanic cavities have been unroofed. The dural roof and lateral wall of the cavernous sinus have been removed. The petrous segment of the internal carotid artery is exposed lateral to the trigeminal nerve. The temporalis muscle is exposed in the temporal fossa lateral to the greater sphenoid wing. **C** The floor of the middle fossa has been removed to show the relationship below the floor. The temporalis muscle descends medial to the zygomatic arch in the temporal fossa to insert on the coronoid process of the mandible. The infratemporal fossa is located medial to the temporal fossa, below the greater sphenoid wing, and contains the pterygoid muscles and venous plexus and branches of the mandibular nerve and maxillary artery. The mandibular condyle rests in the mandibular fossa located below the posterior part of the middle fossa floor. *A*. artery; *Cav*. cavernous; *Clin*. clinoid; *CN* cranial nerve; *Cond*. condyle; *Eust*. eustachian; *Fiss*. fissure; *Gang*. ganglion; *Gen*. geniculate; *Gr*. greater; *Lat*. lateral; *Less*. lesser; *M*. muscle; *Mandib*. mandibular; *Mast*. mastoid; *Max*. maxillary; *N*. nerve; *Ophth*. ophthalmic; *Orb*. orbital; *Pet*. petrosal, petrous; *Plex*. plexus; *Post*. posterior; *Pteryg*. pterygoid; *Pterygopal*. pterygopalatine; *Seg*. segment; *Sphen*. sphenoid; *Sup*. superior; *Temp*. temporal

the petroclival fissure. The posterior edge of the medial wall rests against the lateral edge of the dorsum sellae. The cavernous sinus extends downward and laterally from the lateral margin of the sella, across the sphenoid body to the junction of the body and greater sphenoid wing of the sphenoid, but does not extend laterally to include the margins of the foramina ovale, rotundum, or spinosum, although venous channels coursing through and around these foramina empty into the sinus and are part of the pericavernous venous plexus. The inconsistently occurring sphenoid emissary foramen, situated medial to the foramen ovale, transmits an emissary vein from the cavernous sinus.

The carotid sulcus is the shallow groove on the lateral aspect of the body of the sphenoid bone along

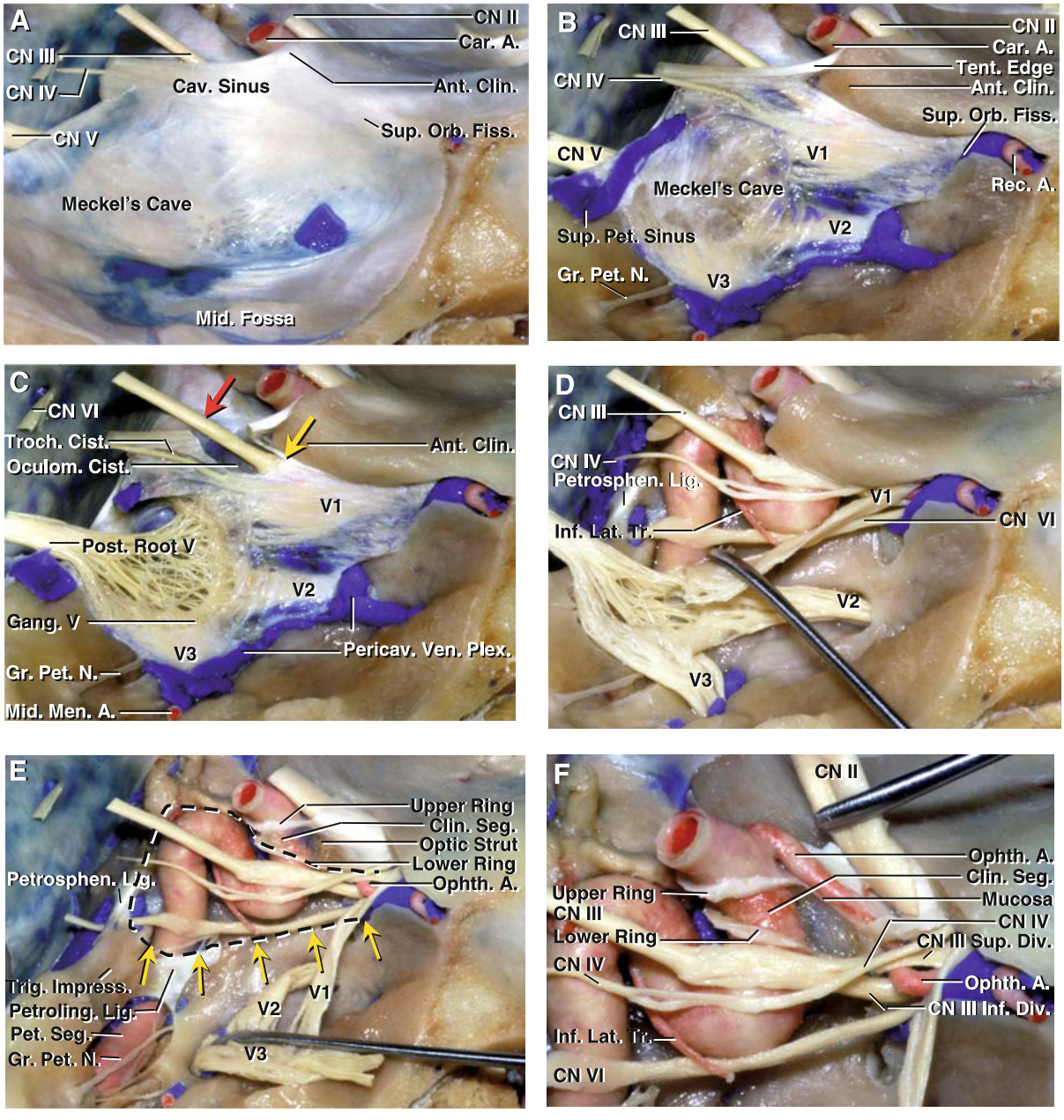

which the intracavernous carotid courses. The artery sits against and is separated from the sulcus by the dura of the medial sinus wall (Fig. 4). The sulcus begins below and lateral to the dorsum sellae at the intracranial end of the carotid canal, turns forward on the body of the sphenoid immediately below the lateral edge of the floor of the sella, and curves upward along the medial to the anterior clinoid process. The segment of the internal carotid artery that courses along the medial side of the clinoid is referred to as the clinoid segment. The carotid sulcus, in well-pneumatized sphenoid bones, forms a serpiginous prominence that can be seen in the lateral wall of the sphenoid sinus below the pituitary fossa. The bone in the lateral wall of the sphenoid sinus may be thin or even absent in some areas, thus allowing the artery to be observed through the sinus wall [9].

The clinoid processes

The anterior clinoid process projects posteriorly from the lesser wing of the sphenoid bone above the anterior part of the roof of the sinus (Fig. 4). The base of the clinoid has three sites of continuity with the adjacent parts of the sphenoid bone. The base is attached anteriorly at the medial edge of the lesser sphenoid wing, and medially to the anterior and posterior roots of the lesser wing. The anterior root of the lesser wing extends medially from the base of the anterior clinoid to the body of the sphenoid bone

Fig. 2. Stepwise dissection of the right cavernous sinus. **A** The lateral wall of the cavernous sinus extends downward from the tentorial edge and blends into the dura covering Meckel's cave and the middle fossa. The oculomotor and trochlear nerves enter the roof of the cavernous sinus. The carotid artery exits the cavernous sinus on the medial side of the anterior clinoid process. **B** The outer layer of dura has been peeled away from the lateral wall of the cavernous sinus and Meckel's cave. This exposes the oculomotor and trochlear nerves entering the roof of the cavernous sinus and passing forward through the superior orbital fissure. The thin layer covering Meckel's cave consists in part of the arachnoid membrane extending forward from the posterior fossa and surrounding trigeminal nerve to the level of the mid portion of the trigeminal ganglion. The superior petrosal sinus passes above the ostium of Meckel's cave and joins the posterior part of the cavernous sinus. **C** The oculomotor nerve enters a short cistern in the sinus roof (red arrow) and does not become incorporated into the lateral sinus wall until it reaches the lower margin of the anterior clinoid process (yellow arrow). The arachnoid covering of Meckel's cave, which extends forward around the posterior trigeminal root to the level of the midportion of the ganglion, has been removed. The cavernous sinus extends from the superior orbital fissure to the petrous apex. It is located medial to the upper third of the gasserian ganglion. The pericavernous venous plexus surrounds the maxillary and mandibular nerves in the region of the foramen rotundum and ovale. **D** The remaining dura covering the lateral sinus wall has been removed. The oculomotor, trochlear, and ophthalmic nerves pass forward and converge on the superior orbital fissure. The segment of the superior petrosal sinus above the posterior trigeminal root has been removed. The venous plexus surrounding the nerves has been removed to expose the trigeminal divisions and the nerves coursing in the wall of the cavernous sinus. The ophthalmic nerve has been depressed to expose the abducens nerve, which passes under the petrosphenoid ligament roofing Dorello's canal, and courses medial to the ophthalmic nerve. The abducens nerve crosses below the ophthalmic nerve as it passes through the superior orbital fissure. **E** The anterior clinoid process has been removed. The optic strut separates the optic canal and superior orbital fissure. The dura extending medially off the upper surface of the anterior clinoid forms the upper dural ring around the internal carotid artery, and the dura lining the lower margin of the clinoid extends medially to form the lower dural ring. The clinoid segment of the carotid artery, located between the upper and lower ring, is enclosed in the dura sheath, referred to as the carotid collar. The trigeminal nerve has been folded downward to expose the petrolingual ligament, which extends above the internal carotid artery, just proximal to where the artery enters the cavernous sinus. The abducens nerve passes around the internal carotid artery and courses medial to the ophthalmic nerve in the lower part of the cavernous sinus. The margins of the cavernous sinus are shown with a broken line. The cavernous sinus does not extend laterally into the area of the trigeminal impression where Meckel's cave sets. **F** Enlarged view. The optic nerve has been elevated to expose the ophthalmic artery coursing within the optic sheath. At the orbital apex, the artery penetrates the optic sheath and enters the orbital apex on the lateral side of the optic nerve. Removal of additional optic strut exposes the mucosa lining the sphenoid sinus on the medial side of the optic strut. *A*. artery; *Ant*. anterior; *Car*. carotid; *Cav*. cavernous; *Cist*. cistern; *Clin*. clinoid; *CN* cranial nerve; *Div*. division; *Fiss*. fissure; *Gang*. ganglion; *Gr*. greater; *Impress*. impression; *Inf*. inferior; *Inf. Lat*. inferolateral; *Lig*. ligament; *Men*. meningeal; *Mid*. middle; *N*. nerve; *Oculom*. oculomotor; *Ophth*. ophthalmic; *Orb*. orbital; *Pericav*. pericavernous; *Pet*. petrosal, petrous; *Petroling*. petrolingual; *Petrosphen*. petrosphenoid; *Plex*. plexus; *Post*. posterior; *Rec*. recurrent; *Seg*. segment; *Sup*. superior; *Tent*. tentorial; *Tr*. trunk; *Trig*. trigeminal; *Troch*. trochlear; *Ven*. venous

and forms the roof of the optic canal. The posterior root of the lesser wing, called the optic strut, extends medially below the optic nerve to the sphenoid body and forms the floor of the optic canal. The base of the anterior clinoid forms the lateral margin of the optic canal.

The segment of the internal carotid artery that courses along the medial aspect of the anterior

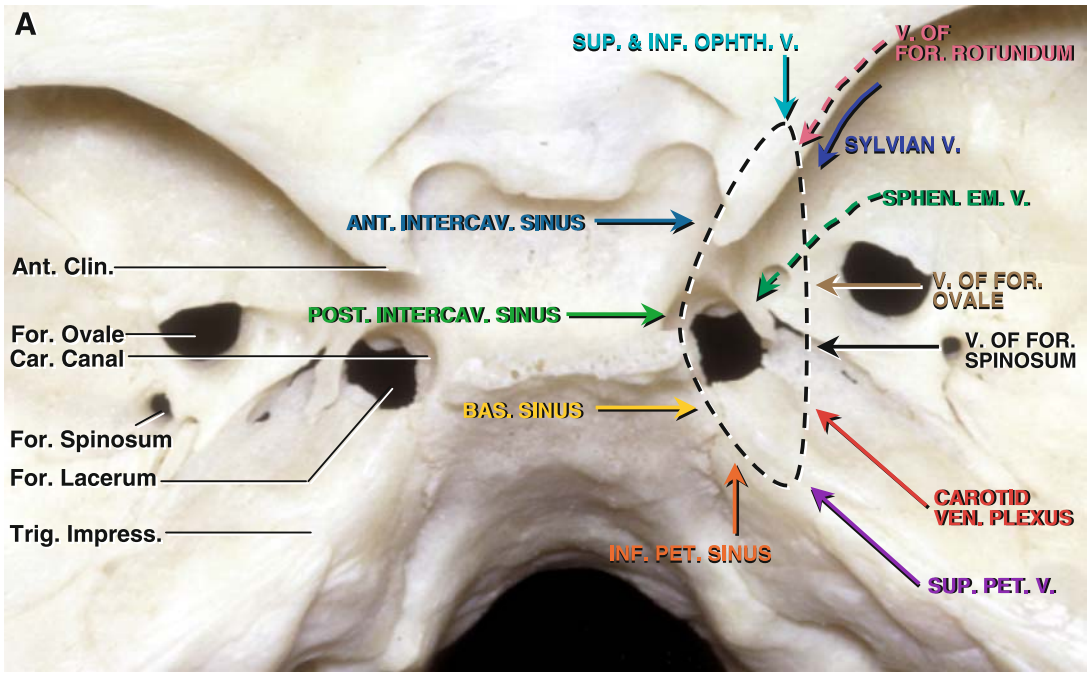

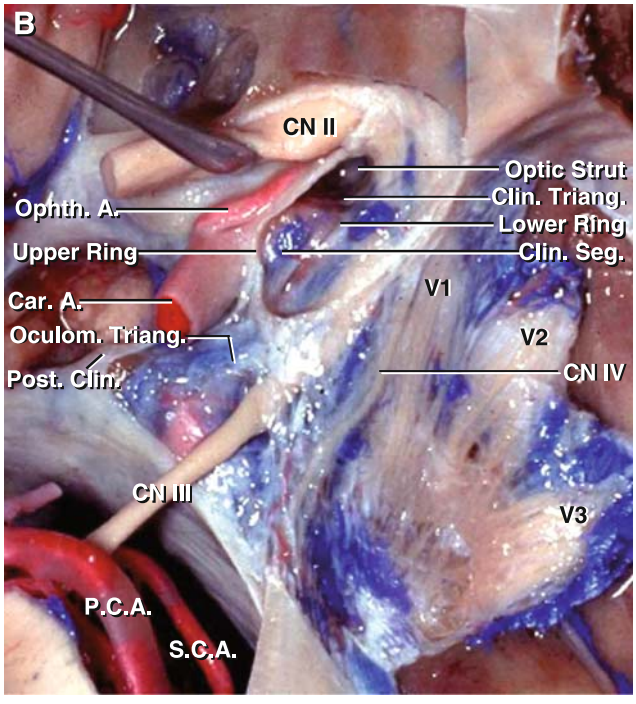

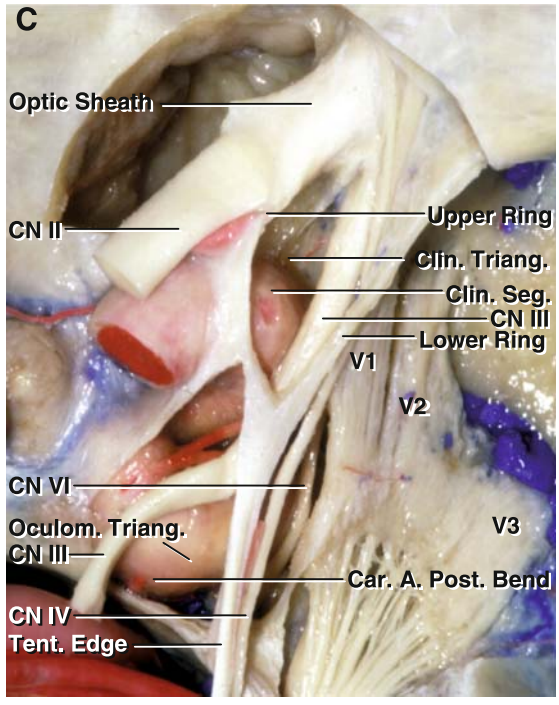

clinoid process and is exposed by removing the anterior clinoid is referred to as the clinoid segment. The clinoid segment courses below the medial half of the lower margin of the clinoid, where it grooves the bone before coursing upward along the medial edge of the clinoid. The medial edge of the clinoid, just behind the base, is frequently the site of a shallow rounded indention that accommodates the lateral surface of the clinoid segment. The posterior tip of the clinoid often projects medially behind the lateral part of the clinoid segment.

Optic strut

The optic strut (posterior root of the lesser wing) is a small bridge of bone that extends from the inferomedial aspect of the base of the anterior clinoid process to the body of the sphenoid just in front of the carotid sulcus (Figs. 2–4) [25]. The strut, from its junction with the clinoid, slopes gently downward and medially as it approaches the body of the sphenoid. The strut separates the optic canal and superior orbital fissure. The superior surface of the strut, which slopes downward and forward from its intracranial edge, forms the floor of the optic canal. The lower surface of the optic strut forms the medial part of the roof of the superior orbital fissure and the anterior part of the roof of the cavernous sinus. The strut sits at the junction of the orbital apex anteriorly, with the superior orbital fissure and optic canal posteriorly. The anterior edge of the strut is a narrow ridge located at the junction of its superior and inferior surfaces. The posterior face of the optic strut, which faces slightly downward, is shaped to accommodate the anterior surface of the anterior bend of the intracavernous carotid, which rests against the posterior surface of the optic strut as it ascends on the medial side of the anterior clinoid process. The air cells in the sphenoid sinus may also extend through the optic strut into the anterior clinoid.

Fig. 3. **A** Superior view of the cranial base in the region of the cavernous sinus. The cavernous sinus extends from the superior orbital fissure anteriorly, to the petrous apex posteriorly, and it is bordered by the sella medially and the middle fossa laterally. It fills the posterior margin of the superior orbital fissure, which is located below the anterior clinoid process and its posterior wall, extends from the lateral edge of the dorsum sellae to the medial margin of the trigeminal impression and Meckel's cave. Numerous venous channels open into the cavernous sinus. These include the basilar, anterior and posterior intercavernous, and the superior and inferior petrosal sinuses; the sylvian and ophthalmic veins, and the veins exiting the foramen ovale, rotundum, and spinosum; and the carotid canal and the sphenoidal emissary foramen. Each structure is shown by colored arrows. The basilar sinus is the largest communicating channel between the cavernous sinuses. **B** Superior view. The anterior clinoid process has been removed. The outer layer of dura covering the roof and lateral wall of the cavernous sinus has been removed while preserving the inner layer in which the nerves course. The roof of the cavernous sinus is formed anteriorly by the dura lining the lower margin of the anterior clinoid and posteriorly by the dura covering the oculomotor triangle. The roof of the optic canal has been opened to facilitate exposure of the ophthalmic artery. Removing the anterior clinoid exposes the clinoidal triangle located between the optic and oculomotor nerves. The dura extending medially off the upper surface of the clinoid forms the upper dural ring. The dura separating the lower surface of the clinoid from the oculomotor nerve and extending medially around the carotid artery, referred to as the carotidoculomotor membrane, forms the floor of the clinoidal triangle and the anterior part of the roof of the cavernous sinus. The carotidoculomotor membrane extends medially to form the lower dural ring. The dura in the floor of the clinoidal triangle and roof of the oculomotor triangle together form the roof of the cavernous sinus. **C** The sinus has been cleared of the material in the venous system and the inner layer of dura has been removed to expose the clinoid segment of the internal carotid artery in the clinoidal triangle and the posterior bend of the intercavernous carotid below the oculomotor triangle. The anterior part of the roof is formed by the dura that separates the anterior clinoid and oculomotor nerve and that extends medially to form the lower dural ring. The posterior part of the roof is formed by the dura forming the oculomotor triangle. **D** The dura has been removed from the roof and lateral wall of another cavernous sinus to expose the passage of nerves through the sinus. The abducens nerve passes below the petrosphenoid ligament and around the lateral surface of the internal carotid artery. **E** Superior view of the cavernous sinus with the anterior clinoid process and roof removed. The lateral wall of the cavernous sinus, in which the oculomotor, ophthalmic, and trochlear nerves course, has been retracted laterally to show the lower margin of the sinus from inside. Numerous ostia of veins drain the surrounding areas open into the cavernous sinus (arrows). The ophthalmic artery enters the optic canal. *A*. artery; *Ant*. anterior; *Bas*. basal; *Car*. carotid; *Cav*. cavernous; *Clin*. clinoid; *CN* cranial nerve; *Em*. emissary; *For*. foramen; *Hyp*. hypophyseal; *Impress*. impression; *Inf*. inferior; *Intercav*. intercavernous; *Lig*. ligament; *Men. Hyp*. meningohypophyseal; *Oculom*. oculomotor; *Ophth*. ophthalmic; *P.C.A*. posterior cerebral artery; *Pet*. petrosal; *Petrosphen*. petrosphenoid; *Post*. posterior; *S.C.A*. superior cerebellar artery; *Seg*. segment; *Sphen*. sphenoid; *Sup*. superior; *Tent*. tentorial; *Triang*. triangle; *Trig*. trigeminal; *V*. vein; *Ven*. venous

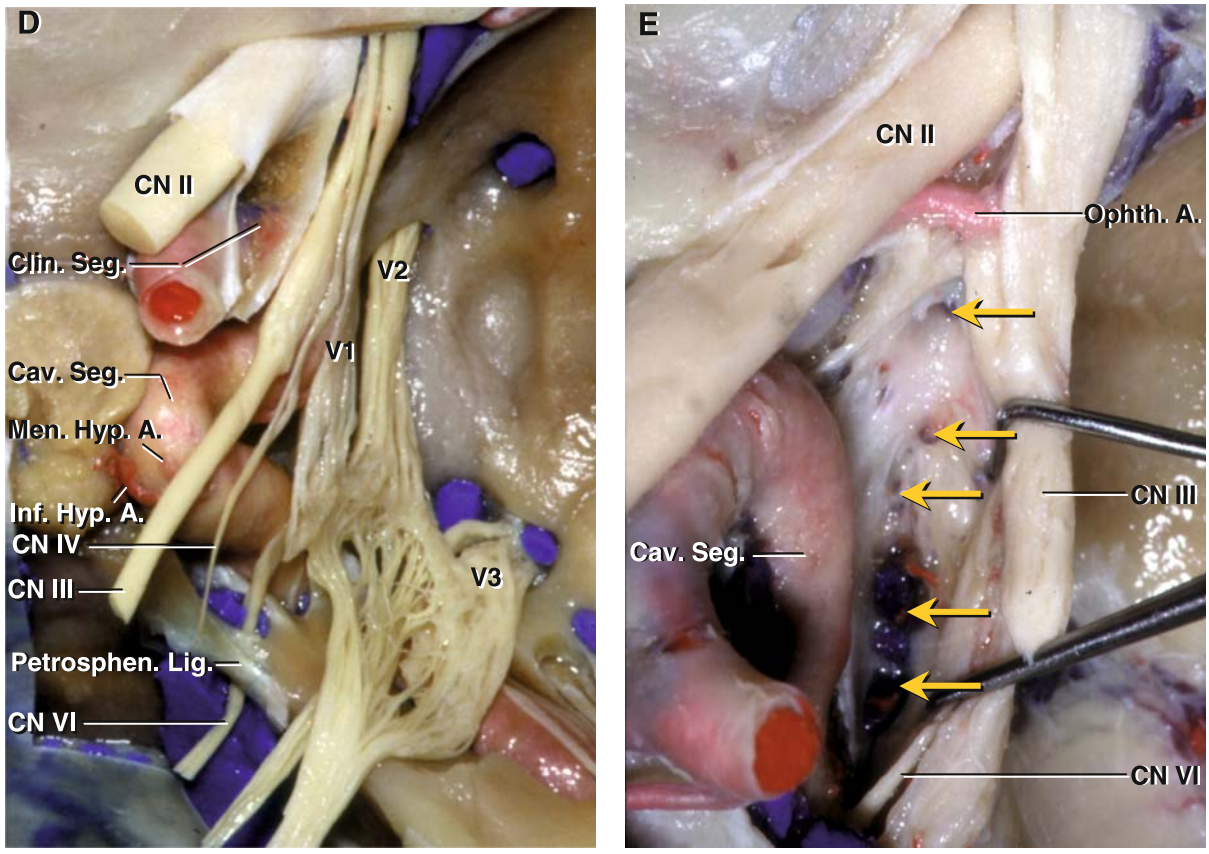

Fig. 3. (*Continued*)

Dural relationships

The consistent nature of the dural layers and folds in the walls and roof of the cavernous sinus provides important landmarks used in surgery. The dural structures include the upper (or distal) and lower (or proximal) carotid dural rings, the carotid collar, and the triangles of the roof and lateral wall of the sinus (Figs. 2 and 3). The dura lining and extending medially from the upper surface of the anterior clinoid forms the lateral part of a dural ring, referred to as the upper or distal ring, which defines the upper margin of the carotid's clinoid segment [29]. The dura forming the lateral part of the upper ring extends forward and medially below the optic nerve to line the upper surface of the optic strut and forms the anterior part of the upper ring. The dura lining the upper surface of the optic strut extends medially and posteriorly at the level of the upper part of the carotid sulcus to form the medial part of the upper ring. Further medially, the dura forming the upper ring blends into the diaphragma sellae.

The lower or proximal dural ring is formed by the layer of dura that lines and extends medially from the lower margin of the anterior clinoid. This layer of dura is called the carotidoculomotor membrane because it separates the lower margin of the clinoid from the oculomotor nerve and extends medially around the carotid artery.

The segment of the internal carotid artery located between the upper and lower dural rings, which is exposed by removing the anterior clinoid process, is referred to as the clinoid segment. It may be necessary to divide the dural rings to mobilize the carotid artery for dealing with aneurysms arising from the internal carotid artery at the level of the roof of the cavernous sinus and origin of the ophthalmic artery.

The dura lining the middle fossa lateral to the cavernous sinus has an inner layer that adheres to the

bone and is called the endosteal layer, and the outer layer faces the brain and is called the meningeal layer (Fig. 5) [35, 36]. The two layers separate at the lower lateral edge of the cavernous sinus and the meningeal layer and outer part of the endosteal extends upward to form the lateral wall of the cavernous sinus, whereas the inner part of the endosteal layer continuous medially to form part of the medial sinus wall. Dissections of the lateral sinus wall reveal that the thicker outer layer (a continuation of the meningeal layer) peels away, leaving the thin inner layer (a continuation of the endosteal layer) that invests the nerves in the lateral wall. The lateral sinus wall blends into the dura covering Meckel's cave. The lower edge of the lateral wall of the cavernous sinus joins the medial wall of the cavernous sinus below the carotid sulcus in a "keel-like" formation at the level of the superior margin of the maxillary nerve.

The medial wall of the cavernous sinus is divided into a sellar part and a sphenoidal part. In our anatomic dissections, we have found the sellar part of the medial wall to be a continuation of the diaphragma sellae that folds downward around the lateral surface of the anterior lobe of the pituitary gland and is constituted by the meningeal layer. The sellar part of the medial wall is not continuous with the sphenoidal part, which is formed by the endosteal layer that covers the body of the sphenoid bone and continues medially across the sellar floor. In our dissections, we found that the sellar part, an extension of the meningeal layer that lines the lower surface of the pituitary gland, is easily separated from the sphenoid part, which lines the floor of the sella and is an extension of the endosteal layer (Fig. 5). The intercavernous sinuses course between the two layers. Therefore, the anterior, posterior, and inferior surfaces of the sella are formed by two layers of dura, and the wall lateral to the pituitary gland is formed by one dural layer, the meningeal layer. Our anatomic dissections allow us to say that the medial sinus wall has one layer that is constituted by the meningeal dura layer on its sellar part and by an endosteal layer (or intracranial periosteum) on its sphenoidal part.

Carotid collar

The dura forming the lower ring, as it approaches the clinoid segment, turns upward inside the bony ring to form a collar (carotid collar) around the artery, which does not adhere or fuse to the wall of the artery until it reaches the level of the upper ring [29]. The upper dural ring, at its junction with the collar, is adherent to the surface of the artery and serves as a barrier between the intra- and extradural spaces. In contrast, the lower dural ring and lower part of the collar are separated from the wall of the artery, creating a narrow space in which courses a thin layer of venous channels that are continuous through the lower part of the collar and lower dural ring with the venous channels within the cavernous sinus. These venous channels extend to just below the level of the upper dural ring. The carotid collar disappears posterior to the tip of the anterior clinoid process, where the dura lining the upper and lower surfaces of the clinoid process fuse into a single dural layer that forms the oculomotor triangle and posterior part of the roof of the cavernous sinus.

Neural relationships

The nerves in the sinus wall or sinus are, from superior to inferior, the oculomotor, trochlear, ophthalmic, and abducens nerves (Figs. 1–3). A sympathetic nerve plexus accompanies the carotid artery through the sinus [10, 11]. The oculomotor, trochlear, and ophthalmic nerves course in the inner part of the lateral sinus wall. The abducens courses medial to the ophthalmic nerve and is adherent to the lateral surface of the intracavernous carotid medially, but it also is adherent laterally to the medial surface of the ophthalmic nerve and the inner part of the lateral sinus wall.

The oculomotor nerve pierces the roof of the cavernous sinus near the center of the oculomotor triangle, and the trochlear nerve enters the dura at the posterolateral edge of the triangle. A short length of both trochlear and oculomotor nerves are surrounded by a dural and arachnoid cuff to create the oculomotor and trochlear cisterns as they pass through the roof of the cavernous sinus and below the anterior clinoid process. Both nerves are situated medial to and slightly beneath the level of the free edge of the tentorium at their point of entry.

The trochlear nerve enters the roof of the sinus posterolateral to the oculomotor nerve and courses below the oculomotor nerve in the posterior part of the lateral wall. Anteriorly, below the base of the anterior clinoid process, it passes upward along the lateral surface of the oculomotor nerve. From there,

the trochlear nerve passes medially between the oculomotor nerve and dura lining the lower margin of the anterior clinoid and optic strut to reach the medial part of the orbit and the superior oblique muscle.

The ophthalmic nerve is the smallest of the three trigeminal divisions. It is inclined upward as it passes forward near the medial surface of the dura, forming the lower part of the lateral wall of the cavernous sinus, to reach the superior orbital fissure. The ophthalmic nerve splits into the lacrimal, frontal, and nasociliary nerves as it approaches the superior orbital fissure.

The superior petrosal sinus passes above the posterior root of the trigeminal root to form the upper margin of the ostium of Meckel's cave, the dural and subarachnoid cavern, which communicates with the subarachnoid space in the posterior fossa. The cave extends forward around the posterior trigeminal root to the midportion of the ganglion.

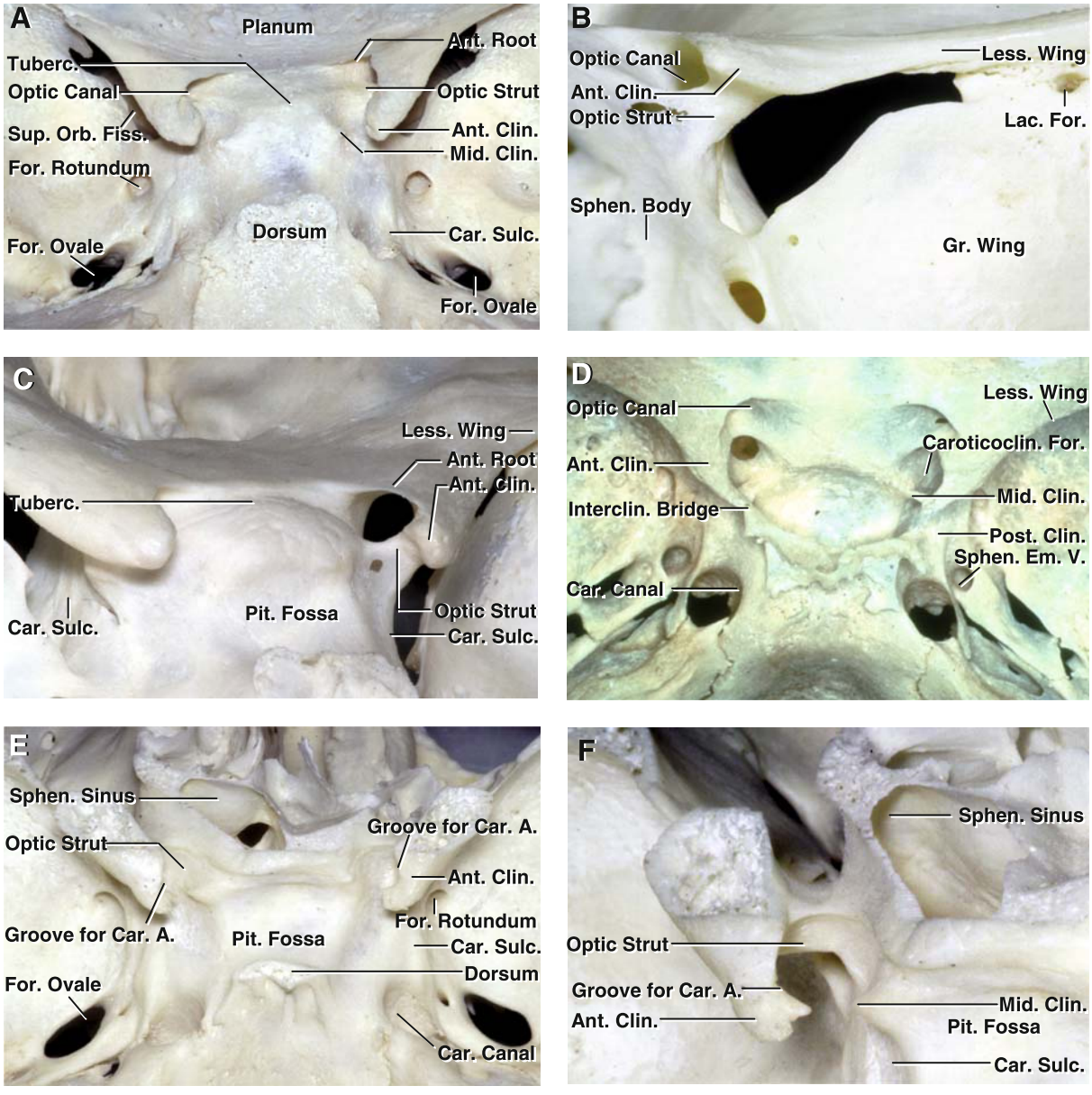

The abducens nerve pierces the dura forming the lower part of the posterior wall of the sinus at the upper border of the petrous apex and enters a dural cave, referred to as Dorello's canal, where it passes below the petrosphenoid ligament (Gruber's ligament). The nerve bends laterally around the proximal portion of the intercavernous carotid and gently ascends as it passes forward inside the cavernous sinus medial to the ophthalmic nerve, on the lateral side of the internal carotid artery. After entering the sinus, it may split into as many as five rootlets as it courses between the internal carotid artery and ophthalmic nerve [10].

Sympathetic fiber bundles large enough to be recognized without a surgical microscope travel on the surface of the carotid as it emerges from the foramen lacerum. Some of the bundles join the VIth nerve within the sinus before ultimately being distributed through the first trigeminal division.

Cavernous sinus and middle fossa triangles

Parkinson [17] described a triangle within the lateral wall of the cavernous sinus through which the intracavernous portion of the carotid artery and its branches might be exposed for the surgical treatment of carotid–cavernous fistulae. Since his pioneering work, a number of significant triangular relationships formed by the convergence and divergence of the cranial nerves in the region of the cavernous sinus and middle fossa have been defined. There are four cavernous sinus triangles, four middle fossae triangles

Fig. 4. Osseous relationships of the cavernous sinus and carotid collar. **A** Superior view. The osseous structures, which nearly encircle the clinoid segment of the internal carotid artery, include the anterior clinoid laterally, the optic strut anteriorly, and the carotid sulcus medially. The carotid sulcus begins lateral to the dorsum sellae at the intracranial end of the carotid canal, extends forward just below the sellar floor, and turns upward along the posterior surface of the optic strut. The anterior clinoid process projects backward from the lesser wing of the sphenoid bone, often overlapping the lateral edge of the carotid sulcus. The anterior root of the lesser sphenoid wing extends medially to form the roof of the optic canal. The posterior root of the lesser wing, referred to as the optic strut, extends from the inferomedial aspect of the anterior clinoid to the sphenoid body. The bony collar around the carotid artery formed by the anterior clinoid, optic strut, and carotid sulcus is inclined downward as it slopes medially from the upper surface of the anterior clinoid to the carotid sulcus. Another small prominence, the middle clinoid process, situated on the medial side of the carotid sulcus at the level of the tip of the anterior clinoid process, projects upward and laterally. In some cases, there is an osseous bridge extending from the tip of the middle clinoid to the tip of the anterior clinoid. In well-pneumatized sphenoid bones, the carotid sulcus is seen as a prominence in the lateral wall of the sphenoid sinus just below the floor of the sella. **B** Posterior view of the optic strut, optic canal, and the superior orbital fissure. The optic strut separates the optic canal and superior orbital fissure and forms the floor of the optic canal and the superomedial part of the roof of the superior orbital fissure. The posterior surface of the strut is shaped to accommodate the anterior wall of the clinoid segment. The artery courses along and may groove the medial half of the lower aspect of the anterior clinoid before turning upward along the medial edge of the clinoid. The air cells in the sphenoid sinus may extend into the optic strut and anterior clinoid. In this case, the sphenoid sinus has pneumatized to a degree that bone is absent over the anterior part of the carotid sulcus, just medial to where the optic strut attaches to the body of the sphenoid bone. The maxillary strut is the bridge of bone separating the superior orbital fissure from the foramen rotundum. **C** Oblique posterior view of the right optic strut. The lateral part of the bony collar around the clinoid segment is formed by the anterior clinoid, the anterior part is formed by the posterior surface of the optic strut and the part of the carotid sulcus located medial to the anterior clinoid process. The posterior surface of the optic strut is wider medially adjacent to the carotid sulcus than it is laterally at the site of attachment to the anterior clinoid process. The optic strut slopes downward from its lateral end so that the medial part of the bony collar is located below the level of the part of the collar joining the anterior clinoid. The inferomedial aspect of the right anterior clinoid is grooved by the artery. **D** Superior view of specimen with bilateral caroticoclinoidal foramen and interclinoidal osseous bridges. An osseous bridge connects the tips of the anterior and middle clinoid processes bilaterally, thus creating a bony ring around the artery, called a caroticoclinoidal foramen, on each side. There is also an interclinoidal osseous bridge connecting the anterior and posterior clinoid processes on both sides. **E** Superior view of another specimen, in which the lesser sphenoid wings and the base of the anterior clinoids and roof of the optic canals have been removed. The remaining part of the anterior clinoid is held in place by its attachment to the optic strut. The medial side of the anterior clinoid is grooved to accommodate the clinoid segment. **F** Enlarged view of the left half of E. The posterior face of the optic strut is shaped to accommodate the anterior surface, and the medial aspect of the anterior clinoid is grooved to accommodate the lateral surface of the clinoid segment. The tip of the anterior clinoid process is the site of a small bony projection directed toward the middle clinoid process, with the anterior and middle clinoids nearly completing a ring around the clinoid segment at the level of the cavernous sinus roof. *A*. artery; *Ant*. anterior; *Car*. carotid; *Caroticoclin*. caroticoclinoid; *Clin*. clinoid; *Em*. emissary; *Fiss*. fissure; *For*. foramen; *Gr*. greater; *Interclin*. interclinoid; *Lac*. lacrimal; *Less*. lesser; *Mid*. middle; *Orb*. orbital; *Pit*. pituitary; *Post*. posterior; *Sphen*. sphenoid; *Sulc*. sulcus; *Sup*. superior; *Tuberc*. tuberculum; *V*. vein [23]

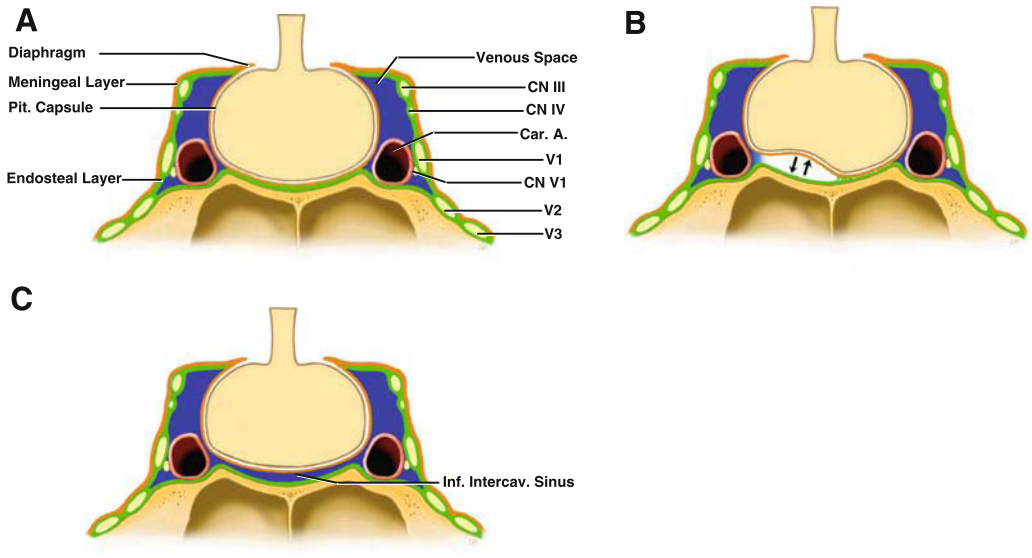

Fig. 5. Diagrams illustrating coronal sections through the cavernous sinus and pituitary gland. **A** Diagram showing the dura divided into a meningeal layer (orange) and an endosteal layer (green). The two layers are tightly adherent in the floor of the middle cranial fossa, but on reaching the upper edge of the second trigeminal division (V2), which is the most inferior limit of the cavernous sinus, they separate into two layers. The meningeal layer extends upward to form the outer layer of the lateral wall and roof of the cavernous sinus and the upper layer of the diaphragma sellae. The endosteal layer, at the level of the upper border of the maxillary nerve, divides into two layers. One layer extends upward to constitute the internal layer of the lateral wall and roof of the cavernous sinus, and the other one adheres to the sphenoid bone, covering the carotid sulcus and the sellar floor. From the free edge of the diaphragma, a thin layer of dura extends downward to wrap around but is easily separable from the pituitary gland. Our dissections suggest that the meningeal layer forms the sellar part of the medial wall of the cavernous sinus and that the endosteal layer (green layer) forms the sphenoidal part of the medial wall. The meningeal and endosteal layers of dura fuse into a single layer on the sellar floor. **B** Diagram illustrating that it is easy to separate the meningeal layer covering the inferior aspect of the pituitary gland from the endosteal layer covering the bony sellar floor. **C** Diagram illustrating an inferior intercavernous sinus that connects the paired cavernous sinuses. These intercavernous sinuses extend across the midline between the meningeal dural layer covering the inferior aspect of the pituitary gland and the endosteal layer covering the osseous sellar floor. *A.* artery; *Car.* carotid; *CN* cranial nerve; *Inf.* inferior; *Intercav.* intercavernous; *Pit.* pituitary [35]

lateral to the cavernous sinus, and two triangles in the paraclival area that are helpful in understanding and planning approaches to the cavernous sinus (Fig. 6). The cavernous sinus triangles are formed by the optic, oculomotor, trochlear, and ophthalmic nerves converging on the optic canal and superior orbital fissure. The middle fossa triangles are formed by the trigeminal divisions diverging as they pass from the gasserian ganglion to reach their foramina.

Cavernous sinus triangles

The roof and lateral wall of the cavernous sinus can be divided into four triangular areas: two in the roof and two on the lateral wall. The triangles in the roof are the clinoidal and oculomotor triangles (Fig. 6). The triangles on the lateral wall are the supratrochlear and infratrochlear triangles (or Parkinson's triangle). The borders of the triangles in the roof of the cavernous sinus are formed by dural folds, whereas the borders of the triangles on the lateral wall are defined by neural structures.

Clinoidal triangle (Dolenc's triangle) This triangle is situated in the interval between the upper and lower dural rings and the optic and oculomotor nerves. This triangle is exposed by removing the anterior clinoid process. The optic strut is in the anterior part, the clinoid segment of the internal

carotid artery is in the midportion, and the thin roof of the cavernous sinus is in the posterior part of this triangle.

Oculomotor triangle This triangle is formed by the triangular patch of dura through which the oculomotor nerve enters the roof of the cavernous sinus. Two margins of this triangle are formed by the anterior and posterior petroclinoidal dural folds that extend, respectively, from the anterior and posterior clinoid processes to the petrous apex. The third side is formed by the interclinoidal dural fold that extends from the anterior to the posterior clinoid process.

Supratrochlear triangle This triangle is situated between the lower surface of the oculomotor nerve and the upper surface of the trochlear nerve. A line joining the points of entrance of these nerves into the dura forms the third margin. This triangle is very narrow.

Infratrochlear triangle (Parkinson's triangle) This triangle is located between the lower margin of the trochlear nerve and the upper margin of the ophthalmic nerve. The third margin is formed by a line connecting the point of entry of the trochlear nerve into the dura to the site where the trigeminal nerve enters Meckel's cave. The posterior bend of the internal carotid artery and the origin of the meningohypophyseal trunk from the posterior bend are located in this triangle, except when the carotid artery is elongated and tortuous, in which case, the origin may be pushed upward into the oculomotor triangle.

Parkinson [16–18] first described the surgical exposure of the intercavernous portion of the carotid artery through this triangle for the treatment of carotid–cavernous fistulas. Parkinson [16], through an incision starting 4 mm beneath the dural entrance of the IIIrd nerve and extending anteriorly approximately 2 cm parallel to the slope of the IIIrd and IVth nerves, exposed the meningohypophyseal trunk and the artery of the inferior cavernous sinus [10]. The VIth nerve at the bottom edge of the exposure was seen on retracting the superior aspect of the trigeminal nerve. Parkinson thought that the triangle would provide access to most spontaneous fistulas, assuming that they are due to ruptured aneurysms developing at the point of departure of the meningohypophyseal trunk or artery of the inferior cavernous sinus.

Middle fossa triangles

Anteromedial middle fossa triangle This triangle is situated between the lower margin of the ophthalmic and the upper margin of the maxillary nerves. The third edge is formed by a line connecting the point where the ophthalmic nerve passes through the superior orbital fissure and the maxillary nerve passes through the foramen rotundum (Fig. 6). Removing bone in the triangular space between the ophthalmic or maxillary nerve opens into the sphenoid sinus.

Anterolateral middle fossa triangle This triangle is located between the lower surface of the maxillary nerve, the upper surface of the mandibular nerve, and a line connecting the foramen ovale and rotundum. Opening the bone in the medial wall of this triangle exposes the lateral wing of the sphenoid sinus.

Posterolateral middle fossa triangle (Glasscock's triangle) This triangle is formed on the anteromedial side by the lateral surface of the mandibular nerve distal to the point at which the greater petrosal nerve crosses below the lateral surface of the trigeminal nerve. On the posterolateral side, it is formed by the anterior margin of the greater petrosal nerve. This triangle opens laterally to encompass the floor of the middle cranial fossa between these two structures. The middle meningeal artery passes through the foramen spinosum in this triangle. Opening the floor of the middle fossa in this triangle exposes the infratemporal fossa.

Posteromedial middle fossa triangle (Kawase's triangle) This triangle is located between the greater petrosal nerve, and the lateral edge of the trigeminal nerve behind the point where the greater petrosal nerve passes below its lateral surface, and a line connecting the hiatus fallopii to the dural ostium of Meckel's cave. The petrous segment of the internal carotid artery crosses the anterior margin of this triangle. The cochlea is located below the floor of the middle fossa in the lateral apex of the triangle. Removing the bone in the lateral part of the posteromedial triangle ex-

poses the cochlea and the anterior wall of the internal auditory canal, and removing the bone in the medial part of the posteromedial triangle exposes the side of the clivus and the inferior petrosal sinus. The approach directed through the petrous apex in this triangle is referred to as an anterior petrosectomy [12].

Paraclinoid triangles

Inferolateral paraclival triangle This triangle is located on the posterior surface of the clivus and temporal bone. The medial margin is formed by a line connecting the dural entry sites of the trochlear and abducens nerves; the upper margin ex-

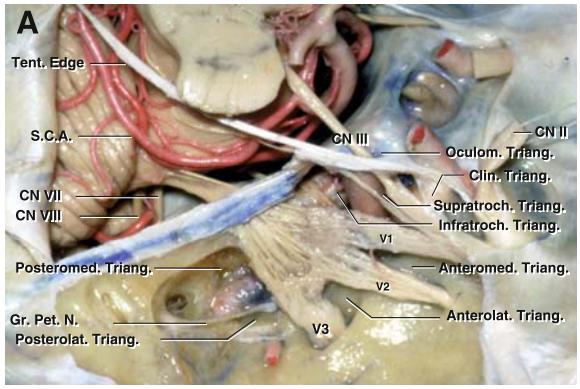

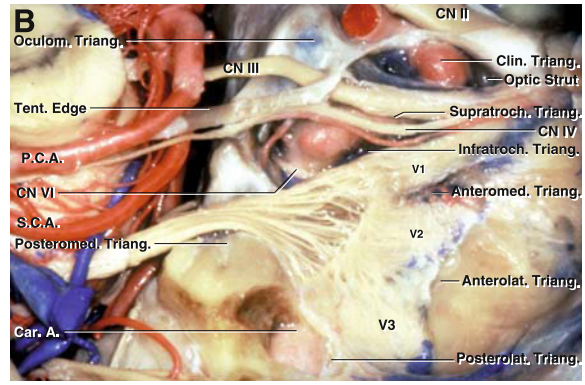

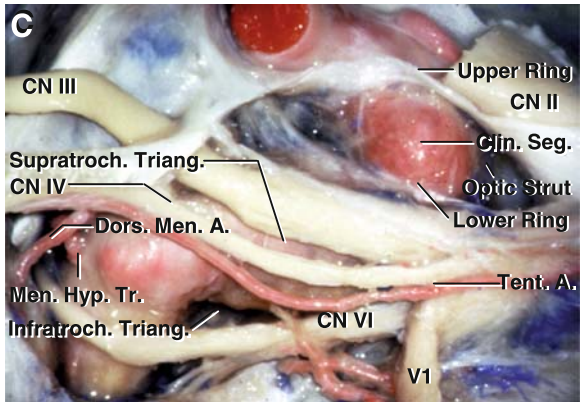

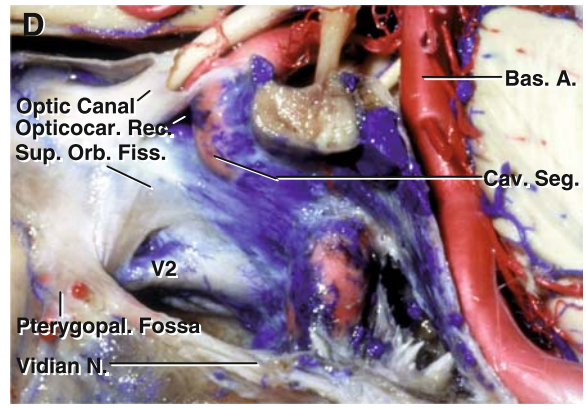

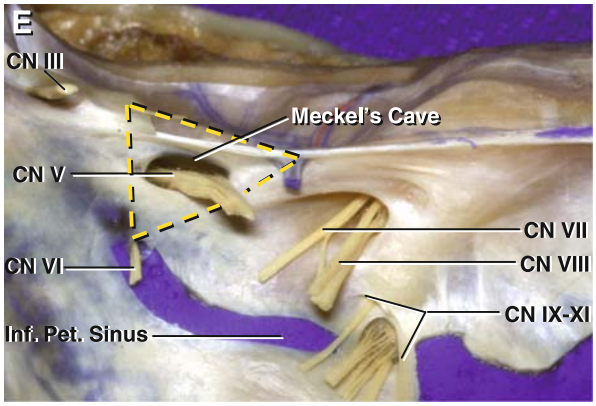

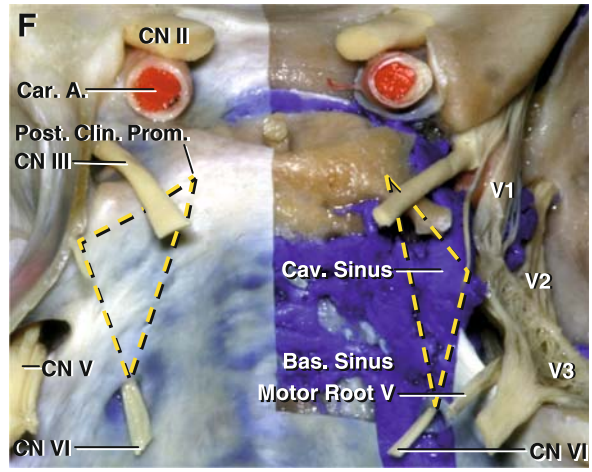

Fig. 6. Triangles in the region of the cavernous sinus and middle fossa formed by the convergence and divergence of the cranial nerves. **A**, **B** Lateral aspect of brainstem and posterior fossa showing the brainstem origin of the cranial nerves, which form the margins of the cavernous sinus and middle fossa triangles. The tentorial edge was preserved in **A** and removed in **B**. There are four cavernous sinus triangles, four middle fossa triangles, and two paraclival triangles. The cavernous sinus triangles are the clinoidal, oculomotor, supratrochlear, and infratrochlear triangle. The clinoidal triangle, exposed by removing the anterior clinoid process, is situated in the interval between the optic and oculomotor nerves. The optic strut is in the anterior part, the clinoid segment is in the midportion and the thin roof of the cavernous sinus is in the posterior part of this triangle. The oculomotor triangle is the triangular patch of dura through which the oculomotor nerve enters the roof of the cavernous sinus. The posterior margin of this triangle is formed by the posterior petroclinoid dural fold, which extends from the petrous apex to the posterior clinoid process. The lateral margin is formed by the anterior petroclinoid dural fold, which extends from the petrous apex to the anterior clinoid process. The medial margin is formed by the intraclinoid dural fold, which extends from the anterior to the posterior clinoid. The supratrochlear triangle is situated between the lower surface of the oculomotor nerve and the upper surface of the trochlear nerve, and has a line joining the points of entrance of these nerves into the dura as its third margin. This triangle is very narrow. The infratrochlear triangle (Parkinson's triangle) is located between the lower margin of the trochlear nerve and the upper margin of the ophthalmic nerve, and has a third margin formed by a line connecting the point of entry of the trochlear nerve into the dura to the site where the trigeminal nerve enters Meckel's cave. The posterior bend of the carotid artery and the origin of the meningohypophyseal trunk are located in this triangle. The middle fossa triangles are the anteromedial, anterolateral, posterolateral, and the posteromedial triangles. The anteromedial triangle is situated between the lower margin of the ophthalmic and the upper margin of the maxillary nerves, and has a third edge formed by a line connecting the point where the ophthalmic nerve passes through the superior orbital fissure and the maxillary nerve passes through the foramen rotundum. Removing bone in the medial wall of this triangle will create an opening into the sphenoid sinus. The anterolateral triangle is located between the lower surface of the maxillary nerve, the upper surface of the mandibular nerve, and a line connecting the foramen ovale and rotundum. Opening the bone in the medial wall of this triangle exposes the sphenoid sinus. The posterolateral triangle (Glasscock's triangle) is formed on the anterolateral side by the lateral surface of the mandibular nerve distal to the point at which the greater petrosal nerve crosses below the lateral surface of the trigeminal nerve, and on the posterolateral side is formed by the anterior margin of the greater petrosal nerve. This triangle encompasses the floor of the middle cranial fossa between these two structures. The middle meningeal artery passes through the foramen spinosum in this triangle. Opening the floor of the middle fossa in this triangle exposes the infratemporal fossa. The posteromedial triangle (Kawase's triangle) is located between the greater petrosal nerve and the lateral edge of the trigeminal nerve behind the point where the greater petrosal nerve passes below the lateral edge of the trigeminal nerve, and a line along the connecting hiatus falopi to the dural ostium of Meckel's cave. The petrous carotid crosses the anterior margin of this triangle. The cochlea is located below the floor of the middle fossa in the lateral apex of the triangle. Drilling the bony floor of the triangle in the area behind the internal carotid artery and medial to the cochlea exposes the lateral edge of the clivus. **C** Enlarged view of the clinoidal, oculomotor, supratrochlear, and infratrochlear cavernous sinus triangles. The optic strut is exposed in the anterior part of the clinoidal triangle, the clinoid segment is exposed in the midportion and the roof of the cavernous sinus is exposed in the posterior part. The upper margin of the clinoid segment is surrounded by the upper dural ring, which is formed by the dura extending medially from the upper surface of the anterior clinoid. The lower margin of the clinoid segment is defined by the lower dural ring, which is formed by the dura extending medially from the lower margin of the anterior clinoid. The dura on the lower margin of the anterior clinoid, referred to as the carotidoculomotor membrane, separates the lower surface of the anterior clinoid from the upper surface of the oculomotor nerve and extends medially to form the lower dural ring. The posterior bend of the internal carotid artery and the origin of the meningohypophyseal trunk, which gives rise to the tentorial and dorsal meningeal arteries, are exposed in the infratrochlear triangle. The abducens nerve passes through Dorello's canal and between the lateral surface of the intracavernous carotid and the medial side of the ophthalmic nerve. **D** View through the sphenoid sinus, of the medial side of the cavernous sinus shown in **B**. On the sphenoid sinus side of the specimen, the optic canal is seen above the opticocarotid recess, which leads into the optic strut. The clinoid segment rests against the posterior aspect of the optic strut in both views. In the lateral view, the superior orbital fissure through which the ophthalmic, trochlear, abducens nerves pass is seen below the optic strut. In the sphenoid sinus, the medial edge of the superior orbital fissure produces a wide rounded prominence below the optic strut, and the maxillary nerve produces a prominence in the lower part of the sphenoid sinus just distal to the foramen rotundum. The lateral wing of the sphenoid sinus extends laterally under the maxillary nerve into the medial part of the floor of the middle fossa. Opening the middle fossa floor in the anteromedial and anterolateral triangles exposes the sphenoid sinus. **E** Posterior view of the inferolateral triangle. The medial edge of the inferolateral triangle extends between the dural entrances of the IVth and VIth nerves. The inferior limb extends from the VIth nerve to where the first vein lateral to Meckel's cave joins the superior petrosal sinus and the superior limb extends from that vein to the dural entrance of the Vth nerve. The ostium of Meckel's cave is located within the inferolateral triangle. **F** Posterior view of the inferomedial triangles. The medial limb of the inferomedial triangle extends from the posterior clinoid to the dural entrance to the VIth nerve. The lateral limb extends between the dural entrances of the IVth and VIth nerves and the superior limb extends from the IVth nerve to the posterior clinoid. On the right side, there is an abnormal projection of the posterior clinoid process, which extends below the oculomotor nerve toward the petrous apex. *A.* artery; *Anterolat.* anterolateral; *Anteromed.* anteromedial; *Bas.* basilar; *Car.* carotid; *Cav.* cavernous; *Clin.* clinoid; *CN* cranial nerve; *Dors.* dorsal; *Fiss.* fissure; *Gr.* greater; *Inf.* inferior; *Infratroch.* infratrochlear; *Men.* meningeal; *Men. Hyp.* meningohypophyseal; *N.* nerve; *Oculom.* oculomotor; *Opticocar.* opticocarotid; *Orb.* orbital; *P.C.A.* posterior cerebral artery; *Pet.* petrosal; *Post.* posterior; *Posterolat.* posterolateral; *Posteromed.* posteromedial; *Prom.* prominence; *Pterygopal.* pterygopalatine; *Rec.* recess; *S.C.A.* superior cerebellar artery; *Seg.* segment; *Sup.* superior; *Supratroch.* supratrochlear; *Tent.* tentorial; *Tr.* trunk; *Triang.* triangle

tends from the dural entrance of the trochlear nerve to the point at which the first petrosal vein lateral to Meckel's cave joins the superior petrosal sinus; and the lower margin is formed by a line connecting the point at which the abducens nerve enters the dura to the site at which the first petrosal vein, lateral to the trigeminal nerve, joins the superior petrosal sinus. The porus through which the posterior trigeminal root enters Meckel's cave is situated in the center of the inferolateral paraclival triangle.

Inferomedial paraclival triangle This triangle is formed above by a line extending from the posterior clinoid process to the dural entrance of the trochlear nerve; laterally by a line connecting the dural entrances of the trochlear and abducens nerves; and medially by a line extending from the dural entrance of the abducens nerve to the posterior clinoid process. The abducens nerve enters the cavernous sinus at the lower edge of this triangle. This triangle extends along the posterior sinus wall. Removing the medial part of the inferomedial triangle behind the internal carotid artery exposes the lateral edge of the dorsum sellae, the upper end of the petroclival suture, and the VIth nerve passing below Gruber's ligament.

Arterial relationships

The cavernous sinus contains the intracavernous segment of the internal carotid artery and its branches (Figs. 1–3 and 6). The internal carotid artery exits the foramen lacerum lateral to the posterior clinoid process where it passes under the petrolingual ligament and turns abruptly forward to course along the carotid sulcus and lateral part of the body of the sphenoid. It passes forward in a horizontal direction for approximately 2 cm and terminates by passing upward along the medial side to the anterior clinoid process and the posterior surface of the optic strut where it penetrates the roof of the cavernous sinus. The clinoid segment of the carotid artery is tightly surrounded by the anterior clinoid process laterally, the optic strut anteriorly, and the carotid sulcus medially, leaving only a narrow space between the bone and artery.

Just proximal to the cavernous sinus in the foramen lacerum the artery lies beneath the trigeminal nerve. In surgical approaches to the trigeminal nerve directed through the middle cranial fossa, there is a tendency to assume that the carotid artery is distant from the trigeminal nerve. However, nearly 85% of carotid arteries are exposed under some portion of Meckel's cave and the trigeminal nerve with only dura, and no bone, separates the nerve from the artery [10]. In the remainder, the bone separating the nerve and artery is often paper-thin. The absence of bone over the carotid often extends to the lateral edge of the trigeminal nerve and, in more than a third, the bone covering the carotid is defective lateral to the edge of the third division. The maximum length of artery exposed lateral to the nerve was 7 mm in our study [10].

The branches of the intracavernous carotid are the meningohypophyseal trunk, the largest branch, present in 100% of our specimens; the artery of the inferior cavernous sinus, present in 84%; and McConnell's capsular arteries, present in 28%. Less frequent branches of the intracavernous carotid were the ophthalmic artery (8%) and the dorsal meningeal artery (6%) [10].

Ophthalmic artery

The ophthalmic artery commonly arises just above the upper ring from the medial half of the anterior wall of the internal carotid artery. From its origin, it runs anteriorly and laterally on the upper surface of the optic strut and below the optic nerve. It runs freely above the optic strut inside the posterior part of the optic canal, but anteriorly it pierces the dura on the upper surface of the optic strut and exits the optic canal outside the optic sheath to course on the inferolateral aspect of the optic nerve and sheath at the orbital apex. The ophthalmic artery may also arise in the cavernous sinus or from the clinoid segment, in which case it usually passes through the superior orbital fissure. It may rarely arise from the middle meningeal artery.

Intracavernous branches

The meningohypophyseal trunk, the most proximal intracavernous branch, arises lateral to the dorsum sellae at or just before the apex of the first curve of the intracavernous carotid where it turns forward

after leaving the foramen lacerum (Figs. 1, 2, and 6). The meningohypophyseal trunk divides near the roof of the cavernous sinus and typically gives rise to three branches: (1) the tentorial artery, also called the artery of Bernasconi-Cassinari, which courses lateral to the tentorium; (2) the inferior hypophyseal, which travels medially to supply the posterior pituitary capsule; and (3) the dorsal meningeal artery, which enters the dura of the posterior sinus wall and supplies the clival dura and VIth nerve [2, 10].

There are two types of meningohypophyseal trunk: complete and incomplete. The complete type gives rise to all three of the usual meningohypophyseal branches. The incomplete type gives rise to one or two of the usual branches, and the other ones arise directly from the intracavernous carotid. Inoue et al. [11] reported 70% of the complete type and 30% of the incomplete type. All three of the usual branches of the meningohypophyseal trunk may infrequently originate directly from the intracavernous carotid artery. The artery of the inferior cavernous sinus, also called the inferolateral trunk, may infrequently arise from the meningohypophyseal trunk [10].

The tentorial artery, the most constant branch of the meningohypophyseal trunk, passes forward to the roof of the cavernous sinus and then posterolaterally along the free edge of the tentorium [2]. The dorsal meningeal artery arises from the meningohypophyseal trunk and passes posteriorly through the cavernous sinus with the abducent nerve to reach the dura over the dorsum and clivus. The inferior hypophyseal artery, the least frequent of the three common branches of the meningohypophyseal trunk passes medially to the posterior pituitary capsule and lobe and anastomoses with its mate of the opposite side after supplying the dura of the sellar floor [10, 11].

The inferolateral trunk (artery of the inferior cavernous sinus) arises from the lateral side of the midportion of the horizontal segment of the intracavernous carotid distal to the origin of the meningohypophyseal trunk. It arises directly from the carotid artery in 84% of cavernous sinuses and from the meningohypophyseal artery in another 6% [10, 11]. It passes above or below the VIth nerve and downward medial to the first trigeminal division to supply the dura of the inferior lateral wall of the cavernous sinus.

McConnell's capsular arteries arise from the medial side of the carotid artery and pass to the capsule of the gland or the dura lining the anterior wall and floor of the sella [14]. They are frequently absent, being found in approximately a quarter of cavernous sinuses [10].

Parkinson [15–20] noted that spontaneous carotid–cavernous fistulas, which are presumed to be due to aneurysm rupture, tend to occur at the junction of one of the branches with the intracavernous carotid. Traumatic fistulas due to tears of the carotid and/or one or more of its intracavernous branches may have several sources, and are commonly located anteriorly in the sinus. Another artery, larger than the meningohypophyseal trunk that may pass through the cavernous sinus, is a persistent trigeminal artery. This artery arises from the carotid artery in the cavernous sinus proximal to the origin of the meningohypophyseal trunk and joins the basilar artery between the superior cerebellar and anteroinferior cerebellar arteries.

Arteriovenous fistulae between the branches of the meningohypophyseal trunk, especially the dorsal meningeal branch and the basilar sinus, may produce all the signs and symptoms associated with a fistula between the internal carotid artery and the cavernous sinus [10]. A fistula between the dorsal meningeal artery and the basilar sinus may be of the low-flow type. The fistulas, because of a communication between a branch of the intracavernous carotid or a branch of the external carotid artery in the floor of the middle fossa, will be more amenable to direct occlusion of the fistula than one in which there has been a traumatic rupture of the carotid artery into a large venous cavern. In dealing with a carotid–cavernous fistula, it is important to remember that the proptosis may occur on the side opposite the cavernous sinus harboring the fistula.

Venous relationships

The cavernous sinus is shaped like a boat, being the narrowest anteriorly near the superior orbital fissure and widest posteriorly lateral to the dorsum sellae where it opens into the venous confluence formed by the junction of the basilar, cavernous, and superior and inferior petrosal sinuses (Figs. 2, 3, and 6). The sinus is connected to the orbit by the

superior and inferior ophthalmic veins, to the cerebral hemispheres through the middle and inferior cerebral veins, to the retina by the central retinal vein, to the dura by tributaries of the middle meningeal veins, to the transverse sinus via the superior petrosal sinus, to the jugular bulb by way of the inferior petrosal sinus, to the pterygoid venous plexus by the emissary veins passing through the cranial foramina, and to the facial veins through the ophthalmic veins. The basilar sinus, the largest and most constant intercavernous connection across the midline, passes posterior to the dorsum sellae and upper clivus and connects the posterior aspect of both cavernous sinuses.

The cavernous sinus has four venous spaces (medial, anteroinferior, posterosuperior, and lateral), which are defined according to their position in relation to the intracavernous carotid. The widest spaces are located posteriorly near the junction with the basilar sinus and anteriorly near the superior orbital fissure. The medial compartment is situated between the pituitary gland and the carotid artery [10]. The anteroinferior space is located in the concavity below the first curve of the intracavernous carotid where the superior and inferior ophthalmic veins commonly open into the sinus. The superior or common trunk of the superior and inferior ophthalmic veins commonly empties into this space. The posterosuperior space is located between the intracavernous carotid and the posterior half of the roof of the sinus. The basilar sinus opens into the posterosuperior space. These three venous spaces are larger than the lateral space located between the carotid artery and the lateral sinus wall. The lateral space is usually so narrow that the VIth nerve that passes through it is adherent to the carotid on its medial side and to the sinus wall on its lateral side. The fact that the medial or posterior spaces are the largest makes them the most suitable areas for entering the sinus. The medial space can be entered through the roof on the medial side of the oculomotor nerve and the posterior space can be entered through Parkinson's triangle.

Intercavernous sinus

The venous sinuses commonly found in the margins of the diaphragma and sella and connecting both cavernous sinuses are termed the intercavernous sinuses [21]. These intercavernous connections within the sella are named on the basis of their relationship to the pituitary gland; the anterior intercavernous sinuses pass anterior to the hypophysis, and the posterior intercavernous sinuses pass behind the gland. These transsellar connections between the cavernous sinuses may exist at any point from the anterior to the posterior wall of the sella, including the diaphragma, or all connections between the two sides may be absent. The anterior intercavernous sinuses are usually larger than the posterior ones. If the anterior and posterior connections coexist and join with the cavernous sinus to form a venous ring around the gland, the whole structure constitutes the "circular sinus" [29].

Fig. 7. **A** Orbitozygomatic craniotomy and transcavernous approach to basilar apex. **A**, the inset (lower left) shows the scalp incision and the inset (lower right) shows the two-piece orbitozygomatic craniotomy. The sylvian fissure has been opened to expose the optic and oculomotor nerves and the anterior and middle cerebral and posterior communicating arteries. **B** The carotid artery has been elevated to expose the basilar artery apex through the interval between the carotid artery and oculomotor nerve. The posterior clinoid process blocks access to the basilar artery. **C** The anterior clinoid process has been removed and the roof of the cavernous sinus have been opened to provide access to the clinoid segment of the internal carotid artery and the posterior clinoid process. The upper dural ring extends medially from the upper margin of the anterior clinoid process. **D** The oculomotor triangle has been opened and the dura removed from the posterior clinoid and adjacent dorsum in preparation for removing the clinoid and adjacent dorsum. **E** The posterior clinoid process and adjacent dorsum has been removed and the anterior part of the tentorial edge has been opened to expose the upper part of the basilar artery. **F** The anterior part of the tentorial edge has been removed to expose the upper margin of the posterior trigeminal root in Meckel's cave and to provide increased access to the upper part of the basilar artery. The trochlear nerve was preserved in opening the anterior part of the tentorial edge. Note the difference in the length of basilar arteries exposed in **B** and **F**. *A.* artery; *A.Ch.A.* anterior choroidal artery; *A.Co.A.* anterior communicating artery; *Bas.* basilar; *Car.* carotid; *Cav.* cavernous; *Clin.* clinoid; *CN* cranial nerve; *Lam.* lamina; *P.Co.A.* posterior communicating artery; *Pit.* pituitary; *Post.* posterior; *S.C.A.* superior cerebellar artery; *Seg.* segment; *Term.* terminalis

Clinoid venous space

The clinoid venous space, the upward extension of the cavernous sinus through the lower dural ring and inside the carotid collar, is widest at the level of the lower ring through which it communicates with the larger venous channels in the anterior part of the cavernous sinus and narrows superiorly to a thin serpiginous venous plexus, which disappears as the upper ring is approached, thus demonstrating that the clinoid segment is intracavernous.

Discussion

A controversy has arisen as to whether the sinus is an unbroken, trabeculated, venous cavern or a plexus of various sized veins that divide and coalesce and

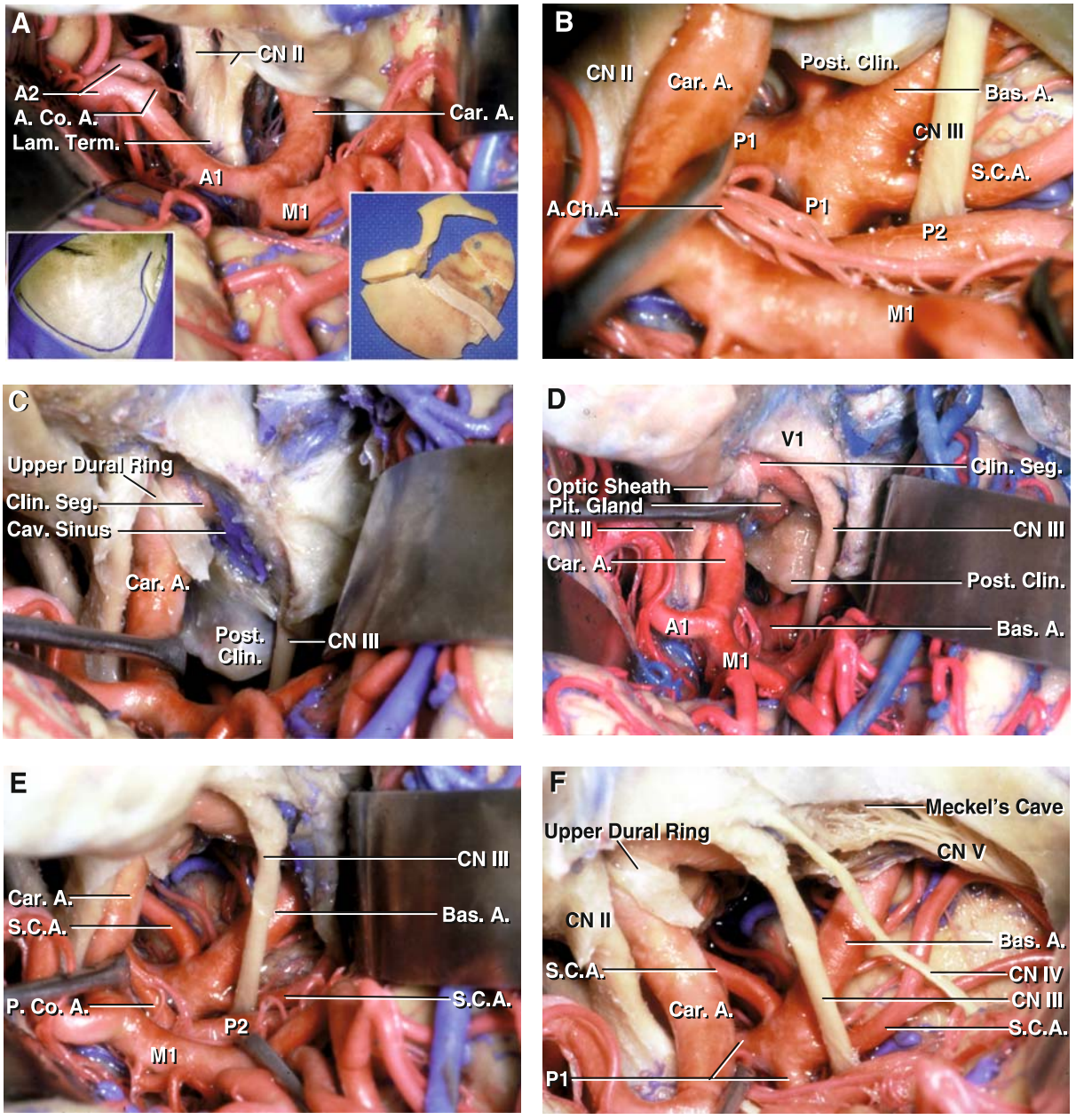

incompletely surround the carotid artery [1, 18, 31]. Both concepts are, in part, correct. Numerous veins, such as those from the orbit, middle fossa dura, and sylvian fissure, maintain their integrity as they wind their way around the carotid arteries and nerves in the sinus wall before opening into the sinus. In other areas, numerous dural sinuses converge and form large venous spaces in the sinus, such as in the area where the basilar and the superior and inferior petrosal sinuses open into the posterior part of the cavernous sinus, or on the medial side of the carotid artery where the intercavernous sinuses join the cavernous sinus. The degree to which a cavern or a venous plexus will predominate varies from sinus

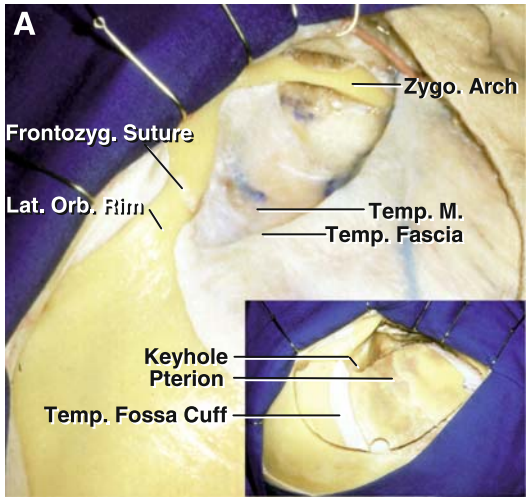

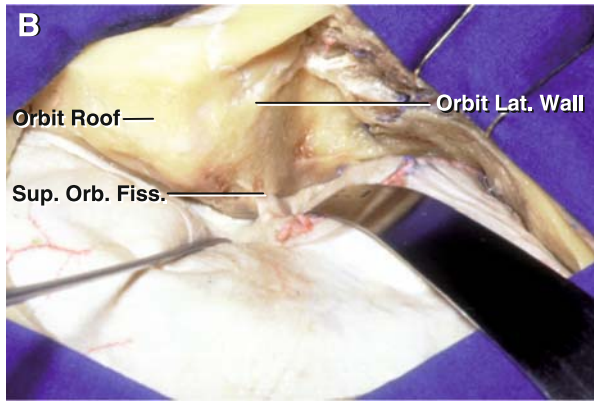

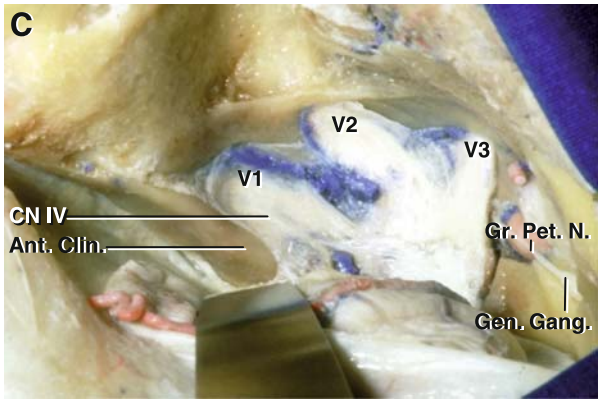

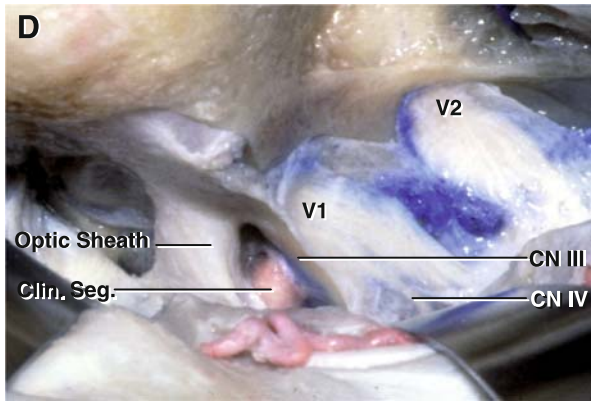

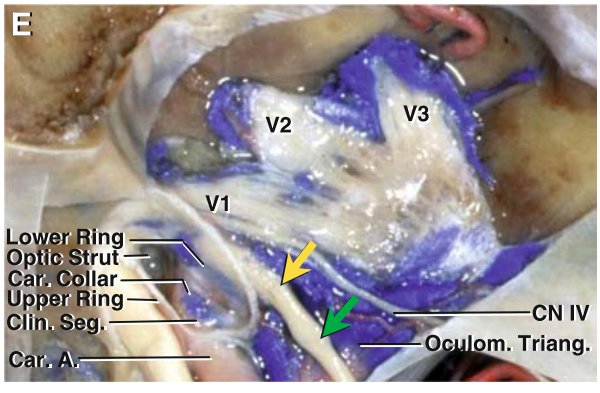

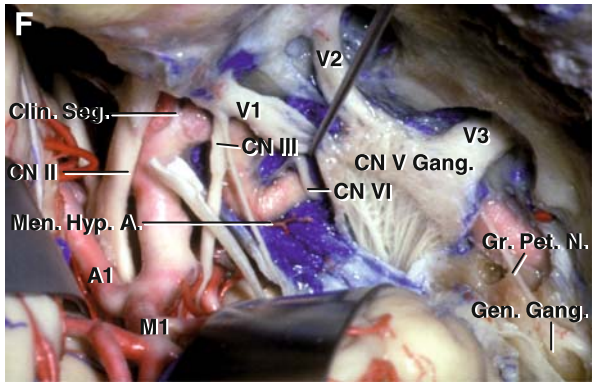

to sinus and from one area to another in the same sinus. The venous plexus predominates anteriorly near the orbital apex and superior orbital fissure, but becomes a cavern where these numerous venous channels join within the dural envelope defining the sinus. The cavern is largest at the junction of the basilar and superior and inferior petrosal sinuses with the cavernous sinus and on the medial side of the carotid where the intercavernous sinus joins the paired cavernous sinuses. Parkinson's observations are valuable in that they form the basis for carefully examining the anatomy of the carotid–cavernous fistulae and identifying those involving the veins in the area that can be repaired with a single clip while preserving the carotid artery.

Operative considerations

The walls of the cavernous sinus are exposed in the operative approaches that reach the infra-, supra-, and parasellar areas [4–8, 26–28, 34]. A pterional (frontotemporal) or orbitozygomatic craniotomy is commonly selected to expose the roof and lateral wall of the sinus and also to provide access to the adjoining orbit and suprasellar area. The lateral sinus wall can also be exposed by the subtemporal route, but reaching the sinus roof by this route often requires significant temporal lobe retraction, and the angle of view is not suitable for examining the roof. The orbitozygomatic approach is a variant of the frontotemporal craniotomy in which a variable amount of the upper and lateral orbital rim and zygomatic arch are elevated as a single piece in continuity with the bone flap or as a second step after elevation of a frontotemporal (pterional) bone flap. The orbitozygomatic craniotomy provides an excellent exposure of the cavernous sinus and orbital contents and the structures passing through the optic canal and superior orbital fissure. The frontotemporal approach without the orbitozygomatic osteotomy is suitable for lesions that are more strictly intracranial in the supra- and parasellar areas.

The cavernous sinus is usually approached through its roof or lateral wall. The approach through the roof involves opening the anterior portion only or the anterior and posterior portions together, depending on the site of pathological findings. If the pathological abnormality is a paraclinoid aneurysm, only the anterior portion of the sinus roof is opened. For the transcavernous approach to a basilar tip aneurysm, the anterior and posterior parts of the roof are opened. The approach through the lateral wall is used for lesions arising from the structures in the lateral wall, such as meningiomas, trigeminal neuromas,

Fig. 8. Pterional craniotomy and extradural approach to the right cavernous sinus. **A** The scalp has been reflected using subgaleal dissection to expose the frontal bone and the temporalis muscle and fascia. The superficial layer of temporalis fascia has been divided just above the fat pad so that the superficial layer of temporalis fascia and the fat pad with the facial nerve branches to the frontalis muscle can be folded downward with the scalp flap to protect the branches of the facial nerve. The inset shows the burr holes and craniotome cuts for the bone flap. The keyhole burr hole is located above and behind the frontozygomatic suture. **B** The sphenoid ridge has been flattened with a drill and a thin shell of bone has been left along the roof and lateral wall of the orbit. The dura has been elevated from the orbital roof and lateral wall to the lateral edge of the superior orbital fissure, where the dura blends into the periorbita. It is often necessary to make a shallow cut in the dura at this lateral apex of the fissure to continue to peel the thick outer layer of dura in the lateral sinus wall from the inner layer investing the nerves. **C** The dura has been elevated from the anterior clinoid process and backward along the sinus wall to expose the three trigeminal divisions and trochlear and greater petrosal nerves and petrous apex. **D** The anterior clinoid process has been removed to expose the clinoid segment and the anterior part of the sinus roof formed by the dura lining the lower surface of the clinoid. **E** The outer layer of dura in the roof and lateral wall of the sinus has been elevated while preserving the inner layer of dura. Removing the anterior clinoid process exposes the clinoid segment of the carotid, the carotid collar, and the dural rings. **F** The sylvian fissure has been opened and the remaining part of the orbital roof, the anterior clinoid, and the roof of the optic canal have been removed. The clinoid segment of the internal carotid artery is exposed in the clinoidal triangle. The site at which the oculomotor nerve passes through the sinus roof medial to the tentorial edge has been preserved. The dura has been elevated from the lateral wall of the cavernous sinus to expose the trigeminal ganglion and the ophthalmic, maxillary, and mandibular nerves. Bone has been drilled from the floor of the middle fossa to expose the facial nerve and geniculate ganglion. The ophthalmic nerve has been depressed to expose the abducens nerve coursing around the lateral surface of the intracavernous carotid. The meningohypophyseal trunk arises from the posterior bend of the internal carotid artery within the cavernous sinus. *A.* artery; *Ant.* anterior; *Car.* carotid; *Clin.* clinoid; *CN* cranial nerve; *Fiss.* fissure; *Frontozyg.* frontozygomatic; *Gang.* ganglion; *Gen.* geniculate; *Gr.* greater; *Lat.* lateral; *M.* muscle; Men. *Hyp.* meningohypophyseal; *N.* nerve; *Oculom.* oculomotor; *Orb.* orbital; *Pet.* petrosal; *Seg.* segment; *Sup.* superior; *Temp.* temporal; *Triang.* triangle; *Zygo.* zygomatic

and pituitary adenomas extending to the cavernous sinus.

The roof of the cavernous sinus has an anterior portion and a posterior portion. The anterior portion has an "upper floor" and a "lower floor." The upper floor is the upper surface of the anterior clinoid process, and the lower floor is the dura that lines the lower surface of the anterior clinoid process and forms the floor of the clinoidal triangle. The approaches through roof use a combination of the extradural and intradural routes. They require a pretemporal fronto-orbitozygomatic craniotomy and removal of the anterior clinoid process intradurally or extradurally to expose the anterior part of the sinus roof, after which the oculomotor triangle in the posterior part of the roof may be opened (see Fig. 7) [4, 5, 26, 30]. The posterior portion of the roof of the cavernous sinus, formed by the oculomotor triangles, is usually entered only after the anterior portion has been exposed by removing the anterior clinoid process. After opening the oculomotor triangle forming the posterior part of the roof, the posterior clinoid process and the upper clivus can be removed to provide additional access to the basilar artery and upper brain stem behind the dorsum sellae.

The approach through the lateral wall of the cavernous sinus involves separating the outer dural layer from the inner dural layer of the lateral wall (Fig. 8). The dissection begins at the greater sphenoid wing and proceeds toward the superior orbital fissure, where the intracranial periosteum is continuous with the periorbit. A shallow cut in the junction of the dura and periorbita at the lateral edge of the superior orbital fissure allows the separation of the dura from the middle fossa floor to proceed medially along the wall of the sinus. The outer layer (meningeal dura) peels away from the inner layer (endosteal layer) exposing Cranial Nerves III, IV, V1, V2, and V3 and the gasserian ganglion. Separating these layers allows visualization of the neural structures within the inner layer of the lateral wall. The lesion is usually accessed at the point where it is nearest or invades and bulges into and deforms the lateral wall. The site of the incision in the lateral wall is usually over the most prominent part of the tumor, which is commonly between the first and second divisions of the trigeminal nerve. Tumors extending into the posterior fossa through an enlarged porus of Meckel's cave can be followed into the posterior fossa through the enlarged porus. In the approach through the lateral area wall, the nerves coursing in the semitransparent inner layer of the lateral wall of the cavernous sinus can be exposed without opening directly into the cavernous sinus [4].

Exposure of the roof of the cavernous sinus requires opening the sylvian fissure and removal of the anterior clinoid process. In addition, the temporal lobe should be freed from its arachnoid attachments on its medial-basal surface to allow retraction of the temporal lobe for adequate exposure of the roof of the cavernous sinus. When removing the anterior clinoid process, part of the lesser sphenoid wing is usually removed extradurally and then the dura is opened to finish the resection. The dura over the anterior clinoid process, exposed intradurally, is opened in four cuts: the first one extends forward across the planum beginning near the medial limit of the optic canal, the second one begins near the clinoid tip and extends forward parallel to the sphenoid ridge, the third one joins the anterior end of the first cut and extends above the orbital roof to join the anterior end of the second cut, and the fourth one joins the posterior ends of the first and second cuts passing through the falciform ligament and the tip of the anterior clinoid process. The anterior clinoidectomy exposes the anterior part of the roof of the cavernous sinus and the clinoidal triangle, without opening its venous plexus. The exposure of the anterior portion of the roof of the cavernous sinus is often combined with opening the optic sheath lateral to the optic nerve and the distal dural ring around the internal carotid artery to allow mobilization of the clinoid segment and origin of the ophthalmic artery.

The medial wall of the cavernous sinus wall may also be exposed in the lateral margin of the transsphenoidal approach by extending the bone removal laterally from the anterior sellar wall to the area of the prominences overlying the carotid arteries, superior orbital fissure, and the maxillary nerve [8, 13]. Some of the posterior ethmoid air cells, located in front of the upper part of the lateral wing of the sphenoid sinus, often have to be removed to gain the lateral exposure in the sphenoid sinus needed to see the wall of the cavernous sinus. Care is required to avoid injury to the optic nerve in the superolateral part of the sphenoid sinus, the nerves passing through the superior orbital fissure in the midportion, and the maxillary nerve in the lower portion, where they may

occasionally be exposed directly under the sphenoid mucosa.

References

1. Bedford MA (1966) The "cavernous" sinus. Br J Ophthalmol 50: 41–46
2. Bernasconi V, Cassinari V (1957) Caratteristische angiografiche dei meningionu del tentorio. Radiol Med (Torino) 43: 1015–1026
3. Browder J (1937) Treatment of carotid artery cavernous sinus fistula. Report of a case. Arch Ophthalmol 18: 95–102
4. Dolenc VV (1983) Direct microsurgical repair of intracavernous vascular lesions. J Neurosurg 58: 824–831
5. Dolenc VV (1985) A combined epi- and subdural direct approach to carotid-ophthalmic artery aneurysms. J Neurosurg 62: 667–672
6. Dolenc VV (1997) Transcranial epidural approach to pituitary tumors extending beyond the sella. Neurosurgery 41: 542–552
7. Dolenc VV (1999) Extradural approach to intracavernous ICA aneurysms. Acta Neurochir 72 [Suppl]: 99–106
8. Dolenc VV, Skrap M, Sustersic J, Skrbec M, Morina A (1987) A transcavernous-transsellar approach to the basilar tip aneurysms. Br J Neurosurg 1: 251–259
9. Fujii K, Chambers SM, Rhoton AL Jr (1979) Neurovascular relationships of the sphenoid sinus: a microsurgical study. J Neurosurg 50: 31–39
10. Harris FS, Rhoton AL Jr (1976) Anatomy of the cavernous sinus. A microsurgical study. J Neurosurg 45: 169–180
11. Inoue T, Rhoton AL Jr, Theele D, Barry ME (1990) Surgical approaches to the cavernous sinus: a microsurgical study. Neurosurgery 26: 903–932
12. Kawase T, van Loveren H, Keller JT, Tew JM (1996) Meningeal architecture of the cavernous sinus: clinical and surgical implications. Neurosurgery 39: 527–536
13. Laws ER Jr, Onofrio BM, Pearson BW, McDonald TJ, Dirrenberger RA (1979) Successful management of bilateral carotid–cavernous fistulae with a transsphenoidal approach. Neurosurgery 4: 162–167
14. McConnell EM (1953) The arterial blood supply of the human hypophysis cerebri. Anat Rec 115: 175–203
15. Parkinson D (1964) Collateral circulation of cavernous carotid artery: anatomy. Can J Surg 7: 251–268
16. Parkinson D (1965) A surgical approach to the cavernous portion of the carotid artery. Anatomical studies and case report. J Neurosurg 23: 474–483
17. Parkinson D (1967) Transcavernous repair of carotid cavernous fistula: Case report. J Neurosurg 26: 420–424
18. Parkinson D (1973) Carotid cavernous fistula: direct repair with preservation of the carotid artery. Technical note. J Neurosurg 38: 99–106
19. Parkinson D (1987) Carotid cavernous fistula: history and anatomy. In: Dolenc VV (ed) The cavernous sinus. Springer, Wien New York, pp 3–29
20. Parkinson D (1990) Surgical anatomy of the lateral sellar compartment (cavernous sinus). Clin Neurosurg 36: 219–239
21. Renn WH, Rhoton AL Jr (1975) Microsurgical anatomy of the sellar region. J Neurosurg 43: 288–298
22. Rhoton AL Jr (2002) The anterior and middle cranial base. Neurosurgery 51[Suppl 1]: S273–S302
23. Rhoton AL Jr (2002) The cavernous sinus, the cavernous venous plexus, and the carotid collar. Neurosurgery 51 [Suppl 1]: S375–S410
24. Rhoton AL Jr, Hardy DG, Chambers SM (1979) Microsurgical anatomy and dissection of the sphenoid bone, cavernous sinus and sellar region. Surg Neurol 12: 63–104
25. Rhoton AL Jr, Natori Y (1996) The skull. In: Rhoton A1 Jr, Natori Y (eds) The orbit and sellar region: microsurgical anatomy and operative approaches. Thieme, New York, pp 4–25
26. Sekhar LN, Burgess J, Akin O (1987) Anatomical study of the cavernous sinus emphasizing operative approaches and related vascular and neural reconstruction. Neurosurgery 21: 806–816
27. Sekhar LN, Moller AR (1986) Operative management of tumors involving the cavernous sinus. J Neurosurg 64: 879–889
28. Sekhar LN, Sen CN, Jho HD, Janecka IP (1989) Surgical treatment of intracavernous neoplasms: a four-year experience. Neurosurgery 24: 18–30
29. Seoane E, Rhoton AL Jr, de Oliveira EP (1998) Microsurgical anatomy of the dural collar (carotid collar) and rings around the clinoid segment of the internal carotid artery. Neurosurgery 42: 869–886
30. Seoane E, Tedeschi H, de Oliveira E, Wen HT, Rhoton AL Jr (2000) The pretemporal transcavernous approach to the interpeduncular and prepontine cisterns: microsurgical anatomy and technique application. Neurosurgery 46: 891–899
31. Taptas JN (1982) The so-called cavernous sinus: a review of the controversy and its implications for neurosurgeons. Neurosurgery 11: 712–717
32. Umansky F, Nathan H (1982) The lateral wall of the cavernous sinus with special reference to the nerves related to it. J Neurosurg 56: 228–234
33. Umansky F, Valarezzo A, Elidan J (1994) The superior wall of the cavernous sinus: a microanatomical study. J Neurosurg 81: 914–920
34. van Loveren H, Keller JT, El-Kalliny M, Scodary DJ, Tew JM Jr (1991) The Dolenc technique for cavernous sinus exploration (cadaveric prosection). Technical note. J Neurosurg 74: 837–844
35. Yasuda A, Campero A, Martins C, Rhoton AL Jr, Oliveira E, Ribas GC (2005) Microsurgical anatomy and approaches to the cavernous sinus. Operat Neurosurg 56: 4–27
36. Yasuda A, Campero A, Martins C, Rhoton AL Jr, Ribas G (2004) The medial wall of the cavernous sinus: Microsurgical anatomy. Neurosurgery 55: 179–189

The transition between the cavernous sinus and orbit

S. Froelich[1], K. M. Abdel Aziz[2], H. R. van Loveren[3], J. T. Keller[4]

[1]Department of Neurosurgery, Strasbourg University, CHU de Hautepierre, Strasbourg, France
[2]Department of Neurosurgery, Allegheny General Hospital, Pittsburgh, PA, USA
[3]Department of Neurosurgery, University of South Florida, Tampa, FL, USA
[4]The Neuroscience Institute, Department of Neurosurgery, University of Cincinnati College of Medicine, and Mayfield Clinic, Cincinnati, OH, USA

Introduction

In 1755, Zinn [26] presented the first accurate three-dimensional view of the junction between the cavernous sinus and orbit (Fig. 1). In subsequent anatomical treatises, this highly complex area was often represented as a two-dimensional bony opening that was composed of a wide medial portion and a lateral narrow portion; both portions were depicted as transgressed by nerves. When cranial base surgeons initially focused on the cavernous sinus, relatively little interest was accorded its communication with the orbit [6, 7, 14, 18, 21, 22]. Morard et al. [11] and Natori and Rhoton [12] more recently presented detailed descriptions of the surgical anatomy of the superior orbital fissure (SOF). Spektor et al. [19] emphasized the continuity between the cavernous sinus and the orbit by describing the orbital venous drainage into the cavernous sinus via the SOF.

However, Parkinson believed that the term *cavernous* was too restrictive; that is, the term emphasized only the venous components of this region but neglected the neural and soft tissue elements. To address this restriction, he introduced the concept of the lateral sellar compartment [13–15]. He considered this compartment, contents of the SOF, and orbit as a continuum – all part of the extradural neural axis compartment. In fact, the venous network of this compartment, first described by Batson and later by Parkinson, provides a continuous link from the coccyx to the orbit. The continuity of the orbital venous drainage with the anterior cavernous sinus (lateral sellar compartment) can be identified early in embryonic development (see Keller et al., in this same issue). Initially the primitive maxillary vein drains the orbit. Subsequently the primitive supraorbital vein, which becomes the superior ophthalmic vein, drains into the anterior cavernous sinus.

To date, most anatomical treatises schematize the complex anatomy of the SOF as a two-dimensional bony opening composed of a wide medial portion and a lateral narrow portion; both portions are transgressed by nerves that course to the orbit. Such representation of the SOF leads to misunderstanding because, as we show, the SOF is actually a three-dimensional anatomical structure. Therefore, we propose that the term SOF refers only to the bony opening. We introduce the term lateral sellar orbital junction (LSOJ) to define the transitional region between the lateral sellar compartment and the orbit via the SOF. This junction is divided into the anterior lateral sellar compartment and the orbital apex. The LSOJ is located at the medial, wide portion of the SOF. The lateral portion of the SOF does not contain

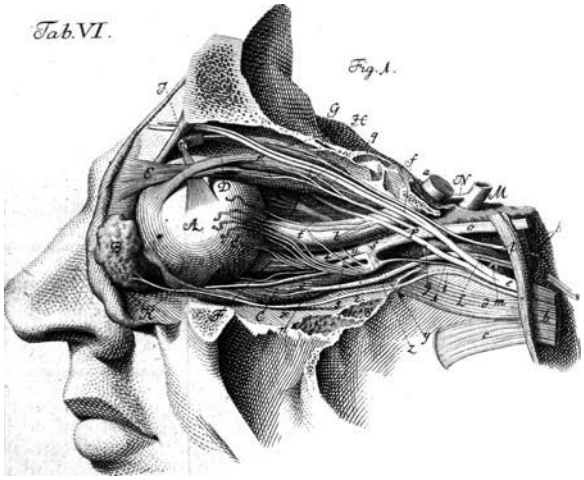

Fig. 1. Original drawing of the orbit from Johannes Zinn's *Descriptio Anatomica Oculi Humani*. Veuve A. Vandenhoeck, Göttingen, 1755

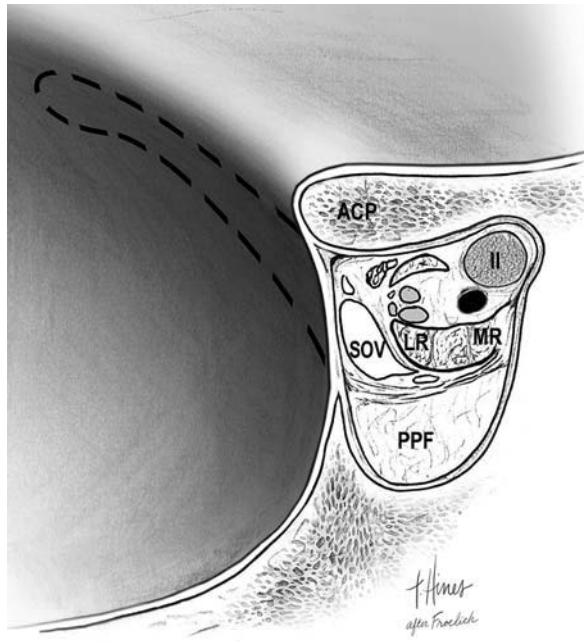

Fig. 2. Drawing (coronal section) through the medial portion of the superior orbital fissure (*SOF*) showing temporal fossa dura that covers its narrow lateral portion (dashed line), which is not transgressed by any nerves. Anterior clinoid process (*ACP*), lateral rectus (*LR*), medial rectus (*MR*), optic nerve (*II*), pterygopalatine fossa (*PPF*), superior orbital vein (*SOV*) (with permission from Mayfield Clinic)

any neural structures but is covered by the temporal fossa dura. The pterygopalatine fossa also extends posteriorly via the inferior aspect of the medial wide portion of the SOF, subjacent to the LSOJ. However, this extension is not part of the extradural neural axis compartment.

The superior orbital fissure

The SOF refers to the bony opening located between the middle cranial fossa and the orbit. It is divided into a wide medial portion and a narrow superolateral portion. The cylindrical-shaped medial portion is located along and bounded medially by the body of the sphenoid bone (basisphenoid). Laterally, the medial portion of the SOF and its contents are covered by the middle cranial fossa dura (Fig. 2). The lateral portion of the SOF is located between the smooth inferior surface of the lesser wing of the sphenoid bone (alisphenoid) and the sharp superomedial border of the greater wing of the sphenoid bone (orbitosphenoid). This lateral portion varies considerably in shape and dimension according to the extent of membranous ossification of the lateral wall of the orbit [16]. The classic two-dimensional representation of the SOF, transgressed by nerves, gives a false impression that the lacrimal, frontal, and trochlear (CN IV) nerves course through the lateral portion of the SOF [4, 12]. According to Hovelacque [5], only the medial wide portion of the SOF should be considered as a connection between the cavernous sinus (lateral sellar compartment) and the orbit. Only the orbitomeningeal artery and the dural veins of the middle cranial fossa contiguous with the orbital venous network cross the lateral portion of the SOF. The lacrimal nerve, the most lateral nerve that courses through the SOF, passes through the medial portion of the SOF above the superior ophthalmic vein, tangential to the lateral portion of the SOF (Fig. 3).

The posterior end of the inferior orbital fissure crosses the medial portion of the SOF just above the maxillary strut. The inferior orbital fissure separates the pterygopalatine fossa from the orbit. Therefore, the medial portion of the SOF contains the lateral sellar orbital junction above the inferior orbital fissure and the posterior extension of the pterygopalatine fossa below the level of the inferior orbital fissure.

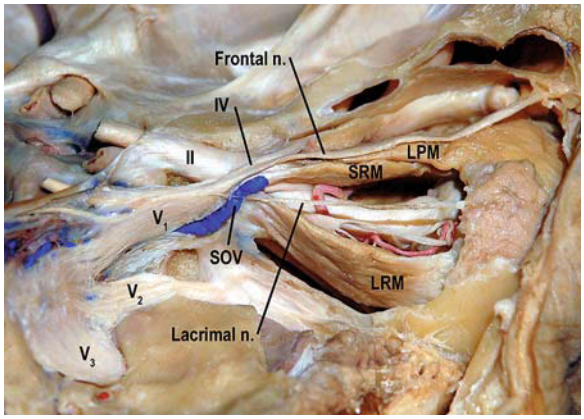

Fig. 3. Cadaveric dissection of the lateral sellar orbital junction. Superior ophthalmic vein (*SOV*) crosses under the common annular tendon laterally. Superior rectus muscle (*SRM*), lateral rectus muscle (*LRM*), levator palpebrae muscle (*LPM*) (with permission from Mayfield Clinic)

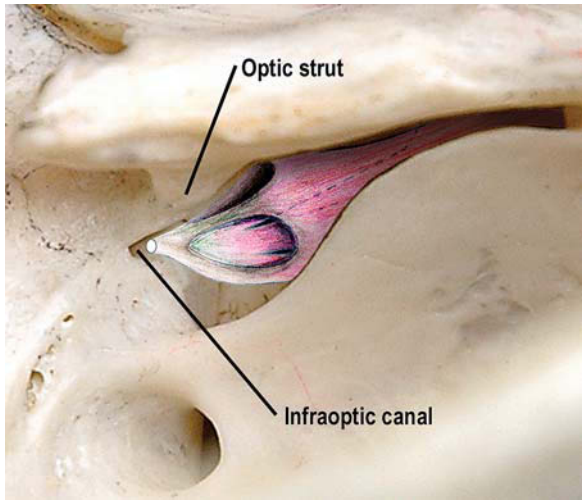

Fig. 4. Common annual tendon inserts on the infraoptic tubercle, which is often found as a canal located beneath the optic strut (with permission from Mayfield Clinic)

Common annular tendon

The four rectus muscles arise from a common tendon called the common annular tendon, which inserts on the infraoptic tubercle. This tendon forms the central structure of the LSOJ. Various terms have been used to define the tendinous origin of the rectus muscles including common annular tendon, annulus of Zinn, tendinous ring, tendon of Zinn, and tendon of Lockwood. We use the term *common annular tendon,* as identified in *Terminologia Anatomica* [20], to define the origin of the rectus muscles.

In *Descriptio Anatomica Oculi Humani*, Zinn described a common tendon for the lateral, inferior, and medial rectus muscles that inserts below the optic strut; a distinct origin was described for the superior rectus muscle [26]. Lockwood identified two separate tendons, a superior tendon (tendon of Lockwood) and an inferior tendon (tendon of Zinn) [10]. The tendon of Lockwood inserts on the superior margin of the optic foramen and gives rise to the superior rectus muscle and the superior head of the lateral rectus muscle. The tendon of Zinn inserts on the infraoptic tubercle and gives rise to the inferior head of the lateral rectus muscle and the inferior and medial rectus muscles (personal observation).

According to some authors [3, 9–12, 25], the common annular tendon inserts not only on the medial aspect of the SOF but on a bony spine (lateral rectus spine) on the lateral aspect of the SOF. As suggested by Wolff [25] and Bisaria et al. [1], this spine is often a groove formed by the superior orbital vein. Morard et al. [11] described two heads of the lateral rectus muscle that delineate the oculomotor foramen.

In our study of the common annular tendon, the oculomotor foramen was delimited by the tendinous fibers of the superior and lateral rectus muscles; this observation is consistent with other descriptions [17, 20]. The four rectus muscles arise from a common tendon called the common annular tendon. This tendon originates from the infraoptic tubercle, which is a small depression in the body of the sphenoid bone located just below the optic strut (Fig. 4). The origin of the common annular tendon is continuous with the periosteum of the sphenoid bone.

Moving anteriorly, the common annular tendon splits into a superior and an inferior tendon; the rectus muscle fibers originate centrally within these tendons. The superior tendon courses anteriorly and gently ascends along the lateral border of the orbital opening of the optic canal where it merges with the periosteum and optic nerve sheath. This tendon progressively crosses over the optic nerve sheath and spreads horizontally to give rise to the superior rectus muscle. The inferior tendon, which serves as the origin for the lateral, inferior, and medial rectus muscles, courses anteriorly and spreads out to form a concave gutter in which the oculomotor (CN III), nasocilliary, and abducens (CN VI) nerves lay (Fig. 5A). The most lateral fibers of the inferior

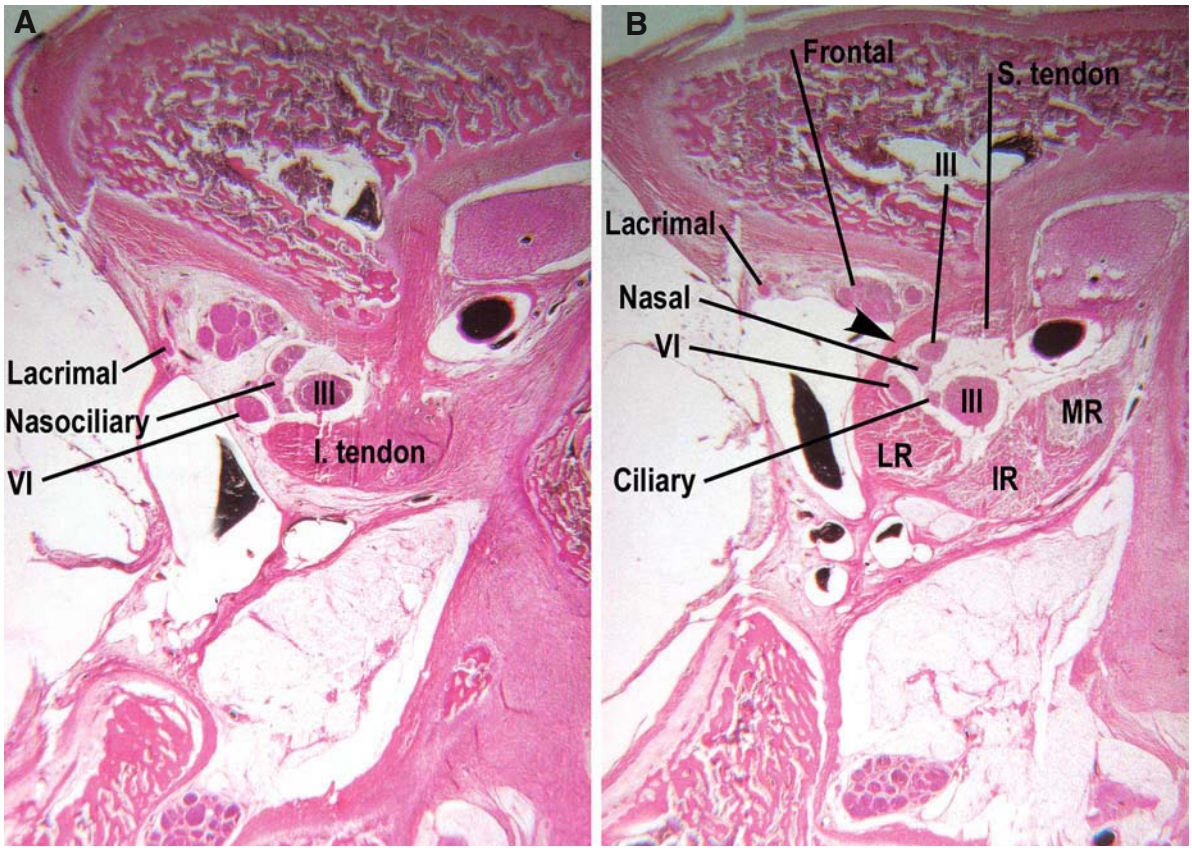

Fig. 5. Coronal histological sections through the superior orbital fissure of a newborn head. **A** Section through the common annular tendon. Inferior tendon forms a concave gutter for the oculomotor (*III*), nasociliary, and abducens (*VI*) nerves. **B** Tendinous fibers of the lateral rectus (*LR*) and superior rectus muscles join to close the superolateral foramen (*arrowhead*). Inferior rectus muscle (*IR*), medial rectus muscle (*MR*) (with permission from Institute of Anatomy of Strasbourg)

tendon, dedicated to the lateral rectus muscle, course laterally and superiorly to join the most lateral fibers of the superior tendon to form a tendinous foramen (Fig. 5B). This tendinous foramen is called the superolateral annular foramen or oculomotor foramen. The most medial fibers of the inferior tendon that give rise to the medial rectus run anteriorly and superiorly along the medial aspect of the optic nerve. These fibers join the most medial fibers of the superior tendon, thus constituting a second tendinous foramen. Through this superomedial annular foramen courses the optic nerve and the ophthalmic artery. The margins of the superomedial annular foramen adhere firmly to the optic nerve sheath. Thus, the common annular tendon forms a tendinous cone inserted posteriorly on the infra-optic tubercle and comprises a superomedial and superolateral annular foramen.

Subdivisions of the lateral sellar orbital junction

The LSOJ, located in the medial portion of the SOF, is composed of the anterior aspect of the lateral sellar compartment and the orbital apex. Inferiorly, the LSOJ is separated from the intracranial extension of the pterygopalatine fossa by the orbital muscle of Müller (Fig. 6).

Anterior lateral sellar compartment

The anterior lateral sellar compartment is that part of the lateral sellar compartment located anterior to the anterior loop of the intracavernous internal carotid artery (ICA). This compartment is covered laterally by the middle cranial fossa dura.

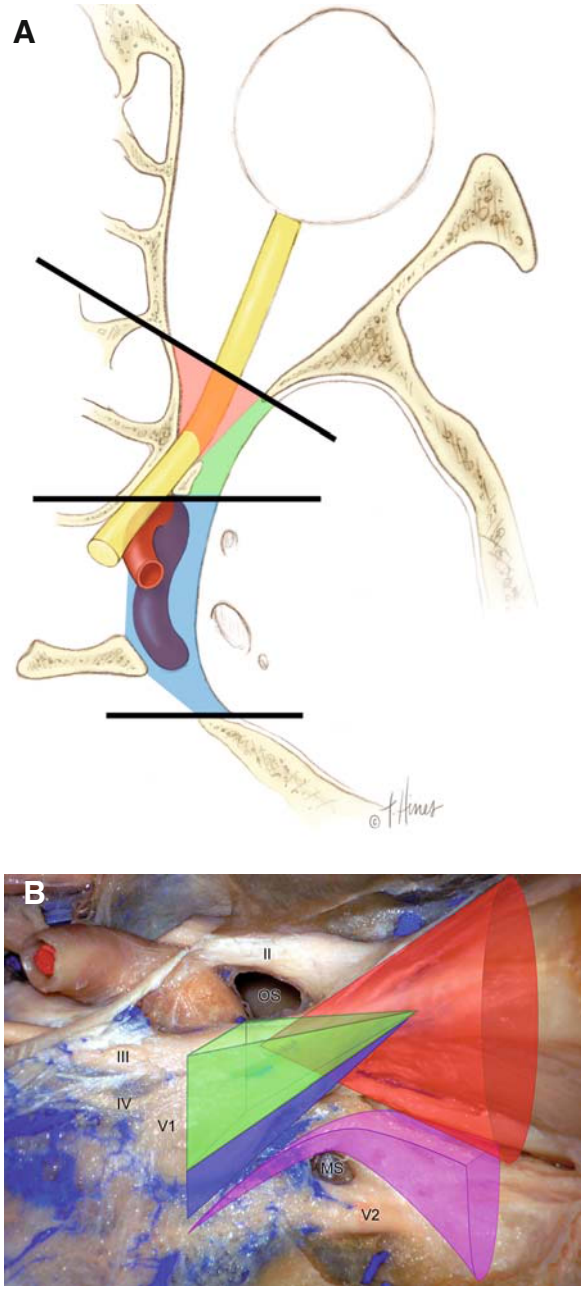

Fig. 6. Compartments of the lateral sellar orbital junction are as indicated: red = orbital cone, green = neural compartment, blue = venous compartment, purple = pterygopalatine compartment. **A** Drawing of the lateral sellar orbital junction in axial cross section. **B** Lateral view of a cadaveric dissection of the lateral sellar orbital junction (with permission from Mayfield Clinic)

Its floor is formed by the orbital muscle of Müller. The anterior lateral sellar compartment itself has a superior nervous component and an inferior venous component. The superior nervous component can be divided into medial and lateral groups of nerves. The medial group is composed of the superior and inferior divisions of CN III, the first division of the trigeminal nerve, the nasociliary branch of V1, and CN VI. These nerves are covered by their own perineurium and are progressively wrapped in a thin connective tissue sheath that blends anteriorly with the margin of the superolateral annular foramen through which they course. The lateral group, situated laterally to the medial group, is composed of the trochlear nerve (CN IV), and the frontal and lacrimal branches of V1. The CN IV and frontal nerve gently ascend and progressively cross over the medial group to enter the orbital apex above the common annular tendon. The lacrimal nerve courses along the inferior aspect of the lesser sphenoid wing just above the superior ophthalmic vein. The inferior venous component is formed by the confluence of the superior and inferior ophthalmic veins that drain into the anterior cavernous sinus [2].

Orbital apex

The orbital apex is divided into the intra- and extraconal compartments. The intraconal compartment is located in the muscular conus formed by the four rectus muscles; it has two posterior openings in the common annular tendon, a superomedial and a superolateral opening. First, the superomedial annular foramen is the opening through which the CN II and ophthalmic artery enter the muscular conus. Second, the superolateral annular foramen is the route through which courses CN III, nasociliary nerve, and CN VI. The LSOJ is located on the medial portion of the SOF. The lateral portion of the SOF is not crossed by any neutral structures and is covered by temporal fossa dura. The extraconal compartment is located circumferentially around the muscular conus. The superior aspect contains fat, orbital veins that drain into the superior ophthalmic vein, CN IV, and the lacrimal and frontal branches of CN VI. The medial and inferior aspects contain fat and orbital veins that drain into the superior orbital vein or directly into the anterior cavernous sinus. Laterally, the superior orbital vein courses tangentially along the lateral

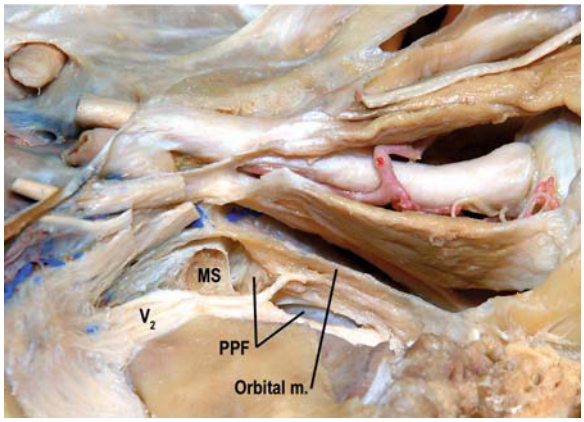

Fig. 7. Cadaveric dissection of the lateral sellar orbital junction. Pterygopalatine fossa (*PPF*) extends posteriorly through the SOF, below the orbital muscle of Müller (with permission from Mayfield Clinic)

portion of the SOF and crosses under the annular tendon [2]. The lacrimal nerve courses immediately above the superior ophthalmic vein. Laterally and posteriorly, the origin of the lateral rectus muscle adheres to the greater sphenoid wing. The extraconal compartment is separated inferiorly from the pterygopalatine fossa by the orbital muscle of Müller.

Pterygopalatine compartment

The pterygopalatine fossa has a posterior extension through the SOF, inferior to the lateral sellar compartment and the orbital muscle of Müller (Fig. 7). This extension is composed of fat, small veins, and nerve fibers associated with the pterygopalatine ganglion [23, 24]. Although this posterior extension is in the medial portion of the SOF, it is not a constituent of the extradural neural axis compartment.

Conclusions

The LSOJ is a component of the extradural neural axis compartment that represents the transition between the lateral sellar compartment and the orbit. This complex three-dimensional region can be further divided into an anterior lateral sellar compartment and an orbital apex. The LSOJ is located in the medial aspect of the SOF. The SOF should refer only to the bony opening between the orbit and the temporal fossa. No cranial nerves pass through the lateral portion of the SOF. In the inferior aspect of the SOF below the LSOJ, lies a posterior extension of the pterygopalatine fossa, which is not part of the extradural neural axis compartment. The four rectus muscles insert posteriorly on the infraoptic tubercle by the common annular tendon that forms the central structure of the LSOJ. This tendon forms a tendinous cone with two openings that we identified as the superomedial and superolateral annular foramina. The optic nerve and ophthalmic artery enter the muscular conus through the superomedial annular foramen. Cranial nerves III and VI and the nasociliary nerves course through the superolateral annular foramen to enter the muscular conus.

References

1. Bisaria KK, Kumar N, Prakesh M, Sharma PK, Agarwal PP, Bisaria SD, Lakhtakia PK, Premesagar IC (1996) The lateral rectus spine of the superior orbital fissure. J Anat 189: 243–245
2. Brismar J (1974) Orbital phlebography III. Topography of intraorbital veins. Acta Radiol Diagn (Stockh) 15: 577–594
3. Dutton JJ (1994) Atlas of clinical and surgical orbital anatomy. W.B. Sanders Co., Philadelphia
4. Govsa F, Kayalioglu G, Erturk M, Ozgur T (1999) The superior orbital fissure and its contents. Surg Radiol Anat 21: 181–185
5. Hovelacque A (1927) Anatomie des nerfs crâniens et rachidiens et du système grand sympathique. Doin et Cie, Paris
6. Inoue T, Rhoton AL, Theele D, Barry ME (1990) Surgical approaches to the cavernous sinus: a microsurgical study. Neurosurgery 26: 903–932
7. Kawase T, van Loveren HR, Keller JT, Tew JM Jr (1996) Meningeal architecture of the cavernous sinus: clinical and surgical implications. Neurosurgery 39: 527–536
8. Keller JT, Leach JL, van Loveren HR, Abdel Aziz KM, Froelich S (2008) Venous anatomy of the lateral sellar compartment. In: Dolenc VV, Rogers L (eds) Cavernous sinus. Springer, Wien New York, pp 35–51
9. Koorneef L (1977) The architecture of the musculofibrous apparatus in the human orbit. Acta Morphol Neerl Scand 15: 35–64
10. Lockwood CB (1886) The anatomy of the muscles, ligaments, fascia of the orbit, including an account of the capsule of Tenon, the check ligaments of the recti, and of the suspensory ligament of the eye. Anat Physiol 20: 1–25
11. Morard M, Tcherekayev V, de Tribolet N (1994) The superior orbital fissure: a microanatomical study. Neurosurgery 35: 1087–1093

12. Natori Y, Rhoton AL (1995) Microsurgical anatomy of the superior orbital fissure. Neurosurgery 36: 762–775
13. Parkinson D (2000) Extradural neural axis compartment. J Neurosurg 92: 585–588
14. Parkinson D (1990) Surgical anatomy of the lateral sellar compartment (cavernous sinus). Clin Neurosurg 36: 219–239
15. Parkinson D (1996) Lateral sellar compartment O.T. (Cavernous sinus): history, anatomy, terminology. Anat Rec 251: 486–490
16. Ray CD (1995) Configuration and lateral closure of the superior orbital fissure. Am J Phys Anthropol 13: 309–321
17. Rouvière H (1981) Anatomie humaine. Tome I, 11ème ed, Masson, Paris
18. Sekhar LN, Burgess J, Akin O (1987) Anatomical study of the cavernous sinus emphasizing operative approaches and related vascular and neural reconstruction. Neurosurgery 21: 806–816
19. Spektor S, Piontek E, Umansky F (1997) Orbital venous drainage into the anterior cavernous sinus space: microanatomic relationships. Neurosurgery 40: 532–540
20. Terminologia Anatomica: International Anatomical Terminology Federative Committee on Anatomical Terminology (1998), Thieme, Stuttgart, New York
21. Testut L, Latarjet A (1949) Traité d'anatomie humaine. 9ème éd, G. Doin et Cie, Paris
22. Umansky F, Nathan H (1982) The lateral wall of the cavernous sinus. With special reference to the nerves related to it. J Neurosurg 56: 228–234
23. Weninger WJ, Pramhas D (2000) Compartments of the adult parasellar region. J Anat 197: 681–686
24. Weninger WJ, Steicher J, Müller GB (1997) Anatomical compartments of the parasellar region: adipose tissue bodies represent intracranial continuations of extracranial spaces. J Anat 191: 269–275
25. Wolff E (1940) The anatomy of the eye and orbit, 2nd ed. The Blakiston Company, Philadelphia
26. Zinn JG (1755) Descriptio anatomica oculi humani. Veuve A. Vandenhoeck, Göttingen

Venous anatomy of the lateral sellar compartment

J. T. Keller[1,2], J. L. Leach[3], H. R. van Loveren[4], K. M. Abdel Aziz[5], S. Froelich[6]

[1]The Neuroscience Institute, Department of Neurosurgery, University of Cincinnati College of Medicine, Cincinnati, OH, USA
[2]Mayfield Clinic, Cincinnati, OH, USA
[3]The Neuroscience Institute, Department of Radiology, University of Cincinnati College of Medicine, Cincinnati, OH, USA
[4]Department of Neurosurgery, University of South Florida, Tampa, FL, USA
[5]Department of Neurosurgery, Allegheny General Hospital, Pittsburgh, PA, USA
[6]Department of Neurosurgery, Strasbourg University, CHU de Hautepierre, Strasbourg, France

Introduction

Parkinson's description of the cavernous sinus (CS) as an anatomical jewel box [44] is well deserved. This complex neurovascular structure is located centrally in the skull base on either side of the basisphenoid bone. The cavernous sinus not only houses cranial nerves (CNs) III through VI and the internal carotid artery (ICA), which is the primary vascular supply for the anterior cerebral circulation but also serves as a pivotal venous drainage route for the orbit and skull base. The venous anatomy has in large part led to misconceptions of the cavernous sinus and thwarted those who attempted to directly enter this structure. The scientific literature is replete with accounts of physicians who have directed attention to the cavernous sinus, especially for the treatment of carotid cavernous fistulas. Hamby [19] attributed this to the "spectacular presenting features of the malady and from the intense disability usually attending it." Carotid cavernous fistulas frequently produce pulsating exophthalmos; it was this syndrome that spawned discussion rather than the underlying cause, arteriovenous aneurysm (arteriovenous fistula), which was initially described by William Hunter in 1762 [21]. According to Hamby, Travers was the first one to successfully treat such a lesion by ligating the common carotid artery in 1809 [19, 62].

Winslow's concept of the venous architecture of this structure prompted him to introduce the term cavernous sinus, which he compared to the corpora cavernosa of the penis. However, the cavernous sinus is neither cavernous nor a sinus. In fact, Parkinson [45] proposed "that this inaccurate and inappropriate term, cavernous sinus, after serving stalworthy for 250 years, misleading students and surgeons alike, has earned retirement and should be considered a leading candidate to join the legion of "OTs" (older terminology). There is no statute of limitation on errors. The lateral sellar compartment is descriptive and accurate." Although the cavernous sinus has been known and studied for centuries, it entails further investigation for those pursuing a better understanding of its microanatomical detail [10, 11, 18, 20, 23, 31, 49]. Umansky and Nathan's illustration depicts diagrams of the cavernous sinus by various authors that appeared on the front cover of the *Journal of Neurosurgery* illustrates the varied understanding of this structure [63].

One name not generally associated with the cavernous sinus is that of Oscar V. Batson

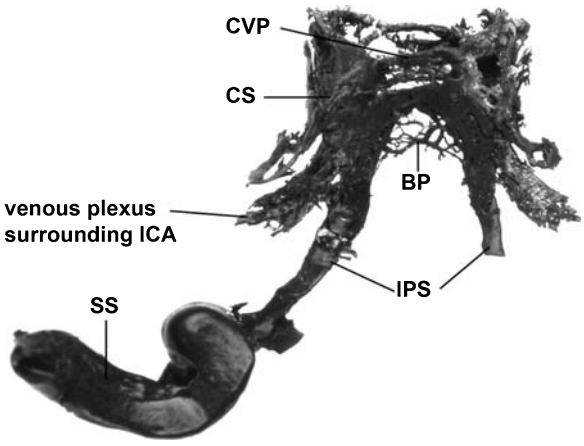

Fig. 1. Cast of the venous system of the cavernous sinus (*CS*) prepared by Dr. Oscar V. Batson. Internal carotid artery (*ICA*) is identified by the venous plexus surrounding its course. *CVP* circular venous plexus, *BP* basilar plexus, *IPS* inferior petrosal sinus, *SS* sigmoid sinus (reprinted with permission from the Mayfield Clinic)

(1894–1979). Dr. Batson, best known for the venous plexus that bares his name, also had an interest in the cavernous sinus [1, 2]. His publication, *More About Veins* [3], demonstrated a pericarotid venous plexus entering the cavernous sinus by a corrosion cast technique that he developed. Subsequently, he presented the author (JTK) with a corrosion cast of this structure (Fig. 1); this cast has served to spawn our interest in attempting to understand and unravel this complex structure within the lateral sellar compartment. Batson understood this venous plexus to be in continuity with the extradural venous plexus of the vertebral column caudally and the orbit rostrally; this understanding served as the basis of Parkinson's [47] concept of the extradural neural axis compartment. On this basis, the authors believe that the addition of Batson to the roster of legends is substantiated as another key contributor toward understanding the cavernous sinus and/or lateral sellar compartment.

A review of the embryology of the cranial venous system in general and veins of this sinus in particular is critical to a presentation of the venous anatomy of the cavernous sinus. In addition to the seminal work of Dorcas Padget [40–42], giants of embryology, including Mall [38], Streeter [58, 59], Evans [14], and Sabin [53], are also referenced since they served as a foundation for Padget's treatise. Streeter and Mall recognized the veins of the cavernous sinus considerably earlier in embryologic development than Padget who first identified a definitive cavernous sinus in Stage 7. Furthermore, the formers' work supports Parkinson's concept of the lateral sellar compartment (older terminology, cavernous sinus) as an enlarged compartment of the extradural neural axis compartment that extends from the coccyx to the orbit [47].

Following our discussion of the relevant venous embryology is a general presentation of the lateral sellar compartment venous anatomy. We explicitly focus on the variations of the venous channels or spaces that contribute to the lateral sellar compartment and those that exit it. Finally, we highlight these anatomical descriptions using current radiographic technology, Three-dimensional (3D) gadolinium-enhanced elliptic-centric-encoded magnetic resonance venography (MRV).

Embryology of the veins of the lateral sellar compartment (cavernous sinus)

Development of the cerebral vessels is a complicated subject; to add insult to injury, its understanding is made even more difficult by the application of inconsistent, antiquated terminology. Dorcas Padget published companion tomes on the development of the cranial arterial and venous systems in human [40–42]. Recognized as seminal papers, they are requisite reading for anyone aspiring to pursue these topics. In our overview of the venous embryology of the cavernous sinus/lateral sellar compartment, we have drawn on not only the classic studies [14, 38, 40–42, 53, 58, 59] but also recent studies of Gilmore [17], O'Rahilly and Mueller [39], and Lasjaunias et al. [36, 37].

When compared with arterial development, venous development is more complicated. According to Padget "there has long been wanting a comprehensive account of veins of the head." Fifty years earlier, Mall [38] recognized that "while the arteries of the brain undergo many changes in their development, their history is relatively simple when compared with the gyrations the veins undergo." To further confound matters, there are discrepancies among authors regarding the terminology and descriptions of the various stages of cerebrovascular development. In addressing these discrepancies, we invoke a statement offered by Padget to define her interpretations of this complicated venous system: "*The author* (*Padget*) *was*

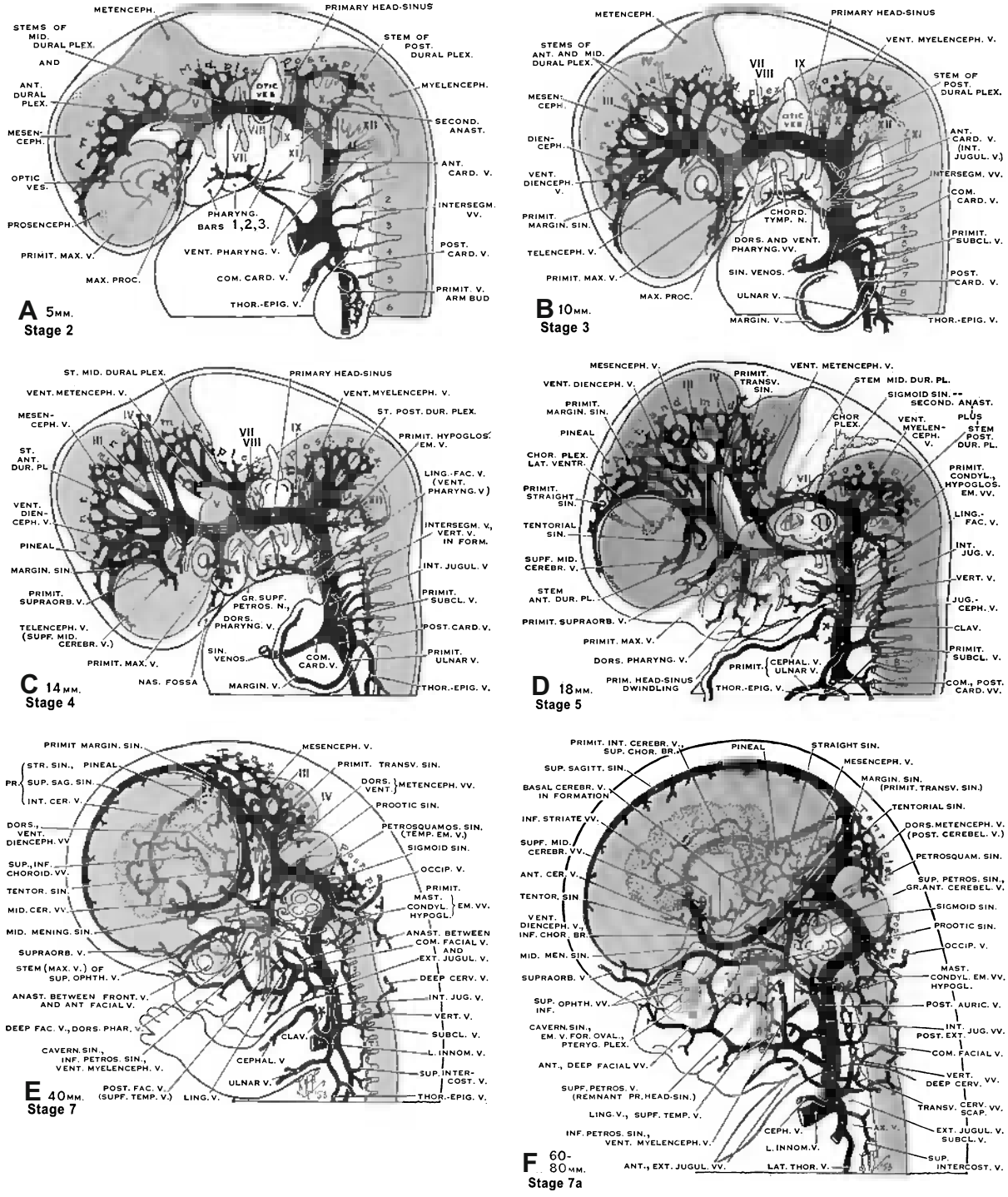

Fig. 2. Padget divided the complex process of venous development into eight stages including the postnatal pattern. Illustrations (lateral view) show progression in stages during the development of the cavernous sinus-lateral sellar compartment, including the major veins and sinuses emptying into and exiting from this region: 2 at 5 mm (**A**), 3 at 10 mm (**B**), 4 at 14 mm (**C**), 5 at 18 mm (**D**), 7 at 40 mm (**E**), 7a at 60–80 mm (**F**) (reprinted from Padget D.H. (1956) Contributions to Embryology No. 247: 79–140)

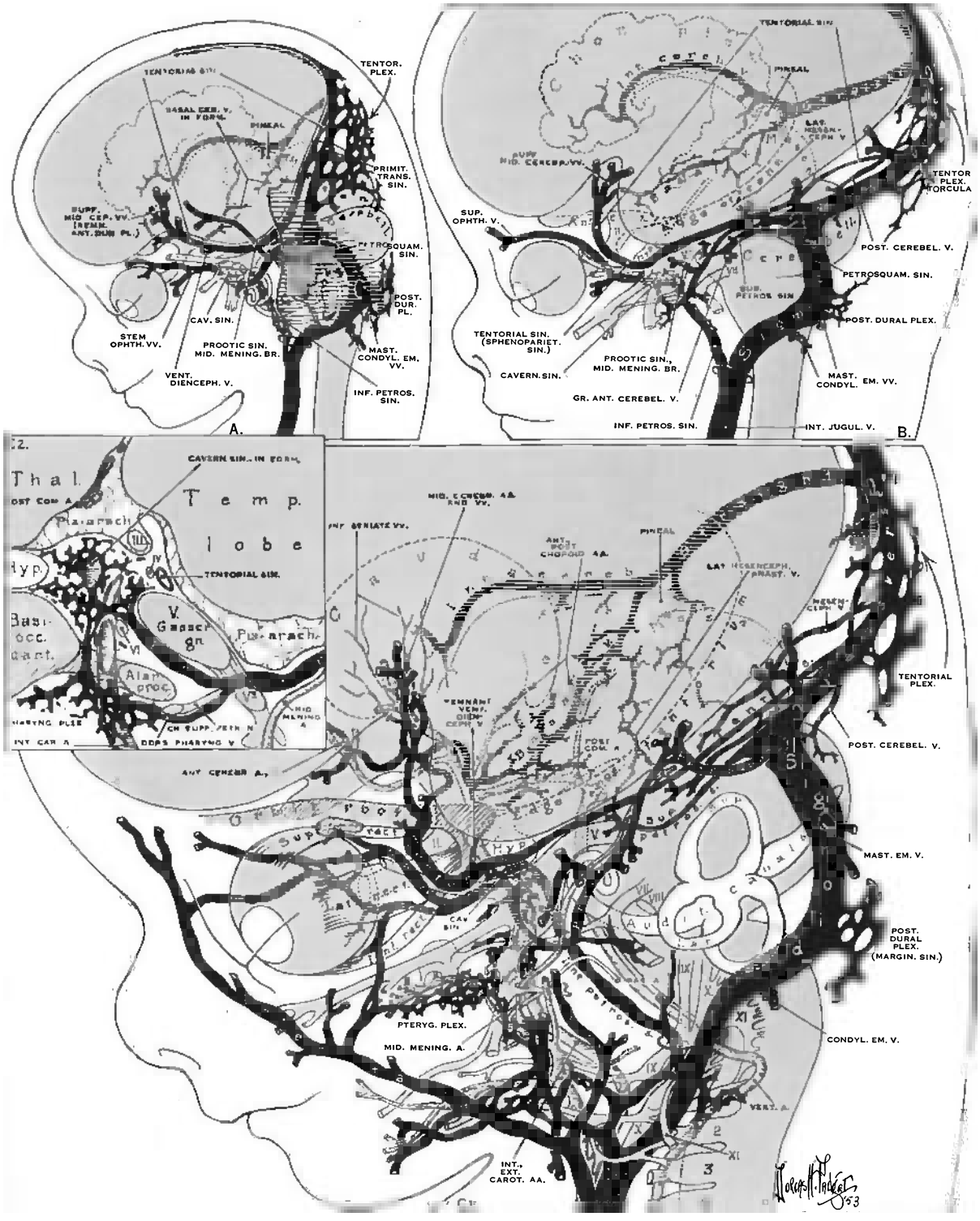

Fig. 3. Lateral reconstruction of three early fetuses by Padget illustrating the post-natal configuration in Stage 7a. **A** Carnegie No. 4193, 48.5 mm. **B** Carnegie No. 234a, 80 mm. **C** Carnegie No. 613, 80 mm; insert C2 details the region of the left cavernous sinus (C1) viewed from the front (reprinted from Padget D.H. (1956) Contributions to Embryology No. 247: 79–140)

faced with a choice between showing the complete or exact graphic reconstructions, which were too complicated to be readily understood, and risking errors of personal judgment by conversion to a semi-diagrammatic picture. The resulting compromise makes no undue sacrifice to either clarity or accuracy" [42].

According to Gilmore [17], "it should be emphasized that the origin of the cavernous sinus is not agreed upon; Streeter for example, considers the cavernous sinus to arise from that portion of the primary head sinus situated medial to the trigeminal ganglion and, as such, considers it to be present from the outset." Padget identified eight stages in cerebral venous development, including the postnatal pattern. She stated that, "for the first time, therefore, one may properly speak of a primitive cavernous sinus, although the part of the pro-otic sinus that is always medial to the 5th nerve ganglion, and is the sole remaining segment of the primary head-sinus of the initial stages, has often been so designated (Streeter [59] and others). The intercavernous sinuses (forming the circular sinus) and the basilar sinus (plexus) of the adult are merely the midline plexiform extensions already beginning to anastomose the bilateral cavernous and inferior petrosal sinuses, respectively" [42]. However, Padget did not identify the cavernous sinus until Stage 7, considerably later than Streeter. Kehrli et al. [28] in their exhaustive and excellent paper on the venous system of the lateral sellar compartment (cavernous sinus) identify a condensation of mesenchyme at 12–14 weeks in this area, which marks the first stage of development of the dura propria of the cavernous sinus.

Using Padget's Figures (Figs. 2 and 3), we give a detailed account of the various stages of venous development and take the liberty to identify the cavernous sinus in earlier stages of development when she did not (Fig. 2A). The basic pattern of cerebrovasculature is established between the ends of the first and third months of gestation. The neural tube is in fact the first of the permanent organs of the body to be vascularized [17, 39]. Current embryology textbooks schematically depict the embryonic vascular system in the fourth week with two dorsal aortae and right and left anterior cardinal veins to the head (Fig. 4). The anterior cardinal vein is continuous cranially with a venous channel called the vena capitis medialis (also called the primordial hind brain channel) [59] that lies medial to all the cranial nerves and is immediately

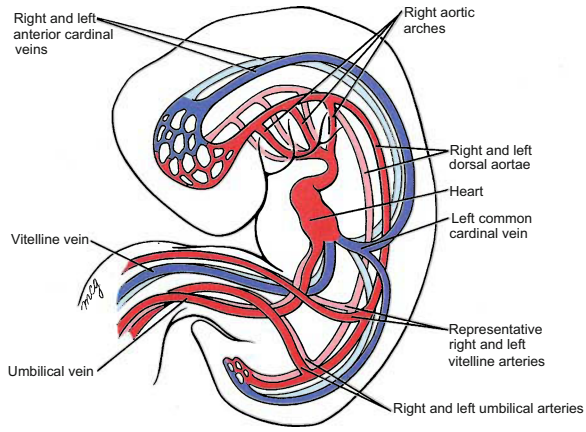

Fig. 4. Schematic depiction of the embryonic vascular system in the middle of the fourth week when the heart has begun to beat and circulate blood. Outflow tract of the heart now includes four pairs of aortic arches and the paired dorsal aortae that circulate blood to the head and trunk. Three pairs of veins (umbilical, vitelline, cardinal veins) deliver blood to the inflow end of the heart (reprinted with permission from Larsen WJ (1993) Human embryology, Churchill Livingstone, New York, Fig. 7.5)

adjacent to the neural tube. This channel is transitory. However, it provides the proliferative endothelial material from which pial arteries and veins are derived. This vena capitis medialis gives rise to a more lateral definitive channel, which constitutes the first true drainage of the craniocervical region, "vena capitis lateralis or primary head vein" [14]. This channel remains medial to CNs V and X but lateral to CNs VII, VIII, IX, and the otocyst. Because the primary head vein is lateral and will drain the neural tube through three dural stems located in the future dural layer, it is also named the primary head sinus (Fig. 2A). The primary head sinus is continuous with the anterior cardinal veins, which become the internal jugular vein beginning at the level of the jugular foramen.

On completion of the first month of gestation, the embryo is 5–8 mm in length (Stage 2); the entire neural tube is surrounded by a primitive capillary plexus. The brain, which develops from the rostral neural tube, is drained by three dural plexuses and stems: anterior, middle, and posterior (Fig. 2A–D). As shown later, these stems play a pivotal role in shaping the adult dural sinuses. The anterior plexus drains the forebrain (telencephalon and diencephalon) and the midbrain (mesencephalon). The anterior dural

stem and the primitive maxillary vein, which drain the ventrocaudal aspect of the optic vesicle, join together and drain into the primary head sinus. The primitive maxillary vein is the only noteworthy ventral tributary of the primary head sinus at Stage 2. The middle plexus drains the metencephalon (pons and cerebellum) while the posterior plexus drains the myelencephalon (medulla).

Stage 3, the foremost part of the anterior dural plexus forms the primitive marginal sinus that will participate in the formation of or contribute to the future superior sagittal and part of the transverse sinuses. Another major tributary of the anterior dural plexus is the telencephalic vein, also named the middle cerebral vein. Its stem is the future tentorial sinus. At the level of the junction between the posterior dural stem and the primary head sinus, the primary head sinus moves laterally to CN X and the posterior dural stem moves more caudally to be directly continuous with the primitive jugular vein. This segment of the head sinus and the posterior dural stem will form the future sigmoid sinus. The remnant of the primary head sinus medial to CN X receives the ventral myeloencephalic vein; its stem will contribute to the inferior petrosal sinus (Fig. 2B–D).

Stage 5, the human face is first recognizable. A new longitudinal channel, located dorsal to the CN roots and the otic capsule, appears as an anastomosis of the anterior, middle, and posterior dural plexuses. This channel will progressively replace the primary head sinus to form two major adult sinuses, the transverse and sigmoid sinuses. The primary head sinus is dwindling ventral to the otic capsule. The part of this longitudinal channel that runs between the middle and posterior dural plexuses to the optic capsule, together with the posterior dural stem, constitutes the definitive sigmoid sinus. The part of the longitudinal channel between the anterior and middle dural plexuses is the primary transverse sinus.

Stage 6, the sigmoid sinus dorsal to the otic capsule constitutes the main brain drainage flow. Because of the dwindling of the primary head sinus ventral to the otic capsule, the flow into the stem of the old middle dural plexus changes direction toward the newly formed sigmoid sinus dorsal to the otic capsule. The stem of the anterior dural plexus that connects to the primitive maxillary vein also dwindles and progressively disappears. Therefore, the blood of the forehead and part of the brain now drains via the superficial middle cerebral vein and tentorial sinus into the primitive transverse sinus. Because of the disappearance of the anterior dural stem and the reversal of flow in the middle dural stem, the pro-otic sinus (unlike the middle dural stem from which it derives that drains the metencephalon (pons and cerebellum)) only drains extracranial veins: the supraorbital and maxillary veins. Therefore, the pro-otic sinus is not a drainage pathway for the forebrain because of the disappearance of the anterior dural stem.

At Stage 6, the primary head sinus has almost entirely disappeared with the exception of a small segment between the anterior dural stem, primitive maxillary vein, and pro-otic sinus medial to CN V. It is the pro-otic sinus that gives rise to the cavernous sinus.

At Stage 7a (Figs. 2F, 3), the inferior petrosal sinus arises from the pro-otic sinus and ventral myeloencephalic vein (remnant of the primary head sinus medial to CN X) and a dural plexiform collateral of this vein that lies in the angle between the otic and basioccipital cartilage. At the level of CN VI, the emerging inferior petrosal sinus is continuous with the emerging cavernous sinus medial to CN V. The cavernous sinus and inferior petrosal sinus form a direct drainage route for the orbit. The cavernous sinus plays essentially no role in the drainage of the brain.

The tentorial sinus drains superficial cerebral veins. At Stages 6, 7, and 7A the tentorial sinus (following the contour of the middle cranial fossa along the cartilaginous lesser sphenoid wing) drains into the medial part of the primary transverse sinus (Figs. 2A–F, 3). The expansion (elongation) of the temporal lobe and fossa cranioventrally pulls the tentorial sinus into the dural mesenchyme. This phenomenon explains the gradual transition of the middle cerebral vein from a subarachnoid vein to a dural vein, and also explains the variable position of the tentorial sinus from a medial to a lateral position on the floor of the middle cranial fossa.

The sphenoparietal sinus of Breschet, its development and anatomy, are enigmatic [41, 42, 56, 61]. According to Padget [41], "the sinus often borders the edge of the cartilaginous lesser sphenoid wing in the position of the adult so-called sphenoparietal sinus." However, the tentorial sinus differs from the sphenoparietal sinus of Breschet; the latter sinus is a meningeal and diploic channel that also drains the ophthalmomeningeal sinus, which follows the orbi-

tomeningeal artery through the superior orbital fissure.

According to Streeter [58], the superior petrosal sinus appears in the 18-mm embryo. Padget identified the superior petrosal sinus at 14–16 mm as early as Stage 4 (Fig. 2C). However, the definitive superior petrosal sinus is the last of the major adult sinuses to be formed. Of note, the superior petrosal sinus has no well-defined communication with the cavernous sinus and any communication that occurs is late in development.

Special attention should be given to the development of the orbital veins. Before Stage 4, the primitive maxillary vein, caudal and ventral to the eye, is the only drainage pathway of the optic region. At Stage 4, a smaller vein, the primitive supraorbital vein, arises from the superficial tissues cranial and dorsal to the eye. This vein will become the superior ophthalmic vein. The primitive supraorbital vein initially drains directly into the stem of the anterior dural plexus between CNs V and IV. Because of the approximation of the two nerves, the stem of the veins is wedged between CNs IV and VI. A new anastomosis appears lateral to the ophthalmic (V1) nerve and CN IV that reroutes the primitive supraorbital vein to the stem of the maxillary vein. This explains the adult trajectory of the superior ophthalmic vein, which laterally crosses the annular tendon and the cranial nerves that course through the superior orbital fissure to drain into the anterior cavernous sinus.

A discussion of the venous system of the cavernous sinus is incomplete without the inclusion of the emissary veins, including its connections to the face and pterygoid plexus. According to Padget, definitive emissary veins are seen at Stage 7 (Fig. 2E), as has been the case for most of the veins associated with the cavernous sinus. A frontal tributary of the primitive supraorbital vein anastomoses with the anterior facial vein at the inner angle of the eye, forming the angular vein. Superficial tributaries of the primitive supraorbital vein also form the definitive supraorbital and frontal veins. Formation of the cavernous sinus at Stage 7, according to Padget, clarifies the origin of the remaining emissary connection commonly found at the base of the adult skull, the sphenoid emissary vein (of the foramen ovale). This vein communicates with the pterygoid plexus, which is derived from the medial components of the primitive maxillary vein present already at an earlier stage. There is also an inconstant accessory sphenoid emissary (foramen of Vesalius). Both the sphenoid and Vesalian emissary veins drain what Padget termed the "lateral wing of the cavernous sinus," a remnant of the pro-otic sinus. Browder and Kaplan refer to the sphenoid emissary vein as the trigeminal plexus [6, 24].

Venous anatomy of the lateral sellar compartment

The lateral sellar compartment can be succinctly defined as the dural envelope that encloses the parasellar internal carotid artery (ICA). However, its exact borders are still the subject of controversy. Anteriorly, the cavernous sinus proper extends to the superior orbital fissure. Posteriorly, the sinus extends to the dorsum sellae medially and the ostium of Meckel's cave laterally. Superiorly, the sinus roof is defined by clinoidal dural folds. Inferiorly, the lateral sellar compartment is limited by the periosteum of the sphenoid bone and sella turcica. The medial limit is still controversial. Some authors do not recognize a medial dural wall of the cavernous sinus and believe that the medial wall is made of the pituitary capsule [9, 30, 66]. Controversy also exists regarding the lateral boundaries of the lateral sellar compartment; specifically, should the periosteal dural compartment containing V2, V3, and associated venous channels be included in the lateral sellar compartment? If we consider Parkinson's concept that the extradural neural axis compartment is a continuum from the sacrum to the orbit along the inner skull base, then V2, V3, and accompanying venous channels should be included in the lateral sellar compartment.

Variably sized venous spaces exist in this region, lying extradurally beneath the inner dural layer (Fig. 5). These spaces communicate with an extensive variety of venous tributaries and pericavernous venous structures (described below). The cavernous sinus essentially forms a venous crossroads in the central skull base; according to the embryology, the primary pathway is from the orbit through the venous channels of the lateral sellar compartment to the inferior petrosal sinus and internal jugular vein.

Another long-standing controversy concerns the exact structure and organization of the venous channels that compose the cavernous sinus. The cavernous sinus has been referred to as a sinus or a plexus. In fact, the venous channels of the lateral sellar compartment vary greatly from one specimen to

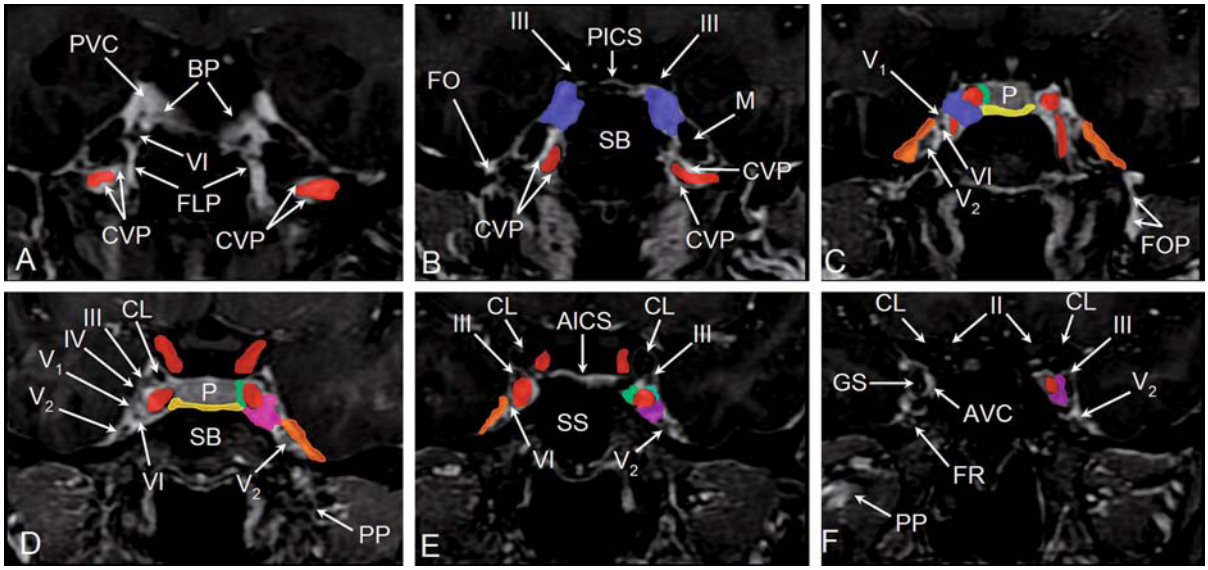

Fig. 5A–F. Lateral sellar venous compartments. (3 Tesla, coronal 3D FSPGR sequence, TR 9.1 msec , TE 3.9 msec, 1.25-mm slice thickness, after 20 cc intravenous gadolinium.) Some slices are same as in Fig. 15. Internal carotid artery (*ICA*) is overlaid in red. *II–VI* cranial nerves, *AICS* anterior intercavernous sinus, *AVC* anterior venous confluence, *BS* basilar sinus, *CL* clinoid, *CVP* carotid venous plexus, *FLP* venous plexus of the foramen lacerum, *FOP* venous plexus of the foramen ovale, *GS* greater wing of sphenoid bone, *M* Meckel's cave, *P* pituitary gland, *PICS* posterior intercavernous sinus, *PP* pterygoid plexus, *PVC* posterior venous confluence, *SS* sphenoid sinus. Spaces of the cavernous sinus are denoted in color overlays. Dark blue: posterior superior space; Green: medial space; Purple: anterior inferior space; Light blue: lateral space; Yellow: inferior intercavernous connections; Orange: lateral pericavernous sinus plexus or laterocavernous sinus. Note how the carotid venous plexus is well seen surrounding the ICA below the skull base and within the petrous bone below the cavernous sinus (**A**,**B**). Venous spaces merge with the spaces of the cavernous sinus as the ICA becomes intracavernous (with permission from the Mayfield Clinic)

another. In the fetal period, the venous channels of the lateral sellar compartment are clearly individual vessels separated by connective tissue and without a muscular layer [32]. Therefore, the macroscopic appearance of the venous channels of the lateral sellar compartment evolves from a network of venous channels of various size veins to a large venous cavity resulting from the coalescence of those veins. In this coalescence of veins, the remnants of the venous walls and surrounding fibrous tissue appear as trabeculae that have historically led to numerous misconceptions [27, 32, 33]. More relevant than the question of the term sinus versus plexus to define the cavernous sinus is the issue of the ultrastructure of the venous wall. The venous channel walls of the cavernous sinus differ from a classic venous wall composed of a basal membrane, smooth muscular media, and adventitia [32, 33]. The junction between the orbital veins and the anterior aspect of the cavernous sinus illustrates this difference. At the level of the orbital apex, the layer of smooth muscle cells disappears and the superior ophthalmic vein progressively takes on a structure identical to a sinus with a basal membrane surrounded by fibrous connective tissue (but without smooth muscle). Therefore, the venous channels of the lateral sellar compartment may have a structure of a plexus or a sinus depending on their macroscopic appearance. However, the ultrastructure of the venous wall is more of a sinus structure.

The presence of arachnoid and arachnoidal granulations that are associated with the venous elements of the lateral sellar compartment is also of import; this was first emphasized by Kricovic [33] and Kehrli et al. [27–30] who proposed a classification of cavernous sinus meningiomas according to the localization of the arachnoidal granulations from which meningiomas arise. They emphasized that such classification, while not clinically applicable, helps to understand some of the features including invasiveness of cavernous sinus meningiomas. Arachnoid tissue is present in several locations within the lateral

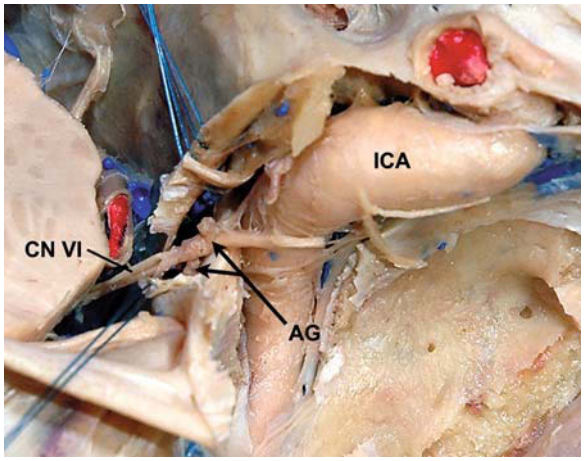

Fig. 6. Anatomical dissection of the lateral sellar compartment of a cadaveric specimen. Lateral wall of the cavernous sinus (right side) has been removed exposing the intracavernous (C4) segment of internal carotid artery (*ICA*) and CN VI. Arrows show arachnoid granulations (*AG*) (with permission from the Mayfield Clinic)

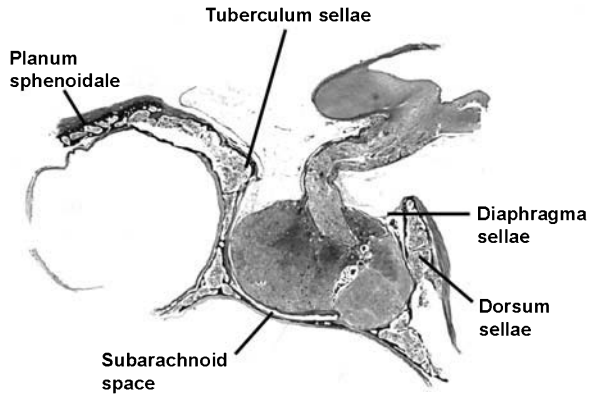

Fig. 7. Illustration of a histologic midline sagittal section (using Masson's trichrome stain, magnification 1×) of a human revealing the sella turcica and adjacent anterior and posterior bony structures, tuberculum sellae, and dorsum sellae as well as the planum sphenoidale. Note the subarachnoid space adjacent to the sella turcica (with permission from the Mayfield Clinic)

sellar compartment. First, arachnoid extends along the cranial nerves as illustrated by Kerli et al. [27]. According to these authors, an arachnoid sleeve with corresponding arachnoidal granulations extends into the lateral sellar compartment along CNs III, IV, and V. Rhoton also recently described an oculomotor sleeve and subarachnoid space that follows CN III into the lateral sellar compartment [50, 51]. Such a sleeve also exists for CN VI. We identified an arachnoidal sleeve and arachnoid granulations of CN VI in the posterior venous cavity of the lateral sellar compartment (Fig. 6). According to Kehrli et al. [27] the arachnoid associated with CN V stops at the level of the trigeminal ganglion within Meckel's cave and does not follow the trigeminal branches (V1–V3) into the lateral sellar compartment. Although we agree with this finding, we have identified a sleeve of arachnoid that followed the trigeminal motor root. Kricovic [33] also described arachnoidal granulations that arose from the arachnoid covering the thin inner wall of Meckel's cave. The arachnoid also extends in front of the pituitary gland, as we identified in several histological sections [52] (Fig. 7).

Several descriptions of the venous spaces of the lateral sellar compartment have been proposed [25, 34, 50, 51, 54, 57]. Rhoton [50, 51] described four venous spaces within the cavernous sinus based on their relationship to the ICA (Fig. 5). The posterior superior space located superior and posterior to the ICA is the largest. This space is connected with the inferior petrosal sinus, which is the main drainage route of the cavernous sinus, basilar sinus, and dorsal intercavernous sinus. The anterior inferior space is located in front of the anterior loop of the ICA; it extends anteriorly to the venous confluence of the superior and inferior ophthalmic veins. The anterior confluence was previously described by Sadasivan et al. [54] as the fifth venous space of the lateral sellar compartment termed the anterior cavernous sinus space. The medial compartment, which lies between the pituitary gland and ICA, varies in size, primarily depending on the artery's tortuosity. A lateral compartment can be identified between the ICA and lateral wall.

The venous spaces of the lateral sellar compartment receive connections from multiple venous structures (Figs. 8–11). Anteriorly, the lateral sellar compartment connects with and receives blood from the superior and inferior ophthalmic veins, either separately or as a common anterior venous confluence within the superior orbital fissure [12, 50, 51, 57]. Using phlebography, Brismar [5] identified a medial ophthalmic vein that drains into the anterior cavernous sinus below the superior ophthalmic vein in 39% and an inferior ophthalmic vein in 65% of cases. Spektor et al. [57] explicitly focused on an inferior ophthalmic vein in 91.7% of cases (24 sides). The superior ophthalmic vein

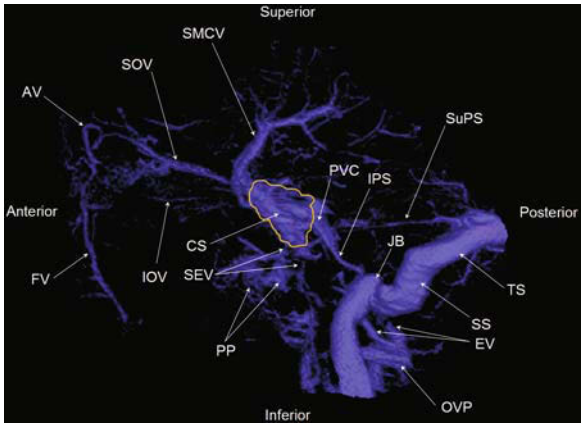

Fig. 8. Venous connections of the lateral sellar venous compartment. Lateral projection, volume rendered image, 3D gadolinium-enhanced elliptic-centric-encoded magnetic resonance venography. Arterial structures and overlapping venous sinuses and veins removed for clarity. *AV* angular vein, *CS* cavernous sinus region (lateral sellar extradural venous compartment), *EV* emissary veins, *FV* facial vein, *IOV* inferior ophthalmic vein, *IPS* inferior petrosal sinus, *JB* jugular bulb, *OVP* occipital venous plexus, *PP* pterygoid plexus, *PVC* posterior venous confluence, *SEV* skull base emissary veins, *SMCV* superficial middle cerebral vein, *SuPS* superior petrosal sinus, *SOV* superior ophthalmic vein, *SS* sigmoid sinus, *TS* transverse sinus. Location of the lateral sellar extradural venous compartment (*CS*) is marked in yellow. Venous flow into the cavernous sinus is from the SOV and IOV anteriorly, and the SMCV and sphenoparietal sinus anterior laterally. Note the multiple skull base emissary veins connecting the CS with the pterygoid plexus. Note the facial vein directly connecting with the superior ophthalmic vein serving as a direct venous route from the face to the cavernous sinus. SMCV in this case enters directly into the cavernous sinus complex. The IPS is usually larger than the SuPS (with permission from the Mayfield Clinic)

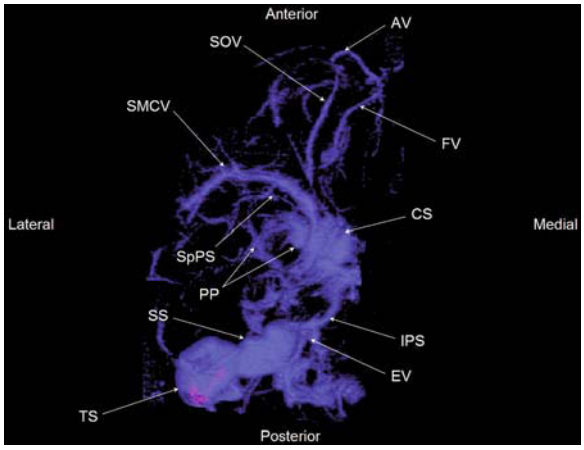

Fig. 9. Venous connections of the cavernous sinus (lateral sellar venous compartment). Direct cranial caudal projection. Volume-rendered image, 3D gadolinium-enhanced elliptic-centric-encoded magnetic resonance venography. Arterial structures and overlapping venous sinuses and veins removed for clarity. Left cavernous sinus and venous structures have been removed. *AV* angular vein, *CS* lateral sellar venous compartment, *EV* emissary veins, *FV* facial vein, *IPS* inferior petrosal sinus, *JB* jugular bulb, *PP* pterygoid plexus, *SMCV* superficial middle cerebral vein, *SS* sphenoid sinus, *SOV* superior ophthalmic vein, *SS* sigmoid sinus, *TS* transverse sinus. Note small size of the sphenoparietal sinus in this case where the superficial middle cerebral vein directly enters the cavernous sinus (with permission from the Mayfield Clinic)

receives an important tributary, the angular vein, which directly connects the veins of the face with the lateral sellar compartment. Inferiorly, the lateral sellar compartment connects with the pterygoid plexus via multiple skull base foramina. The most prominent connection is the plexus within the foramen ovale extending along the mandibular nerve as it exits Meckel's cave. Other skull base foraminal connections to the pterygoid plexus include venous structures that extend through the foramen rotundum, foramen lacerum, and foramen of Vesalius.

The superficial middle cerebral vein is a vital cortical venous structure that drains the majority of the perisylvian region including portions of the temporal, parietal, and frontal lobes [50, 51]. Embryologically, the superficial middle cerebral vein drains into the tentorial sinus, which ultimately drains into the transverse sinus. Preservation of the superficial middle cerebral veins is often difficult when opening the Sylvian fissure because of their variability [16, 26, 50, 51, 55, 60, 61]. Using fat-suppressed contrast-enhanced 3D fast gradient-echo MR, Tanoue et al. classified the drainage patterns of the superficial middle cerebral vein into four types (Fig. 12) [61]. The superficial middle cerebral vein usually drains into the proximal part of the sphenoparietal sinus or directly into the lateral part of the cavernous sinus. The authors also described three variations of the sphenoparietal sinus of Breschet (Fig. 13).

Controversies also exist regarding the sphenoparietal sinus of Brechet. As stated by Padget [41, 42], the sphenoparietal sinus should not be confused with the tentorial sinus because they have distinct origins. Ruiz et al. [55] noted that the superficial middle

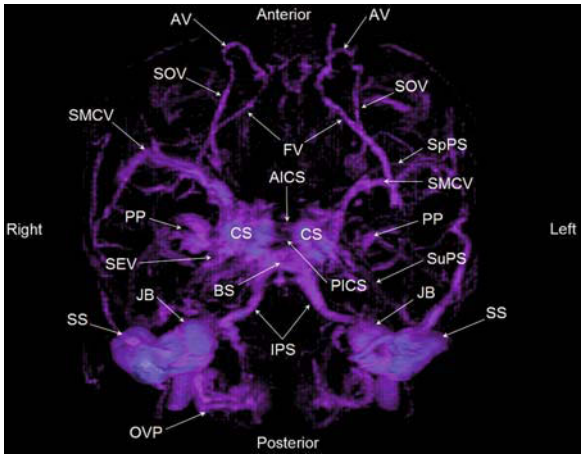

Fig. 10. Venous connections of the cavernous sinus (*CS*) (lateral sellar venous compartment). Frontal oblique caudal projection. Volume-rendered image, 3D gadolinium-enhanced elliptic-centric-encoded magnetic resonance venography. Arterial structures and overlapping venous sinuses and veins removed for clarity. Frontal oblique projection nicely demonstrates the intercavernous connections, anterior intercavernous sinus (*AICS*) and basilar sinus (*BS*). Small dot of enhancement between the AICS and posterior intercavernous sinus (*PICS*) is the infundibular stalk. On the left a moderate-sized superficial middle cerebral vein (*SMCV*) joins a small sphenoparietal sinus (*SpPS*) to become a common trunk joining the CS. Large right-sided SMCV overlaps the very small SpPS on this side. *AV* angular vein, *FV* facial vein, *IPS* inferior petrosal sinus, *JB* jugular bulb, *OVP* occipital venous plexus, *PP* pterygoid plexus, *PVC* posterior venous confluence, *SEV* skull base emissary veins, *SS* sigmoid sinus, *SuPS* superior petrosal sinus, *SOV* superior ophthalmic vein, *TS* transverse sinus (with permission from the Mayfield Clinic)

cerebral vein never drains into the sphenoparietal sinus. The sphenoparietal sinus drains branches of the middle meningeal veins, diploic veins of the lesser sphenoid wing, and orbital veins that follow the orbitomeningeal artery through the lateral part of the superior orbital fissure [41, 42, 55]. The sphenoparietal sinus courses along the inferior aspect of the lesser sphenoid wing, crosses over the superior ophthalmic vein, and drains into the most anterior aspects of the venous channel of the lateral sellar compartment.

Ruiz et al. [55] also commented on a laterocavernous sinus located between the two layers of the lateral wall of the cavernous sinus and a paracavernous sinus located laterally along the temporal fossa floor. Gailloud et al. [16], using cerebral angiograms (Fig. 14), then described three types of drainage patterns of the superficial middle cerebral vein. In 20% of cases, it drains into a laterocavernous sinus, which in turn either drains into the superior petrosal sinus (18%), pterygoid plexus (27%), cavernous sinus (32%), or a combination of those (23%). In 39% of cases, the superficial middle cerebral vein drains into the paracavernous sinus, which in turn either drains into the superior petrosal sinus (33%), pterygoid plexus (44%), cavernous sinus (5%), or a combination of those (18%). Embryologically, connections between the cavernous sinus and the derivatives of the tentorial sinus (superficial middle cerebral vein, laterocavernous sinus, paracavernous sinus) are established late in the fetal period [16, 32].

Posteriorly, the cavernous sinus connects broadly with a venous confluence that we dealt with earlier, the posterior venous confluence. This confluence connects the large basilar plexus along the dorsum sellae, inferior petrosal sinus along the clival margin, and superior petrosal sinus along the petrous ridge, with the posterior cavernous sinus. Destrieux [8] termed this connection the petroclival venous confluence while Iaconetta [22] called it the sphenopetroclival venous gulf. Importantly, CN VI courses through this region as it enters the cavernous sinus. The inferior petrosal sinus is the main venous drainage route of the lateral sellar compartment. It extends inferiorly along the clivus and connects the cavernous sinus to the jugular bulb or lower sigmoid sinus. The inferior petrosal sinus is usually much larger than the superior petrosal sinus, which connects the cavernous sinus to the transverse sinus along the petrous ridge. The superior petrosal sinus also receives bridging veins from the cerebellum and brainstem [51]. According to Padget [41, 42], no connection exists between the superior petrosal sinus and the cavernous sinus until late in development. Knosp et al. [32] opined that the superior petrosal sinus was always superior to the porous trigeminus; a connection was also identified between the superior petrosal sinus and cavernous sinus in 60% of cases. They emphasized that the diameter of the superior petrosal sinus increases distal to the entry of the superior petrosal vein; the superior petrosal sinus represents drainage for this vein rather than the cavernous sinus.

The paired lateral sellar compartments connect with each other primarily via a large basilar sinus or plexus posterior to the upper clivus and dorsum

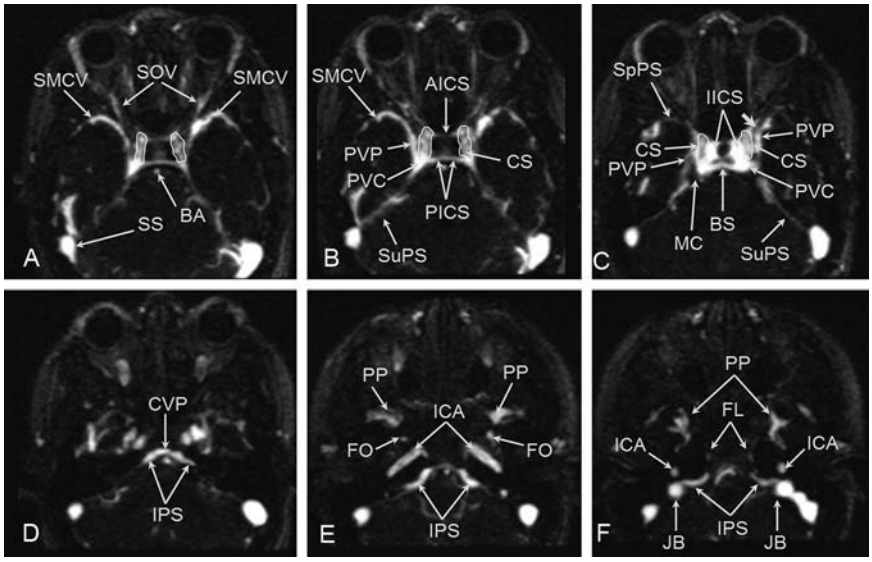

Fig. 11. Axial reformatted source images from 3D gadolinium-enhanced elliptic-centric-encoded magnetic resonance venography (**A–F**, superior to inferior). Classically described location of the lateral sellar extradural venous compartment (yellow) lying near the ICA location. Note the prominent venous opacification along the lateral margin of the lateral sellar venous compartment (*CS*), appearing separate from the sinus in part on the left by a linear cleft (arrow, **C**); this likely represents in part the so-called paracavernous venous plexus or laterocavernous sinus, receiving blood from skull base foraminal plexus, sphenoparietal sinus (*SPS*), or superficial middle cerebral vein (*SMCV*). Small venous channels extend through the skull base within the foramen lacerum (*FL*). Paired inferior petrosal sinuses (*IPS*) in this patient are large extending along the clivus to the jugular bulb (*JB*). *AICS* anterior intercavernous sinus, *BS* basilar sinus, *EV* emissary veins, *FLP* venous plexus of the foramen lacerum, *FOP* venous plexus of the foramen ovale, *FV* facial vein, *IICS* inferior intercavernous sinus, *IOV* inferior ophthalmic vein, *M* Meckel's cave, *OVP* occipital venous plexus, *PICS* posterior intercavernous sinus, *PP* pterygoid plexus, *PVC* posterior venous confluence, *PVP* paracavernous venous plexus, *SuPS* superior petrosal sinus, *SOV* superior ophthalmic vein, *SS* sigmoid sinus (with permission from the Mayfield Clinic)

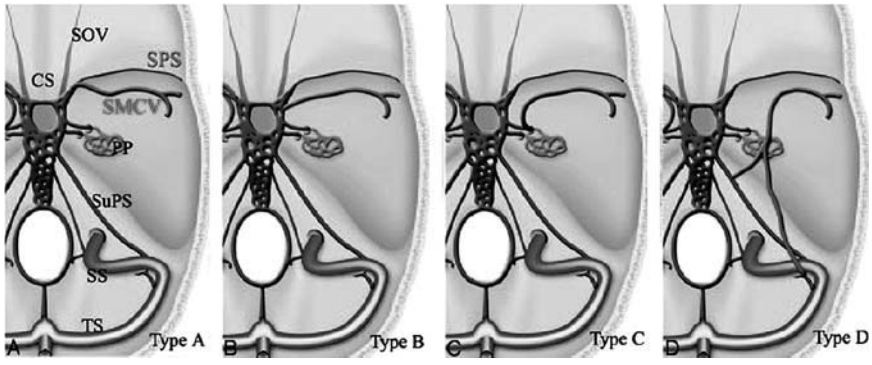

Fig. 12. Schematic drawings of variations of connections of the superficial middle cerebral vein (*SMCV*). Type A, vein connects with the proximal sphenoparietal sinus (*SPS*) and flows into the frontal aspect of the cavernous sinus (*CS*). Type B, vein connects with the lateral aspect of the cavernous sinus independently. Type C, vein turns downward and connects with the pterygoid plexus through the middle cranial fossa. Type D, vein runs across the pyramidal ridge and connects with the superior petrosal sinus or transverse sinus via the tentorial sinus. *SOV* indicates the superior orbital vein, *PP* pterygoid plexus, *SuPS* superior petrosal sinus, *SS* sigmoid sinus, *TS* transverse sinus (with permission from Tanoue S et al. (2006) AJNR 27: 1083–1089, Fig. 1)

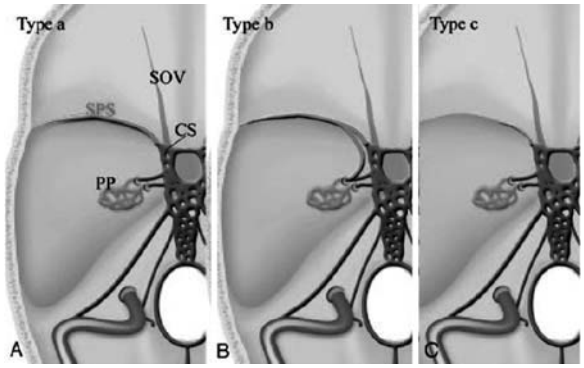

Fig. 13. Schematic drawings of variations (Types a–c) of the sphenoparietal sinus (*SPS*). Type a, SPS runs along the lesser sphenoid wing and connects to the anterior aspect of the cavernous sinus (*CS*). Type b, SPS runs along the lesser sphenoid wing and connects with the foramen ovale plexus or pterygoid plexus (*PP*). Type c, hypoplastic SPS connects with the CS. *SOV* superior orbital vein (with permission from Tanoue S et. al. (2006) AJNR 27: 1083–1089, Fig. 3)

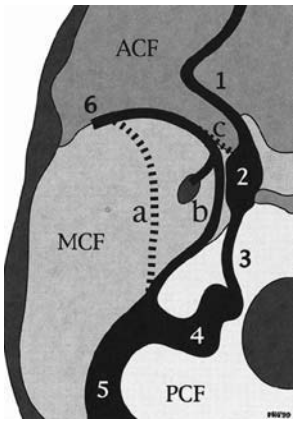

Fig. 14. Schematic representation of the three basic drainage pathways of the superficial middle cerebral vein (*SMCV*) according to San Millan Ruiz et al. [55]. Superior view of the anterior (*ACF*), middle (*MCF*), and posterior cranial fossae (*PCF*). The SMCV may continue as a paracavernous sinus coursing laterally over the MCF (*a*), may run as a laterocavernous sinus enclosed within the lateral wall of the cavernous sinus (*b*), or may terminate into the anterosuperior aspect of the cavernous sinus (*c*). Venous outflow toward the pterygoid plexus via a skull base foramen is shown for the LCS. *1* Superior ophthalmic vein, *2* cavernous sinus, *3* inferior petrosal sinus, *4* sigmoid sinus, *5* transverse sinus, *6* SMCV (with permission from Gailloud P et al. (2000) AJNR 21: 1923–1929, Fig. 1)

sellae. Additional connections are rendered with multiple intercavernous sinuses, which can occur along any surface of the pituitary gland. These are usually visible as a larger posterior intercavernous sinus, a smaller anterior intercavernous sinus, and a variable inferior intercavernous sinus connection [32] (Figs. 10 and 11). The entire complex of intercavernous connections is termed the "circular sinus" [50].

Imaging of the venous part of the cavernous sinus

With improvement of MR imaging techniques, the venous and soft tissue components of the lateral sellar compartment can be demonstrated in vivo with unprecedented detail [13, 36, 37, 48, 64, 65]. Our demonstration of the complex venous anatomy of the lateral sellar compartment was feasible at 3 Tesla as well as 3D MRV [15] by high-resolution MR imaging. This imaging shows the soft tissue components and venous relationships of the lateral sellar compartment by using noninvasive imaging techniques most commonly used for evaluating skull base and sellar lesions.

On contrast-enhanced T1-weighted MR images, parasellar venous structures enhance intensely, outlining the cranial nerves as filling defects or impressions on the enhancing sinus components (Figs. 5, 15). The dura also variably enhances, defining the outer wall of the sinus. Other filling defects, such as intracavernous arterial vessels and dural reflections, are variably seen [13, 65]. CNs III, VI, V2, and V1 are well visualized and their anatomic relationships can be outlined routinely. Because of the small size of CN IV and its position adjacent to CN III, it is less well delineated [65]. The complex internal venous structure of the lateral sellar extradural venous compartment is difficult to detect on MR imaging. Early dynamic CT studies have, however, successfully increased our understanding of different compartments that enhance in different sequence after contrast administration [4]. Although compartmentalized dural fistula drainage has been described [7], descriptions of lateral sellar compartments have been more important in determining potential conduits for surgical therapy of lesions in this region [51].

The venous connections of the cavernous sinus proper have traditionally been demonstrated by catheter angiography. In spite of being requisite for rapid sequence imaging of fistulas and other vascular lesions of the lateral sellar compartment, the incom-

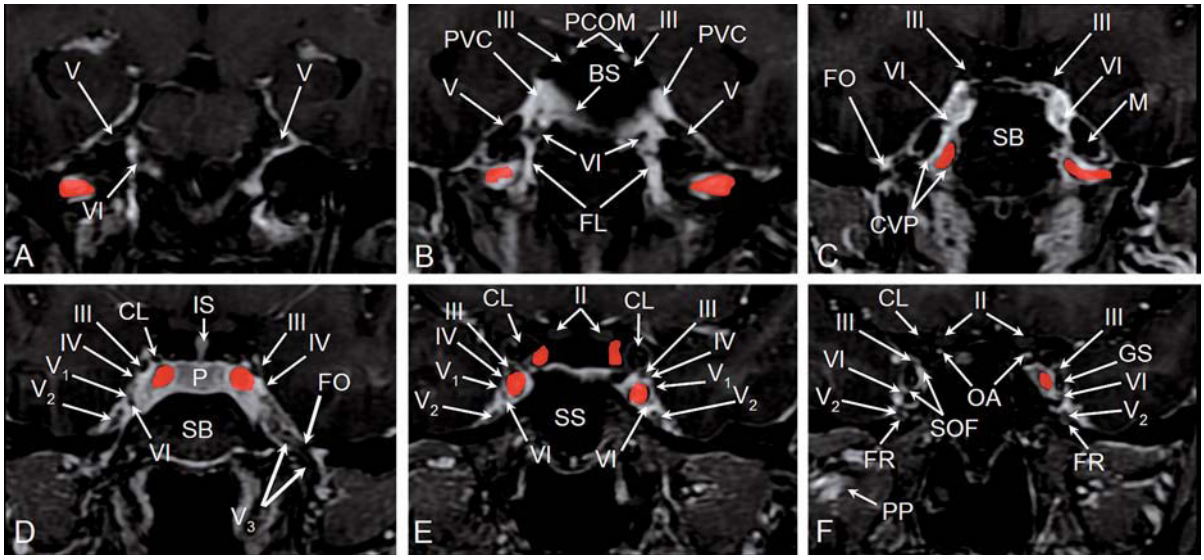

Fig. 15. Soft tissue anatomy of the lateral sellar compartment (3T, coronal 3D FSPGR sequence, TR: 9.1 msec, TE: 3.9 msec, 1.25 mm slice thickness, after 20 cc intravenous gadolinium) from posterior (**A**) to anterior (**F**). Internal carotid artery (ICA) is traced and overlaid in red to aid in identification. Venous compartments of the lateral sellar region enhance intensely, outlining the ICA, and cranial nerves (CNs). CN III can be identified entering the cavernous sinus superiorly (**C**), extending to lie beneath the clinoid process (**D**), superior to the ICA (**E**), and extending into the upper SOF anteriorly (**F**). CN IV is very small in the lateral wall of the sinus producing a subtle impression and filling defect, variably seen just below CN III (**D**, **E**). CN V_1 can be identified exiting the superior margin of Meckel's cave lying along the lateral wall of the sinus. Initially at the level of CN VI, V_1 ascends anteriorly entering the SOF along with CNs III and IV. Meckel's cave is visualized lying posterior and inferior to the cavernous sinus (**C**), accepting the CN V root as it extends through the cistern (**A**,**B**). Posterior venous confluence, connecting the inferior petrosal sinus, superior petrosal sinus, and basilar sinus with the posterior cavernous sinus, lies just above and medial to Meckel's cave (**B**). CN V_2 keeps an inferior position outside of the cavernous sinus, bordered laterally by enhancing dura and lateral paracavernous venous plexus (**D**, **E**), entering the foramen rotundum anteriorly along with a small enhancing venous plexus (**F**). CN V_2 lies outside the dural envelop of the cavernous sinus. CN V_3 exits Meckel's cave inferiorly, seen as a filling defect among the rich venous plexus in the foramen ovale (**D**). CN VI enters the cavernous sinus from the cistern through the basilar venous plexus/posterior venous confluence (**A**), through Dorello's canal deep to the petrosphenoid ligament (**B**), entering the cavernous sinus deep to the outer dural layer (**C**, **D**) (investing CNs III–V_1), eventually lying directly lateral to the ICA (**E**). Venous plexus of the foramen lacerum (**B**) and foramen ovale (**D**) appear as lobular areas of intense enhancement extending into the foramina. Pituitary gland is visible as a zone of slightly diminished enhancement within the sella. Dura of the medial cavernous sinus wall is not well seen on this sequence. *II–IV* Cranial nerves *II–IV*, *V_1–V_3* first through third divisions of CN V (ophthalmic, maxillary, and mandibular nerves, respectively), *V* retrogasserian trigeminal root at the level of the porous trigeminus, *CL* clinoid process, *CVP* pericarotid venous plexus (carotid venous plexus), *FL* foramen lacerum plexus, *FO* foramen ovale, *FR* foramen rotundum, *GS* greater wing of the sphenoid bone marginating the superior orbital fissure, *IS* infundibular stalk, *M* Meckel's cave, *P* pituitary gland, *PCOM* posterior communicating artery, *PP* pterygoid plexus, *PVC* posterior venous confluence, *SOF* superior orbital fissure, *SS* sphenoid sinus, *SB* sphenoid bone, *OC* optic chiasm, *OS* optic strut, *OT* optic tract (with permission from the Mayfield Clinic)

plete filling of the cavernous sinus secondary to inflow effects limits its ability to completely opacify and define the sinus three-dimensionally. Three-dimensional gadolinium-enhanced elliptic-centric-encoded MRV is a newer technique [15] that we have used extensively to evaluate patients with suspected venous occlusion. It provides high-resolution evaluation, with the acquisition timed to coincide with maximal venous contrast opacification. The production of selected multiplanar reformations and volume rendered images in any plane or rotation is a significant benefit of this technique.

Conclusions

The value of this discussion is to enhance the understanding of the complex anatomy of the lateral

sellar compartment to better serve patients by the effective and safe treatment of pathologies within this region. Knowledge of the embryology, particularly of the venous anatomy, which is considerably more complex and variable than the arterial, is requisite. Furthermore, the technological advancements currently afforded the medical community, 3D MRV enables visualization and/or identification of soft tissue and vascular anatomy in the greatest detail. Thus, a keen appreciation of the myriad embryological variants will be invaluable in the interpretation of the vascular imagery.

References

1. Batson OV (1940) Function of the vertebral veins and their role in the spread of metastases. Am Surg 112: 139–149
2. Batson OV (1956) The vertebral vein system. Caldwell Lecture 1956. Am J Roentgenol Radium Ther Nucl Med 78: 195–212
3. Batson OV (1975) More about veins. Acta Anat Nippon 50: 299–309
4. Bonneville J, Cattin F, Racle A, Boucharaeb M, Boulard D, Potelon P, Tang YS (1989) Dynamic CT of the laterosellar extradural venous spaces. Am J Neuroradiol 10: 535–542
5. Brismar J (1974) Orbital phlebography III. Topography of intraorbital veins. Acta Radiol Diagn (Stockh) 15: 577–594
6. Browder J, Kaplan HA (1976) Cerebral dural sinuses and their tributaries. Charles C Thomas, Springfield, IL, pp 05–88
7. Chaloupka J, Goller D, Goldberg R, Duckwiller G, Martin N, Vinuela F (1993) True anatomical compartmentalization of the cavernous sinus in a patient with bilateral cavernous dural arteriovenous fistulae. J Neurosurg 79: 592–595
8. Destrieux C, Velut S, Kakou M, Lefrancq T, Arbeille B, Santini J (1997) A new concept in Dorello's canal microanatomy: the petroclival venous confluence. J Neurosurg 87: 67–72
9. Dietemann JL, Kehrli P, Maillot C, Diniz R, Reis M Jr, Neugroschl C, Vinclair L (1998) Is there a dural wall between the cavernous sinus and the pituitary fossa? Anatomical and MRI findings. Neuroradiology 40: 627–630
10. Dolenc VV (1983) Direct microsurgical repair of intracavernous vascular lesions. J Neurosurg 58: 824–831
11. Dolenc VV (1989) Anatomy and surgery of the cavernous sinus. Springer, Wien New York, pp 1–344
12. Doyon D, Aron-Rosa D, Ramee A (1974) Orbital veins and cavernous sinus. Chap. 76. In: Newton TH, Potts DG (eds) Radiology of the skull and brain, Vol 2, Book 3. CV Mosby, St. Louis
13. Ettl A, Zwrtek K, Daxter A, Salomonowitz E (2000) Anatomy of the orbital apex and cavernous sinus on high-resolution magnetic resonance images. Surv Ophthalmol 44: 303–323
14. Evans HM (1912) The development of the vascular system. Chap. III. In: Kerbel F, Mall FP (eds) Manual of human embryology. J.B. Lippincott, Philadelphia, pp 570–709
15. Farb RI, Scott JN, Willinsky RA, Montanera WJ, Wright GA, terBrugge KG (2003) Intracranial venous system: gadolinium-enhanced three-dimensional venography with auto-triggered elliptic centric-ordered sequence-initial experience. Radiology 226: 203–209
16. Gailloud P, San Milan Ruiz D, Muster M, Murphy KJ, Fasel JHD, Rugenacht DA (2000) Angiographic anatomy of the laterocavernous sinus. Am J Neuroradiol 21: 1923–1929
17. Gilmore SA (1996) Developmental anatomy of the intracranial venous system: a review of dural venous sinus development. In: Hakuba A (ed) Surgery of the intracranial venous system. Springer, Tokyo, pp 3–13
18. Hakuba A, Ohata K, Nakaniski N, Bae HG, Soares SB (1996) Developmental anatomy of the cavernous sinus. In: Hakuba A (ed) Surgery of the intracranial venous system. Springer, Berlin, pp 26–35
19. Hamby WB (1966) Carotid-cavernous fistula. Charles C Thomas, Springfield, IL, pp 1–139
20. Harris FS, Rhoton AL (1976) Anatomy of the cavernous sinus: a microsurgical study. J Neurosurg 45: 169–180
21. Hunter W (1762) Further observations upon a particular species of aneurism M. Observations and inquiries 2: 390–414
22. Iaconetta G, Fusco M, Samii M (2003) The sphenopetroclival venous gulf: a microanatomical study. J Neurosurg 99: 366–375
23. Inoue T, Rhoton AL, Theele D, Barry ME (1990) Surgical approaches to the cavernous sinus. A morphological study. Neurosurgery 26: 903–932
24. Kaplan HA, Browder J, Krieger AJ (1976) Intercavernous connections of the cavernous sinuses. J Neurosurg 45: 166–168
25. Kawase T, van Loveren H, Keller JT, Tew JM (1996) Meningeal architecture of the cavernous sinus: clinical and surgical implications. Neurosurgery 39: 527–534
26. Kazumata K, Kamiyama H, Ishikawa T, Takizawa K, Maeda T, Makino K, Gotoh S (2003) Operative anatomy and classification of the Sylvian veins for the distal transylvian approach. Neurol Med Chir (Tokyo) 43: 427–434
27. Kehrli P, Maillot C, Wolff Quenot MJ (1995) Sheaths of cranial nerves in the lateral wall of the cavernous sinus. An embryological and anatomical study. Neurochirurgie 41: 403–412 (in French)
28. Kehrli P, Maillot C, Wolff MJ (1996) The venous system of the lateral sellar compartment (cavernous sinaus): a

histological and embryological study. Neurol Res 18: 387–393
29. Kerhli P, Maillot C, Wolff MJ (1997) Anatomy and embryology of the trigeminal nerve and its branches in the parasellar area. Neurol Res 19: 57–65
30. Kehrli P, Ali M, Reis M Jr, Maillot C, Dietemann JL, Dujovny M, Ausman JI (1998) Anatomy and embryology of the lateral sellar compartment (cavernous sinus) medial wall. Neurol Res 20: 585–592
31. Kim JM, Romano A, Sanan A, van Loveren HR, Keller JT (2000) Microsurgical anatomic features and nomenclature of the paraclinoid region. Neurosurgery 46: 670–682
32. Knosp E, Müller G, Perneczky A (1987) Anatomical remarks on the fetal cavernous sinus and the veins of the middle cranial fossa. In: Dolenc VV (ed) The cavernous sinus: a multidisciplinary approach to vascular and tumorous lesion. Springer, Wien New York, pp 104–116
33. Krivosic I (1987) Histoarchitecture of the cavernous sinus. In: Dolenc VV (ed) The cavernous sinus: a multidisciplinary approach to vascular and tumorous lesion. Springer, Wien New York, pp 117–129
34. Lang J, Kageyama I (1990) Clinical anatomy of the blood spaces and blood vessels surrounding the siphon of the internal carotid artery. Acta Anat (Basel) 139: 320–325
35. Larson WJ (1993) Human Embryology, 2nd ed. Churchill Livingstone, New York
36. Lasjaunias P, Berenstein A (1987) Angiographic protocol of the parasellar region. In: Lasjaunias P, Berestein A (eds) Surgical neuroangiography 3: functional anatomy of craniofacial arteries. Springer, Berlin, pp 341–354
37. Lasjaunias P, Berenstein A, Raybaud (1987) Intracranial venous system. In: Lasjaunias P, Berestein A (eds) Functional vascular anatomy of brain, spinal cord and spine. Springer, Berlin, pp 223–266
38. Mall FP (1905) On the development of blood vessels of the brain in the human embryo. Am J Anat 4: 1–18
39. O'Rahilly R, Mueller F (1987) Developmental stages in human embryos including a revision of Streeter's "Horizons" and a survey of the carnegie collection. Carnegie Institute No. 637
40. Padget DH (1948) The development of the cranial arteries in the human embryo. Contrib Embryol 212: 205–261
41. Padget DH (1956) The cranial venous system in man in reference to development, adult configuration, and relation to the arteries. Am J Anat 98: 307–355
42. Padget DH (1956) The development of the cranial venous system in man, from the viewpoint of comparative anatomy. Contrib Embryol 247: 79–140
43. Parkinson D (1965) A surgical approach to the cavernous portion of the carotid artery: anatomical studies and case report. J Neurosurg 23: 474–483
44. Parkinson D (1987) Carotid cavernous fistula. History and anatomy. In: Dolenc VV (ed) The cavernous sinus: a multidisciplinary approach to vascular and tumorous lesions. Springer, Wien New York, pp 120–138
45. Parkinson D (1990) Surgical anatomy of the lateral sellar compartment (cavernous sinus). Clin Neurosurg 36: 219–239
46. Parkinson D (1998) Lateral sellar compartment O.T. (Cavernous sinus): history, anatomy, terminology. Anat Rec 251: 486–490
47. Parkinson D (2000) Extradural neural axis compartment. J Neurosurg 92: 585–588
48. Pinker K, Ba-SSalamah A, Wolsberger S, Mlynarik V, Knosp E, Trattnig S (2005) The value of high-field MRI (3T) in the assessment of sellar lesions. Eur J Rad 54: 327–334
49. Renn WH, Rhoton AL (1975) Microsurgical anatomy of the sellar region. J Neurosurg 43: 288–298
50. Rhoton AL (2002) The cavernous sinus, the cavernous venous plexus, and the carotid collar. Neurosurgery 51 (Suppl 1): SI-375–SI-410
51. Rhoton AL (2002) The cerebral veins. Neurosurgery 51 (Suppl 1): 159–205
52. Romano A, Zuccarello M, van Loveren HR, Keller JT (2001) Expanding the boundaries of the transsphenoidal approach: a microanatomic study. Clin Anat 14: 1–9
53. Sabin FR (1917) Origin and development of the primitive vessels of the chick and of the pig. Carnegie Inst Wash Pub 226, Contrib Embryol 6: 61–124
54. Sadasivan B, Ma H, Dujovny M, Ausman JI, Zamaro L, Dragovic L (1991) The anterior cavernous sinus. Acta Neurochir (Wien) 108: 154–158
55. San Milan Ruiz D, Gailloud P, De Miguel Miquel MA, Muster DM, Dolenc VV, Rufenacht DA, Fasel JHD (1999) Laterocavernous sinus. Anat Rec 25: 7–12
56. San Milan Ruiz D, Fasel JHD, Rufenacht DA, Gailloud P (2004) The sphenoparietal sinus of Breschet: does it exist? An anatomic study. Am J Neuroradiol 25: 112–120
57. Spektor S, Piontek E, Umansky F (1997) Orbital venous drainage into the anterior cavernous sinus space: microanatomic relationships. Neurosurgery 40: 532–540
58. Streeter GL (1915) The development of the venous sinuses of the dura mater in human embryo. Am J Anat 18: 145–178
59. Streeter GL (1918) The development of alterations in the vascular system of the brain of the human embryo. Contrib Embryol 271: 5–38
60. Suzuki Y, Matsumoto K (2000) Variations of the superficial middle cerebral vein: classification using three-dimensional CT angiography. Am J Neuroradiol 21: 932–938
61. Tanoue S, Kiyosue H, Okahara M, Sagara Y, Hori Y, Kashiwagi J, Mori H (2006) Para-cavernous sinus venous structures: anatomic variations and pathologic condi-

tions evaluated on fat-suppressed 3D fast gradient-echo MR images. Am J Neuroradiol 27: 1083–1089
62. Travers B (1811) A case of aneurism by anastomosis in the orbit, cured by ligation of the common carotid artery. Med Chir Tr 2: 1–16
63. Umansky F, Nathan H (1982) The lateral wall of the cavernous sinus: with special reference to the nerves related to it. J Neurosurg 56: 228–234
64. Wolfsberger S, Ba-Ssalamah A, Pinker K, Mlynarik V, Czech T, Knosp E, Trattnig S (2004) Application of three-tesla magnetic resonance imaging for diagnosis and surgery of sellar lesions. J Neurosurg 100: 278–286
65. Yagi A, Sato N, Taketomi A, Nakajima T, Morita H, Koyama Y, Aoki J, Endo K (2005) Normal cranial nerves in the cavernous sinuses: contrast-enhanced three-dimensional constructive interference in the steady state MR imaging. Am J Neuroradiol 26: 946–950
66. Yilmazlar S, Kocaeli H, Aydiner F, Korfali E (2005) Medial portion of the cavernous sinus: quantitative analysis of the medial wall. Clin Anat 18: 416–422

Central skull base anatomy as seen through the endoscope

M. Tschabitscher[1], R. J. Galzio[2]

[1]Microsurgical & Endoscopic Anatomy, University of Vienna, Vienna, Austria
[2]Department of Neurosurgery, University of L'Aquila, L'Aquila, Italy

Introduction

The endoscope may provide new effective therapeutic strategies and less invasive approaches. This instrument, however, provides quite a different perspective of the anatomical structures normally seen with the operating microscope, thus requiring different reference points. The "keyhole concept" dictates that anatomical variation from patient to patient often requires different endoscopic approaches to the same target. The best approach to various lesions of the central skull base is determined only after precise analysis of a given patient's anatomy and clinical circumstances. The following describes three different endoscopic approaches.

Material and method

The equipment used throughout the preparation of the anatomical studies consisted of the HOPKINS® rod lens telescope, 0°, 30° and 45° view, diameter 4 mm of Karl Storz Company, Tuttlingen, Germany, Cold Light Fountains and Accessories for Video Documentation, KARL STORZ Endovision, IMAGE-1 Video Camera System and Accessories for Illumination, Documentation and Data Storage.

Fresh (non-fixed) cadaver heads were employed, and only the arterial system was injected with colored rubber. Access to each region was similar to that achieved by standard neurosurgical techniques.

Supraorbital–subfrontal approach

Certain anatomical conditions are required for exploring central skull base structures endoscopically (Fig. 1):

1. The window between the pituitary stalk, the 2nd cranial nerve and the internal carotid artery or the 3rd cranial nerve must be of sufficient size;
2. The dorsum sellae must not be too prominent. The anterior cranial fossa is bordered posteriorly by the lesser wing of the sphenoid, which also marks the junction of the frontal and temporal lobes, or direct access to the sylvian fissure. After splitting the arachnoid, the entire M1 segment may be seen endoscopically.

The 3rd cranial nerve comes into view medially. It enters the roof of the cavernous sinus (through Lang's "trough") (Fig. 2). Between the 3rd cranial nerve and the internal carotid Liliequist's membrane may be split, giving access to the posterior cranial fossa. Depending on how medially or how laterally the supraorbital craniotomy is placed, the interpeduncular fossa is accessed along the posterior communicating artery (Fig. 3). There, the tip of the basilar artery (and its terminal branches), the mammillary bodies, and tuber cinereum are seen. In keeping with the keyhole concept, the midline is better visualized from a more lateral approach than medially.

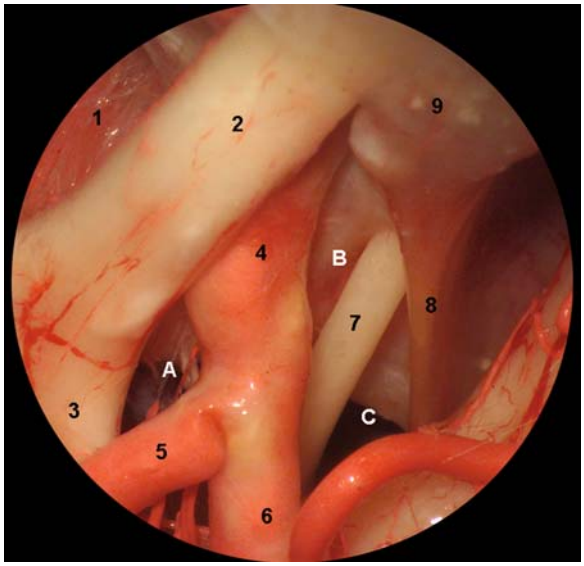

Fig. 1. Right supraorbital approach (0° optic). *1* Diaphragma sellae, *2* cn II, *3* optic tract, *4* ICA, *5* A1, *6* M1, *7* C. N.III, *8* anterior petroclinoid fold, *9* anterior clinoid process. *A* Opto-carotid window, *B* window between ICA and cn III, *C* window lateral of cn III

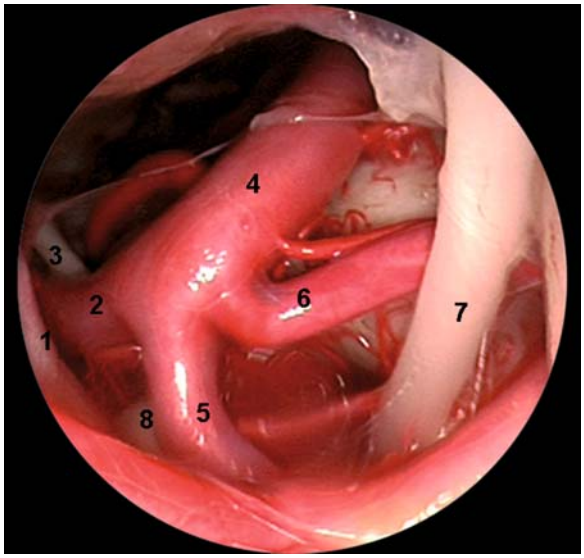

Fig. 2. Right supraorbital approach (30° optic). Window between ICA and cn III : *1* tuber cinereum, *2* left P1, *3* left cn III, *4* BA, *5* right P1, *6* right SCA, *7* right cn III

The window between the ICA and the 2nd cranial nerve provides a view into the posterior cranial fossa similar to that described above.

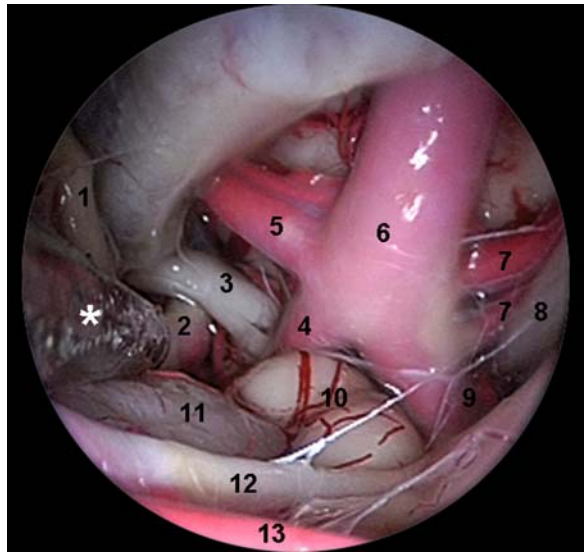

Fig. 3. Right supraorbital approach (30° optic). Window between cn II and ICA: *1* left PCoA, *2* left P2, *3* left cn III, *4* left P1, *5* left SCA, *6* BA, *7* doubled right SCA, *8* right cn III, *9* right P1, *10* mammillary bodies, *11* tuber cinereum, *12* right PCoA, *13* right M1.* sucker

If the dorsum sellae is sufficiently low, the route between the pituitary stalk and the 2nd cranial nerve provides maximum medial exposure of the interpeduncular fossa and the upper third of the basilar artery and its branches.

Transnasal–transsphenoidal approach

When the two sphenoidal orifices are widened and connected and the anterior wall of the sphenoid sinus is removed, the remaining sinus walls may be distinguished, i.e. the sphenoid planum anterior-superiorly, the bulge of the pituitary fossa centrally, and the clivus postero-inferiorly (Fig. 4). The distinct bulges in the lateral wall are caused by the 2nd cranial nerve, the ICA and the second portion of the 5th cranial nerve. At the junction of the lateral wall and the floor, the pterygoid canal (the Vidian canal) produces another, possibly less distinct, bulge. This midline orientation allows three levels to be distinguished after removing the roof and the posterior wall of the sphenoid sinus (Fig. 5):

1. After removing the planum sphenoidale, the optic chiasm is seen centrally, providing two alternative routes for the endoscope:

(a) Above the chiasm, with the lamina terminalis and the anterior communicating artery complex in full view (Fig. 6) or
(b) Below the chiasm and above the sellar diaphragm, providing an excellent view of the pituitary stalk, and, lateral to it, the posterior cranial fossa and the optic tract.

2. Removing pituitary fossa bone exposes its periosteal lining, then a dense venous plexus, finally the pituitary gland itself.
3. After removing Blumenbach's clivus, the periosteum is encountered, followed by a venous plexus, then dura mater (Fig. 7). When these three layers, plus the arachnoid, are split, the full length of the basilar artery (and its branches) comes into view (Fig. 8) within the interpeduncular fossa, and caudally the confluence of the vertebral arteries and, depending on the dissection, the foramen magnum. In Fig. 9, depending on the endoscope employed (0° or 45°), the 6th and 4th nerves may be seen as well.

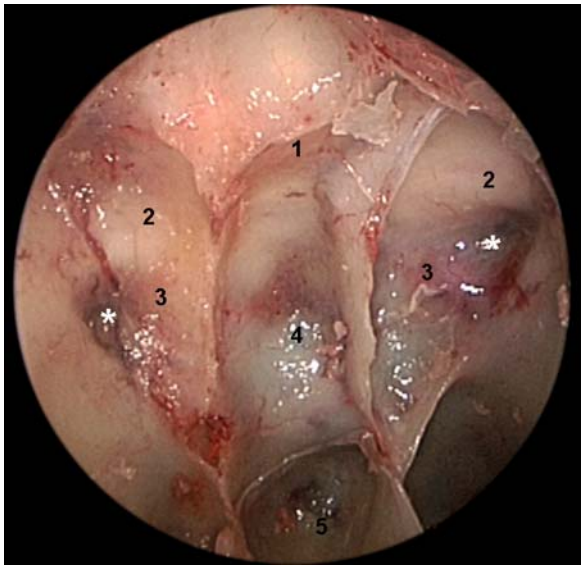

Fig. 4. Transsphenoidal approach (0° optic). Overview of the inner shaping of the sinus after opening and removing the anterior-inferior walls. *1* Planum sphenoidale, *2* optic protuberance, *3* carotid protuberance, *4* pituitary protuberance, *5* clival inclination; *opto-carotid recess (corresponds to the region of anterior clinoid process)

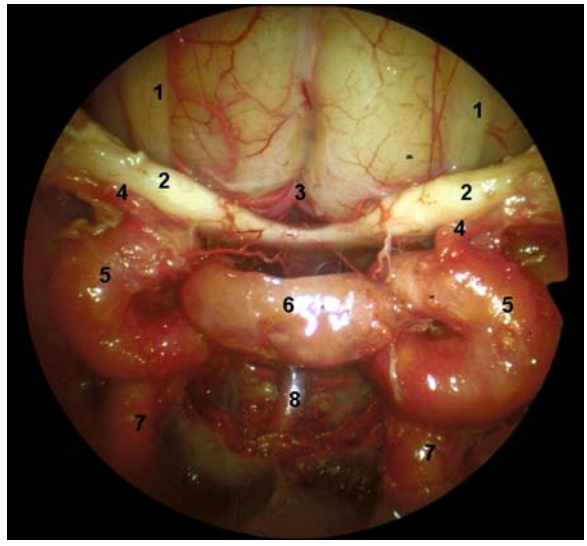

Fig. 5. Transsphenoidal approach (0° optic). *1* cn I, *2* cn II, *3* ACA-ACoA complex, *4* Ophth A, *5* intracavernous ICA, *6* pituitary gland, *7* intrapetrous ICA, *8* BA

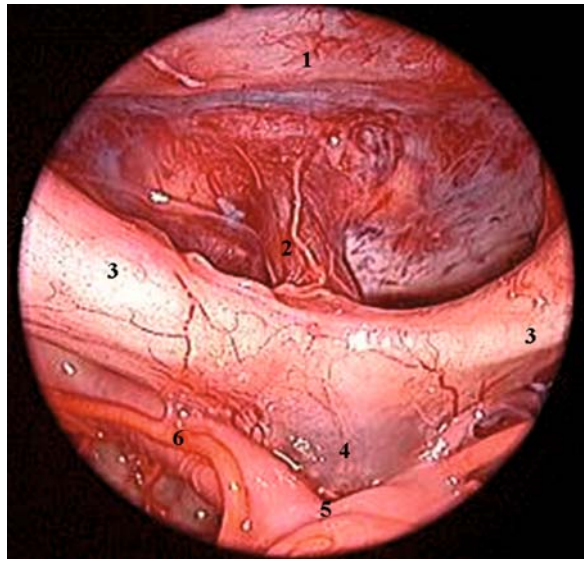

Fig. 6. Right supraorbital approach (0° optic). *1* Planum sphenoidale, *2* pituitary stalk, *3* cn II, *4* lamina terminalis, *5* ACoA, *6* Heubner artery

Retrosigmoidal approach

As with all other approaches, the craniotomy must be placed at the appropriate site and the jugular tubercle (which may hide a superior jugular bulb) should not be too prominent.

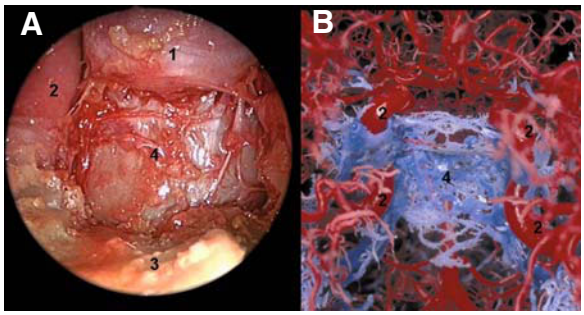

Fig. 7. Transsphenoidal approach (0° optic). **A** After removing the clivus the periostal layer is seen: *1* pituitary gland, *2* ICA, *3* remnant of clivus, *4* periosteal layer. **B** Corrosion cast (Technovit®) *2* ICA, *4* dense venous plexus between periosteal layer and dura mater

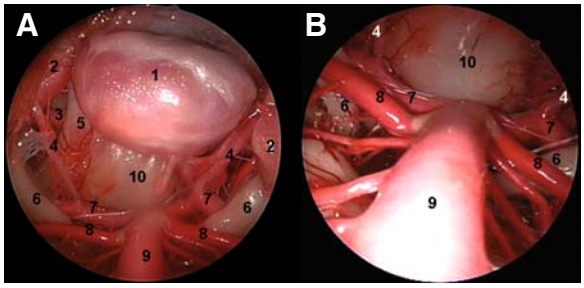

Fig. 8. Transsphenoidal approach. **A** 30° optic, **B** 45° optic. *1* Pituitary gland, *2* ICA, *3* A1, *4* PCoA, *5* optic tract, *6* cn III, *7* PCA, *8* SCA, *9* BA, *10* infundibulum

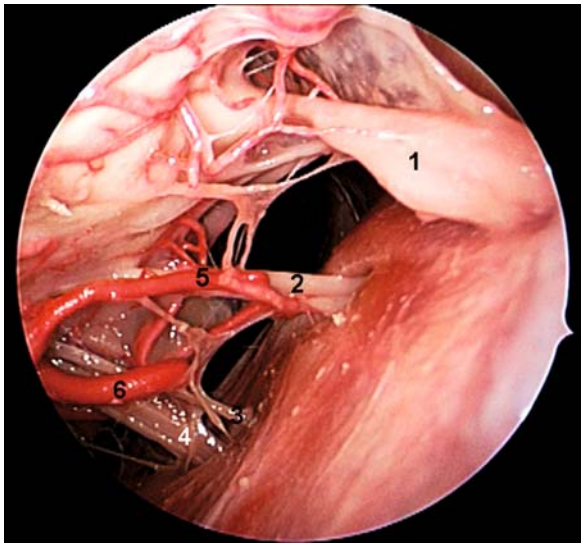

Fig. 9. Right retrosigmoid approach (0° optic). *1* cn V, *2* cn VII–VIII, *3* cn IX, *4* cn X, *5* AICA, *6* PICA

The retrosigmoid approach provides two routes for the endoscope: (1) Along the posterior surface of the petrous pyramid from the jugular foramen, passing the internal auditory meatus to the entrance into Meckel's space, and beyond it, deep to the tentorium into the ambient cistern, exposing its structures (Fig. 10) and (2) with an angled endo-

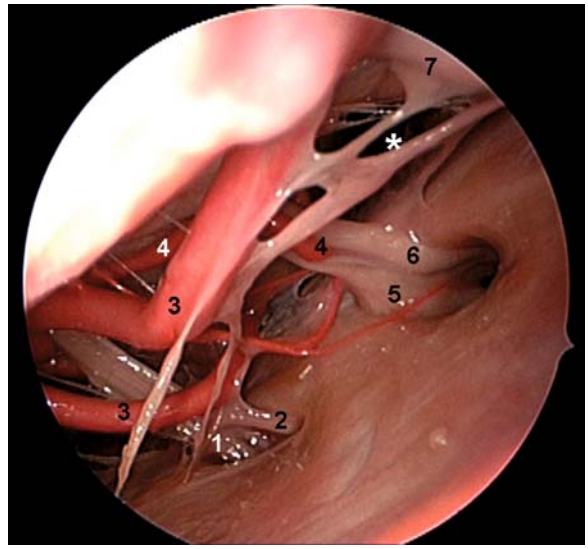

Fig. 10. Right retrosigmoid approach (0° optic). *1* cn X, *2* cn IX, *3* PICA, *4* AICA, *5* inferior vestibular nerve, *6* superior vestibular nerve, *7* cn V. * ambient cistern in the depth

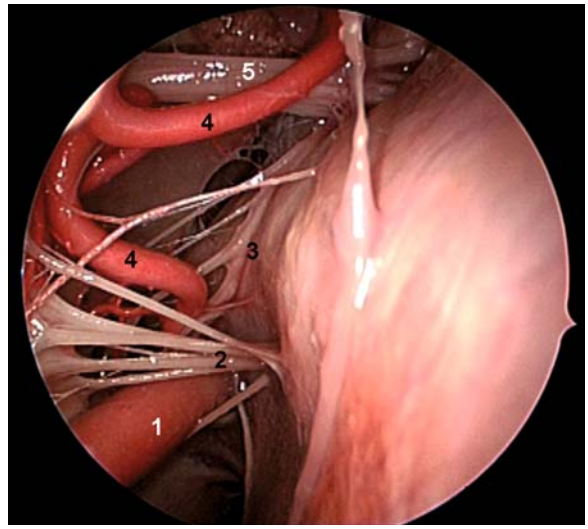

Fig. 11. Right retrosigmoid approach (0° optic). *1* Right VA, *2* cn XII, *3* cn XI, *4* PICA, *5*cn X-IX

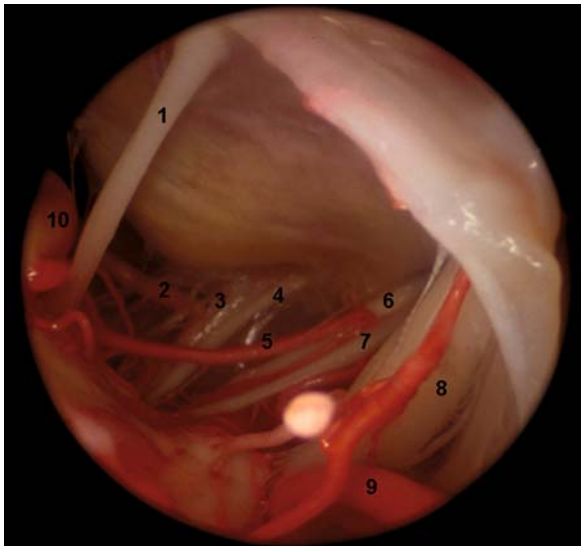

Fig. 12. Right supraorbital approach (0° optic). Window between cn II and cn III: *1* cn VI, *2* PICA, *3* cn X, *4* cn IX, *5* AICA, *6* superior vestibular nerve, *7* inferior vestibular nerve, *8* cn V, *9* SCA, *10* basilar artery

scope, advanced medially, exposing the entire brainstem as far as the infundibulum.

The roots of the 12th cranial nerve may exit via up to three separate dural passages, before leaving the cranium altogether through the hypoglossal canal (Fig. 11). The posterior triad is characterized by the spinal root of the 11th cranial nerve plus the transverse jugular ligament (Hayek's bridge) between the 9th and 10th cranial nerves. The anterior triad is quite distinct at the site of the 9th and 10th cranial nerves exiting the brainstem. While the 8th cranial nerve takes its origin from a rectangular area, the 7th cranial nerve emerges from a conical area and forms three distinct bundles. The extradural intracranial course of the 6th nerve is the longest of all cranial nerves (Fig. 12). Coursing over the clivus, is it crossed by the AICA. The 5th cranial nerve is easily distinguished from the anterior triad because it consists of a number of densely packed bundles. A look upward beneath the tentorial ridge provides a view the 4th cranial nerve. The 3rd cranial nerve is seen in its typical position between the superior cerebellar and posterior cerebral arteries, lying parallel to the posterior communicating artery.

Abbreviations

A1	first segment of the anterior cerebral artery
ACA	anterior cerebral artery
ACoA	anterior communicating artery
AICA	anterior inferior cerebellar artery
BA	basilar artery
ICA	internal carotid artery
M1	first segment of the middle cerebral artery
OphthA	ophthalmic artery
P1	first segment of posterior cerebral artery
PCA	posterior cerebral artery
PCoA	posterior communicating artery
PICA	posterior inferior cerebellar artery
SCA	superior cerebellar artery
VA	vertebral artery
cn	cranial nerve

References

1. Alfieri A, Jho HD, Tschabitscher M (2002) Endoscopic endonasal approach to the ventral cranio-cervical junction: anatomical study. Acta Neurochir (Wien) 144: 219–225
2. Cappabianca P, Cavallo LM, Esposito F, de-Divitiis E, Tschabitscher M (2002) Endoscopic examination of the cerebellar pontine angle. Clin Neurol Neurosurg 104: 387–391
3. Cavallo LM, Messina A, Cappabianca P, Esposito F, de-Divitiis E, Gardner P Tschabitscher M (2005) Endoscopic endonasal surgery of the midline skull base: anatomical study and clinical considerations Neurosurg Focus 19: E2 1–14
4. Perneczky A, Tschabitscher M, Resch KDM (1993) Endoscopic anatomy for neurosurgery. Thieme, Stuttgart
5. Perneczky A, Müller-Forell W, van Lindert E, Fries G (1999) Keyhole concept in neurosurgery. Thieme, Stuttgart
6. Terminologia Anatomica (1998) International Anatomical Terminology. Federative Committee on Anatomical Terminology (FCAT). Thieme, Stuttgart
7. Tschabitscher M, Galzio RJ (2003) Endoscopic anatomy along the transnasal approach to the pituitary gland and the surrounding structures. In: de Divitiis E, Cappabianca P (eds) Endoscopic endonasal transsphenoidal surgery. Springer, Wien New York

Chapter 2. Surgical approaches to the central skull base

Evolution from the classical pterional to the contemporary approach to the central skull base

V. V. Dolenc, R. Pregelj, I. Kocijančič

International Institute for Neurosurgery and Neuroresearch (IINN), Ljubljana, Slovenia

Introduction

Pioneer surgery of vascular lesions in the cavernous sinus (CS), carried out by Parkinson, marks the beginning of a direct surgical approach to the region [22–26]. Extracorporeal circulation, which was required in order to be able to conduct such surgery, represented a technical difficulty, and this made the direct approach unpopular at the time. Technical innovations in neuroradiology, which introduced endovascular techniques into the area, had practically brought the direct surgical approach to a standstill [1–4, 19, 20, 27, 33].

Of extreme importance for the direct surgical approach to the CS was the idea of temporary segmental exclusion of the circulation through the ICA at the central skull base (CSB), initiated on the basis of previous anatomical studies of the ICA in the petrous canal [18]. This meant that a direct neurosurgical approach to the region was also feasible without extracorporeal circulation, thus leading to a new era in the CSB [5, 7]. It is clear that preoperative cross-circulation studies are mandatory in each case when a temporary or permanent occlusion of the ICA is attempted.

There are very few topics in neurosurgery, if any, which have been discussed so much as the pathologies in the CS have been over the past 20 years. The early anatomical studies by Taptas first threw light on the CS region [28–31]. Parkinson's initial direct surgical approach to the CS was like the opening of a Pandora's Box, and caused much controversy over the CS surgery [21–26]. However, the controversy – which still exists about the direct surgical approach to the region – has had a positive impact, i.e. numerous microanatomical studies made of the CS, detailed control over neurosurgical procedures, and objective comparison of neuroradiological vs. neurosurgical end results [7, 17, 32]. Finally, the controversy surrounding CS surgery has led to well coordinated teamwork.

Positioning of the patient and craniotomy

The patient is positioned supine, and his/her head is fixed in a tripoint headrest with a 30 to 35° rotation to the opposite side of the lesion – the junction point of the orbital rim and the upper leg of the zygoma being the highest point of the head's initial position. During the course of the surgical procedure, the operating table is tilted from its initial position to the Trendelenburg position and to the reverse Trendelenburg's position, and also rotated to the left and/or to the right side. The position of the head is changed through the use of a combination of different degrees of tilting and rotating of the operating table in all four directions, so that "the target area" – in the CSB – is put into the microscope's central beam alignment. It is evident that changing the position of the operative microscope compensates for any extensive changes of the position of the operating table.

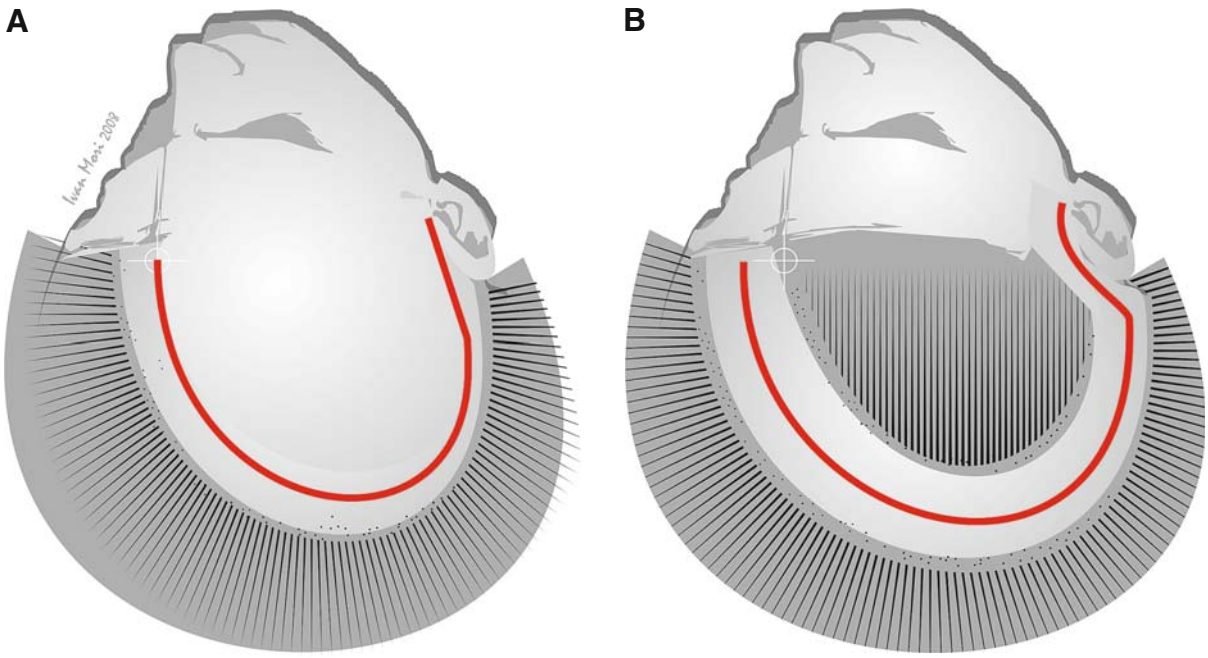

Fig. 1. **A** The initial position of the patient is as for the pterional approach. The anterior quadrant of the head is shaved and the skin incision is coursing from the ear to the midline behind the hairline with the concavity facing anteriorly. **B** In the contemporary approach, skin incision starts approximately 2 cm over the midline, behind the hairline and runs posteriorly over the frontal and parietal region toward the tragus of the ear. In contrast to the initial preparation, now, the head is shaved but only in a 2-cm wide strip. The most important change is the enlargement of the skin incision by beginning the incision over the midline behind the hairline and by turning the incision from front of the ear, around the ear posteriorly. These changes have been introduced in order to explore a larger part of the temporalis muscle

Once the patient's head has been positioned and fixed, a 2-cm wide strip is shaved from the ear, ipsilateral to the lesion in a curvilinear fashion to the midline and slightly beyond it, behind the hairline (Fig. 1B). The shaved area of the skin is then prepped and draped.

The skin incision is made from in front of the tragus of the ear, coursing firstly in an upward direction and then posteriorly around the ear and then to the midline and approximately 2 cm beyond it (Fig. 1B). It should – whenever possible – run behind the front line of the hair. The skin flap is reflected anteriorly over the ipsilateral eye. The periosteum is cut in a curvilinear fashion from the pterion – with the incision running peripheral to and around the insertion line of the temporalis muscle, so that it crosses the coronary suture line – into the parietal bone region. The temporalis muscle is cut in its posterior portion in a radial direction toward the squama of the temporal bone region, and is fixed with stay sutures to the fascia covering the temporalis muscle (Fig. 2B). Only in elderly patients is the temporalis muscle stripped from the junction of the upper leg of the zygoma and the orbital rim in order to expose the pterion (Fig. 2A). The first burr hole is made into the parietal bone approximately 2 cm behind the coronal suture line, and the second into the frontal bone (Fig. 2A and B). In elderly patients, two more burr holes at the pterion and in the squama of the temporal bone are made (Fig. 2A). Drilling of the bone at the pterion involves the use of a diamond drill in order to avoid damage to the dura over the frontal and/or temporal lobes and the periorbita. The bone is then cut from the burr hole in the parietal bone in an anterior direction across the burr hole in the frontal bone, involving the basal area of the frontal bone as far as the pterion. Next, part of the parietal bone and squama of the temporal bone are cut in basal direction and slightly anteriorly (Fig. 2A and B). On each side of the bone cut, corresponding holes are made into the bone to ensure appropriate fixation of the bone flap at the end of surgery and

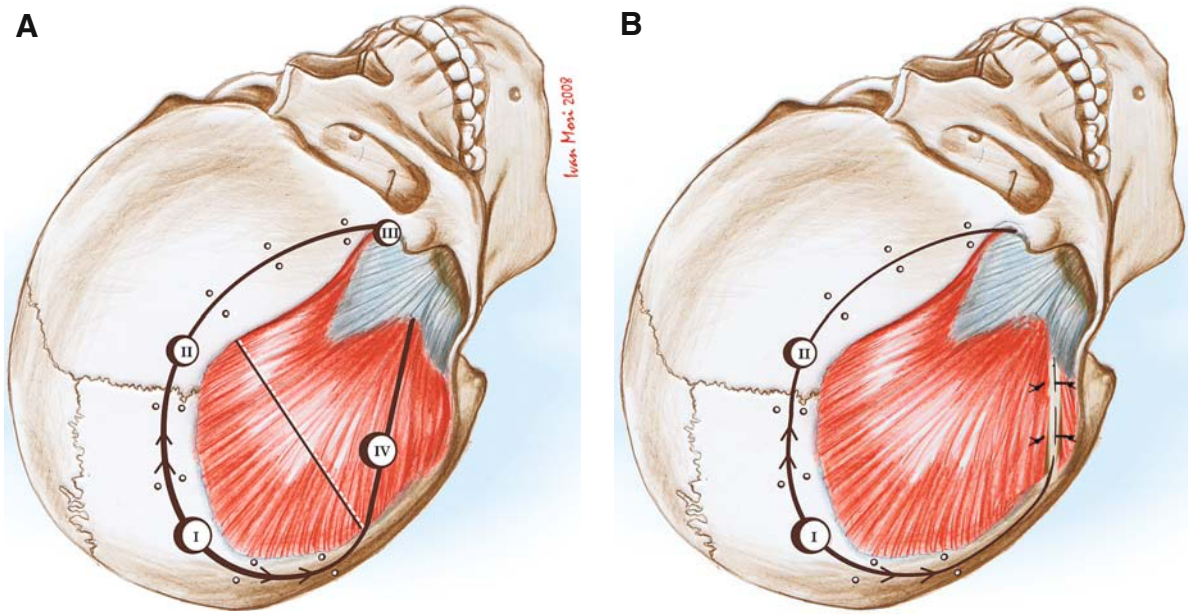

Fig. 2. **A** The old design of the bone flap is shown. In most cases, a burr hole was also performed at the pterion so that the frontal and temporal fossa as well as the orbit were opened at the same time. The fourth burr hole was close to the squama of the temporal bone underneath the temporalis muscle. The temporalis muscle was cut transversal to the direction of muscle fibers, so that the insertion of the temporalis muscle was left on the bone flap and the central part of the muscle was peeled away from the bone flap and fixed with fish-hooks laterally. **B** Currently only two burr holes – posteriorly and anterirorly – to the coronal suture line are made peripherally to the temporalis muscle. The temporalis muscle is cut (divided) in its posterior portion along the muscle fibres. Burr holes at the pterion and at the squama of temporal bone are placed only occasionally. Bone cut is commenced from the burr hole posterior to the coronal suture, and runs anteriorly from the parietal bone over the frontal bone toward the pterion. The bone cut posteriorly runs peripheral to and around the temporalis muscle, and then caudal to the squama of the temporal bone. The squama of the temporal bone is then broken and the base of the squama of the temporal bone is trimmed additionally, so that the fish hooks might be placed accordingly

adequate tension of the temporalis muscle (Fig. 2B). The osteo-muscular flap is lifted as a single flap, so that the squama of the temporal bone is broken. The temporalis muscle is additionally carefully stripped from the base of the squama of the temporal bone in order to preserve the vasculature of the temporalis muscle, which serves as a vascular pedicle to the bone flap (Fig. 3B). In turn, the bone flap, attached to the temporalis muscle, guarantees for the "anatomic" repositioning of the temporalis muscle at the end of surgery. The temporal bone is further nipped in a downward direction toward the base of the middle cranial fossa. The dura is fixed with stay sutures to the edges of the frontal and parietal bones in order to prevent epidural oozing during surgery and epidural hematoma postoperatively (Fig. 3B). Next, the dura is peeled from the bone of the middle cranial fossa, whereby the foramen rotundum (FR with V_2), the foramen ovale (FO with V_3), and the foramen spinosum (FS with MMA) are visualized (Fig. 4A and B).

Unroofing of the orbit

The roof of the orbit is opened by using the diamond drill. Only in this way is damage to the periorbita avoided. The periorbita is separated from the orbital surface of the orbital roof with a dissector, and the dura is separated from the orbital roof on the intracranial side, so that the orbital roof is seen from both sides – orbital and intracranial – and can be resected. The orbital branch of the middle MMA is visualized, coagulated and cut. The dura over the pole of the temporal lobe is dissected from the orbital roof on the posterior aspect of the superior orbital fissure (SOF), and the periorbita is further dissected

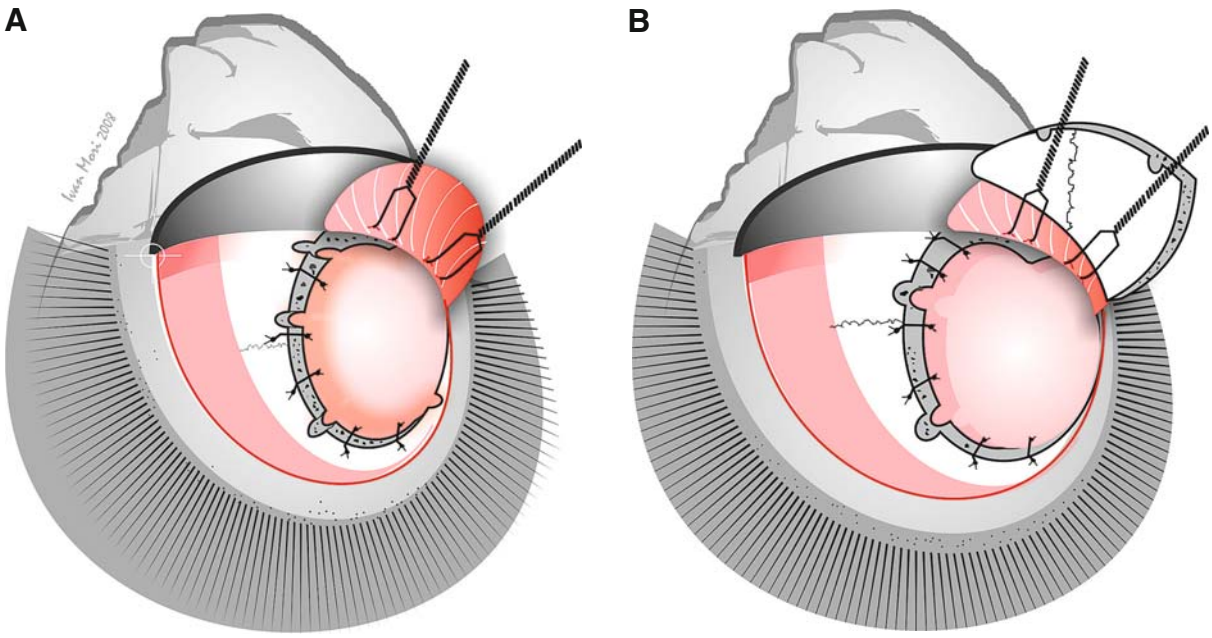

Fig. 3. **A** The bone flap with the peripheral part of the temporalis muscle insertion is removed for the time of surgery. The central part of the temporalis muscle is fixed laterally with fish hooks. **B** The bone flap and the temporalis muscle are not separated. The insertion of the temporalis muscle to the temporal bone is preserved intact and does provide good vascularization of the bone via muscular vascularization after surgery. From the other side, putting the peripheral part of the bone flap back into the bed and properly fixing it at the end of surgery, does provide normal tension of the temporalis muscle and hence causes no atrophy of the temporalis muscle postoperatively

from the intraorbital surface of the orbital roof, which is then removed, so that the dorsal aspect of the SOF is entirely exposed (Fig. 4A and B). More laterally and basally, i.e. on the medial aspect of the FR, the bone becomes thicker and cannot be nipped with a rongeur but should be carefully drilled with the diamond drill in order to avoid entering the bony sinus. Following the unroofing of the orbit dorsolateral to the SOF, the orbital roof is further removed by drilling in the antero-medial aspect to the SOF. Care

Fig. 4. **A** The situation following the removal of the bone flap in the old approach to the cavernous sinus is shown. The optic nerve (ON), anterior loop (AL) of the ICA in the antero-medial triangle is visualized, the duplicature of the dura coursing from the dura of the anterior-medial side of the temporal lobe through the superior orbital fissure (SOF) is preserved intact. The foramen rotundum (FR) with V_2 in front of it, and foramen ovale (FO) with V_3, are shown. Foramen spinosum (FS) and proximal stump of the middle meningeal artery (MMA) in it, and posterior loop (PL) of the ICA in the petrous bone are shown. The dotted line shows the directions of the dural incision: first along the sylvian fissure, and then in anterior direction over the ON and the other arm coursing in posterior direction behind the SOF laterally, and then over the lateral borders of the dura at the base of the middle cranial fossa over V_2 and V_3, and posteriorly to the petrous bone. After cutting of the dura, the brain (temporal lobe) is retracted and lateral wall of the CS covered with the dura is visualized. **B** This figure shows almost identical exposure of the ON, ICA, AL, peripheral end of V_2 in front of FR, and V_3 in front of FO, as well as FS with MMA as seen in **A**. However, in this figure the duplicature of the dura running over from the temporal lobe through the SOF to the orbit is cut, and cranial nerves (CNs) III, IV, and V_1 are visualized by peeling the dura on the under aspect of the temporal lobe away from the lateral wall of the CS. With this manoeuvre, CNs III, IV, V_1, and V_2 in the lateral wall of the CS are visualized as well as V_3 and GG further postero-medially from the epidural side. The dura is intermittently pulled and lifted by stay sutures while dissecting from the underlying structures of the lateral wall of the CS. No tension is placed on the brain, since the brain is protected by the dura and gentle pulling of it in upward and medial-ward direction

should be taken not to enter the frontal sinus (in cases where it is larger than normal), and not to remove the orbital roof in a downward direction toward the peripheral end of the optic canal without in advance carefully inspecting the bone on either side: intracranially and intraorbitally. Only in this manner can damage to the optic nerve (ON) be avoided.

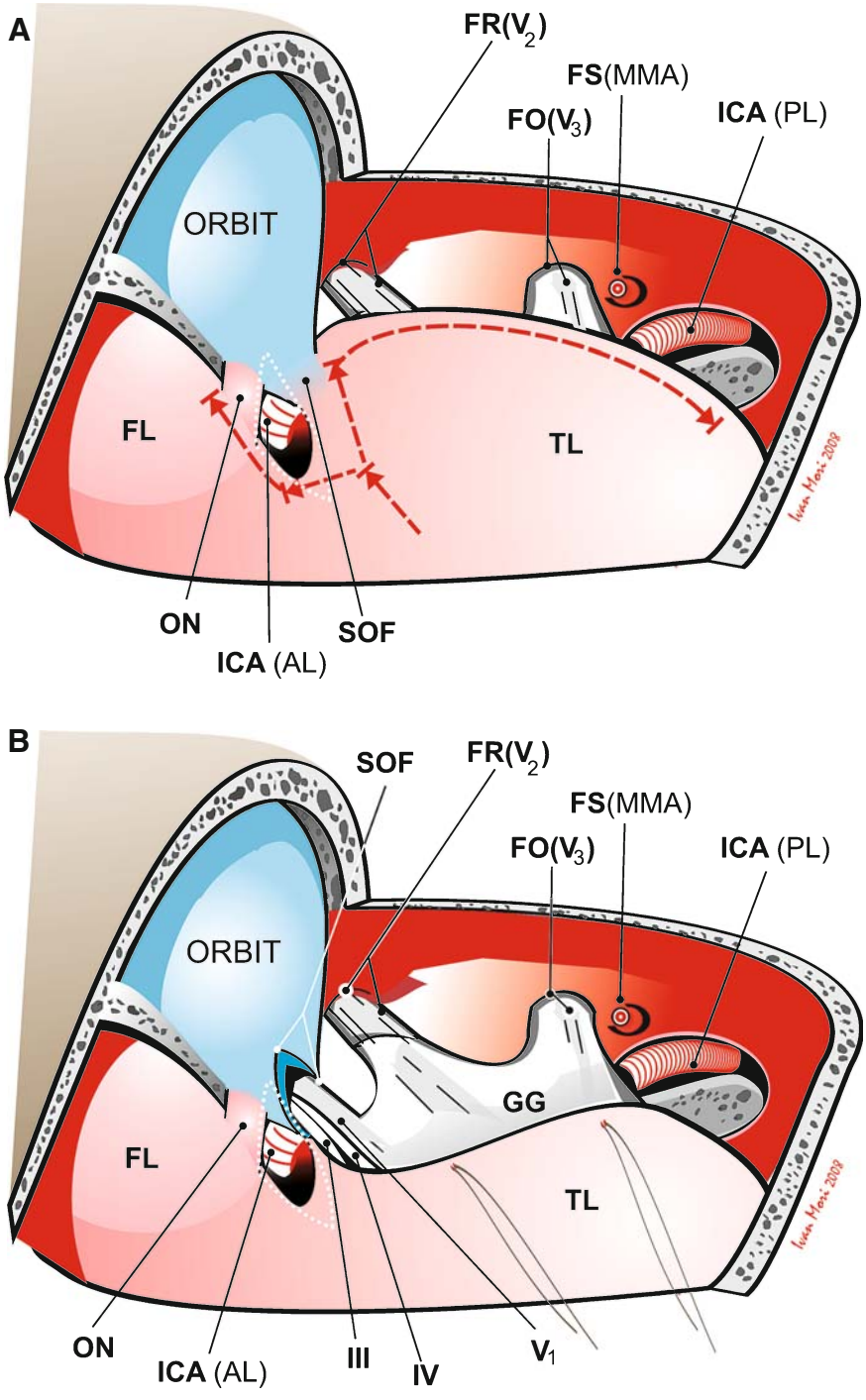

Resection of the sphenoid wing and the dural duplicature

The duplicature of the dura in the SOF, extending from the middle cranial fossa to the orbit, should be separated very gently from the sphenoid wing. After being removed from the bone anteriorly and posteriorly, it is cut with curved microscissors pointing in a posterior direction in order to avoid damage to CNs (III, IV, and V_1). When the dura has been separated from the posterior aspect of the sphenoid wing, the sphenoid wing can be resected. The cleavage line between the two layers of the lateral wall of the CS is entered, and separation of the outer layer from the inner layer and from CNs III, IV, V_1, and V_2 is thus made possible (Fig. 4B). Care should be taken to ensure that these CNs are not damaged during the procedure.

Resection of the anterior clinoid process, opening of the optic canal and the optic strut

Following the removal of the sphenoid wing, the dura on the inferolateral side of the anterior clinoid process (ACP) is gently dissected from the ACP with a microdissector. The ACP is drilled with a diamond drill from its inferolateral surface medialward, thus removing the bulk of the ACP. The drilling of the midportion of the ACP is safe providing that it proceeds in short bursts of drilling and under constant irrigation of the tip of the drill with saline. When the ACP is divided from the optic strut and from the lateral wall of the optic canal, it can be mobilized by microdissection circumferentially from the surrounding dura and thereafter removed without traction. Occasionally, the tip of the ACP is connected with the wall of the sphenoid sinus, consequently forming a canal for the ICA. Removal of the ACP by force may result either in entering the sphenoid sinus, and/or damaging the ICA and/or CNs III and IV. For that reason, removal of the final part of the ACP should be conducted with utmost care (by drilling, but under no condition by pulling). In some cases, the very tip of the ACP, in the under aspect of the ICA, is sharp as a blade and by pulling it the ICA can easily be cut.

Drilling of the ACP from the lateral wall of the optic canal should be performed with great care in order to avoid damage to the ON mechanically and/or by heat. Drilling with short intervals and providing constant irrigation of the tip of the diamond drill are prerequisites for preserving the ON undamaged, not only morphologically but also functionally. When the ACP has been completely removed, the ICA – coursing under the membrane on the floor of the antero-medial triangle – is exposed in its entire length from the lateral to the medial border of the triangle that is from the proximal ring (PR) to the distal ring (DR). If the ICA cannot be appropriately visualized at this stage, additional drilling toward the anterior corner of the antero-medial triangle is necessary so that the membrane overlying the anterior loop of the ICA is visualized entirely, and the ICA can then be dissected from the wall of the sphenoid sinus, with care being taken not to enter the bony sinus and/or CS.

The dura is additionally separated from the bone of the tuberculum sellae in a medialward direction, i.e. medial to the optic canal, in order to keep the dura wall away from the drill and thus protect it from damage while drilling is performed on the proximal and lateral walls of the optic canal. Care should be taken not to drill too far medially at the region where the sphenoid sinus may be entered (again). While the proximal wall of the optic canal is being drilled, it is important that the tip of the diamond drill be constantly irrigated, the drilling frequently interrupted, and the drilling periods should be brief in order to avoid overheating of the drill. The bone, covering the optic canal, should be removed more by "rubbing" than by drilling it away from the ON with a new (sharp) diamond drill. In this way, the bone is thinned and finally made transparent, so that it is much less likely that the ON might be mechanically damaged. The paper-thin, transparent bone can then be removed with a microdissector. The proximal wall of the optic canal should be drilled medialward so far that the canal is completely opened in its whole length and width. Once the optic canal has been opened, both on the superior and lateral aspects, the ON in the canal, covered by the dura propria, can be mobilized and slightly lifted upward so that the optic strut is better visualized and additionally resected when necessary. To conduct the final resection (drilling) of the optic strut, the operating table should be rotated to the opposite side of the lesion and the microscope accordingly adjusted closer to the temporal side and directed from the lateral side in a medial direction toward the under aspect of the ON. While drilling the optic strut, the smallest diamond

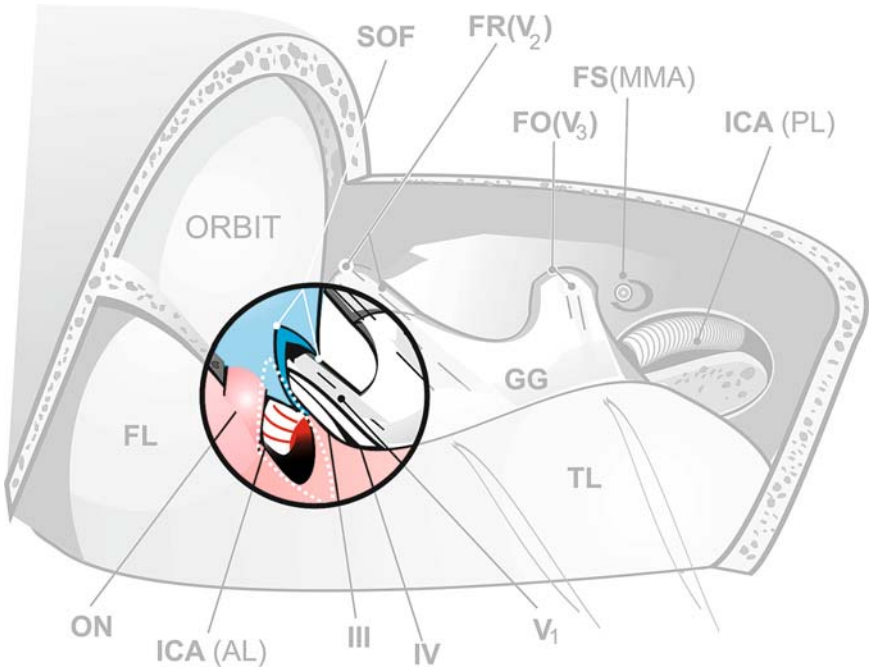

Fig. 5. The final situation of the current general epidural approach to the central skull base from the right side is shown. The encircled area indicates the region where the anterior corridor through the antero-medial triangle is possible. The antero-medial triangle is limited between the ON medially, CNs III, IV, and V_1 laterally and the dura posteriorly. Through this entry point, it is possible to eradicate intrasellar as well as medial parasellar tumors. With a dural cut along the Sylvian fissure, the access to the posterior clinoid process (PCP) is easy and in addition, this bony structure can be removed and then the access to the upper clival region as well as to the basilar tip of the basilar artery is made possible without endangering the neighboring neural and vascular structures. The approach to the intradural segment of the ICA is ideal from this side – in cases of L/G ICA aneurysms – since the proximal control of the flow through the ICA is possible

drill should be used and the drilling commenced from the side of the ICA toward the ON. It is essential that the drilling be carried out in very short bursts and not at high speed, and the tip of the drill constantly irrigated. Care should be taken not to damage the periosteum and fascia overlying the ICA, or the DR, or the dura propria of the ON, and – equally important – not to damage the wall of the sphenoid sinus, which would inevitably lead to CSF leak after surgery. The optic strut should be removed in its entirety in dealing with lesions in the sella and/or in the area of the ACP and/or posterior clinoid process (PCP). Complete removal of the optic strut enables mobilization of the distal half of the anterior loop of the ICA, which is extremely important in surgery for carotid-ophthalmic aneurysms. After complete removal of the ACP, of the lateral and superior walls of the optic canal, and of the optic strut, the antero-medial triangle is exposed in its entirety and so is the distal segment of the anterior loop of the extradural ICA (Fig. 5).

Dissection of the outer layer of the lateral wall of the CS and exposure of CNs III–V

Complete separation of the two layers of the lateral wall of the CS necessitates fixation of the outer (dural) layer with stay sutures. The initial stay suture is placed in the dura on the medial side of the pole of the temporal lobe where the dural duplicature, coursing toward the orbit, has been transsected. The stay sutures enable "dynamic" traction of the dura, by which the brain is better protected than by continuous retraction with spatulas. Using upward traction with stay sutures, the outer layer of the lateral wall of the CS can be separated from the underlying inner layer of the lateral wall of the CS

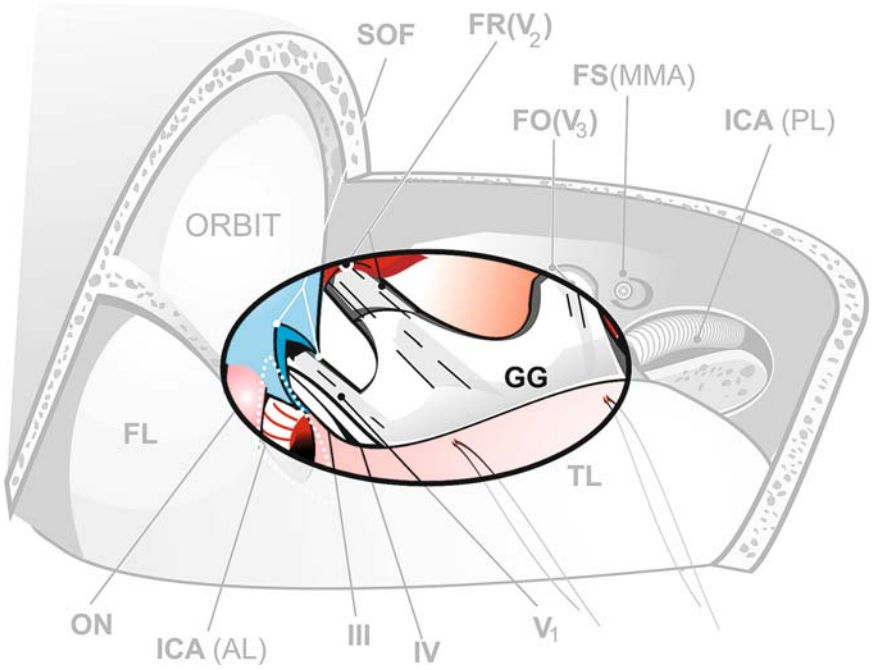

Fig. 6. After completion of the general epidural approach to the central skull base, the encircled area shows the region which is accessible via extradural approach to the tumorous and vascular lesion in the right CS. All the triangles: antero-medial, paramedial, Parkinson's, antero-lateral, lateral, and also postero-lateral are exposed, and through all these windows the tumorous and vascular lesions from the parasellar space (CS) might be eradicated without opening the dura. In addition, the posterior and anterior loops of the ICA – convenient for clipping and/or anastomosing – are well exposed. Following placing of proximal and distal clips, dissection of the tumorous and/or vascular lesions in the whole parasellar space is possible without confronting a significant bleeding. Any lesion confined to the parasellar space can be eradicated through this approach

and CNs III–V (Fig. 6). The dural outer layer should be cut along the lateral border of the CS over V_2 and further in posterior direction over V_3, in order that as little pressure as possible be exerted on the under surface of the temporal lobe while the dura is being pulled. The table should be rotated in the opposite direction from the pathology. In this way, the cleavage line is better visualized and the two layers of the lateral wall of the CS are more easily separated, with less traction over the outer layer of the CS wall. A rather large vein usually traverses the outer layer of the lateral wall of the CS into the space between the two layers of the lateral wall of the CS, and enters the CS at the point medial to the V_2 and lateral to V_1, i.e. through the antero-lateral triangle [7]. This vein should be cut at its entry point into the CS and plugged with Surgicel, whereas the vein in the dura of the temporal lobe should be coagulated. The dural and thin inner layers of the lateral wall of the CS are separated entirely. In this way, CNs III–V, and the antero-lateral border of the Gasserian ganglion (GG), are visualized (Fig. 6). Further exposure of the GG is obtained by dissecting the dura from the GG in a posterior and medial direction so that eventually only the arachnoidal layer still covers the plexiform segment of the root of CN V and the root of nerve V proper. Visualization of the plexiform portion of the root of CN V is only possible after transsection of the middle meningeal artery (MMA) in front of the foramen spinosum (FS). The proximal stump of the MMA is coagulated and packed into the FS, which should be plugged with Surgicel and bone wax. By dissection of the dura from the anterior surface of the petrous bone, and cutting the dura along the posterior aspect of the GG toward the apex of the pyramid, care should be taken not to damage the greater petrosal nerve (GPN) or the genticulate ganglion of the facial nerve while the dura is being separated from the anterior side of the petrous bone.

Exposure of the intrapetrous ICA

After transsection of the MMA, dissection of the dura from the anterior surface of the pyramid, exposure of the GPN and separation of the dura from the dorsal aspect of V_3 and Meckel's cave, drilling can be commenced on the roof of the petrous carotid canal. Drilling of the wall of the petrous carotid canal is conducted with a medium size diamond drill, and is started at a distance of 5–8 mm antero-medially to the FS, on the posterior aspect of V_3 and the GG, direction of drilling being from the postero-lateral to the antero-medial side. If drilling is started too laterally and the tensor tympani muscle is encountered first, it should be continued medialward in order not to open the Eustachian tube. When the medial aspect of the ICA is sufficiently exposed, the bone needs to be additionally drilled underneath V_3 along the ICA to allow better exposure of the horizontal portion of the ICA between the posterior and the lateral loops. It is important not to drill too far posteriorly – around the posterior loop of the ICA – as there is a risk of entering of the middle and/or the inner ear. When the ICA in the petrous canal has been exposed supero-laterally to 1/3 of its circumference, it should be dissected from the walls of the canal around its entire circumference. Use of a microdissector is essential in peeling the periosteum away from the bone in order not to damage the ICA wall proper. The segment of the ICA to be exposed should be 1 cm long. In the initial description of the exposure of the ICA in the petrous canal, exenteration of the Eustachian tube was suggested [18]. However, the present belief is that the Eustachian tube should be preserved intact at all costs, even in cases where the wall between the petrous carotid canal and the Eustachian tube canal has been incomplete or damaged by the surgeon.

Dissection of the periosteum from the walls of the petrous carotid canal circumferentially allows for temporary occlusion of the ICA with clip(s) or better with a balloon. Completeness of the occlusion of the ICA with clip(s) should be tested at this step of surgery. However, in cases where grafting of the ICA from the petrous portion to the infra- or supraclinoid portion is planned, the periosteum around the ICA should be dissected proximal to the unroofed segment of the canal, i.e. in the direction toward the tip of the posterior loop of the ICA, in order to provide sufficient space for insertion of a catheter with a

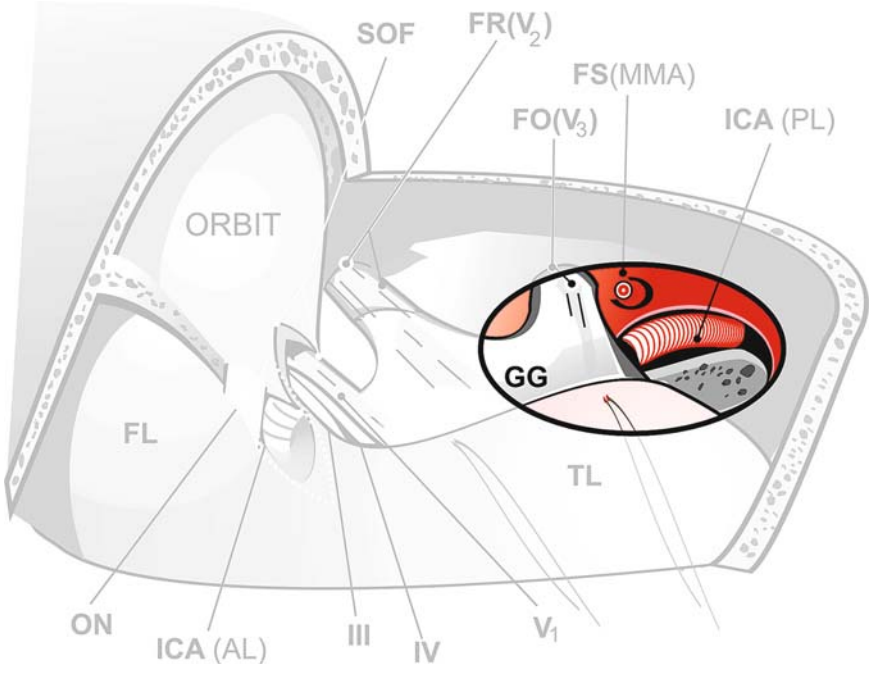

Fig. 7. The posterior – transpetrous approach (corridor) is used when the pathology is at the petro-clival region. The extent of the lesion may also necessitate additional use of the transcavernous and/or anterior corridors

balloon into the space between the bony wall and the ICA. Inflation of the balloon provides temporary occlusion of the ICA and reconstruction (grafting) will be easier because the proximal clip is not needed and the space gained is very useful while performing the end-to-end suture of the graft and the ICA.

Resection of the apex of the pyramid and unroofing of the inner auditory canal

Removal of the apex of the pyramid involves drilling the bone in an antero-medial direction from the exposed ICA in the petrous canal (Fig. 7). It is essential that the drilling be started in the immediate vicinity of the apex of the pyramid, i.e. from the postero-lateral to antero-medial direction, underneath the GG and the dura covering the floor of Meckel's cave, in order not to damage the dura of the inner auditory canal. Drilling the apex of the pyramid underneath Meckel's cave allows for exposure of the dura on the medial aspect of the apex of the pyramid – in the posterior cranial fossa – anterior to the entry into the inner auditory canal, and lateral to the entry into Dorello's space. When the apex of the pyramid has been transsected, the pyramid can be drilled in a posterior direction toward the superior petrous sinus, which at this stage should remain intact (Fig. 8A and B). Drilling of the bone toward the inner auditory canal should be performed in short bursts, and the drill should constantly be irrigated with saline in order to prevent damage to CNs VII and VIII by heat. When the dura propria of the inner auditory canal is exposed, the bone between the inner auditory canal and the superior petrous sinus is drilled off, so that the inner auditory canal is unroofed on the supero-lateral side (Fig. 8D). In addition, a similar area of the bone is drilled off on

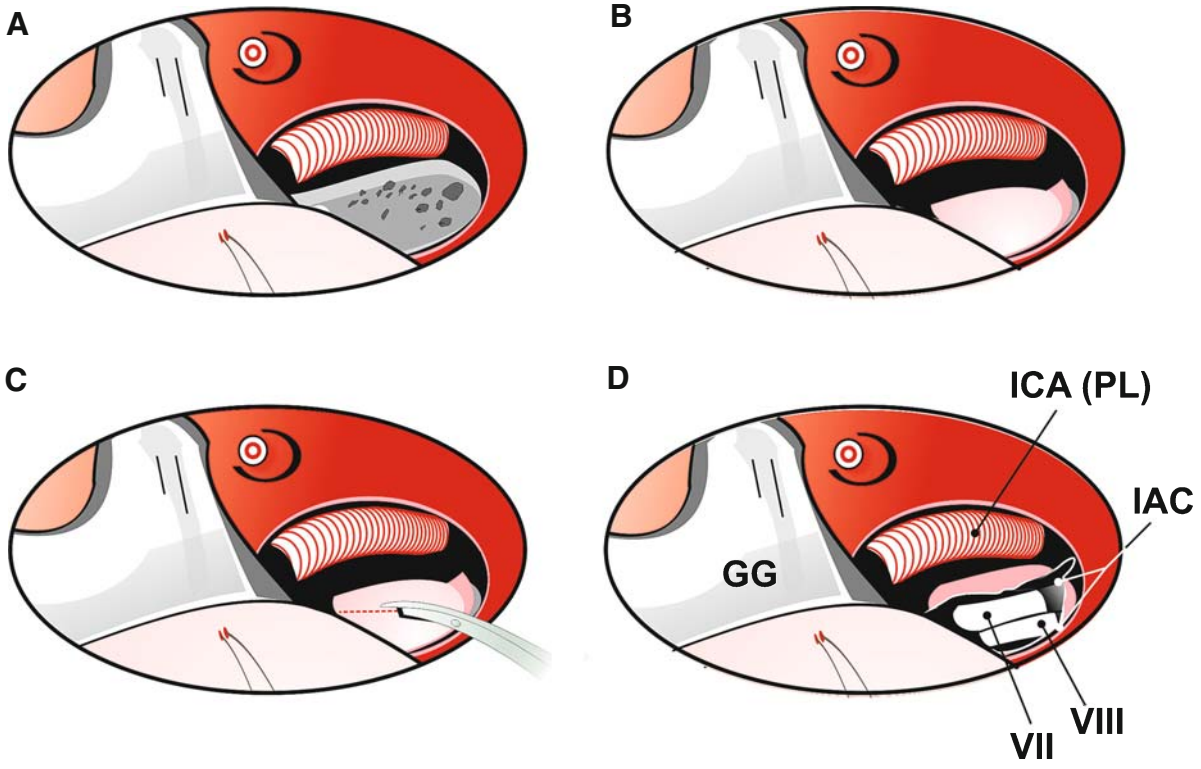

Fig. 8. (**A**–**D**) The posterior (transpetrous) corridor includes the exposure of the ICA in the segment of its PL, and then drilling of the apex of the pyramid behind Meckel's cave medially to the Gasserian ganglion and in front of the inner auditory canal. When the bone is resected and the dura in the medial aspect of the apex of the pyramid (that is in the posterior cranial fossa) is met, then this dura is cut and the posterior fossa is entered. After opening the dura of the posterior fossa, the root of CN V is anteriorly exposed, and posteriorly CNs VII and VIII in front of the inner auditory canal are visualized. Again, according to the extent of the lesion, this posterior transpetrous corridor might be enlarged accordingly

the infero-lateral aspect of the inner auditory canal, which will leave the bone of the inner auditory canal only on its postero-medial side. Careful dissection of the dura from the medial side of the apex of the pyramid and at the entry point of CN VI into Dorello's space will ensure the integrity of CN VI morphologically and functionally. Further resection of the clival bone between Dorello's space and the horizontal segment of the ICA coursing toward the lateral loop can endanger CN VI even more; this is why the periosteum should be preserved at all costs. In cases where the very apex of the pyramid cannot be drilled off and completely resected through this approach, i.e. from the postero-medial side of CN V, it is left in place and is removed later on when the dura on the antero-medial aspect of Meckel's cave has been transsected through Parkinson's triangle, and the root of CN V has been gently displaced posteriorly. By this manoeuvre, an ample space will be gained and the very apex of the pyramid will be entirely exposed and then easily removed. This exposure is very important for resection of the meningiomas at this location as well as for trigeminal neurinomas and aneurysms of the trunk of the basilar artery.

Changing of surgical approach to the CS during the last two decades

The initial position of the patient's head in surgery of the parasellar region has not been changed over the period of 20 years [5–17]. During the first 10 years of direct surgery in the CS, the anterior quadrant of the patient's head was shaved in all cases, whereas during the following 10 years it has been common practice for only a rather narrow strip of the head to be shaved (Fig. 1A and B). In earlier approaches, the skin incision was practised more anteriorly than it is currently (Fig. 1A). In the present approach, the skin incision begins from very close to the ear, so that it is not only posterior to the frontal branch of the facial nerve but also posterior to the auriculo-temporal nerve, the superficial temporal artery and the superficial temporal vein. It then runs more posteriorly around the ear and then in a semicircular line in upward direction ending 2 cm beyond the midline on the contralateral side (Fig. 1B). Since with this approach the skin flap is larger than it was in earlier operations, when it is reflected anteriorly, a larger part of the temporalis muscle is revealed than the area exposed by the previous skin flap. In order for the temporalis muscle to be preserved undamaged, the formerly used transverse cutting of the muscle close to its insertion to the bone is no longer practised (Fig. 2A). Instead, the muscle is cut in its posterior portion in the parallel direction of the muscle fibers so that the fibers are minimally damaged if at all (Fig. 2B). Only in elderly patients, anteriorly, the muscle is stripped from the pterion where simultaneous opening of the orbit, the middle cranial fossa, and the anterior cranial fossa is performed with a diamond drill (Fig. 2A). The osteomuscular flap is made as a single flap, so that the temporalis muscle is not detached from its insertion in the bone flap (Fig. 3B). The bone flap and the temporalis muscle remain vascularized and the temporalis muscle under normal tension when osteomuscular flap is placed back in its bed and fixed accordingly at the end of the operation. In this way, the muscle is normally functional immediately after surgery. At previous craniotomy, the temporalis muscle was transversally cut and could not be accordingly repaired at the end of surgery – which resulted in most cases with marked atrophy of the temporalis muscle and unpleasant cosmetic defect. Using new type of craniotomy – provided that the motor branch of the trigeminal nerve has also been preserved – there is no postoperative atrophy of the temporalis muscle. The extent to which the craniotomy is performed anteriorly has not been changed: the bone flap is cut close to the rim of the orbit (Fig. 2A and B). The initial unroofing of the orbit anterior and posterior to the SOF, and the resection of the temporal bone centralward, also do not differ from those previously practised, as seen in (Fig. 4A and B). The epidural exposure of the SOF on its posterior side, as well as the exposure of the FR, FO, and FS, is the same as described initially, and the same is also transsection of the MMA in front of the FS (Fig. 4A and B). However, further unroofing of the orbit anterior to the SOF, removal of the sphenoid wing, and unroofing of the optic canal – as well as removal of the ACP and the optic strut – have been largely modified, since the introduction of transsection of the dural duplicature covering the neural structures which course from the CS to the orbit. Separation of the two layers of the lateral wall of the CS is essential in order to have access to the ACP from its infero-lateral aspect, and to remove it with-

out injuring the surrounding structures (Fig. 4A and B). It is likewise essential to remove the optic strut, and the lateral and superior walls of the optic canal, so that no pressure is exerted on the dura toward the ICA and the ON intradurally, as used to occur with the initial version of the approach [5]. One of the main shortcomings of the previous approach was that it was difficult – due to the insufficient space – to resect the ACP without exerting pressure on the dura (Fig. 4A), and this was why many neurosurgeons had reservations about the resection of the ACP from the extradural side, especially in cases of carotid-ophthalmic aneurysms, as there was a probability of premature rupture of the aneurysm. By splitting the layers of the lateral wall of the CS, access to the ACP is made possible from the infero-lateral side, which is much safer because there is no pressure on the dura toward the aneurysm – this holds both for carotid-opthalmic aneurysm and for large and giant distal ICA aneurysms; and is even more important in those carotid-ophthalmic aneurysms which are on both sides of the dura.

Separation of the layers of the lateral wall of the CS is the most important improvement in the approach, since this allows for an entirely epidural approach (Fig. 4B). The initial approach (Fig. 4A) to the CS was in reality intradural [5, 7–11]. As a result of long-standing retraction of the temporal lobe with spatulas, the temporal lobe suffered a massive contusion and later on inevitable atrophy followed. Owing to the splitting of the lateral wall of the CS, the temporal lobe can be dynamically lifted together with the dura, a procedure which is much less traumatic for the temporal lobe. Consequently, there is no surgery-related atrophy of the temporal lobe, since the dura provides optimum protection for the brain.

Drilling the apex of the pyramid is carried out from the extradural side (Figs. 7 and 8), which is also less traumatic for the temporal lobe than performing it intradurally, which involves forceful retraction of the temporal lobe, and thus endangers the temporal lobe directly (locally) and if the vein of Labbe is torn, then a large area of the brain suffers. However, this does not happen anymore by using the extradural approach. Since the beginning of our practice, the unroofing the petrous carotid canal has always been practised in such a way that the tensor tympani muscle and the Eustachian tube are preserved intact, unlike Glasscock's initial suggestion of exenterating the Eustachian tube entirely [18]. Initially, the ICA in the petrous canal was exposed in the treatment of all tumorous lesions in the CS, all intracavernous ICA aneurysms, and even in cases of carotid-ophthalmic aneurysms. Following the new epidural approach to the CS, exposure of the ICA in the petrous carotid canal was not practised in most cases of trigeminal neurinomas, pituitary tumors extending into the CS, the carotid-ophthalmic aneurysms, small intracavernous ICA aneurysms, and in tumors inside the CS, unless the diameter of the ICA is reduced.

Owing to the epidural exposure of the CS, trigeminal neurinomas are now all treated exclusively through the epidural approach; only when a tumor of CN V extends into the posterior fossa is the dura opened (Fig. 8C and D) around the root of CN V behind the GG and anteriorly to CNs VII, VIII [12]. A similar approach is also used in juxta-sellar pituitary adenomas extending into the CS, as this approach provides a much better possibility for complete removal of the lateral extension of the tumor, and the tumor from the ipsilateral side of the floor of the sella (Fig. 6). The tumors which occupy only that part of the CS, regardless of their nature, are also treated through an exclusively epidural approach (Figs. 5–7). These are: meningiomas in Dorello's space and in the posterior part of the CS, as well as those located lateral and anterior to the medial loop and the horizontal segment of the intracavernous ICA. Almost all chordomas and certain chondrosarcomas can also be resected solely through the extradural approach to the CS, and then through the CS and further down and medially in the clivus.

Vascular lesions, dealt with through use of the extradural approach only, include small intracavernous ICA aneurysms, large intracavernous ICA aneurysms, all low-flow CCFs and most of the high-flow CCFs.

The presence of a meningioma, both intradurally and extradurally, and in the CS requires a combined extra- and intradural approach. The epidural approach, as described in this report, is practised in all such cases as well, and has a great advantage over the intradural approach in removing the intradural part of the meningioma. Thus, the intradural part of a meningioma is left completely devascularized, and resection of the dura infiltrated by the tumor and of the intradural extension of meningioma is made much easier. In each case of an intradural and intracavernous meningioma, two distinctive steps of tumor resection are currently being used: extradural and intradural.

The splitting of the lateral wall of the CS, after resection of the dura infiltrated by the tumor, in many cases ensures the retention of a useful portion of normal dura at the latero-basal border of the temporal lobe, which can then be unfolded and fixed to the dura around V_2, V_3, and to the dura on the posterior aspect of the SOF and/or to the periorbita. The dural closure at the end of surgery is notably better than it used to be in the initial intradural approach.

The epidural approach, as described here, either in its complete or partial form, can scarcely be avoided in surgery of intracavernous pathologies unless one is contemplating only a "biopsy" of an intracavernous tumor or trapping of an intracavernous ICA aneurysm and/or a CCF and the ICA itself, rather than resection of the lesion and reconstruction of the ICA (whenever necessary). In comparison with the initial approach [5, 7], this procedure is safer, easier to perform, carries fewer risks of perioperative complications, and ensures better end results in surgical treatment of tumorous and vascular lesions in CS. And much more, following the corridors: anterior transclinoidal (Fig. 5), lateral transcavernous (Fig. 6), and posterior transpetrous (Fig. 7), brings you into posterior fossa and gives you the chances to fix the basilar tip and basilar artery aneurysms as well as petro-clival tumors. In order to be able to practise this approach in live surgeries, one has to possess practical knowledge of the anatomy of the region, which can only be gained through repeated laboratory anatomical dissections.

References

1. Berenstein A, Ransohoff J, Kupersmith M, Flamm E, Graeb D (1984) Transvascular treatment of giant aneurysms of the cavernous carotid and vertebral arteries. Functional investigation and embolization. Surg Neurol 21: 3–12
2. Debrun G (1978) Detachable balloon and calibrated leak balloon technique in the treatment of cerebral vascular lesions. N Neurosurg 49: 635
3. Debrun G (1983) Treatment of traumatic carotid-cavernous fistula using detachable balloon catheters. Am J Neuroradiol 4: 355–365
4. Debrun GM (1987) Embolization techniques in the treatment of vascular lesions involving the cavernous sinus. In: Dolenc VV (ed) The cavernous sinus: a multidisciplinary approach to vascular and tumorous lesions. Springer, New York, pp 1973–1981
5. Dolenc VV (1983) Direct microsurgical repair of intracavernous vascular lesions. J Neurosurg 58: 824–831
6. Dolenc VV (1985) A combined epi- and subdural approach to carotid-ophthalmic artery aneurysm. J Neurosurg 62: 667
7. Dolenc VV (1989) Anatomy and surgery of the cavernous sinus. Springer, Wien New York
8. Dolenc VV (1990) Surgery of vascular lesions of the cavernous sinus. Clin Neurosurg 36: 236–240
9. Dolenc VV (1991) The necessity for intracavernous ICA reconstruction In: Sato K (ed) Neurosurgeons 10. Proceedings of the Japanese Congress of Neurological Surgeons, Tokyo, pp 299–307
10. Dolenc VV (1992) Cavernous sinus masses. In: Apuzzo MLJ (ed) Brain surgery, vol 1. Churchill Livingstone, New York, pp 601–614
11. Dolenc VV (1992) Surgery of tumors originating in or invading the cavernous sinus. In: Long DM (ed) Surgery of skull base tumors, vol 12. Blackwell, Boston, pp 211–221
12. Dolenc VV (1994) Frontotemporal epidural approach to trigeminal neurinomas. Acta Neurochir (Wien) 130: 55–56
13. Dolenc VV (1994) Intracavernous carotid artery aneurysms. In: Spetzler RF, Carter LP (eds) Neurovascular surgery. McGraw-Hill, New York, pp 659–673
14. Dolenc VV (1994) Carotid ophthalmic aneurysms. In: Spetzler RF, Carter LP (eds) Neurovascular surgery. McGraw-Hill, New York, pp 673–686
15. Dolenc VV, Valavanis A (1997) Cavernous carotid aneurysm: Direct vs. indirect approaches, In: Batjer HH (ed) Cerebrovascular disease. Lippincott-Raven Publishers, Philadelphia, pp 939–955
16. Dolenc VV (1997) Approaches to and techniques of surgery within the cavernous sinus. In: Torrens M, Al Mefty O, Kobayashi S (eds) Operative skull base surgery. Churchill Livingstone, New York, pp 207–236
17. Dolenc VV (2003) Microsurgical anatomy and surgery of the central skull base. Springer, Wien NewYork
18. Glasscock ME (1969) Exposure of the intra-petrous portion of the carotid artery. In: Hamberger CA, Wersaal J (eds) Disorders of the skull base region. Proceedings of the 10th Nobel Symposium. Almqvist and Wiksell, Stockholm, pp 135–143
19. Kupersmith MJ, Berenstein A (1984) Percutaneous transvascular treatment of giant carotid aneurysms. Neuro-ophthalmologic findings. Neurology 34: 328–335
20. Lasjaunias P, Berenstein A (1987) Aneurysms of the cavernous segment of the internal carotid artery. In: Lasjaunias P, Berenstein A, TerBrugge K, Willinsky RA (eds) Surgical Neuroangiography, vol 2. Endovascular treatment of craniofacial lesions. Springer, Berlin, pp 248–264
21. Parkinson D (1964) Collateral circulation of cavernous carotid artery: anatomy. Can J Surg 7: 251–268
22. Parkinson D (1965) A Surgical approach to the cavernous portion of the carotid artery. Anatomical studies and case report. J Neruosurg 23: 474–483
23. Parkinson D (1969) Transcavernous repair of carotid cavernous fistula. J Neurosurg 26: 420

24. Parkinson D (1973) Carotid cavernous fistula: direct repair with preservation of the carotid artery. Technical note. J Neurosurg 38: 99–106
25. Parkinson D (1987) Carotid cavernous fistula. History and anatomy. In: Dolenc VV (ed) The cavernous sinus: a multidisciplinary approach to vascular and tumorous lesions. Springer, New York, pp 3–29
26. Parkinson D (1988) Surgical management of internal carotid artery aneurysms within the cavernous sinus. In: Schmidek HH et al. (eds) Operative neurosurgical techniques. Indications, methods and results. Grune & Stratton, Orlando, FL, pp 837–844
27. Serbinenko F (1974) Wound catheterization and occlusion of major cerebral vessels. J Neurosurg 41: 125–145
28. Taptas JN (1949) La loge du sinus caverneux, sa constitution et les rapports des éléments qui la traversent. Paris Semin Hop 25: 1719
29. Taptas JN (1960) Loge du sinus caverneux et sinus caverneux. Rapports meninges de nerfs craniens et de l'arterie carotide interne dans leur traversée de la fosse cérébrale moyenne. Paris Semin Hop 36: 1853
30. Taptas JN (1982) The so-called cavernous sinus: a review of the controversy and its implications for neurosurgeons. Neurosurgery 11: 712
31. Taptas JN (1987) Must we still call cavernous sinus the parasellar vascular and nervous crossroads? The necessity of a definite topographical description of the region. In: Dolenc VV (ed) The cavernous sinus: a multidisciplinary approach to vascular and tumorous lesions. Springer, New York, pp 30–40
32. Umansky F, Nathan H (1982) The lateral wall of the cavernous sinus, with special reference to the nerves related to it. J Neurosurg 56: 228
33. Viunuela F, Lylyk P (1987) Endovascular therapy of vascular lesions of the cavernous sinus. Experience with 192 cases. In: Dolenc VV (ed) The cavernous sinus: a multidisciplinary approach to vascular and tumorous lesions. Springer, New York, pp 182–197

Extended endoscopic endonasal transsphenoidal approach to supra-parasellar tumors

E. de Divitiis, F. Esposito, P. Cappabianca, L. M. Cavallo, O. de Divitiis

Department of Neurological Sciences, Division of Neurosurgery, Università degli Studi di Napoli Federico II, Naples, Italy

Introduction

The extended transsphenoidal route, a very versatile approach [13], affords the possibility of exposing the entire midline skull base from below, passing through a less noble structure (the nasal cavity) in order to reach a more noble one (the brain and its neurovascular structures). In contrast to standard skull base surgical approaches, the transsphenoidal technique offers a direct and minimally invasive approach which provides excellent midline access and visibility into the suprasellar, retrosellar and retroclival spaces, obviating brain retraction [9, 13, 14, 27, 34, 36, 37, 39, 42, 49, 52]. Owing to its location, the cranial base extending from the posterior planum sphenoidale to the upper two-thirds of the clivus may be exposed through the sphenoid sinus so long as it is sufficiently pneumatized.

Furthermore, the endoscope provides neurosurgeons with a minimally invasive option for resecting suprasellar, parasellar, retrosellar and infrasellar tumors under direct visual control. Since all surgical actions, including intradural dissection, are accomplished under direct vision, even when forced to operate "around the corner," such operations are potentially safer while allowing the surgeon to see better and therefore do more. The following describes our experience with the extended endoscopic endonasal approach, the latest advancement in skull-base surgery.

Patients and methods

Expanding our 480-patient experience with the standard endoscopic endonasal approach to the pituitary area [4, 5, 12], in 2004 we began to use the extended endonasal transsphenoidal approach for a variety of lesions involving the midline skull base, primarily the suprasellar area, the cavernous sinus, and the retroclival prepontine region. Thirty-three procedures were performed in 20 males and 13 females, ranging in age between 24 and 70 years (median 49.8 years) with a mean follow-up of 14.6 months (ranging from 3 to 27 months). Of patients with suprasellar lesions, 4 had pituitary adenomas (3 non-functioning lesions and 1 PRL-secreting adenoma which did not respond to medical treatment), 10 had craniopharyngiomas, 3 had a suprasellar Rathke's cleft cysts, and 4 harbored tuberculum sellae meningiomas. Other anterior midline skullbase lesions included 1 chiasmatic astrocytoma and 1 neuroendocrine tumor. In addition, 3 patients had anterior cranial base meningoencephaloceles. Of 2 patients with tumors in the cavernous sinus, both had non-functioning pituitary adenomas, one of which had been operated on several years previously via the microsurgical transsphenoidal approach. Five patients had clival tumors: 3 chordomas (1 previously operated elsewhere via the transpetrosal approach), 1 retrosellar–retroclival prepontine meningioma, and 1 fibro-osseous dysplasia.

Presenting symptoms, pre- and post-operative endocrine function, and ophthalmologic evaluations were recorded in all patients. Pre-operative radiological investigations included magnetic resonance imaging (MRI) and computed tomography (CT). These examinations provided information about the tumors themselves and the bone structures involved with the approach.

On the 4th post-operative day all patients underwent endoscopic exploration of the nasal cavity under local anesthesia in order to determine the position and effectiveness of reconstruction materials and to check the integrity of the nasal mucosa. All had a post-operative 1.5 Tesla MRI after 3 months.

Endoscopic equipment and instruments

The endoscopic endonasal approach employs a 0-degree endoscope, 4-mm in diameter (or 2.7-mm for narrow nostrils), and 18-cm in length (Karl Storz Endoscopy, Tuttlingen, Germany). Angled endoscopes (30° and 45°) can be employed to permit an even wider angle of vision on the parasellar area. A digital endoscopic 3-CCD video camera connected to the endoscope provides clear endoscopic images, and the capacity for digital archiving. A DVD-based recording system was employed for image and video documentation (AIDA – Karl Storz Endoscopy, Tuttlingen, Germany) integrated in an informatized operative room (OR1, Karl Storz Endoscopy, Tuttlingen, Germany). A high-resolution flat monitor (>750 lines) and a Xenon light source were also used.

The extended approach requires image-guided systems, providing information for midline orientation and trajectory, and offering precision in defining the extent of planum removal. The neuronavigator (VectorVision^2 Compact; BrainLab, Kirchheim-Heimstetten, Germany) is placed behind the patient's head, with the screen near the endoscopic cart, providing the surgeon a view of both screens simultaneously.

An intraoperative microDoppler ultrasonography system (Mizuho America, Beverly, MA, USA) is employed to insonate major vascular structures prior to opening the dura and initiating sharp dissection, enhancing the safety of the procedure.

Surgical instruments for the extended approach must be straight in order that they may be inserted parallel to the endoscope, sliding along it. They must be equipped with variously angled tips in order to provide vision at corners. We employ a high-speed electric microdrill to open bone (Anspach, Palm Beach Gardens, Florida, USA). It is equipped with an extra long, low-profile handpiece (3–4 mm diameter, 15 cm long and 20° angle attachment), and a diamond burr of small diameter (2–4 mm).

Instruments used for the standard endoscopic transsphenoidal approach (Karl Storz Endoscopy, Tuttlingen, Germany) are used for extended approaches, and others have been specifically designed for this purpose, equipped with longer and variously-shaped tips for the removal of pathological material wherever found [11].

Operative technique

The patient is under general anesthesia with endotracheal intubation and is placed supine or in slight anti-Trendelenburg's position. For the extended approaches, in order to employ neuronavigation systems, the patient's head is placed in 3-point Mayfield–Kees skeletal fixation and turned 10°–15° toward the surgeon, who usually is on the patient's right side, in front of him. The neck is extended or flexed for approximately 10°–15°. Extension is useful primarily for suprasellar approach, which requires a more anterior trajectory, in order for the endoscope and surgical instruments to avoid the patient's chest. The neck is flexed for transclival approach, since the trajectory of that route is inferior and downward.

Different from the standard endoscopic endonasal transsphenoidal approach to sellar lesions [4, 5, 12], the extended approaches require the following modifications for the purpose of increasing working space and the manoeuvrability of instruments: (i) removal of the middle turbinate on one side; (ii) lateralization of the middle turbinate in the other nostril; and (iii) removal of the posterior portion of the nasal septum. These variations allow the use of both nostrils, with two or three instruments inserted plus the endoscope, which is used hand-free by the assistant, since it requires continuous movement in order to expose and access all the possible corners (the "four-hand" technique).

Once the posterior nasal cavity is exposed, the choana, the spheno-ethmoid recess, and the sphenoid ostium, which sometimes is hidden by the

superior turbinate, are identified. They are important landmarks for orientation.

Then the anterior sphenoidotomy is begun by either coagulating the posterior nasal mucosa from 5 mm above the choana superiorly to the sphenoid ostium, and extending the coagulated area to the corresponding portion of the nasal septum (1–5–2 cm circa), or through progressive enlargement of the sphenoid ostium to access the contralateral one. Using a microdrill with a 4-mm diamond burr, the sphenoid rostrum and bone of the posterior nasal septum are removed and the nasal septum is elevated from the sphenoid rostrum.

Depending on its degree of pneumatization, a series of protuberances and depressions are visible on the posterior wall of the sphenoid sinus. Their precise location is of considerable importance for the correct orientation and bone opening required by the approach: the sellar floor is at the center, the sphenoethmoid planum above it and the clival indentation below; lateral to the sellar floor the bony prominences of the intracavernous carotid artery (ICA) and the optic nerve can be seen and, between them, the lateral opto-carotid recess, moulded by pneumatization of the optic strut of the anterior clinoid process.

Exposing the anterior cranial base

Bone removal begins by thinning the tuberculum sellae, employing a microdrill equipped with a 2-mm diamond burr. The upper half of the sella is removed in order to expose the superior intercavernous sinus (or anterior sinus). Injury to this sinus results in venous bleeding, which, if not avoidable, can be controlled with haemostatic material and gentle pressure.

The tuberculum sellae is freed from the two medial opto-carotid recesses and from the planum sphenoidale, then gently dissected from dura and removed. Using a 2-mm Kerrison's rongeur, bone is removed from the planum, exposing the falciform ligament. This is a useful landmark and usually represents the anterior limit of the bony and dural opening.

The bone opening in the planum is extended postero-anteriorly approximately 1.5–2 cm but not beyond the level of the anterior wall of the sphenoid sinus. This is important to avoid (a) damaging the cribriform plate and olfactory nerve fibers, and (b) injury to the posterior ethmoidal arteries. The lateral extension of the opening is limited by the protuberances of the optic nerves.

Two horizontal dural incisions are made a few millimeters above and below the superior intercavernous sinus, between the two medial opto-carotid recesses, to avoid internal carotid artery injury. The sinus is then closed between the tips of the bipolar forceps, coagulated and incised with microscissors. The dural opening is then enlarged.

After achieving precise hemostasis, dissection and resection of supra sellar lesions are carried out using low-profile instruments and specially designed bipolar forceps. The strategy for tumor removal is tailored to each lesion. Techniques will be different for craniopharyngiomas, meningiomas, etc.

Exposing the cavernous sinus

The technique of exposing the cavernous sinus is dependent upon whether the medial compartment or the lateral compartment is to be entered.

Access to the medial compartment, exposing the proximal segments of the oculomotor and trochlear nerves, may be achieved through the loop of the parasellar intracavernous carotid artery, via the fibrous trabecular structures forming the parasellar portion of the medial wall of the sinus. The endonasal route is via the contralateral nostril. The sellar floor is opened, extending the opening much as possible toward the lesion's parasellar extension. Dura is incised in a cruciate fashion, avoiding the additional risk of extending it too close to the parasellar compartment. Extending the dural incision in such a way does not benefit the exposure of the medial wall of the cavernous sinus. After the sellar–suprasellar portion of the lesion has been completely removed and the suprasellar cistern has descended into the sella, suction curettes and angled suction cannulas are employed under endoscopic visual control to remove the parasellar extension of the lesion through the medial wall of the cavernous sinus. That the parasellar portion of the lesion has been removed completely is usually confirmed by the onset of venous bleeding. This is easily controlled with gentle irrigation and temporarily packing the sella with cottonoids or haemostatic materials.

With lesions involving the entire cavernous sinus and extending toward the lateral recess of the sphe-

noid sinus, the approach is homolateral to the parasellar extension of the lesion. The standard endonasal approach until the exposure of the posterior wall is performed. Then a lateral transethmoidal route is created with the removal of the middle turbinate, the bulla ethmoidalis and the anterior and posterior ethmoid, allowing the exposure of the lateral wall of the sphenoid sinus through a direct trajectory, creating a wide surgical corridor between the nasal septum and the lamina papiracea. Care should be taken to preserve the medial wall of the orbit and the anterior and posterior ethmoidal arteries.

If required, wide removal of the medial wall of the maxillary sinus (middle meatotomy) may be performed to expose the posterior maxillary sinus wall, infraorbital nerve, and orbital floor. The limits of such an opening are: the orbital floor superiorly, the inferior turbinate inferiorly, the sphenopalatine foramen posteriorly, and the nasolachrymal duct anteriorly. Direct access to the lateral recess of the sphenoid sinus may be gained by a trans-pterygoid approach.

Neuronavigation and microDoppler are useful for identifying the ICA's precise location. Dura is opened as far as possible from the ICA, which, with pituitary adenomas, allows the lesion to emerge under pressure. Delicate curettage and suction usually affords the removal of the parasellar parts of the lesion. Only after the resection is complete will some bleeding begin, which is usually easily controlled with hemostatic material.

Exposing the clivus

Access to the clivus requires a lower trajectory than that required for the sellar region. Nasal mucosa is elevated from the vomer and along the inferior wall of the sphenoid sinus bilaterally, allowing identification of the Vidian nerves, which represents the lateral limits of the surgical corridor. The vomer and the inferior wall of the sphenoid sinus are removed completely, exposing the sphenoidal and rhinopharyngeal parts of the clivus. The mucosal flap resulting from the dissection of the vomer and the inferior wall of the sphenoid sinus is transected along the floor of the nasal cavity inferiorly and the Vidian nerves bilaterally, thus creating a mucosal flap which will be useful for closing the surgical defect. At this point, the clivus is exposed from the level of the pituitary gland to the level of the eustachian tubes. The amount of clival bone removed depends on the extent of the lesion. With the endoscopic endonasal approach, the limits of the clival fenestration are the sella superiorly and the paraclival tracts of the intracavernous carotid artery laterally. Laterally, below the level of paraclival carotid arteries, there are no relevant vascular structures limiting removal of clival bone, thus allowing a wider exposure. After the opening the dura, the basilar artery and its branches, plus the upper cranial nerves, are well seen along their courses in the posterior cranial fossa.

Closure

A relatively extensive osteodural defect remains after the tumor has been removed, whatever approach has been employed, anterior cranial base, parasellar compartment, or clival. Its reconstruction can be challenging and sometimes time-consuming and frustrating for a surgeon fatigued by a prolonged intradural dissection. Nevertheless, a watertight reconstruction is extremely important if post-operative CSF leakage is to be avoided. The residual cavity is lined with a single layer of collagen sponge or dural substitute. Next, a large piece of dural substitute is placed in the extradural space, bridging the dural defect. Finally, a sized sheath of resorbable solid material (LactoSorb, Lorenz Surgical, Jacksonville, Florida, USA) is used to overlap the layer of the dural substitute, tucking its borders beneath the edges of intact dura. This is very important since these layers represent the only solid barrier between the intradural and extradural compartments. After closing the dural defect in this manner, the reconstruction is reinforced with multiple layers of dural substitute and/or mucoperichondrium of the middle turbinate, which was removed during the approach to the tumor. These layers may be placed over the posterior and superior walls of the sphenoid sinus. The use of surgical glue (Tisseel®, BioGlue®) further strengthens the repair. Additional reinforcement is achieved by inflating a Fogarty catheter (usually a 12–14 French) in the posterior nasal cavity, immediately in front of the sphenoidal packing. It is left in place for 48–72 h. Lumbar drainage may be avoided if the reconstruction described above is optimal, and remains watertight.

Illustrative cases

Case #1: tuberculum sellae meningioma (Figs. 1, 2)

A 50-year-old female complained of headache and progressive visual loss. Formal visual field examination revealed a bitemporal hemianopia. The sellar MRI showed the presence of a suprasellar lesion extending over the planum sphenoidale, which was suggestive of a tuberculum sellae meningioma. Endocrine testing was normal.

After discussing all possible surgical options with the patient, emphasizing advantages and disadvantages of each, an endonasal transsphenoidal approach to the tuberculum sellae and the posterior portion of the planum sphenoidale was carried out.

After coagulating and removing the dura over the tuberculum sellae and the posterior planum, the tumor was debulked and the remainder removed gradually in piecemeal fashion, finally dissecting remnants from suprasellar neurovascular structures.

The post-operative course was uneventful. After 1 month her visual field examination was improved, and at 3 months her MRI confirmed total tumor removal. There was no evidence of endocrine dysfunction.

Case #2: recurrent non-functioning pituitary macroadenoma with cavernous sinus invasion (Figs. 3, 4)

A 33-year-old male had been operated in our institute 14 years earlier via a transseptal transsphenoidal microscopic approach for a non-functioning macroadenoma. After being lost to follow-up, he was referred again with a huge recurrence of his pituitary adenoma, now involving the entire left cavernous

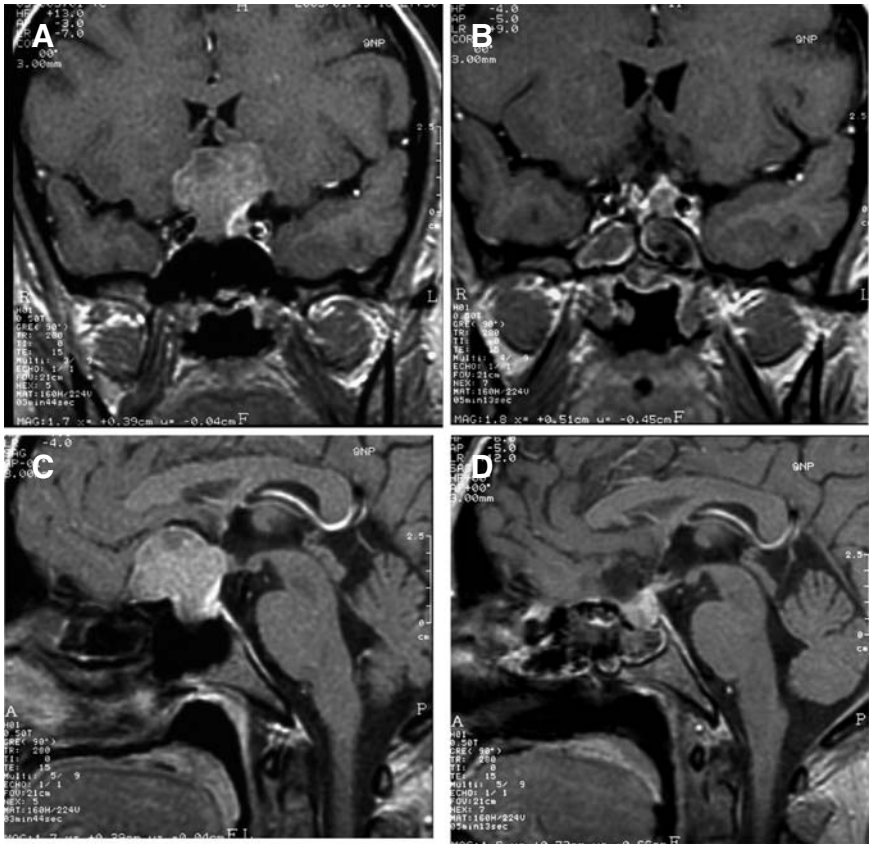

Fig. 1. A, C Coronal and sagittal pre-operative MRI images of a patient with a tuberculum sellae meningioma. **B, D** Coronal and sagittal post-operative MRI images of the same patient confirming gross total tumor resection

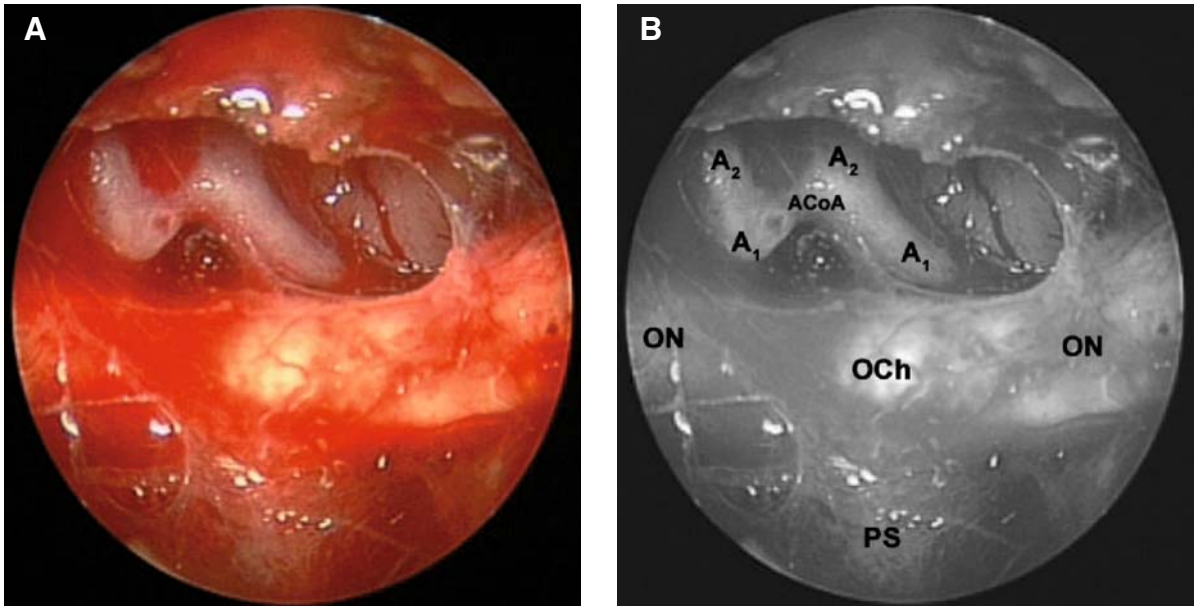

Fig. 2. Intraoperative pictures of the suprasellar meningioma shown in Fig. 1. **A** After removing the lesion, suprasellar neurovascular structures are visibly free of tumor. **B** Structures present in **A**. *A_1* First segment of the anterior cerebral artery; *ACoA* anterior communicating artery; *A_2* second segment of the anterior cerebral artery; *OCh* optic chiasm; *ON* optic nerve; *PS* pituitary stalk

sinus. He underwent an endoscopic endonasal approach, drilling away the medial pterygoid process and extending the opening to the ethmoid, thus creating a route to the lateral cavernous sinus. The lesion was totally resected from the cavernous sinus. The post-operative course was complicated by *Alicagenes* spp. meningitis, which resolved with intravenous antibiotic therapy. The post-operative MRI revealed subtotal tumor removal, with only a small remnant remaining within the sella. The left cavernous sinus was free of tumor.

Case #3: retrosellar–retroclival–prepontine meningioma (Figs. 5, 6)

A 34-year-old female had secondary amenorrhea since age 8. A few weeks prior to admission she developed a right sixth nerve palsy. An MRI revealed a retrosellar, retroclival, prepontine mass consistent with the diagnosis of meningioma. Hormonal testing demonstrated hyperprolactinemia. The tumor was removed through an endoscopic endonasal transsphenoidal approach extending to the upper two-thirds of the clivus. The prepontine region, including the upper basilar artery, was exposed. From fear of injuring the paraclival ICA, the procedure was stopped at that point.

Post-operative MRI confirmed subtotal tumor resection, with some persistent tumor behind the dorsum sellae. Several weeks after discharge the patient returned with a CSF leak, which required reoperation.

Results

Three-month post-operative 1.5 Tesla MRIs demonstrated complete tumor removal in 13 of 23 patients with suprasellar lesions (1/4 pituitary adenomas, 6/10 craniopharyngiomas, 3/3 Rathke's cleft cyst, 4/4 tuberculum sellae meningiomas) and in 1 patient with a non-functioning adenoma involving the cavernous sinus. Subtotal (>80%) removal was achieved in 3 patients with giant pituitary adenomas with suprasellar extension (2 non-functioning and 1 PRL-secreting), in 3 patients with craniopharyngiomas, in 1 patient with a chiasmatic pilocytic astrocytoma, in 1 patient with a neuroendocrine tumor, and with 1 patient with a pituitary adenoma extending into the cavernous sinus. Of the 2 patients with clival

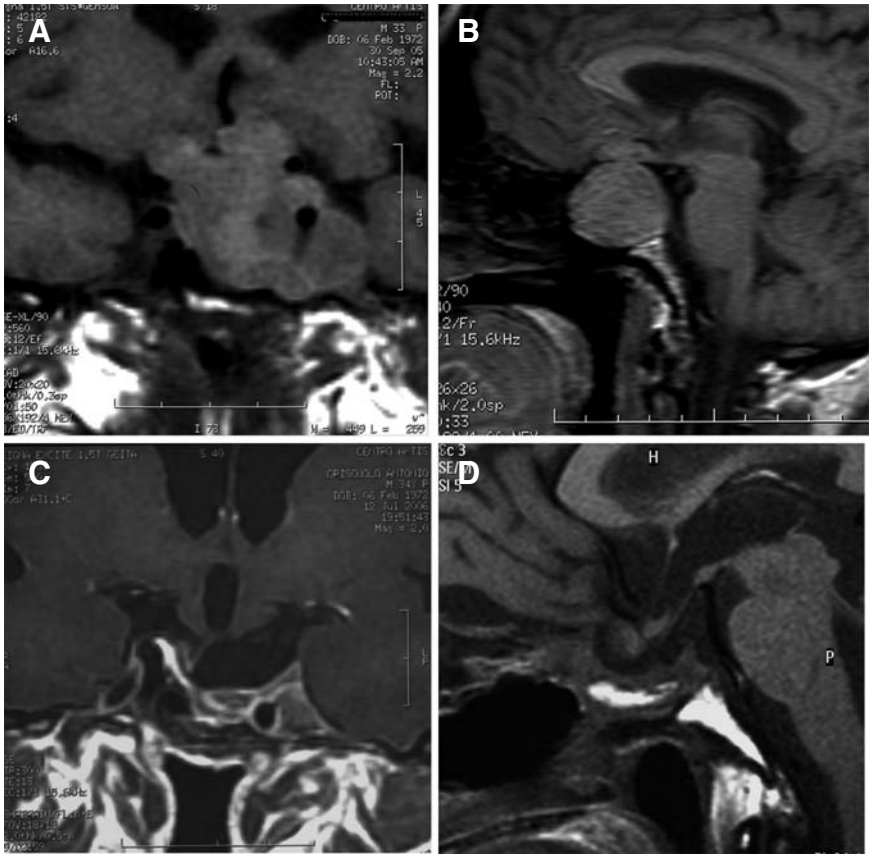

Fig. 3. A, B Pre-operative coronal and sagittal MRI images revealing a recurrent intrasuprasellar non-functioning pituitary adenoma filling the entire left cavernous sinus. **C, D** Post-operative coronal and sagittal MRI images of the same patient revealing the subtotal removal of the lesion

tumors, both had subtotal removals. One suprasellar craniopharyngioma could be removed only partially. Among the clival tumors, the meningioma and 1 of the chordomas were subtotally removed, while the other 2 chordoma and 1 fibro-osseous dysplasia could only be partially debulked. All 3 patients with anterior cranial base meningoencephaloceles were successfully treated by removing the sac and closing the dura.

Of 16 subjects with pre-operative visual field defects, 5 of 16 recovered completely and 10 of 16 improved. Only 1 of 16 experienced worsening vision after surgery. That patient had a giant non-functioning pituitary macroadenoma with a severe bitemporal haemianopia prior to surgery. After surgery her vision worsened in the left eye, and only light perception remained on the right. With respect to surgical complications, 3 patients – 1 with a craniopharyngioma, 1 with a recurrent non-functioning pituitary adenoma involving the cavernous sinus, and 1 with a retrosellar retroclival meningioma – developed a post-operative CSF leak, requiring a second operation for repair. One of them had bacterial meningitis requiring intravenous antibiotic therapy. One patient with extrasellar extension of a non-functioning adenoma experienced generalized epileptic seizures a few hours after the surgical procedure, presumed to be related to the presence of intracranial air after massive CSF loss during surgery.

One patient, with a suprasellar intraventricular craniopharyngioma, died (3.2%). Four patients developed de novo diabetes insipidus after surgery (3 of whom were treated for craniopharyngiomas). The mean post-op stay of the entire series was of 5.9 days.

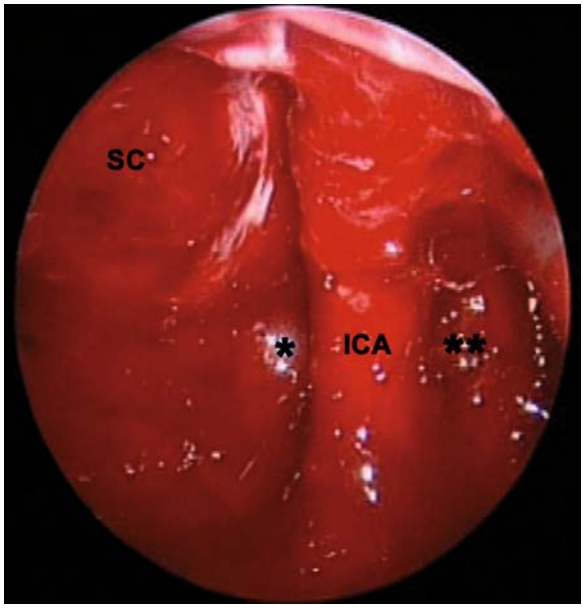

Fig. 4. Intraoperative photographs of the recurrent intrasuprasellar craniopharyngioma demonstrated in Fig. 3. *ICA* internal carotid artery; *SC* suprasellar cistern; * medial compartment of the cavernous sinus; ** lateral compartment of the cavernous sinus

Discussion

The area extending from the anterior limit of the anterior cranial fossa to the anterior limit of the foramen magnum is considered to be the *midline skull base*. The base of the skull is among the most fascinating and complex areas, from both an anatomical and surgical perspective. The skull base may be involved with a variety of lesions, neoplastic and non-neoplastic, benign and malignant. Many such pathologies are highly invasive. Successful treatment of skull base lesions is extremely difficult to achieve without paying a very high price in terms of morbidity and mortality. A variety of innovative craniofacial approaches to skull base lesions – including anterior, antero-lateral, and postero-lateral routes – have been developed to access lesions of the anterior midline skull base or those ventral to the brainstem [1, 7, 8, 15, 18–26, 32, 33, 35, 38, 40, 41, 44–48, 50]. For extensive tumors such methods have been used either alone, or in combination as "staged" operations. Often such operations require both extensive bone removal and neurovascular dissection, resulting in serious repercussions in terms of perioperative morbidity and mortality. The evolution of surgical techniques plus methods of diagnosis, post-anesthetic and perioperative care, plus the advent of the endoscope have led in recent decades to improving the plight of patients affected by these pathologies. Such factors, including recent anatomical studies of the transsphenoidal route and related matters [2, 3, 6, 10, 13, 14, 16, 17, 28–31, 37, 42, 43, 51] have contributed to extending the previous transsphenoidal approach to the entire midline skull base. Furthermore, during the past decade, the extended transsphenoidal approach has benefited from important diagnostic and technical advances, including frameless neuronavigation, Doppler ultrasonography and intraoperative magnetic resonance imaging.

With the endoscope, the extended approaches provide a wider view of the surgical field and improved identification of many surgical landmarks, both in the sphenoid sinus and intradurally. The high quality of vision provided by the endoscope promotes the preservation of crucial neurovascular structures.

Nevertheless, not all cases are suitable for such techniques. Several variations, either with respect to parasellar anatomy or morphology of the lesion itself, may either simplify or complicate a given lesion's dissection and removal.

First is the *grade of pneumatization of the sphenoid sinus*. In a well pneumatized sphenoid sinus all bony landmarks of its posterior wall are easily recognized. This is important for the surgeon gaining and maintaining his orientation [11]. A conchal-type sphenoid sinus, however, is not ideal for the extended approach. For the trans-tuberculum trans-planum sphenoidale approach especially, bony prominences of the optic nerves and the intracavernous carotid arteries, plus the lateral opto-carotid recesses are important landmarks for the surgeon drilling the medial opto-carotid recesses and removing the tuberculum sellae. For accessing the lateral compartment of the cavernous sinus, pneumatization of the infero-lateral recess of the sphenoid cavity is very important. Drilling away a thin clivus makes the trans-clival approach faster.

The second anatomical variation is the *size of the sella*. A normal (or small) sella dictates that the two intracavernous carotid arteries lie closer to each other, necessitating a narrower approach between the two medial opto-carotid recesses. This requires particular care when opening dura overlying, above, or beneath the sella turcica.

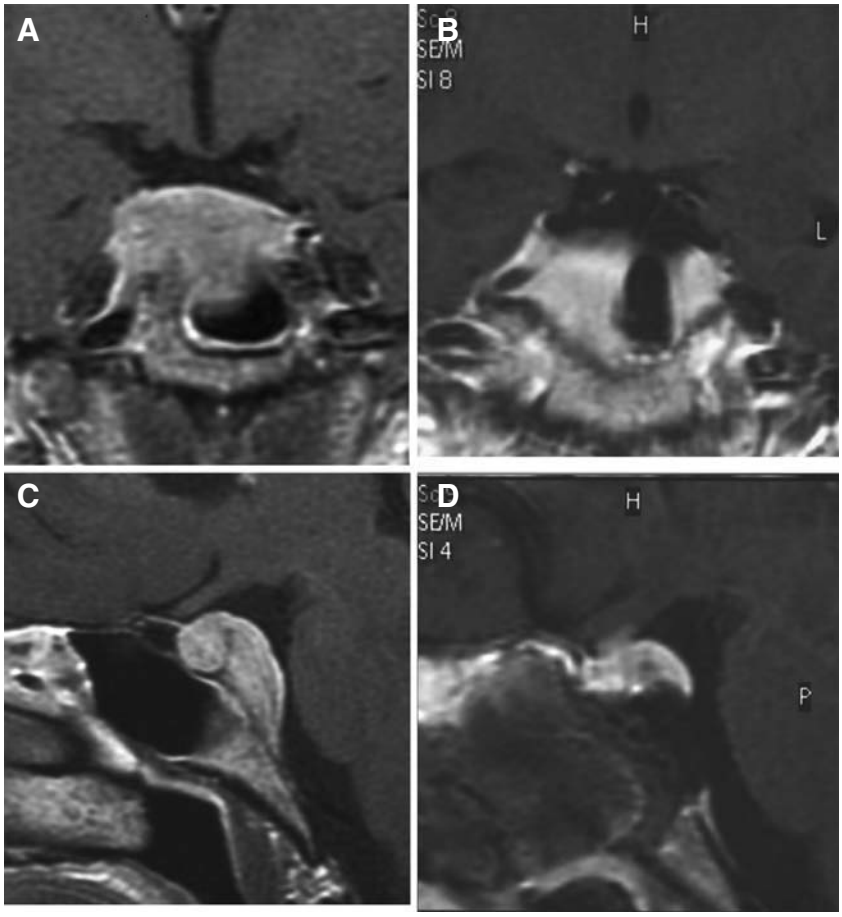

Fig. 5. A, C Pre-operative coronal and sagittal MRI images showing a retrosellar, retroclival prepontine meningioma. **B, D** Post-operative coronal and sagittal MRI images of the same patient confirming a subtotal tumor resection

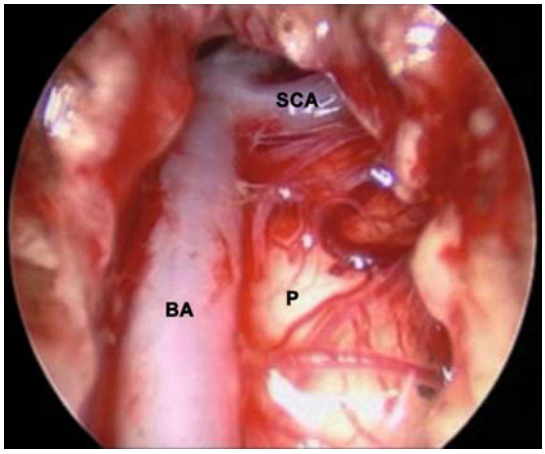

Fig. 6. Intraoperative photograph of the retroclival meningioma in Fig. 5. *P* Pons; *BA* basilar artery; *SCA* left superior cerebellar artery

The *direction of the long axis of the tumor*, especially for suprasellar masses and those inside the third ventricle, is important. If the orientation of the axis of the approach is identical to the long axis of the tumor, resection may be carried out without further enlarging bone and dural openings. In addition, post-fixed or posteriorly displaced optic chiasms simplify tumor resections. By contrast, if the optic chiasm is pre-fixed or anteriorly displaced, access to the suprasellar and supradiaphragmatic areas is more difficult since bone resection and dural opening must be carried out very carefully since the chiasm lies immediately behind the tuberculum sella.

With respect to intradural lesions, *encasement of neurovascular structures* renders the operation more dangerous. Sometimes such structures are displaced but not encased by the mass, making tumor removal

possible with cautious dissection, whether blunt or sharp. When neurovascular elements are even partially encased, however, the transsphenoidal approach is generally not a good choice.

Finally, for retrosellar masses, the *height of the dorsum sellae and the dimensions of the posterior clinoid processes* are important factors to consider carefully. Large dorsum sellae or hypertrophic posterior clinoid processes make access to the retrosellar area more difficult.

One challenge of the extended approach is finding reliable instruments to control bleeding and reconstruct the relatively large bony and dural defects. Working space is decidedly limited. Low-profile endonasal bipolar forceps are currently available for coagulating vessels of the tumor capsule. It is important to use the microDoppler probe before and during sharp dissection in certain areas in order to lessen the risk of injury to vessels like the internal carotid artery, from which bleeding is typically extremely difficult to control.

Several methods and materials (autologous, heterologous and synthetic) have been employed to reconstruct the skull base defect, minimizing the likelihood of a post-operative CSF leak. At this time we use a heterologous substance (collagen sponges) held in place by a solid or semisolid resorbable buttress constructed by placing additional pieces of collagen sponge extradurally and infusing them with various surgical glues. Using this technique we have not observed a post-operative CSF leak in our last nine operations. Even lumbar drainage, employed with our first three cases, no longer seems to be required. Our only instance of a post-op CSF leak was with a recurrent craniopharyngioma. In that patient, a clear defect in the reconstruction was confirmed at the time of reoperation.

Conclusions

The endoscopic extended transsphenoidal approach to suprasellar and parasellar tumors, once thought operable only by transcranial routes, seems to be a promising treatment alternative for these lesions. The method is minimally invasive, the route primarily extracranial, and only minimal neurovascular manipulations are required. A patient undergoing such operations may expect a quicker recovery.

Longer operative times, at least for surgeons beginning their learning curves, and a higher incidence of post-op CSF leak and related complications (meningitis and tensive pneumocephalus) are current disadvantages. Improved closure techniques are needed. This approach requires adequate endoscopic technology, neuronavigation systems, microDoppler instruments, low-profile surgical tools (including coagulation forceps), plus considerable experience and confidence with the endoscope and the transsphenoidal route. Follow-up currently is too short to compare the extent of tumor removal and rates of recurrence with intracranial methods.

References

1. Al-Mefty O, Ayoubi S, Smith RR (1991) The petrosal approach: indications, technique, and results. Acta Neurochir Suppl (Wien) 53: 166–170
2. Alfieri A, Jho HD, Schettino R, Tschabitscher M (2003) Endoscopic endonasal approach to the pterygopalatine fossa: anatomic study. Neurosurgery 52: 374–378; discussion 378–380
3. Alfieri A, Jho HD, Tschabitscher M (2002) Endoscopic endonasal approach to the ventral cranio-cervical junction: anatomical study. Acta Neurochir (Wien) 144: 219–225; discussion 225
4. Cappabianca P, Cavallo LM, de Divitiis E (2004) Endoscopic endonasal transsphenoidal surgery. Neurosurgery 55: 933–940; discussion 940–931
5. Cappabianca P, de Divitiis E (2004) Endoscopy and transsphenoidal surgery. Neurosurgery 54: 1043–1048; discussions 1048–1050
6. Cavallo LM, Cappabianca P, Galzio R, Iaconetta G, de Divitiis E, Tschabitscher M (2005) Endoscopic transnasal approach to the cavernous sinus. Anatomical study. Neurosurgery 90: 111–133
7. Chanda A, Nanda A (2002) Partial labyrinthectomy petrous apicectomy approach to the petroclival region: an anatomic and technical study. Neurosurgery 51: 147–159; discussion 159–160
8. Cho CW, Al-Mefty O (2002) Combined petrosal approach to petroclival meningiomas. Neurosurgery 51: 708–716; discussion 716–718
9. Cook S, Smith Z, Kelly DF (2004) Endonasal transsphenoidal removal of tuberculum sellae meningiomas: technical note. Neurosurgery 55: 239–246
10. Couldwell WT, Weiss MH, Rabb C, Liu JK, Apfelbaum RI, Fukushima T (2004) Variations on the standard transsphenoidal approach to the sellar region, with emphasis on the extended approaches and parasellar approaches: surgical experience in 105 cases. Neurosurgery 55: 539–547; discussion 547–550

11. de Divitiis E, Cappabianca P (2004) Endoscopic pituitary surgery. Anatomy and surgery of the transsphenoidal approach to the sellar region. Endo-Press, Tuttlingen
12. de Divitiis E, Cappabianca P, Cavallo LM (2003) Endoscopic endonasal transsphenoidal approach to the sellar region. In: de Divitiis E, Cappabianca P (eds) Endoscopic endonasal transsphenoidal surgery. Springer, Wien New York, pp 91–130
13. de Divitiis E, Cappabianca P, Cavallo LM (2002) Endoscopic transsphenoidal approach: adaptability of the procedure to different sellar lesions. Neurosurgery 51: 699–705; discussion 705–697
14. de Divitiis O, Conti A, Angileri FF, Cardali S, La Torre D, Tschabitscher M (2004) Endoscopic transoral–transclival approach to the brainstem and surrounding cisternal space: anatomic study. Neurosurgery 54: 125–130; discussion 130
15. Donald PJ (1998) Transoral approach to the clivus and upper cervical spine. In: Donald PJ (ed) Surgery of the skull base. Lippincott-Raven Publishers, Philadelphia, pp 507–532
16. Dusick JR, Esposito F, Kelly DF, Cohan P, DeSalles A, Becker DP, Martin NA (2005) The extended direct endonasal transsphenoidal approach for nonadenomatous suprasellar tumors. J Neurosurg 102: 832–841
17. Esposito F, Becker DP, Villablanca JP, Kelly DF (2005) Endonasal transsphenoidal transclival removal of prepontine epidermoid tumors: technical note. Neurosurgery 56: E443; discussion E443
18. Fahlbusch R, Schott W (2002) Pterional surgery of meningiomas of the tuberculum sellae and planum sphenoidale: surgical results with special consideration of ophthalmological and endocrinological outcomes. J Neurosurg 96: 235–243
19. Goel A, Desai K, Muzumdar D (2001) Surgery on anterior foramen magnum meningiomas using a conventional posterior suboccipital approach: a report on an experience with 17 cases. Neurosurgery 49: 102–106; discussion 106–107
20. Goel A, Muzumdar D, Desai KI (2002) Tuberculum sellae meningioma: a report on management on the basis of a surgical experience with 70 patients. Neurosurgery 51: 1358–1363; discussion 1363–1354
21. Grisoli F, Diaz-Vasquez P, Riss M, Vincentelli F, Leclercq TA, Hassoun J, Salamon G (1986) Microsurgical management of tuberculum sellae meningiomas. Results in 28 consecutive cases. Surg Neurol 26: 37–44
22. Hakuba A, Liu S, Nishimura S (1986) The orbitozygomatic infratemporal approach: a new surgical technique. Surg Neurol 26: 271–276
23. Hakuba A, Nishimura S, Jang BJ (1988) A combined retroauricular and preauricular transpetrosal–transtentorial approach to clivus meningiomas. Surg Neurol 30: 108–116
24. Jallo GI, Benjamin V (2002) Tuberculum sellae meningiomas: microsurgical anatomy and surgical technique. Neurosurgery 51: 1432–1439; discussion 1439–1440
25. James D, Crockard HA (1991) Surgical access to the base of skull and upper cervical spine by extended maxillotomy. Neurosurgery 29: 411–416
26. Javed T, Sekhar LN (1991) Surgical management of clival meningiomas. Acta Neurochir Suppl (Wien) 53: 171–182
27. Jho HD (1999) Endoscopic endonasal skull base surgery for midline lesions from olfactory groove to distal clivus. In: 67th Annual Meeting of the American Association of Neurological Surgeons. New Orleans, Louisiana
28. Jho HD, Alfieri A (2002) Endoscopic glabellar approach to the anterior skull base: a technical note. Minim Invasive Neurosurg 45: 185–188
29. Jho HD, Ha HG (2004) Endoscopic endonasal skull base surgery: Part 1 – The midline anterior fossa skull base. Minim Invasive Neurosurg 47: 1–8
30. Jho HD, Ha HG (2004) Endoscopic endonasal skull base surgery: Part 2 – The cavernous sinus. Minim Invasive Neurosurg 47: 9–15
31. Jho HD, Ha HG (2004) Endoscopic endonasal skull base surgery: Part 3 – The clivus and posterior fossa. Minim Invasive Neurosurg 47: 16–23
32. Kawase T, Shiobara R, Toya S (1991) Anterior transpetrosal–transtentorial approach for sphenopetroclival meningiomas: surgical method and results in 10 patients. Neurosurgery 28: 869–875; discussion 875–866
33. Lakhdar A, Sami A, Naja A, Achouri M, Ouboukhlik A, El Kamar A, El Azhari A (2003) [Epidermoid cyst of the cerebellopontine angle. A surgical series of 10 cases and review of the literature]. Neurochirurgie 49: 13–24
34. Lalwani AK, Kaplan MJ, Gutin PH (1992) The transsphenoethmoid approach to the sphenoid sinus and clivus. Neurosurgery 31: 1008–1014; discussion 1014
35. Lang DA, Neil-Dwyer G, Iannotti F (1993) The suboccipital transcondylar approach to the clivus and craniocervical junction for ventrally placed pathology at and above the foramen magnum. Acta Neurochir (Wien) 125: 132–137
36. Laws ER (1993) Clivus chordomas. In: Sekhar LN, Janecka IP (eds) Surgery of cranial base tumors. Raven Press, New York, pp 679–685
37. Liu JK, Decker D, Schaefer SD, Moscatello AL, Orlandi RR, Weiss MH, Couldwell WT (2003) Zones of approach for craniofacial resection: minimizing facial incisions for resection of anterior cranial base and paranasal sinus tumors. Neurosurgery 53: 1126–1135; discussion 1135–1127
38. MacDonald JD, Antonelli P, Day AL (1998) The anterior subtemporal, medial transpetrosal approach to the upper basilar artery and ponto-mesencephalic junction. Neurosurgery 43: 84–89
39. Maira G, Pallini R, Anile C, Fernandez E, Salvinelli F, La Rocca LM, Rossi GF (1996) Surgical treatment of clival chordomas: the transsphenoidal approach revisited. J Neurosurg 85: 784–792

40. Miller E, Crockard HA (1987) Transoral transclival removal of anteriorly placed meningiomas at the foramen magnum. Neurosurgery 20: 966–968
41. Nakamura M, Samii M (2003) Surgical management of a meningioma in the retrosellar region. Acta Neurochir (Wien) 145: 215–219; discussion 219–220
42. Puxeddu R, Lui MW, Chandrasekar K, Nicolai P, Sekhar LN (2002) Endoscopic-assisted transcolumellar approach to the clivus: an anatomical study. Laryngoscope 112: 1072–1078
43. Rabadan A, Conesa H (1992) Transmaxillary–transnasal approach to the anterior clivus: a microsurgical anatomical model. Neurosurgery 30: 473–481; discussion 482
44. Reisch R, Bettag M, Perneczky A (2001) Transoral transclival removal of anteriorly placed cavernous malformations of the brainstem. Surg Neurol 56: 106–115; discussion 115–116
45. Samii M, Ammirati M (1988) The combined supra-infratentorial pre-sigmoid sinus avenue to the petroclival region. Surgical technique and clinical applications. Acta Neurochir (Wien) 95: 6–12
46. Sano K (1980) Temporo-polar approach to aneurysms of the basilar artery at and around the distal bifurcation: technical note. Neurol Res 2: 361–367
47. Seifert V, Raabe A, Zimmermann M (2003) Conservative (labyrinth-preserving) transpetrosal approach to the clivus and petroclival region–indications, complications, results and lessons learned. Acta Neurochir (Wien) 145: 631–642; discussion 642
48. Sepehrnia A, Knopp U (2002) The combined subtemporal-suboccipital approach: a modified surgical access to the clivus and petrous apex. Minim Invasive Neurosurg 45: 102–104
49. Spencer WR, Levine JM, Couldwell WT, Brown-Wagner M, Moscatello A (2000) Approaches to the sellar and parasellar region: a retrospective comparison of the endonasal-transsphenoidal and sublabial-transsphenoidal approaches. Otolaryngol Head Neck Surg 122: 367–369
50. Talacchi A, Sala F, Alessandrini F, Turazzi S, Bricolo A (1998) Assessment and surgical management of posterior fossa epidermoid tumors: report of 28 cases. Neurosurgery 42: 242–251; discussion 251–252
51. Weiss M (1987) The transnasal transsphenoidal approach. In: Apuzzo MLJ (ed) Surgery of the third ventricle. Williams & Wilkins, Baltimore, pp 476–494
52. Zada G, Kelly DF, Cohan P, Wang C, Swerdloff R (2003) Endonasal transsphenoidal approach for pituitary adenomas and other sellar lesions: an assessment of efficacy, safety, and patient impressions. J Neurosurg 98: 350–358

Chapter 3. Neuromonitoring in central skull base surgery

Neuromonitoring in central skull base surgery

W. Eisner, T. Fiegele

Neurosurgical Department, Medical University Innsbruck, Innsbruck, Austria

Introduction

Intraoperative electrophysiological monitoring has become increasingly common in neurosurgery. Such methods prevent postoperative deficits by warning the surgeon of the imminent injury to neuronal structures. Monitoring sensorimotor, cognitive (language and short term memory), and cranial nerve function (except hearing) during cerebellopontine angle operations has been well established. Yet monitoring the function of nuclei and fiber tracts in the floor of the fourth ventricle and cranial nerves traversing the central skull base is more demanding – ranging from recording site challenges (e.g., within the orbit) to interpreting the more subtle electrophysiological findings. Preserving motor cranial nerve function has long been a problem for skullbase surgeons. Currently, however, the continuous recording of compound muscle action potentials (CMAPs) from muscles enervated by cranial nerves III–XII makes it possible to monitor skull base and cavernous sinus operations as reliably as those performed in the cerebellopontine angle.

Problems in central skull base surgery

Space occupying lesions occurring at the central skull base endanger three primary systems: (1) cranial nerves I–VI include four motor nerves, two sensory nerves, and one of the mixed functions. Lesions extending from the central skull base to the foramen magnum may affect any or all cranial nerves, I–XII. (2) The vascular system of the anterior circulation, including connections with the posterior circulation, as it impacts the cerebral hemispheres and basal ganglia. (3) The hypothalamic and hypophyseal system (concerned with endocrine function) is beyond the scope of this article.

The basis for intraoperative electrophysiological monitoring involves stimulating various cranial motor nerves, then recording subclinical contractions of the muscles they innervate. Continuous recording of muscle activity during surgical dissection has the capacity to reveal contact with or injury to a cranial nerve. The percentage reduction of a supramaximal CMAP compared to that at the beginning of the operation indicates the percentage of functional neuron loss.

Historical overview

On 14 July 1898, Dr. Fedor Krause in Berlin first described the use of cranial nerve monitoring during posterior fossa surgery to section a cochlear nerve for tinnitus. He noted that ". . .unipolar faradic irritation of the facial nerve trunk with the weakest possible current of the induction apparatus resulted in contractions of the right facial region, especially of the orbicularis oculi, as well as of the branches supplying the nose and the mouth . . ." [65]. The patient exhibited facial paresis immediately following surgery which almost completely resolved by the next day. Krause also noted contractions of the shoulder,

which he thought were due to the stimulation of the spinal accessory nerve that "...had undoubtedly been reached by the current, because it was, together with the acusticus, bathed in liquor that had trickled down...". Thus, Krause was not only the first to describe locating a cranial nerve by electrical stimulation; but also the first to encounter the confounding problem of an artifact being produced by the spread of current!

Frazier used a similar technique during an operation for the relief of vertigo, and pointed out the importance of preserving the facial nerve, which he noted could be identified by "galvanic current" [36].

Table 1. Electromyography – a historical overview

1791	Luigi Galvani observed muscle twitch following the application of an electrostatic spark by conducting atmospheric electricity to muscle by contact with various metals in animals. The following year Galvani demonstrated the existence of bioelectricity and published "On Electrical Powers in the Movement of Muscles."
1794	Luigi Galvani placed the free end of a nerve across a muscle and elicited muscle contractions without utilizing metal, proving that electricity could be generated by animal tissue.
1833	G.B.A. Duchenne invented surface electrodes, and thus percutaneous electrical stimulation. He was the first to use alternating current and introduced the name "Faradic".
1838	Carlo Matteucci demonstrated that proximal stimulation of a ligated or sectioned nerve does not elicit muscle contraction.
1844	Carlo Matteucci introduced the nerve–muscle preparation. He observed muscle contractions in bare frog muscles when the sciatic nerve from the opposite leg was placed in contact with the muscles. When the muscles of one leg contracted, muscles in the opposite leg contracted after a delay, so long as the nerve was not insulated from the bare muscle.
1849	Du Bois Reymond was the first to record voluntary elicited electrical signals from contractions of arm muscles causing a potential difference between two fingers immersed in the cups of saline.
1857	H. von Ziemssen demonstrated that "motor points" coincided with the entrance of nerves into muscles. He mapped the entire body, marking motor points (on the skin of terminally ill patients) with silver nitrate. He proved by immediate post mortem dissection that the clinical markings corresponded to the entrance of nerves into muscles.
1870	Engelmann described the relationship between the intensity and duration of current flow by recording the strength–duration curve in laboratory animals.
1898	Fedor Krause was first to stimulate the facial nerve intraoperatively and described the current spread via the liquor cerebrospinalis.
1901	Einthoven recorded millivolt potentials with speed, accuracy, and permanency.
1909	L. Lapicque defined "rheobase" as the threshold of excitation, and "chronaxie" as the minimal value of current duration at double the rheobase intensity required to cause excitation.
1912	H.E. Piper published Elektrophysiologie menschlicher Muskeln (the first electromyography book) and introduced metal surface electrodes. He performed frequency analysis and recorded compound muscle action potentials following ulnar nerve stimulation and action potentials following voluntary contractions.
1916	E.D. Adrian recorded strength–duration curves in healthy and diseased human muscles. He noted a shift of the curve with the degeneration and fairly constant changes with the regeneration.
1920	Forbes and Thatcher were the first to use a vacuum tube to amplify the action potential and a string galvanometer to record it.
1922	Gasser and Erlanger combined an amplifying circuit with a Braun (cathode ray) tube to identify bioelectric potentials, eliminating the mechanical limitations of galvanometers.
1925	Liddell and Sherington introduced the concept of the "motor unit".
1929	Lord Adrian and Bronk introduced the concentric needle electrode and the loudspeaker. They also described the motor unit potential.
1934	Matthews introduced the differential amplifier. Thus making small muscle potential recording possible since it minimized electrical interference from other sources.
1944	Jasper and Notman introduced the monopolar needle electrode.
1962	Basmajian introduced fine wire bipolar recording electrodes for functional muscle studies.
1979	TE Delgado visualized for the first time intraoperative facial nerve CMAPs on the oscilloscope [23].
1983	AR Moller described evoked potentials in intraoperative monitoring.
1986	CW Hess introduced transcranial magnetic stimulation.

Later, similar methods were described by Givre and Olivecrona [42], Hullay and Tomits [50], Rand and Kurze [109], Pool [106], and Albin et al. [3]. The old nomenclature and differentiation between galvanic and faradic shocks or stimulation refers to the fact that a galvanic shock or stimulus is of long duration and a faradic shock or stimulus is of short duration. This nomenclature disappeared with the advent of electronic stimulators.

From the 1940s through the 1960s, some surgeons resected vestibular swannomas (acoustic neuromas) under local anesthesia in order to facilitate the assessment of facial nerve function [42, 50]. Observing the face for visible contractions after electrical stimulation remained the state of the art for facial nerve monitoring until 1979, when intraoperative facial electromyography (EMG) was introduced by Delgado et al. [23].

During the 1980s a combination of analog data processed by the simple computers and electron beam oscilloscope presentation of EMG signals and CMAPs (compound muscle action potential, a curve produced by the stimulation of a certain latency and amplitude) in combination with rudimentary surface and needle electrodes postulated specialized monitoring by a neurophysiological team in the operation room.

Poor or total absence of shielding of operating room equipment (such as coagulation devices, lasers, cusa, anesthesia machines, even electric lights and the operating microscope) created artifacts obscuring or destroying electrophysiological signals. With the early 1990s came not only superior shielding technology but also digital multipurpose machines allowing up to eight channels of simultaneous examinations of different modalities (for instance, evoked potentials and continuous muscle recordings in combination). Then the standards of intraoperative electrophysiological monitoring (IOM) were determined (Table 1).

Electrophysiological methods

The advent of microneurosurgery and technical innovations in neuroradiology led to the precise localization and classification of neuronal structures and pathological lesions, which ultimately resulted in reduced surgical morbidity and mortality. The capacity to identify neuronal functions by electrophysiological methods was also an important advance. It is possible to identify electrophysiologically the distribution of normal cranial motor nerves as they traverse the central skull base (also nuclei and fiber tracts within the floor of the fourth ventricle) as they are affected by space-occupying pathologies. Sensorimotor, auditory, and visual systems are also useful components of intraoperative multimodal monitoring.

Various electrophysiological techniques are employed simultaneously or in close temporal relationship. Before describing the techniques currently available with intraoperative electrophysiological units, the requirements of intraoperative electrophysiological monitoring (IOM) must be addressed.

In order to reduce postoperative deficits, IOM must reflect surgical events the instant they occur. If the correlation between surgical action and recording event is clear and precise, a potential neurological deficit is identified by a change in the continuous electrophysiological record. Then the surgeon's noxious actions must be stopped immediately, at least altered, if a permanent neurological deficit is to be avoided.

A minimum of eight channels of simultaneous recording is necessary. Evoked potentials confirm the integrity of the lemniscal system, disappearing in ischemic areas associated with developing strokes. Neurographic methods – compound muscle action potentials – identify cranial motor nerves by direct stimulation of the nerve and recording electrical activity from its target muscle. The activity is characterized by latency and amplitude. Supramaximal stimulation refers to increased intensity or current while not increasing the amplitude of the potential. Continuous activity recorded from muscles innervated by a cranial motor nerve may indicate contact of a surgical instrument with that nerve if such activity ceases when mechanical contact is discontinued. Such activity is referred to as "contact activity".

Activity persisting longer than the mechanical stimulation reflects "pathological activity", indicating partial damage to the nerve. The degree of such a nerve's functional loss is proportional to the percentage reduction of the amplitude of a potential generated by supramaximal stimulation, compared to its baseline (that amplitude resulting from an identical stimulation of the nerve prior to its surgical manipulation [91]).

We utilize a bipolar recording system employing isolated and not insulated needle electrodes of 1–5 cm in length. Preferred recording sites are: inferior oblique m. (N.III), superior oblique m. (N.IV), masseter m. (N.V), lateral rectus m. (N.VI), orbicular oculi m. and orbicular oris m. (N.VII), stylopharyngeal m. (N.IX), vocal m. (N.X), trapetius m. (N.XI), lingual m. (N.XII). Needle electrodes must be placed with great precision. We will demonstrate anatomical studies and strategies to achieve that end. Directly stimulating motor cranial nerves/nuclei/fiber tracts (mapping) is accomplished at 4.6 stimuli per second, square wave impulse, 0.2 ms duration, 0.1–3 mA via isolated coagulation forceps. We prefer bipolar concentric stimulation electrodes. Recording parameters include: analysis time of 10–20 ms, amplification 200–500 μV, with filtering (low pass: 2–5 Hz and high pass: 1.5 kHz). Direct nerve contact is identified by the stimulation intensities lower than 0.3 mA (see Table 2).

Continuous monitoring is accomplished by recording free running activity from selected muscles. Acoustic transformation of the electrophysiological signal (loudspeaker warnings) indicates motor cranial nerve manipulation and impending injury. A free running mode is chosen using higher amplification (50–200 μV). Preferable analysis time is 100 ms, (filtering as above). Our focus is not only potential latency and amplitude, but also height, density, duration, and form of activity. Correlations with surgical manipulations are observed carefully. Activity lasting no longer than surgical actions is not considered indicative of damage to neural structures (see Table 3).

Table 2. Compound muscle action potentials (CMAPs)

Stimulation electrode	Bipolar concentric or bipolar forceps
Stimulation intensity	0.1–2 mA
Stimulus duration	0.2 ms
Stimulus frequency	4.7 s
Filter bandpass	2.5–1500 Hz
Input gain	200 μV/unit to 500 μV/unit
Averages	No

Table 3. Free running muscle response

Input gain	50 μV/unit
Filter bandpass	2.5–1500 Hz
Mode	Free running

Electrode placement

Preserving an intact oculomotor system (oculomotor, trochlear, and abducens nerves) is a goal of every skull base operation. Electrophysiological monitoring employing CMAPs and continuous EMG recording have improved surgical strategies [90, 123], and reduced postoperative cranial motor nerve deficits [35]. Precise placement of the recording needle electrodes is crucial. Descriptions of pertinent anatomy and various strategies to achieve that end will be discussed below.

Electrophysiological monitoring of facial nerve function during cerebellopontine angle surgery has been demonstrated to preserve facial nerve function, becoming a goal for intraoperative electrophysiological monitoring of all cranial motor nerves. Such monitoring results in reducing or avoiding altogether postoperative cranial motor nerve deficits. Intraoperative methods of protecting the oculomotor system by electrophysiological methods have been reported only rarely. Special ring electrodes [124] are required. Standard surface electrodes become easily displaced and often record potential muscles innervated by the facial nerve ("far field potentials"). We have circumvented this problem by utilizing common needle electrodes to record compound muscle action potentials (CMAPs) and free running electromyographic activity in intraorbital extraocular muscles. The following anatomical descriptions of electrode placement are designed to enhance the technique in the neurosurgical operation theatre. The technique is safe and easily performed, obviating the necessity for ultrasound and neuronavigational guidance.

Our methods for needle placement include selecting the ideal muscles for recording activities of the oculomotor, trochlear, and abducens nerves. Important anatomical structures are identified, and strategies for puncturing orbital muscles with minimal risk of injury are discussed. Technical data, such as required needle length and various recording parameters, are given.

It is essential to record from intraorbital muscles innervated by different cranial nerves at maximal distances from each other in order to avoid mixing electrophysiological signals. The oculomotor nerve innervates the superior rectus m, inferior rectus m, medial rectus m, inferior oblique m, superior levator palpepral m, ciliar m, sphincter pup. m, while the

trochlear nerve innervates only the oblique superior m. and the abducens nerve innervates only the lateral rectus m.

Criteria for selecting muscle from which to record is dictated by the distribution of muscles within the orbit. For electrophysiological monitoring purposes, it would be ideal if intraocular muscles innervated by a given cranial nerve were located discretely, isolated from muscles influenced by other nerves. Nevertheless, direct recordings must be made from muscles not covered by muscles innervated by other cranial nerves, if "far field recordings" from other nerves is to be avoided. Far field potentials are electrophysiological activities recorded from distant electrophysiological sources.

Muscle selection for monitoring the trochlear and abducens nerves is simple since each nerve supplies only a single muscle. For oculomotor nerve monitoring, on the other hand, we must choose from seven different muscles. In order to avoid confusion with recordings of trochlear and abducens nerve stimuli, it is best to avoid recording from structures in the lateral, superior, and medial parts of the orbit. Two muscles supplied by the oculomotor nerve, the inferior rectus m. and inferior oblique m., lie in the inferior part of the orbit. The larger and more superficially located muscle is the inferior oblique m., making it the ideal site for recording.

Therefore, we prefer recording CMAPs and free running EMGs from the inferior oblique muscle for the oculomotor nerve, the superior oblique muscle for the trochlear nerve, and the lateral rectus muscle for abducens nerve.

Figure 1 illustrates intraorbital anatomy, including bone elements, the bulb of the eye, and the extraocular muscles we target for recording electrodes. In children, there is very little space between the bulb of the eye and orbital bone, making electrode placement much more difficult than in adults. We execute all punctures by the free hand technique.

Description of electrode placement

For purposes of description it is useful to consider the ocular bulb as an eye-ball with a pupil in its center. Figure 2 illustrates the orbit being

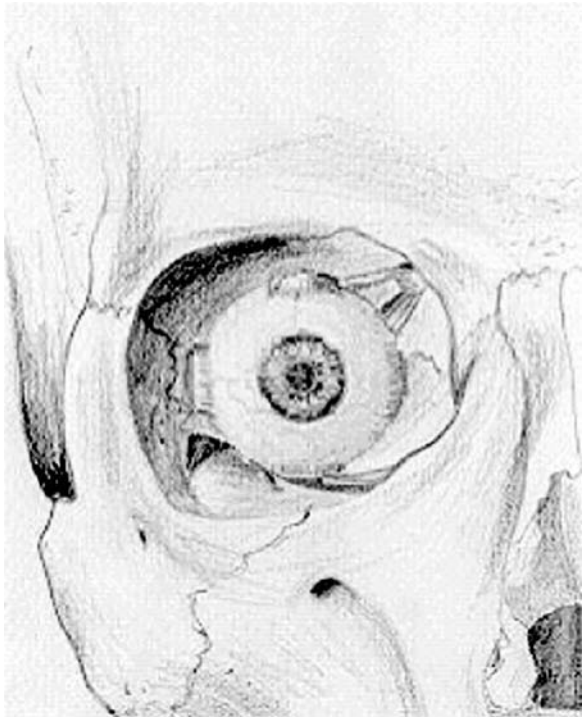

Fig. 1. Eye bulb, bony orbita and selected muscles

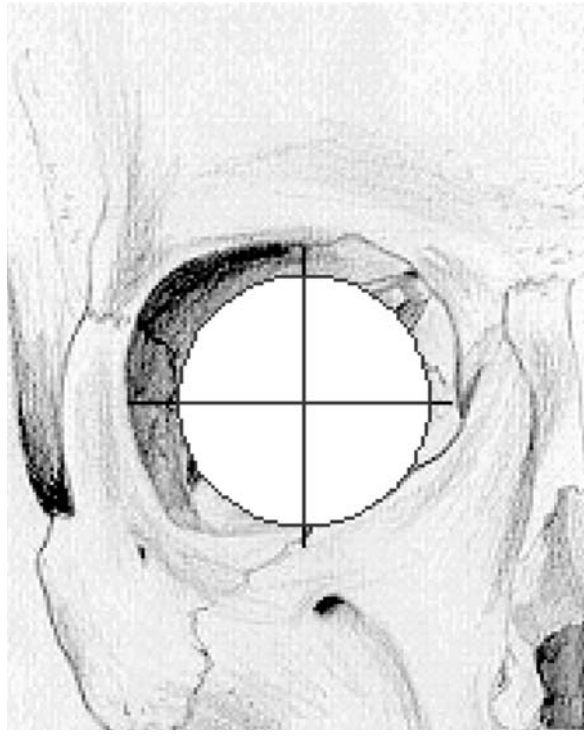

Fig. 2. The orbit separated in four quadrants

divided into four quadrants with the pupil in its center.

Oculomotor nerve – inferior oblique muscle

The inferior oblique is the only muscle inferior to the ocular bulb that is oriented transversely. Immediately inferior to the pupil, this muscle is 3–5 mm from the ocular bulb. The bulb is the only structure endangered by puncturing the orbit. If the needle electrode is placed closer to the eye bulb additional activity from the inferior rectus muscle may be recorded as "far field potentials," but both muscles are innervated by the oculomotor nerve. The ideal time for puncture is between 5 and 6 o'clock on the analog watch (Fig. 3). Of the three electrodes to be placed into intraorbital muscles, only the one to monitor the oculomotor nerve system is placed through the lower two quadrants (Figs. 2, 4, 5).

The inferior oblique muscle should be punctured perpendicular to the pupil through the inferior palpebral sulcus. With the second finger of the left hand contacting the inferior rim of the bony orbit one can palpate the ocular bulb through the skin with a fingernail. The needle electrode is inserted directly through the skin, and then the electrode is bent to the side of the nose and fixed with tape.

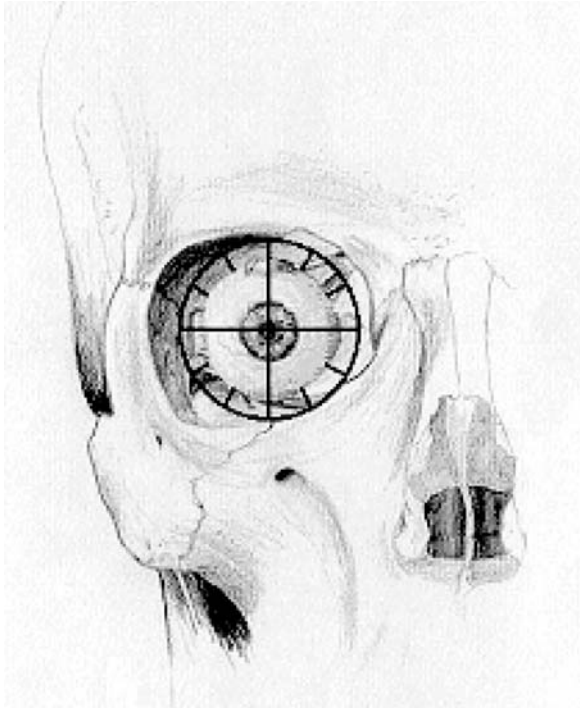

Fig. 3. The bulb of the eye as an analogue watch

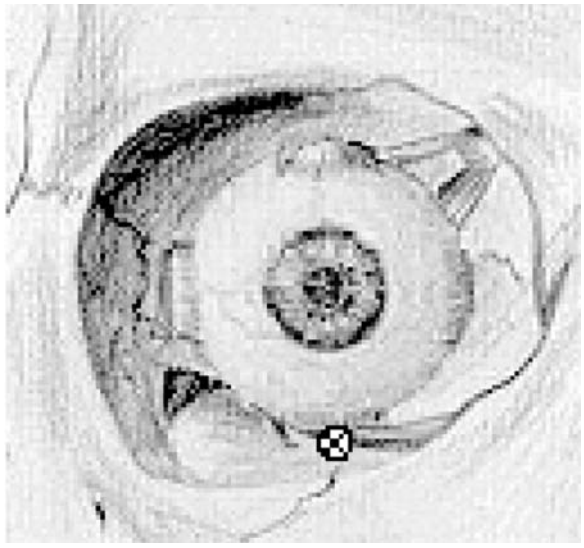

Fig. 4. Anatomical drawing (right eye) for puncturing the inferior oblique muscle

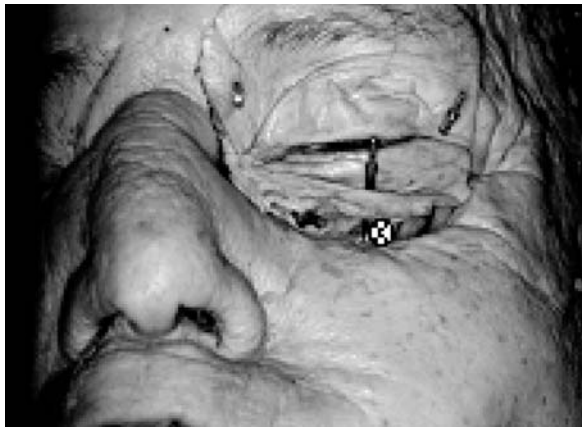

Fig. 5. Cadaver preparation with inserted needle electrodes (left)

Trochlear nerve – superior oblique muscle

The superior oblique is the largest muscle in the superior medial quadrant of the orbit. It consists of two bellies looped around a "pulley" (the trochlea). Deeper and closer to the ocular bulb, at the junction of the superior and inferior medial quadrants, lies the

medial rectus muscle, which is innervated by the oculomotor nerve. Similarly, the superior rectus muscle, also innervated by the oculomotor nerve, is superior to and perpendicular to the pupil.

Endangered structures are angular vein and angular artery, which are adjacent to the dorsal nasal vein and the dorsal nasal artery, all near the bulb of the eye (Figs. 6 and 7).

The superior oblique muscle is best punctured at the medial third of the superior medial quadrant of the orbit. Skin should be punctured in the lateral part of the superior eye-lid, with the needle directed toward orbital bone medially. After contacting the bone, the needle electrode is redirected deeper by angling its tip downward. The electrode should be placed perpendicular to the frontal incision and fixed to the nose with tape.

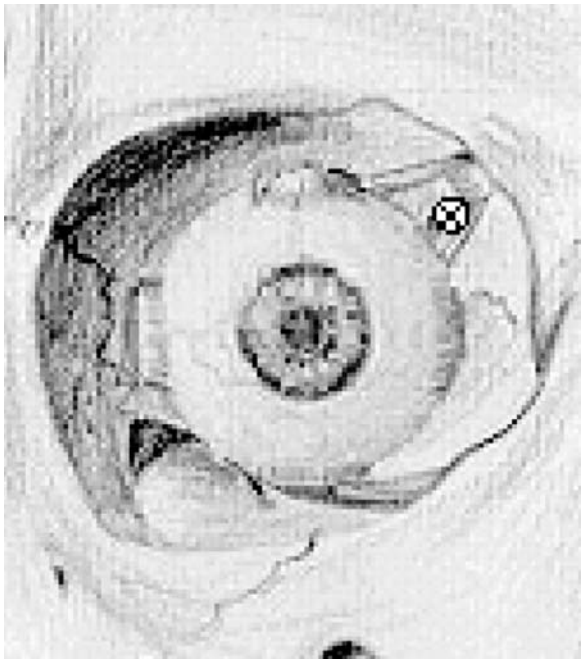

Fig. 6. Sketch of the right orbit

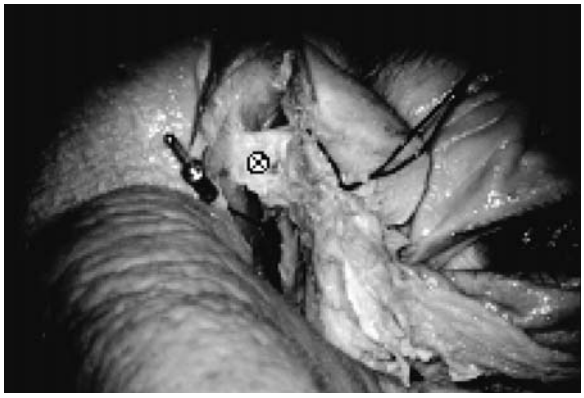

Fig. 7. Cadaver preparation of the left orbit and best puncture site, exposing the superior oblique muscle and trochlea

Abducens nerve – lateral rectus muscle

The lateral rectus muscle is the only muscle lateral to the ocular bulb. Like all rectus muscles, it inserts into the bulb near its equator. The bulb is the only structure placed at risk by inserting an electrode into the lateral rectus, but such risk is low since the electrode-wire is very fine.

The lateral rectus muscle should be punctured through the lateral palpebral ligament. Imagining a horizontal line through the pupil of the eye may be helpful. After inserting the electrode, its proximal end is bent and fixed to the skin with tape.

With all three targeted muscles it is best to insert each needle electrode from the rim of the eye lid

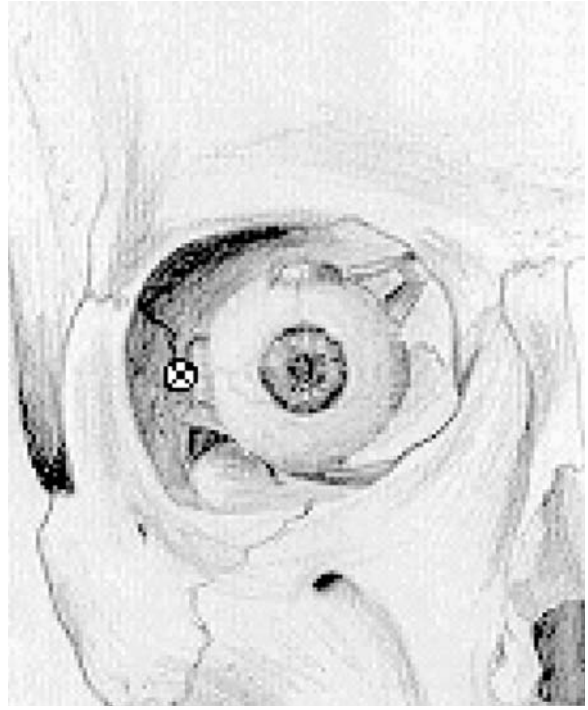

Fig. 8. Anatomical drawing of the right orbit: the preferred site for puncturing the lateral rectus muscle

toward orbital bone. This will ensure avoiding the angular artery and vein and the bulb of the eye. Contacting a known structure (orbital bone) first inspires confidence, making it easier to approach the appropriate muscle deeper in the orbit. For puncturing the skin, one should first recall the periorbital surface anatomy illustrated in Figs. 9 and 10. It is necessary to identify the inferior palpebral sulcus, the lateral palpebral ligament, and the frontal incision in the bony orbit (Fig. 11).

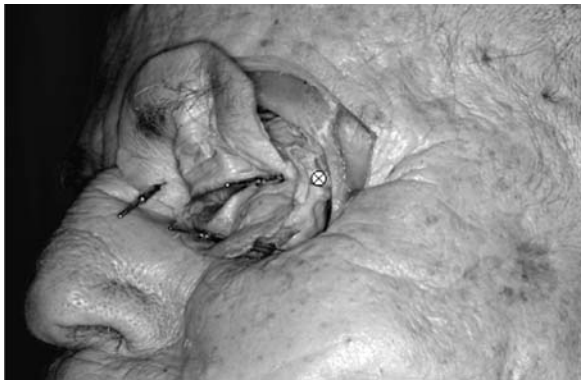

Fig. 9. Cadaver preparation of the left orbit, exposing the lateral rectus muscle

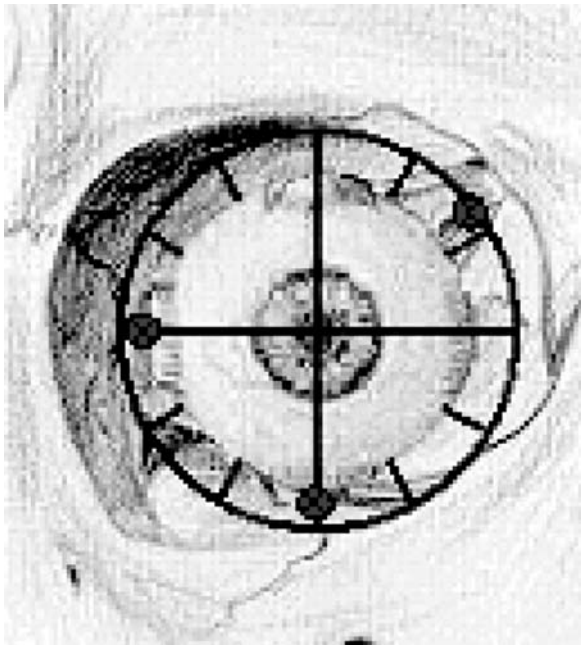

Fig. 10. Best strategy for puncturing the right orbit (summary)

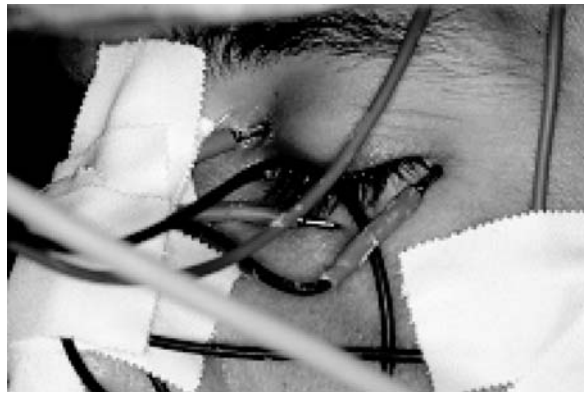

Fig. 11. Intraoperative needle electrodes placed in the left orbit

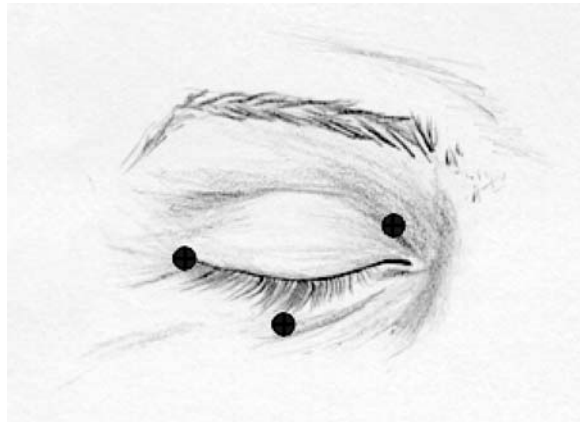

Fig. 12. Skin puncture

Figures 12 and 13 illustrate pertinent skin landmarks for inserting electrodes and a "watch face", which is useful in locating pertinent intraorbital anatomy. The superior lateral quadrant should never be punctured in order to avoid injuring the lacrimal gland, which could result in a percutaneous fistula and ectopic lacrimal gland cells.

Puncturing the bulb of the eye is virtually impossible since electrodes currently available internationally for intraoperative neurophysiological monitoring are too delicate to cause injury. Typically they bend rather than puncture the ocular bulb. Sclera covering the eye consists of very strong collagenous tissue. Furthermore, our experience recording from intraorbital muscles in well over 400 cases (of several thousand monitored neurosurgical procedures) since 1993, neither the surgical approach

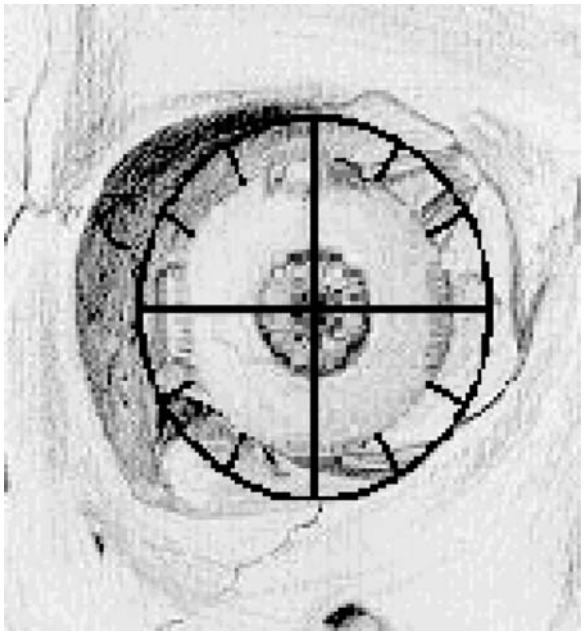

Fig. 13. Correlating structures

(despite the sometimes unusual positioning requirements of skull base surgery) nor IOM was hindered by intraorbital electrode placement.

After switching to eight channel digitized multimodal monitoring in 1991 (from four channel technology), we quickly became aware that a wide range cranial motor nerves are subject to injury, not only from the mechanical manipulation but also from thermal spread associated with coagulating blood vessels. At that time we began routinely monitoring all cranial motor nerves. The following pertains to electrode placement for monitoring the trigeminal, facial, glossopharyngeal, vagus, spinal accessory, and hypoglossal nerves.

Monitoring motor elements of the trigeminal nerve is best done by recording from the masseter muscle. It is located one fingerbreadth anterior to angle of the mandible. We insert two angular electrodes (approximately 20 mm in length) roughly 10 mm apart. The tip of each electrode is stripped of Teflon. Longer electrodes increase the risk of traversing the masseter muscle into the mouth, even into the tongue.

For facial nerve monitoring, we employ the orbicularis oculi and the orbicularis oris muscles. Both are large, surrounding each orbit and the mouth with minimum diameters of 20 mm. We place the negative electrode in the upper part of each muscle, and the positive electrode in the inferior part.

For glossopharyngeal nerve monitoring we place an electrode in the stylopharyngeal muscle, lateral to the velum palatinum bilaterally, ensuring that the negative electrode is on the right and the positive electrode is on the left, therefore requiring only a single channel for both glossopharyngeal nerves. Electrical activity from the right glossopharyngeal muscle will create a negative deflection of the potential and activity from the left will result in a positive (downward) deflection.

Monitoring the vagus nerve is accomplished by monitoring from the ipsilateral vocal chord or the pharyngeal constrictor muscle. Placing the electrode in the vocal chord requires a special applicator. The pharyngeal constrictor muscle is located lateral and superior to the vellum palatinum. For practical purposes, electrodes for recording from the stylopharyngeal muscle will suffice since in the absence of activity in glossopharyngeal system, so called "far field potentials" from the pharyngeal constrictor muscle result. Theoretically, activity requiring stopping surgical manipulations could occur from both cranial nerve systems simultaneously. Which nerve is at risk is of little practical importance, however, since surgical manipulations should be interrupted at the first sign of such activity in order to avoid a permanent neurological deficit.

Monitoring the spinal accessory nerve system requires recording from the superior part of the trapezius muscle. The lower elements of the trapezius are innervated by the ansa cervicalis.

For the hypoglossal nerves (right and left), the same polarity is set up as for recordings from the soft palate, activity from the right hypoglossal nerve producing an upward deflection and activity from the left, a downward deflection.

Needle electrodes/required needle length

We employ custom made recording electrodes. Fixed-needle electrodes remain firmly in place and resistant to perspiration. Without pushing, pulling, or otherwise manipulating skin, an electrode is inserted into each of the three extraocular muscles to be monitored (some 5–15 mm beneath the skin surface). Distances from the orbital rim and the maximum depths to the surface of each muscle vary very

little. We recommend a 20–40-mm needle for each muscle. In order to reduce (or avoid altogether) "far field potentials" from structures innervated by the facial nerve (such as orbicularis oculi muscle), it is helpful to use recording needles insulated with teflon. We strip Teflon from each electrode with a scalpel, exposing it 7–10 mm from the tip. This tends to separate targeted muscles electrophysiologically from surrounding orbital muscles. Various systems may be differentiated by their characteristic latencies.

Reference electrodes should be inserted in the scalp some distance from muscles innervated by the facial nerve. Utilizing a single reference electrode for all three orbital muscles will produce parallel excursions in artefacts. To gain similar amplitudes of CMAPs, corresponding electrodes should be equidistant.

Electrophysiological findings

As stated previously, it is important that an electrophysiological baseline is recorded after exposing the pathology and before surgical dissection begins. Distortions reflecting the effect of a space-occupying lesion on a given cranial motor nerve must be distinguished from subsequent changes, distortions likely indicating surgical manipulation or heat damage. In the early stages of the surgical approach, free running EMG recordings should reveal no electrical changes unless spikes or bursts indicate some contact with or damage to neural tissue.

Compared to awake patients, where electrophysiological bursts reflect spontaneous muscle activity, spontaneous activity is seen in *anesthesized patients* (*not on muscle relaxants*) indicating that a nerve is being surgically contacted or has been injured. "Contact activity" persists no longer than the nerve is contacted with a surgical instrument. "Pathological activity" refers to electrophysiological change persisting beyond the period of observed surgical contact.

When the surface of the pathological lesion is exposed, "macro-mapping" is accomplished, essentially determining where neural tissue can and cannot be demonstrated electrophysiologically. Such mapping is helpful since space-occupying lesions may hide neural tissue that is to be preserved. This simplifies the identification of cranial motor nerves later, or "micro-mapping." A cranial motor nerve is identified by stimulating it electrically and recording the resulting potentials from the target muscle. Initial stimulation intensities between 0.5 mA and 2 mA are sufficient to cause recordable activity even when the nerve stimulated is covered by minimal amounts of tissue. Fifteen years ago we confirmed that any cranial motor nerve might be stimulated by intensities even less than 0.3 mA. Stimulating cranial motor nerves at different sites will result in different latencies of recorded potentials. The farther the impulse must be conducted through the nerve, the longer it will take for the potential to appear.

Every cranial motor nerve has its own characteristic conduction velocity. The facial nerve, for example, has a conduction velocity of 50 m per second, requiring approximately 0.7 ms for neuromuscular transmission. Injured cranial motor nerves have decreased conduction velocities (Moller AR, 1995), making it necessary to obtain baseline values at the beginning of an operation, including latencies from proximal and distal stimulation sites of exposed nerves or nerve fibers. The amplitude of supramaximal stimulation is also very important. Functional neuron loss within a nerve during surgery is identified by the percentage reduction of the supramaximal stimulation amplitude. It is necessary to stimulate an exposed nerve at varying stimulation sites. One site should be distal to the tumor, or between tumor and the recording muscle. Another stimulation site should be proximal to the tumor, or between tumor and brainstem. Stimulating the nerve at each site will result in different latencies. The latency resulting from stimulating a nerve between brainstem and recording site is necessarily longer than that resulting from stimulating between the tumor and the recording muscle. Even after a cranial motor nerve is destroyed, it remains possible to record stimulations of the distal nerve trunk from intraorbital muscles. Stimulating proximal to the tumor is not recordable, however, since the integrity of the nerve has been interrupted, producing a flat line on the screen.

Current may be conducted through surrounding spinal fluid or irrigation fluid to the distal nerve stump resulting in a potential. In such circumstances it is necessary to know the latencies from the different sites of the stimulation. When the nerve has been

Fig. 14. Spikes and bursts, free running activity

destroyed, the latency from stimulating the stump will be identical to that resulting from stimulating the nerve distal to the site of injury. Proof of nerve integrity requires different latencies from different sites of stimulation. The surgical field must be free of fluid to avoid such artefacts, but they may be identified by synchronous identical activities on multiple recording channels.

Typical waveforms are shown in Fig. 14.

These types of waveforms are encountered during surgery. Loudspeaker warnings (acoustic transformation of the EMG) simplify communications between electrophysiologist and surgeon [107].

Continuously recording free running activities from innervated muscle is of proven value in identifying emerging neuronal damage. Surgically contacting the nerve or nerve fibers being monitored results in activity, which does not persist beyond the time the nerve is contacted by a surgical instrument. Strauss et al. verified that high frequency, high amplitude signals recorded from innervated muscle which persist beyond the time the nerve is subject to contact or thermal injury correlate well with postoperative deficits [130]. This observation has been confirmed by many others, including ourselves, and is currently generally accepted. The loss of functional fibers within a nerve was examined by Moller. He developed an optimal procedure for monitoring cranial motor nerves, which has since become the international standard.

After the nerve is exposed, it is supramaximally stimulated, and the resulting latency and amplitude are recorded. Increasing the stimulation intensity further will not result in a higher potential. Functional neurone loss during surgery is monitored by repeatedly stimulating the nerve at risk at the same site with the same intensity. The percentage of decrease in amplitude is directly proportional to the functional nerve fiber loss. Optimal stimulation parameters for compound muscle action potentials (CMAPs) are listed in Table 2 and for free running recording in Table 3 (Fig. 15).

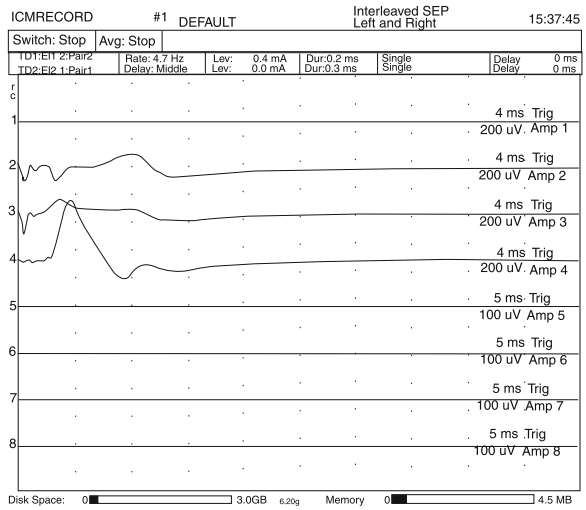

Fig. 15. CMAPs from the inferior oblique muscle (channel 4) and "far field potentials" from the superior oblique muscle (channel 2) and the lateral rectus muscle (channel 3)

Discussion and outlook

Cranial motor nerve monitoring is ideal for skull base surgery. Sekhar and Møller [123] point out its special value for procedures in and around the cavernous sinus. Others and we could demonstrate that surgery even within the brainstem is made safe by monitoring cranial motor nerves electrophysiologically during surgery.

Monitoring within the sinus cavernosus and its environs may very well be more important than monitoring cerebellopontine angle operations since the oculomotor nerve appears to be even more sensitive to the manipulation than the facial nerve. Oculomotor nerve deficits seem to occur simply by "looking at the nerve!".

Cranial motor nerves are frequently unseen, hidden beneath the surface of various tumors, making the recording of cmap's and free running muscle activity from intraorbital muscles of considerable value to tumor surgeons. The techniques are also

important to vascular neurosurgeons. Basilar apex aneurysm operations carry the risk of postoperative oculomotor palsies, which may even occur present bilaterally. Since 1993 we have routinely recorded from both inferior oblique muscles, allowing us to anticipate oculomotor nerve injuries in early stages. Detecting such a problem prior to concluding an operation allows the surgeon to prevent oculomotor deficits in some cases simply by repositioning the aneurysm clip.

Recording the result of supramaximally stimulating a cranial motor nerve before and after it has been surgically manipulated makes it possible to quantify its functional fiber loss from partial injury [91]. Supramaximal stimulation is accomplished by increasing the intensity until no change in the compound muscle action potential's amplitude is apparent. Recording free running muscle activity from intraorbital extraocular muscles cannot quantify functional loss from surgical injury, but it can indicate injury to nerves and neural tissue [31, 130] by identifying new electrophysiological activity. We distinguish between "contact activity" and "pathological activity" in that the former persists no longer than the period of surgically manipulating the nerve, while the latter continues after surgical manipulation has ceased. "Pathological activity" is also of high amplitude and high intensity, and reflects serious damage if it persists until the operation ends. "Contact activity", on the other hand is generally harmless.

Intraoperative electrophysiological monitoring of cranial motor nerves III, IV, and VI is still considered to be very difficult. Some employ ultrasound guidance or neuronavigation to position the needle electrodes. This is time consuming, particularly in comparison to our method, which may be performed in less than 30 min. We have recorded from intraorbital eye muscles in over 400 cases without once damaging the eye or surrounding structures or causing a single recording site infection.

But, like the operating microscope, intraoperative electrophysiological monitoring is only a tool. The electrophysiologist's familiarity with the operation and respect between him or her and the surgeon are keys to avoiding postoperative cranial nerve deficits. This is similar to a great jazz ensemble's simultaneously hearing and reacting to a single musician's improvisation. Disasters occur when all participants are not on the same page.

Acknowledgements

Special thanks to Sonja Scholz, M.D., for making drawings of the eye and orbit, and to Adolf Müller, M.D., for preparing the anatomical cadaver specimens.

References

1. Akagami R, Dong CC, Westerberg BD (2005) Localized transcranial electrical motor evoked potentials for monitoring cranial nerves in cranial base surgery. Neurosurgery 57(1 Suppl): 78–85; discussion 78–85
2. Alberti O, Sure U, Riegel T, Bertalanffy H (2001) Image-guided placement of eye muscle electrodes for intraoperative cranial nerve monitoring. Neurosurgery 49: 660–663; discussion 663–664
3. Albin MS, et al. (1976) Anesthetic management of posterior fossa surgery in the sitting position. Acta Anaesthesiol Scand 20: 117–128
4. Aravabhumi S, Izzo KL, Bakst BL (1987) Brainstem auditory evoked potentials: intraoperative monitoring technique in surgery of posterior fossa tumors. Arch Phys Med Rehabil 68: 142–146
5. Baker GS (1965) Physiologic abnormalities encountered after removal of brain tumors from the floor of the fourth ventricle. J Neurosurg 23: 338–343
6. Bejjani GK, Nora PC, Vera PL, Broemling L, Sekhar LN (1988) The predictive value of intraoperative somatosensory evoked potential monitoring: review of 244 procedures. Neurosurgery 43: 491–498; discussion 498–500
7. Benson DF (1988) Classical syndromes of aphasia. In: Boller F, Grafmann J (eds) Handbook of neuropsychology. 1. Elsevier, Amsterdam
8. Berger MS, Ghatan S, Haglund MM, Dobbins J, Ojemann GA (1993) Low-grade gliomas associated with intractable epilepsy: Seizure outcome utilizing electrocorticography during tumor resection. J Neurosurg 79: 62–69
9. Berger MS, Ojemann GA, Lettich E (1989) Brain mapping techniques to maximize resection, safety, and seizure control in children with brain tumors. Neurosurgery 25: 786–792
10. Black P, Ronner SF (1987) Cortical mapping for defining the limits of tumor resection. Neurosurgery 20: 914–919
11. Bogen J, Bogen G (1975) Wernicke's region – where is it? Ann NY Acad Sci 280: 834–843
12. Bricolo A, Turazzi S, Cristophori L, Talacchi A (1991) Direkt surgery for brainstem tumors. Acta Neurochir (Wien) [Suppl] 53: 148–158
13. Broca P (1861) Remarques sur le siège de la faculté du language articulé, survie d'une observation d'aphémie (perte de la parole). Bull Soc Anat Paris 36: 330–357
14. Broggi G, Scaioli V, Brock S, Dones I (1995) Neurophysiological monitoring of cranial nerves during

posterior fossa surgery. Acta Neurochir [Suppl] 64: 35–39
15. Burchiel KJ, Clark H, Ojemann G (1989) Use of stimulation mapping and corticography in the excision of arteriovenous malformations in sensorimotor and language related neocortex. Neurosurgery 24: 323–327
16. Castilla-Garrido JM, Murga-Oporto L (1999) Intraoperative electroneurophysiological monitoring of basal cranial nerve surgery. Rev Neurol 28: 573–582
17. Chyatte D (1989) Vascular malformations of the brainstem. J Neurosurg 70: 847–852
18. Colletti V, Fiorino FG (1998) Advances in monitoring of seventh and eighth cranial nerve function during posterior fossa surgery. Am J Otol 19: 503–512
19. Cushing H (1909) A note upon the Faradic stimulation of the postcentral gyrus in conscious patients. Brain 32: 44–54
20. Damasio AR (1992) Aphasia. New Engl J Med 326: 531–539
21. Daube JR (1991) Intraoperative monitoring of cranial motor nerves. In: Schramm J, Moller AR (eds) Intraoperative neurophysiologic monitoring in neurosurgery. Springer, Berlin, pp 246–267
22. Deletis V, Vodusek DB, Abbot R, Epstein FJ, Turndorf H (1992) Intraoperative monitoring of the dorsal sacral roots: minimizing the risk of iatrogenic micturition disorders. Neurosurgery 30: 72–75
23. Delgado TE, Buchheit WA, Rosenholz HR (1979) Intraoperative monitoring of facial muscle evoked responses obtained by intracranial stimulation of the facial nerve: a more accurate technique for facial nerve dissection. Neurosurgery 4: 418–421
24. Dickins JR, Graham SS (1991) A comparison of facial nerve monitoring systems in cerebellopontine angle surgery. Am J Otol 12: 1–6
25. Dong CC, Macdonald DB, Akagami R, Westerberg B, Alkhani A, Kanaan I, Hassounah M (2005) Intraoperative facial motor evoked potential monitoring with transcranial electrical stimulation during skull base surgery. Clin Neurophysiol 116: 588–596
26. Ebeling U, Reulen HJ (1995) Space occupying lesions of the sensorimotor region. Adv Tech Stand Neurosurg 22: 137–181
27. Ebeling U, Schmid U, Reulen HJ (1990) Tumor-surgery within the central motor strip: surgical results with the aid of electrical motor cortex stimulation. Acta Neurochir 101: 100–107
28. Ebeling U, Schmid U, Ying Z (1991) Mapping bei Tumorpatienten in der Zentralregion. Schweiz Rundsch Med Praxis 47: 1318–1323
29. Eisner W (2001) Elektrophysiologisches Monitoring in der Neurochirurgie. J Neurol Neurochir Psychiat 3: 38–56
30. Eisner W, Reulen HJ, Ilmberger J, Swozil U, Bise K (1999) Intraoperative mapping of eloquent brain areas. Front Radiat Ther Oncol 33: 28–36
31. Eisner W, Schmid UD, Reulen HJ, Oeckler R, Olteanu V, Gall C, Kothbauer K (1995) The mapping and continuous monitoring of the intrinsic motor nuclei during brainstem surgery. Neurosurgery 37: 255–265
32. Epstein F, McCleary EL (1986) Intrinsic brainstem tumors of childhood: surgical indications. J Neurosurg 64: 11–15
33. Fahlbusch R, Strauss C, Huk W, Röckelein G, Kömpf D, Ruprecht KW (1990) Surgical removal of pontomesencephalic cavernous hemangiomas. Neurosurgery 26: 449–457
34. Fasano VA, Urciuoli R, Ponzio RM, Lanotte MM (1986) The effect of new technologies on the surgical management of brainstem tumors. Surg Neurol 25: 219–226
35. Foerster O (1931) The cerebral cortex of man. Lancet 109: 309–312
36. Frazier CH (1912) Intracranial division of the auditory nerve for persisting aural vertigo. Surg Gynecol Obstet 15: 524–529
37. Friedman WA, Kaplan BJ, Gravenstein D, Rhoton AL Jr (1985) Intraoperative brain-stem auditory evoked potentials during posterior fossa microvascular decompression. J Neurosurg 62: 552–557
38. Fritsch G, Hitzig E (1870) Über die elektrische Erregbarkeit des Großhirns. Archiv für Anat Physiol Wiss Med 37: 300–332
39. Fritschi J, Reulen H, Spetzler R, Zabramski J (1994) Cavernous malformation of the brainstem. Acta Neurosurg (Wien) 130: 35–46
40. Gentili F, Lougheed WM, Yamashiro K, Corrado C (1985) Monitoring of sensory evoked potentials during surgery of skull base tumours. Can J Neurol Sci 12: 336–340
41. Geschwind N (1967) The varieties of naming errors. Cortex 3: 97–112
42. Givre A, Olivecrona H (1949) Surgical experiences with acoustic neuroma. J Neurosurg 396–407
43. Grundy BL (1982) Monitoring of sensory evoked potentials during neurosurgical operations: methods and applications. Neurosurgery 11: 556–575
44. Grundy BL, Nelson PB, Doyle E, Procopio PT (1982) Intraoperative loss of somatosensory potentials and loss of spinal chord function. Anesthesiology 57: 321–322
45. Haldeman S, Bradley WE, Bhatia NN, Johnson BK (1982) Pudendal evoked responses. Arch Neurol 39: 280–283
46. Harner S, Daube J, Ebersold M, Beatty C (1987) Improved facial nerve function with use of electrical monitoring during removal of acoustic neuromas. Mayo Clin Proc 62: 92–102
47. Heffez DF, Zinreich SJ, Long DM (1990) Surgical resection of intrinsic brainstem lesions: an overview. Neurosurgery 27: 789–798
48. Huber W, Poeck K, Weniger D, Willmes D (1989) Aphasie. In: Poeck K (ed) Klinische Neuropsychologie. Poeck K, Stuttgart
49. Huber W, Poeck K, Weniger D, Wilmes D (1983) Der Aachener aphasie test. Hogrefe, Gottingen

50. Hullay J, Tomits GH (1965) Experiences with total removal of tumors of the acoustic nerve. J Neurosurg 22: 127–135
51. Jackson LE, Roberson JB Jr (1999) Vagal nerve monitoring in surgery of the skull base: a comparison of efficacy of three techniques. Am J Otol 20: 649–656
52. James HE, Mulcahy JJ, Walsh W, Kaplan GW (1979) Use of anal sphincter electromyography during operations on the conus medullaris and sacral nerve roots. Neurosurgery 4: 521–523
53. Jasper HH (1958) The ten–twenty electrode system of the international federation. Electroenphalogr Clin Neurophysiol 10: 371
54. Jones NS (1997) Visual evoked potentials in endoscopic and anterior skull base surgery: a review. J Laryngol Otol 111: 513–516
55. Jünemann KP, Schmid RA, Melchior H, Tanagho EA (1987) Neuroanatomy and clinical significance of the external urethral sphincter. Urol Int 42: 132–136
56. Kalmanchey R, Avila A, Symon L (1986) The use of brainstem auditory evoked potentials during posterior fossa surgery as a monitor of brainstem function. Acta Neurochir (Wien) 82: 128–136
57. Kartush JM, Bouchard KR (1992) Intraoperative facial nerve monitoring. In: Kartush JM, Bouchard KR (eds) Neuromonitoring in otology and head and neck surgery. Raven Press, New York, pp 99–120
58. Kartush JM (1989) Electroneurography and intraoperative facial monitoring in contemporary neurootology. Otolaryngol Head Neck Surg 101: 496–503
59. Kawaguchi M, Ohnishi H, Sakamoto T, Shimizu K, Touho H, Monobe T, Karasawa J (1995) Intraoperative electrophysiologic monitoring of cranial motor nerves in skull base surgery. Surg Neurol 43: 177–181
60. Kertesz A (1983) Localisation of lesions in Wernicke's aphasia. In: Kertesz A (ed) Localisation in neuropsychologia. Kertesz A, New York
61. Kohn SE, Goodglas H (1985) Picture-naming in aphasia. Brain Lang 24: 266–283
62. Kombos T, Suess O, Kern BC, Funk T, Pietila T, Brock M (2000) Can continuous intraoperative facial electromyography predict facial nerve function following cerebellopontine angle surgery? Neurol Med Chir (Tokyo) 40: 501–505; discussion 506–507
63. Kothbauer K, Deletis V, Epstein FJ (1997) Intraoperative spinal chord monitoring for intramedullary surgery: an essential adjunct. Pediatr Neurosurg 26: 247–254
64. Kothbauer K, Schmid UD, Seiler RW, Eisner W (1993) Intraoperative motor and sensory monitoring of the cauda equina. Neurosurgery 34: 702–707
65. Krause F (1912) Surgery of the brain and spinal cord, Vol II. Rebman Co., New York
66. Kyoshima K, Kobayashi S, Gibo H, Kuroyanagi T (1993) A study of save entry zones via the floor of the fourth ventricle for brainstem lesions. J Neurosurg 78: 987–993
67. Lang JJ, Ohmachi N, Lang JS (1991) Anatomical landmarks of the rhomboid fossa (floor of the 4th ventricle), its length and width. Acta Neurochir (Wien) 113: 84–90
68. Legatt AD, Schroeder CE, Gill B, Goodrich JT (1992) Electrical stimulation and multichannel EMG recording for identification of functional neural tissue during cauda equina surgery. Childs Nerv Syst 8: 185–189
69. Lenarz T, Ernst A, Plinkert P (1994) Intraoperative facial nerve monitoring in the infratemporal fossa approach: improved preservation of nerve function. Eur Arch Otorhinolaryngol: S319–S320
70. Leonetti JP, Brackmann DE, Prass RL (1989) Improved preservation of facial nerve function in the infratemporal approach to the skull base. Otolaryngol Head Neck Surg 101: 74–78
71. Leonetti JP, Jellish WS, Warf P, Hudson E (1996) Intraoperative vagal nerve monitoring. Ear Nose Throat J 75: 489–491, 495–496
72. Lesser RP, Raudzens P, Luders H, Nuwer MR, Goldie WD, Morris HH, Dinner DS, Klem G, Hahn JF, Shetter AG, et al. (1986) Postoperative neurological deficits may occur despite unchanged intraoperative somatosensory evoked potentials. Ann Neurol 19: 22–25
73. Lesser RP, Hahn J, Lueders H, Rothner AD, Ehrenberg G (1981) The use of chronic subdural electrodes for cortical mapping of speech. Epilepsia 22: 240
74. Lesser RP, Lueders H, Dinner DS, et al. (1984) The location of speech and writing functions in the frontal language area. Results of extraoperative cortical stimulation. Brain 107: 275–291
75. Lesser RP, Lueders H, Hahn J, Dinner DS, Morris HH, Klem G (1983) Afterdischarge and functional alteration thresholds in the frontal and temporal lobes: extraoperative testing. Epilepsia 24: 518–519
76. Levesque MF, Sutherland WW, Risinger M, Becker DP, Crandall PH (1989) Variability of speech cortex during functional localisation – implication for plasticity. J Neurosurg 70: 329–330
77. Levine DN, Sweet E (1983) Localisation of lesions in Broca's motor aphasia. In: Kertesz A (ed) Localisation in neuropsychology. Kertesz A, New York
78. Linden RD, Tator CH, Benedict C, Charles D, Mraz V, Bell I (1988) Electrophysiological monitoring during acoustic neuroma and other posterior fossa surgery. Can J Neurol Sci 15: 73–81
79. Lueders H, Lesser RP, Dinner DS, et al. (1983) Inhibition of motor activity by elicited electrical stimulation of the human cortex. Epilepsia 24: 519
80. Lueders H, Lesser RP, Hahn J, et al. (1986) Basal temporal language area demonstrated by electrical stimulation. Neurology 36: 505–510
81. Magliulo G, Petti R, Vingolo GM, Cristofari P, Ronzoni R (1994) Facial nerve monitoring in skull base surgery. J Laryngol Otol 108: 557–559

82. Magliulo G, Petti R, Vingolo GM, Ronzoni R, Cristofari P (1994) Facial nerve monitoring of skull base and cerebellopontine angle lesions. Eur Arch Otorhinolaryngol: S314–S315
83. Magliulo G, Zardo F (1997) Intra-operative facial nerve monitoring. Its predictive value after skull base surgery. J Laryngol Otol 111: 715–718
84. Mann WJ, Maurer J, Pelster H, Riechelmann H, Wolfensberger M, Amedee RG (1993) Modifications of a nerve integrity monitor useful in skull base surgery. Otolaryngol Head Neck Surg 109: 777–779
85. Matthies C, Samii M (1997) Direct brainstem recording of auditory evoked potentials during vestibular schwannoma resection: nuclear BAEP recording. Technical note and preliminary results. J Neurosurg 86: 1057–1062
86. Matthies C, Samii M (1997) Management of vestibular schwannomas (acoustic neuromas): the value of neurophysiology for evaluation and prediction of auditory function in 420 cases. Neurosurgery 40: 919–929
87. Merton PA, Hill DK, Morton HB, Marsden CD (1982) Scope of a technique for electrical stimulation of human brain, spinal cord, and muscle. Lancet 2(8298): 597–600
88. Mohr JP (1976) Broca's area and Broca's aphasia. In: Whitaker H, Whitaker HA (eds) Studies in neuroliguistics. Whitaker, New York, pp 201–236
89. Moller A, Jannetta P (1985) Monitoring of facial nerve function during removal of acoustic tumor. Am J Otol Suppl 11: 27–29
90. Moller AR (1988) Intraoperative Monitoring of cranial motor nerves. In: Moller AR (ed) Evoked potentials in intraoperative monitoring. Williams & Wilkins, Baltimore, pp 99–120
91. Moller AR (1995) Intraoperative neurophysiological monitoring. Harwood Academic Pub
92. Moller AR (1991) Neuromonitoring in operations in the skull base. Keio J Med 40: 151–159
93. Ojemann GA (1988) Effect of cortical and subcortical stimulation in human language and verbal memory. In: Plum F (ed) Language communication and the brain. Plum F, New York, pp 101–115
94. Ojemann GA (1983) Brain organisation for language from the perspective of electrical stimulation mapping. Behav Brain Sci 6: 189–206
95. Ojemann GA (1983) Electrical stimulation and the neurobiology of language. Behav Brain Sci 6: 221–230
96. Ojemann GA (1979) Individual variability in cortical localisation of language. Brain Lang 6: 239–260
97. Ojemann GA, Ojemann J, Lettich E, Berger MS (1989) Cortical language localisation in left, dominant hemisphere. An electrical stimulation mapping investigation in 117 Patients. J Neurosurg 71: 316–326
98. Ojemann GA, Whitaker HA (1978) Language localisation and variability. Brain Lang 6: 239–260
99. Ojemann GA, Whitaker HA (1978) The bilingual brain. Arch Neurol 35: 409–412
100. Oldfield RC (1971) The assessment and analysis of handedness: the Edinburgh inventory. Neuropsychologia 7: 97–113
101. Owen JH (1991) Evoked potential monitoring during spinal surgery. In: Bridwell KH, DeWald RL (eds) The textbook of spinal surgery. Lippincott, Philadelphia, J.B., pp 31–64
102. Pang D, Casey K (1983) Use of anal sphincter pressure monitor during operations on the sacral spinal cord and nerve roots. Neurosurgery 13: 562–568
103. Penfield W, Jasper HH (1954) In: Penfield W (ed) Epilepsy and the Functional Anatomy of the Human Brain. Penfield W, Boston
104. Penfield W, Roberts L (1959) Speech and brain mechanism. University Press, Princeton
105. Piatt JH Jr, Radtke RA, Erwin CW (1985) Limitations of brain stem auditory evoked potentials for intraoperative monitoring during a posterior fossa operation: case report and technical note. Neurosurgery 16: 818–821
106. Pool JL (1966) Suboccipital surgery for acoustic neurinomas: advantages and disadvantages. J Neurosurg 24: 483–492
107. Prass RL, Lüders H (1986) Acoustic (loudspeaker) facial electromyographic monitoring: evoked electromyographic activity during acoustic neuroma surgery. Neurosurgery 19: 392–400
108. Radtke RA, Erwin CW, Wilkins RH (1989) Intraoperative brainstem auditory evoked potentials: significant decrease in postoperative morbidity. Neurology 39: 187–191
109. Rand RW, Kurze TL (1965) Facial nerve preservation by posterior fossa transmeatal microdissection in total removal of acoustic tumors. J Neurol Neurosurg Psychiat 28: 311–316
110. Rank JB Jr (1975) Which elements are excited in electrical stimulation of mammalian central nervous system. Brain Res 98: 417–440
111. Reulen HJ, Schmid DU, Ilmberger J, Eisner W, Bise K (1997) Tumor surgery of the speech cortex in local anesthesia. Neuropsychological and neurophysiological monitoring during operations in the dominant hemisphere. Nervenarzt 68: 813–824
112. Romstöck J, Strauss C, Fahlbusch R (2000) Continuous electromyographic monitoring of motor cranial nerves during cerebellopontine angle surgery. J Neurosurg 93: 586–593
113. Rostomily RC, Berger MS, Ojemann GA, Lettich E (1991) Postoperative deficits and functional recovery following removals of tumors involving the dominant hemisphere supplementary motor area. J Neurosurg 75: 62–68
114. Samii M, Matthies C (1997) Mangement of 1000 vestibular schwannomas (acoustic neuromas): the facial nerve-preservation and restitution of function. Neurosurgery 40: 684–694

115. Sasaki T, Suzuki K, Kodama N (2000) Intraoperative monitoring of electrooculograms. J Neurosurg 92: 1077–1079
116. Schipper J, Ridder GJ, Arapakis I, Gellrich NC, Spetzger U, Maier W (2004) Neurophysiologic intraoperative monitoring to preserve cranial nerve function in base of skull surgery. HNO 52: 897–907
117. Schlake HP, Goldbrunner R, Milewski C, Siebert M, Behr R, Riemann R, Helms J, Roosen K (1999) Technical developments in intra-operative monitoring for the preservation of cranial motor nerves and hearing in skull base surgery. Neurol Res 21: 11–24
118. Schlake HP, Goldbrunner R, Siebert M, Behr R, Roosen K (2001) Intra-operative electromyographic monitoring of extra-ocular motor nerves (Nn. III, VI) in skull base surgery. Acta Neurochir (Wien) 143: 251–261
119. Schlake HP, Goldbrunner RH, Milewski C, Krauss J, Trautner H, Behr R, Sorensen N, Helms J, Roosen K (2001) Intra-operative electromyographic monitoring of the lower cranial motor nerves (LCN IX–XII) in skull base surgery. Clin Neurol Neurosurg 103: 72–82
120. Schmid UD, Moller AR, Schmid J (1992) Transcranial magnetic stimulation of the facial nerve: intraoperative study on the effect of stimulus parameters on the excitation site of man. Muscle Nerve 15: 829–836
121. Schramm J, Mokrusch T, Fahlbusch R, Hochstetter A (1988) Detailed analysis of intraoperative changes monitoring brain stem acoustic evoked potentials. Neurosurgery 22: 694–702
122. Schramm J, Watanabe E, Strauss C, Fahlbusch R (1989) Neurophysiologic monitoring in posterior fossa surgery. I. Technical principles, applicability and limitations. Acta Neurochir (Wien) 98: 9–18
123. Sekhar LN, Moller AR (1986) Operative management of tumors involving the cavernous sinus. J Neurosurg 64: 879–889
124. Sekiya T, Hatayama T, Iwabuchi T, Maeda S (1993) Intraoperative recordings of evoked extraocular muscle activities to monitor ocular motor nerve function. Neurosurgery 32: 227–235; discussion 235
125. Shinomiya K, Fuchioka M, Matsuoka T, Okamoto A, Yoshida H, Mutoh N, Furuya K, Andoh M (1991) Intraoperative monitoring for tethered spinal cord syndrome. Spine 16: 1290–1294
126. Sloan TE (1997) Evoked responses in neurosurgery. In: Albin M (ed) Textbook of neuroanesthesia: with neurosurgical and neuroscience perspectives. McGraw Hill, New York, pp 221–276
127. Soustiel JF, Hafner H, Chistyakov AV, Guilburd JN, Zaaroor M, Yussim E, Feinsod M (1993) Monitoring of brain-stem trigeminal evoked potentials. Clinical applications in posterior fossa surgery. Electroencephalogr Clin Neurophysiol 88: 255–260
128. Stechison MT (1994) Neurophysiologic monitoring during cranial base surgery. J Neurooncol 20: 313–325
129. Stöhr M (1989) Physiologie und Pathophysiologie der Impulsleitung. In: Stöhr M, Dichgans J, Diener HC, Buettner UW (eds) Evozierte Potentiale. Springer, Berlin, pp 1–128
130. Strauss C, Romstöck J, Nimsky C, Fahlbusch R (1993) Intraoperative identification of motor areas of the rhomboid fossa using direct stimulation. J Neurosurg 79: 393–399
131. Uziel A, Benezech J, Frerebeau P (1993) Intraoperative facial nerve monitoring in posterior fossa acoustic neuroma surgery. Otolaryngol Head Neck Surg 108: 126–134
132. Van Buren JM, Fedio P, Frederick GC (1978) Mechanism and localisation of speech in parietotemporal cortex. Neurosurgery 2: 233–239
133. Wada J, Rasmussen T (1960) Intracarotid injection of sodium amytal for the lateralisation of speech dominance. J Neurosurg 17: 266–282
134. Wee AS, al-Mefty O, Ashley RA (1990) Electrophysiologic monitoring of the facial nerve during basal cranial and posterior fossa surgeries. J Miss State Med Assoc 31: 251–254
135. Wernicke C (1874) Der aphasische Symptomenkomplex. Universitätsschrift, Breslau
136. Whitaker HH, Ojemann GA (1978) Graded localisation of naming from electrical stimulation mapping of left cerebral cortex. Nature 270: 50–51
137. Wolf SR, Schneider W, Suchy B, Eichhorn B (1995) Intraoperative facial nerve monitoring in parotid surgery. HNO 43: 294–298
138. Zimmermann R, Spetzler RF, Lee KS, Zabramski JM, Hargraves W (1991) Cavernous malformations of the brainstem. J Neurosurg 75: 32–39

Chapter 4. Surgical treatment of vascular lesions in the central skull base

Surgical treatment of large/giant carotid–ophthalmic and other intradural internal carotid artery aneurysms

E. de Oliveira[1,3], E. G. Figueiredo[2,3,4], W. M. Tavares[2], A. L. Rhoton Jr[5]

[1]Department of Neurological Surgery, State University of Campinas and Instituto de Ciencias Neurologicas, Sao Paulo, Brazil
[2]Department of Neurological Surgery, University of Sao Paulo School of Medicine, Sao Paulo, Brazil
[3]Microsurgery Laboratory Hospital de Beneficencia Portuguesa, Sao Paulo, Brazil
[4]Instituto de Doencas Neurologicas, Sao Paulo, Brazil
[5]Department of Neurological Surgery, University of Florida, Gainesville, FL, USA

Introduction

Surgical approaches to paraclinoid aneurysms (PCAs) have evolved considerably since the early 1980s, when Dolenc's work clarified the anatomy of the cavernous sinus and the paraclinoid region. An improved understanding of this anatomy has led to the area no longer being considered prohibited territory for surgeons [1, 2, 6, 7]. The Dolenc method has revolutionized the management of PCAs, dividing thought about their treatment into distinct eras, pre-Dolenc and post-Dolenc [6, 7].

In addition to the complex regional anatomy [3–6], the surgery of paraclinoid aneurysms is further complicated by considerations of the size and shape of the lesion, the safest and most efficient approach to it, the most feasible site to gain proximal control of the internal carotid artery, and the risk of deteriorating vision with surgery [6, 7]. Here we present a comprehensive review of pertinent surgical anatomy and nuances of the surgical techniques employed by the senior author for these demanding aneurysms.

Microsurgical anatomy

PCAs occur at the site where the internal carotid artery (ICA) enters the skull, establishing an intricate relationship with structures in the vicinity of the roof of the cavernous sinus. Commonly considered "ophthalmic segment" aneurysms, they are better termed "paraclinoid" lesions because of the typically close relationship with the anterior clinoid process (ACP). The ophthalmic segment of the ICA extends from the origin of the ophthalmic artery to the origin of the posterior communicating artery. In many cases, the presence of the ACP makes the origin of the ophthalmic artery difficult to establish, either radiographically or surgically (Fig. 1).

The ACP, the medial end of the lesser sphenoid wing, forms the roof of the cavernous sinus anteriorly. It also limits the optic canal laterally. The optic strut is a bony bridge extending from the lower margin of the ACP to the body of the sphenoid bone, separating the optic canal from the superior orbital fissure. Since the ACP may be pneumatized, and communicate with the sphenoid sinus, its removal may expose the mucous membrane of the sphenoid sinus. More commonly, however, the ACP is solid bone which is bulky or very long, projecting into the cavernous sinus posterior to the anterior loop of the ICA [6, 7].

A bony or fibrous bridge may unite the anterior and posterior clinoid processes, which may compli-

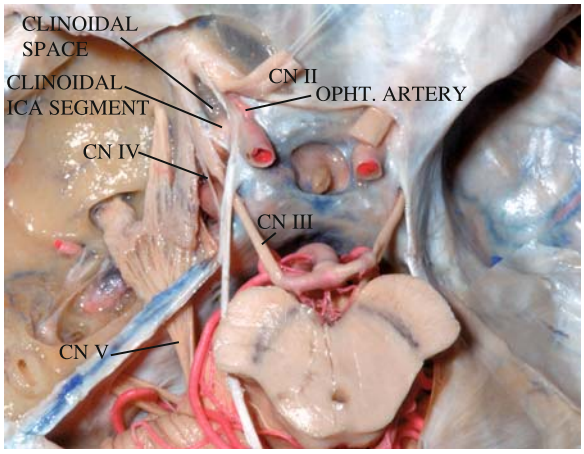

Fig. 1. Anatomical view of dissection of the clinoidal segment of the internal carotid artery. Dura mater has been removed over the optic canal, the middle fossa and lateral surface of the cavernous sinus. The tentorium cerebelli has been incised and reflected posteriorly to show the course of the cranial nerves within the cavernous sinus. The anterior clinoid process has been removed to expose the clinoidal segment of the ICA. Bone has been drilled posterior to the intrapetrous ICA to expose the superior semicircular canal, the cochlea, and the geniculate ganglion. *CN II* Optic nerve; *CN III* oculomotor nerve; *CN IV* trochlear nerve; *CN V* trigeminal nerve; *ICA* internal carotid artery; *Opht. Artery* ophthalmic artery

cate removal of the ACP. In addition, the anterior and middle clinoid processes may be bridged by bone forming the caroticoclinoid foramen at the distal end of the clinoidal segment of the ICA. Here bone surrounds the ICA inferomedial to the ACP, posterolateral to the optic strut, and lateral to the wall of the sphenoid sinus. Removing the ACP exposes the anteromedial triangle, dural folds covering the optic nerve medially, the oculomotor nerve laterally, and dura posteriorly. The anterior loop of the ICA (the clinoidal segment), in the anteromedial corner of the cavernous sinus, may be exposed through the anteromedial triangle [7].

The superior orbital fissure is limited superiorly by the lesser sphenoid wing, below by the greater sphenoid wing, and medially by the body of the sphenoid bone. Removal of the ACP unveils the clinoidal segment of the ICA, which is surrounded by a pair of distinct dural rings and is continuous with the ICA's anterior vertical segment. These dural rings define the anatomical limits of the clinoidal segment. The proximal ring, the carotid-oculomotor membrane, is composed of tenuous connective tissue constituting the roof of the cavernous sinus. It extends from the oculomotor nerve to the lateral surface of the ICA and to the posterior clinoid process. This membrane separates venous contents of the cavernous sinus from the space occupied by the ACP [7].

Dura at the base of the skull extends to the ACP, tightly enveloping the ICA as it enters the subarachnoid space to form the distal ring. The supraclinoid ICA enters the subarachnoid space medial and inferior to the ACP. Dura forming the distal ring is contiguous medially with dura of the diaphragma sellae, and laterally with dura adjacent to the ACP. Usually the ophthalmic artery arises immediately above the clinoidal segment, from the anteromedial or superomedial surface of the ICA and beneath the medial half of the optic nerve. This artery typically lies within the subarachnoid space throughout its intracranial course, attached to the inferior surface of the optic nerve by a loose mesh of connective tissue. It then courses anterolaterally within the dural sheath of the optic canal, ultimately reaching the orbital apex on the inferolateral surface of the optic nerve. Occasionally it arises from the clinoidal segment or even from the intracavernous ICA in the oculomotor triangle, between the posterior clinoid process and the anterior edge of the tentorium, then passing along the lower margin of the ACP to the superior orbital fissure.

Removing the ACP plus a section of the distal ring is an important step, providing a site for temporary clipping of the ICA for the purpose of gaining proximal control of the vessel in the event of arterial bleeding, and to allow better visualization of the proximal part of the neck of the aneurysm. Care must be taken to avoid damaging the oculomotor nerve as the ACP is removed [6, 7].

Types of aneurysms

Paraclinoid aneurysms arise from the superomedial surface of the ICA, near the origin of the ophthalmic artery and the optic nerve. They may project superiorly or superomedially ("true" ophthalmic aneurysms), or may take origin from the posterior or posteromedial surfaces of the carotid artery, then project either inferiorly to the para-

sellar region, or medially underneath the optic chiasm (following the course of the superior hypophyseal arteries). However, these lesions may arise from any location throughout the circumference of the ICA wall. They are defined by the relationship between the neck of the aneurysm and its site of origin from the internal carotid artery [6, 7].

These aneurysms may also project inferomedially. Such lesions demand arterial reconstruction procedures. There are two basic variants: (1) the aneurysm is directed upward, and (2) it projects downward. Any other projection should be considered a variant of these two types. Clinical symptoms, surgical planning, and clip application technique, including choice of clip design, all depend upon the direction of projection [6, 7].

Like other aneurysms, PCAs usually present with subarachnoid hemorrhage; nonetheless, the percentage of unruptured PCAs causing neurologic deficits is much higher than in any other group of aneurysms. The specific neurological deficit that occurs depends on the aneurysm's location, projection, and size. Aneurysms projecting superiorly usually produce visual symptoms by trapping the optic nerve superiorly against the falciform ligament anteriorly and posteriorly against the A1 segment of the anterior cerebral artery. Even though these aneurysms are not in the proximity of perforating branches of the ICA, their surgical management requires manipulating the optic nerve, placing vision at risk.

Aneurysms arising from the posterior or posteromedial surfaces of the ICA, projecting inferiorly to the parasellar region or medially beneath the optic chiasm, usually have a close relationship with ICA perforating branches. Such aneurysms often are large or even giant lesions, typically presenting as masses adherent to dura at the base of the skull. Whether or not perforating branches can be preserved is one of the most important factors predictive of surgical outcome. Often the sacs of such aneurysms, which typically are found adherent to skull base dura, must be opened and emptied of blood and debris, requiring that the ICA be reconstructed. In order to assure accurate dissection and manipulation of these aneurysms, it is mandatory to completely expose the clinoidal segment and section the dural rings. Only then can the proximal ICA be fully mobilized and clips applied which occlude the aneurysm without narrowing the lumen of the ICA [6, 7].

Surgical technique

Treatment of PCAs using the approach described by Dolenc involves removing the orbital roof, sphenoid wing, and optic canal; drilling away the ACP; and exposing the clinoidal segment of the ICA [1, 2, 4, 5]. Dolenc also exposes the intrapetrous segment of the ICA extradurally in the middle fossa in order to provide proximal control of arterial bleeding [1, 2].

The superior and medial walls of the orbit are removed through a standard pterional craniotomy in order to expose the superior orbital fissure completely. The superior and medial walls of the optic canal are carefully removed, exposing the clinoidal segment of the ICA and permitting the optic nerve to be mobilized medially.

Removal of the medial wall of the optic canal implies significant risk of postoperative cerebrospinal fluid (CSF) leak because the sphenoid sinus may be violated during drilling. The inferior wall of the optic canal is formed by the so-called optic strut, the removal of which makes it possible to section the dural rings [6, 7] (Fig. 2).

This technique may be tailored to specific cases. For true ophthalmic aneurysms, i.e., those with superior or superomedial projections, the extradural approach may be combined with intradural resection of the ACP under direct visualization of the aneurysm. As previously mentioned, a broad aneurysm neck sometimes penetrates the clinoidal space. In addition, for those aneurysms projecting superolaterally, the dome of the aneurysm may be positioned in such a way that it projects into the ACP, making its extradural removal quite risky. If removal of the clinoid process is to be completed intradurally, the basal cisterns should be opened first and the supraclinoid ICA identified [6, 7]. This allows ready access to the supraclinoid segment of the carotid artery if an inadvertent rupture occurs.

In the classic extradural exposure, after the ACP is removed and the optic canal unroofed, the dura mater is opened. The dural incision starts by following the superficial sylvian vein toward the superior orbital fissure, then proceeds to the clinoidal space. In the clinoidal space, the incision changes direction, proceeding medially and exposing the extra- and

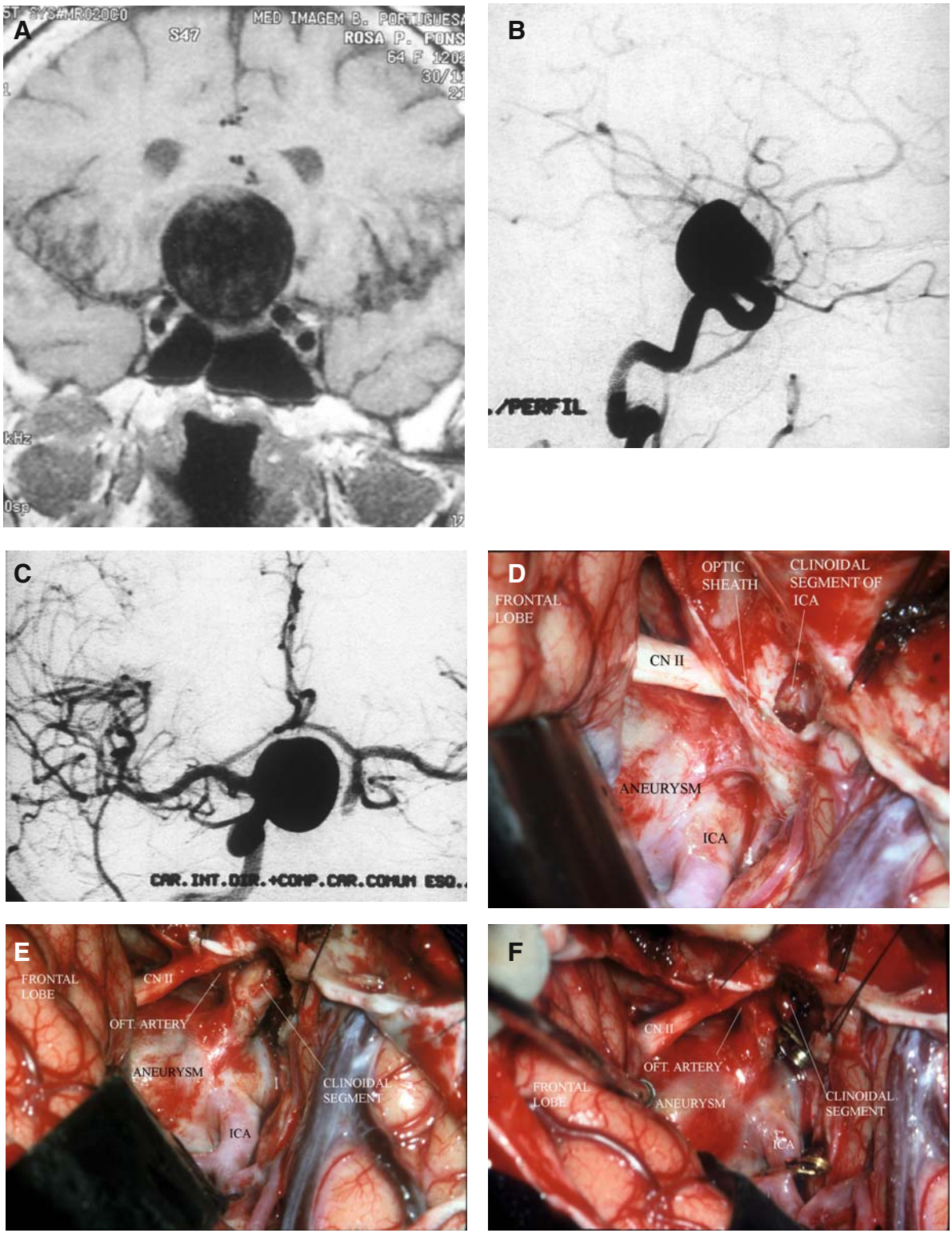

Fig. 2. *(Continued)*

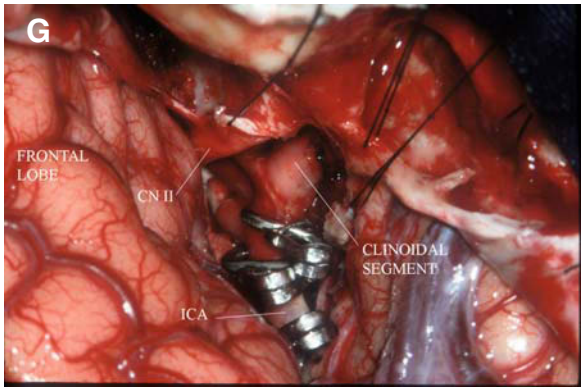

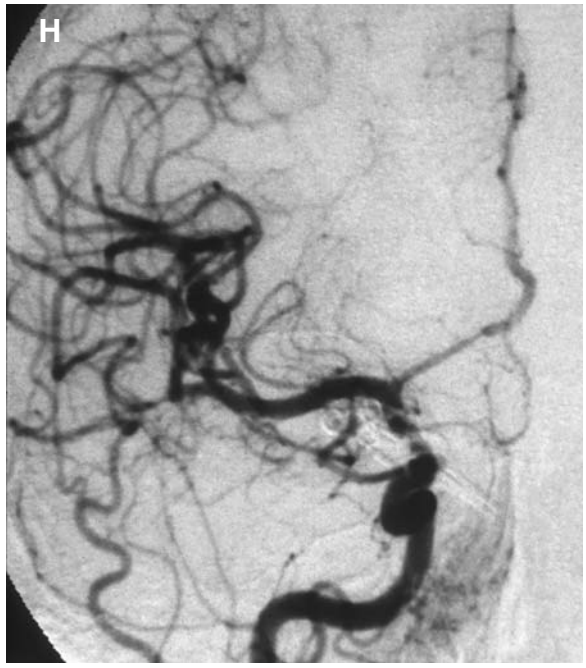

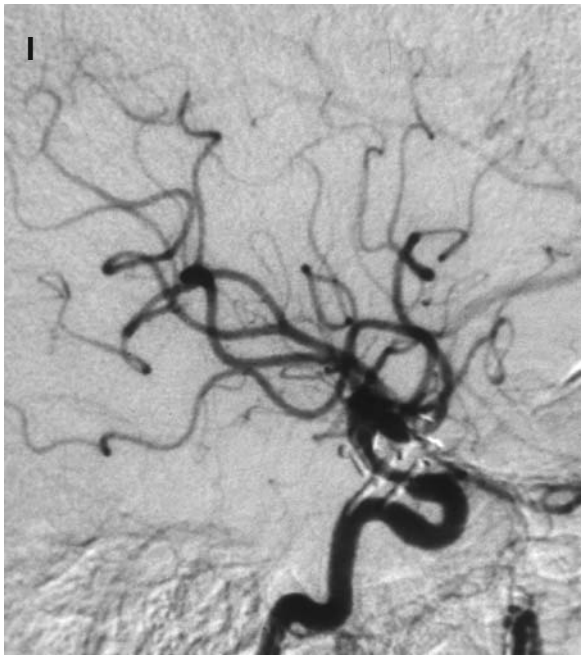

Fig. 2. **A** A magnetic resonance image showing a giant, partially-thrombosed paraclinoid aneurysm. **B** Antero-posterior right carotid angiogram revealing a paraclinoid aneurysm projecting medially. **C** Lateral view. **D** Intraoperative view. The orbital roof and the anterior clinoid process have been removed, and the clinoidal segment of the internal carotid artery has been exposed. **E** The optic sheath has been opened and the ophthalmic artery has been exposed. *CN II* Optic nerve; *ICA* internal carotid artery; *Opht. Artery* ophthalmic artery. **F, G** Aneurysm has been deflated and clipped. **H** Postoperative lateral carotid angiogram showing obliteration of the aneurysm. **I** Postoperative antero-posterior carotid angiogram

intradural portions of the optic nerve and the extra- and intradural course of the ICA. After the dura is opened, the sylvian and basal cisterns are widely dissected to minimize brain retraction.

Then the lateral surface of the dural sheath enveloping the optic nerve is carefully incised. Because of the potential for the ophthalmic artery to be adherent to the optic sheath as it courses laterally beneath the optic nerve, care must be taken not to injure it. The optic nerve may then be displaced medially, allowing identification of the ophthalmic artery and access to the proximal part of the neck of the aneurysm.

The clinoidal segment of the ICA is denuded of its covering (the carotid-oculomotor membrane) and prepared for temporary clipping. At this point, any bleeding from the cavernous sinus may be controlled by packing with Surgicel^{TM}. Excessive packing

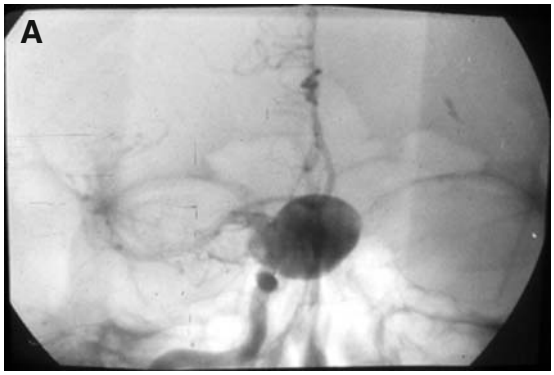
A

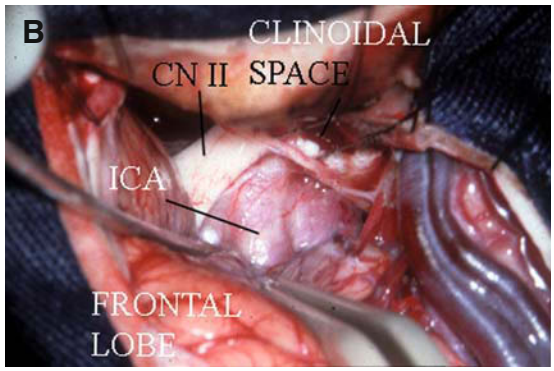
B
CLINOIDAL
CN II SPACE
ICA
FRONTAL
LOBE

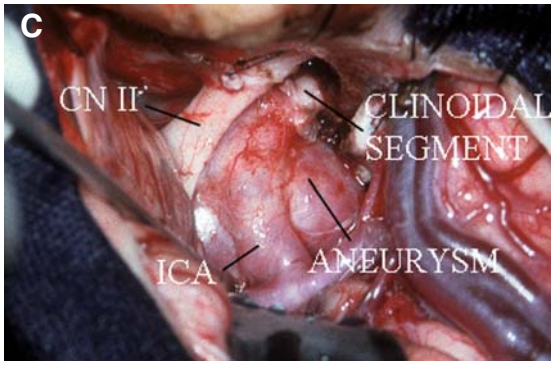
C
CN II
CLINOIDAL
SEGMENT
ICA
ANEURYSM

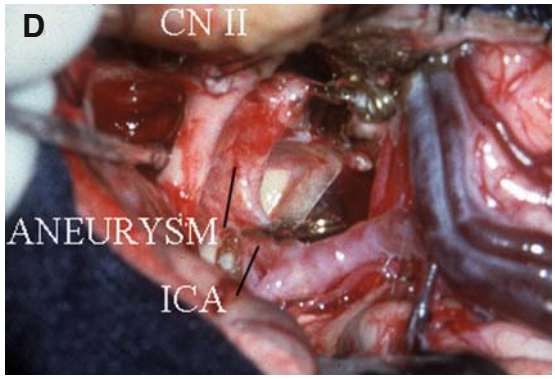
D
CN II
ANEURYSM
ICA

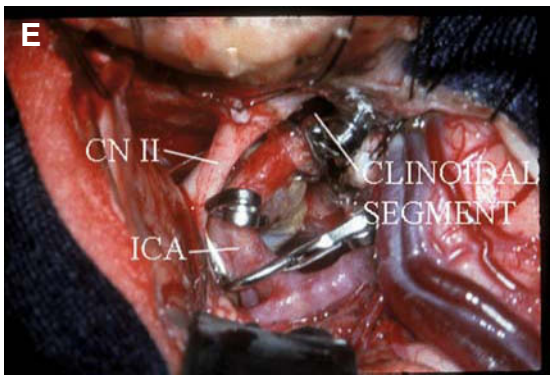
E
CN II
CLINOIDAL
SEGMENT
ICA

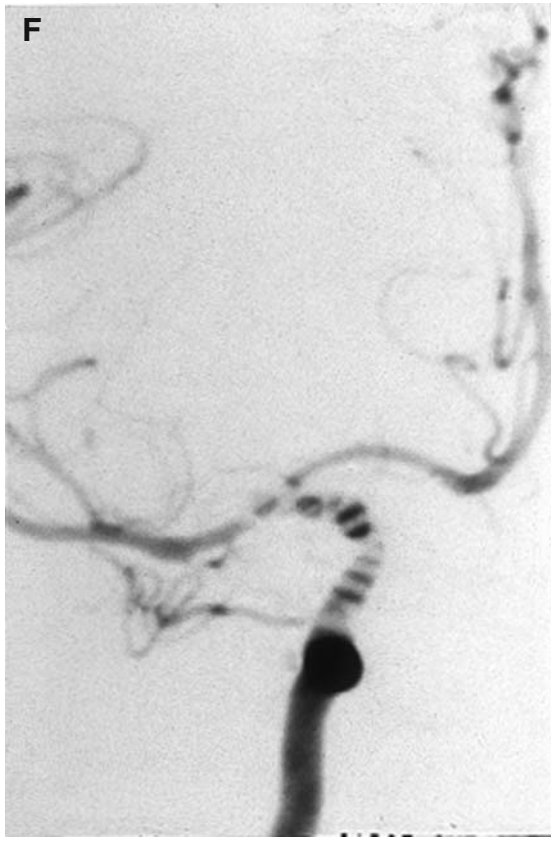
F

should be avoided, however, since it may produce stenosis of the carotid artery within the cavernous sinus (Fig. 3).

Then the distal dural ring surrounding the carotid artery is completely incised to allow mobilization of its anterior vertical segment. This is of paramount importance in exposing the proximal part of the neck, therefore ensuring proper clip placement. For those aneurysms projecting superiorly or superomedially, complete incision of the dural ring avoids narrowing the parent vessel after clipping. This arterial narrowing is to be expected if the inferior

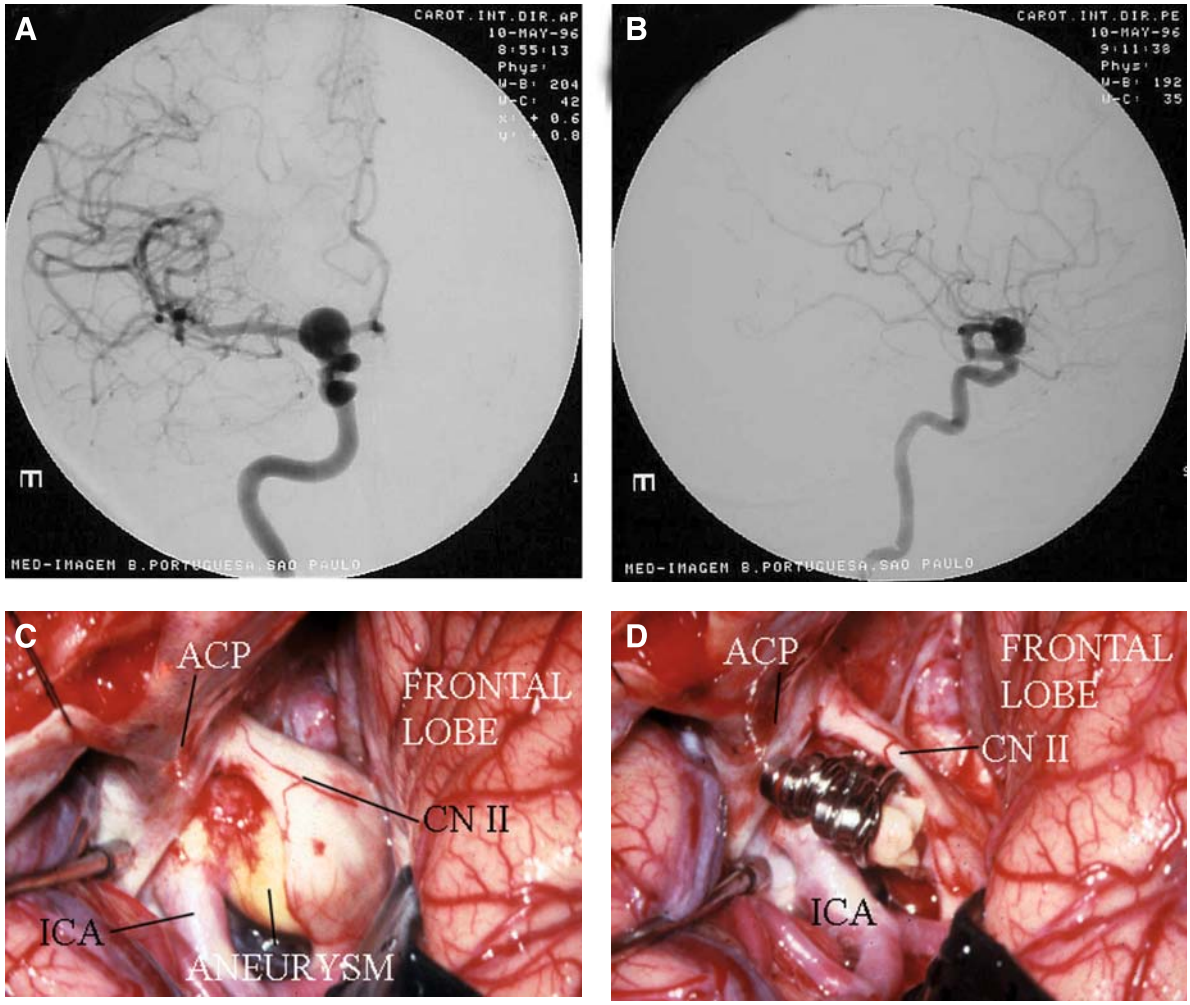

Fig. 4. Digital right carotid angiogram of a paraclinoid aneurysm projecting superiorly. **A** Frontal view, **B** lateral view, **C** intraoperative view. As the aneurysm projects superiorly, the orbital roof and the anterior clinoid process have not been removed. **D** The aneurysm has been clipped and opened. *ACP* Anterior clinoid process; *CN II* optic nerve; *ICA* internal carotid artery; *Opht. Artery* ophthalmic artery

Fig. 3. **A** Digital right carotid angiogram of a paraclinoid aneurysm projecting posteriorly. **B** Intraoperative view after removal of the orbital roof and the anterior clinoid process. **C** The orbital roof and the anterior clinoid process have been removed, and the clinoidal segment of the internal carotid artery has been exposed. **D** The optic sheath has been opened. **D, E** The aneurysm has been clipped and the ICA reconstructed. *CN II* Optic nerve; *ICA* internal carotid artery. **F** Postoperative digital right carotid angiogram showing obliteration of the aneurysm

wall of the artery is left fixed to dura at the base of the skull. A similar situation relative to sectioning the dural ring occurs with those aneurysms with inferior or inferomedial projections [6, 7]. These aneurysms usually present with broad necks extending to the level of the dural ring, making its incision mandatory for proper clip placement and complete obliteration of the aneurysmal neck. If the proximal and inferior surfaces of neck are not freed from their attachments to the dural ring, and if the inferior surface of the anterior vertical segment of the ICA is not properly exposed, completely closing the blades of the clip will result in stenosis of the parent vessel (Fig. 4).

The ophthalmic segment of the ICA is the site of origin of several perforating branches which arise from the inferior or inferomedial walls of the artery and supply the optic nerve, pituitary stalk, and chiasm. Several perforating branches also originate from the posterior communicating and choroidal segments of the ICA. These arteries can be displaced by large or giant carotid–ophthalmic aneurysms, and must always be preserved. Sacrificing them results in high rates of surgical morbidity.

After the perforating vessels are dissected from the walls of the aneurysm and sufficient space is obtained from the proximal exposure of the neck, we often place a fenestrated right-angled clip, directed from proximal to distal, to first occlude the proximal part of the neck. After that, depending on other factors, the artery is reconstructed with clips of various types (Fig. 3). Temporarily clipping the clinoidal segment and the distal ICA below the level of the posterior communicating artery permits the aneurysmal sac to be deflated and evacuated of its contents prior to definitive clip placement.

In cases of very small paraclinoid aneurysms, we often use an intradural approach. The only difference is that we use a wider dural incision, which allows the optic canal to be unroofed and the ACP removed, fully exposing the clinoidal segment of the ICA [6, 7]. The intradural approach may be tailored depending on anatomical features of the aneurysm, insuring a safer removal of the ACP.

Because angiographic examinations provide only indirect information about the anatomy of the ICA and the neck of the aneurysm, the probability of direct clipping is difficult to predict prior to surgical intervention. Large lesions have, at times, surprisingly small necks that cannot be detected preoperatively.

For those patients who show any risk of permanent occlusion of the ICA after four-vessel angiography, or those who have insufficient collateral circulation, a high-flow bypass procedure (a long saphenous vein graft from the external carotid artery to the sylvian middle cerebral artery) should be considered. A bypass should also be performed when an excessive interval of temporary clipping is anticipated. Maintaining flow distal to the lesion via a venous graft permits a safer operation without imposing time limits for temporarily interrupting flow in the ICA.

Proximal control

Proximal control of arterial bleeding may be achieved at three different sites: the cervical segment, the petrous segment, or the clinoidal segment of the ICA. We differ from Dolenc in that we expose the common, internal, and external carotid arteries in the neck before performing the craniotomy. We believe that exposing the extracranial carotid bifurcation is a much safer means of obtaining early proximal control of arterial bleeding than exposing the petrous ICA segment because anatomical variants sometimes encountered with the latter procedure are difficult to predict. Although extremely important, exposing the clinoidal segment of the ICA for proximal control (by temporary clipping) of bleeding from inadvertent aneurysmal rupture cannot always be achieved readily [6, 7].

Visual impairment

It is well known that untreated aneurysms tend to continue to grow and compress the optic apparatus. Surgery or other methods of treatment do not assure visual recovery or improvement; yet, direct surgery remains the only treatment that provides the reduction of an aneurysm's mass effect, offering the possibility for visual recovery or for the arrest of visual deterioration. Nevertheless, visual deficits may worsen even after surgery. Possible causes of postoperative visual deterioration are: (a) damage to the optic nerve during removal of the ACP and optic strut, (b)

optic nerve injury while unroofing the optic canal (from heat or direct injury caused by the high-speed drill), (c) excessive manipulation of the optic nerve during dissection, and (d) damaging branches of the ICA supplying the optic nerve and chiasm while the aneurysm is being dissected or clipped. There are instances, however, in which the cause of visual deterioration cannot be identified.

Other methods of treatment, such as endovascular procedures, are promising but have not proven to be capable of dealing with large aneurysmal necks or of obliterating larger lesions without sacrificing the ICA. Moreover, endovascular procedures cannot alleviate an aneurysm's mass effect and carry a significant risk of major complications, primarily from thromboembolic events.

Conclusion

The preferred treatment of paraclinoid aneurysms is direct clipping of the aneurysmal neck with reconstruction of the carotid artery and decompression of the optic apparatus, whenever possible. This applies to both symptomatic and asymptomatic patients whenever the aneurysm seems to be amenable to clipping, whether or not the aneurysm has ruptured, because these lesions tend to continue to grow and produce neurological impairment due to mass effect. Those patients whose clinical conditions result in a contraindication to surgical intervention should be considered for alternative methods of treatment [6, 7].

References

1. Dolenc VV (1983) Direct microsurgical repair of intracavernous vascular lesions. J Neurosurg 58: 824–831
2. Dolenc VV (1985) A combined epi- and subdural approach to carotid–ophthalmic artery aneurysms. J Neurosurg 62: 667–672
3. Figueiredo EG, Gomes M, Vellutini E, Rosemberg S, Marino R Jr (2005) Angioleiomyoma of the cavernous sinus: case report. Neurosurgery 56: E411
4. Figueiredo EG, Zabramski JM, Deshmukh P, Crawford NR, Preul MC, Spetzler RF (2006) Anatomical and quantitative description of the transcavernous approach to interpeduncular and prepontine cisterns. J Neurosurg 104: 1–8
5. Figueiredo EG, Zabramski JM, Deshmukh P, Crawford NR, Spetzler RF, Preul MC (2006) Comparative analysis of anterior petrosectomy and transcavernous approaches to retrosellar and upper clival basilar artery aneurysms. Neurosurgery 58: 13–21
6. Oliveira E, Tedeschi H, Rhoton AL Jr, Peace DA (1996) The treatment of giant aneurysms of the carotid ophthalmic artery: coils vs. decompression clipping technique. In: Al-Mefty O, Origitano TC, Harkey HL (eds) Controversies in neurosurgery, Thieme, New York, pp 175–181
7. Oliveira E, Tedeschi H, Rhoton AL Jr (1997) Paraclinoid aneurysms – Management update – surgical treatment. Surg Cereb Stroke 25: 83–90

Surgical treatment of basilar apex aneurysms – surgical approaches and techniques

E. de Oliveira[1,3], E. G. Figueiredo[2,3,4], W. M. Tavares[2], A. L. Rhoton Jr.[5]

[1]Department of Neurological Surgery, State University of Campinas and Instituto de Ciencias Neurologicas, Sao Paulo, Brazil
[2]Department of Neurological Surgery, University of Sao Paulo School of Medicine, Sao Paulo, Brazil
[3]Microsurgery Laboratory Hospital de Beneficencia Portuguesa, Sao Paulo, Brazil
[4]Instituto de Doencas Neurologicas, Sao Paulo, Brazil
[5]Department of Neurological Surgery, University of Florida, Gainesville, FL, USA

Introduction

Basilar artery bifurcation aneurysms account for 5–8% of intracranial aneurysms [15] and constitute a major surgical challenge, due mainly to their depth within an extremely narrow surgical field, their intimate relationship with thalamoperforating arteries, and the difficulty gaining sufficient exposure of the basilar artery [11, 12, 16]. With the increasing number of endovascular procedures being performed, previously unsuccessfully coiled aneurysms have become more commonplace [24]. Furthermore, giant or wide-necked aneurysms and those which involve the posterior cerebral artery (PCA) at its neck generally are not embolized but are directly clipped. Thus, endovascular techniques have in a sense "raised the bar" for surgical expertise by selecting out a group of patients that have more difficult aneurysms [1].

The most popular approaches to treat basilar bifurcation aneurysms are via the subtemporal route [7, 8] and the pterional route [25, 26]. The advantages and disadvantages of each are well known [9, 10, 11, 20]. Variations of these conventional techniques [1–5, 13, 14, 17, 19, 21, 23] have resulted as attempts to overcome obvious limitations. However, such variations have not provided adequate solutions to problems presented by limited working space at the depths of the interpeduncular and prepontine cisterns. Surgical approaches to BBAs must overcome the additional complexities presented when such lesions are hidden by posterior clinoid processes or the dorsum sellae and upper clivus. In such cases, the pterional or subtemporal approaches or their variants rarely provide sufficient working space.

More "dramatic" skull base approaches have been described to deal with such aneurysms, including anterior petrosectomy and the transcavernous approach [1, 2, 6, 18, 22]. These may be considered basal extensions of subtemporal and pterional approaches, respectively. However, anterior petrosectomy provides a restricted surgical field and carries considerable risk of damaging the vein of Labbé, the internal carotid artery (ICA) and IV–VIIIth cranial nerves. The transcavernous approach was devised by Dolenc [6] as a means of increasing the working space in the vicinity of the interpenducular and prepontine cisterns. This involves removing the anterior clinoid process, incising the distal and proximal dural rings, opening the cavernous sinus, and drilling the dorsum sellae and clivus to varying extents. Such actions provide a wider exposure of the deep anatomy plus a better means of mobilizing the ICA.

The senior author has used a pretemporal approach to treat basilar artery aneurysms since 1985 [4, 5, 9]. A similar technique was first described by Sano [19] (temporopolar approach), also known as the half-and-half approach [14]. This technique takes advantage of several possible surgical routes offered by the same operation. A view of the interpeduncular fossa may be achieved via a trans-sylvian, subtemporal, or pretemporal perspective. The surgeon may choose the ideal trajectory and change the angle of view, depending on the peculiarities of each specific case [9]. However, changing the angle of view does not provide additional space at the deep limits of the exposure [11, 12].

The authors usually associate the orbitozygomatic osteotomy with high basilar bifurcation aneurysms and the transcavernous-transsellar approach with low-lying lesions [4, 5, 9]. The latter approach is also used for complex and giant basilar artery aneurysms. The orbitozygomatic resection permits visualizing the lesion from a more caudal perspective. On the other hand, we present a transcavernous approach from a pretemporal perspective to treat low-lying, complex, or giant basilar artery aneurysms. In the following, we will detail its anatomical principles and technical nuances of the method, as well as present our clinical experience with it.

Pretemporal approach – technical description

The patient is placed in the supine position with the head turned slightly to the opposite side (Fig. 1A). The incision begins immediately in front of the tragus and courses slightly posterior, behind the hairline and superior to the highest point of the external ear. It curves medially and anteriorly to finish just beyond the midline in the opposite frontal area (Fig. 1A). After retracting the skin flap anteriorly, the temporal muscle is dissected interfascially, then retracted caudally (Fig. 1B). A frontotemporosphenoidal craniotomy is performed, differing from the pterional approach in that the exposure of the temporal lobe is augmented posteriorly and inferiorly (Fig. 1B). After removing the bone flap, the lesser wing of the sphenoid bone is drilled away. The squamousal portion of temporal bone is removed completely in order to reach the level of the middle fossa floor (Fig. 1C), which allows adequate mobilization of the temporal lobe. A zygomatic osteotomy is performed when a particularly thick temporal muscle limits exposure or when operating on giant or complex aneurysms.

The dura mater is opened in an S-shaped fashion and the sylvian fissure is widely dissected (Fig. 1D). The bridging vein to the sphenoparietal sinus is preserved when possible. Arachnoid adhesions between the frontal and temporal lobes are divided. Basal cisterns are opened, and arachnoid connections with the temporal lobe, uncus, frontal lobe, oculomotor nerve, carotid artery, and its branches are transected (Fig. 1E). This is a key feature of this approach since it allows mobilizing the temporal pole without exerting traction on surrounding neurovascular structures. The temporal pole may be elevated from the floor of the middle fossa, making a number of routes to the region of the interpeduncular fossa possible (Fig. 1F). The vein of Labbé is not disturbed. Several surgical windows may be used to reach the basilar bifurcation, such as the opticocarotid or the carotid–oculomotor spaces. It is also possible to work lateral to the oculomotor nerve (Fig. 1F). An orbitozymogatic osteotomy is added to the pretemporal approach when the neck of the aneurysm is greater than 5 mm above the posterior clinoid process.

Pretemporal transcavernous-transsellar approach

The transcavernous-transsellar approach, described by Dolenc [6] and later with minor variations by others, was developed as a means of expanding exposures within the vicinity of the interpeduncular and prepontine cisterns, compared to what is possible via the pterional approach [2, 10, 18, 22]. The transcavernous-transsellar approach opens a route to the interpeduncular and prepontine cisterns through the anterior wall of the anterior incisural space.

The authors started using this approach in 1997 for low-lying, complex, or giant basilar artery aneurysms. We have combined the transcavernous approach with a pretemporal technique in order to enhance the surgical exposure of the interpeduncular and prepontine cisterns (Figs. 2A, B and 3) [9].

After performing the pretemporal craniotomy and drilling the lesser wing of the sphenoid bone, the orbital roof and anterior clinoid process are removed extradurally and the optic canal is unroofed

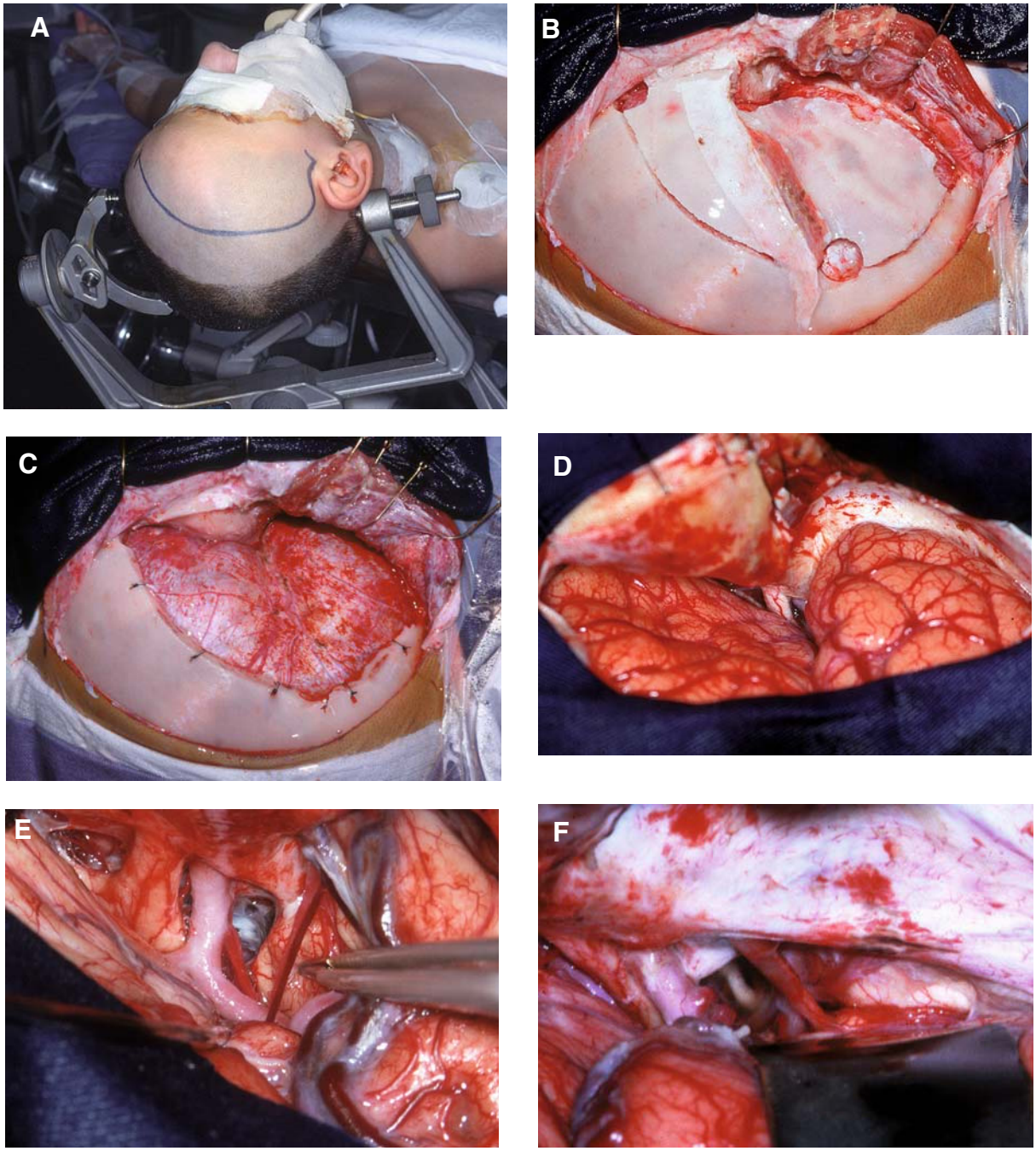

Fig. 1. **A** Skin incision and positioning of the patient. **B** The temporalis muscle has been reflected inferiorly, and a cuff of muscle has been left for closure. **C** Pretemporal extradural exposure. **D** Pretemporal exposure after the dura has been completely opened. **E** Cisternal opening. **F** The basal cisterns have been opened and the interpeduncular cistern and basilar artery bifurcation are exposed

(Fig. 4A). This step is carried out as classically described by Dolenc for aneurysms of the parasellar region (Fig. 4B). The distal dura ring of the internal carotid artery is divided to allow full mobilization of the ICA. The third nerve is dissected along its length, from its emergence in the interpeduncular fossa to its

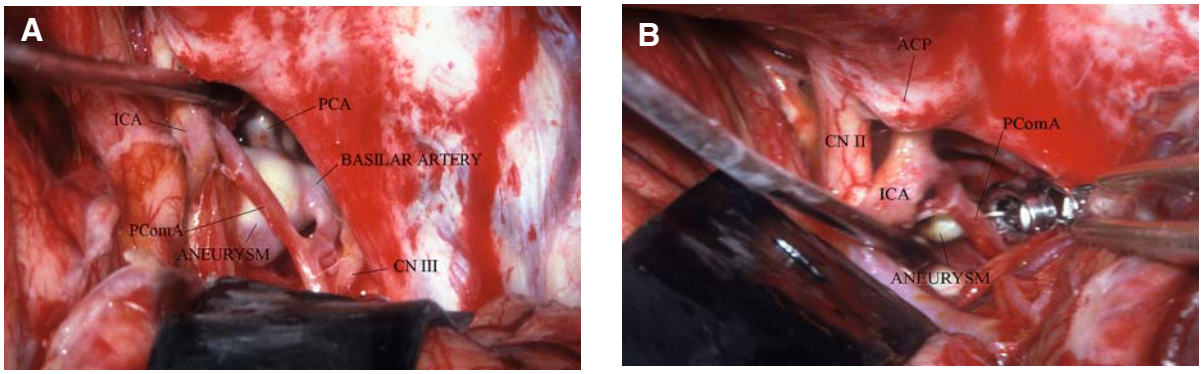

Fig. 2. **A** A right pretemporal approach has been performed and the basal cisterns have been widely dissected. All the arachnoid adhesions between the medial temporal lobe with the internal carotid artery, oculomotor nerve, posterior communicating artery, and anterior choroidal artery have been divided, allowing the displacement of the temporal pole from the middle fossa floor. The tentorial edge is exposed. The interpeduncular fossa and its contents, including the basilar bifurcation aneurysm, are exposed. **B** The aneurysm has been clipped successfully after dissection and preservation of the parent vessels. The contralateral P1 segment of the posterior cerebral artery is well visualized and the ipsilateral posterior communicating artery is preserved. *ACP* Anterior clinoid process; *CN II* optic nerve; *CN III* oculomotor nerve; *ICA* internal carotid artery; *PCA* posterior cerebral artery; *PComA* posterior communicating artery

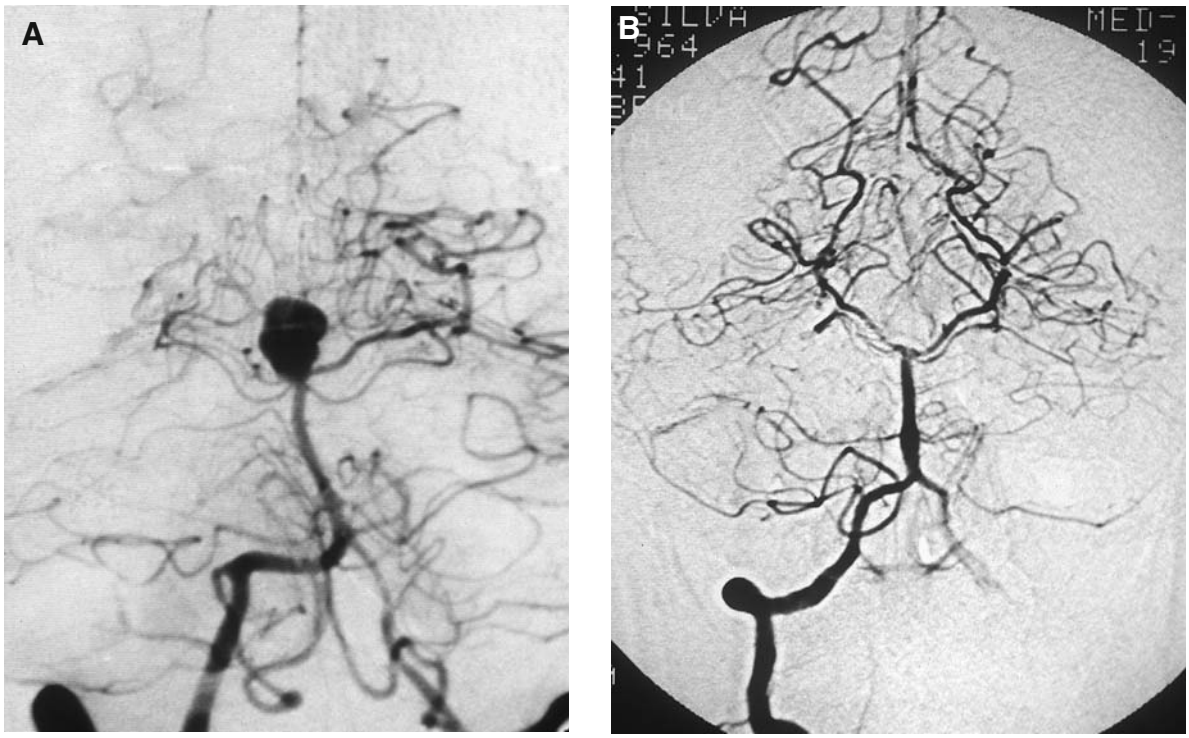

Fig. 3. **A** Antero-posterior view of preoperative digital subtraction vertebral angiograms of a basilar apex aneurysm arising well below the level of the posterior clinoid process. **B** Postoperative view depicting complete obliteration of the lesion

penetration of the posterior portion of the roof of the cavernous sinus, within the so-called oculomotor triangle (Fig. 4C). Dura medial to oculomotor nerve as it penetrates the roof of the cavernous sinus is incised, and the third nerve is dissected distally, towards the superior orbital fissure, proximal to the

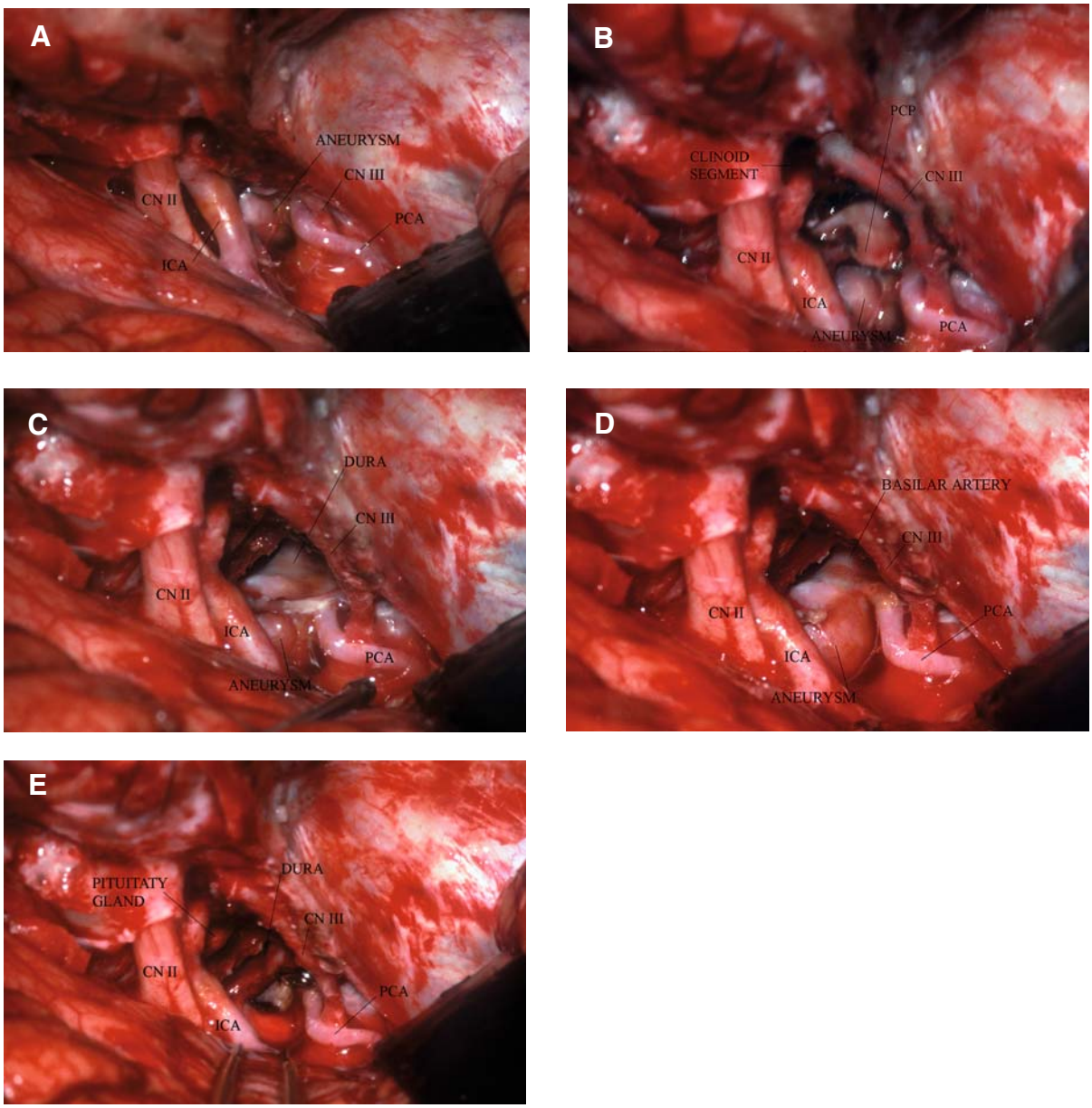

Fig. 4. Intraoperative view of the case depicted in Fig. 3. The aneurysm was approached through a right-sided pretemporal transcavernous craniotomy. **A** The orbital roof and the anterior clinoid process have been removed, and the optic canal has been unroofed. The temporal lobe has been retracted to expose the posterior clinoid process covered by dura and the entrance of the oculomotor nerve into the posterior part of the roof of the cavernous sinus. **B** The optic sheath has been opened, and the dura over the oculomotor nerve has been incised toward the apex of the orbit to expose the nerve on the lateral wall of the cavernous sinus, upper clivus, and posterior clinoid process. **C** The posterior clinoid process has been removed along with the superior part of the clivus; clival dura has been preserved, and the pituitary gland may be seen inferior and medial to the internal carotid artery. **D** The dura of the clivus and over the posterior clinoid process has been removed to expose the basilar artery apex and the aneurysm. **E** Final view after the aneurysm has been clipped. *ACP* Anterior clinoid process; *CN II* optic nerve; *CN III* oculomotor nerve; *ICA* internal carotid artery; *PCA* posterior cerebral artery; *PCP* posterior clinoid process

site of the trochlear nerve's crossing above the third nerve. This exposes the venous channels inside the cavernous sinus and necessitates meticulous packing of the sinus with small pieces of absorbable knitted fabric (Surgicel, Johnson & Johnson, New Brunswick, NJ).

No cranial nerves are present medial to the third nerve's entrance into the oculomotor triangle or medial to the horizontal segment of the intracavernous carotid artery. Cranial nerves IV–VI lie lateral to the oculomotor nerve, making damage to these structures unlikely. The posterior bend of the intracavernous carotid artery and the meningohypophyseal trunk are usually inferior and lateral of the oculomotor nerve's entrance into the cavernous sinus. Nevertheless, the intracavernous carotid may be medial to the third nerve, bulging into the medial half of the oculomotor triangle. It must be identified and scrupulously preserved.

Dura adjacent to the posterior clinoid process is coagulated and incised, exposing the entire posterior clinoid process and the upper portion of the clivus. The entire posterior clinoid process is removed along with varying amounts of the upper clivus (Fig. 4C). The clival resection may be tailored inferiorly, depending on how much of the basilar artery trunk and its branches the individual case deems necessary to expose. Such bone removal increases the anteroposterior dimension of the deepest part of the exposure. More lateral exposure may be achieved by gently displacing the oculomotor nerve laterally. This increases the width of the space available to manipulate the aneurysm or apply a temporary clip (Fig. 4D, E).

Opening the medial side of the oculomotor triangle and removing the posterior clinoid process gives access to a space bounded by the horizontal portion of the intracavernous internal carotid artery laterally, by the clinoid segment of the internal carotid artery anteriorly, the supraclinoid segment of the internal carotid artery medially, and by the interpeduncular fossa posteriorly. The pituitary gland is also identified, inferomedial to the supraclinoid carotid artery.

Although more time-consuming and technically difficult, this approach is safe and provides a wide working space within the interpeduncular fossa. Transient oculomotor nerve palsy, observed in all patients postoperatively, was the only complication related to the approach. All patients recovered full oculomotor function within 2 months.

Pretemporal transcavernous approach to the upper third of the basilar artery

Anatomical considerations

The upper portion of the basilar artery lies in the interpeduncular and prepontine cisterns, deep in the central skull base. The proximity of vital neurovascular structures within this confined area creates considerable difficulty for the neurosurgeon, particularly when dealing with basilar apex aneurysms.

By observing the basic principle of avoiding brain retraction by increasing bone removal, these approaches employ wider craniotomies to provide unobstructed views of pertinent anatomy at the base of the skull [9]. However, such techniques have contributed little to expanding the working space at the deepest levels of the exposure. The exposure provided by conventional approaches is further restricted when the basilar aneurysm is large or its neck lies below the dorsum sellae.

Dolenc's transcavernous-transsellar approach [6] was designed to increase the surgical exposure provided by traditional techniques. Superior exposure results, particularly at the deeper levels. The primary anatomical structures encountered in the transcavernous-transsellar approach to the interpeduncular and prepontine cisterns are contained in the anterior incisural space. Understanding their relationships with cavernous sinus components is of paramount importance to the neurosurgeon.

The anterior part of the tentorial incisura, the *anterior incisural space*, lies anterior to the midbrain and pons. Its superior limit is the floor of the third ventricle, which is formed, from posterior to anterior, by the posterior perforated substance, the mammillary bodies, the tuber cinereum, the infundibulum, and the chiasm. The inferior limit corresponds to a plane in the infratentorial compartment connecting the entrance of both trochlear nerves into the dura. The anterior limit is formed by the clivus, the dorsum sellae, and the posterior clinoid processes. The anterior incisural space ends in the suprasellar region at the level of the pituitary stalk. The uncus, the anterior end of the tentorium, and a parasagittal plane that connects cranial nerves IV and VI make up its lateral limit [22].

The primary cisterns in this area are the interpeduncular, chiasmatic, and prepontine. The

interpeduncular cistern is limited anteriorly and inferiorly by the diencephalic and mesencephalic portions of Liliequist's membrane and by the floor of the third ventricle and the brainstem superiorly and posteriorly. The chiasmatic and prepontine cisterns lie in front of and below the interpeduncular cistern. The main vascular structures in the anterior incisural space are the basilar artery and its terminal branches, the posterior cerebral and the superior cerebellar arteries.

The posterior communicating arteries are oriented posteriorly and medially from the ICA, giving rise to the anterior thalamoperforating arteries before joining the posterior cerebral artery. The posterior thalamoperforating arteries, arising from the posterior surface of the P1 segment, are the most difficult vascular structures to preserve during basilar apex aneurysm surgery [9, 22].

Depending on its height relative to the upper part of the dorsum sellae, the basilar artery bifurcation may be divided into three types: low, normal and high. The basilar artery bifurcation is considered normal when it is within 5 mm above or below the level of the dorsum sellae (40% of cases). A high bifurcation is present in 32% of cases, and a low bifurcation in 28% of cases [22].

The clinoid segment of the ICA is encased almost entirely by bone: the anterior clinoid process laterally, the optic strut anteriorly, and the sphenoid carotid sulcus medially. Two dural rings form its superior, inferior, and posterior limits. The distal dural ring, formed by the union of the outer and inner layers of the lateral wall of the cavernous sinus, corresponds to the superior and posterior limits of the clinoid segment. The proximal dural ring, which is formed only by the inner layer, corresponds to the inferior limit. The inner layer of dura envelopes the clinoid segment completely. The posterior part of the roof of the cavernous sinus is formed mainly by the oculomotor triangle, a space between the dural folds which invests the anterior and posterior clinoid processes and the petrous apex.

After opening the outer and inner layers of the roof of the cavernous sinus, the horizontal segment of the intracavernous carotid artery may be exposed to the pituitary gland and the posterior clinoid process and medial to the nerves in the lateral wall of the cavernous sinus. The space between the horizontal petrous carotid segment and the pituitary gland is filled with blood from the cavernous sinus, but it contains no important vascular or neural structures.

Surgical technique

A question-mark-shaped incision is extended beyond the midline, and an interfascial dissection of the temporalis muscle is carried out. After reflecting the temporalis muscle inferiorly, an orbitozygomatic craniotomy is performed. Middle and anterior fossa dura is dissected, exposing the superior orbital fissure. Beginning at the frontal limit of the craniotomy, a curving dural incision is carried to the level of the impression of the lesser sphenoid wing, where it is directed 90° anteriorly along the bone impression toward the orbitomeningeal artery. Upon reaching the temporal pole, the incision is directed along the inferior limit of the craniotomy. After opening the dura, the sylvian fissure and the basal cisterns are dissected (Fig. 5A).

Outer and inner layers of middle fossa dura are separated by blunt dissection to the superior border of the superior orbital fissure. Here, where the two dural layers meet periorbita, is where the orbitomeningeal artery enters the orbit. Blunt dissection is continued medially, exposing the anterior clinoid process and the anterior part of the lateral wall of the cavernous sinus. Then the orbital roof, the anterior clinoid process, and the optic strut are removed, exposing the clinoid segment of the carotid artery (Fig. 5B). Dura is incised medially toward the optic sheath and the distal dural ring is divided laterally, anteriorly, and posteriorly, making it possible to mobilize the carotid artery. The roof of the cavernous sinus is opened anteriorly along the third nerve toward the superior orbital fissure, then posteriorly and medially, thus exposing the posterior clinoid process and the horizontal, clinoid and intradural segments of the carotid artery (Fig. 5C, D).

Retracting the intradural segment of the ICA medially, the horizontal, clinoid, intradural segments form an arch which is concave posteriorly. The space separating this arterial arch from the pituitary gland medially, the lateral wall of the cavernous sinus laterally, and the posterior clinoid process and dorsum sellae posteriorly (Fig. 5D) is safe territory since it is free of important vascular and neural structures. Removing the posterior clin-

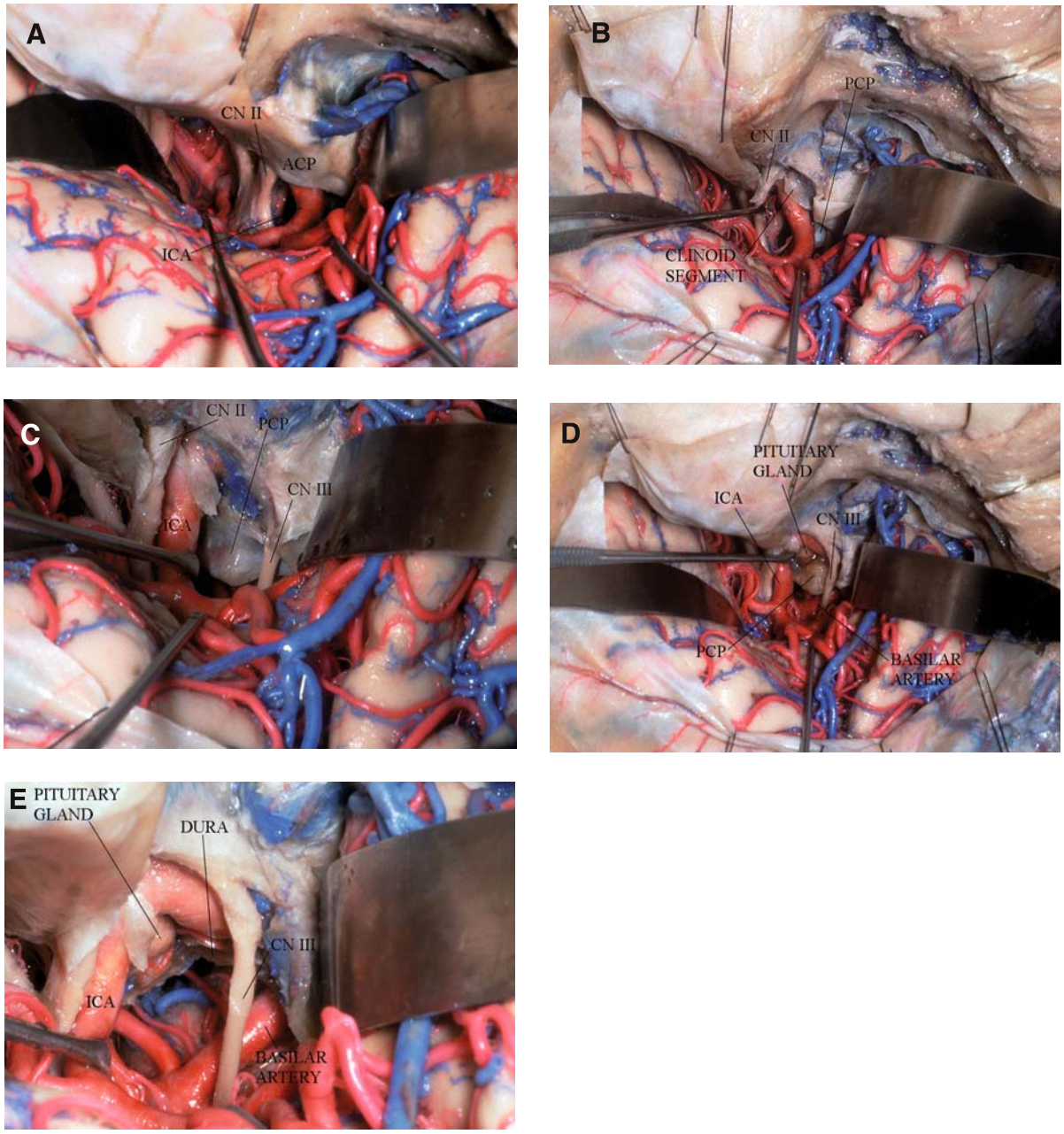

Fig. 5. Anatomical view illustrating the stepwise progression of the transcavernous approach. **A** Dura mater has been opened and basal cisterns have been widely dissected. **B** The optic nerve has been unroofed and ACP has been removed to expose the clinoidal segment of the ICA. **C** Oculomotor nerve has been exposed and dissected towards its entrance into the cavernous sinus. Posterior clinoid process may be well visualized. **D** The roof of the cavernous sinus has been opened medial to the third cranial nerve to further expose the posterior clinoid process and upper clivus. The pituitary gland may be seen medial to the ICA. **E** Posterior clinoid process and part of the upper clivus have been removed and dura has been opened. Basilar apex and the interpeduncular and prepontine cistern are adequately exposed. *ACP* Anterior clinoid process; *CN II* optic nerve; *CN III* oculomotor nerve; *ICA* internal carotid artery; *PCP* posterior clinoid process

oid process and dorsum sellae gives access to neurovascular structures in the interpeduncular cistern and the upper part of the prepontine cistern (Fig. 5E). Displacing the temporal pole posteriorly and resecting the anteromedial edge of the tentorium between cranial nerves IV and V allows exposure of the lower segment of the basilar artery when necessary.

Surgical considerations

Combining the transcavernous-transsellar approach with an orbitozygomatic craniotomy provides the surgeon a wider exposure (Fig. 4A–E). Removing the anterior clinoid process, exposing the clinoid segment of the ICA, then incising the dural rings around the vessel are important steps, facilitating mobilization of the ICA and improving exposure of the posterior clinoid process, the dorsum sellae, and the upper part of the clivus. Opening the roof of the cavernous sinus requires considerable manipulation of the third cranial nerve. However, the third nerve palsy which typically follows (occurring in every patient in our series) is temporary, subsiding within 2 weeks to 3 months. Continuous bleeding associated with opening the cavernous sinus may be controlled by gently packing the sinus with Surgicel^{TM}. The horizontal, clinoid, and intradural segments of the carotid artery form a C-shaped vascular structure which is oriented posteriorly, toward the posterior clinoid process, dorsum sellae, the clivus and pituitary gland. Resecting the posterior clinoid, the dorsum sellae, and upper part of the clivus and their dural coverings substantially improves exposure of [11] the basilar artery and facilitates its proximal control when treating giant or low-lying basilar bifurcation aneurysms.

Conclusion

Despite its surgical complexity, the pretemporal transcavernous-transsellar approach is a valuable alternative to more traditional routes to basilar artery lesions. It enhances the exposure of intra-axial and extra-axial lesions in this region, including posterior circulation aneurysms, brainstem cavernomas, petroclival meningiomas, and posterior fossa extensions of craniopharyngiomas. It is particularly useful for treating giant or low-lying basilar artery bifurcation aneurysms.

References

1. Aziz KMA, van Loveren HR, Tew JM Jr, Chicoine MR (1999) The kawase approach to retrosellar and upper clival basilar aneurysms. Neurosurgery 44: 1225–1236
2. Chanda A, Nanda A (2002) Anatomical study of the orbitozygomatic transsellar-transcavernous-transclinoidal approach to the basilar artery. J Neurosurg 97: 151–160
3. Day JD, Giannotta SL, Fukushima T (1994) Extradural temporopolar approach to lesions of the upper basilar artery and infrachiasmatic region. J Neurosurg 81: 230–235
4. de Oliveira E, Siqueira M, Tedeschi H, Peace DA (1993) Surgical approaches for aneurysms of the basilar artery bifurcation. In: Matushima T (ed) Surgical anatomy for Microsurgery VI. Cerebral aneurysms and skull base lesions. Sci Med Publications, Fukuoka City, pp 34–42
5. de Oliveira E, Tedeschi E, Siqueira M, Peace DA (1995) The pretemporal approach to the interpeduncular and petroclival regions. Acta Neurochir (Wien) 136: 204–211
6. Dolenc VV, Skrap M, Sustersic J, Skrbec M, Morina A (1987) A transcavernous-transellar approach to the basilar tip aneurysms. Br J Neurosurg 1: 251–259
7. Drake CG (1961) Bleeding aneurysms of the basilar artery. J Neurosurg 18: 230–238
8. Drake C (1968) The surgical tratment of aneurysms of the basilar artery. J Neurosurg 29: 790–791
9. Ferreira MAT, Tedeschi H, Wen HT, de Oliveira E (2000) Posterior circulation aneurysms: guidelines to management. Oper Techn Neurosurg 3: 169–178
10. Figueiredo EG, Gomes M, Vellutini E, Rosemberg S, Marino R Jr (2005) Angioleiomyoma of the cavernous sinus: case report. Neurosurgery 56: E411
11. Figueiredo EG, Zabramski JM, Deshmukh P, Crawford NR, Preul MC, Spetzler RF (2006) Anatomical and quantitative description of the transcavernous approach to interpeduncular and prepontine cisterns. J Neurosurg 104: 1–8
12. Figueiredo EG, Zabramski JM, Deshmukh P, Crawford NR, Spetzler RF, Preul MC (2006) Comparative analysis of anterior petrosectomy and transcavernous approaches to retrosellar and upper clival basilar artery aneurysms. Neurosurgery 58: 13–21
13. Hakuba A, Liu S, Nishimura S (1986) The orbitozygomatic infratemporal approach: a new surgical technique. Surg Neurol 26: 271–276
14. Heros R, Lee S (1993) The combined pterional/anterior temporal approach for aneurysms of the upper basilar complex: technical report. Neurosurgery 33: 244–251
15. Le Roux PD, Winn HR (1998) Surgical approaches to basilar bifurcation aneurysms. Neurosurg Clin N Am 9: 835–849

16. Lozier AP, Kim GH, Sciacca RR, Connolly ES Jr, Solomon RA (2004) Microsurgical treatment of basilar apex aneurysms: perioperative and long-term clinical outcome. Neurosurgery 54: 286–299
17. Matsuyama T, Shimomura T, Okumura Y, Sakaki T (1997) Mobilization of the internal carotid artery for basilar artery aneurysms surgery. Technical note. J Neurosurg 86: 294–296
18. Nutik SL (1998) Pterional craniotomy via a transcavernous approach for the treatment of low-lying distal basilar aneurysms. J Neurosurg 89: 921–926
19. Sano K (1980) Temporo-polar approach to aneurysms of the basilar artery at and around the distal bifurcation: technical note. Neurol Res 2: 361–367
20. Samson DS, Hodosh RM, Clark WK (1978) Microsurgical evaluation of pterional approach to aneurysms of the distal basilar circulation. Neurosurgery 3: 135–141
21. Sato S, Sato M, Oizumi T, Nishizawa M, Ishizawa M, Inamasu G, Kawase T (2001) Removal of anterior clinoid process for basilar tip aneurysm: clinical and cadaveric analysis. Neurol Res 23: 298–303
22. Seoane E, Tedeschi E, de Oliveira E, Wen HT, Rhoton AL Jr (2000) The pretemporal transcavernous approach to the interpeduncular and prepontine cisterns: microsurgical anatomy and technique application. Neurosurgery 46: 891–899
23. Sugita K, Kobayashi S, Takemae T, Tada T, Tanaka Y (1987) Aneurysms of the basilar artery trunk. J Neurosurg 66: 500–505
24. Veznedaroglu E, Benitez RP, Rosenwasser RH (2004) Surgically treated aneurysms previously coiled: lessons learned. Neurosurgery 54: 300–305
25. Yaşargil MG (1984) Microneurosurgery: clinical considerations, surgery of the intracranial aneurysms and results, vol. II. Thieme, Stuttgart
26. Yaşargil MG, Antic J, Laciga R, Jain KK, Hodosh RM, Smith RD (1976) Microsurgical pterional approach to aneurysms of the basilar bifurcation. Surg Neurol 6: 83–91

Aneurysms of the intracavernous ICA: current treatment

L. N. Sekhar[1], S. K. Natarajan[1], G. W. Britz[1,2], B. Ghodke[1,2]

[1]Department of Neurological Surgery, University of Washington, Seattle, WA, USA
[2]Department of Radiology, University of Washington, Seattle, WA, USA

Introduction

Intracavernous aneurysms make up approximately 5% of all intracranial aneurysms. Their location makes them notoriously difficult to treat. Management of such lesions has evolved over the past decade through a better understanding of their natural history and advances in endovascular techniques. At the present time the senior author relies on bypasses and endovascular therapy rather than direct surgery for aneurysms confined to the cavernous sinus. We still favor intracavernous operations for paraclinoid aneurysms and small intracavernous aneurysms with extracavernous components.

Description

The term "intracavernous aneurysm" refers to those arising from the ICA between the petrolingual ligament and the anterior clinoid process (excluding the clinoid segment). According to the classification proposed by Bouthillier et al. [1], the cavernous segment begins at the superior margin of the petrolingual ligament and ends at the proximal dural ring, which incompletely surrounds the ICA. Those authors classify the C1 as the cervical ICA, the C2 is the petrous ICA, the C3 is the lacerum segment, the C4 is the cavernous segment, the C5 the clinoid segment, the C6 the ophthalmic segment, and the C7 the supraophthalmic segment. We prefer to think of the ICA by its anatomical location rather numbering its segments. In practice, the management of petrous and cavernous ICA segment aneurysms is similar (endovascular treatment and microsurgical bypass). Similarly, clinoidal and ophthalmic segment aneurysms are managed by endovascular coiling, microsurgical clipping, or occasionally, by performing a bypass and trapping the lesion. Recent work by Ziyal et al. [4] refutes the designation, "lacerum segment".

This series specifically excludes aneurysms arising from the clinoidal and ophthalmic segments of the ICA. Some large aneurysms extend both into and out of the CS, though, and some patients have a clinoidal or an ophthalmic aneurysm in addition to an intracavernous aneurysm, lesions which may be treated together.

Natural history and treatment indications

Intracavernous ICA aneurysms may either: (a) produce progressive neuropathies of cranial nerves II–VI, or (b) rupture, resulting in a carotid–cavernous fistula, a subarachnoid hemorrhage, or a posterior fossa subdural hematoma [2]. The ISUIA study [3], the best available analysis of the natural

history of unruptured intracranial aneurysms, indicates that no cavernous carotid aneurysm with a diameter of 7–12 mm ruptured in 5 years, and that only 3% of 13–24 mm diameter lesions and 6.4% of those with diameters greater than 25 mm ruptured during that period of time. When considering treatment options, the surgeon must also weigh the disabilities associated with progressive cranial neuropathy against the morbidity of treatment.

For aneurysms fully within the CS, our current indications for surgery are as follows: (a) significant growth of lesions $\leq$10 mm usually receive an endovascular procedure, and (b) symptomatic aneurysms $\geq$11 mm (even lesions $\geq$25 mm) are treated either by endovascular techniques or by trapping with a microsurgical bypass. Asymptomatic aneurysms $\geq$11 mm (including those $\geq$25 mm) are managed by observation only, endovascular therapy, or with bypass and trapping, depending on the patients' personal preference.

Endovascular treatment

Giant fusiform intracavernous aneurysms may be managed by proximal endovascular occlusion following a balloon-occlusion test which includes neurological evaluation, Transcranial Doppler evaluation, SPECT scanning, and induced hypotension (optional). In our institution, we perform the test as shown in Fig. 1.

We prefer to treat intracavernous aneurysms with necks (which are usually broad) with a Neuroform® stent, followed by endovascular coiling. Early in our experience, two incompletely coiled aneurysms recurred, and one developed severe trigeminal neuralgia from the mass of the coil. Both were treated subsequently by bypass and trapping, and the patient with trigeminal neuralgia was relieved of facial pain when the coil was removed.

Surgical treatment

Although the senior author (LNS) previously performed direct intracavernous surgery for CS aneurysms, he switched to bypass and trapping, noting immediately less cranial nerve morbidity. Initially, bypasses were constructed with grafts from the petrous ICA to the supraclinoid ICA, but since 1992 we have preferred bypasses between the cervical ICA or ECA (selection depending on collateral circulation) to the MCA, or bypasses from the cervical ICA or ECA to the supraclinoid ICA (if the MCA is not suitable for anastamosis) (Figs. 2–9). Both the radial artery and the saphenous vein have been used as inter. position grafts (Table 1). Of our series of 105 bypasses for aneurysms from 1984–1987/2006 (Figs. 10, 11), 30 patients were treated for intracavernous aneurysms by proximal occlusion or trapping. Of these, one bypass graft was occluded, a casualty of a hypercoagulable state, the patient suffering a stroke and disability. Two others treated very early in our experience suffered minor strokes because of prolonged temporary ICA occlusion. Both were left with mild residual disabilities.

Table 1. Bypass surgery for cavernous ICA aneurysms (1988–2006)

Total number	30 cases	
Types of bypass		
Cervical ECA-MCA	4	
Cer. ECA-sup. clinoid ICA	1	
Cervical ICA-MCA	23	
Petrous ICA-sup. clin. ICA	2	
	Early	Late
Patency	29/30 (96.7%)	28/30 (93.3%)
Complications		
Operative death	0	
Minor stroke	3 (Recovery GOS in all)	
Brain swelling	1	
Delayed occlusion	1	
Int. op. revision angioplasty	1	
Outcome, early		
Glasgow Outcome Scale 5	27	
Glasgow Outcome Scale 4	3	
Outcome, late		
Death from Marfan's dis.	2	
suicide	1	

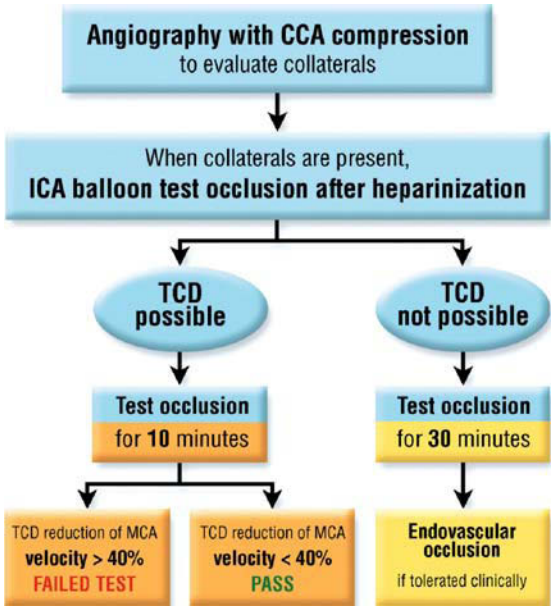

Fig. 1. Diagnosis of intracavernous aneurysms

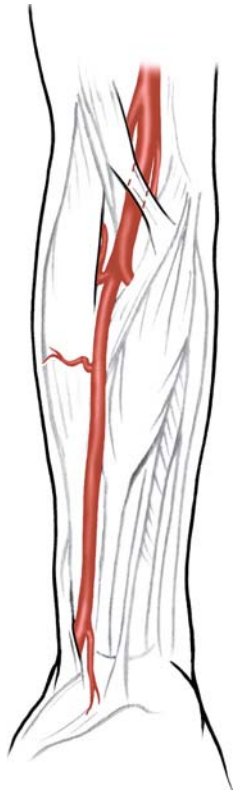

2

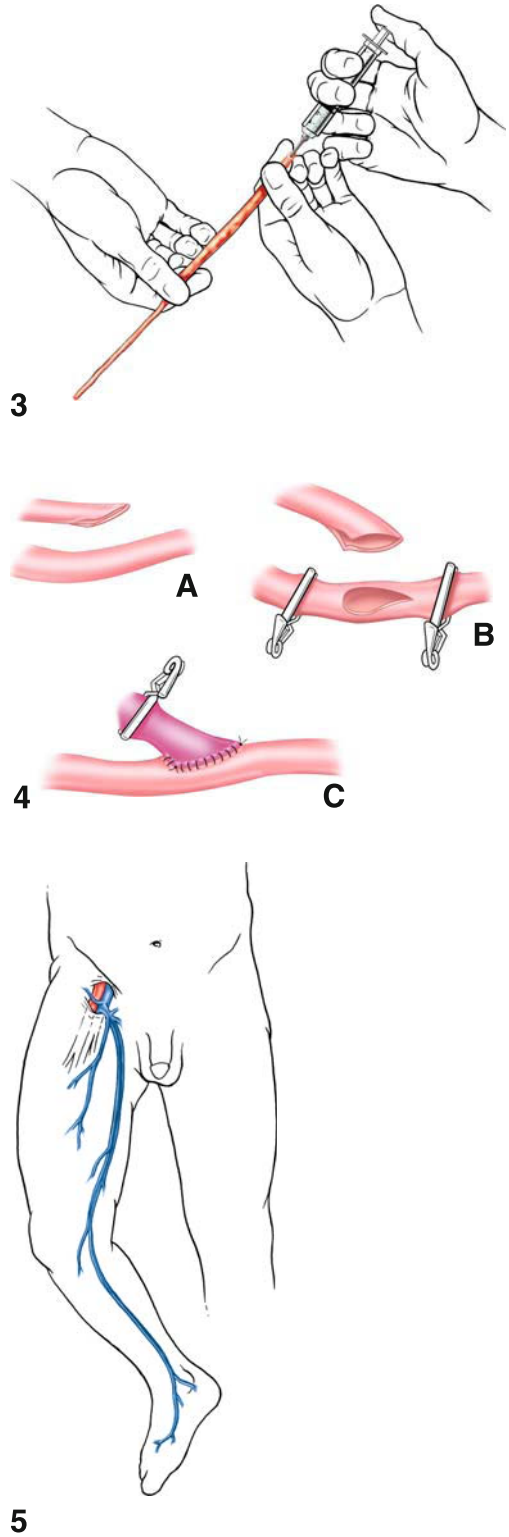

Figs. 2–5. Construction of bypass (I) (see text for details)

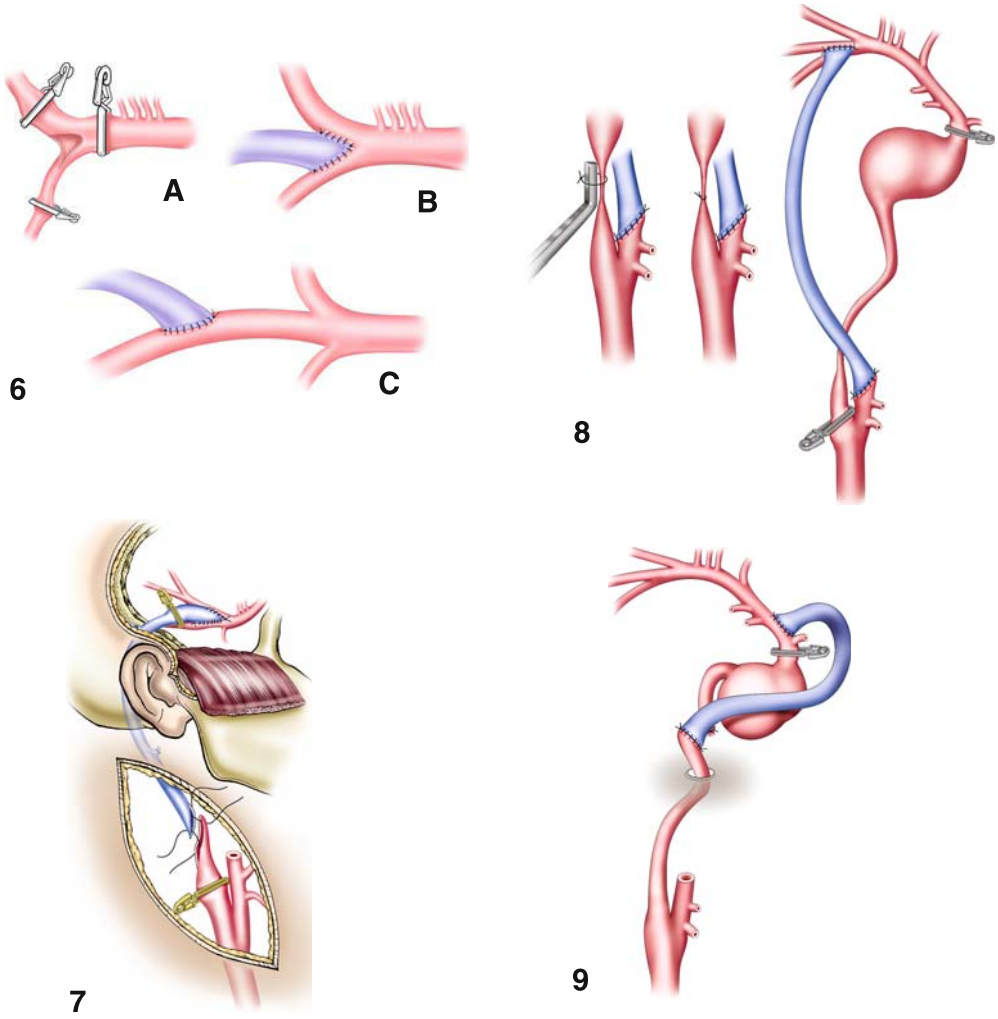

Figs. 6–9. Construction of bypasses (II) (see text for details)

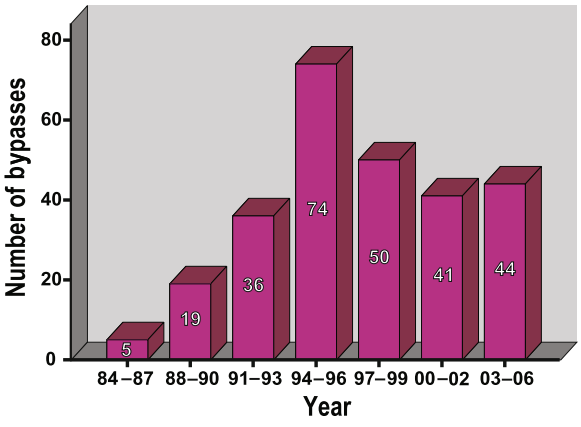

Fig. 10. Bypass surgery (1984–2006)

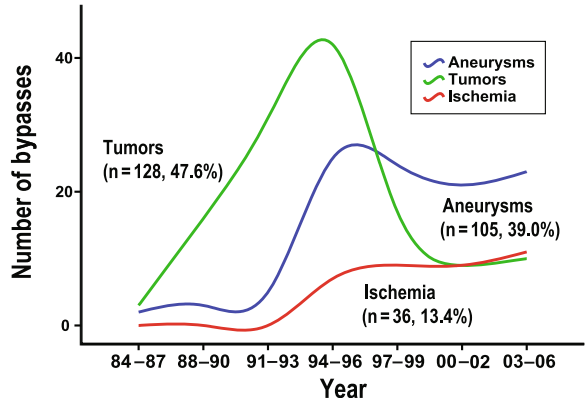

Fig. 11. Correlation between bypass surgery, aneurysms, tumors, and ischemia

Illustrative cases

Case #1 (Figs. 12–14)

This patient presented in 1992 with a giant intracavernous aneurysm and underwent endovascular ICA occlusion after passing a trial balloon-occlusion test which revealed good collateral flow to the hemisphere ipsilateral to the occluded ICA.

Case #2 (Figs. 15, 16)

This patient presented in 1992 with an abducens palsy and underwent trial balloon-occlusion, failing quickly and completely. No treatment was offered, only follow-up. Today, because of our subsequent success with bypass surgery, this patient would be considered for an ECA to MCA bypass followed by proximal occlusion of the ICA if the bypass was successful.

Case #3 (Figs. 17–19)

This patient presented in 1990 with bilateral intracavernous aneurysms. The one on the left was a giant, symptomatic lesion, extending into the clinoid segment. She underwent trial balloon occlusion of the ICA. During testing she developed a dissection of the cervical ICA dissection which led to total occlusion, plus an embolus to the MCA, leaving her with a right hemiparesis. Following emergent embolectomy and aneurysm exploration (leading to ICA repair by aneurysmorrhaphy) she made a complete recovery. Subsequently she declined treatment for the large contralateral intracavernous aneurysm.

Case #4 (Figs. 20–23)

This patient presented in 2005 with acute onset of oculomotor palsy and confusion from a heavily thrombosed left intracavernous aneurysm. Collateral circulation was determined to be poor by carotid cross-compression testing, disqualifying her as a candidate for stent-assisted coiling. Her ICA at the origin of the aneurysm was stenotic. A radial artery bypass graft was interposed between the cervical ECA and the MCA. Intraoperative graft revision was required to relieve a proximal thrombosis. She also developed vasospasm 9 days after surgery which required an endovascular angioplasty. Her recovery was excellent, with resolution of the oculomotor palsy and confusion, and the graft remained patent with excellent flow 11 months after surgery.

Case #5 (Figs. 24–26)

This patient presented with an abducens palsy from a giant petrocavernous aneurysm plus a small carotid-ophthalmic aneurysm. Since her radial artery was not available because of an inadequate palmar arch, a saphenous vein graft was interposed betweens her cervical ICA and MCA. The ophthalmic aneurysm was then clipped, and the cavernous ICA was trapped. As the petrocavernous ICA aneurysm clotted, she developed facial, trigeminal, and abducens paralysis which ultimately cleared completely. Approximately 7 months later, she developed multiple seizures which resolved with anticonvulsants. Her subsequent recovery was excellent.

Case #6 (Figs. 27, 28)

This 71-year-old woman presented in 2006 with third and sixth cranial nerve palsies related to a heavily thrombosed intracavernous ICA aneurysm. She underwent stent-assisted coiling, with no ill effects postoperatively.

Results

Between 1984 and 1990, the senior author evaluated 43 intracavernous aneurysms, and recommended no treatment for 20. Twenty-three patients underwent balloon-occlusion testing to determine the adequacy of ICA collateral flow. Four failed the test, two of whom had no further treatment. Of the remaining two, one lesion was clipped directly, and the other was trapped after bypass surgery. Of those remaining, 13 underwent endovascular treatment and 8 had surgery. Of those undergoing endovascular treatment, two could not be treated satisfactorily. Between 1985 and 7/2006, a total of 30 bypasses were performed for intracavernous ICA aneurysms (Fig. 29) as discussed above.

During the past 2 years, we have evaluated approximately 40 patients with intracavernous aneur-

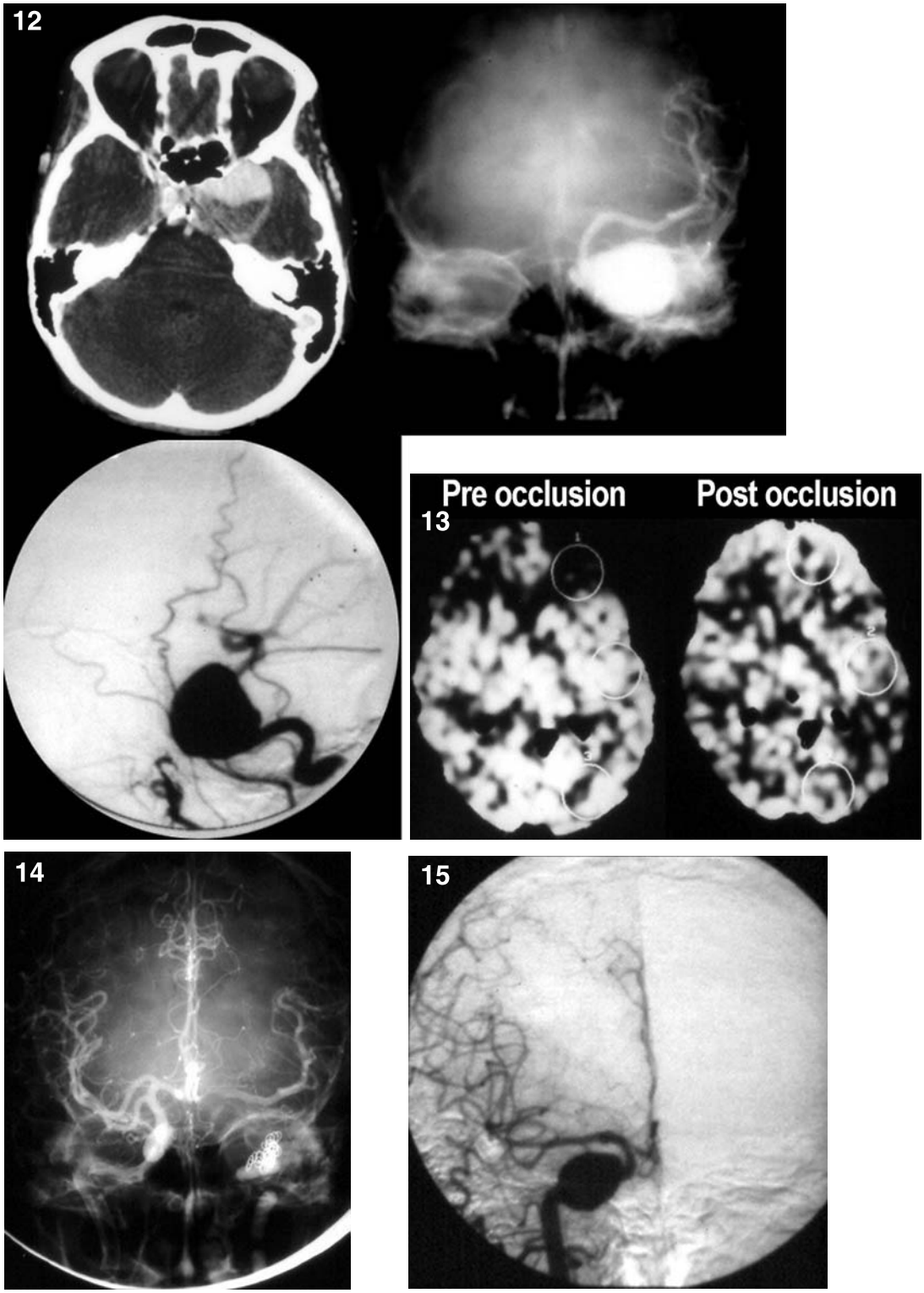

Figs. 12–14. Case 1: diagnosis and treatment of a giant intracavernous aneurysm (see text for details)
Figs. 15, 16. Case 2: (see text for details)

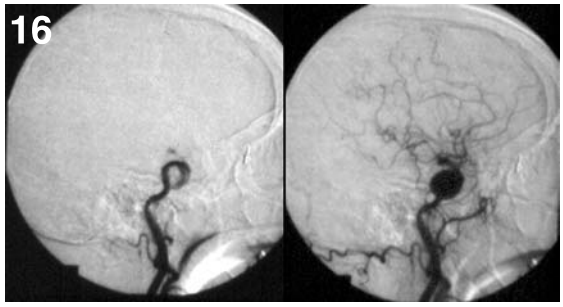

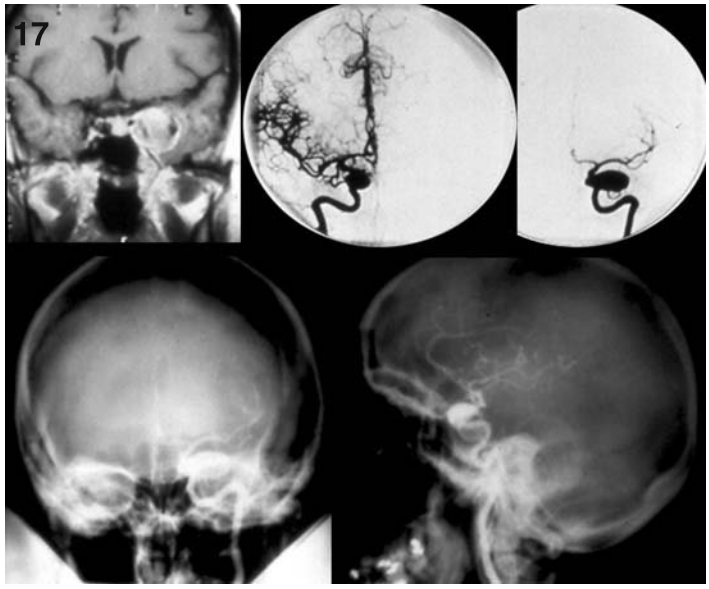

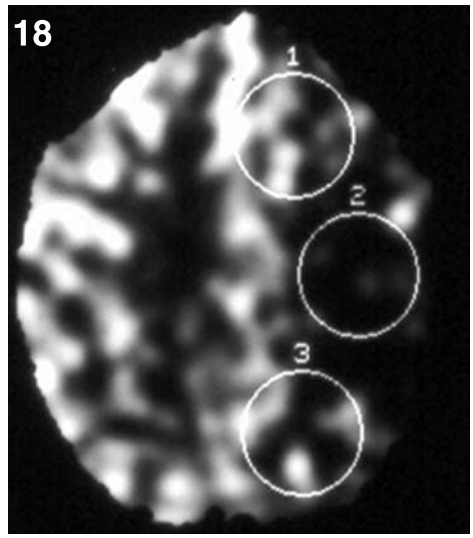

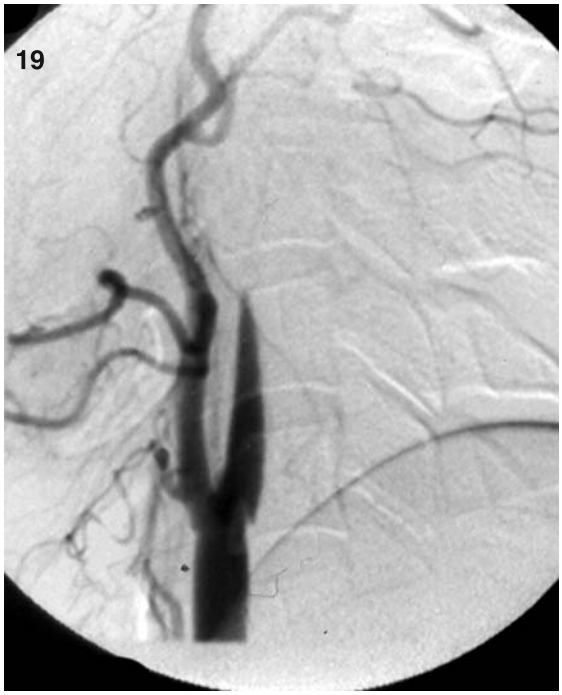

Figs. 17–19. Case 3: diagnosis and treatment of bilateral intracavernous aneurysms

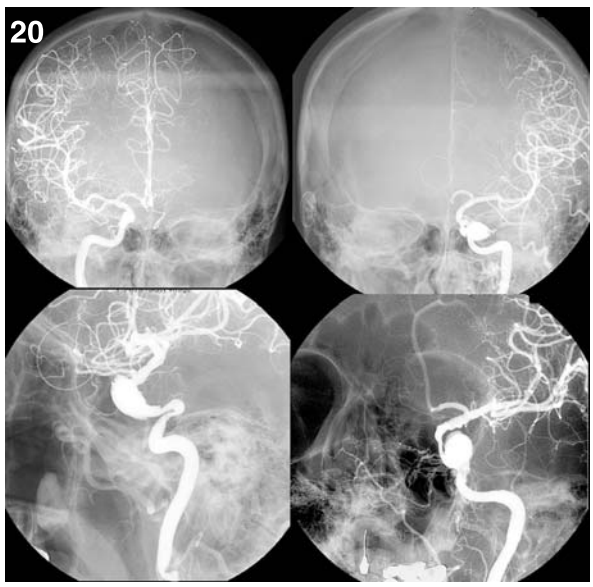

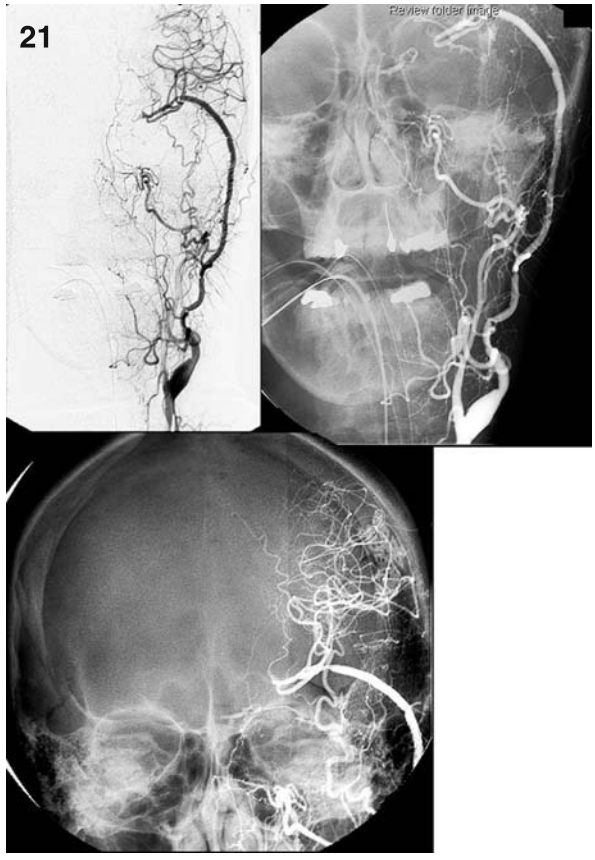

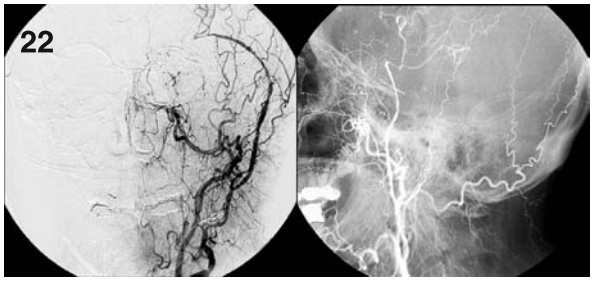

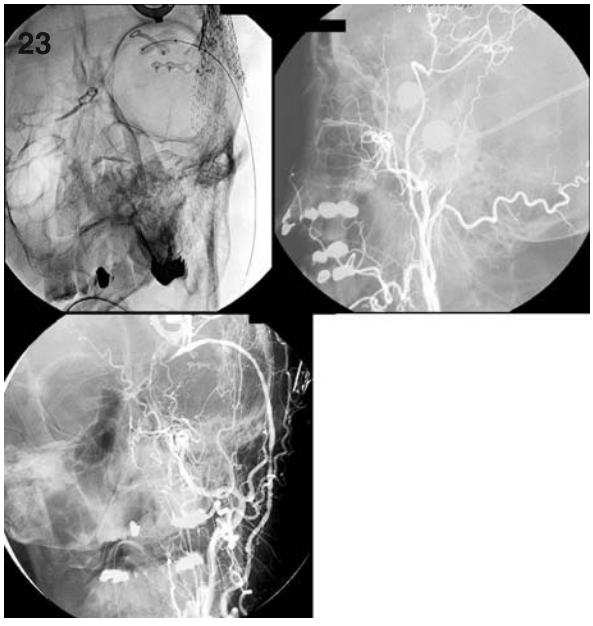

Figs. 20–23. Case 4: diagnosis and treatment of intracavernous aneurysms (see text for details)

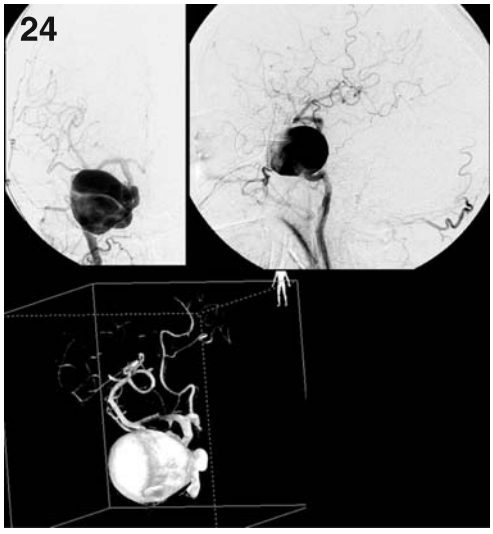

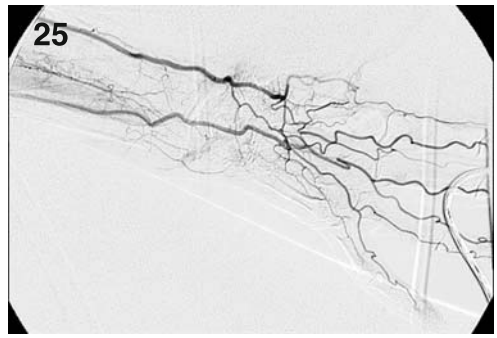

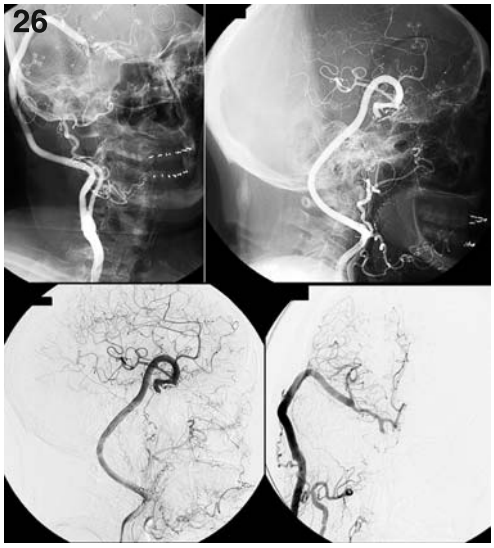

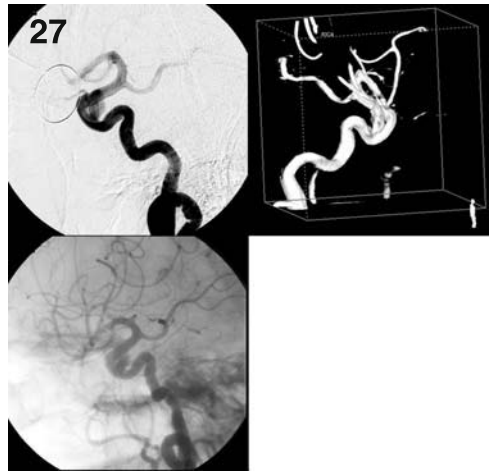

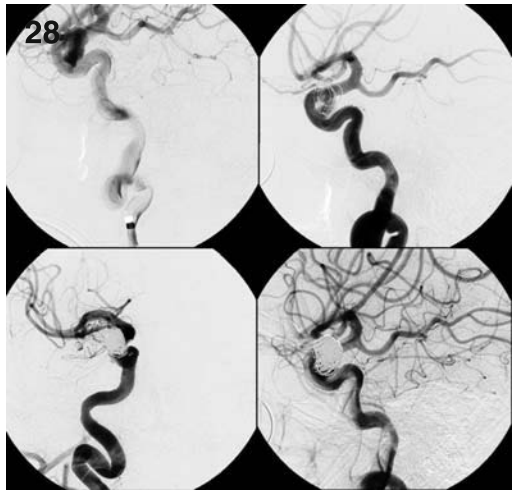

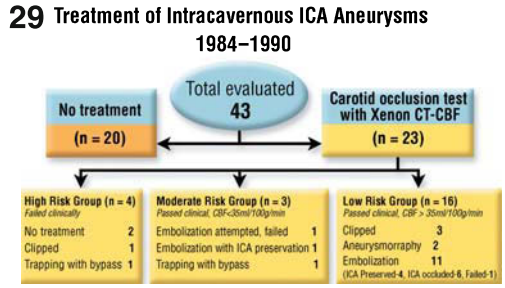

Figs. 24–26. Case 5: diagnosis and treatment of a giant petrocavernous meningioma
Figs. 27, 28. Case 6: treatment of a heavily thrombosed intracavernous ICA aneurysm (see text for details)
Fig. 29. Overview of intracavernous ICA aneurysms

ysms. Two were selected for bypass and trapping, and two for endovascular treatment. Currently a number of such patients are being followed, without specific treatment.

References

1. Bouthillier A, van Loveren HR, Keller JT (1996) Segments of the internal carotid artery: a new classification. Neurosurgery 38: 425–432; discussion 432–423
2. De Jesus O, Sekhar LN, Riedel CJ (1999) Clinoid and paraclinoid aneurysms: surgical anatomy, operative techniques, and outcome. Surg Neurol 51: 477–487; discussion 487–478
3. Wiebers DO, Whisnant JP, Huston J III, Meissner I, Brown RD Jr, Piepgras DG, Forbes GS, Thielen K, Nichols D, O'Fallon WM, Peacock J, Jaeger L, Kassell NF, Kongable-Beckman GL, Torner JC (2003) Unruptured intracranial aneurysms: natural history, clinical outcome, and risks of surgical and endovascular treatment. Lancet 362: 103–110
4. Ziyal IM, Ozgen T, Sekhar LN, Ozcan OE, Cekirge S (2005) Proposed classification of segments of the internal carotid artery: anatomical study with angiographical interpretation. Neurol Med Chir (Tokyo) 45: 184–190; discussion 190–191

Chapter 5. Surgical treatment of tumorous lesions in the central skull base

Cavernous sinus meningiomas

O. Al-Mefty[1], J. A. Heth[2]

[1]Department of Neurosurgery, University of Arkansas for Medical Sciences, Little Rock, Arkansas, USA
[2]Department of Neurosurgery, University of Michigan Health System, Ann Arbor, Michigan, USA

Introduction

Meningiomas look simple. Neurosurgeons have enjoyed great success in treating them, because the majority of meningiomas are readily accessible benign tumors and complete resection usually proves curative. Their simplicity evaporates when they recur, when they are attached to major draining sinuses, or when they are insinuated among critical neural structures. Such is the case with meningiomas involving the cavernous sinus (CSM). Within this compact space run the carotid artery and the ocular motor nerves, and nearby lie the optic nerve and pituitary body. As neurosurgeons pursue the goal of total resection, the risks to vision, ocular function, appearance, and stroke are ever-present.

Historically, such CSMs were thought to be in a surgical "no man's land." Effective skull base approaches and techniques began to emerge in the 1980s. Since that time, experience continues to accumulate using these approaches, and stereotactic radiosurgery (SRS) has been introduced and developed into another effective treatment. Yet, debate exists as to what constitutes "successful" treatment of CSMs: Is it tumor eradication? Absence of neurological deficits? Lack of tumor growth? This article outlines the experiences of one surgically oriented center and the techniques used in the evaluation and treatment of patients with CSM.

Presentation and physical examination

Meningiomas arise primarily in the cavernous sinus or involve the cavernous sinus secondarily. Not surprisingly, presenting symptoms are related to the neurovascular structure involved. Tumors in the cavernous sinus most frequently present with ocular motor deficits – ptosis, diplopia, anisocoria, or complete ophthalmoplegia. Trigeminal nerve dysfunction can be present with facial numbness or facial pain. Tumors can compress the optic nerve to result in visual field deficits. Carotid artery compression can result in ischemic deficits. Although involvement of the pituitary body or stalk does not frequently appear as a primary presenting symptom, pituitary dysfunction can occur and such dysfunction should prompt a complete laboratory evaluation.

Past medical history is always critical when evaluating patients with suspected CSM. Information about any prior treatment including surgical resection (including operative report), radiation, medical treatment, and a pathology report should be obtained, if available. Several other tumors can metastasize to the dura and mimic meningioma [12, 34] including lymphoma, breast carcinoma, and paranasal sinus carcinomas. For women, recent mammography results should be obtained because a potential association between meningiomas and breast carcinoma has been reported [32] (although this may represent two tumor types with common risk factors [3, 11]). Prior cranial radiation is associ-

ated with secondary development of meningiomas and should be queried [10, 30]. Patients should also be questioned for manifestations of neurofibromatosis such as café-au-lait spots, hearing loss, cutaneous neurofibromas, or family history of neurofibromatosis. A history of using birth control medications or hormone replacement therapy should be elicited as there is a suspected hormonal

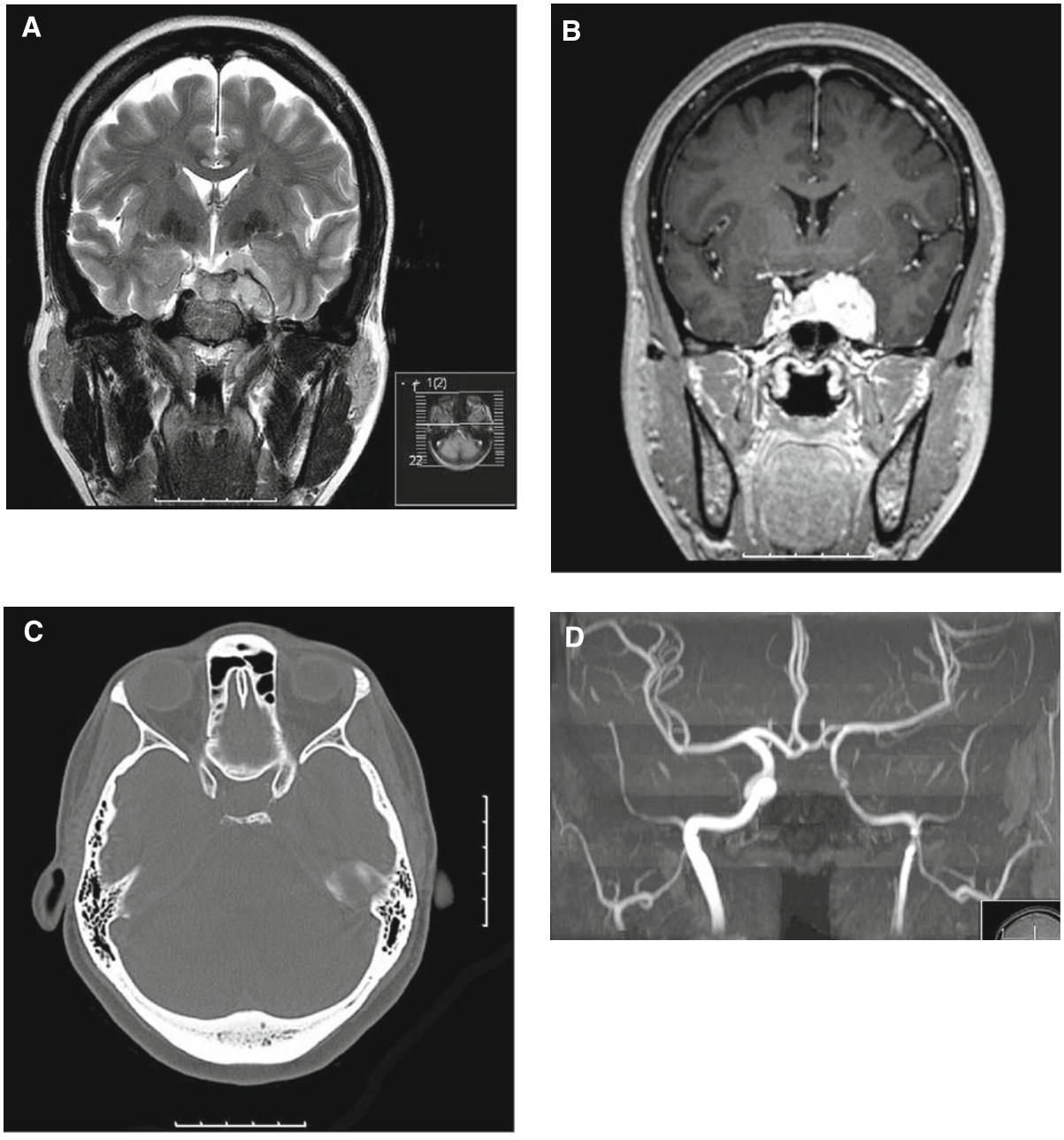

Fig. 1. Patient with tumor originating in the cavernous sinus. **A** T2 coronal MRI showing a hyperintense mass in left cavernous sinus pushing the lateral dural margin of the cavernous sinus outward (dark band). **B** T1 coronal post-contrast MRI showing enhancing mass in left cavernous sinus. **C** Axial CT showing hyperostosis of the left anterior clinoid process. **D** MRA showing constriction of left internal carotid artery

association to meningioma development and growth [1, 28, 31, 33].

Physical examination should include a complete and thorough neurological work-up. Deficits of cranial nerves III, IV, and VI are extremely common, as are trigeminal nerve deficits. Visual fields should be scrutinized and any suspicion of a field deficit should prompt acquisition of a complete neuro-ophthalmological examination with visual fields. The remaining cranial nerves should be examined as well. Examination of coordination and motor, sensory, and cerebellar functions assists with assessment of any tumor extension into the posterior fossa with brainstem compression.

Imaging

Magnetic resonance imaging (MRI) is currently the best method for evaluation of a suspected CSM. Meningiomas are typically dural-based masses that are isointense on T1, variable on T2, densely enhanced, and generally have a dural tail (Fig. 1A,B). Calcifications may be seen as hypointense regions within the tumor. Computed tomography (CT) is also important, as it displays the presence of any associated hyperostosis (Fig. 1C). Magnetic resonance angiography (MRA) generally reveals the intracranial circulation without the risks of conventional angiography (Fig. 1D). Conventional angiography with cross-compression, however, should be considered in situations where there is any question about the integrity of the ipsilateral carotid artery or the intracranial circulation in general, or in a patient who received prior irradiation to the cavernous sinus. Thorough study is recommended to identify patients in which the carotid artery is at excess risk. In these cases, a balloon test occlusion with single-photon emission computed tomography and acetazolamide challenge might be considered in order to assess the collateral circulation. Patients with poor collateral circulation should undergo a bypass procedure.

Treatment options and indications

There are three primary treatment options for patients with CSM: observation, microsurgical resection, and SRS. Observational treatment is based on the fact that meningiomas can remain quiescent for long periods of time, and some grow only very slowly [15, 24, 35]. Patients with asymptomatic or minimally symptomatic CSMs with cranial nerve deficit may be candidates for observation.

CSMs that demonstrate growth on serial imaging or become progressively more symptomatic require intervention. These characteristics constitute the primary indications for microsurgical resection. SRS can be utilized in these patients as well as in asymptomatic patients. It is also wise to inform the patient of alternative medical regimens, such as hydroxyurea, mifepristone, or tamoxifen; however, none of these regimens has been proven to treat meningiomas in toto [7, 8, 13, 16, 19, 21]. There are some situations where surgical resection should be considered over SRS, such as for tumors with significant extracavernous components in which symptomatology is secondary to neural compression by the tumor (e.g., hydrocephalus from brainstem compression). Tumors that compress the optic nerves, chiasm, or tracts should be considered for resection, owing to the risk of radiation-induced optic neuropathy [27]. Some authors advocate a "safety margin" of 2–3 mm of tumor separation from the optic tract to treat the tumor with stereotactic radiosurgery while minimizing the risk of radiation-induced optic neuropathy [22, 25]. Others formulate dose plans to keep the radiation dose to the optic apparatus under 10 Gy [17, 29]. Tumors greater than 3–3.5 cm in diameter are not suitable candidates for SRS [18].

None of these options are without potentially significant risks. Neurosurgeons, oncologists, and radiation oncologists have been trained to discuss treatment options and recommendations with patients, but the medico-legal atmosphere now demands that practitioners present a full and fair accounting of treatment options, their aims, risks, and benefits. Patient requests for second opinions of proposed surgical, SRS, or medical treatments should be readily honored.

Guiding principles of CSM resection

Skull base approaches are used to provide greater visualization while attempting to minimize neural retraction. Bone removal facilitates this wide exposure. Approaches to the cavernous sinus are designed to provide vascular control of the carotid artery. Meningiomas quite frequently respect arachnoid

planes and, when they do, it is critical to exploit these planes to preserve normal structures. These planes become scarred and obliterated after initial resection or irradiation, making re-operation much more difficult. Therefore, total removal of the tumor at the first operation is recommended. Carotid artery preservation is sought at our centers, and again, there is often an arachnoid plane separating the tumor from the artery that can be exploited to spare the artery. If necessary, when no plane is encountered, small remnants of adherent tumor are left rather than sacrifice the artery. The same philosophy is true regarding the cranial nerves. Attempts should be made to remove all affected dura, and any affected dura that cannot be resected should be electrocoagulated, if possible. All involved or hyperostotic underlying bone should be drilled away. Any submucosal tumor spread within the sinuses should be removed. Sphenoid sinus defects must be repaired with extreme care during the reconstruction.

Surgical approaches to the cavernous sinus

Two primary surgical approaches to the cavernous sinus are used by the authors: the cranio–orbito–zygomatic approach (COZ), and the extended middle cerebral fossa (EMCF) transzygomatic approach. The COZ approach affords wide exposure of the entire cavernous sinus, proximal and distal carotid artery, and minimal cerebral retraction. The EMCF approach is used for tumors present in the posterior cavernous sinus, anterior petrous apex, and medial clival masses. This approach is more limited, does not offer readily obtainable distal control, and does not expose the medial or superior cavernous sinus as easily as does the COZ approach.

COZ approach

Extensive set-up is required prior to skin preparation (Fig. 2). The endotracheal tube is secured to the side of the mouth contralateral to the approach. A lumbar drain is placed for cerebrospinal fluid (CSF) drainage later. The upper body and head are slightly elevated. The head is positioned after application of 3-pin skeletal fixation. The frameless stereotactic system is registered, and intraoperative electrophysiologic electrodes are applied. Somatosensory evoked potentials and cranial nerve V and VII electrodes are placed at this time. Incisions are proposed for a coronal scalp flap over the cervical carotid artery in the event that more proximal control is required, and over the left lower quadrant and lateral left thigh to obtain fat and/or fascia during the reconstruction. After preparation, a sterile microphone and electrode are placed in the ipsilateral ear for brainstem auditory evoked response recording.

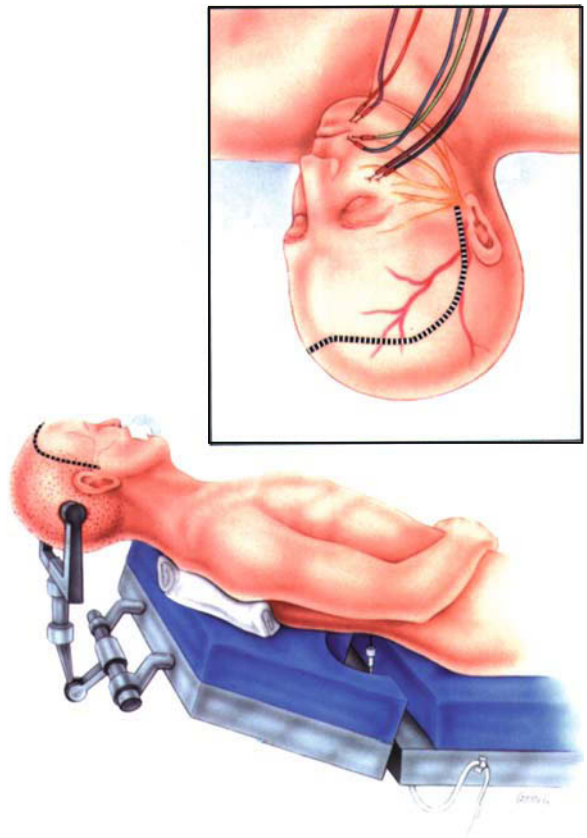

Fig. 2. Operative set-up for the COZ approach. Main illustration shows head and body positioning, Mayfield pin placement, and lumbar drainage. Inset shows proposed scalp incision and monitoring electrode placement. Reprinted with permission from Al-Mefty, *Operative Atlas of Meningiomas*. Lippincott, Williams & Wilkins, 1998

The anterior superficial temporal artery is located and carefully protected during the coronal incision. This maintains vascular supply to the flap and provides a donor vessel should an extracranial-to-intracranial bypass be required in the future. A temporal subfascial dissection is performed to

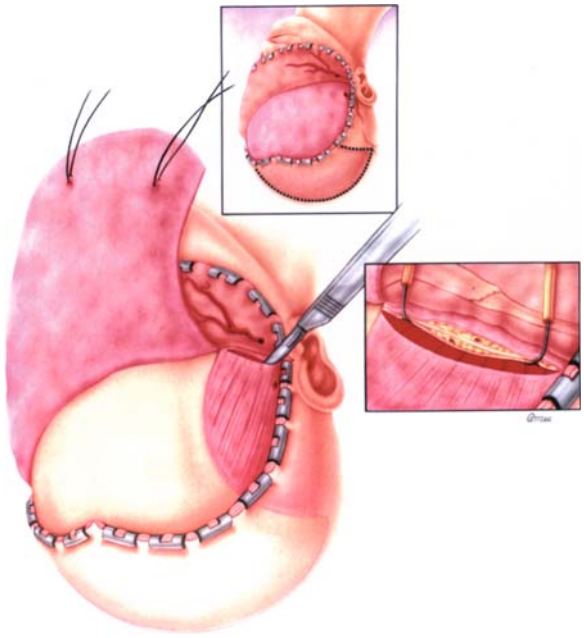

Fig. 3. Superficial soft tissue dissection. Upper inset shows dissection of the anterior and posterior scalp flaps while leaving the galeopericranial flap adherent to the calvarium. The main illustration shows elevation of the galeopericranial flap and the temporal fascia incision. *Right inset* subfascial dissection to preserve the facial nerve branches to the frontalis muscle. Reprinted with permission from Al-Mefty, *Operative Atlas of Meningiomas*. Lippincott, Williams & Wilkins, 1998

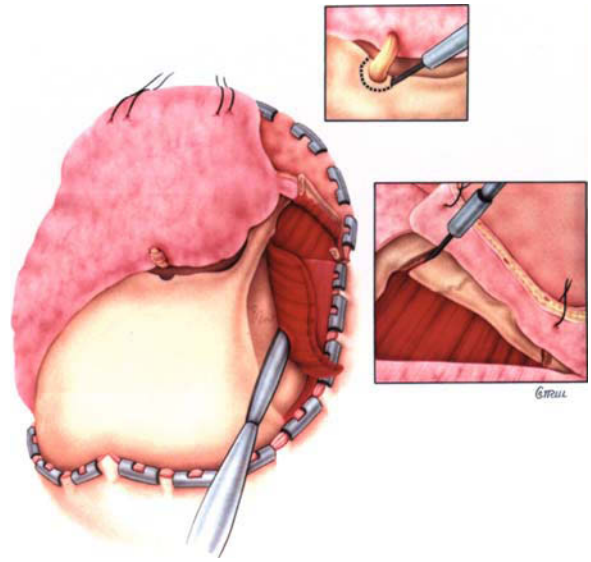

Fig. 4. Management of the temporalis muscle and zygomatic arch. *Upper inset* use of the air drill to preserve the supraorbital nerve. *Right inset* osteotomies at either end of the zygoma, which allows the temporalis muscle, shown in the main illustration, to be elevated off the calvarium and retracted inferiorly. Reprinted with permission from Al-Mefty, *Operative Atlas of Meningiomas*. Lippincott, Williams & Wilkins, 1998

preserve the frontal branches of facial nerve (Fig. 3). The frontoparietal pericranium is maintained as a vascularized flap for the reconstruction and can be raised from beneath the posterior flap (Fig. 3). As the scalp flap is elevated, the superficial and deep temporal fasciae are incised at first appearance of the temporal fat pad and are subsequently raised with the cutaneous flap. After dissecting the lateral orbit and zygomatic arch, the zygoma is divided at either end and displaced inferiorly on its masseteric pedicle (Fig. 4). The temporalis muscle is elevated off the calvarium in subperiosteal fashion, beginning low on the temporal squama and ending by disinserting the muscle at the superior temporal line (Fig. 4).

The cranio–orbital flap is elevated as a single piece (Fig. 5). A burr hole is placed in the keyhole to gain simultaneous entrance into the cranium and orbit. A second burr hole is placed posteriorly, adjacent to the temporal floor. A cut is made from the medial aspect of the lateral orbital wall to its lateral aspect and is continued to the keyhole. The keyhole is then connected to the posterior burr hole by cutting through the temporal fossa. A cut starting at this burr hole is then brought superiorly to the frontal bone, then anteriorly through the supraorbital rim, taking care to protect orbital contents during any cuts involving the bony orbit. Care must be taken to ensure that the posterior wall of the frontal sinus is cut, if the sinus has been entered. A cut is made from the first burr hole through the orbit, again taking care to protect the orbital contents. A notched osteotome is used to incise the orbital roof from the second burr hole toward the nasion, while protecting the orbital contents during this cut. The bone flap is now elevated. Remaining portions of the orbital roof, lateral orbital wall, and sphenoid wing can be removed with the craniotome for later reconstruction (Fig. 6). With the orbit now exposed, electromyographic electrodes may be directly placed into the superior oblique, superior rectus, and lateral rectus muscles to monitor cranial nerves III, IV, and VI.

Proximal control of the carotid artery is the next objective (Fig. 7). The middle fossa dura is elevated in

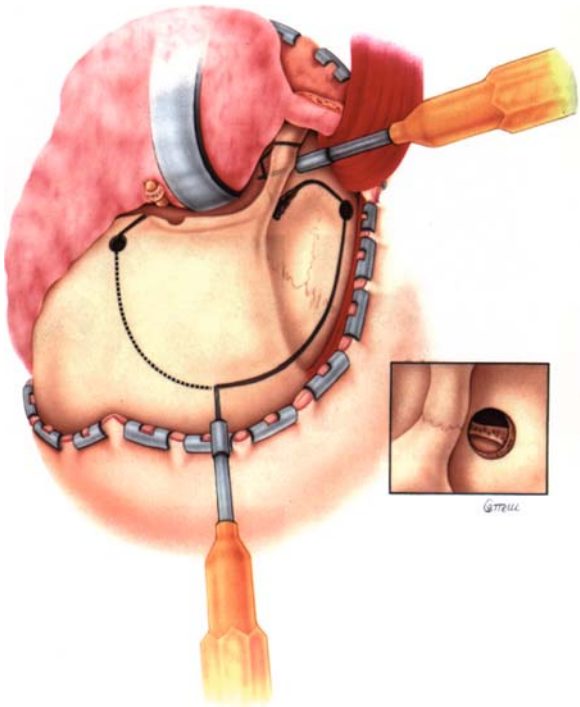

Fig. 5. Creating the cranio–orbital flap. Burr holes are placed in the keyhole and posteroinferiorly in the temporal squama. A cut is made across the lateral orbital wall, then brought up to the keyhole. The keyhole is connected posteriorly to the posterior burr hole. The cut is then continued up to the frontal bone and through the supraorbital bar. If the frontal sinus is entered, the posterior wall of the sinus must be cut as well. Orbital contents must be protected when drilling the bony orbit. A V-chisel is then used to cut the orbital roof from the keyhole (right inset) to the medial cut behind the supraorbital bar. Reprinted with permission from Al-Mefty, *Operative Atlas of Meningiomas*. Lippincott, Williams & Wilkins, 1998

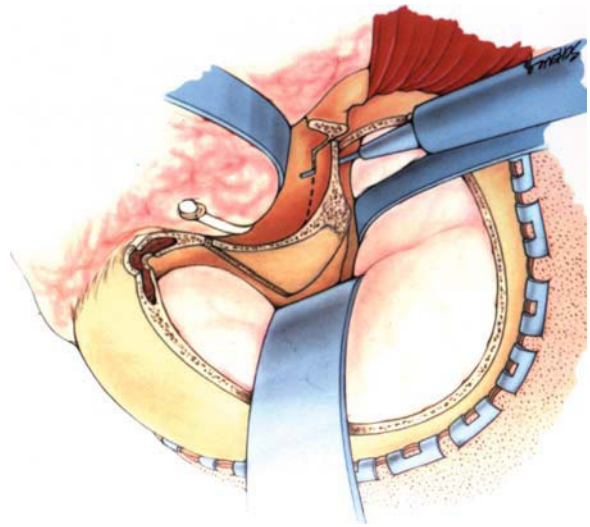

Fig. 6. Remaining portions of the orbital roof, sphenoid wing, and lateral orbital wall can be removed and used during reconstruction. Reprinted with permission from Al-Mefty, *Operative Atlas of Meningiomas*. Lippincott, Williams & Wilkins, 1998

a posterior-to-anterior direction. The greater superficial petrosal nerve (GSPN) emerges from the facial hiatus and should be dissected free of the dura. Traction of the GSPN is avoided to alleviate transmission to the geniculate ganglion, which can lead to facial palsy. The middle meningeal artery is identified, thoroughly electrocoagulated, and divided. Continued dural elevation reveals V3 and foramen ovale. The apices of Glasscock's triangle are now exposed: the facial hiatus, the anterior aspect of the foramen ovale, and the intersection of the GSPN and the lateral aspect of the V3. This triangle overlies the carotid artery, and drilling here with a diamond bit and constant irrigation exposes the carotid artery. In 62% of cases, the absence of bone between the carotid artery and the trigeminal ganglion extends to the lateral edge of the ganglion, and in 38% it extends lateral to the third division [9]. This may be sufficient for proximal control of the artery or to allow drilling posterolaterally from the known location of the artery. Proximal control may be obtained by sufficient exposure for placement of a temporary clip on the petrous carotid artery, if necessary. Alternatively, a Fogarty catheter may be inserted into the carotid canal. Should vascular control be required, the catheter balloon can be inflated to occlude the carotid artery in the carotid canal [36].

Medial exposure of the cavernous sinus and exposure of the subclinoid carotid artery is obtained by drilling out the remainder of the orbital roof, the superior orbital fissure, the anterior clinoid process, and the optic strut (Fig. 8). Drilling adjacent to the orbital apex and optic canal mandates a diamond burr and copious irrigation to dissipate the heat of drilling. The optic canal is opened first. The superior orbital fissure is opened by drilling along the lesser sphenoid wing. The anterior clinoid process is cored out with the drill and then disarticulated by drilling out the optic strut. The clinoid is subperiosteally dissected and resected. This procedure exposes the

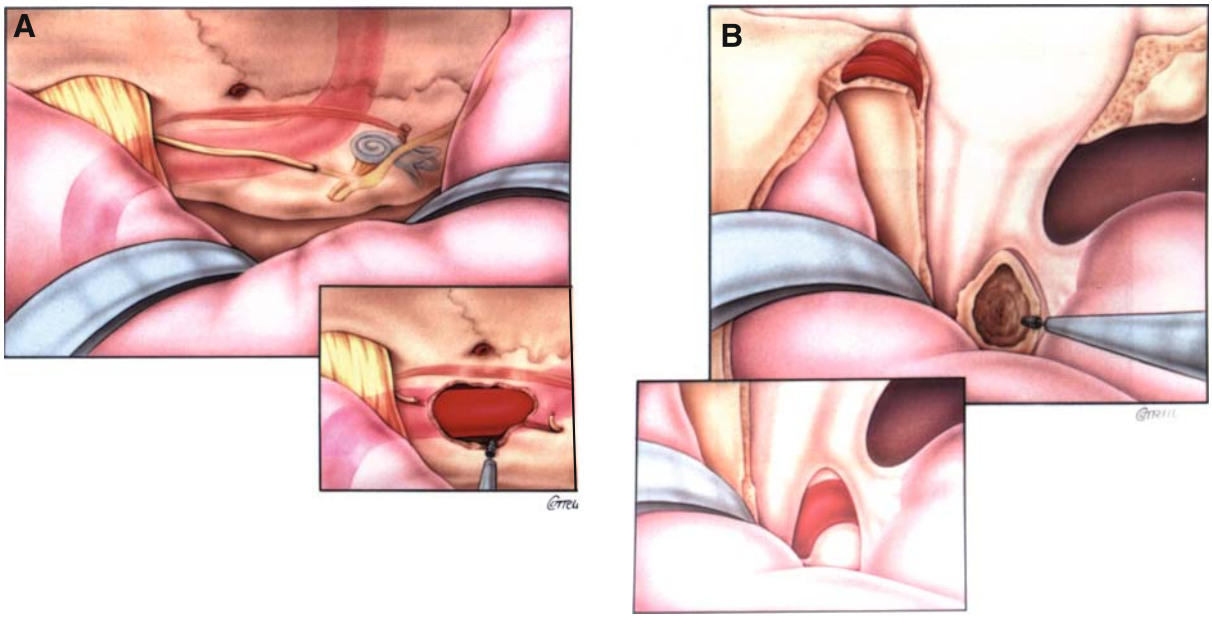

Fig. 7. **A** Middle fossa dissection. The main illustration shows anatomy of the floor of the middle fossa. *Lower inset* drilling lateral to V3 and posterior to the GSPN dissection reveals the petrous carotid artery, thereby providing proximal control. **B** Drilling to obtain medial cavernous sinus exposure. The main illustration (upper image) shows opening of the optic canal and drilling of the anterior clinoid process. *Inset* appearance of the anterior clinoid process and optic strut after resection. Reprinted with permission from Al-Mefty, *Operative Atlas of Meningiomas*. Lippincott, Williams & Wilkins, 1998

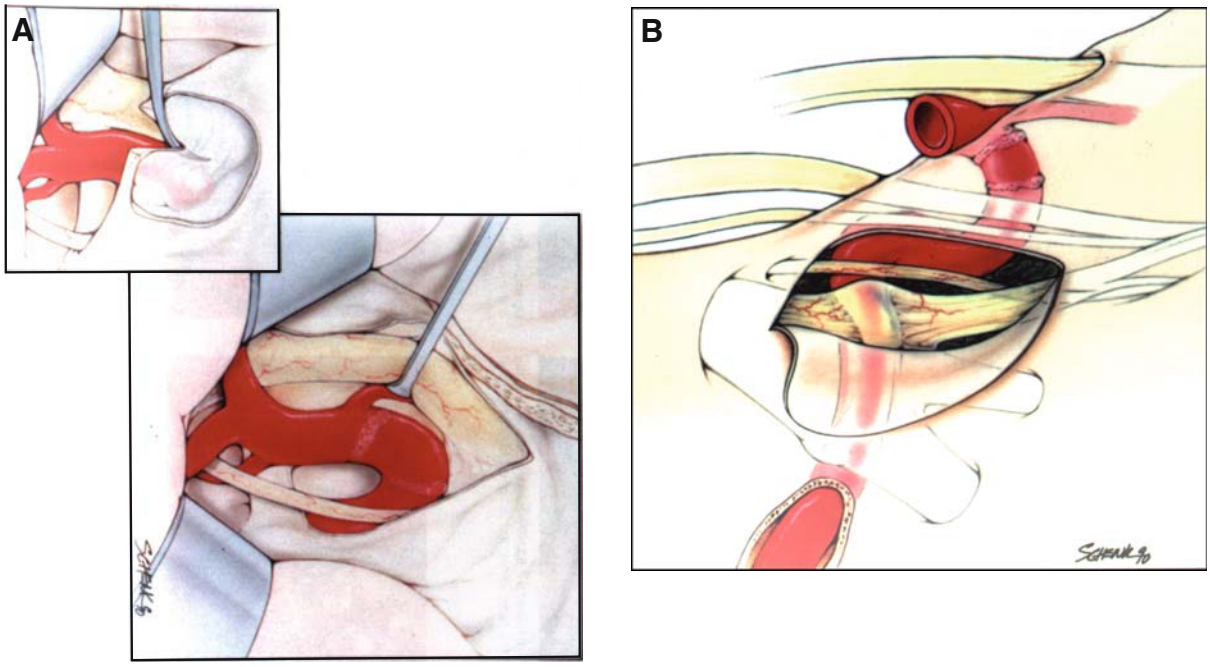

Fig. 8. **A** Superior entry into the cavernous sinus. *Inset* incising the dura over the optic nerve and the medial cavernous sinus. Main illustration shows the superior exposure obtained. **B** Intradural lateral entry into the cavernous sinus through Parkinson's triangle. Reprinted with permission from Al-Mefty, *Operative Atlas of Meningiomas*. Lippincott, Williams & Wilkins, 1998

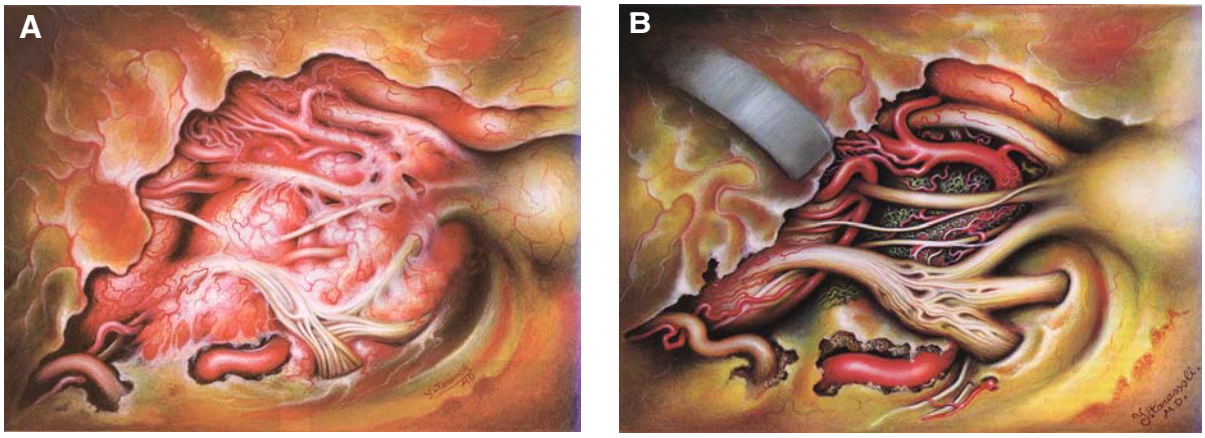

Fig. 9. **A** Illustration demonstrating extradural and intradural from both the superior and lateral entry of the cavernous sinus. The carotid artery is identified behind the gasserian ganglion proximally and in the anterior superior cavernous sinus distally. **B** Illustration demonstrating preservation of the cavernous sinus neurovascular structures after the removal of meningioma. Reprinted with permission from Al-Mefty, *Operative Atlas of Meningiomas*. Lippincott, Williams & Wilkins, 1998

subclinoid portion of the carotid artery, which is both extradural and extra-cavernous, and provides distal control of the carotid artery.

Entrance into the cavernous sinus has been described in relationship to the intervals between the neurovascular structures of the cavernous sinus. These intervals have been expressed in terms of 10 triangles distributed among the parasellar, middle fossa, and paraclival locations. The actual approach taken depends on the anatomy of the lesion in relationship to the cavernous sinus structures and must be individualized for each patient. In general, there are two approaches for entry into the cavernous sinus: a superior and a lateral approach. The superior approach is particularly suited to those lesions adjacent to the anterior loop of the carotid artery, and those that are superior and/or medial to the cavernous carotid artery. The lateral approach lends itself well to exposing those lesions lateral and/or inferior to the carotid artery and those that are posteriorly located within the cavernous sinus. Frequently these approaches are combined for lesions widely involving the sinus.

Superior entry (Fig. 9) After exposing the superior surface of the cavernous sinus, the dura overlying the optic nerve is divided over the length of the optic canal to free the optic nerve. The distal carotid ring is now divided. The dura is then incised toward the oculomotor nerve, providing initial entry into the cavernous sinus. Exposure can be increased by dissecting along the length of the carotid artery. Further exposure can be obtained by subperiosteal dissection of the posterior clinoid process and drilling off the process, the dorsum sellae, and the superior clivus. These maneuvers allow increased exposure of the posterior fossa.

For tumors with medial extension, the planum sphenoidale can be drilled away. This allows exposure of the sphenoid sinus. Dissection and incision of the diaphragma sellae allows visualization of the pituitary gland. Great care must be taken during closure to obliterate any communication between the cavernous sinus and sphenoid sinus in order to prevent CSF leakage.

Lateral entry Lateral entry into the cavernous sinus can be intradural or extradural. Extradural entry begins by incising the dura propria overlying V3. The dura propria is peeled away from the trigeminal branches and ganglion with superiorly directed traction. This will initially expose the third division and lateral ganglion followed by the second division and the majority of the remainder of the ganglion. Anterior extension from the region of Meckel's cave can be addressed by drilling away bone around the foramina rotundum and ovale to allow exposure of the sphenoid sinus and infratemporal fossa. Drilling bone here will also free the trigeminal branches that will, in turn, allow greater mobility of these

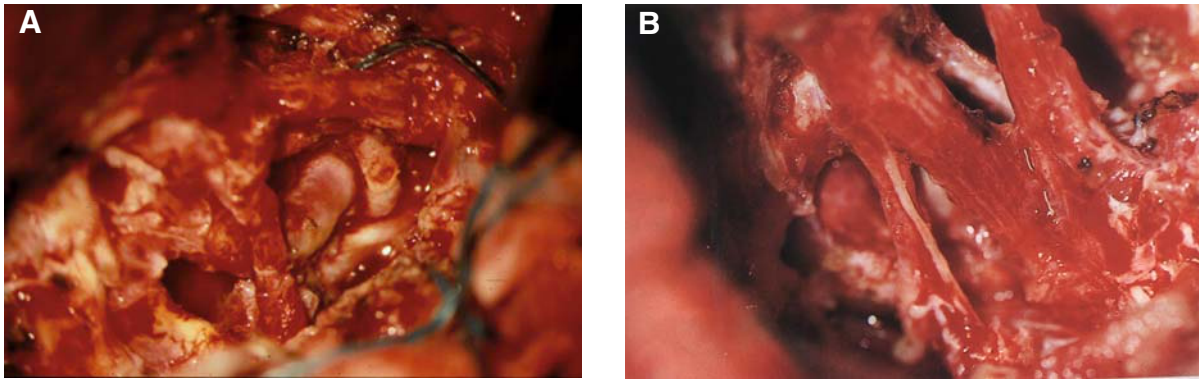

Fig. 10. **A** Operative photograph during the dissection of a meningioma through the lateral and superior wall of the cavernous sinus. The IIIrd nerve is in the middle of field and the VIth nerve is seen crossing over the carotid as it enters the cavernous sinus through Dorello's canal. **B** Operative photograph where the tumor has been entirely dissected and all cranial nerves and the carotid artery are preserved. Reprinted with permission from Al-Mefty, *Operative Atlas of Meningiomas*. Lippincott, Williams & Wilkins, 1998

branches and the ganglion. A mass beginning to enter the posterior fossa can be further exposed by drilling the petrous apex. This drilling also allows greater exposure around and under the trigeminal ganglion.

For lesions requiring intradural exposure, intradural entry into the cavernous sinus is achieved through Parkinson's triangle [26] (Fig. 10). Cranial nerves III and IV are identified over the tentorial edge. An incision beneath the anticipated position of the fourth nerve is fashioned and extended approximately 8 mm anteriorly and 8 mm inferiorly. The external dural layer is peeled away from the thin inner dural layer in which nerves III–V are found. The dural flap can be further dissected from the trigeminal ganglion to expose Meckel's cave. Exposure can be increased posteriorly and into the posterior fossa by drilling the petrous apex. The trigeminal nerve can be mobilized by drilling the foramina rotundum and ovale.

The inner dural layer between the fourth nerve and the ophthalmic division can be incised to expose the lateral space of the cavernous sinus, the posterior bend and the horizontal segment of the intracavernous carotid artery, and the lateral cavernous and meningohypophysial arteries. The abducens nerve is the only cranial nerve coursing inside the cavernous sinus proper, often appearing in fascicles of 2–5 nerves, and should be carefully located and protected [9, 20]. Frequently meningiomas necessitate the combination of extra and intradural cavernous sinus dissection with combining superior and lateral entry (Figs. 9 and 10).

Reconstruction after the COZ approach begins by directing attention toward prevention of CSF leaks by searching for and obliterating any feature of the dissection that may result in a CSF leak. Any entrance into the paranasal sinuses or the Eustachian tube should be obliterated with fat and fascia. Any tenuous or incomplete dural closures should be reinforced with tissue – preferably autologous – such as fascia, muscle, or fat. Fibrin glue can be used for further reinforcement. The galeopericranial flap is now brought down under the frontal lobe, over the orbit, and over any sinus entries in the middle fossa or petrous apex. The orbital roof is reconstructed to prevent late enophthalmos. Dural tack-up sutures are placed circumferentially, including in the subtemporal region, to obliterate dead space and prevent postoperative development of epidural hematomas. If the frontal sinus has been entered, the mucosa should be exenterated and the cavity packed with fat or tissue to prevent mucocele formation and CSF leakage. The cranio–orbital flap is secured in place with titanium miniplates. Bony defects can be obliterated with titanium plates or mesh, or any of a number of cranioplastic materials, such as hydroxyapatite cement. The temporalis muscle is sutured to the superior temporal line. The zygoma is plated into position with titanium miniplates. The scalp is closed in layers and a craniotomy headwrap is applied to decrease postoperative fluid collection under the flap.

EMCF approach

Scalp incision, temporalis dissection, and zygomatic osteotomies are performed as previously described (Figs. 3–5). Four burr holes are now placed (Fig. 11): the first in the keyhole, the second low and anterior in the middle fossa, the third low and posterior in the middle fossa, and the last along the superior temporal line. These four burr holes are connected using a craniotome. Residual bone along the sphenoid wing or temporal squama can be removed with the craniotome as well. Dissection along the middle fossa floor (dural elevation, middle meningeal artery division, GSPN dissection, and acquisition of proximal carotid artery control) is performed as previously described (Fig. 7). Further dural elevation exposes the confines of the petrous apex: the lateral aspect of V3, the GSPN, and the facial hiatus. If exposure of the petroclival area is required, then the petrous apex is drilled down. Lateral entrance is similar to the extradural lateral cavernous sinus entrance previously described. The dura propria overlying V3 is incised and peeled away from the trigeminal branches and ganglion. Further dissection of the dura propria reveals V1 and the fourth cranial nerve. Anterior extension from Meckel's cave is exposed by drilling bone around the foramina rotundum and ovale to allow exposure of the sphenoid sinus and infratemporal fossa. If intradural extension of the tumor is discovered, such as with invasion into the temporal lobe and cisterns anterior to the brainstem, then intradural exposure can be easily obtained using this approach (Fig. 10). Lateral intradural entrance as described above can also be performed using this approach, although distal control of the carotid artery cannot be obtained.

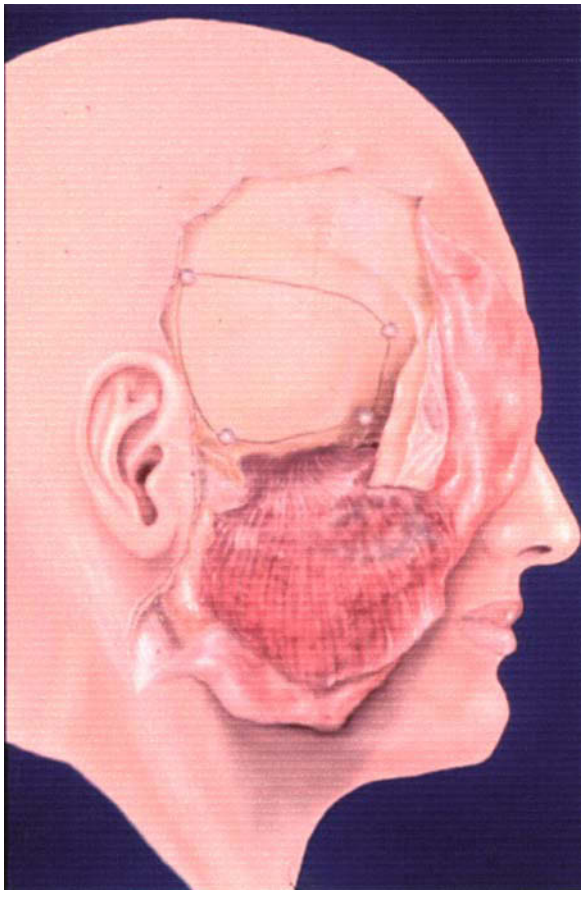

Fig. 11. Four burr holes are placed using the EMCF approach

Closure of the EMCF approach requires meticulous attention to prevention of CSF leak, as described. A strip of posterior temporalis muscle is placed along the petrous apex to prevent leakage. The remainder of the closure is similar to that of the COZ closure.

Dissection within the cavernous sinus

Dissection within the cavernous sinus is performed with microdissectors and microscissors. Sharp dissection is performed, whenever possible, to prevent traction of intracavernous cranial nerves and arteries. Coagulation, where necessary, should be bipolar. As mentioned, once the cavernous sinus is entered, the abducens nerve should be located and preserved. Venous bleeding can be controlled using head elevation and judicious packing with hemostatic agents. Any cranial nerve that is frankly severed should be directly repaired. If a tension-free direct repair is not possible, an interposition graft should be performed. Injury to the carotid artery can be addressed in several ways. Temporary clipping and direct repair of tears can be performed with 8–0 suture; more severe carotid injury can be treated by vein graft repair.

Surgical results

Surgical resection of tumors within the cavernous sinus is not the prohibitive procedure it once was.

Table 1. Results of surgical resection of cavernous sinus meningiomas

Series	Number of patients	Mean follow-up (range)	Complete removal	Gross total removal	Tumor recurrence	Progression-free interval	New cranial nerve deficits	Mortality
Kosp et al. [14]	29	(3 months–7 years)		5 (17%)			III – 14% IV – 14% VI – 3.4% V1 – 3.4% V2 – 10% V3 – 17%	3 (10%)
Delmonte et al. [5]	38	45 months (2 months–10 years)		31 (82%)	13%		7 patients (18%) 10 nerves	6 (16%)
De Jesus et al. [4]	119	33.8 months		73 (61%)	10%	3 years – 87% 5 years – 62%		
O'Sullivan et al. [23]	39	24 months (6 months–5.3 years)		8 (21%)	5%		23 of 192 normal nerves at risk (12%)	
Cusimano et al. [2]	89	28 months		59 (66%)	7%			5 (6%) died from tumor
Dolenc [6]	511		89 (17%)	179 (35%)			34 patients[a] (7%)	3 (0.6%)

[a]Number of patients with cranial nerve deficits persisting longer than 6 months.

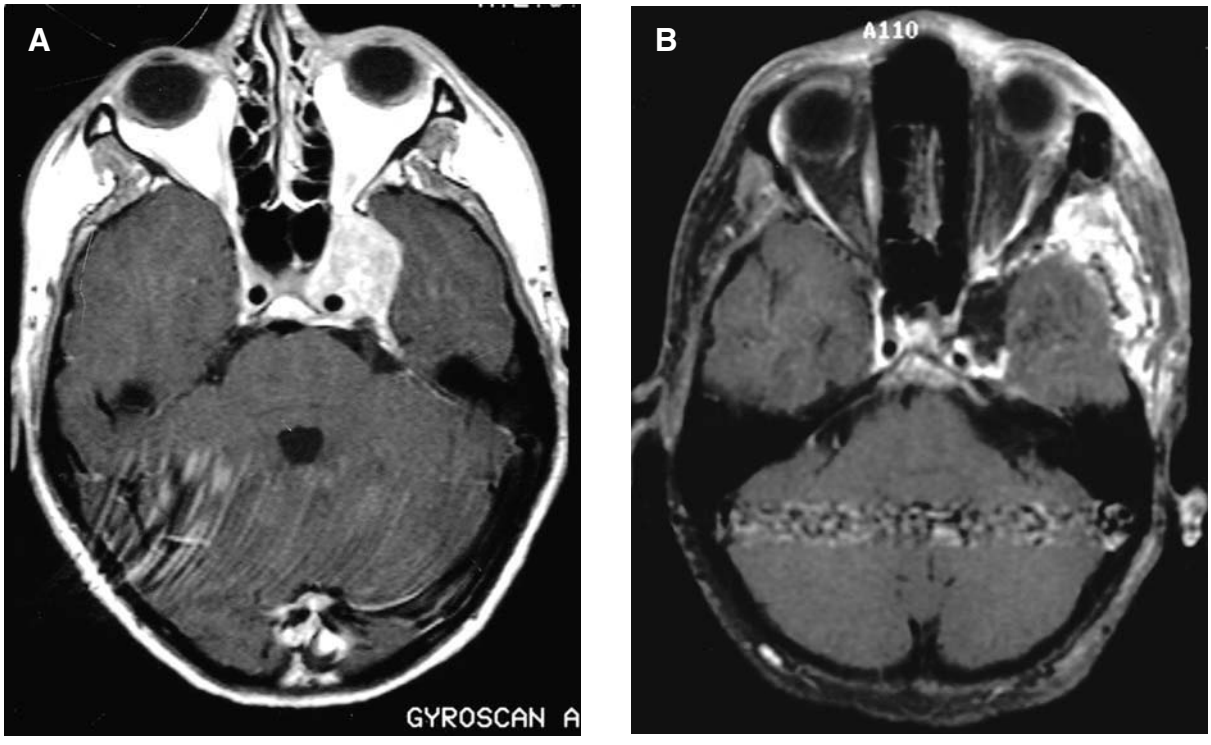

Fig. 12. MRIs of a patient with a left cavernous sinus meningioma. **A** Preoperative image. **B** Image showing complete resection

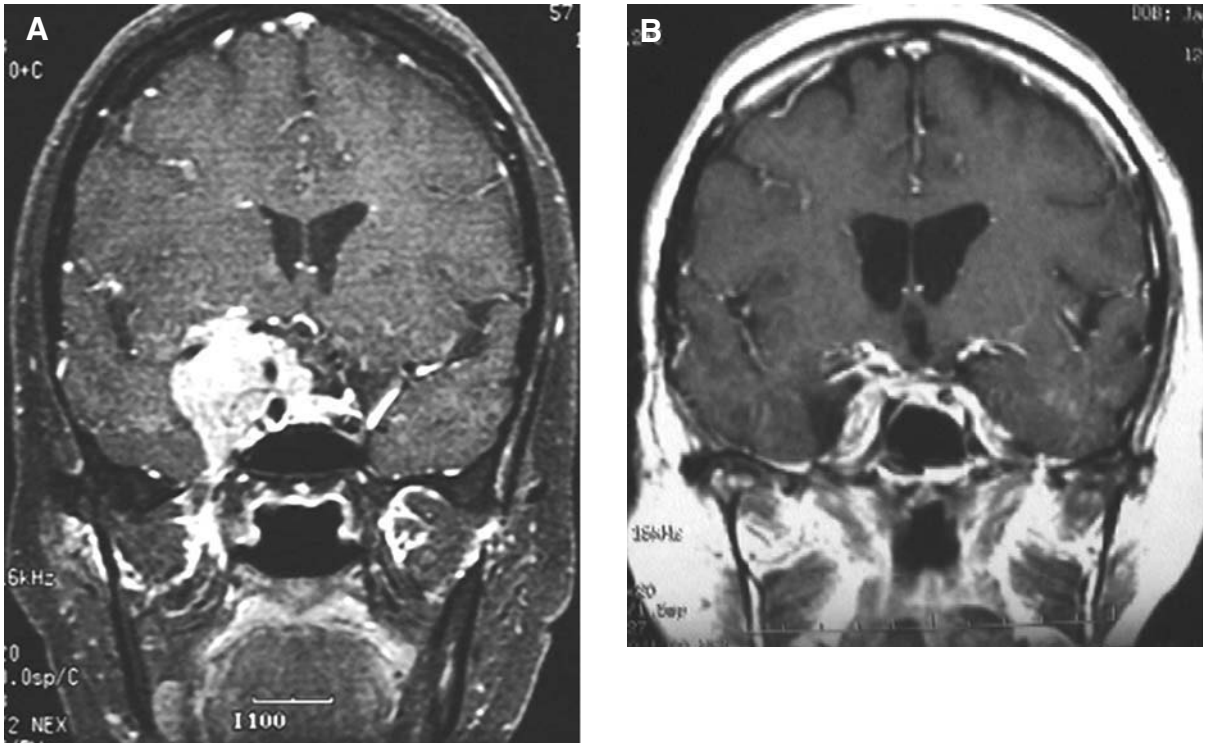

Fig. 13. MRIs of a patient with a right cavernous sinus meningioma. **A** Preoperative image. **B** Image showing incomplete resection with a small portion of residual tumor

Many refinements in skull-based surgical approaches, neuroanesthesia, neuroimaging, and nerve monitoring make surgical resection of the cavernous sinus a more tractable problem. Published series reporting gross total resections of the cavernous sinus vary widely (21–76%) [2, 4–6, 14, 23] (Table 1). Total resection has been achieved in 71 of 163 cases (44%) in the senior author's experience (Fig. 12). At the University Hospital of Arkansas, the overall recurrence rate is 26%, with 12% rate of recurrence in cases of total resection and 86% in cases of residual tumor (Fig. 13). De Jesus et al. reported 87% progression-free survival at 3 years and 62% at 5 years [4]. Therefore, centers working routinely with CSMs have reported reasonable rates of gross total resection and progression-free survival. In his series of 511 CSMs Dolenc [6], first to operate regularly on cavernous sinus lesions without the assistance of cardiac-arrest, reports resecting 286 either "completely" or "gross totally" with a gold-standard mortality rate of less than 1%, all three deaths occurring among 71 patients who had had recurrences from operations performed elsewhere.

Stroke is a significant concern when working around or with the carotid artery in the cavernous sinus. Ischemic stroke is not a frequent complication in the resection of CSMs [5, 14, 23]. At the University Hospital of Arkansas, seven of 188 patients (3.7%) experienced ischemic stroke. Cusimano et al. [2] reported four disabling strokes in 89 patients, and De Jesus et al. [4] reported 6 strokes (5%); however, this group's operative philosophy includes bypass and resection of an invaded carotid artery.

Cranial nerve morbidity is a critical issue in resecting CSMs. Table 1 shows reported incidences of new cranial nerve deficits following resection of CSMs. In general, existing preoperative cranial nerve deficits infrequently improve or resolve following resection, and the majority of new cranial nerve deficits postoperatively resolve. DeMonte et al. reported improvements in 14% of preoperatively affected cranial nerves, while 80% remained stable [5]. They reported 10 new neuropathies in seven (18%) patients. In a recent re-evaluation of the cases operated on by one author (O.A.-M.), 21 of 163

patients (12.8%) experienced new cranial nerve deficits, 14 of 163 operated patients (8.5%) experienced worsening of a preoperative deficit, while 11 of 163 patients (6.7%) experienced both a new cranial nerve deficit and a deterioration of existing deficits. O'Sullivan et al. [23] reported 4 of 17 patients (24%) with preoperative optic nerve deficits improved, while 1 of 17 patients (6%) with normal preoperative vision suffered a new visual field deficit. Five of twenty four extraocular nerves (21%) with preoperative deficits improved, while 14 of 78 (18%) preoperatively normal cranial nerves at risk suffered a new deficit. They reported an overall 12% risk of new cranial nerve morbidity. Knosp et al. [14] report that 43% of impaired oculomotor deficits improved, 50% of sixth nerve deficits improved, and 33% and 28% of V2 and V3 deficits improved, respectively. Preoperative deficits in nerves IV and V1 improved rarely (0% and 7%, respectively). In their experience, no patient who had intact cranial nerves experienced any postoperative deficits. There were no new third nerve palsies, one new sixth nerve palsy, one new V1 nerve palsy, two new fourth nerve palsies, three new V2 palsies, and five new V3 palsies.

Conclusions

CSMs can be very difficult tumors to treat. A thorough understanding of the patient's history, physical examination, radiographic findings, and other evaluations (visual fields, pituitary function, etc.) is crucial to proper treatment of CSMs. It is also critical that the CSM patient understand the natural history, options, and risks with every treatment. Further, it is important to understand the patient's goals for treatment.

Skull base techniques have rendered the resection of CSMs a viable treatment option. Currently, microsurgical resection of CSM stands alone as the only treatment capable of providing total tumor removal. No other treatment option can provide total removal or disappearance of the meningioma with any consistency. Critics warn of dire consequences of traversing this region. The main problem encountered in the pursuit of total resection is cranial neuropathy. Most neuropathies encountered in these patients are evident at presentation, while a minority occurs postoperatively and are permanent; many that do occur are sensory in nature or can be treated with strabismus surgery. Optic nerve deficits are infrequently encountered. All of these morbidities are tractable, however. Multiple surgical centers world-wide have extensive expertise in treating such tumors, and techniques and outcomes are in continual evolution. Therefore, a balanced presentation of options to patients with CSM should include surgical resection.

References

1. Bozzetti C, Camisa R, Nizzoli R, Manotti L, Guazzi A, Naldi N, Mazza S, Nizzoli V, Cocconi G (1995) Estrogen and progesterone receptors in human meningiomas: biochemical and immunocytochemical evaluation. Surg Neurol 43: 230–233; discussion 234
2. Cusimano MD, Sekhar LN, Sen CN, Pomonis S, Wright DC, Biglan AW, Jannetta PJ (1995) The results of surgery for benign tumors of the cavernous sinus. Neurosurgery 37: 1–9; discussion 9–10
3. Custer BS, Koepsell TD, Mueller BA (2002) The association between breast carcinoma and meningioma in women. Cancer 94: 1626–1635
4. De Jesus O, Sekhar LN, Parikh HK, Wright DC, Wagner DP (1996) Long-term follow-up of patients with meningiomas involving the cavernous sinus: recurrence, progression, and quality of life. Neurosurgery 39: 915–919; discussion 919–920
5. DeMonte F, Smith HK, Al-Mefty O (1994) Outcome of aggressive removal of cavernous sinus meningiomas. J Neurosurg 81: 245–251
6. Dolenc VV (2003) Microsurgical anatomy and surgery of the central skull base. Springer, Wien New York, pp 162–177
7. Goodwin JW, Crowley J, Eyre HJ, Stafford B, Jaeckle KA, Townsend JJ (1993) A phase II evaluation of tamoxifen in unresectable or refractory meningiomas: a Southwest Oncology Group study. J Neurooncol 15: 75–77
8. Grunberg SM, Weiss MH, Spitz IM, Ahmadi J, Sadun A, Russell CA, Lucci L, Stevenson LL (1991) Treatment of unresectable meningiomas with the antiprogesterone agent mifepristone. J Neurosurg 74: 861–866
9. Harris FS, Rhoton AL (1976) Anatomy of the cavernous sinus. A microsurgical study. J Neurosurg 45: 169–180
10. Harrison MJ, Wolfe DE, Lau TS, Mitnick RJ, Sachdev VP (1991) Radiation-induced meningiomas: experience at the Mount Sinai Hospital and review of the literature. J Neurosurg 75: 564–574
11. Jacobs DH, Holmes FF, McFarlane MJ (1992) Meningiomas are not significantly associated with breast cancer. Arch Neurol 49: 753–756
12. Johnson MD, Powell SZ, Boyer PJ, Weil RJ, Moots PL (2002) Dural lesions mimicking meningiomas. Hum Pathol 33: 1211–1226
13. Kaba SE, DeMonte F, Bruner JM, Kyritsis AP, Jaeckle KA, Levin V, Yung WK (1997) The treatment of recurrent

unresectable and malignant meningiomas with interferon alpha-2b. Neurosurgery 40: 271–275
14. Knosp E, Perneczky A, Koos WT, Fries G, Matula C (1996) Meningiomas of the space of the cavernous sinus. Neurosurgery 38: 434–442; discussion 442–444
15. Kuratsu J, Kochi M, Ushio Y (2000) Incidence and clinical features of asymptomatic meningiomas. J Neurosurg 92: 766–770
16. Lamberts SW, Tanghe HL, Avezaat CJ, Braakman R, Wijngaarde R, Koper JW, de Jong H (1992) Mifepristone (ru 486) treatment of meningiomas. J Neurol Neurosurg Psychiatry 55: 486–490
17. Leber KA, Bergloff J, Pendl G (1998) Dose–response tolerance of the visual pathways and cranial nerves of the cavernous sinus to stereotactic radiosurgery. J Neurosurg 88: 43–50
18. Lee JY, Niranjan A, McInerney J, Kondziolka D, Flickinger JC, Lunsford LD (2002) Stereotactic radiosurgery providing long-term tumor control of cavernous sinus meningiomas. J Neurosurg 97: 65–72
19. Mason WP, Gentili F, Macdonald DR, Hariharan S, Cruz CR, Abrey LE (2002) Stabilization of disease progression by hydroxyurea in patients with recurrent or unresectable meningioma. J Neurosurg 97: 341–346
20. Nathan H, Ouaknine G, Kosary IZ (1974) The abducens nerve. Anatomical variations in its course. J Neurosurg 41: 561–566
21. Newton HB, Slivka MA, Stevens C (2000) Hydroxyurea chemotherapy for unresectable or residual meningioma. J Neurooncol 49: 165–170
22. Nicolato A, Foroni R, Alessandrini F, Bricolo A, Gerosa M (2002) Radiosurgical treatment of cavernous sinus meningiomas: experience with 122 treated patients. Neurosurgery 51: 1153–1159; discussion 1159–1161
23. O'Sullivan MG, van Loveren HR, Tew JM Jr (1997) The surgical resectability of meningiomas of the cavernous sinus. Neurosurgery 40: 238–244; discussion 245–247
24. Olivero WC, Lister JR, Elwood PW (1995) The natural history and growth rate of asymptomatic meningiomas: a review of 60 patients. J Neurosurg 83: 222–224
25. Pamir MN, Kilic T, Bayrakli F, Peker S (2005) Changing treatment strategy of cavernous sinus meningiomas: experience of a single institution. Surg Neurol 64 [Suppl 2]: S58–S66
26. Parkinson D, West M (1990) Lesions of the cavernous plexus region. In: Youmans JR (ed) Neurological surgery. W.B. Saunders, Philadelphia, pp 3351–3370
27. Pendl G, Schrottner O, Eustacchio S, Ganz JC, Feichtinger K (1998) Cavernous sinus meningiomas – what is the strategy: upfront or adjuvant gamma knife surgery? Stereotact Funct Neurosurg 70[Suppl 1]: 33–40
28. Piper JG, Follett KA, Fantin A (1994) Sphenoid wing meningioma progression after placement of a subcutaneous progesterone agonist contraceptive implant. Neurosurgery 34: 723–725; discussion 725
29. Pollock BE, Stafford SL (2005) Results of stereotactic radiosurgery for patients with imaging defined cavernous sinus meningiomas. Int J Radiat Oncol Biol Phys 62: 1427–1431
30. Ron E, Modan B, Boice JD Jr, Alfandary E, Stovall M, Chetrit A, Katz L (1988) Tumors of the brain and nervous system after radiotherapy in childhood. N Engl J Med 319: 1033–1039
31. Schlehofer B, Blettner M, Wahrendorf J (1992) Association between brain tumors and menopausal status. J Nat Cancer Inst 84: 1346–1349
32. Schoenberg BS, Christine BW, Whisnant JP (1975) Nervous system neoplasms and primary malignancies of other sites. The unique association between meningiomas and breast cancer. Neurology 25: 705–712
33. Surawicz TS, McCarthy BJ, Kupelian V, Jukich PJ, Bruner JM, Davis FG (1999) Descriptive epidemiology of primary brain and CNS tumors: results from the Central Brain Tumor Registry of the United States, 1990–1994. Neuro-Oncol 1: 14–25
34. Tagle P, Villanueva P, Torrealba G, Huete I (2002) Intracranial metastasis or meningioma? An uncommon clinical diagnostic dilemma. Surg Neurol 58: 241–245
35. Van Havenbergh T, Carvalho G, Tatagiba M, Plets C, Samii M (2003) Natural history of petroclival meningiomas. Neurosurgery 52: 55–62; discussion 62–54
36. Wascher TM, Spetzler RF, Zabramski JM (1993) Improved transdural exposure and temporary occlusion of the petrous internal carotid artery for cavernous sinus surgery. Technical note. J Neurosurg 78: 834–837

Surgery of cavernous sinus meningiomas: advantages and disadvantages

M. Samii, V. M. Gerganov

International Neuroscience Institute-Hannover, Hannover, Germany

Introduction

Meningiomas of the cavernous sinus (CS) are extremely difficult to treat surgically with acceptable morbidity and mortality. Risks are rooted primarily in tumor location, particularly with respect to the proximity of important neurovascular structures. Dramatic advances in skull base techniques in recent decades have made radical resection of these lesions possible. Complex approaches to specific sites within the CS through various anatomical triangles have been described [5, 9, 15], and the rates of total resection have improved [4–7, 9, 43]. But rushing to aggressive surgery is to ignore the potentially high costs exacted from patients in terms of functional loss and reduced quality of life. Furthermore, the high recurrence rates associated with increasing periods of follow-up after presumed total resection raises the question of whether surgical cure is actually possible. Currently, treatment options range from attempts at radical resection to radiosurgery [13, 17, 19, 20, 27, 33].

The senior author's (MS) treatment philosophy has evolved over the course of treating more than 1600 skull base meningiomas, including 242 involving the CS. Here we focus on the two largest CS groups: (a) medial sphenoid wing meningiomas involving the CS, or sphenocavernous meningiomas (SCM), and (b) petroclival meningiomas with CS involvement (PCCSM). We discuss clinical features, methods of treatment, and outcomes shaping our current management philosophy. Understanding the advantages and disadvantages of CS surgery is vital to selecting the most appropriate treatment.

Clinical material and methods

Patients with meningiomas involving the CS treated surgically by the senior author were studied retrospectively by analyzing clinical records, neuroradiological findings, operative reports, and follow-up data. Age, sex, clinical presentation, site of tumor origin and growth pattern, operation performed, and therapeutic outcome were examined. A patient's outcome was established by postoperative CT and/or MR imaging, neurological status, specific postoperative complaints, and the presence or absence of surgical complications.

Operative approaches were determined by the individual patient's neurological status, plus imaging findings with respect to tumor origin, size, and predominant pattern of growth. Since the surgical techniques employed have been described elsewhere [30, 37, 39, 40, 47, 49], only the primary steps of the fronto-temporal approach are discussed. A standard fronto-temporal craniotomy was performed in each case, removing the sphenoid ridge with a high-speed drill and opening dura in a semicircular manner over the sylvian fissure. With large tumors, the sylvian cistern was opened initially in order to avoid injuring the internal carotid artery (ICA). Tumor enucleation

followed, along with exposing middle cerebral artery branches surrounding the tumor capsule retrograde in order to identify the main trunk of the ICA. The most delicate and dangerous part of this process involved manipulations posterior to the ICA, within the tentorial notch. After identifying the ICA and the optic nerve, attention was directed to the posterior communicating artery, the anterior choroidal artery, and the oculomotor nerve. Only when space sufficient for a good view of the oculomotor and trochlear nerves was achieved, did we expose the CS. The lateral wall of the sinus was incised along the course of the oculomotor nerve, paying close attention to the trochlear and trigeminal nerves nearby. The 4th and 5th cranial nerves might be displaced by the tumor in different directions, while the ICA is most frequently displaced toward the medial wall of the CS. We injected highly vascular meningiomas with fibrin glue through the CS wall before incising it, thus minimizing subsequent bleeding. After tumor resection, the sinus cavity was lined with one or two layers of Surgicel, then filled with fibrin sponges in order to assure hemostasis.

Occasionally surgery was performed in two stages, initially decompressing the brainstem by resecting tumor via the retrosigmoid–suprameatal or retrosigmoid approach (Figs. 1, 2), then removing the supratentorial component by a fronto-temporal approach in a separate operation (Fig. 3).

Results

Patient data

Of 242 patients with meningiomas involving the CS, 10% occurred there primarily and 90% invaded the CS secondarily (Table 1). Meningiomas arising from the medial sphenoid wing and spreading to the CS were most common, making up 38.4% of all CS meningiomas and 66.4% of all medial sphenoid wing meningiomas in the series. The mean age was 56 years, ranging from 23 to 80.5 years, and the male (29%) to female (71%) ratio was 1:2.5. Petroclival meningiomas involving the CS accounted for 36.8% of all CS meningiomas and 48.4% of all petroclival meningiomas. Among such lesions the male (40%) to female (60%) ratio was 1:1.5.

Table 1. Site of origin of the meningiomas with CS involvement in the series

Site of origin of the meningioma	Incidence (%)
Primary CS	10
Sphenocavernous	38.4
Anterior clinoid	2
Tuberculum sellae	4.6
Petrous apex	4.1
Cerebellopontine angle	4.1
Petroclival	36.8

For SCMs, a neuroradiological diagnosis was achieved from 2 weeks to 8 years following the initial symptom (mean 19 months), compared to from 1 month to 8 years (mean 17.6 months) for PCCSMs. The most common presenting symptoms are listed in Table 2. Patients with SCMs presented most frequently with visual disturbances (54.8%) and double vision (28%), while among those with PCCSMs, trigeminal nerve dysfunction (43%), hearing loss (43%), and ataxia (30%) predominated. The mean tumor diameter among SCM lesions was 4.7 cm, and bone involvement was documented by CT examination in 34%. Previous operations for the same tumor had taken place in 30.1% of patients with SCMs and in 20% of those with PCCSMs.

Surgical treatment and outcome

SCMs were approached fronto-temporally (92.5%) and fronto-laterally (7.5%). Approaches to PCCSMs most frequently were the retrosigmoid route with suprameatal extension (53.3%) and the pure retrosigmoid route (40%). Occasionally the fronto-lateral, fronto-temporal, and combined infra-supratentorial presigmoid approaches were employed. Surgery was accomplished in two stages in 16.6% of the recently operated patients with PCCSM. Total resection (Simpson grade 1 + 2) was achieved in 14% of patients with SCM and in 3.4% of those with PCCSMs, although resecting all CS tumor among the latter was not a surgical goal.

The function of nerves innervating extraocular muscles before and after treatment is summarized in Table 3. The highest risk of new postoperative dysfunction among patients in the SCM group involved the third cranial nerve. Oculomotor palsy occurred in 12.3% of such patients, but on follow-up these deficits resolved or improved in more than 89%. Vision improved immediately in 24.7% of those with

newly diagnosed tumors, while improving in only 8.6% of patients with recurrent meningiomas. One patient developed pituitary insufficiency. Hemiparesis present prior to surgery resolved in 80% of cases, and new postoperative hemiparesis occurred in 4.3%

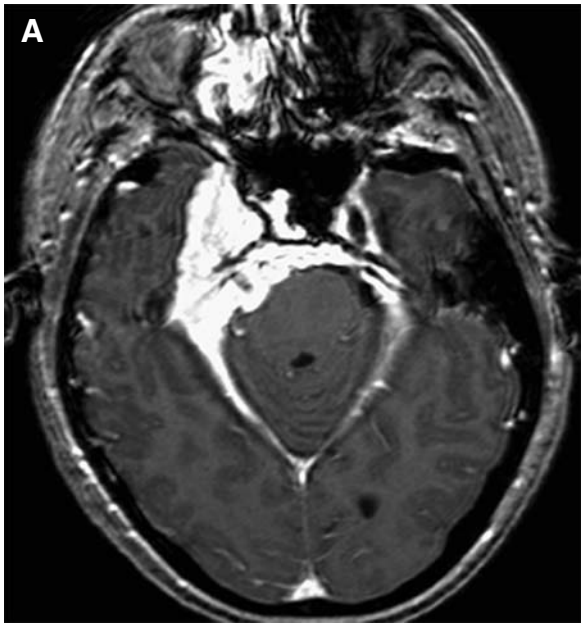

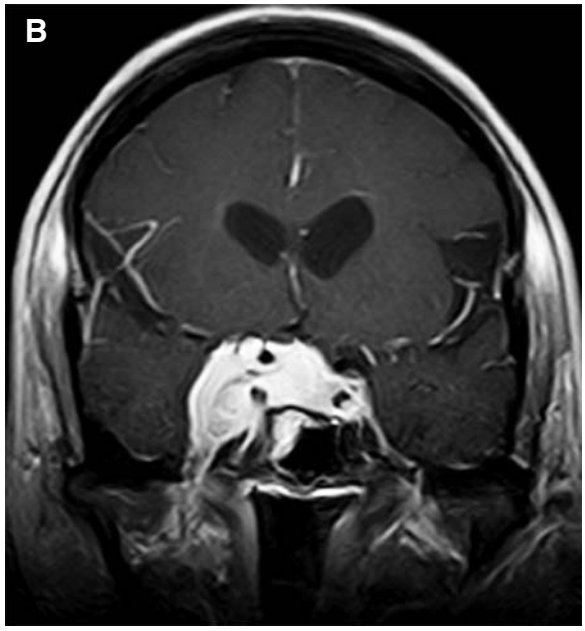

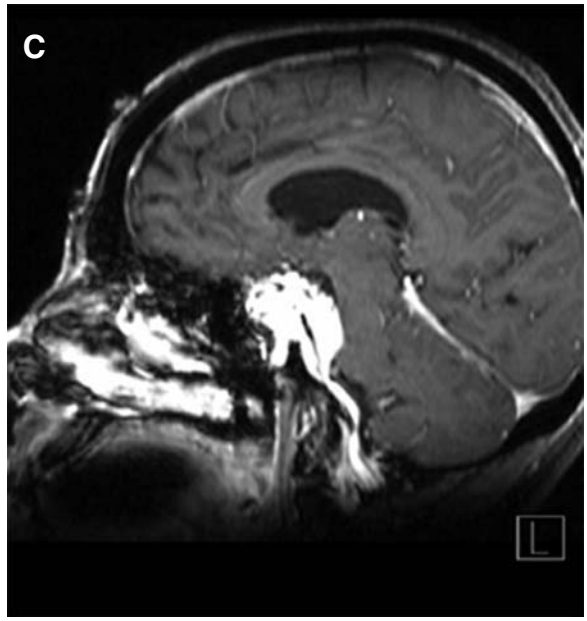

Fig. 1. **A–C** T1-weighted MRI images with contrast enhancement of a 58-year-old female patient with a petroclival meningioma, involving the cavernous sinus

patients. One-half of patients developing hemiparesis postoperatively harbored recurrent tumors already operated on several times. All patients developing hemiparesis during treatment improved on long-term follow-up. Two patients developed aphasia which resolved. Postoperative hematomas occurred in 3.2%, but only one patient required surgical evacuation.

The most frequent postoperative extraocular muscle impairment among PCCSM patients involved the trochlear nerve (6.6%). Twenty-nine percent of patients with abducent palsies present prior to surgery improved or completely resolved following decompression. One patient developed a new partial facial nerve palsy in the early postoperative period; one, hypacusis; another, dysphagia; and still another, transient diabetes insipidus. A CSF leak occurred in one patient and required surgery. Hydrocephalus developed in one patient (on the 10th postoperative day), requiring a shunt. No deaths occurred within 30 days of surgery in either group.

Discussion

Cavernous sinus meningiomas originate primarily within the sinus or infiltrate it from adjacent regions. CS tumors make up a heterogeneous group, with respect to both biological behavior and ana-

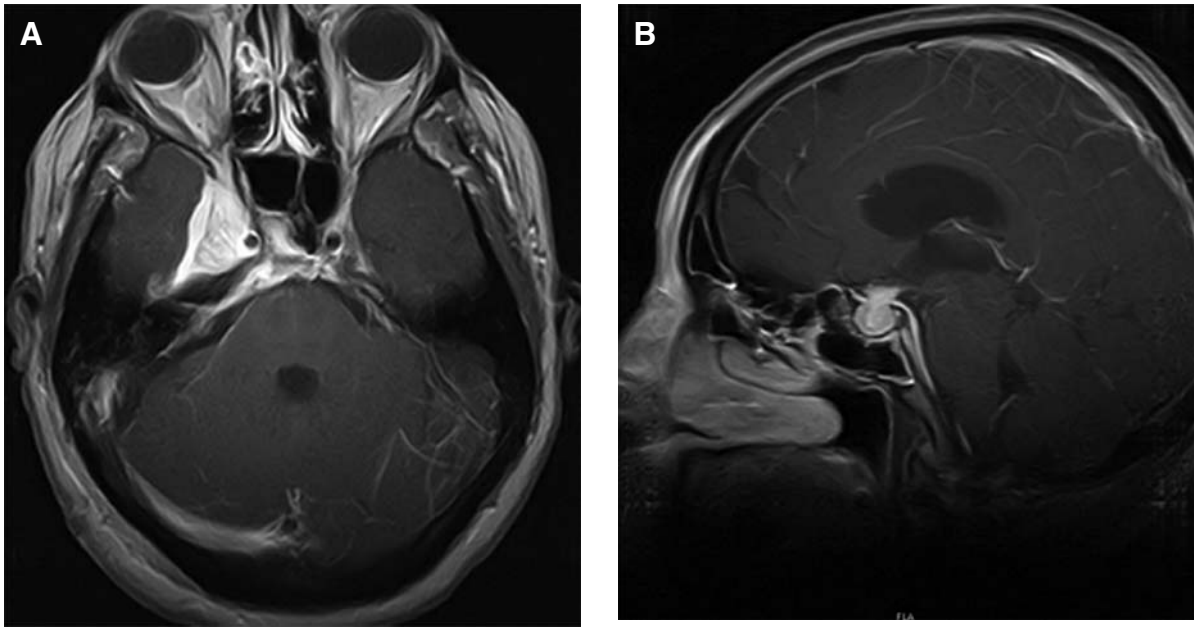

Fig. 2. A, B T1-weighted MRI images with contrast enhancement of the same patient after first surgery – removal of the infratentorial tumor part and decompression of the brain stem via a retrosigmoid-suprameatal approach

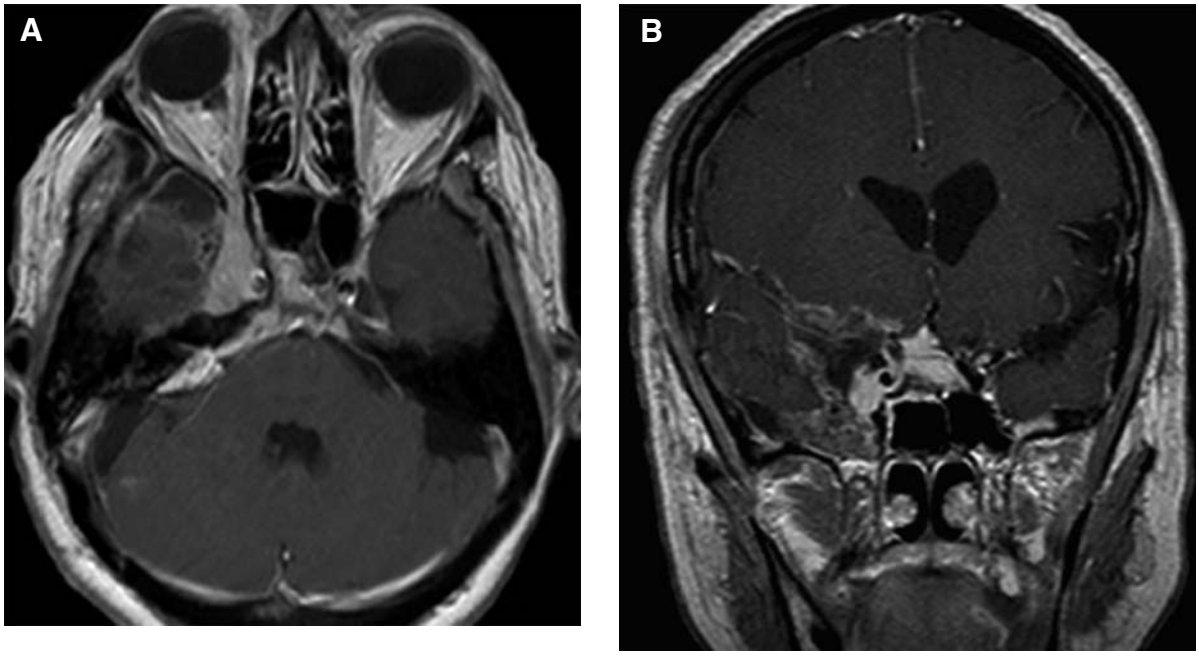

Fig. 3. A, B T1-weighted MRI images with contrast enhancement of the same patient after the second surgery – the supratentorial part has been removed via a fronto-temporal approach. The intracavernous sinus portion of the tumor is removed partially

Table 2. Clinical presentation in two groups

Clinical presentation	SCM (%)	PCCSM (%)
Visual disturbance	54.8	13.3
Double vision:	28	21.7
Oculomotor nerve	22.6	3.3
Trochlear nerve	10.7	3.3
Abducent nerve	14	23.3
Proptosis	24.7	0
Headache	38.7	6.6
Trigeminal nerve dysfunction	21	43
Dizziness	10.7	16.6
Seizure	10.7	0
Hemiparesis	10.7	6.6
Hearing loss	8.7	43
Ataxia	4.3	30

tomical location. The natural history of such lesions remains uncertain, making the selection of optimal treatment difficult. Primary management options include observation, surgical resection, and stereotactic radiosurgery [17]. Recently combined treatment, including resection of the extracavernous component followed by radiosurgery, has gained wide acceptance [27, 33]. Primary indications for surgery include progressive tumor growth on imaging studies and/or increasing symptoms. An important factor pointing to surgical treatment is the extension of the lesion – is it confined to the CS or are other brain structures involved? Loss of vision and symptoms and signs of brainstem compression constitute absolute indications for surgery.

Female preponderance, mean age, and clinical presentations described here are similar to previous reports [6, 7, 32]. It is no surprise that presenting symptoms among patients in the SCM group involved the optic nerve and nerves supplying extraocular muscles, while patients in the PCCSM group typically manifested trigeminal nerve signs, hearing loss, and ataxia. Since neurological symptoms usually result from neurovasacular structures being directly affected by the lesion, preoperative neurological status is important in determining appropriate treatment.

Proven skull base approaches to the CS include: the combined epidural and subdural approach [8–10], the cranioorbitozygomatic approach [17], the extended middle cranial fossa zygomatic approach [17], the combined orbitozygomatic infratemporal approach [16], and the preauricular infratemporal approach [42]. It is presumed that such wide bone resections provide adequate visualization of the lesion and minimize the risk of nerve injury. Others, however, report that such extensive skull base approaches do little to influence the extent and safety of resection, contending that such methods only increase the approach-related morbidity [21].

The operative approaches employed in this series were determined by (a) the lesion's location, size, and pattern of spread, and (b) the patient's neurological status. For SCMs, the frontotemporal approach was preferred, but several different routes were favored for lesions of the PCCSM group. At the outset we employed the frontotemporal approach for PCCSMs, resecting the tentorium and petrous apex. Later we utilized the combined infratentorial supratentorial presigmoid approach, and, more recently, the retrosigmoid–suprameatal approach (resecting the petrous apex and, sometimes, part of the tentorium). With particularly large tumors involving both middle and posterior cranial fossae, we prefer to operate in stages. Initially the component occupying the cerebellopontine angle, the clivus, and/or Meckel's cave is removed via a retrosigmoid–suprameatal approach. The residual

Table 3. Postoperative outcome: function of nerves innervating extraocular muscles

Extraocular muscle nerves	Preoperative deficit	New deficit
SCM:		
• Oculomotor nerve	• Improved – 9.5% Resolved – 4.6%	• 12.3%: Improved or resolved in 89%
• Trochlear nerve	• Improved – 10% Resolved – 10%	• 2.4%: Resolved in 100%
• Abducent nerve	• Improved – 15.4%	• 3.6%: Improved in 33.3%
PCCSM:		
• Oculomotor nerve	• Improved – 0%	• 3.3%
• Trochlear nerve	• Improved – 0%	• 6.6%
• Abducent nerve	• Improved or resolved – 28.6%	• 3.3%

Table 4. Microsurgical series of cavernous sinus meningiomas: literature review

Series-microsurgery	No. of cases	Mean follow-up (months)	New deficit CN	Ischemic stroke (%)	Morbidity	Mortality (%)	Recurrences (%)	Progression-free survival
De Monte et al. [7]	41	45	18%	7.3	CSF leak – 4.9%	7.3	10.7	85.7%
Cusimano et al. [4]	89	28		4.5	CSF leak – 30.3% Meningitis – 7.9% Pit. Dysf. – 37%	6	7	
De Jesus et al. [6]	119	33.8		5	CSF leak – 21% Pit. Dysf. – 14%	9.2	10	62% at 5 years
Knosp et al. [21]	29	3–62	41%			10		
O'Sullivan et al. [32]	24	24	67%	12.8		0	5	
Heth and Al-Mefty [17]	163			4			7	
Dolenc [10]	123 (pure CS)		0%		CSF leak – 2% Epilepsy – 4.9% Other deficit – 5%	0		
Dolenc [10]	388 (CS and adjacent areas)		8.8	1.3	CSF – 2.3% Epilepsy – 1.8% Other deficit – 3%	1		

Pit. dysf. pituitary dysfunction, *CS* cavernous sinus.

(supratentorial) component, adjacent to and within the CS, is removed as a second stage via a frontotemporal approach.

Despite increasing experience with CS meningiomas, appropriate treatment remains controversial. Some favor an aggressive approach, aimed at radical tumor removal with or without carotid artery reconstruction [5–7, 14, 17, 32, 43]. If the ICA is infiltrated by tumor, it is resected and a bypass operation performed [4, 22, 45]. Associated cerebral ischemia occurs by several different mechanisms [41]. In our view, the high morbidity rates and risk of death associated with such an aggressive approach make it unacceptable. Furthermore, devascularising cranial nerves within the CS courts devastating functional results [3].

Table 4 lists series published over the past decade. De Monte et al. [7] report complete removal in 76% of 41 CS meningiomas. New cranial nerve deficits occurred in 18%, and preoperative deficits deteriorated in 6%. Improvement was noted only in 13%. Ischemic stroke occurred in 7.3%, and the mortality rate was 7.3%. The recurrence rate after a mean follow-up of less than 4 years was 10.7%. It is surprising, in view of their outcome data, that these authors state that complete removal of CS meningiomas is possible with acceptable mortality and morbidity.

De Jesus et al. [6] came to a similar conclusion. They reported their experience with 119 CS meningiomas. Total removal was achieved in 61% with a 9.2% mortality rate, and complications included CSF leakage (21%) and pituitary dysfunction (14%). No mention was made of cranial nerve status. Ten percent of their tumors recurred during a mean follow-up of 33.8 months.

Of those operated by Cusimano et al. [4] 7% of tumors recurred within 28 months. Day and Fukushima [5] describe operating on 154 patients with CS tumors, approximately half of which were meningiomas, with permanent extraocular motor nerve palsies developing in 68%, trigeminal nerve deficits in 84%, and visual loss in 5%. Heth and Al Mefty [17] report 44% total resection (71 of 163 patients), with ischemic strokes occurring in 4%, and tumor recurrences in 7%.

In a recently published large series including 123 purely cavernous meningiomas, Dolenc [10] achieved complete tumor removal in 31%. However, there was no mortality and the morbidity rate was remarkably low: 4.9% of the patients had epilepsy requiring anticonvulsive therapy, 5% had other deficits, and 2% experienced CSF leaks. Furthermore, no new cranial nerve deficit developed after surgery. Six months following surgery persisting preoperative cranial nerve deficit was noted in 19%.

Intracavernous dissection is associated with a high risk of directly injuring nerves or disrupting their delicate blood supply [3, 15]. In addition, since meningiomas tend to invade cranial nerves and the adventitia of the intracavernous segment of the ICA [22, 24, 32, 41, 44], it is not clear that CS meningiomas can be totally excised without incurring neurological deficits. But, despite high surgical morbidity and mortality rates, aggressive surgery for CS meningiomas is still recommended [13, 17]. Proponents of radical CS meningioma surgery focus on techniques to achieve radical resection, rather than its costs with respect to preserving neurological function and quality of life. Progression-free survivals even after total removal are only 62–86% and short-term recurrences are 5–11% [6, 7].

Recent reports tend to substantiate our strategy of more conservative surgery for such lesions [1, 3, 12, 20, 33]. Achieving the goals of reducing the tumor volume and decompressing the optic nerve and/or brain stem, thereby providing a safe distance between the optic apparatus and the residual meningioma, makes radiosurgery safe. Couldwell et al. [3] advocate decompressing the CS and facilitating cranial nerve improvement by limiting the piecemeal removal of CS meningiomas to "safe" locations only. Similarly, Abdel-Aziz et al. [1] propose removing only the lateral elements of CS meningiomas, a strategy which enabled them to reduce the incidence of extraocular nerve impairment from 55% prior to surgery to 16% well after surgery. For sphenoorbital meningiomas secondarily involving the CS, Shrivastava et al. [46] do not recommend exploring the CS because the regrowth rates of residual CS meningiomas are low. Similar views are shared by Maroon et al. [26] and Brotchi et al. [2].

We favor individualizing the management of CS meningiomas, tailoring treatment to tumor characteristics and the expectations of each patient. Both factors are important in our decisions. Biological characteristics of the extracavernous tumor component – e.g., infiltrative vs. circumscribed growth patterns, invasion vs. mere compression of the sinus – along with a given patient's neurological

status and personal expectations, should determine how aggressive one should be with the intracavernous component. If a patient has an increasing eye-movement disorder, we recommend attempting to decompress involved nerves as much as possible. With patients experiencing optic nerve or brain stem symptoms and/or signs, but no loss of extraocular muscle function, we favor decompressing only the structures with clinical manifestations. Aggressively resecting the intracavernous component is to be avoided, in order that new extraocular muscle deficits do not occur.

Preoperative neuroimaging findings are sometimes misleading, leaving the question of the extent of resection to be determined in the operating room. Occasionally the CS appears to be invaded when, at surgery, the lateral wall of the sinus is demonstrated to be only compressed. Such lesions can easily be removed.

When meningiomas infiltrate a cranial nerve or the carotid artery, no attempt should be made to remove the most adherent portion. Such remnants can be effectively treated by radiosurgery. With cases of tumor recurrence or progression after radiosurgery/radiotherapy, the risk of ICA and extracranial nerve injury is much higher. In such circumstances treatment should be limited to decompress the optic nerve and/or brainstem.

Multiple studies have proven the value of radiosurgery as a primary or adjuvant tool for treating CS meningiomas [11, 18, 23, 29, 31, 34, 36]. Although radiosurgery cannot produce a cure, it does provide long-term tumor control, and is therefore an acceptable option for small meningiomas limited to or invading the CS. Refinements in neuroimaging and treatment planning dramatically reduced the incidence of radiation-induced morbidity in the major radiosurgery series (Table 5). Reported tumor growth control rates for CS meningiomas were greater than 90% [25, 28, 31, 34, 36]. Tumor volumes were decreased in 31–61% of the cases. Reported progression-free survival rates of 80–96.5% were considerably longer than those reported after even the most aggressive surgery. On the other hand, tumor progression was observed in 0–8% and the rate of permanent morbidity was as high as 8.2% [35]. Some complications, such as pituitary insufficiency, occurred several years after radiotherapy [38], indicating that much longer follow-up studies are required to assess the actual safety of the method.

Some evidence suggests that neurological improvement would be more likely if radiosurgery were employed as primary treatment, rather than as an adjunct to microsurgery [31, 48]. Nevertheless, with larger tumors with significant extracavernous components, surgery remains the only effective option to decompress cranial nerves or brain structures. Furthermore, the risk of radiation-induced complications is directly proportional to tumor volume. Radiosurgery is safely performed only if a separation of 3–5 mm between tumor and optic apparatus is provided [3, 33]. Most authors agree that radiosurgery should be applied to the residual intracavernous tumor components in order to obviate recurrences [1, 3, 27, 33]. Whether radiosurgery should be performed immediately after surgery or later remains controversial. Cellular atypia, proliferative index, patient age, and clinical condition have been suggested as having prognostic value [1]. We doubt, however, the reliability of such parameters, and recommend follow-up MRI studies 3–6 months after surgery.

Table 5. Radiosurgical series of cavernous sinus meningiomas: literature review

Series-radiosurgery	No. of cases	Mean follow-up (months)	Transient morbidity (%)	Permanent morbidity (%)	Clinical improvement (%)	Stable tumor (%)	Decreased size (%)	Progression-free survival
Pendl et al. [34]	41	39	0	0		63	37	
Roche et al. [36]	80	30.5	2.5	0		64	31	92% at 5 years
Lee et al. [25]	159	35	1.9	5	29	60.4	34	93.1% at 10 years
Nicolato et al. [31]	122	48.9	3	1	65	36	61.5	96.5% at 5 years
Iwai et al. [18]	42	49	0	2.4	29	31.5	59.5	92% at 5 years
Pollock and Stafford [35]	49			8.2	26	41	59	80% at 7 years[a]
Mettelus et al. [28]	36	63.6	2.8	0	58.3	41.7	52.7	94.4% at 10 years

[a] Event-free survival at 7 years.

Conclusion

The treatment of cavernous sinus meningiomas should be tailored to the tumor's biological characteristics plus the individual patient's personal expectations. Both factors should be considered when determining how aggressive to be surgically. Limiting the goals of surgery to reducing the tumor volume and decompressing the optic nerve and/or brainstem (thus enhancing the safety of radiosurgery) will result in preserving or improving affected patients' neurological function and quality of life. The treatment of CS meningiomas should provide an outcome which is superior to the lesion's natural history.

References

1. Abdel-Aziz KM, Froelich SC, Dagnew E, Jean W, Breneman JC, Zuccarello M, van Loveren HR, Tew JM Jr (2004) Large sphenoid wing meningiomas involving the cavernous sinus: conservative surgical strategies for better functional outcomes. Neurosurgery 54: 1375–1383
2. Brotchi J, Levivier M, Raftopoulos C, Noterman J (1991) Invading meningiomas of sphenoid wing. What must we know before surgery? Acta Neurochir (Wien) [Suppl] 53: 98–100
3. Couldwell WT, Kan P, Liu JK, Apfelbaum RI (2006) Decompression of cavernous sinus meningioma for preservation and improvement of cranial nerve function. Technical note. J Neurosurg 105: 148–152
4. Cusimano MD, Sekhar LN, Sen CN, Pomonis S, Wright DC, Biglan AW, Jannetta PJ (1995) The results of surgery for benign tumors of the cavernous sinus. Neurosurgery 37: 1–9
5. Day JD, Fukushima T (1996) Cavernous sinus neoplasms. In: Youmans JR (ed) Neurological surgery: a comprehensive reference guide to the diagnosis and management of neurosurgical problems, vol 4, 4th ed. Saunders, Philadelphia, pp 2862–2882
6. De Jesus O, Sekhar LN, Parikh HK, Wright DC, Wagner DP (1996) Longterm follow-up of patients with meningiomas involving the cavernous sinus: recurrence, progression, and quality of life. Neurosurgery 39: 915–919
7. DeMonte F, Smith HK, Al-Mefty O (1994) Outcome of aggressive removal of cavernous sinus meningiomas. J Neurosurg 81: 245–251
8. Dolenc VV (1979) Microsurgical removal of large sphenoidal bone meningiomas. Acta Neurochir (Wien) [Suppl] 28: 391–396
9. Dolenc VV, Kregar T, Ferluga M, Fettich M, Morina A (1987) Treatment of tumors invading the cavernous sinus. In: Dolenc VV (ed) The cavernous sinus. Springer, New York, pp 372–391
10. Dolenc VV (2003) Microsurgical anatomy and surgery of the central skull base. Springer, Wien New York, pp 162–177
11. Duma CM, Lunsford LD, Kondziolka D, Harsh GRt, Flickinger JC (1993) Stereotactic radiosurgery of cavernous sinus meningiomas as an addition or alternative to microsurgery. Neurosurgery 32: 699–704
12. Friedlander RM, Ojemann RG, Thornton AF (1999) Management of meningiomas of the cavernous sinus: conservative surgery and adjuvant therapy. Clin Neurosurg 45: 279–282
13. George B, Ferrario CA, Blanquet A, Kolb F (2003) Cavernous sinus exenteration for invasive cranial base tumors. Neurosurgery 52: 772–780
14. Goel A, Muzumdar DP, Nitta J (2001) Surgery on lesions involving cavernous sinus. J Clin Neurosci 8 [Suppl 1]: 71–77
15. Hakuba A, Suzuki T, Jin TB, Komiyama M (1987) Surgical approaches to the cavernous sinus: Report of 52 cases. In: Dolenc VV (ed) The cavernous sinus. Springer, Wien New York, pp 302–327
16. Hakuba A, Tanaka K, Suzuki T, Nishimura S (1989) A combined orbitozygomatic infratemporal epidural and subdural approach for lesions involving the entire cavernous sinus. J Neurosurg 71: 699–704
17. Heth JA, Al-Mefty O (2003) Cavernous sinus meningiomas. Neurosurg Focus 14: e3
18. Iwai Y, Yamanaka K, Ishiguro T (2003) Gamma knife radiosurgery for the treatment of cavernous sinus meningiomas. Neurosurgery 52: 517–524
19. Kleinpeter G, Bock F (1990) Invasion of the cavernous sinus by medial sphenoid meningioma – radical surgery and recurrence. Acta Neurochir (Wien) 103: 87–91
20. Klink DF, Sampath P, Miller NR, Brem H, Long DM (2000) Long-term visual outcome after nonradical microsurgery in patients with parasellar and cavernous sinus meningiomas. Neurosurgery 47: 24–32
21. Knosp E, Perneczky A, Koos WT, Fries G, Matula C (1996) Meningiomas of the space of the cavernous sinus. Neurosurgery 38: 434–442
22. Kotapka MJ, Kalia KK, Martinez AJ, Sekhar LN (1994) Infiltration of the carotid artery by cavernous sinus meningioma. J Neurosurg 81: 252–255
23. Kurita H, Sasaki T, Kawamoto S, Taniguchi M, Terahara A, Tago M, Kirino T (1997) Role of radiosurgery in the management of cavernous sinus meningiomas. Acta Neurol Scand 96: 297–304
24. Larson JJ, van Loveren HR, Balko MG, Tew JM Jr (1995) Evidence of meningioma infiltration into cranial nerves: clinical implications for cavernous sinus meningiomas. J Neurosurg 83: 596–599
25. Lee JY, Niranjan A, McInerney J, Kondziolka D, Flickinger JC, Lunsford LD (2002) Stereotactic radiosurgery providing long-term tumor control of cavernous sinus meningiomas. J Neurosurg 97: 65–72

26. Maroon JC, Kennerdell JS, Vidovich DV, Abla A, Sternau L (1994) Recurrent spheno-orbital meningioma. J Neurosurg 80: 202–208
27. Maruyama K, Shin M, Kurita H, Kawahara N, Morita A, Kirino MDT (2004) Proposed treatment strategy for cavernous sinus meningiomas: a prospective study. Neurosurgery 55: 1068–1075
28. Metellus P, Regis J, Muracciole X, Fuentes S, Dufour H, Nanni I, Chinot O, Martin PM, Grisoli F (2005) Evaluation of fractionated radiotherapy and gamma knife radiosurgery in cavernous sinus meningiomas: treatment strategy. Neurosurgery 57: 873–886
29. Morita A, Coffey RJ, Foote RL, Schiff D, Gorman D (1999) Risk of injury to cranial nerves after gamma knife radiosurgery for skull base meningiomas: experience in 88 patients. J Neurosurg 90: 42–49
30. Nakamura M, Roser F, Jacobs C, Vorkapic P, Samii M (2006) Medial sphenoid wing meningiomas: clinical outcome and recurrence rate. Neurosurgery 58: 626–639
31. Nicolato A, Foroni R, Alessandrini F, Bricolo A, Gerosa M (2002) Radiosurgical treatment of cavernous sinus meningiomas: experience with 122 treated patients. Neurosurgery 51: 1153–1159
32. O'Sullivan MG, van Loveren HR, Tew JM Jr (1997) The surgical resectability of meningiomas of the cavernous sinus. Neurosurgery 40: 238–244
33. Pamir MN, Kilic T, Bayrakli F, Peker S (2005) Changing treatment strategy of cavernous sinus meningiomas: experience of a single institution. Surg Neurol 64: 58–66
34. Pendl G, Schrottner O, Eustacchio S, Ganz JC, Feichtinger K (1998) Cavernous sinus meningiomas – what is the strategy: upfront or adjuvant gamma knife surgery? Stereotact Funct Neurosurg 70 [Suppl 1]: 33–40
35. Pollock BE, Stafford SL (2005) Results of stereotactic radiosurgery for patients with imaging defined cavernous sinus meningiomas. Int J Radiat Oncol Biol Phys 62: 1427–1431
36. Roche PH, Regis J, Dufour H, Fournier HD, Delsanti C, Pellet W, Grisoli F, Peragut JC (2000) Gamma knife radiosurgery in the management of cavernous sinus meningiomas. J Neurosurg 93 [Suppl 3]: 68–73
37. Roser F, Nakamura M, Jacobs C, Vorkapic P, Samii M (2005) Sphenoid wing meningiomas with osseous involvement. Surg Neurol 64: 37–43
38. Rush S, Cooper PR (1997) Symptom resolution, tumor control, and side effects following postoperative radiotherapy for pituitary adenomas. Int J Radiat Oncol Biol Phys 37: 1031–1034
39. Samii M, Knosp E (1992) Approaches to the Clivus – approaches to no man's land. Springer, Berlin, pp 83–140
40. Samii M, Tatagiba M, Carvalho GA (2000) Retrosigmoid intradural suprameatal approach to Meckel's cave and the middle fossa: surgical technique and outcome. J Neurosurg 92: 235–241
41. Shaffrey ME, Dolenc VV, Lanzino GL, Wolcott WP, Shaffrey CI (1999) Invasion of the internal carotid artery by cavernous sinus meningiomas. Surg Neurol 52: 167–171
42. Sekhar LN, Altschuler EM (1991) Meningiomas of the cavernous sinus. In: Al-Mefty O (ed) Meningiomas. Raven, New York, pp 445–460
43. Sekhar LN, Patel S, Cusimano M, Wright DC, Sen CN, Bank WO (1996) Surgical treatment of meningiomas involving the cavernous sinus: evolving ideas based on a 10 year experience. Acta Neurochir (Wien) [Suppl] 65: 58–62
44. Sen C, Hague K (1997) Meningiomas involving the cavernous sinus: histological factors affecting the degree of resection. J Neurosurg 87: 535–543
45. Sen CN, Sekhar LN (1992) Direct vein reconstruction of the cavernous, petrous, and upper cervical internal carotid artery: lessons learned from 30 cases. Neurosurgery 30: 732–743
46. Shrivastava RK, Sen C, Costantino PD, Della Rocca R (2005) Sphenoorbital meningiomas: surgical limitations and lessons learned in their long-term management. J Neurosurg 103: 491–497
47. Sepehrnia A, Samii M, Tatagiba M (1991) Management of intracavernous tumours: an 11-year experience. Acta Neurochir (Wien) [Suppl] 53: 122–126
48. Spiegelmann R, Nissim O, Menhel J, Alezra D, Pfeffer MR (2002) Linear accelerator radiosurgery for meningiomas in and around the cavernous sinus. Neurosurgery 51: 1373–1379
49. Yaşargil MG, Fox JL (1975) The microsurgical approach to intracranial aneurysms. Surg Neurol 3: 7–14

Trigeminal neurinomas: surgical considerations

A. Goel, D. Muzumdar

Department of Neurosurgery, King Edward VII Memorial Hospital and Seth G.S. Medical College, Parel, Mumbai, India

Introduction

Trigeminal neurinomas, second only to acoustic lesions in incidence among neurinomas, exhibit characteristic clinical, radiographic, and anatomical features the understanding of which is crucial to accurate diagnosis and efficient surgical planning. Compared to other lesions of the region, the surgery of trigeminal neurinomas demands unique consideration. Others have stressed the importance of radical surgery (emphasizing that only total resection leads to 'cure'), and recurrence rates following partial resection, particularly of cystic tumors, is higher for trigeminal neurinomas than acoustic neurinomas [15].

These lesions account for 0.2% of all intracranial tumors [1, 4, 5, 9, 20, 21, 25, 28, 31, 33, 35, 38]. Improved surgical outcomes and long-term growth control rely on precise diagnosis, understanding the tumor's anatomical complexity, and modern skull base techniques [3, 6, 10, 12, 26, 27, 36, 39–42, 44, 46, 47]. Jefferson has classified trigeminal schwannomas with respect to location [21]: those in the middle fossa (Type A) (Figs. 1, 2), those involving posterior fossa cranial nerve roots (Type B) (Fig. 3) where the tumor lies anterior to the brain stem, and dumbbell lesions with components in both the middle and the posterior fossa (Type C) (Fig. 4). Less commonly these tumors spread extracranially (Type D) (Figs. 5–12) [25]. Yoshida et al. divided extracranial trigeminal neurinomas into orbital, infratemporal, and pterygopalatine fossa types [47]. Below we will discuss 123 trigeminal neurinomas treated surgically between 1989 and 2006.

Anatomical considerations

After the fifth cranial nerve exits the medial surface of the middle cerebellar peduncle, it passes beneath the tentorium and later over the petrous apex where it forms the Gasserian ganglion. The Gasserian ganglion divides into three divisions, the first and second forming the lateral wall of the cavernous sinus, and the third exiting the cranial cavity through the foramen ovale. It has a short intracranial course. The fifth cranial nerve overlying the petrous apex is covered by a dural and arachnoid sheath, Meckel's cave. The large subarachnoid space above the Gasserian ganglion within Meckel's cave contains cerebrospinal fluid. Apart from this dural and arachnoidal envelope, which is continuous with layers within the posterior fossa, the trigeminal nerve is covered laterally by middle fossa dura. This dural sheath is closely approximated, but separable from the inner dural layers. The large subarachnoid space renders these dural layers easily dissected from the Gasserian ganglion. Individual dural layers merge with sheaths enveloping divisions of the nerve at the foramen ovale, foramen rotundum, and the superior orbital fissure, where dissecting dura from neural structures becomes difficult. The superior petrosal sinus traverses layers of dura superior to the root of the fifth nerve at its entry into Meckel's cave. The precavernous segment of the carotid artery lies posteromedial to the Gasserian ganglion. Here, in two-thirds of cases, the only barrier between ganglion and the internal carotid artery is a tough layer of dura and cartilage.

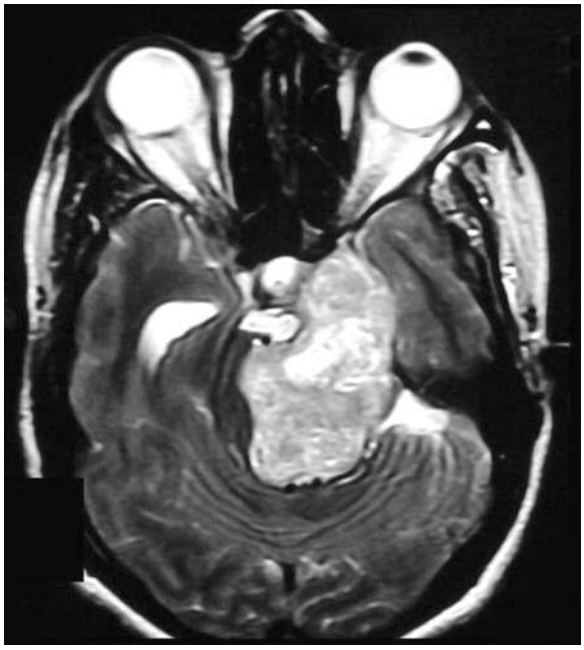

Fig. 1. Dumbbell-shaped trigeminal neurinoma with components in both middle and posterior cranial fossae

Tumors arise from a segment of the trigeminal nerve, and other nerve components become displaced as growth of the mass advances. Our experience suggests that these tumors generally originate near the trigeminal nerve's site of entry into Meckel's cave [11]. Most trigeminal neurinomas, whatever their routes of spreading, are associated with this segment of the nerve.

Clinical presentation

Table 1 lists the presenting clinical features. There was no sexual predilection, the male to female ratio being 1:1.2. Age of presentation varied between 6 months and 75 years. The trigeminal neurinoma presenting at 6 months (previously reported by us) is the youngest case ever reported [17]. Neurofibromatosis is less commonly associated with trigeminal neurinomas [2, 3, 7, 8, 14, 18, 22, 23, 29, 30, 34, 37, 43, 45], only 13 of our series presenting such features. Since early symptoms, which develop subtly over long periods of time, typically are neglected by illiterate and ignorant patients so common in our series, most tumors were quite large at the time of diagnosis.

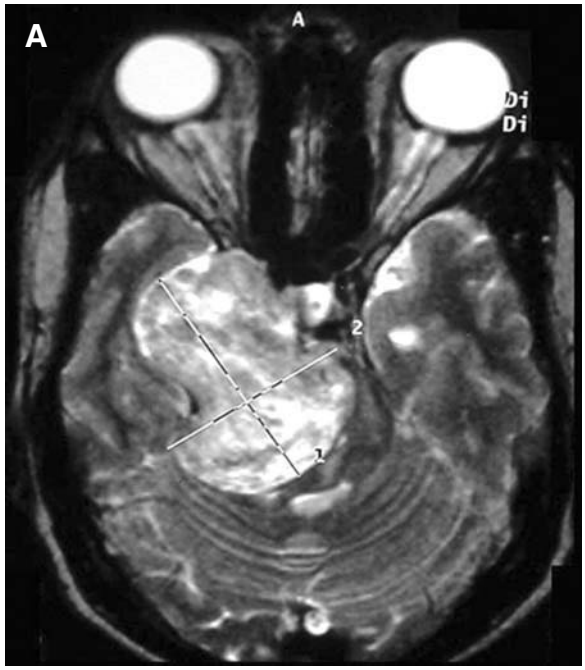

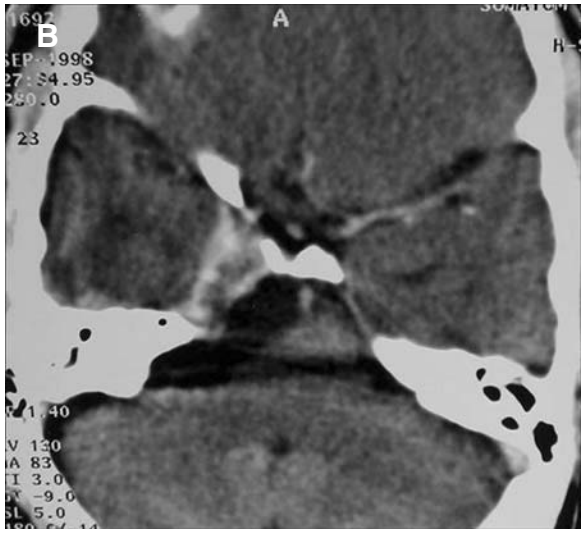

Fig. 2. A Axial T_2-weighted MRI showing a dumbbell-shaped trigeminal neurinoma. **B** Postoperative computed tomography showing excision of the tumor

Paresthesias (usually involving more than one trigeminal division) are common presenting symptoms. Severe or neuralgic pain, on the other hand, is uncommon, observed in only seven of our cases. Temporalis and pterygoid muscle atrophy, present in 56.1% of our patients, was often diagnostic. The corneal reflex was depressed in 74 (60.2%), while

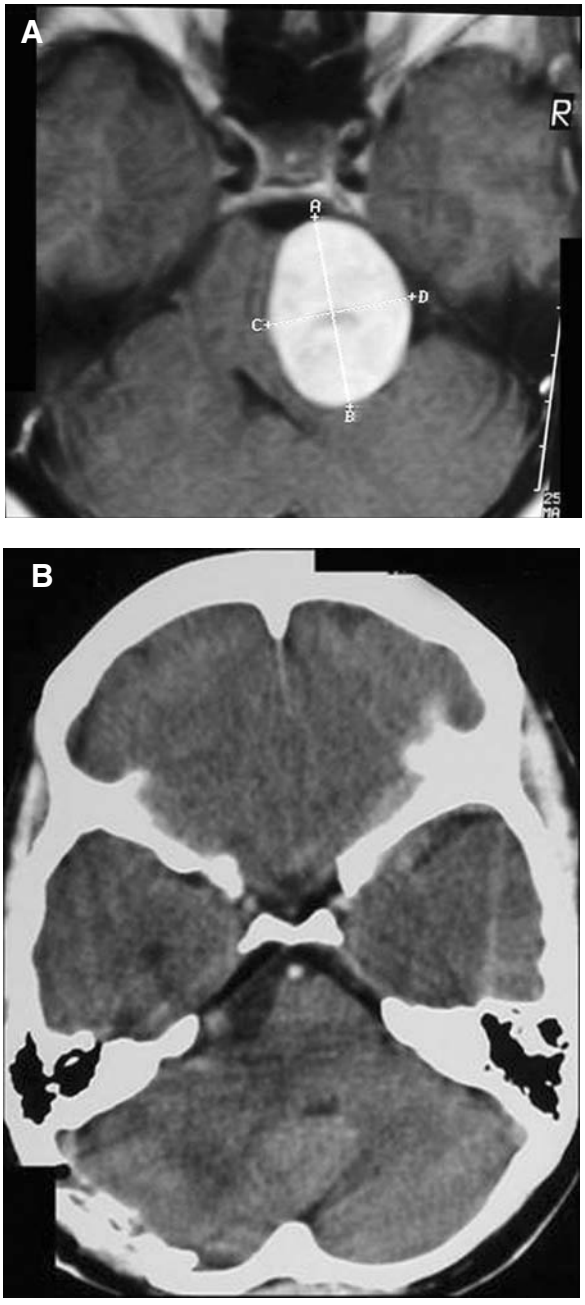

Fig. 3. A Axial contrast-enhanced T_1-weighted magnetic resonance imaging showing a trigeminal neurinoma located in the posterior cranial fossa. **B** Postoperative computed tomography showing excision of the tumor via a retrosigmoid approach

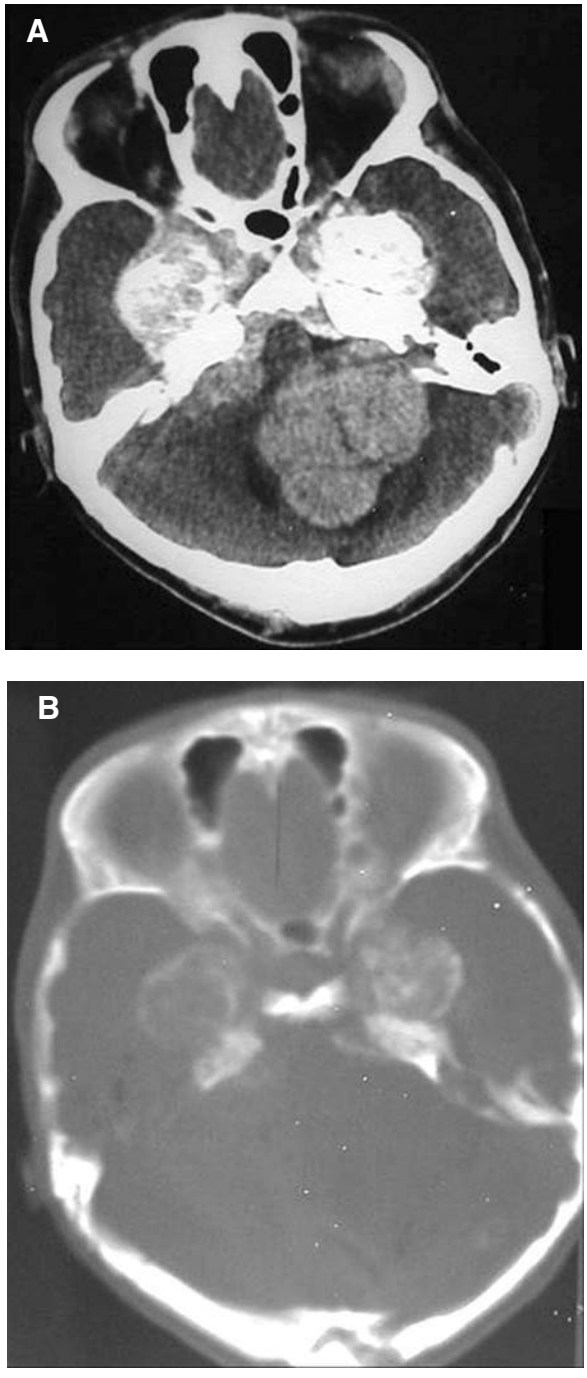

Fig. 4. A Axial CT scan showing large bilateral calcified trigeminal neurinomas. **B** Bone window vividly depicting calcification within the tumor

dense motor and sensory deficits, including complete absence of corneal sensation, are uncommon, but suggestive of malignant degeneration when present. We did not witness such a deficit in this series. Although symptoms involving adjacent cranial nerves within the cavernous sinus and the

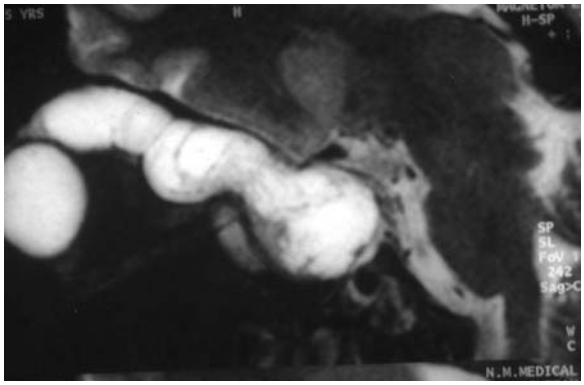

Fig. 5. Sagittal T_2-weighted MRI showing a trigeminal neurinoma extending from the middle fossa into the orbit

cerebellopontine angle have been reported frequently, they occur primarily because the tumors causing them are so large at the time of presentation. Six patients presented with proptosis. The unusual phenomenon of pathological laughter, with or without affecting elements of higher brain function, was observed in nine patients in association with large, dumbbell-shaped tumors [22]. Although the physiological basis for pathological laughter remains uncertain, the literature suggests that a complex combination of brainstem displacement and compression of medial temporal lobe elements may be responsible. Pathological laughter may indicate the presence of a massive trigeminal schwannoma. A slowly developing picture dominated by trigeminal nerve dysfunction, such as facial numbness and atrophy of any of the muscles of mastication, is usually diagnostic.

Radiological and anatomical features

Tumors in our series ranged from 8 mm to 8 cm in size. Physical characteristics are listed in Table 2. Bilateral trigeminal neurinomas rarely occur [21]. In this series the only four cases of bilateral tumors were always associated with features of neurofibromatosis (Fig. 12). The contralateral tumor resulted in no symptoms in any of the four. Tumors limited to the middle fossa and dumbbell-shaped tumors occupying both the middle fossa and the posterior fossa were more common than tumors occurring in the posterior fossa only. Nineteen tumors had spread extracranially. All tumors with extracranial components had a middle fossa presence. Tumors

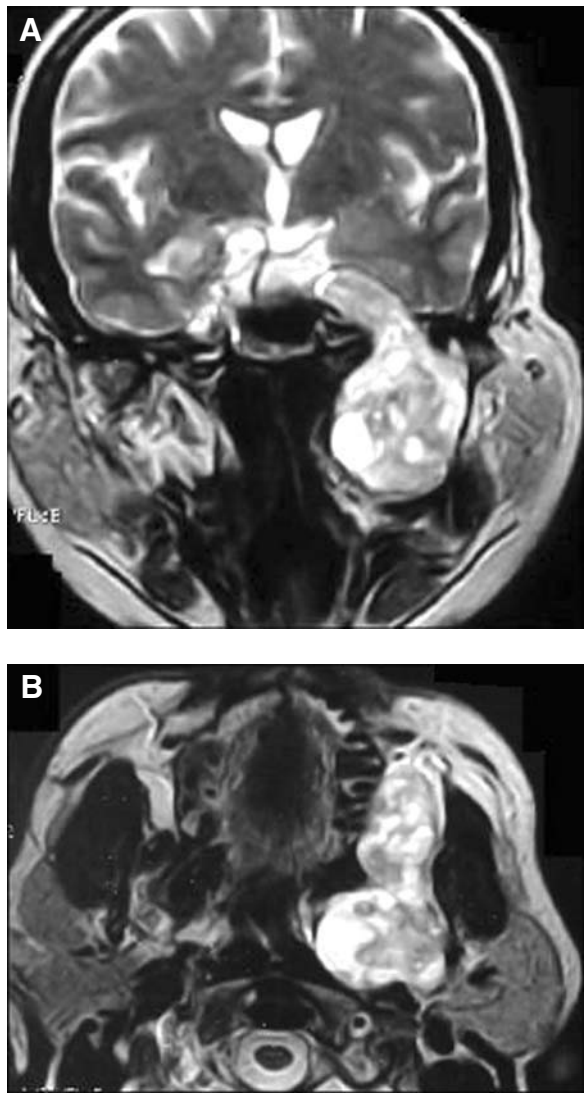

Fig. 6. MRI showing a trigeminal neurinoma extending from the middle fossa into the orbit. **A** Coronal-T_2-weighted image. **B** Axial T_1-weighted image

extending into the orbit were observed in six cases, and those extending into the infratemporal/terygopalatine fossa were seen in 13. Two tumors spreading into the orbit likely arose from the lacrimal division of the fifth cranial nerve [30]. Trigeminal neurinomas were typically soft and moderately vascular. Predominantly cystic changes were seen in 34 tumors, and six lesions had multiple cysts. Although rarely seen in acoustic neurinomas [29], multiple cysts have never been reported with trigeminal neurinomas. Cysts with

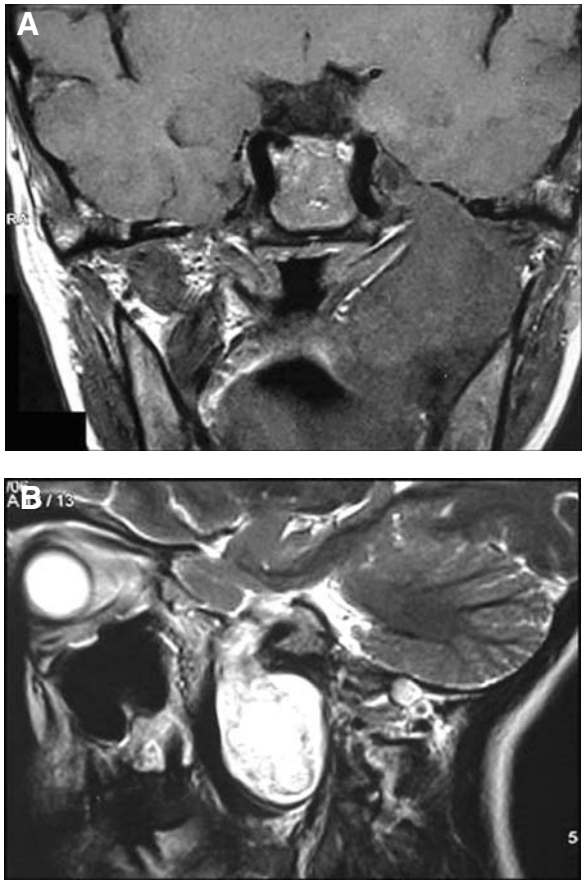

Fig. 7. MRI showing a trigeminal neurinoma with infratemporal fossa extension. **A** Coronal T_1-weighted image. **B** Sagittal T_2-weighted image

fluid levels were encountered in five lesions (Fig. 13). Calcifications within trigeminal neurinomas, not reported previously, were encountered in four tumors. Petrous apex erosion (on plain X-ray or CT) was uniformly associated with larger tumors, and was of diagnostic significance. Although malignant trigeminal neurinomas have been reported [7, 18, 21–25, 45], none were seen in this series.

However large the tumor becomes, it will seldom erode dura and enter the venous spaces of the cavernous sinus or engulf precavernous or cavernous segments of the internal carotid artery. Despite their size, none of our middle fossa tumors violated dura, making them essentially 'interdural' in location [28, 34, 37]. Displacing the internal carotid artery was a characteristic of diagnostic importance [14]. Even when the carotid artery was in close approximation with the tumor, a well-defined dural sheath separating

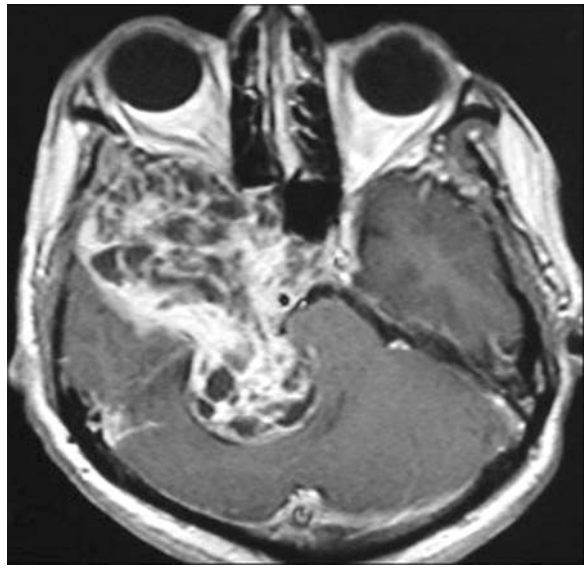

Fig. 8. Axial T_1-weighted contrast enhanced MRI showing multiple cysts within the tumor

carotid artery and tumor remained. Therefore, if the surgeon limits his work to within the confines of the tumor capsule, he faces little risk of injuring the carotid artery. Therefore, there is seldom need for perioperative proximal and distal control of the carotid artery. In the posterior fossa, tumors located anterolateral to the pons were, like acoustic neurinomas, 'extra-arachnoidal' in nature. However, in several cases, the arachnoidal layer was observed to be quite thick in such cases. Even when present extracranially these tumors were well defined, and covered by a membrane continuous with dura near Meckel's cave (Fig. 14). Typically these tumors involve adjacent cranial nerves, blood vessels and brain by displacement rather than by invasion.

Operative approaches

All operations were carried out by the senior author personally or under his direct supervision. In our early experience dumbbell-shaped tumors were operated in two stages, through the middle fossa and the posterior fossa, the larger component operated on first. Although recommended at that time, the sigmoid and transverse sinuses were never sectioned. With better understanding of the subtleties of dural and local anatomy, exposure times and total operating times were reduced considerably [11].

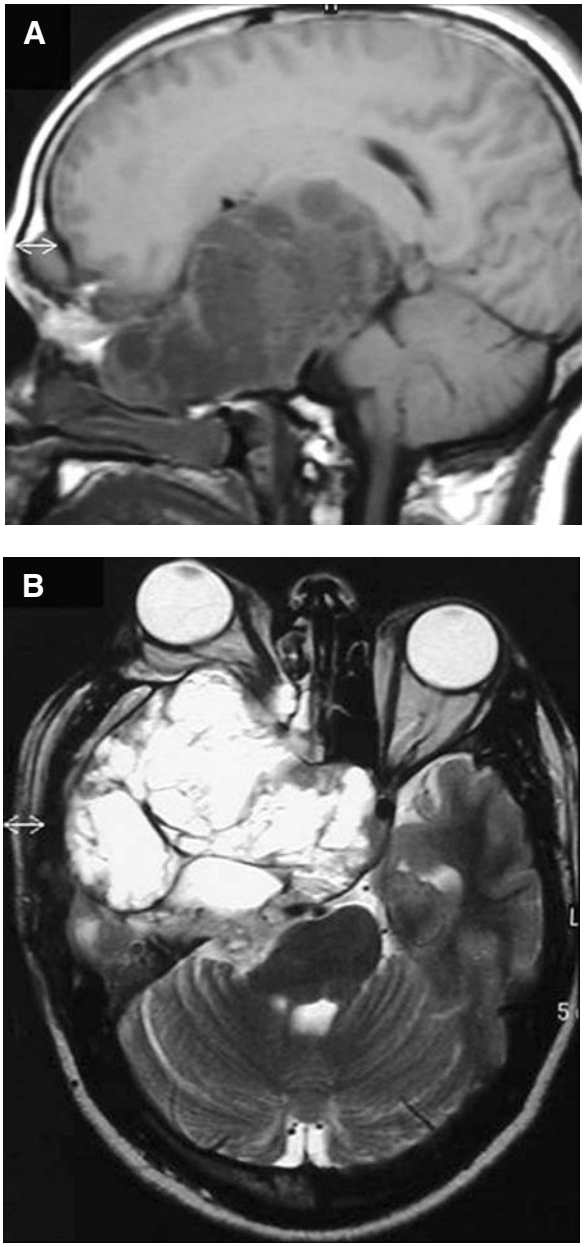

Fig. 9. **A** Sagittal T_1-weighted MRI showing a predominantly cystic trigeminal neurinoma. **B** Axial T_2-weighted MR image showing multiple cysts within the tumor

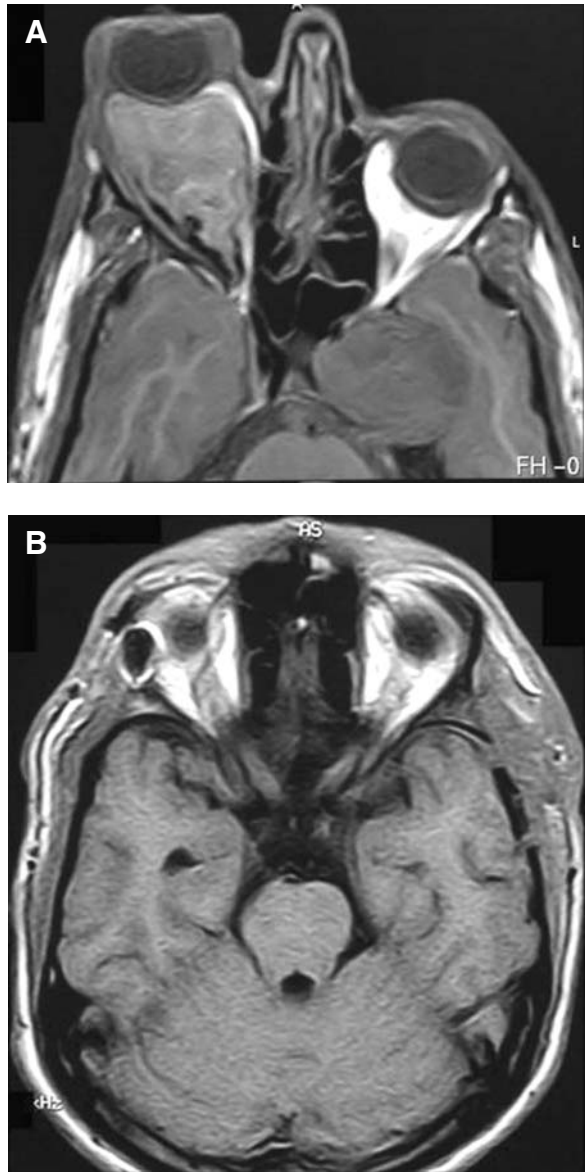

Fig. 10. **A** Axial T_1-weighted MRI showing a right retro-orbital hemangiopericytoma and a left middle fossa trigeminal neurinoma. **B** Postoperative axial T_1-weighted MRI showing excision of both tumors

Infratemporal fossa interdural approach [15]

Indications This approach may apply for small tumors limited to the middle cranial fossa or where the posterior fossa component of a dumbbell-shaped tumor is relatively small.

Surgical technique The patient is positioned with his/her neck extended and head rotated to the contralateral side. Regardless of the side of the lesion, the right-handed surgeon stands to the patient's right, at chest-level (Fig. 15). Head rotation is adjusted as appropriate. A linear incision is made over the zygomatic arch, which is resected complete-

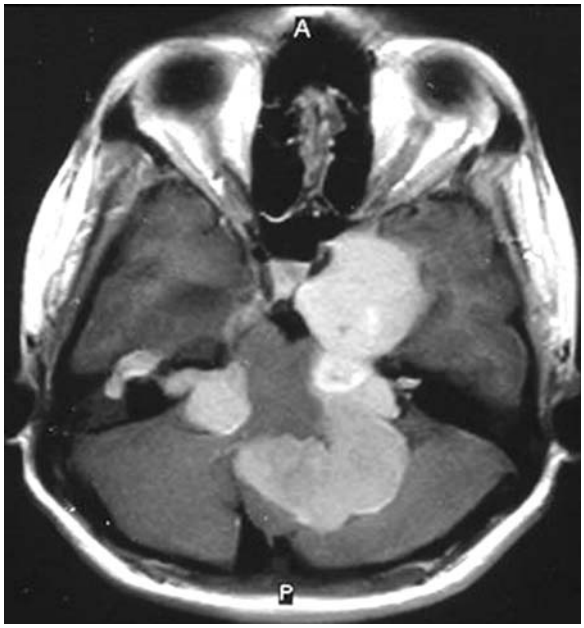

Fig. 11. Axial T_1-contrast enhanced MRI showing a large left middle fossa trigeminal neurinoma. Bilateral acoustic neurinomas and left trochlear nerve neurinoma can also be seen

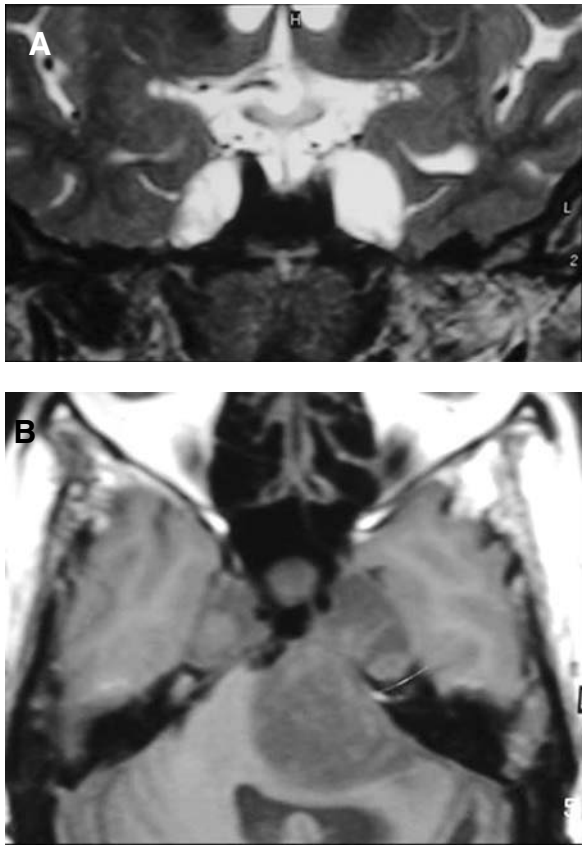

Fig. 12. **A** Coronal T_2-weighted MRI showing bilateral trigeminal neurinomas. **B** Axial T_1-weighted MRI of the same tumors. The one on the left is large and symptomatic

ly. Temporalis muscle is either split parallel to the incision or reflected inferiorly. Muscles of the infratemporal fossa are detached from bone by sharp subperiosteal dissection, exposing the foramen ovale. Temporalis and pterygoid muscle atrophy, seen often with trigeminal neurinomas, makes dissecting the infratemporal fossa easier and the exposure wider. With a microdrill a small craniectomy (approximately 3×3 cm) is performed in the infratemporal fossa, incorporating the foramen ovale. An incision is made along the lateral surface of the dural sheath covering the mandibular nerve at or beyond the level of the foramen ovale and extended posteriorly to the inferior and lateral surfaces of the dural sheaths of the Gasserian ganglion. Dura overlying the Gasserian ganglion and the lateral wall of cavernous sinus is reflected, exposing the middle fossa component of the tumor. This approach obviates exposing the temporal lobe and opening dura of the floor of the middle fossa floor. After the debulking the tumor the exposure may be widened further, and the lesion is followed into the posterior fossa along Meckel's cave. Tumor bulk has widened Meckel's cave, resulting in a large window for resecting the posterior fossa component of the tumor. The cavernous sinus portion of the tumor usually may be resected by angling the microscope anteriorly.

The direction of approach and the surgeons' position (relative to the patient) is altered in order to gain low, direct access to the lesion. Although the carotid artery at the petrous apex, usually covered by a dural sheath, is not exposed, there is sufficient room to accomplish that with relative ease if desirable. The tumor's softness may be helpful in circumventing the disadvantage of confronting tumor before the brainstem is exposed. Approaching tumor anterior to the brainstem is entirely infratentorial. In our hands this exposure was entirely adequate for safely and completely resecting the tumor. The entire procedure could be performed quickly and the cosmetic result was appealing.

Table 1. Clinical features

Clinical features	Number of patients	Percentage
Age		
0–10 years	04	03.3
11–20 years	18	14.6
21–30 years	42	34.1
31–40 years	27	22.0
41–50 years	17	13.8
>50 years	15	12.2
Sex		
Male	54	43.9
Female	69	56.1
Duration of symptoms		
<1 month	14	11.4
1–6 months	56	45.5
6 months – 1 year	23	18.7
1–2 years	18	14.6
>2 years	12	09.8
Presenting symptoms		
Facial numbness	81	65.9
Facial pain	42	34.1
Headaches	83	67.5
Gait disturbance	72	58.5
Pathological laughter	09	07.3
Hearing deterioration	36	29.3
Diplopia	38	30.9
Visual deterioration	19	15.4
Proptosis	06	04.9
Limb weakness	14	11.4
Seizures	05	04.1
Cranial nerve involvement		
Trigeminal nerve		
Sensory		
V1	74	60.2
V2	66	53.6
V3	42	34.1
Motor	69	56.1
Abducens	26	21.1
Oculomotor	12	09.8
Facial	17	13.8
Hearing	25	20.3
Lower cranial nerves	09	07.3
Cerebellar signs	47	38.2
Pyramidal signs	16	13.0

Table 2. Physical characters of the tumor

Tumor characters	Number of patients	Percentage
Location of tumor		
Type A	45	36.6
Type B	17	13.8
Type C	42	34.1
Type D	19	15.4
Tumor size		
<2 cm	10	08.1
2–4 cm	39	31.7
4–6 cm	55	44.7
>6 cm	19	15.4
Nature of tumor		
Predominantly solid	39	31.7
Predominantly cystic	34	27.6
Mixed	54	43.9
Calcification	04	03.3

Basal lateral subtemporal approach [13]

Indications This is for large middle fossa tumors and dumbbell-shaped tumors. Subtemporal craniotomy centered on the external ear canal was found to be suitable for dealing with larger tumors within middle fossa or located in both middle and posterior cranial fossae. This approach is simple, relatively quick, and is familiar to general neurosurgeons.

Surgical technique With the patient in a lateral position, a system for continuously draining CSF via a lumbar subarachnoid catheter is established. The

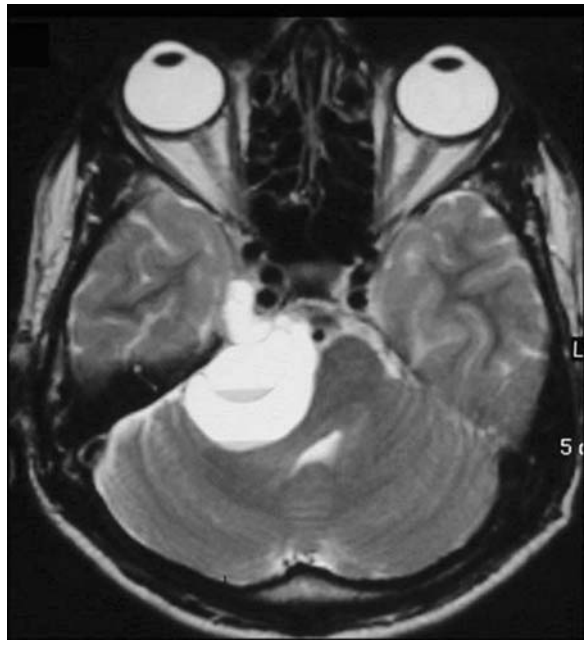

Fig. 13. Axial T_2-weighted MRI showing a fluid level within a trigeminal neurinoma

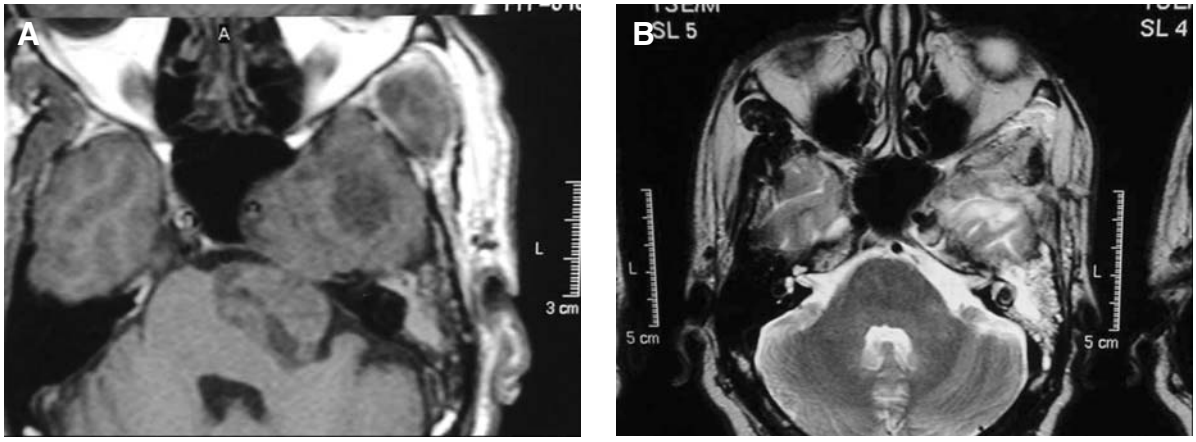

Fig. 14. **A** Axial T_1-weighted MRI showing a multicompartmental trigeminal neurinoma. It is in the extracranial compartment plus the middle and posterior cranial fossae. **B** Axial T_2-weighted MRI showing excision of the tumor

scalp incision, illustrated in Fig. 16a, begins 1.5–2 cm anterior to the tragus of ear and approximately 1.5 cm inferior to the zygomatic arch. This is well anterior to the trunk of superficial temporal artery (by working deep to the temporalis and masseteric fascia, displacing these soft tissues anteriorly protects the frontal and zygomatic branches of the facial nerve, which lie within it). The incision curves initially superiorly, then posteriorly, exposing the temporal squama and posterior parietooccipital bone, the posterior one-third of the temporalis muscle, the roots of the zygomatic arch, the supramastoid crest, and the base of the mastoid process (Fig. 16b). The incision may be extended farther posteriorly and curved inferiorly, enhancing the temporal, occipital and mastoid process exposure. The wide base of the scalp flap preserves all feeding arteries, ensuring sufficient vascularity. The posterior edge of the temporalis muscle is mobilized subperiosteally from the temporal bone and the sharp superior border of the zygomatic arch. This muscle is then rotated anteriorly.

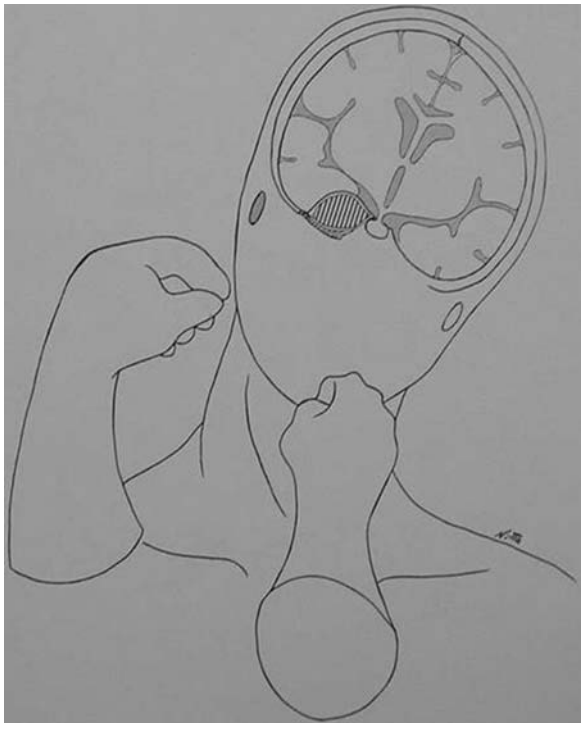

Fig. 15. A line drawing of the surgeon's hands indicating the direction of approach. Shaded ipsilateral zygomatic arch and infratemporal fossa bone reveal the extent of bone removal required for a trigeminal neurinoma (indicated by oblique lines). The zygomatic arch will be replaced after tumor resection

A low temporal craniotomy with its base centered on the external ear canal is performed. The anterior and posterior roots of the zygomatic arch, the glenoid fossa, and the lateral half of the roof of the external ear canal are removed with a power saw as a single piece, or resected with rongeurs and power drill (Fig. 16c). Removing the bone flap as a single piece is frequently difficult and may result in inadvertently opening the external ear canal, which may render the field no longer sterile. The external ear canal is protected by separating periosteum sharply from its bony roof. The external ear canal has loose fibrous connections to its bony and cartilaginous wall. Soft tissues are more firmly attached to the spine of

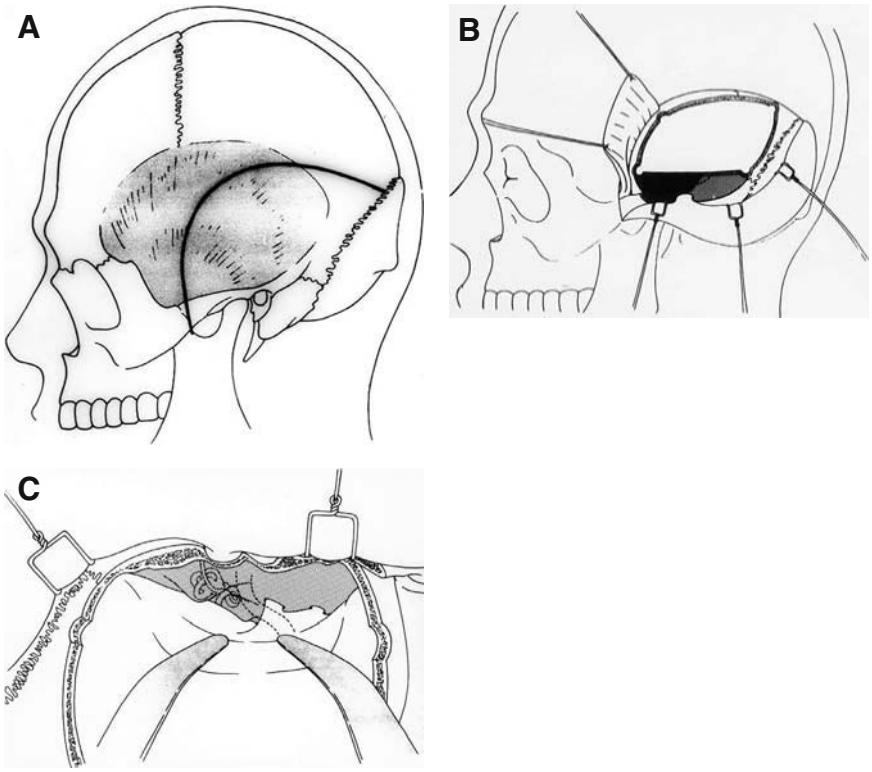

Fig. 16. **A** Line drawing indicating the scalp incision for the lateral basal subtemporal approach. **B** Drawing showing a low temporal craniotomy and its basal extension. The roots of the zygomatic arch and the glenoid fossa are preferably removed as a single piece with an electric saw. The mastoid bone and roof of the external ear canal (shaded area), can be removed with a microdrill. **C** The condyle and superior half of the external ear canal have been unroofed, and the superior one-third of the mastoid has been drilled away in order to achieve a basal extradural exposure. Elevating the middle fossa dura, exposes the foramen spinosum, foramen ovale, foramen rotundum, and dura covering Meckel's cave and the anterior surface of the petrous bone

Henle, where sharp dissection may be necessary to expose the canal. The meniscus of the temporomandibular joint is exposed but not removed. With tumors limited to the middle cranial fossa, or smaller lesions, the glenoid fossa may not require removal and mastoidectomy may be avoided. The superior one-third or one-half (approximately 1.5–2 cm below and medial to the supramastoid crest) of the mastoid air cells are drilled. The mastoid antrum may or may not be opened. Drilling the mastoid process farther medially results in exposing the bony labyrinth surrounding the superior and posterior semicircular canals. The sigmoid sinus and the site of its junction with the transverse sinus are not exposed and a thin plate of bone is preserved between the sinus and the mastoid. After sectioning the middle meningeal artery, dura is elevated from the floor of the middle fossa floor, providing a basal extradural exposure.

Tumors limited to or mostly within the middle fossa may be removed extradurally after exposing the foramen ovale and dissecting the outer sheath of dura. An intradural exposure is preferred for large tumors and those with a significant posterior fossa component. The intradural route (after elevating the temporal lobe) exposes the floor of the middle fossa and the tentorium. The lesion is identified as a bulging mass in the middle fossa floor. A transverse incision is made in dura overlying it and tumor is progressively removed, while carefully preserving displaced trigeminal nerve fibers. In some cases the posterior fossa component of the tumor is exposed by following the middle fossa portion through the window created by erosion of the petrous apex beneath the tentorial edge.

When the posterior fossa component is larger, the tentorium is incised, beginning at its free edge, adjacent to the posterior surface of the cerebral

peduncle, proceeding anterolaterally toward the lateral surface of the superior petrosal sinus.

A triangular flap of tentorium is then reflected over the superior petrosal sinus, or resected by incising it parallel to the sinus, providing a window of access to infratentorial structures. This results in wide exposure of the posterior fossa while protecting the fourth and fifth cranial nerves and the petrosal vein from inadvertent injury. Whether or not more exposure is required is determined by the tumor's consistency, vascularity and growth characteristics.

Maximum exposure is achieved by transecting the superior petrosal sinus between clips (or packing cut ends after incising it). If the surgeon has sufficient space to work anterior, posterior and inferior to the sinus, sacrificing it is not necessary. Angling the microscope anteriorly, exposes tumor in the lateral dural walls of the cavernous sinus, while tilting it posteriorly provides a view into the cerebellopontine angle.

This entire approach is through the middle cranial fossa. When necessary, exposure may be expanded in various directions. The tumor is resected, beginning at its inferolateral pole, adjacent to the third division of the fifth nerve, proceeding superiorly, taking special care to avoid injuring its first division.

Prior to closure, exposed mastoid air cells are packed with bone wax, free muscle, or fat. The posterior one-third of the temporalis muscle and its fascia may be rotated as appropriate to strengthen the reconstruction as a pedicle graft [16]. The bone plate, including the roots of the zygomatic arch, the glenoid fossa, and the lateral surface of the roof of the external ear, is replaced and secured with sutures. The external auditory meatus is packed with cotton pledgets in order to avoid cicatricial stenosis.

The directly lateral approach, parallel to the external ear canal (with its essentially transverse orientation), is the shortest route to the petrous apex, while the basal subtemporal route provides easy access to both the middle fossa and the infratentorial compartment. It is suitable for all varieties of trigeminal neurinomas. The basal extension of the classical temporal craniotomy, as described, improves the horizontal exposure toward the petrous apex. It neither affects hearing nor places the facial nerve at risk. Temporomandibular joint function is not affected since the condyle is not manipulated or displaced. As the temporal squama is removed, the distance to the tumor is reduced by 1.5–2 cm. Following mastoidectomy and removing the roof of the external ear canal and glenoid fossa, another 1.5–2 cm of space is gained inferiorly and posteriorly. Gently depressing the external ear canal, the condyle, and the meniscus inferiorly provides even more space. Relaxing the temporal lobe by draining CSF provides sufficient exposure for manipulating instru-

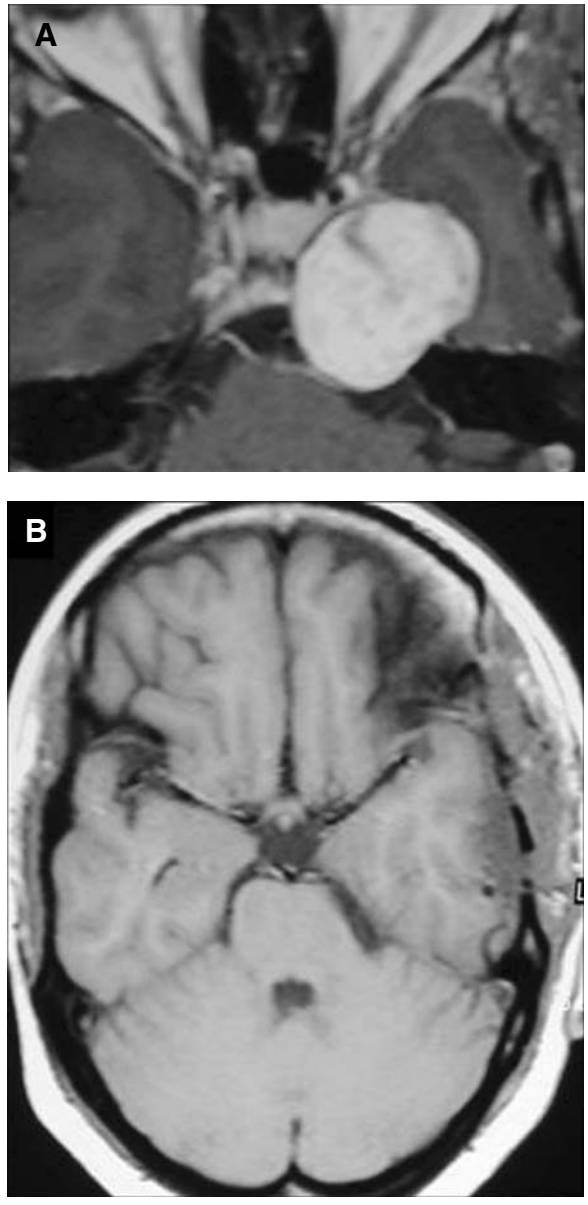

Fig. 17. **A** Axial T_1-weighted contrast enhanced MRI showing an enhancing trigeminal neurinoma in the Meckel's cave. **B** Post-operative T_1-weighted MRI confirming tumor removal

ments and safely dissecting tissues under direct vision at suitable angle.

For lesions primarily of the middle fossa, the inferolateral route is superior to the frontotemporal approach (with its anterolateral trajectory) for preservating of the first division of the fifth nerve. This route also seems safer for dissecting tumor from the brainstem since it can be done under direct vision. It is also relatively quick and easy to execute since it is not necessary to expose the superior bend of the sigmoid sinus, or to take the elaborate steps necessary to mobilize the sigmoid sinus, as required by the petrosal approach. Temporalis muscle is displaced anteriorly, where it no longer obstructs the surgeon's view, making resection of the entire zygomatic arch unnecessary. Furthermore, expanding the initial exposure anteriorly, posteriorly, medially and inferiorly is not difficult. Reconstruction is easy and compact and may be achieved with pedicle-based flaps of temporalis muscle.

The advantages described above make the basal lateral subtemporal approach quite useful (Figs. 17–19). A partial mastoidectomy further enhances the space provided. The ease of expanding

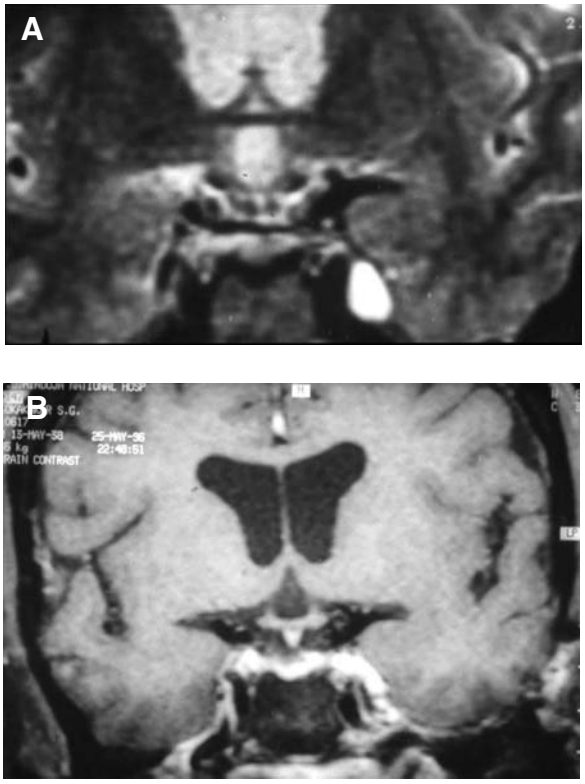

Fig. 18. **A** Coronal T_2-weighted MRI showing the trigeminal neurinoma within the dural walls of Meckel's cave. **B** Coronal T_1-weighted MRI showing excision of the tumor

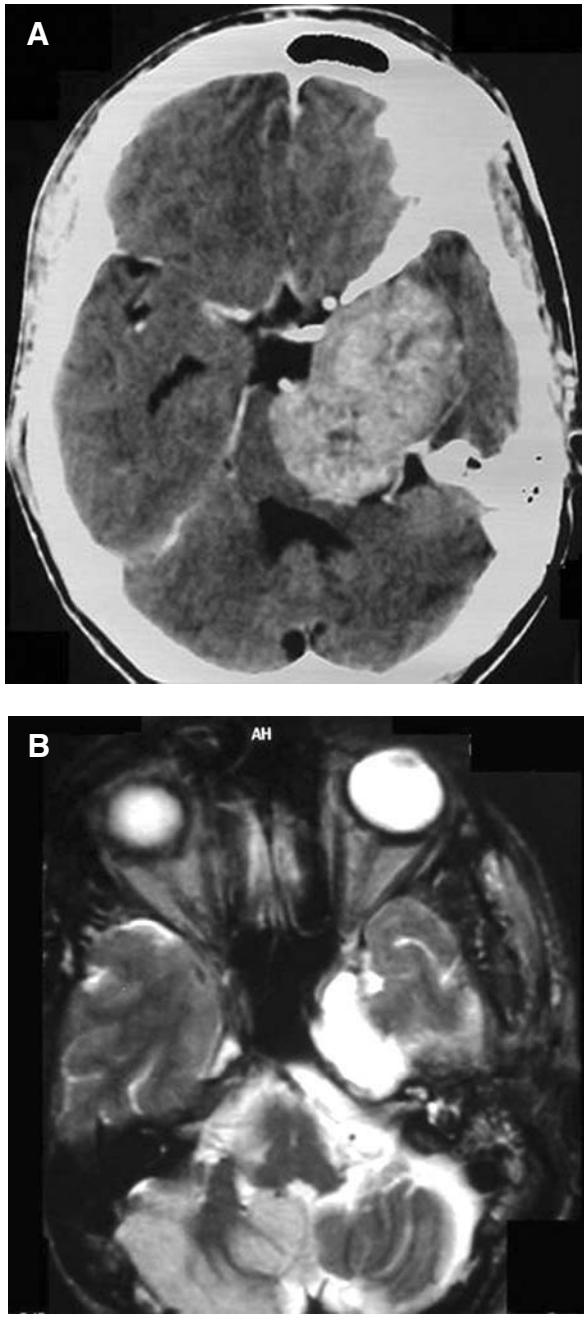

Fig. 19. **A** Axial CT showing a large dumbbell-shaped trigeminal neurinoma. **B** Post-operative axial T_2-weighted MRI showing excision of the tumor

the exposure, either before or during tumor resection, lends this approach considerable versatility.

Anterior basal temporal extradural approach: Recently, with tumors located entirely within the middle cranial fossa, or with only small extensions into the posterior fossa, we have come to prefer the anterior basal temporal approach over the lateral basal subtemporal approach. An anterior basal temporal craniotomy is performed over the anterior part of zygomatic arch. Dura is elevated along the pole of the temporal lobe, beneath the lesser wing of the sphenoid, exposing the superior orbital fissure. From there, extradural dissection proceeds posteriorly along the lateral wall of the cavernous sinus.

Retrosigmoid approach: This route is indicated for trigeminal neurinomas located entirely within the posterior cranial fossa, or those with relatively small extension into the middle fossa.

Multicompartmental tumors: Sometimes trigeminal neurniomas are present in more than two compartments, as those with elements in the posterior fossa, middle fossa, and in the infratemporal fossa or the orbit. Usually such tumors can be removed completely by way of the lateral basal subtemporal approach in a single stage.

Summary of our surgical experience

Early in this series we employed the frontotemporal pterional approach, with or without orbitozygomatic osteotomy and the petrosal approaches. The primary methods preferred after 1992–1993 were the infratemporal fossa interdural approach [15], the lateral basal subtemporal approach [13], the anterior temporal basal extradural approach, and the retrosigmoid approach. The surgical results from various methods are listed in Table 3. Early in this series, seven patients were operated in two stages, combining either the frontotemporal or lateral basal subtemporal approach with the retrosigmoid approach.

Total tumor resection was achieved in 101 cases (82.1%). Extensive but incomplete removal was accomplished in 14 patients (11.4%), with part of the tumor (no more than 5%) deliberately left behind because of difficulties dissecting it from cranial nerves, blood vessels, or the brainstem. In eight patients a subtotal excision was achieved. All patients with partial or a subtotal resection were treated early in the series. Later, over the past 5 years, all tumors have been totally resected. Histology was benign in every tumor, demonstrating both Antoni type A and B tissue.

The fourth cranial nerve was inadvertently transected in two patients, the ipsilateral sixth nerve injured in one, and the facial-auditory nerve complex in two. Two patients died after surgery, one on the first post-operative day of brainstem infraction which was confirmed at autopsy. The other death occurred suddenly on the fifth day after surgery. That patient's post-operative course was otherwise uncomplicated, and an MRI had confirmed total

Table 3. Operative approaches and the outcome after surgery

	No. of Patients	Percentage
Operative approach		
Lateral basal subtemporal	82	66.7
Retrosigmoid	16	13.0
Infratemporal fossa interdural	10	08.1
Petrosal	05	04.1
Fronto temporal	07	05.7
Frontotemporal + Orbito-zygomatic	09	07.3
Tumor excision		
Total	101	82.1
Subtotal	08	06.5
Near-total	14	11.4
Post-operative new cranial nerve Deficits		
Abducens	03	2.4
VII–VIII complex	02	1.6
Other complications		
CSF leak	1	0.8
Meningitis	1	0.8
Osteomyelitis	1	0.8
Extradural hematoma	1	0.8

Symptomatic improvement	Preop	Post-op	Percentage improvement
Facial pain	42	10	76.2
Facial numbness	81	37	54.3
Diplopia	38	12	70.6
Hearing disturbances	36	18	52.0
Visual disturbances	18	06	70.0
Gait difficulty	72	07	91.2
Pathological Laughter	09	00	100.0
Headaches	83	07	92.7
Lower cranial nerves	09	00	100.0

Preop preoperative; *Post-op* post-operative.

tumor resection. No post-mortem examination was performed.

Other post-operative complications were limited to the following: a CSF leak in one patient, requiring lumbar CSF drainage for control. Another developed an acute extradural hematoma which led to emergency re-operation. Two patients experienced worsening sixth nerve deficits after surgery, and two, both with facial weakness and hearing loss prior to surgery, manifest facial paralysis and deafness after surgery.

Lost sixth and eighth nerve function did not return, but facial function improved significantly, although incompletely, with further follow-up. One patient (with a post-operative sixth nerve deficit) developed keratitis and permanent corneal opacity 2 months after surgery. Although sensory return could not be quantified, every patient with preoperative facial numbness continued to have at least some trigeminal hypesthesia, but 44 of 81 improved subjectively after surgery. No patient with unimpaired facial sensation prior to surgery developed facial numbness. Nineteen patients experienced worsening of facial sensation, developing anesthesia in one or more divisions of the fifth nerve. Twenty-eight patients reported increased strength of temporalis and masseter muscles after surgery. No patient with muscular atrophy experienced improved motor function. Hearing returned to normal in 18 patients after surgery and subjectively improved in four. Diplopia resolved in 26 of 38 patients affected prior to surgery, the remaining 12 continuing to have at least some diplopia. Sixty-seven patients (91.2%) ataxic preoperatively could walk normally after surgery, and others improved. Pathological laughter resolved immediately after surgery in all nine patients who experienced this symptom. During follow-up ranging from 6 months to 10 years (average 52 months) all 121 patients improved with respect to preoperative symptoms and functional ability, each returning to his or her previous occupation and independent living.

Four patients required re-operation for tumor-recurrence following partial resections. One of them was treated early in the series with an operation limited to cyst evacuation and partial removal of the tumor capsule. Among all patients with total or near-total resections, only three tumors returned.

Of four patients with bilateral tumors, only the symptomatic tumor was treated surgically. No growth of non-operated tumors was observed during the follow-up period.

Stereotactic radiosurgery, as alternative primary or adjuvant treatment for trigeminal neurinomas, controlled tumor growth, caused no new deficits, was associated with improved rates of cranial nerve preservation, and often improved presenting symptoms [19, 32].

Our experience indicates that radical surgery for trigeminal neurinomas is safe and results in excellent neurological outcomes and long-term tumor control [11].

References

1. Arseni C, Dumitrescu L, Constantinescu A (1975) Schwannomas of the trigeminal nerve. Surg Neurol 4: 497–503
2. Bhatjiwale MG, Nadkarni TD, Desai KI, Goel A (2000) Pathological laughter as a presenting symptom of massive trigeminal neuromas. Report of four cases. Neurosurgery 47: 469–471
3. Bordi L, Compton J, Symon L (1989) Trigeminal schwannoma. A report of eleven cases. Surg Neurol 31: 272–276
4. Cantini R, Giorgetti W, Valleriani AM, Burchianti M (1987) Trigeminal schwannomas in adolescence. Pediatr Neurosci 13: 198–201
5. Cerillo A, Bianco M, Narciso N, Carraturo S, Bucciero A, Cirillo S, Briganti F, De Caro ML (1995) Trigeminal cystic schwannoma in the cavernous sinus. Case report. J Neurosurg Sci 39: 165–170
6. Daspit CP, Spetzler RF, Pappas CT (1991) Combined approach for lesions involving the cerebellopontine angle and skull base. Experience with 20 cases – preliminary report. Otolaryngol Head Neck Surg 105: 788–796
7. Day JD, Fukushima T (1998) The surgical management of trigeminal neuromas. Neurosurgery 42: 233–241
8. Dolenc VV (1994) Frontotemporal epidural approach to trigeminal schwannomas. Acta Neurochir (Wien) 130: 55–65
9. Findler G, Feinsod M, Sahar A (1983) Trigeminal schwannoma with unusual presentation. Report of a case with trigeminal somatosensory-evoked response. Surg Neurol 19: 351–353
10. Fisch U (1982) Infratemporal fossa approach for glomus tumors of the temporal bone. Ann Otorhinolaryngol 9: 474–479
11. Goel A, Muzumdar D, Raman C (2003) Trigeminal neuroma: analysis of surgical experience with 73 cases. Neurosurgery 52: 783–790
12. Goel A, Gupta S (2000) Reconstruction of skull base. A review of personal techniques. Neurol India 48: 208–215

13. Goel A, Nadkarni TD (1999) Basal lateral subtemporal approach for trigeminal neurinomas. Report of an experience with 18 cases. Acta Neurochir (Wien) 141: 711–719
14. Goel A (1998) Impact of arterial displacements on strategy for cavernous sinus surgery. Neurol India 46: 94–101
15. Goel A (1995) Infratemporal fossa interdural approach for trigeminal schwannomas. Acta Neurochir (Wien) 136: 99–102
16. Goel A (1994) Vascularlised osteomyoplastic flaps for skull base reconstruction. Br J Neurosurg 8: 79–82
17. Goel A, Ranade D, Nagpal RD (1994) An unusual trigeminal schwannoma. Br J Neurosurg 8: 369–371
18. Horie Y, Akagi S, Taguchi K, Yoshino T, Hayashi K, Takahashi K, Akagi T (1990) Malignant schwannoma arising in the intracranial trigeminal nerve. A report of an autopsy case and a review of literature. Acta Pathol Jpn 40: 219–225
19. Huang CF, Kondziolka D, Flickinger JC, Lunsford LD (1999) Stereotactic radiosurgery for trigeminal schwannomas. Neurosurgery 45: 11–16
20. Iwai Y, Hakuba A, Noguchi K, Nishimura S (1988) A gigantic neurilemoma originating in the pterygopalatine fossa. A case report. Surg Neurol 30: 452–456
21. Jefferson G (1955) The trigeminal schwannomas with some remarks on malignant invasion of the gasserain ganglion. Clin Neurosurg 1: 11–54
22. Karmody CS (1979) Malignant schwannoma of the trigeminal nerve. Otolaryngol Head Neck Surg 87: 594–598
23. Konovalov AN, Spallone A, Mukhamedjanov DJ, Tcherekajev VA, Makhmudov UB (1996) Trigeminal schwannomas. A series of 111 cases from a single institution. Acta Neurochir (Wien) 138: 1027–1035
24. Koyye RT, Mahadevan A, Santosh V, Chickabasaviah YT, Govindappa SS, Hegde T, Shankar SK (2003) A rare case of cellular schwannoma involving the trigeminal ganglion. Brain Tumor Pathol 20: 79–83
25. Lesoin F, Rousseaux M, Villette L, Autricque A, Dhellemmes P, Pellerin P, Vaneecloo JM, Leys D, Jomin M (1986) Schwannomas of the trigeminal nerve. Acta Neurochir (Wien) 82: 118–122
26. Lunardi P, Missori P, Gagliardi FM, Fraioli B (1989) Trigeminal schwannoma with infratemporal extension. Case report. J Neurosurg Sci 33: 293–295
27. Martini D, Har-El G, Johnson C (1994) Trigeminal schwannoma. Ann Otol Rhinol Laryngol 103: 652–654
28. McCormick PC, Bello JA, Post KD (1988) Trigeminal schwannoma. Surgical series of 14 cases with review of literature. J Neurosurg 69: 850–860
29. Muzumdar DP, Goel A, Pakhmode CK (2002) Multicystic acoustic neurinoma: report of two cases. J Clin Neurosci 9: 453–455
30. Nadkarni T, Goel A (1999) A trigeminal schwannoma involving the lacrimal nerve. Case report. Br J Neurosurg 13: 75–76
31. Nager GT (1984) Schwannomas of the trigeminal nerve. Am J Otolaryngol 5: 301–333
32. Nettel B, Niranjan A, Martin JJ, Koebbe CJ, Kondziolka D, Flickinger JC, Lunsford LD (2004) Gamma knife radiosurgery for trigeminal schwannomas. Surg Neurol 62: 435–444
33. Page RD, Lye RH (1988) Trigeminal schwannomas. Has the "new technology" made any difference? Br J Neurosurg 2: 67–71
34. Paillas JE, Grisoli F, Farnarier P (1974) Neurinomes du trijumeau. A propos de 8 cas. Neurochirurgie 20: 41–54
35. Pollack IF, Sekhar LN, Jannetta PJ, Janecka IP (1989) Neurilemomas of the trigeminal nerve. J Neurosurg 70: 737–745
36. Post KD, McCormick PC (1990) Trigeminal schwannomas. In: Wilkins RH, Renagchary SS (eds) Neurosurgery update I: diagnosis, operative technique and neuro-oncology. McGraw-Hill, New York, pp 346–353
37. Samii M, Migliori MM, Tatagiba M, Babu R (1995) Surgical treatment of trigeminal schwannomas. J Neurosurg 82: 711–718
38. Schisano G, Olivocrona H (1960) Neurinomas of the Gasserian ganglion and trigeminal root. J Neurosurg 17: 306–322
39. Sepehrnia A, Samii M, Tatagiba M (1991) Management of intracavernous tumours. An 11-year experience. Acta Neurochir (Wien) 53(Suppl): 122–126
40. Sindou M, Pelissou I (1987) Trigeminal schwannomas. A special type of cavernous sinus tumors. In: Dolenc VV (ed) The cavernous sinus: a multidisciplinary approach to vascular and tumorous lesions. Springer, Wien New York, pp 355–376
41. Taha JM, Tew JM Jr, van Loveren HR, Keller JT, El-kalliny M (1995) Comparison of conventional and skull base approaches for the excision of trigeminal schwannomas. J Neurosurg 82: 719–725
42. Wetmore SJ, Suen JY, Snyderman NL (1986) Preauricular approach to infratemporal fossa. Head Neck Surg 9: 93–103
43. Yamada K, Ohta T, Miyamoto T (1992) Bilateral trigeminal schwannomas associated with von Recklinghausen disease. Am J Neuroradiol 13: 299–300
44. Yamasaki T, Nagao S, Kagawa T, Takamura M, Moritake K, Tanaka Y, Kida T, Kobayashi T (1996) Therapeutic effectiveness of combined microsurgery and radiosurgery in a patient with a huge trigeminal schwannoma. No To Shinkei 48: 845–850 (in Japanese)
45. Yamashiro S, Nagahiro S, Mimata C, Kuratsu J, Ushio Y (1994) Malignant schwannoma associated with xeroderma pigmentosum – case report. Neurol Med Chir (Tokyo) 34: 817–820
46. Yasui T, Hackbut A, Kim SH, Nishimura S (1989) Trigeminal schwannomas. operative approach in eight cases. J Neurosurg 71: 506–511
47. Yoshida K, Kawase T (1999) Trigeminal schwannomas extending into multiple fossae. surgical methods and review of literature. J Neurosurg 91: 202–211

Bypasses for cavernous sinus tumors: history, techniques, and current status

L. N. Sekhar[1], S. K. Natarajan[1], G. W. Britz[1,2], B. Ghodke[1,2]

[1]Department of Neurological Surgery, University of Washington, Seattle, WA, USA
[2]Department of Radiology, University of Washington, Seattle, WA, USA

Introduction

Many cavernous sinus (CS) tumors affect the intracavernous internal carotid artery (ICA-CS) enough result in its occlusion, with or without bypass surgery. Here we discuss the management of such lesions.

History of bypasses for the ICA-CS

The surgical treatment of lesions inside the cavernous sinus was pioneered by Parkinson, and later revived by Dolenc armed with microsurgical and skull base techniques [8, 9]. Dolenc's landmark report created wide interest in treating CS lesions directly with surgery, resulting in the pioneering efforts of Hakuba et al. [12, 13], Kawase et al. [18], Al-Mefty and co-workers [1–7, 10, 16], Rhoton and co-workers [14, 15, 17, 25, 26, 33, 39, 40], Umansky and co-workers [34, 37, 38], Kobayashi and co-workers [20] and Fukushima and co-workers [11, 35, 36] in this area. The senior author developed an early interest in CS lesions while working in Pittsburgh with Joseph Maroon and Peter Janetta, then subsequently with Professors Madjid Samii in Hannover and M. Gazi Yaşargil in Zurich.

Following early ancient experience operating on CS tumors and early laboratory work, it became apparent that the best solution for some tumors and aneurysms was to replace the cavernous segment of the ICA with a graft (Figs. 1, 2). Anatomical studies of the cavernous sinus and related structures were performed in an effort to devise new types of carotid bypasses [27]. In humans, bypasses between the petrous ICA and the supraclinoid ICA using saphenous vein grafts (SVGs) were described by Sekhar et al. [31] and Fukushima and co-workers [35]. A short vein graft was an attractive idea, but disadvantages of the procedure included the need to expose the petrous ICA, to work at considerable depths for both anastomoses, and the need to occlude the ICA for approximately 90 min.

We ultimately abandoned the procedure in favor of interposing a long SVG between the cervical ICA or ECA and the M_2 segment of the MCA, or the supraclinoid ICA [22, 28, 30, 32]. Such vein grafts (from the extracranial ICA or ECA) subsequently were anastomosed to the bifurcation of the M_1 segment in order to provide a greater volume of flow (Figs. 3, 4). More recently, after solving the problem of postoperative vasospasm, the radial artery has increasingly replaced the SVG, and the technique has been successfully employed by many cerebrovascular surgeons. Yet, in some patients, the radial artery is either insufficiently large, or unavailable, requiring that a SVG still be utilized.

When to revascularize

When the ICA is invaded or encased by tumor, two controversies continue to rage. The first is

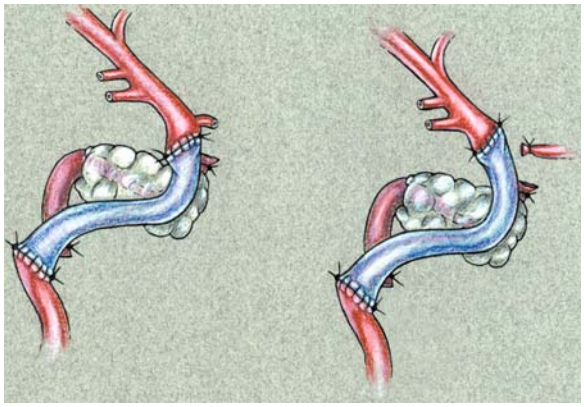

Fig. 1. Bypasses for cavernous sinus tumors: replacing the cavernous segment of the ICA with a graft

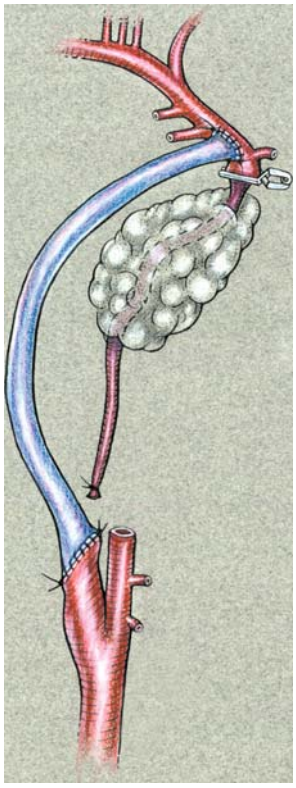

Fig. 2. Bypass for the ICA-CS

whether one should attempt to skeletonize the vessel by removing tumor or whether the vessel should be resected. The second concerns the question of whether all patients should be revascularized, or only those whose collateral circulation is demonstrated to be limited.

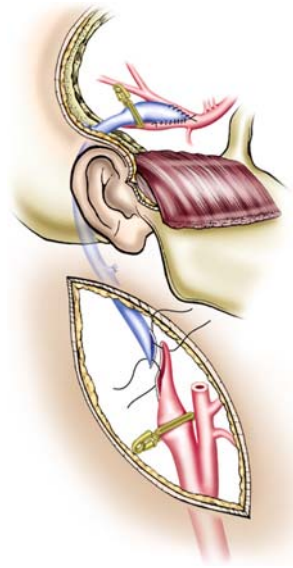

Fig. 3. Interposing a saphenous vein grafts (SVG)

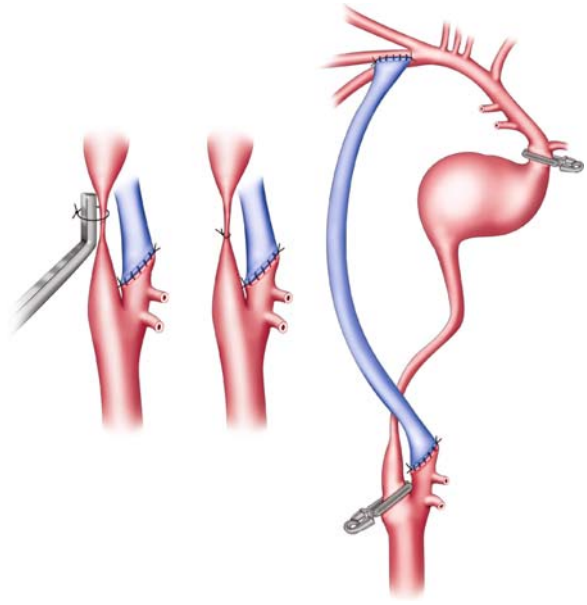

Fig. 4. Examples of SVGs

Whether or not the ICA should be left intact depends on the surgeon's attitude and the nature of the tumor. Benign tumors other than meningiomas (e.g. schwannoma, pituitary adenoma) may usually be dissected from the ICA. With meningiomas, however, encasement and narrowing of the ICA frequently indicates that the vessel wall has been

invaded by tumor. This has been confirmed by histological study of removed arteries [19]. Therefore, total resection often requires ICA resection. Of course, the surgeon may choose to leave tumor behind and treat it with radiosurgery. Generally, chordomas and chondrosarcomas can be dissected from the ICA, but some require replacing the artery with a bypass graft. With slowly growing malignant tumors such as adenoid cystic carcinomas, total tumor removal requires resection of the ICA-CS. Furthermore, resecting and replacing the artery encased with tumor allows the surgeon to give the task of preserving cranial nerves his full attention.

Should a revascularization procedure be performed in every patient where tumor resection creates jeopardy for the ICA, or only in those who fail preoperative balloon-occlusion testing? This is a hotly debated issue, but the occurrence of stroke even when excellent collateral circulation is present [21, 23, 24, 29] convinces us that a bypass should be performed every time tumor resection places the ICA at risk.

Preoperative imaging

We obtain an MRI scan (without and with contrast) to evaluate the extent and special characteristics of the tumor in all patients. The relationship of the tumor to the ICA (inside and outside the CS) is studied, along with the major ICA branches, including whether or not such vessels are encased and/or narrowed. Generally, the presence of an arachnoid plane allows certain tumors to be dissected from the supracavernous ICA and its branches so long as no previous surgery has been performed.

Our patients also undergo cerebral angiography. Collateral circulation and tolerance to temporary occlusion is assessed by compressing the ipsilateral common carotid while injecting contrast material into the contralateral ICA and the dominant vertebral artery. We no longer perform balloon occlusion tests since we revascularize all patients in whom ICA resection or injury seems likely.

Operative technique

After exposing the ICA in the neck, a craniotomy plus an orbital or orbitozygomatic osteotomy is performed and the cavernous sinus tumor is exposed. When it is determined that the tumor cannot be removed without jeopardizing the ICA, the decision is made to proceed with a bypass. A radial artery graft (the entire artery, from the brachial artery bifurcation to the wrist) or a saphenous vein graft (from the upper leg and lower thigh) is removed, flushed with heparinised saline, and distended under pressure in order to minimize the risk of subsequent vasospasm. The patient is placed under burst suppression with propofol to protect the brain, the mean arterial pressure is raised 20% to improve collateral circulation, and 3000–5000 units of heparin are given intravenously.

The distal anastomosis is performed first, to the MCA (M_1 bifurcation or M_2 segment) or to the supraclinoid ICA, then the proximal anastomosis to the ECA (if collateral circulation is poor) or to the ICA (if some collaterals are present). If intraoperative Doppler angiography confirms satisfactory flow through the graft, the cavernous ICA is trapped between clips. The length of the operation plus the fact that anticoagulants were used requires that the operation be terminated at this point. An angiogram is performed the following day, and the tumor is removed as a second stage after 3–7 days.

Postoperative management and complications

Graft occlusion may occur, either during the operation or within the first 24 h after surgery. If occlusion occurs during surgery, the problem is corrected immediately. If the occlusion occurs postoperatively, the patient is reoperated. Rarely is endovascular thrombolysis helpful. Despite intraoperative pressure distension of the graft, vasospasm occurs occasionally with radial artery grafts, and can be treated successfully by endovascular angioplasty.

Patients are maintained on oral aspirin (82 mg daily), and currently patients older than 40 and/or those with hypercholesterolemia are placed on a statin drug. All patients are followed with CT angiography, and/ or Duplex Doppler imaging to measure flow in the graft.

Results of bypasses for tumors

Tables 1–5 indicate the total number of cavernous sinus tumor operations between 1988 and 2005, also

Table 1. Patient characteristics

	Cavernous sinus bypass	Total
Number	65	320
Average	43.39	47.50
Male:Female	17:48	93:227
Average tumor diameter	4.6 cm	3.3 cm
Prior treatment	14	66
Prior surgery	10	51
Prior radiotherapy	12	40
Meningioma	42	203
Chordoma	5	22
Chondrosardoma	5	17
Adenoid cystic CA	5	7
Osteogenic sarcoma	2	2
Secreting adenoma	1	21
Spindle cell sarcoma	1	1
Schwannoma	1	23
Lymphoma	1	1
Hemangioma	1	1
Hemangiopericytoma	1	1
Metastatic adenoCA	0	8
Inflamm. fibrous mass	0	3
Epidermoid	0	2
Giant cell tumor	0	2
Glomus jugulare	0	2
Miscellaneous	0	8

Table 2. Treatment characteristics

	Cavernous sinus bypass	Total
Preoperative embolization	26	120
Preoperative Karnofsky performance score	78.5±9.6	79.7±9.5
Karnopsky performance score at one year	72.4±14.2	79.8±12.8
Recent Karnofsky performance score	75.8±14.8	79.6±13.6
Total operations	115	450
Three operations	6	20
Two operations	38	90
One operation	21	210
Gross total resection	41 (63%)	130 (41%)
Subtotal resection	18 (28%)	88 (28%)
Partial resection	6 (9%)	102 (31%)

specifying those in which bypass surgery was performed in an effort to facilitate resection (Figs. 5, 6) plus the results and complications. Three major complications occurred, two patients with graft oc-

Table 3. Bypass operations performed

Type procedure	Number
Radial artery graft	11
Saphenous vein graft	54
Cervical common carotid artery to middle cerebral artery	1
Cervical external carotid artery to middle cerebral artery	9
Cervical internal carotid artery to middle cerebral artery	38
Cervical internal carotid artery to supraclinoid internal carotid artery	6
Petrous internal carotid artery to supraclinoid internal carotid artery	9
Petrous internal carotid artery to middle cerebral artery	1
Superficial temporal artery to middle cerebral artery	1

Table 4. Surgical outcome

Results	Number of patients
Lost to follow-up	4
No evidence of disease	26
Alive with disease	28
Died of disease	4
Died of complications	3
Died of disease – details	*Length of survival*
(1) Disease progression	24 months
(2) Preop wheelchair bound; Postop cranial nerve IX, X, and XI palsies	7 months
(3) Disease progression	20 months
(4) Disease progression	23 months
Died of complications – details	
(1) Postop Glasgow coma score of 3; major stroke; graft functioning	7 days
(2) Major stroke; graft occlusion; replacement of saphenous vein graft	27 months
(3) Major stroke; graft occlusion; replacement of radial artery graft	20 months

Table 5. Other complications

Complication	Number
New cranial nerve palsy	15
Hydrocephalus	8
Cerebrospinal fluid leak	3

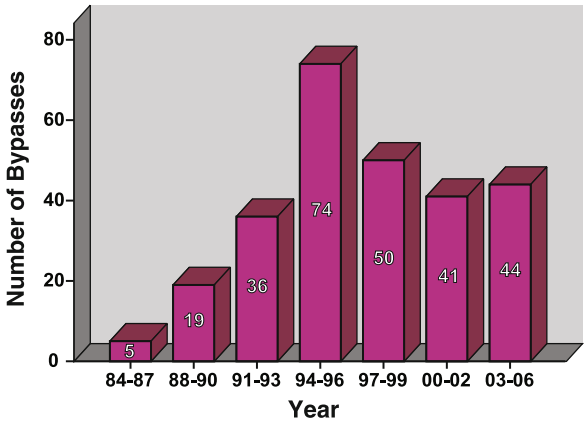

Fig. 5. Bypass surgery (1984–2006)

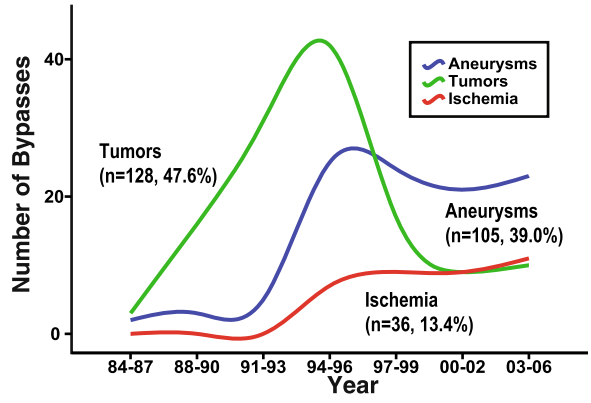

Fig. 6. Correlation between bypass surgery, aneurysms, tumors and ischemia

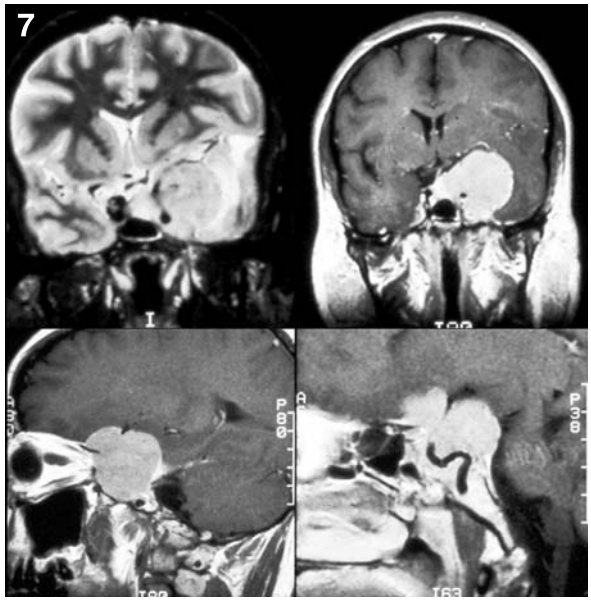

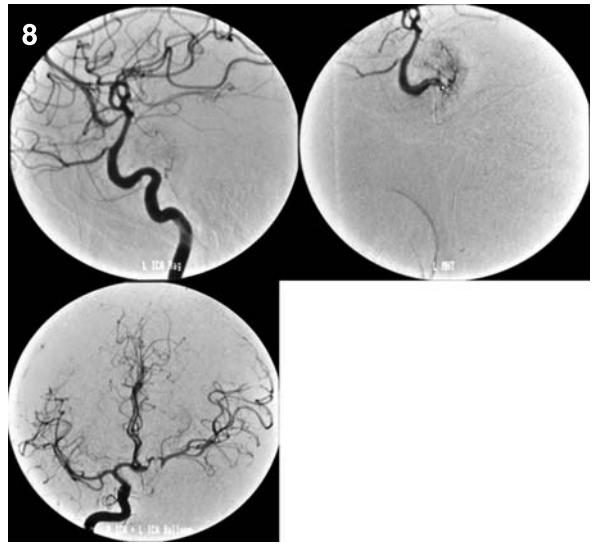

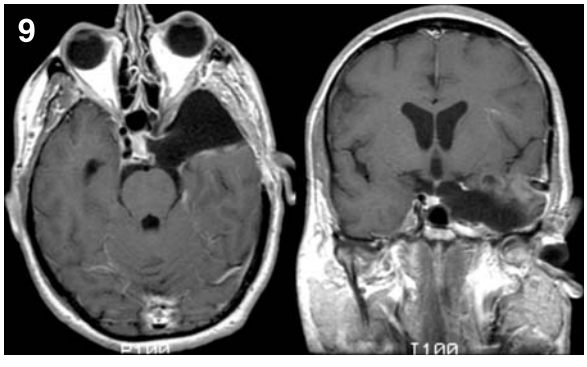

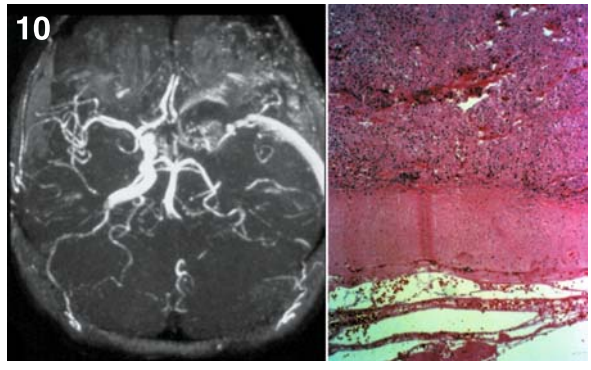

Figs. 7–10. Case 1: diagnosis and treatment of giant sphenocavernous meningiomas. See text for details

clusions and strokes, and others as listed in Table 3. One patient, operated on for a recurrent meningioma (with previous surgery and radiotherapy), had a caudate stroke. In the midst of a good recovery, he developed idiopathic thrombocytopenic purpura and died.

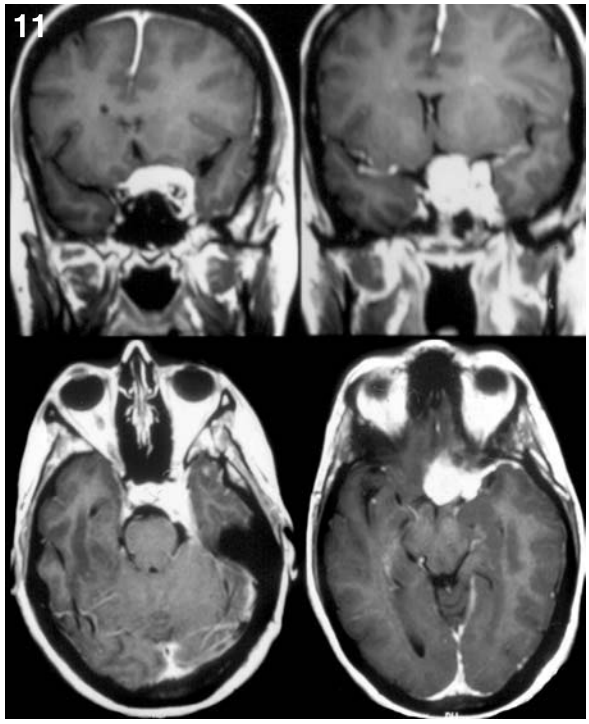

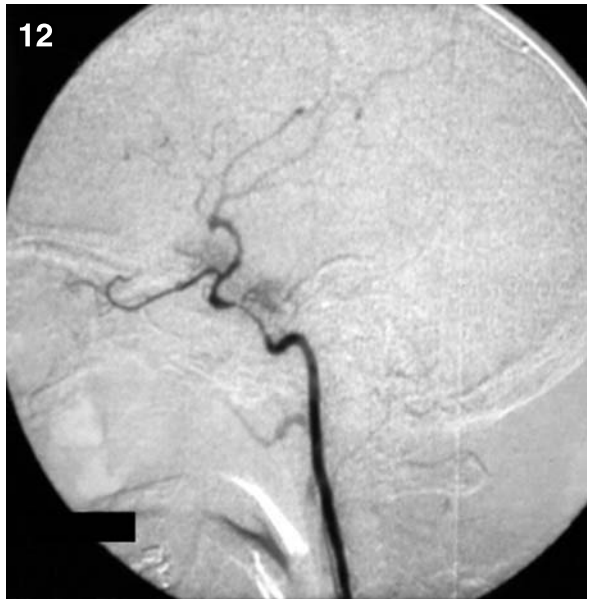

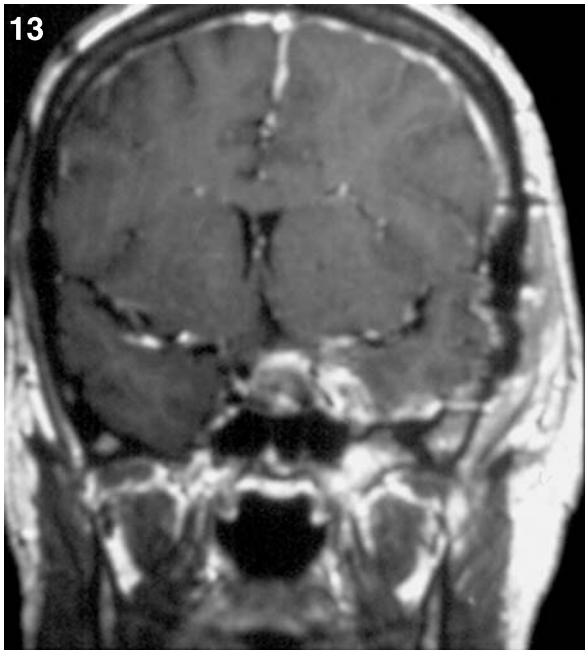

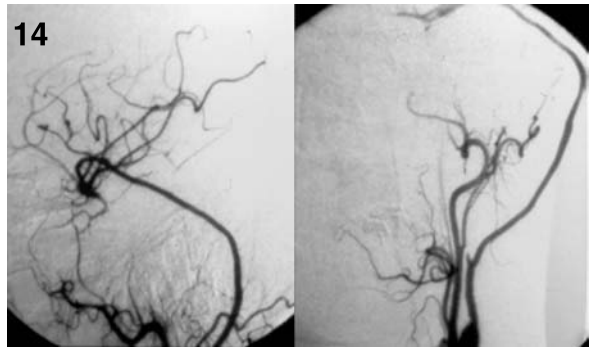

Figs. 11–14. Case 2: diagnosis and treatment of planum sphenoidale-sphenocavernous meningioma. See text for details

Illustrative cases

Case #1

A 40-year-old man (Figs. 7–10) with giant sphenocavernous meningiomas underwent total resection after a SVG was interposed between the cervical ECA and the MCA (M_2 branch). He had third and sixth cranial nerve palsies preoperatively, which were slightly worse after surgery. He had no other deficits and continues to function normally. The tumor has not recurred for 12 years.

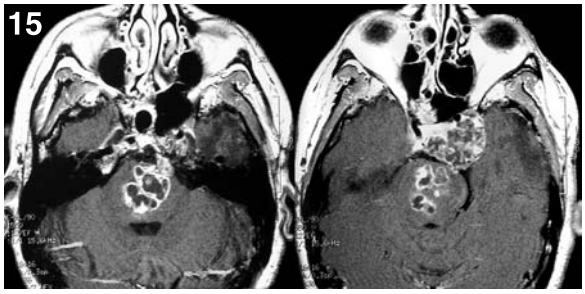

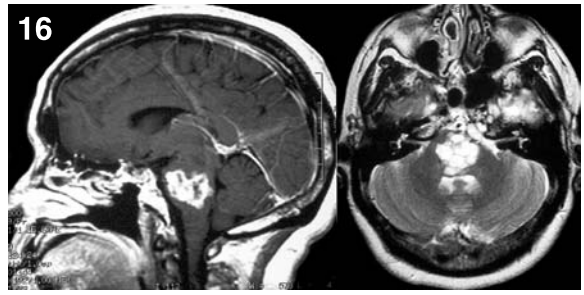

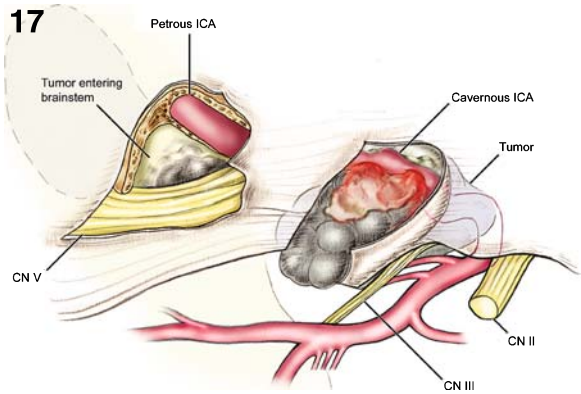

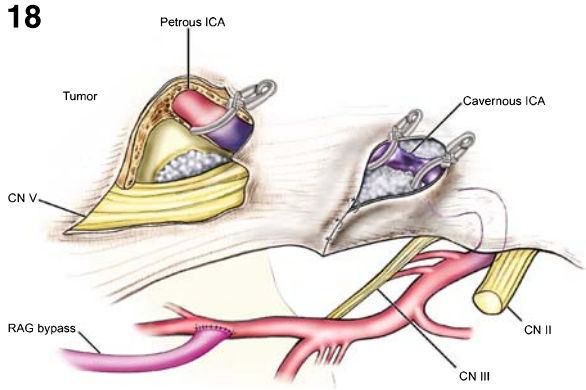

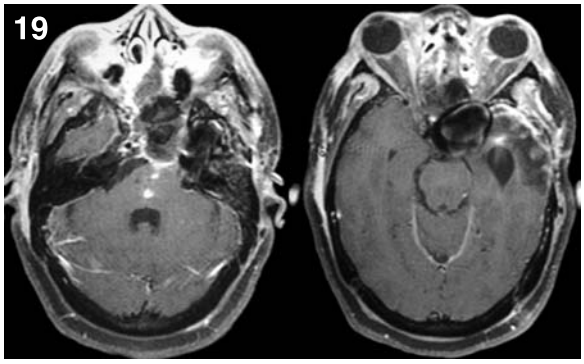

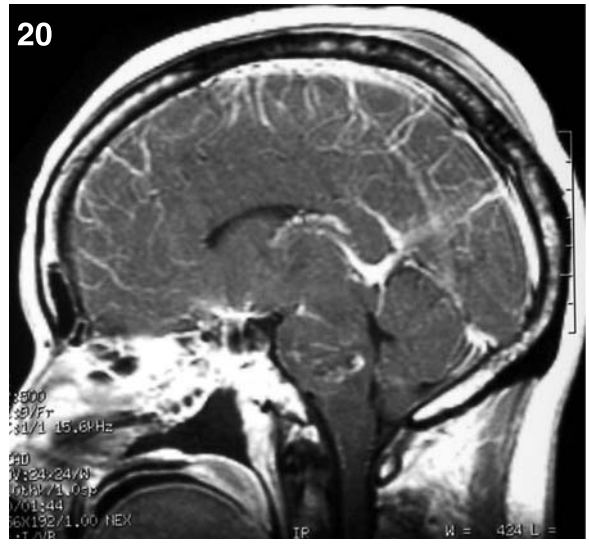

Figs. 15–20. Case 3: diagnosis and treatment of recurrent chondrosarcoma. See text for details

Case #2

A 41-year-old woman (Figs. 11–14) presented with visual loss and the planum sphenoidale-sphenocavernous meningioma as shown. Preoperative angiography revealed a severely narrowed intracavernous ICA with poor collaterals. After an ICA-to-MCA bypass with a radial artery graft, a subtotal tumor resection was carried out, followed by Gamma Knife radiosurgery. She remains free of regrowth after 6 years.

Case #3

Figures 15–20 show a patient with a recurrent chondrosarcoma involving the cavernous sinus and the brainstem. During the operation to remove the tumor, the intracavernous ICA was found to be severely invaded, and could not be preserved. An emergent radial-artery bypass was performed and the tumor was removed totally in two operations. Severe visual loss present preoperatively deteriorated to blindness, but she made an otherwise uneventful recovery. She remains tumor-free after 3 years.

Case #4

Figures 21–23 demonstrate a hemangioma of the cavernous sinus which had recurred after an incomplete prior resection. A RAG-bypass was per-

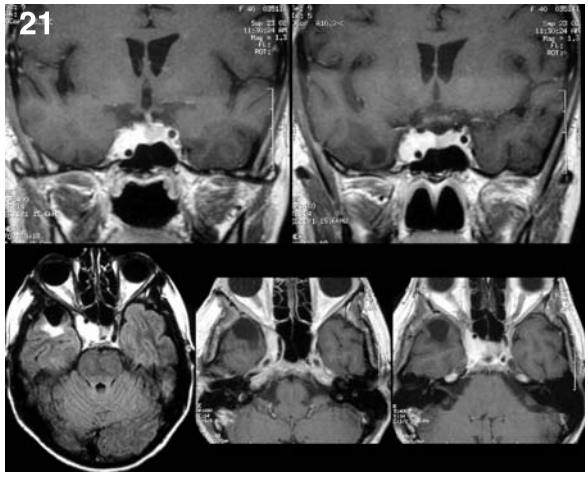

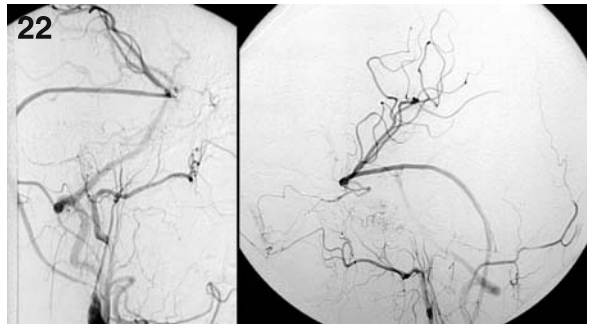

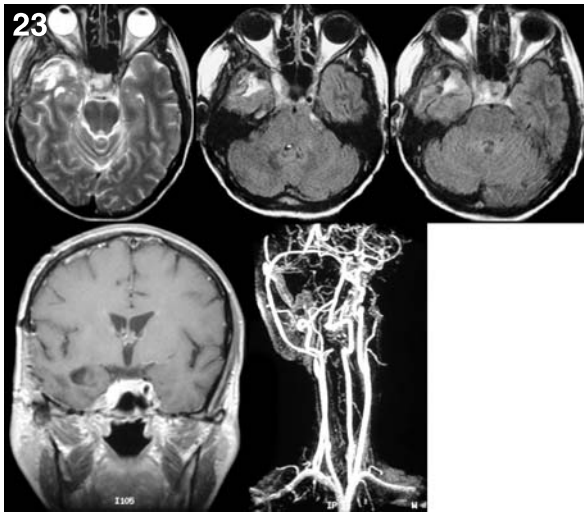

Figs. 21–23. Case 4: diagnosis and treatment of recurrent hemangioma of the cavernous sinus. See text for details

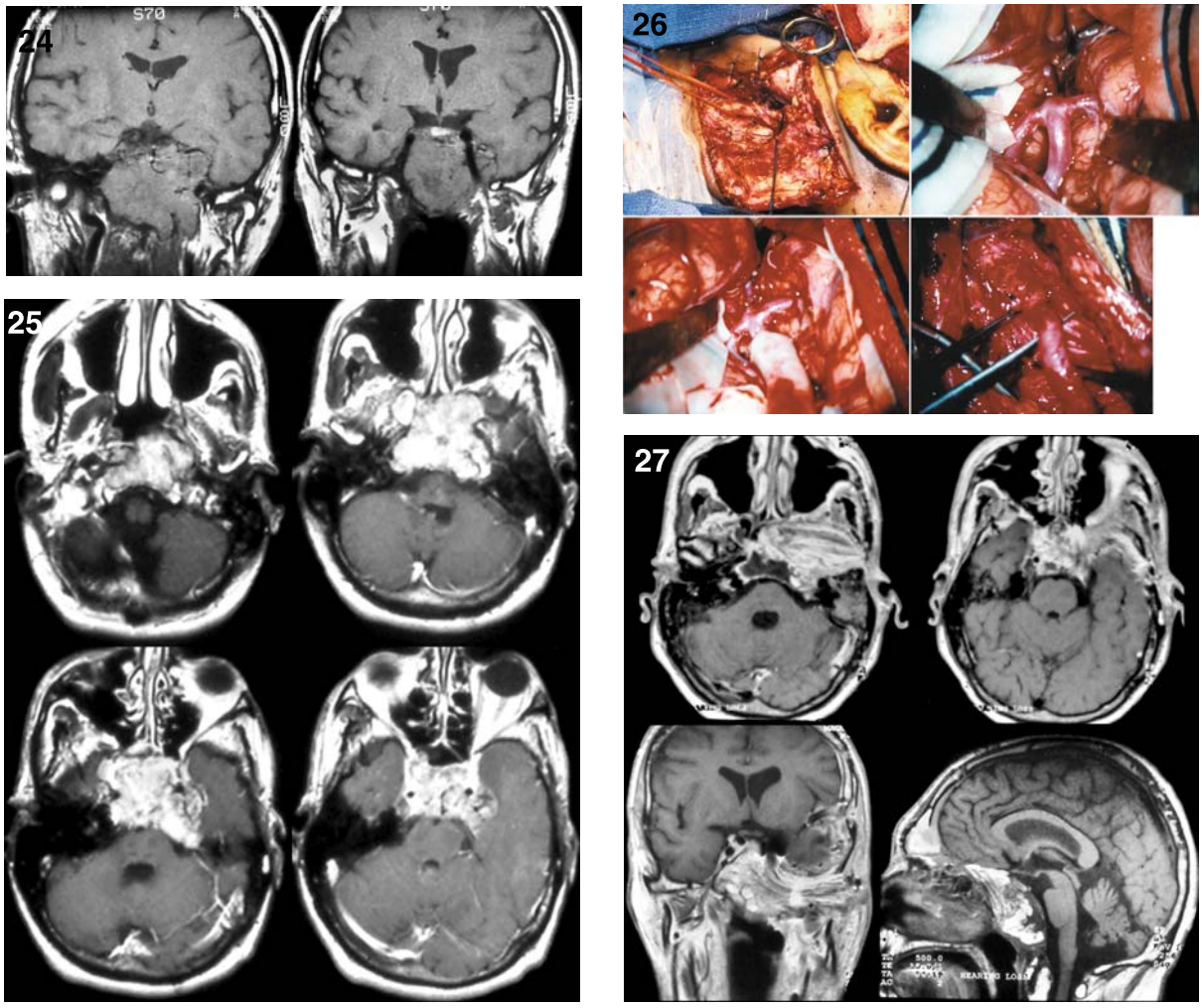

Figs. 24–27. Case 5: diagnosis and treatment of a recurring adenoid cystic carcinoma. See text for details

formed in order to achieve complete tumor removal, and an excellent recovery followed.

Case #5

Figures 24–27 show a patient with adenoid cystic carcinoma which recurred after prior radiotherapy, the tumor involving the sphenoid, cavernous sinus, and infratemporal fossa. A saphenous vein graft bypass was installed between the ICA and the MCA, and the tumor was resected completely. The skull base was reconstructed with a vascularized rectus abdominis muscle flap, and the patient made a nice recovery from surgery only to die 5 years later with systemic metastases.

Conclusions and future trends

With the advent of Gamma Knife radiosurgery, far fewer meningiomas involving the cavernous sinus are being treated surgically, and bypasses are performed only rarely. They may be of value in the future, however, for meningiomas recurring after radiotherapy. For other tumors invading the cavernous sinus, bypasses are sometimes necessary and can be crucial for some patients. For malignant tumors invading the

cavernous sinus, we believe bypasses remain important for lesions which can be potentially cured or controlled for years by resection plus adjuvant radiotherapy or chemotherapy. Even though the value of resection is uncertain in some such patients, their survival should be assumed until proven impossible.

The techniques of bypass surgery have greatly improved, and we have seen fewer complications such as graft-occlusions and strokes. Our experience confirms that previously irradiated patients face a high risk with surgery.

References

1. Al-Mefty O (1991) Management of the cavernous sinus and carotid siphon. Otolaryngol Clin North Am 24: 1523–1533
2. Al-Mefty O, Ayoubi S, Smith RR (1991) Direct surgery of the cavernous sinus: patient selection. Acta Neurochir Suppl (Wien) 53: 117–121
3. Al-Mefty O, Khalil N, Elwany MN, Smith RR (1990) Shunt for bypass graft of the cavernous carotid artery: an anatomical and technical study. Neurosurgery 27: 721–727; discussion 727–728
4. Al-Mefty O, Smith RR (1988) Surgery of tumors invading the cavernous sinus. Surg Neurol 30: 370–381
5. Anand VK, House JR, III, Al-Mefty O (1991) Management of benign neoplasms invading the cavernous sinus. Laryngoscope 101: 557–564
6. Bowles AP Jr, Al-Mefty O (1995) The cavernous carotid artery: preservation is the best means of reconstruction. Clin Neurosurg 42: 154–170
7. DeMonte F, Smith HK, Al-Mefty O (1994) Outcome of aggressive removal of cavernous sinus meningiomas. J Neurosurg 81: 245–251
8. Dolenc V (1979) Microsurgical removal of large sphenoidal bone meningiomas. Acta Neurochir Suppl (Wien) 28: 391–396
9. Dolenc V (1983) Direct microsurgical repair of intracavernous vascular lesions. J Neurosurg 58: 824–831
10. Eisenberg MB, Al-Mefty O, DeMonte F, Burson GT (1999) Benign nonmeningeal tumors of the cavernous sinus. Neurosurgery 44: 949–954; discussion 954–955
11. Fukushima T (1995) Techniques of carotid reconstruction. Clin Neurosurg 42: 119–134
12. Hakuba A, Nishimura S, Shirakata S, Tsukamoto M (1982) Surgical approaches to the cavernous sinus. Report of 19 cases (author's transl). Neurol Med Chir (Tokyo) 22: 295–308
13. Hakuba A, Tanaka K, Suzuki T, Nishimura S (1989) A combined orbitozygomatic infratemporal epidural and subdural approach for lesions involving the entire cavernous sinus. J Neurosurg 71: 699–704
14. Harris F, Rhoton AL Jr (1975) Microsurgical anatomy of the cavernous sinus. Surg Forum 26: 462–463
15. Harris FS, Rhoton AL (1976) Anatomy of the cavernous sinus. A microsurgical study. J Neurosurg 45: 169–180
16. Heth JA, Al-Mefty O (2003) Cavernous sinus meningiomas. Neurosurg Focus 14: e3
17. Inoue T, Rhoton AL Jr, Theele D, Barry ME (1990) Surgical approaches to the cavernous sinus: a microsurgical study. Neurosurgery 26: 903–932
18. Kawase T, van Loveren H, Keller JT, Tew JM (1996) Meningeal architecture of the cavernous sinus: clinical and surgical implications. Neurosurgery 39: 527–534; discussion 534–536
19. Kotapka MJ, Kalia KK, Martinez AJ, Sekhar LN (1994) Infiltration of the carotid artery by cavernous sinus meningioma. J Neurosurg 81: 252–255
20. Kudo T, Ueki S, Kobayashi H, Torigoe H, Tadokoro M (1989) Experience with the ultrasonic surgical aspirator in a cavernous hemangioma of the cavernous sinus. Neurosurgery 24: 628–631
21. Larson JJ, Tew JM Jr, Tomsick TA, van Loveren HR (1995) Treatment of aneurysms of the internal carotid artery by intravascular balloon occlusion: long-term follow-up of 58 patients. Neurosurgery 36: 26–30; discussion 30
22. Linskey ME, Sekhar LN, Horton JA, Hirsch WL Jr, Yonas H (1991) Aneurysms of the intracavernous carotid artery: a multidisciplinary approach to treatment. J Neurosurg 75: 525–534
23. McIvor NP, Willinsky RA, TerBrugge KG, Rutka JA, Freeman JL (1994) Validity of test occlusion studies prior to internal carotid artery sacrifice. Head Neck 16: 11–16
24. Origitano TC, Al-Mefty O, Leonetti JP, DeMonte F, Reichman OH (1994) Vascular considerations and complications in cranial base surgery. Neurosurgery 35: 351–362; discussion 362–363
25. Rhoton AL Jr (2002) The cavernous sinus, the cavernous venous plexus, and the carotid collar. Neurosurgery 51: S375–S410
26. Rhoton AL Jr, Hardy DG, Chambers SM (1979) Microsurgical anatomy and dissection of the sphenoid bone, cavernous sinus and sellar region. Surg Neurol 12: 63–104
27. Sekhar LN, Burgess J, Akin O (1987) Anatomical study of the cavernous sinus emphasizing operative approaches and related vascular and neural reconstruction. Neurosurgery 21: 806–816
28. Sekhar LN, Linskey ME, Sen CN, Altschuler EM (1991) Surgical management of lesions within the cavernous sinus. Clin Neurosurg 37: 440–489
29. Sekhar LN, Patel SJ (1993) Permanent occlusion of the internal carotid artery during skull-base and vascular surgery: is it really safe? Am J Otol 14: 421–422
30. Sekhar LN, Pomeranz S, Sen CN (1991) Management of tumours involving the cavernous sinus. Acta Neurochir Suppl (Wien) 53: 101–112
31. Sekhar LN, Sen CN, Jho HD (1990) Saphenous vein graft bypass of the cavernous internal carotid artery. J Neurosurg 72: 35–41

32. Sen C, Sekhar LN (1992) Direct vein graft reconstruction of the cavernous, petrous, and upper cervical internal carotid artery: lessons learned from 30 cases. Neurosurgery 30: 732–742; discussion 742–743
33. Seoane E, Rhoton AL Jr, de Oliveira E (1998) Microsurgical anatomy of the dural collar (carotid collar) and rings around the clinoid segment of the internal carotid artery. Neurosurgery 42: 869–884; discussion 884–886
34. Spektor S, Piontek E, Umansky F (1997) Orbital venous drainage into the anterior cavernous sinus space: microanatomic relationships. Neurosurgery 40: 532–539; discussion 539–540
35. Spetzler RF, Fukushima T, Martin N, Zabramski JM (1990) Petrous carotid-to-intradural carotid saphenous vein graft for intracavernous giant aneurysm, tumor, and occlusive cerebrovascular disease. J Neurosurg 73: 496–501
36. Tokimura H, Atsuchi M, Tokimura Y, Sato E, Todoroki K, Asakura T, Fukushima T (1991) Direct surgical management of aneurysms in the cavernous sinus: a report of 5 cases. No Shinkei Geka 19: 15–20
37. Umansky F, Nathan H (1982) The lateral wall of the cavernous sinus. With special reference to the nerves related to it. J Neurosurg 56: 228–234
38. Umansky F, Valarezo A, Elidan J (1994) The superior wall of the cavernous sinus: a microanatomical study. J Neurosurg 81: 914–920
39. Yasuda A, Campero A, Martins C, Rhoton AL Jr, Oliveira E, Ribas GC (2005) Microsurgical anatomy and approaches to the cavernous sinus. Neurosurgery 56: 4–27; discussion 24–27
40. Yasuda A, Campero A, Martins C, Rhoton AL Jr, Ribas GC (2004) The medial wall of the cavernous sinus: microsurgical anatomy. Neurosurgery 55: 179-189; discussion 189–190

Giant pituitary tumors: surgical treatment of 265 cases

A. Goel, T. D. Nadkarni

Department of Neurosurgery, King Edward Memorial Hospital, Seth G.S. Medical College, Parel, Mumbai, India

Introduction

Giant and 'invasive' pituitary tumors are among the more complex challenges facing neurosurgeons today [11, 13, 14, 24]. Although histologically benign, some achieve massive size and invade diverse anatomical structures [25, 44]. Their invasiveness and size make surgery difficult, sometimes dangerous [1, 5, 13, 18, 23, 44, 47], and the results of radiation therapy are inconsistent [13, 27, 34, 46].

The diagnosis of pituitary tumors is usually achieved by correlating clinical features with imaging characteristics, rendering biopsy hardly relevant. Subtotal or partial resections are dangerous since bleeding frequently occurs within residual tumor and may result in death. Clinical outcomes following successful partial resection are generally unsatisfactory. Precise understanding of the anatomical extent of the tumor is crucial to the accurate planning of surgery and its execution. Successful radical resections, however, may lead to rapid recovery from symptoms and excellent long-term clinical outcomes. While recurrence rates following radical resection are reported to be low, they are significantly higher than with smaller pituitary adenomas. The following analysis is an update of our previous experience with 118 giant pituitary tumors [13].

Materials and methods

We treated 1,935 pituitary tumors between 1995 and April 2006, including 265 hormonally inactive lesions with maximum diameters greater than 3 cm (Fig. 1). All were treated surgically. *Patients with giant pituitary tumors operated upon previously for were not included here because their growth patterns were not consistent with patients not selected for surgery at that time.*

Results

Clinical and radiological features

Tumors were divided into four grades. *Grade I* pituitary tumors were confined to the sella and remained beneath an elevated diaphragma sellae and did not invade the cavernous sinus. There were 110 such tumors (Figs. 2 and 3). The diaphragma sellae was elevated to or beyond the level of corpus callosum in 11 patients. In three, tumor extended anteriorly, elevating tuberculum sellae and planum sphenoidale dura. *Grade II* pituitary tumors invaded the cavernous sinus. Eighty-nine patients harbored such lesions (Figs. 4 and 5), 61 invading the cavernous sinus unilaterally, and 28 bilaterally. *Grade III* pituitary tumors elevated the roof of the cavernous sinus as shown in the Figs. 6 and 7. There were 48 Grade III lesions, 37 elevating the cavernous sinus superior wall unilaterally (Fig. 6) and 11 bilaterally (Fig. 7). Twenty-five elevated both the diaphragma sellae and one cavernous sinus roof, while four elevated the diaphragma sellae and the cavernous sinus roof bilaterally, each such extensions resulting in distinct 'necks'

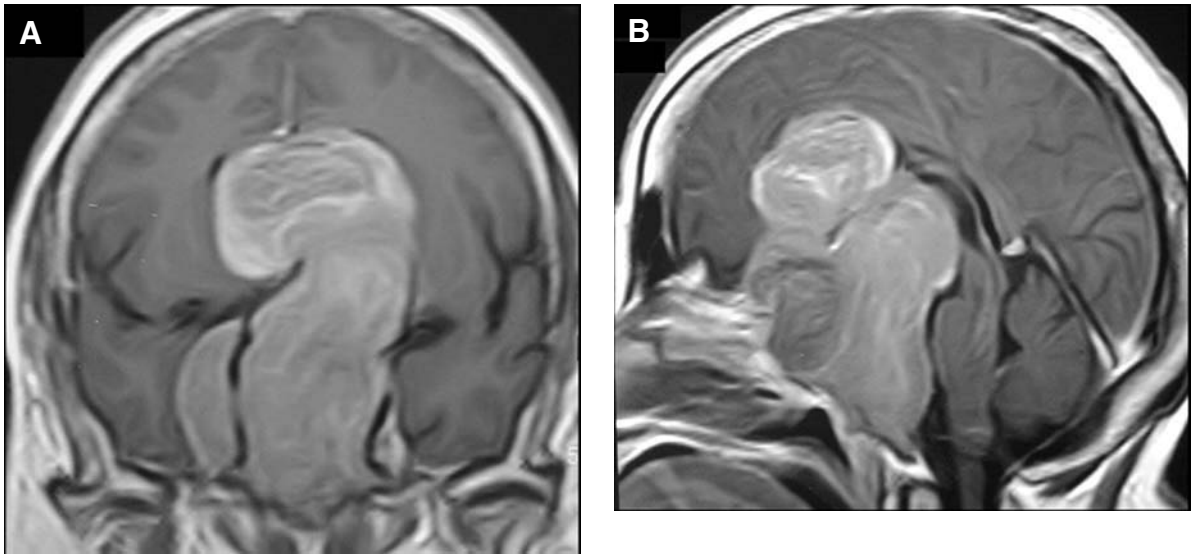

Fig. 1. A Post-contrast T1-weighted coronal MR image showing a giant pituitary adenoma with bilateral cavernous sinus invasion. **B** Contrast enhanced T1-weighted sagittal MR image showing massive vertical extension of the tumor beyond the corpus callosum

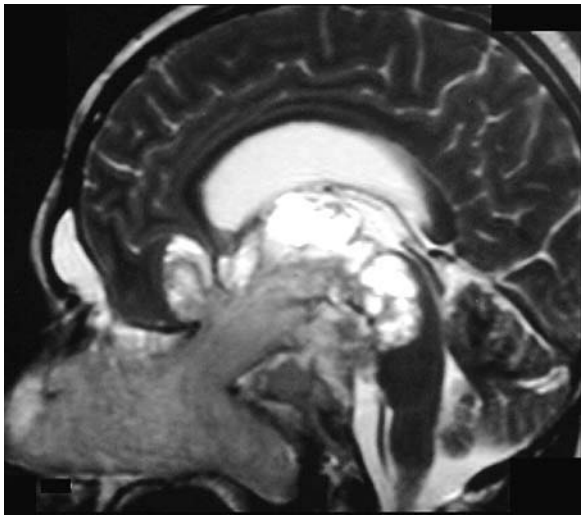

Fig. 2. T2-weighted sagittal image shows a giant pituitary adenoma to have breached the floor of the sella and spread into the nasopharynx. The superior pole contains many cysts

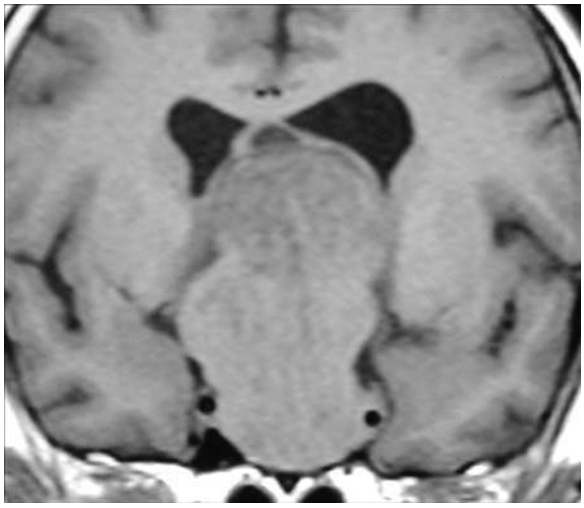

Fig. 3. T1-weighted MR image showing a Grade I giant pituitary tumor which does not invade into the cavernous sinus

of tumor. *Grade IV* pituitary tumors transgressed the diaphragma sella or the cavernous sinus roof, entering the subarachnoid space and encasing arteries of the circle of Willis. Eighteen patients had such lesions (Figs. 8 and 9).

Radiographic and surgical evidence of tumor transgressing sellar dura and extending into paranasal air sinuses was present in 15 cases, seven of which were Grade I lesions, six Grade II, and two Grade III.

Maximum tumor size ranged between 3 and 9 cm, with a mean of 4.5 cm. Each tumor was divided into thirds: the proximal one-third (nearest the sella), middle one-third, and distal one-third. Cysts of

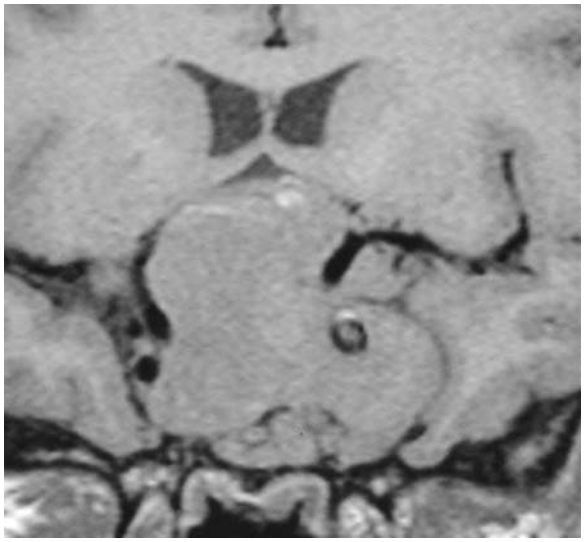

Fig. 4. T1-weighted MR image showing Grade II pituitary tumor with unilateral cavernous sinus invasion. The cavernous segment of the internal carotid artery is encased by the tumor, but its diameter is not compromised

varying sizes were present in 112 tumors, predominantly in the proximal one-third in 15, in the middle one-third in 39, and in the distal one-third in 58. Intratumoral hemorrhage (noted as well-defined liquefication or organized clot) was observed in 52 cases.

Clinical features

Presenting clinical features are listed in Table 1. The mean age was 43.6 years, with a range between 10 and 70 years. Tumors occurred in 144 males and 121 females. Visual deterioration was the primary presenting symptom in 260 patients, occurring bilaterally in 222, of which 9 were blind in one eye and 28 bilaterally. Field defects were predominantly bitemporal, and menstrual irregularities were present in 63 patients. Of 171 patients who had preoperative hormonal data, a hormonal deficiency was detected in 75, 50 of which were hypothyroid and 30 hypocortisolemic. Forty-six had mild to moderate hyperprolactinemia.

Surgery and outcome

Grade I pituitary tumors Transsphenoidal surgery was effective and relatively safe (Figs. 10 and 11). Surgical strategy was to expose and debulk the in-

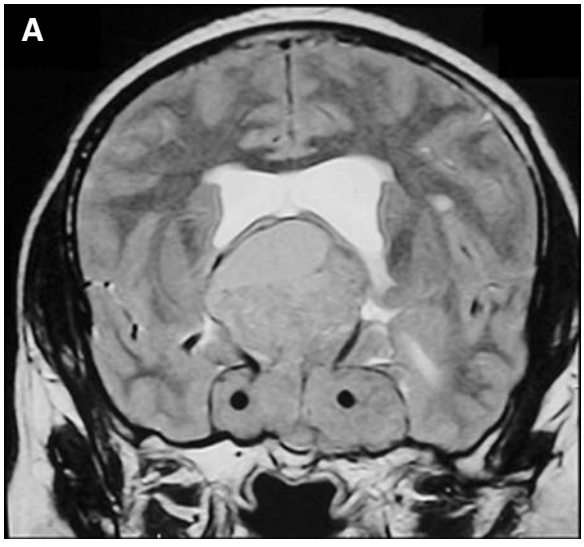

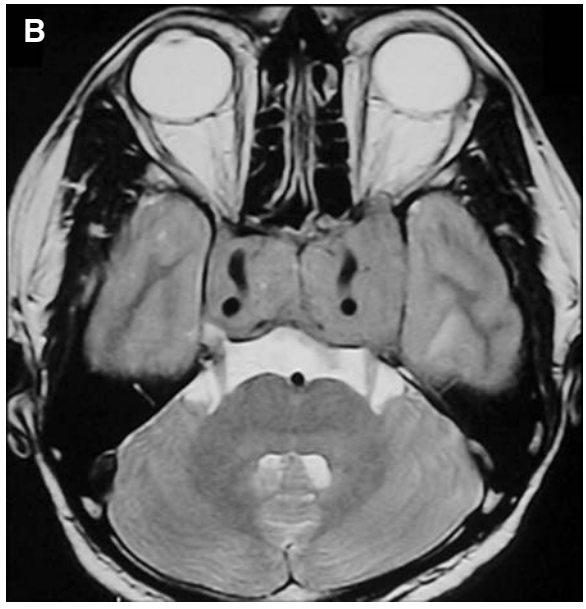

Fig. 5. **A** T2-weighted MR image showing Grade II pituitary tumor with bilateral cavernous sinus invasion. Both cavernous carotid arteries are encased without luminal compromise. **B** T2-weighted axial image shows the bilateral involvement of the cavernous sinus

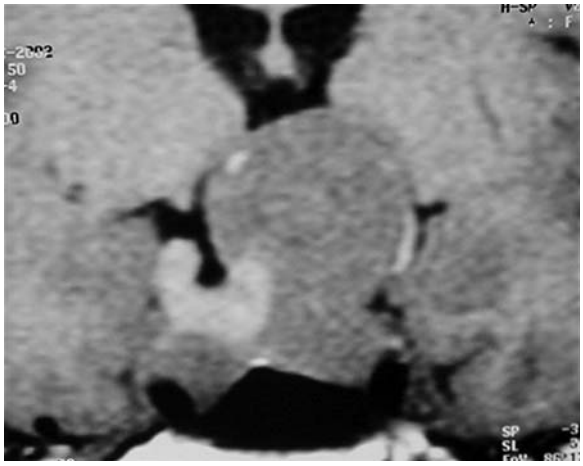

Fig. 6. T1-weighted coronal MR image shows a Grade III tumor which has elevated the roof of the cavernous sinus

trasellar component of the tumor, then to resect the suprasellar component as it progressively fell into view. Valsalva maneuvers facilitated the descent of the suprasellar component. When difficulty exposing the dome of the mass was encountered, additional tuberculum sella and planum sphenoidale bone was removed and dura was incised. The extent of tumor resection following initial transsphenoidal operations was confirmed by post-operative imaging. Radical gross tumor excision was achieved in 79 cases, and relatively small amounts of tumor were left behind in 31. After surgery, 78 experienced improved vision, with two patients worsening. Six died, and six developed CSF leaks which stopped following lumbar punctures for CSF drainage. Two patients developed diabetes insipidus after surgery, either transient or permanent. Radiotherapy was avoided with Grade I tumors. Patients with known residual tumor who were asymptomatic were observed clinically and radiologically. Residual tumor increased in size in six, two of whom were treated with radiation and four required additional surgery.

Grade II pituitary tumors Tumor beneath the elevated diaphragma sellae was resected easily and safely by the transsphenoidal approach. Later in the series attempts were made to resect tumor from the cavernous sinus by rerouting the angle of vision through the microscope, but post-operative imaging generally revealed residual cavernous sinus tumor in such patients. Tumor was totally removed from the cavernous sinus in eight cases. Fifty patients' vision improved after surgery, and one died. One patient was hemiplegic after surgery but experienced progressive but incomplete recovery after 19 months' follow-up. The patient who did not survive died at home 2 months after surgery, and further details are not available. Radiation therapy was given when relatively large amounts of tumor remained in the cavernous sinus and/or visual symptoms or symptoms of cranial nerve compression were present. Of Grade II patients, 28 received post-operative radiation therapy, of which 13 experienced tumor mass

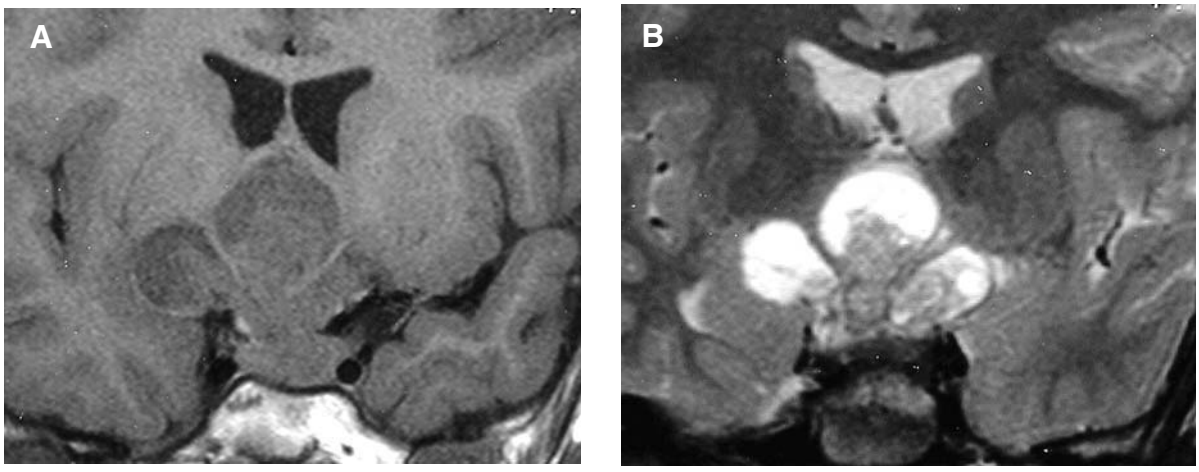

Fig. 7. **A** Coronal MR image demonstrates a Grade III giant pituitary adenoma with bilateral cavernous sinus invasion. The tumor elevates roofs of both cavernous sinuses and diaphragma sella. **B** T2-weighted coronal image shows the trifoliate tumor

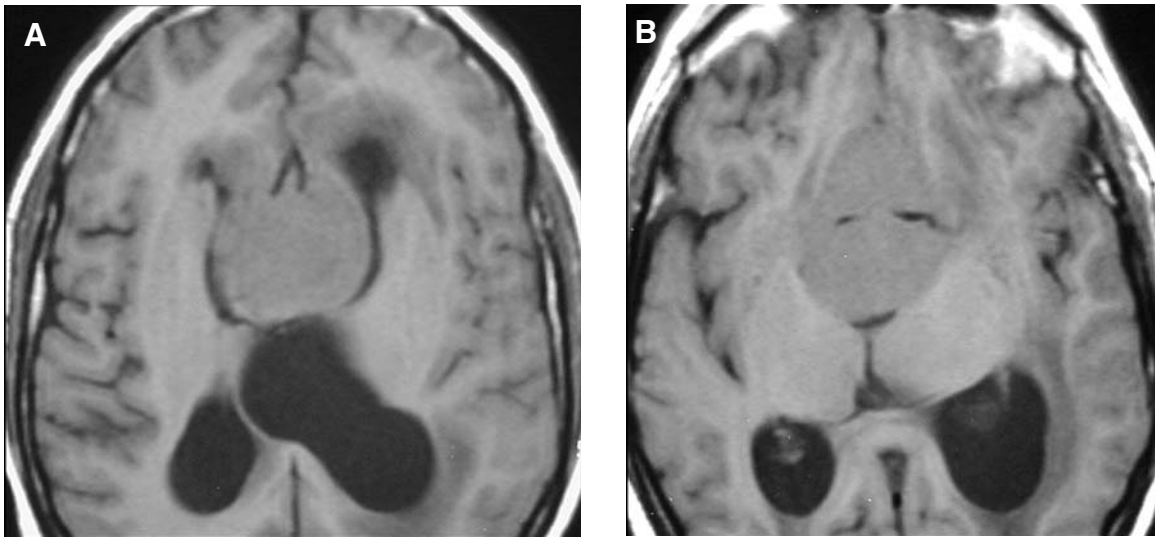

Fig. 8. Grade IV giant pituitary adenoma. **A** Axial T1-weighted MR image shows the encasement of the anterior communicating artery complex within the superior pole of the tumor. **B** Coronal T1-weighted image and **C** Coronal T2-weighted image show both anterior cerebral arteries encased by the giant adenoma

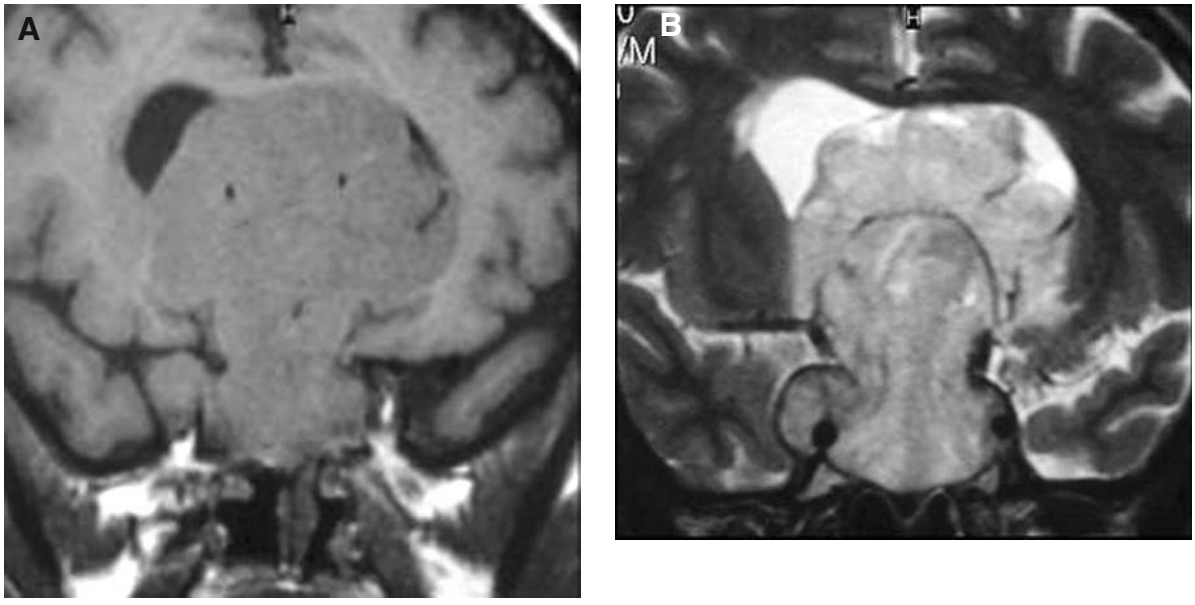

Fig. 9. A, B Post-contrast axial images show Grade IV giant pituitary adenoma encasing the anterior communicating artery complex

reduction and 15 had no change. Vision and diplopia improved in two patients after radiotherapy.

Grade III pituitary tumors Transsphenoidal operations were effective. The angles of approach dictated by the typically narrow necks of tumor expanding the cavernous sinus roof made resection of such tumor extensions difficult. Complete or radical resection in such instances was achieved in three cases (Figs. 12–16). If the mass of residual

Table 1. Clinical presentation

Clinical features	Grade I (110)	Grade II (89)	Grade III (48)	Grade IV (18)
Headaches	92	69	40	18
Diminution of vision	110	85	47	18
Hypothalamic changes	17	19	4	18
Hormonal deficiencies	33	19	23	–
Hemiparesis	–	1	3	–
Epistaxis	–	–	3	–
Seizures	–	–	–	1
Cranial nerves involved				
Third nerve	3	8	4	–
Sixth nerve	3	8	4	–
Fifth nerve	–	9	4	–

tumor was either large or symptomatic, as in six cases, it was explored transcranially. Two were found to have the third cranial nerve displaced medially by the elevated cavernous sinus roof. Asymptomatic patients with significant residual tumor were treated with radiation. Post-operative tumor irradiation was carried out in 34 cases, resulting in radiologic evidence of tumor reduction in 11, with no change in the remainder. Four residual tumors not large enough to be treated with radiation initially increased in size with further follow-up, and ultimately required radiation therapy. One of these four had additional surgery.

Grade IV pituitary tumors Of two patients undergoing an attempt at radical resection, both died soon after surgery. After this experience, the remaining Grade IV tumors were only biopsied and treated with radiation therapy. Four of them died, and three were lost to follow-up. Additional tumor growth occurred in two, and one required multiple readmissions for the management of uncontrolled generalized convulsions.

Follow-up for the entire series ranged from 3 months to 11 years (average 36 months). The outcomes with respect to vision 3 months after surgery are presented in Table 2.

Histological examination confirmed all lesions to be pituitary adenomas, and no patient manifested evidence of malignancy.

Discussion

Pituitary tumors have been classified with respect to size, radiographic appearance, cytogenesis, staining properties, and endocrine function. Hardy classified them with respect to biological behavior [16]. Large pituitary tumors have been described as invasive adenomas [30], malignant adenomas [3] and carcinomas [7], but no consensus terminology currently exists [9]. Some authors refer to pituitary tumors as "giant" if they are in excess of 40 mm in size or extend within 6 mm of the foramen of Monro, irrespective of their invasiveness [8]. Jefferson reported that giant pituitary tumors occur in

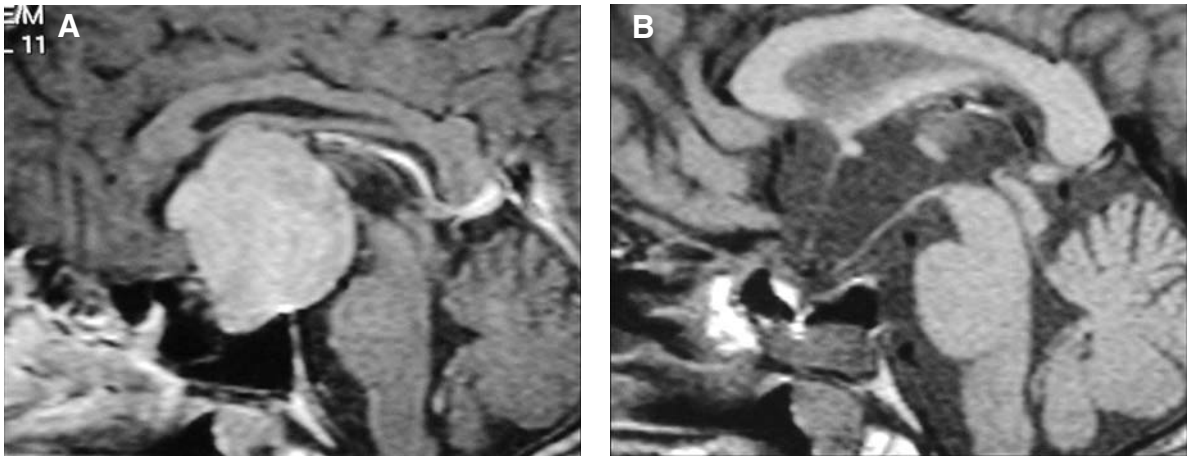

Fig. 10. A, B T1-weighted sagittal and T2-weighted coronal MR images show a Grade I giant pituitary adenoma. **C, D** Post-operative sagittal and coronal T1-weighted MR images show complete excision of the mass

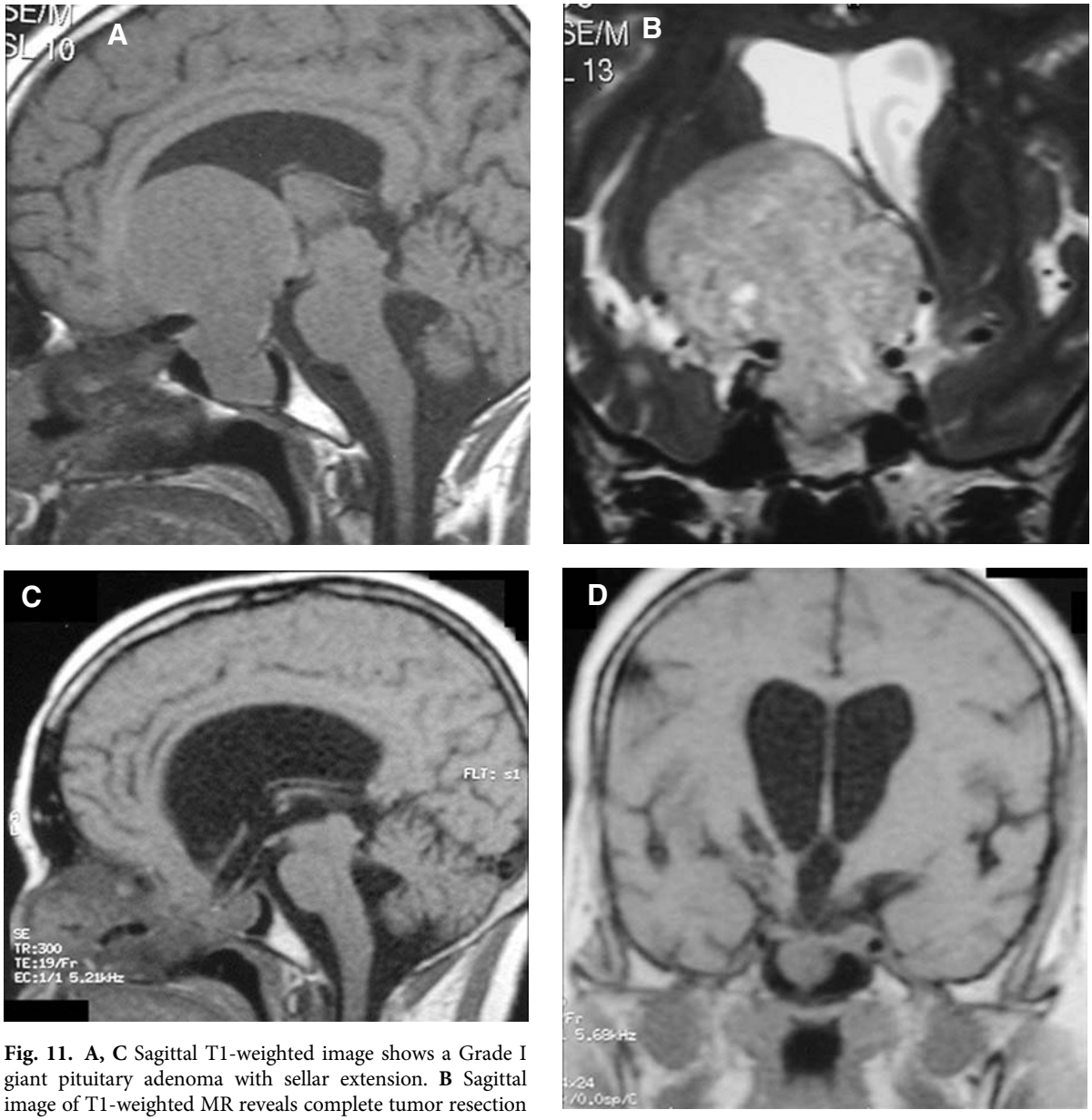

Fig. 11. A, C Sagittal T1-weighted image shows a Grade I giant pituitary adenoma with sellar extension. **B** Sagittal image of T1-weighted MR reveals complete tumor resection (also see **D**)

approximately 6% of all cases [19]. The histological nature of giant pituitary tumors apparently has no correlation with gross features, and most are composed of benign cells [22, 26, 28, 39, 44, 49].

Here we consider pituitary tumors with maximum diameters of at least 30 mm as 'giant' lesions [8, 13, 14, 24, 42–44]. Such tumors account for 13.7 % of the total number of pituitary tumors we have seen during the same period. The relatively large percentage of giant pituitary tumors in our series may be related to our patients' failure to seek medical attention soon after the onset of symptoms because of the high illiteracy rates and poverty in our country, and our citizens' generally poor access to specialized medical care. With all varieties of giant pituitary tumors, the extent of tumor resection increases and clinical outcome improves with increasing experience.

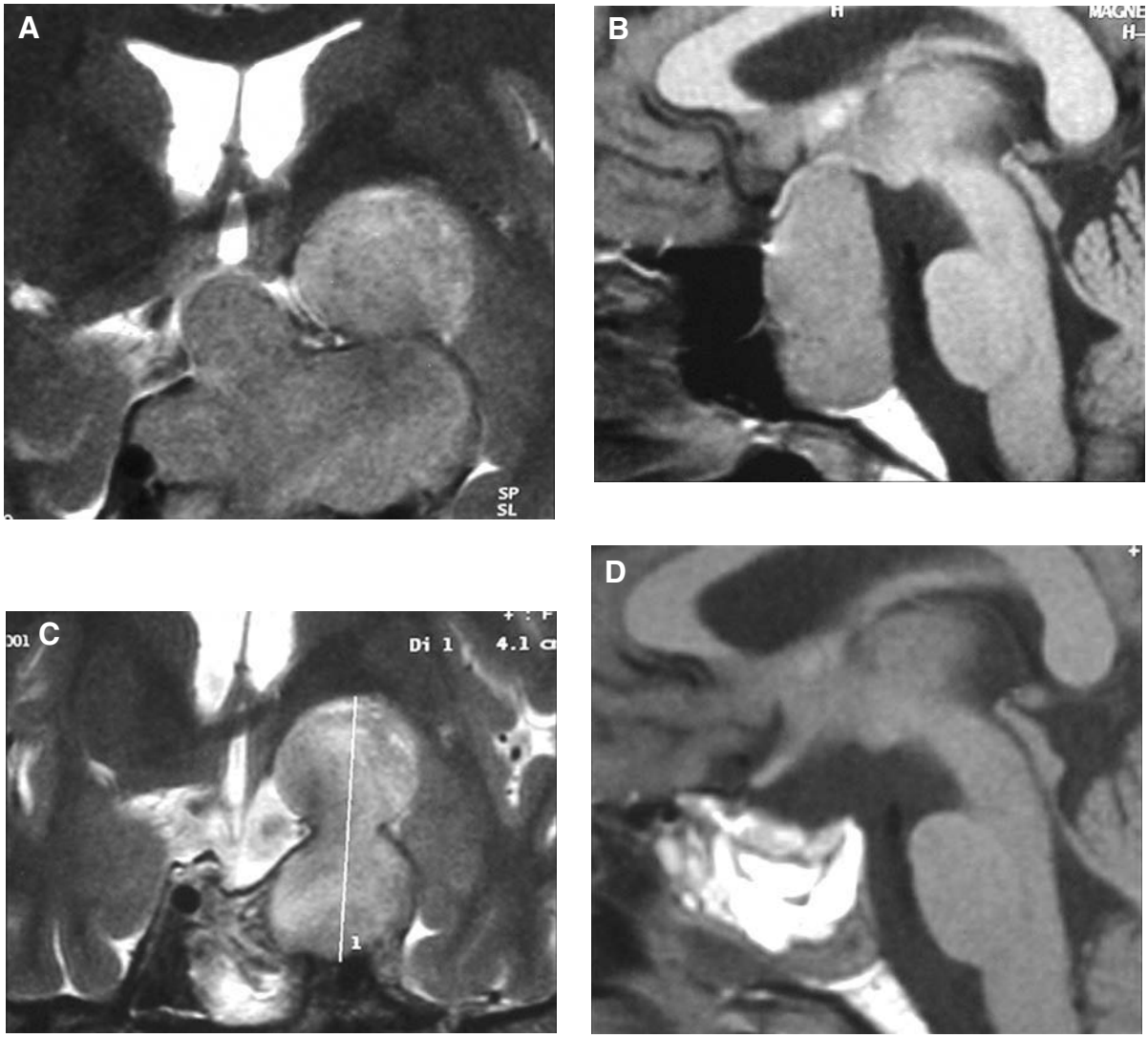

Fig. 12. **A** Coronal T2-weighted image shows a Grade III giant pituitary adenoma. **B** Sagittal T1-weighted image demonstrates the midline portion of the Grade III giant adenoma elevating the diaphragma sella. **C** Post-operative coronal T2-weighted image reveals a tumor remnant in the cavernous sinus. **D** Post-operative sagittal T1-weighted shows excision of the midline tumor. Fat is noted packed in the sphenoid sinus

Giant non-functioning pituitary tumors are frequently soft and slow growing, hence their massive size with relatively innocuous presenting symptoms. The growth of pituitary tumors is typically limited to the sella, which becomes enlarged and ballooned [24, 29, 33]. The diaphragma sellae is elevated with further growth. This series includes 110 Grade I tumors, those confined within sellar dura, beneath elevated diaphragma sellae, the lateral extension of which is limited by intact medial walls of the cavernous sinus. In Grade I tumors the diaphragma sellae has been noted to be quite thin in places, frequently resulting in the formation of large or small daughter balloons. Rounded superior tumor walls suggest that the diaphragma sellae is intact. The fact that an intact diaphragma sellae provides an effective barrier to extension allows Grade I tumors to be resected radically through the limited exposures afforded by the transsphenoidal route [13, 15, 17, 33, 36, 38, 48]. Gross tumor resection was achieved 72% in our

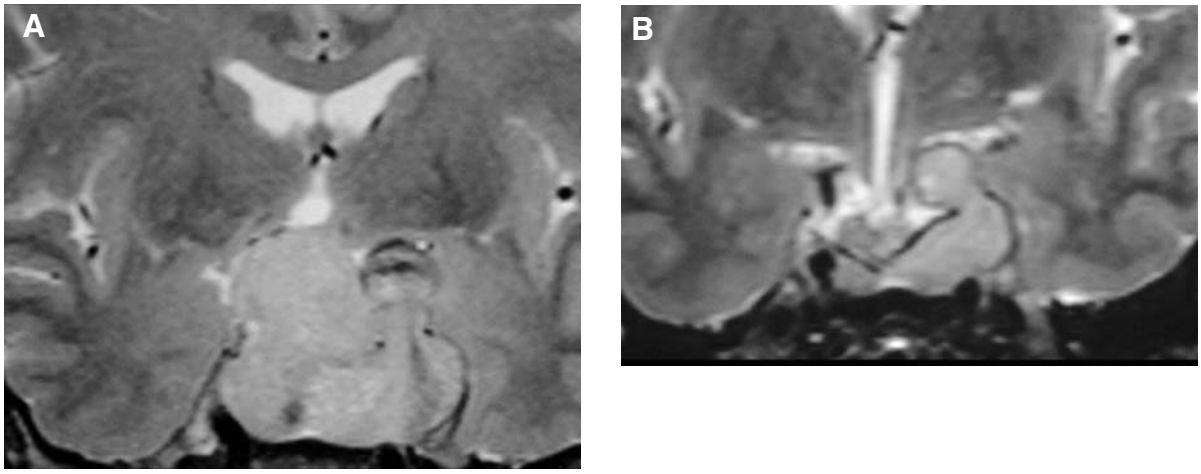

Fig. 13. A Coronal T2-weighted image shows a Grade III giant pituitary adenoma. Elevation of the diaphragma sella and cavernous sinus roof are noted. **B** Post-operative coronal MR image reveals residual tumor within the cavernous sinus, beneath its roof

series, with 71% experiencing symptomatic improvement after surgery.

Grade II giant pituitary tumors cross sellar dura and the medial wall of the cavernous sinus [1, 5, 13, 35]. Cavernous sinus invasion is confirmed by MR imaging if tumor is apparent on both sides of the carotid artery. Carotid artery encasement as a true indication of cavernous sinus invasion has also been reported [10, 20, 41, 43]. When the artery is displaced, the entire cavernous sinus (especially its medial wall) is usually displaced laterally. Although bulging laterally, the lateral dural wall of the cavernous sinus is not observed to be transgressed by Grade II lesions, suggesting that this structure provides considerable resistance [10]. Even when intracavernous tumor encases the internal carotid artery, its vessel wall is seldom compromised. Stenosis of the cavernous carotid segment was not observed in our series. Notwithstanding invasion of the cavernous sinus, cranial nerve symptoms are relatively rare. Most patients who do experience symptoms of cranial nerve involvement have an acute clinical course. The fact that cavernous sinus invasion was observed even in some small or moderately large pituitary tumors suggests that the medial wall of the cavernous sinus may not actually be dura [38]. This observation could lend support to authors who have considered the cavernous sinus an extradural structure. However, neither the cases described here nor those presented previously [11, 13] actually elevated the entire cavernous sinus [1, 5] or elevated middle fossa dura, or extended beyond the dura mater. This suggests that the medial wall of the cavernous sinus allows tumor to enter the 'compartment' of the cavernous sinus but not into the 'extradural' space.

Completely resecting tumor from the cavernous sinus was possible in 11% cases. Removing tumor from the cavernous sinus requires a wide exposure of the entire cavernous sinus and places associated cranial nerves at risk. A medial route, as an extension of the transsphenoidal approach, seems most appropriate for resecting elements of pituitary tumors from the cavernous sinus. However, extensions lateral to the carotid artery are difficult to resect since they necessitate displacing the internal carotid artery. Our anatomical and surgical experience reveals that manipulating the anterior and medial loop of the artery is difficult since this segment of the artery is resistant to mobilization, particularly without proximal and distal control. It is therefore a formidable task. Mobilizating the artery also subjects the sixth cranial nerve to possible injury. For patients with hormonally 'active' tumors, where resection of intracavernous components is necessary to cure hormonal dysfunction, we attempt radical resections by the transsphenoidal route. In selected patients we have employed the lateral extradural approach as described by Dolenc [4], but such cases are not discussed here.

Extension of tumor into the sphenoid or other paranasal air sinuses as a result of transgressing sellar dura occurred infrequently, despite the massive

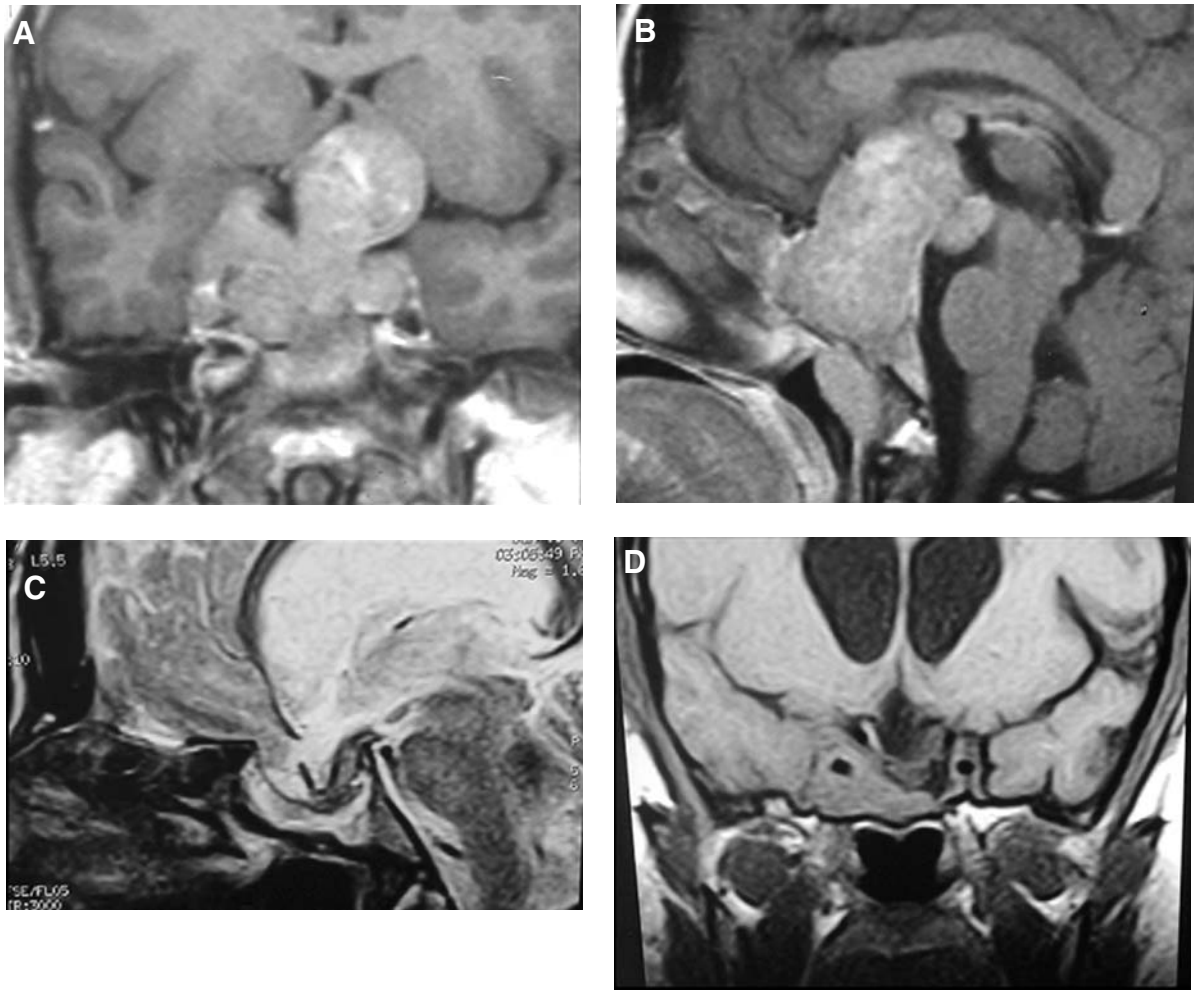

Fig. 14. A, B Post-contrast MR image shows a Grade III giant pituitary adenoma. **C, D** Post-contrast post-operative image confirms partial resection, with residual tumor in the cavernous sinus

tumors in this series. Generally, sellar dura remained intact, although sometimes it did balloon widely. A thin rim of sellar bone was also preserved in most cases.

'Weakness' of the cavernous sinus roof and its elevation by intracavernous masses has been described previously [21]. A significant number of the giant pituitary tumors reported here invaded the cavernous sinus and elevated its roof. Such lesions were labeled Grade III pituitary tumors. Reviewing our previous series [11, 13], and analyzing radiographic information from other reported cases, indicates that a significant number of giant pituitary tumors labeled 'intracranial subarachnoid extensions' may actually be Grade III tumors. In every case the dural roof of the cavernous sinus covered the dome of the mass. In most, where the roof of the cavernous sinus was bloated upward, the extent of roof involvement is small, resulting in localized ballooning. This suggests that the cavernous sinus roof is thinner in some places than others, resulting in foci which are less resistant to pressure [21]. The elasticity of the cavernous sinus roof seems similar to that of the diaphragma sellae, although it is significantly thinner. We employed the transsphenoidal approach to resect the majority of these tumors. An attempt was made to remove that portion of tumors extending into the cavernous sinus and along its roof, but radical resections were possible in only three cases. This is because exposure of the

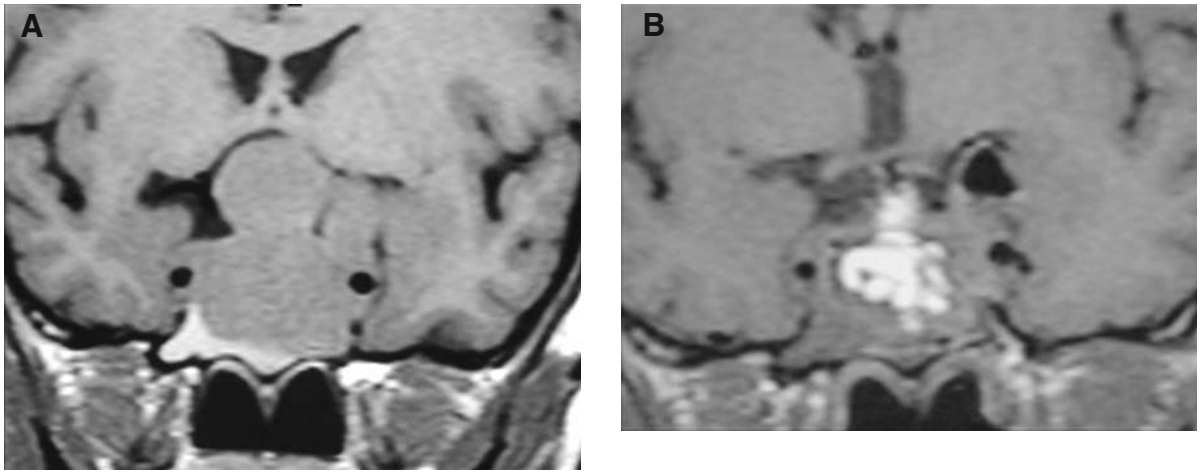

Fig. 15. A Coronal T2-weighted image shows a Grade III giant pituitary adenoma. **B** Immediate post-operative MR scan confirms tumor resection with air in the roof of cavernous sinus

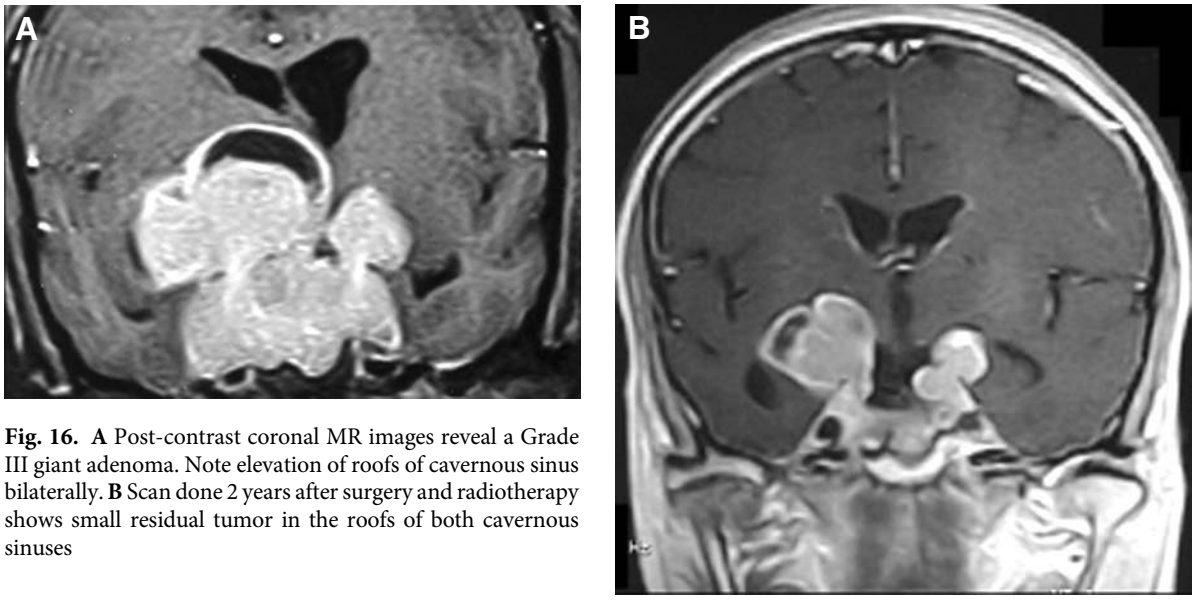

Fig. 16. A Post-contrast coronal MR images reveal a Grade III giant adenoma. Note elevation of roofs of cavernous sinus bilaterally. **B** Scan done 2 years after surgery and radiotherapy shows small residual tumor in the roofs of both cavernous sinuses

Table 2. Visual outcome 3 months after surgery

Visual status	Grade I	Grade II	Grade III	Grade IV
Improvement	78	50	17	–
Same	24	16	12	7
Deteriorated	2	12	9	9

tumor mass was limited by the narrow neck of dura at the level of the cavernous sinus roof. Transcranial surgery was employed in patients where the intracranial extension was large or symptomatic.

Generally either diaphragma sellae or the dural roof of the cavernous sinus continued to cover intracranial extensions of giant pituitary tumors. The rarity of cerebral parenchymal edema associated with intracranial spread supports physiological encapsulation of these intracranial extensions. Giant pituitary tumors transgressing the diaphragma sellae and encasing arteries of the circle of Willis and perforating vessels were considered to be Grade IV lesions. The precise site of dural dehiscence could not be confirmed. Such invasive-

ness is similar to that of epidermoid tumors, spreading into available spaces, surrounding vessels and cranial nerves without actually invading them, rarely compromising the lumens of arteries and displacing them only moderately. Radical resection was attempted in two of such cases but was complete in neither and both patients died postoperatively with cerebral hemorrhages. Both operations were quite difficult. Vascular dissection likely led to the compromise of perforating vessels. After this experience, surgery for Grade IV lesions was limited to biopsy.

There was no histological evidence of malignancy in any case, or significant histological differences among the different grades of these tumors. Immunohistochemical studies were not carried out. Yokoyama et al. reported no statistical difference between tumors encasing and those not encasing the cavernous carotid artery with respect to Ki-6, cathepsin B, and matrix metalloproteinase-9 immunostaining [51]. Others have found that pituitary adenomas invading the cavernous sinus expressed high Ki-67 labeling and DNA indices, plus a high percentage of cells in S-phase [23, 31, 32, 45].

There was evidence of recent or old hemorrhage within 20% of giant tumors and single or multiple cysts in 42%. Cysts were more frequent in the one-third of the tumor mass most distant from the sella, suggesting that a more tenuous vascular supply and necrosis may be responsible for cystic degeneration. The majority of frontal, temporal, and retrosellar extensions contained cysts, suggesting that necrosis likely resulted from tumor constriction at the roof of the cavernous sinus.

Reports of poor clinical courses and surgical results associated with treatment of giant pituitary adenomas are well known [11, 12, 17, 24, 33, 37]. Most lesions in this series were approached transsphenoidally [13], quite different from our previous report where the transcranial route was favored [11]. Understanding that these tumors are covered by dura, plus our increased experience with the transsphenoidal route led to this change. Currently the literature favors either the transcranial method alone for giant pituitary tumors or in combination with the transsphenoidal approach [2, 6, 11, 13, 17, 33, 40, 48]. High surgical mortality has been attributed to a breach of the subarachnoid space and ischemia of the hypothalamus, brainstem, or cerebral hemisphere secondary to small and large vessel compromise [12, 17, 24]. Subtotal resections may lead to infarction and edema of residual tumor from vessel traction, a phenomenon we previously reported as 'post-operative pituitary apoplexy' [12]. Such tumor swelling may result in compression of adjacent vital neural structures or acute obstructive hydrocephalus.

In this series, indications for radiation therapy varied among the four grades of giant pituitary tumors [8, 13, 50]. Because of the ease of resecting Grade I tumors, radiotherapy was generally avoided, and re-exploration was preferred when large or symptomatic tumors remained or recurred. Small and asymptomatic residual tumors were observed clinically and radiographically. Radiotherapy has been proven to be effective in the long-term control of non-functioning pituitary adenomas. More precise stereotactic techniques carry the potential of minimizing radiotherapy-induced morbidity [8, 13, 50]. Among patients with Grade II or Grade III tumors, radiotherapy was employed for residual cavernous sinus tumors of significant size or if associated with symptoms. Otherwise, re-exploring the cavernous sinus was avoided. Radiation was recommended for Grade IV tumors. Overall, 29% of patients received radiation. Radiation therapy was effective in inhibiting tumor growth in the large majority of patients undergoing such treatment. Currently we strongly prefer radiation treatment for tumors larger than 5 cm, those associated with hemorrhage and/or multiple cysts, and where symptomatic residual tumor exists following surgery.

The growth rate, growth potential, pattern of clinical course, and management issues with respect to giant pituitary adenomas are not yet clear and hinge on the results of larger series with longer follow-up periods. Aided by understanding anatomical subtleties, aggressive surgical resection may lead to satisfactory clinical outcomes. Giant pituitary tumors are usually covered by dura and extend along well-defined anatomical pathways.

References

1. Ahmadi J, North CM, Segall HD, Zee CS, Weiss MH (1985) Cavernous sinus invasion by pituitary adenomas. AJNR 6: 893–898
2. Alleyne CH Jr, Barrow DL, Oyesiku NM (2002) Combined transsphenoidal and pterional craniotomy

approach to giant pituitary tumors. Surg Neurol 50: 380–390
3. Bailey OT, Cutler EC (1940) Malignant adenomas of the chromophobe cells of the pituitary body. Arch Pathol 29: 368–399
4. Dolenc VV (1997) Transcranial epidural approach to pituitary tumors extending beyond the sella. Neurosurgery 41: 542–550
5. Fahlbusch R, Buchfeler M (1988) Transsphenoidal surgery of parasellar pituitary adenomas. Acta Neurochir (Wien) 92: 93–99
6. Fahlbusch R, Ganslandt O, Buchfelder M, Schott W, Nimsky C (2001) Intraoperative magnetic resonance imaging during transsphenoidal surgery. J Neurosurg 95: 381–390
7. Feiring EH, Davidoff LM, Zimmerman HM (1953) Pituitary carcinoma of the pituitary. Neuropathol Exp Neurol 12: 205–223
8. Fisher BJ, Gasper LE, Noone B (1993) Giant pituitary adenomas: role of radiotherapy. Int J Radiat Oncol Biol Phys 15: 677–681
9. Garibi J, Pomposo I, Villar G, Gaztambide S (2002) Giant pituitary adenomas: clinical characteristics and surgical results. Br J Neurosurg 16: 133–139
10. Goel A (1998) Meningeal architecture of the cavernous sinus: clinical and surgical implications. Neurosurgery 42: 430–431
11. Goel A, Nadkarni T (1996) Surgical management of giant pituitary tumors – a review of 30 cases. Acta Neurochir (Wien) 138: 1042–1049
12. Goel A, Deogaonkar M, Desai K (1995) Fatal postoperative pituitary apoplexy: its case and management. Br J Neurosurg 9: 37–40
13. Goel A, Nadkarni T, Desai K, Muzumdar D, Phalke U, Sharma P (2004) giant pituitary tumors: a study based on surgical treatment of 118 cases. Surg Neurol 61: 436–446
14. Grote E (1982) Characteristics of giant pituitary adenomas. Acta Neurochir (Wien) 60: 141–153
15. Hardy J (1978) Transsphenoidal hypophysectomy. Neurosurgical techniques. J Neurosurg 48: 13–22
16. Hardy J (1979) Transsphenoidal microsurgical treatment of pituitary tumors. In: Linfoot JA (ed) Recent advances in the diagnosis and treatment of pituitary tumors. Raven, New York, pp 375–388
17. Hashimoto N, Handa H, Yamashita J, Yamagami T (1986) Long term follow up of large or invasive pituitary adenomas. Surg Neurol 25: 49–54
18. Hashimoto N, Kikuchi H (1990) Transsphenoidal approach to infrasellar tumors involving the cavernous sinus. J Neurosurg 73: 513–517
19. Jefferson G (1940) Extrasellar extensions of pituitary adenomas. Proc R Soc Med 33: 433–458
20. Kaufman B, Kaufman BA, Arafah BUM, Rossemann U, Selman WR (1987) Large pituitary gland adenomas evaluated with magnetic resonance imaging. Neurosurgery 21: 540–546
21. Kawase T, van Loveren H, Keller JT, Tew JM (1996) Meningeal architecture of the cavernous sinus: clinical and surgical implications. Neurosurgery 39: 527–536
22. Kernohan JW, Sayre GP (1956) Tumors of the pituitary gland and infundibulum. In: Atlas of tumor pathology. Sect X., Fasc 36. Armed Forces Institute of Pathology, Washington, DC, 81
23. Knosp E, Kitz K, Steiner E, Matula C (1991) Pituitary adenomas with parasellar invasion. Acta Neurochir (Wien) 53: 65–71
24. Krisht AF (1999) Giant invasive pituitary adenomas. In: Krisht AF, Tingdall GT (eds) Pituitary disorders: comprehensive management. Lippincott, Baltimore, pp 287–294
25. Krisht AF (1999) Giant invasive pituitary adenomas: management plan. Contemp Neurosurg 21: 1–6
26. Landolt AM, Wilson CB (1982) Tumors of the sella and parasellar area in adults. In: Youmans JR (ed) Neurological surgery. Saunders, Philadelphia, pp 3107–3162
27. Lawson LJ (1958) Intranasal chromophobe adenocarcinoma. Report of a case. Arch Otolaryngol (Chicago) 68: 704–709
28. Lundberg PO, Drettner B, Hemmingsson A, Stenkvist B, Wide L (1977) The invasive pituitary adenoma. A prolactin – producing tumour. Arch Neurol 34: 742–749
29. Majos C, Coll S, Aguilera C, Acebes JJ, Pons LC (1998) Imaging of giant pituitary adenomas. Neuroradiology 40: 651–655
30. Martins AN, Hayes GJ, Kempe LG (1965) Invasive pituitary adenomas. J Neurosurg 22: 268–276
31. Mastronardi L, Guiducci A, Buttari FM, Cristallini EG, Puzilli F, Maira G (2001) Relationships among DNA Index, S-Phase, and invasive behavior in anterior pituitary adenomas: a cytometric study of 61 cases with Feulgen-positive DNA analysis. Surg Neurol 56: 27–32
32. Mastronardi L, Guiducci A, Spera C, Puzilli F, Liberati F, Maira G (1999) Ki-67 labelling index and invasiveness among anterior pituitary adenomas: analysis of 103 cases using the MIB-1 monoclonal antibody. J Clin Pathol 52: 107–111
33. Mohr G, Hardy J, Comtois R, Beauregard H (1990) Surgical management of giant pituitary adenomas. Can J Neurol Sci 17: 62–66
34. Newton TH, Burhenne HJ, Palubinskas AJ (1962) Primary carcinoma of the pituitary. Am J Roentgenol 87: 110–120
35. Nichols DA, Laws ER, Houser OW, Abboud CF (1988) Comparison of MRI and computed tomography in the preoperative evaluation of pituitary adenomas. Neurosurgry 22: 380–385
36. Oruckaptan HH, Senmevsim O, Ozcan OE, Ozgen T (2000) Pituitary adenomas: results of 684 surgically treated patients and review of the literature. Surg Neurol 53: 211–219
37. Pia HW, Grote E, Hilderbrandt G (1985) Giant pituitary adenomas. Neurosurg Rev 8: 207–220
38. Post KD, Biller BJ, Adelman LS, Molitch ME, Wolpert SM, Reichlin S (1979) Selective transsphenoidal adeno-

mectomy in women with galactorrhea–amenorrhea. J Am Med Assoc 242: 158–162
39. Russel DS, Rubenstein LJ (1977) Tumors of adenohypophysis. In: Russel DS, Rubenstein LJ (eds) Pathology of tumors of the nervous system, 4th ed. Williams and Wilkins, Baltimore, pp 312–323
40. Sandeman D, Moufid A (1998) Interactive image-guide pituitary surgery. Neurochirurgie 44: 331–338
41. Scotti G, Yu CY, Dillon WP, Norman D, Newton TH, DeGroot J, Wilson CB (1988) MR imaging of cavernous sinus involvement by pituitary adenomas. Am J Neuroradiol 9: 657–664
42. Shrivastava RK, Arginteanu MS, King WA, Post KD (2002) Giant prolactinomas: clinical management and long-term follow up. J Neurosurg 97: 299–306
43. Steiner E, Imhof H, Knosp E (1989) Gd- DTPA enhanced high resolution MR imaging of pituitary adenomas. Radiographics 4: 587–598
44. Symon L, Jakubowski J, Kendall B (1979) Surgical treatment of giant pituitary adenomas. J Neurol Neurosurg Psychiatry 42: 973–982
45. Thapar K, Kovacs K, Scheithauer BW, Stefaneanu L, Horvarth E, Pernicone PJ, Murray D, Laws ER Jr (1996) Proliferative activity and invasiveness among pituitary adenomas and carcinomas: an analysis using MIB-1 antibody. Neurosurgery 38: 99–107
46. Terry RD, Hayams VJ, Davidoff LM (1959) Combine non-metastasizing fibrosarcoma and chromophobe tumor of the pituitary. Cancer 12: 791–798
47. Wilson CB (1979) Neurosurgical management of large and invasive pituitary tumors. In: Tindall GT, Collins WF (eds) Clinical management of pituitary disorders, Raven, New York, pp 335–342
48. Wilson CB (1984) A decade of pituitary microsurgery. The Herbert Olivecrona lecture. J Neurosurg 61: 814–833
49. Wise BL, Brown HA, Naffziger HC, Boldrey EB (1955) Pituitary adenomas, carcinomas, and craniopharyngiomas. Surg Gynec Obstet 101: 185–193
50. Yildiz F, Zorlu F, Erbas T, Atahan L (1999) Radiotherapy in the management of giant pituitary adenomas. Radiother Oncol 52: 233–237
51. Yokoyama S, Hirano H, Moroki K, Goto M, Imamura S, Kuratsu JI (2001) Are nonfunctioning pituitary adenomas extending into the cavernous sinus aggressive and/or invasive? Neurosurgery 49: 857–863

Chapter 6. Radiosurgery in treatment of central skull base tumors

The role of Gamma Knife surgery in the management of non-meningeal tumors of the cavernous sinus

Ch. Lindquist

Gamma Knife Centre, The Cromwell Hospital, London, UK

Introduction

Metastases, pituitary adenomas, and a number of uncommon neoplasms may be found in the cavernous sinus. The majority of them invades the sinus from outside origins and are large at the time of diagnosis. Surgery is therefore usually the first treatment of choice. It has been suggested that non-meningeal benign tumors are more likely to be totally removed from the cavernous sinus with low morbidity than meningiomas [10, 33]. A number of factors determine the morbidity of surgery in the cavernous sinus, including the nature of the pathology, the aggressiveness of the surgeon, and the surgical approach selected. Despite the contributions of Vinko Dolenc in improving surgical techniques for cavernous sinus operations, a recent series of 42 patients confirms the achievement of radical removal in only 50% of tumors from the cavernous sinus. The degree of surgical resection is in large part determined by the pathology of the lesion, with pituitary adenomas and chordomas being the most difficult to resect radically even though such resections are achievable with acceptable morbidity [33]. Another recent report concludes that epidural or epidural–transdural approaches to skull base tumors offer satisfactory outcomes [51]. What is acceptable clearly relates to the preoperative condition of the patient and the impact of the procedure on his or her future health and activities of daily living. Even a severe disturbance of oculomotor function may be an acceptable price to pay for radical removal of a skull base chordoma or hemangiopericytoma, while complete facial anaesthesia may not be an acceptable outcome for resecting a trigeminal schwannoma. Some of the complications listed in surgical series indicate that less radical resection followed by adjuvant therapy may be preferred. The following is to encourage surgeons to consider Gamma Knife surgery an adjuvant to, and in some cases an alternative to, open surgery for selected tumors invading the cavernous sinus.

Radiotherapy has been advocated to prevent recurrences of malignant lesions and to treat benign tumor remnants. Conventional fractionated radiotherapy and, more recently, stereotactic radiotherapy are often used as adjunctive forms of treatment. In some centers, protons and other heavy particle beams are available as radiotherapy and radiosurgery. Pituitary tumors, chordomas, and chondrosarcomas have been treated successfully with heavy particles. Radiotherapy may prolong recurrence-free survivals and infrequently results in a significant decrease in tumor volume. Since it is associated with fewer side effects and carries the potential for significant effect on tumor volume and possibly result in permanent cure, radiosurgery is an attractive alternative. From its inception the Gamma Knife has been employed to treat many skull base tumors that typically invade the cavernous sinus (Table 1). Although the number of such patients, even with rare skull base tumors, is relatively large, the number of Gamma Knife treatment reports remains small. Although the diagnosis of some tumors treated with the Gamma Knife was established by imaging stud-

Table 1. Number of patients treated by Gamma Knife surgery for tumors which may grow in the cavernous sinus (end of 2005)

Pituitary adenoma	
Secreting	18,044
Non-Secreting	10,264
Trigeminal schwannoma	2,014
Chordoma	1,460
Chondrosarcoma	382
Hemangiopericytoma	849
Adenoid cystic carcinoma	?
Metastatic tumors	120,915
Hemangioblastoma	1,438
Cavernous angioma	1,082
Paraganglioma	931
Epidermoid	?
Angiofibroma	?

ies alone, in most treatment was initiated as adjunctive therapy after a histological diagnosis had been made.

Pituitary adenomas

Tumors originating from cells of the pituitary gland are the most common tumors invading the cavernous sinus. Most pituitary adenomas are successfully removed by microsurgical techniques. When non-secreting tumors pose a threat to vision, surgery is recommended because it is the quickest way to relieve pressure on the optic apparatus. Hormones produced by secreting tumors constitute a long-term threat by placing strain on the cardiovascular system and/or producing diabetes, osteoporosis and other problems. The relatively long delay required to return hormone levels to normal is a disadvantage of radiation therapy. Surgical removal by the transsphenoidal route is the preferred means of dealing with pituitary adenomas, and failure of total removal is often related to invasion of one or both of the cavernous sinuses.

Drugs for controlling the release of, or the effect of, hypersecreted hormones play an increasing role in the management of secreting pituitary adenomas. For prolactinomas in particular, drug treatment may constitute sufficient treatment. But medical treatment is expensive, lifelong and sometimes not tolerated. Gamma Knife surgery, on the other hand, offers more definitive treatment with some cases of secreting adenomas and non-secreting lesions.

Cushing's disease

The ACTH production of Cushing's disease usually emanates from a microadenoma of the pituitary gland. An experienced pituitary surgeon can usually identify a microadenoma from surrounding pituitary tissue and successfully remove it. However, at times surgery fails to lower the ACTH level adequately, often resulting in the use of postoperative radiation. Many avoid conventional radiotherapy because of its more global and delayed effects on the brain.

Backlund and Rähn pioneered the use of Leksell's Gamma Knife for treating Cushing's disease, publishing their initial experiences in 1978 and long-term results in 1986 [8]. Experienced pituitary neurosurgeons, most notably Laws in Virginia and Landolt in Switzerland, currently prefer Gamma Knife radiosurgery as the complementary treatment of choice following failed transsphenoidal operations. A publication from Virginia describes 44 Gamma Knife treatments in 43 patients previously operated upon for Cushing's disease [42]. In 27 (63%), 24-h free urinary cortisol levels returned to normal. Seven developed new endocrinological deficits, but only one was a different type of deficit.

Kobayashi's Gamma Knife group in Komaki, Japan, report results in 25 patients followed for more than 2.5 years (mean 5.3 years) of whom 35% had previous surgery [21]. Serum ACTH and cortisol levels decreased in 85%, significantly so in 60%, and returned to normal in 35%. Kobayashi acknowledged that very high doses are required to stop hormone production. Best results were obtained with peripheral tumor doses of 40 Gy or more. Among six patients with Nelson's syndrome the response rate was only 33%, although all tumors were controlled. A fulminant course of Cushing's disease predisposes to the development of Nelson's syndrome.

Figure 1 illustrates a case of an aggressive ACTH-producing tumor in which Gamma Knife surgery afforded palliation. Prior to Gamma Knife treatment this patient had not only undergone conventional radiotherapy but also transsphenoidal surgery three times. She was severely hyperpigmented and the tumor was noted to invade her cavernous sinus (Fig. 1A). This tumor was treated with a lower than desirable dose, 20 Gy, in order to limit the dose to the optic nerve to 8 Gy, which, in our experience, is always tolerated. Nevertheless, her skin color returned to near

normal, and her tumor volume decreased (Fig. 1B). However, 3.5 years later the hyperpigmentation returned and the tumor had advanced in size (Fig. 1C). A second treatment with only 14 Gy reduced the volume of the tumor, but it later metastasised to the posterior fossa and spinal canal.

Acromegaly

Growth hormone producing tumors constitute 25–30% of pituitary tumors in recent surgical series [32]. Of secreting adenomas, GH-producing tumors most frequently invade the cavernous sinus. The cure rate of 668 patients with acromegaly, based on stringent biochemical criteria, was evaluated [32]. Of 506 patients undergoing transsphenoidal surgery as primary treatment, 57.3% fulfilled the criteria of cure. In smaller series from centers with less experience, the cure rate has been reported to be even lower [25, 40]. It has been suggested that experience with pituitary surgery is an important predictor of success [25], also with macroadenomas [25, 29, 40].

The ability of the Gamma Knife to return GH and/or IGF1 to normal after conventional surgery has been variable. In a series of 82 patients treated in Marseilles only 17% were endocrinologically cured, but hormonal symptoms improved in additional 23% [4]. At the Prague Gamma Knife Centre 50% of 96 patients treated for acromegaly were cured [19]. Landolt observed less favorable results in patients on octreotide and suggested that such drugs should be withheld a few months prior to Gamma Knife surgery [23]. The same observation was made in

A

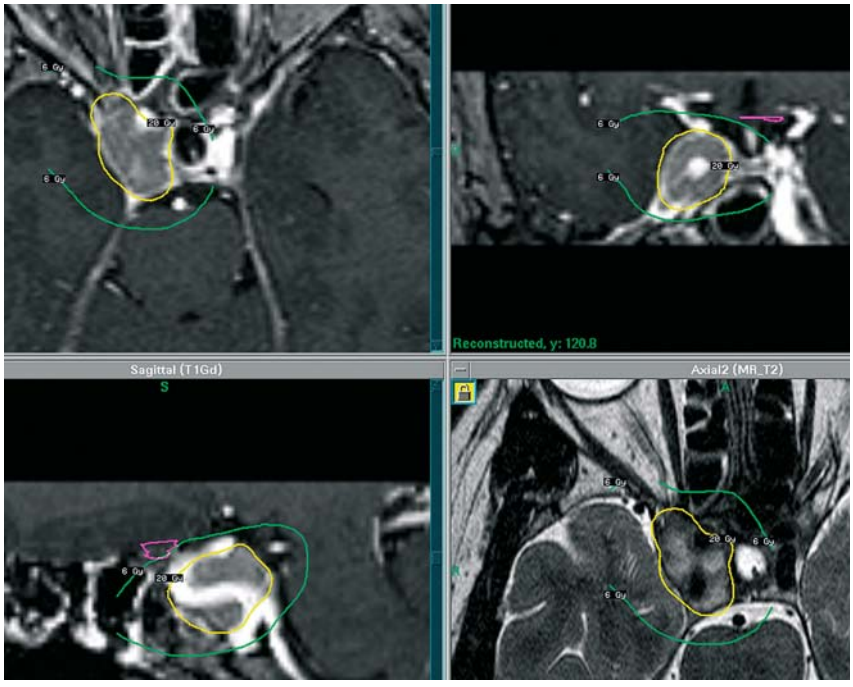

Fig. 1. Female treated by Gamma Knife surgery (GKS) in 2002 at age 50 for Cushing's disease with Nelson's syndrome. Diagnosed in 1992. Transsphenoidal surgery (TSS) 1993 and 1998, radiotherapy 1998, bilateral adrenalectomy 2001. TSS 2001. Severe hyperpigmentation, Cushingoid features, mild diplopia and very high ACTH (1244) on presentation for GKS. **A** Intracavernous tumor with outline (yellow) of 20 Gy prescription isodose and 6 Gy (green) isodose. Optic chiasm outlined in magenta. Upper left: T1W Gd axial image, upper right: coronal, lower left: sagittal, lower right: T2W axial image. Tumor volume is 2.9 cc. **B** Same as **A**, 1 year after GKS. Tumor volume is 1.7 cc. Clinically much improved: normal pigmentation, physically much stronger. Normal ACTH. **C** Three years five months after initial GKS at time of 2nd GKS. The patient is six months post 4th TSS for decompression of optic chiasm. Complete CN III palsy and complete CN VI deficit on the right, hyperpigmentation, visual field defects. Pictures display as **A** & **B**. Prescription dose 14 Gy (yellow line). Tumor volume 10.3 cc

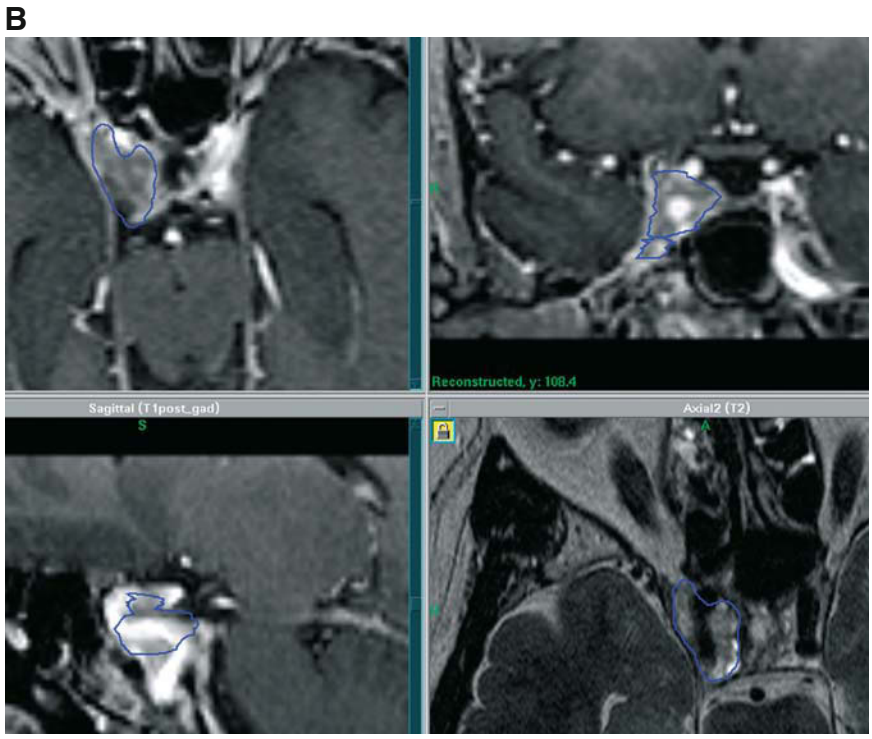

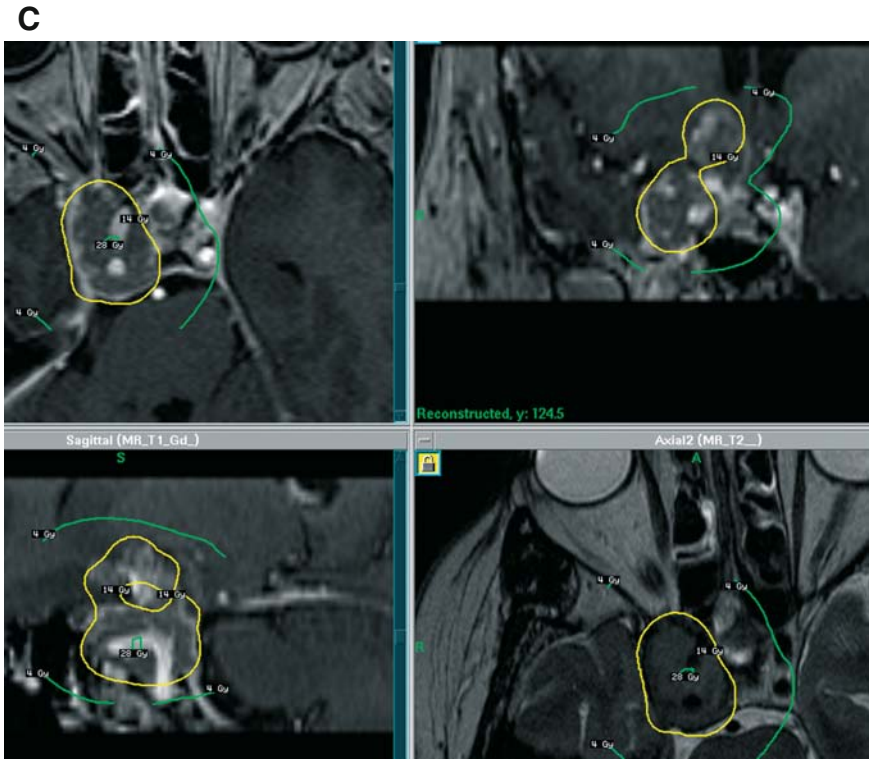

Fig. 1 (*Continued*)

patients on dopaminergic drugs when undergoing Gamma Knife treatment of prolactinomas [24]. Pollock et al., in a multivariate analysis of secreting pituitary adenoma management, also found a correlation between outcome and absence of hormone-suppressive medications at the time of Gamma Knife surgery [37]. It remains to be confirmed that results can be improved further by withholding such drugs.

Trigeminal schwannomas

Trigeminal schwannomas are second only to vestibular schwannomas as the most common of the cranial nerve schwannomas. Yet this tumor accounts for less than 10% of intracranial schwannomas. Consequently, reports of large series of patients treated with conventional or Gamma Knife surgery do not exist. These tumors frequently invade the cavernous sinus and may originate within and remain confined to it. Most commonly trigeminal schwannomas present with facial numbness, and less commonly with trigeminal pain. Samii et al. reported their surgical experience with 12 solitary trigeminal schwannomas in patients with no family history of neurofibromatosis, eight of which invaded the cavernous sinus [38]. They concluded that total tumor removal with preservation of important neural structures is possible in most patients, but they emphasised that "follow-up monitoring is mandatory to exclude recurrence in the cavernous sinus".

The frontotemporal epidural approach described by Dolenc [9] opened the possibility of successfully dealing with these tumors [27]. Al-Mefty reported that all 25 of the lesions he encountered had tumor within the cavernous sinus [1]. With a mean follow-up of 33 months he reported three recurrences after an average of 22 months. Trigeminal nerve sensory deficits improved in 44% of patients and facial pain decreased in 73%. Such results set the benchmark for treatment of trigeminal schwannomas.

Gamma Knife surgery must match these results if its use is to be justified as a *primary* treatment modality. In larger tumors Goel et al. reported radical removal in 51 of 73 patients (70%) with only one recurrence over an average follow-up of 38 months [15]. In five of eight patients Moffat et al. elected to leave a tumor remnant in order to minimize the postoperative neurological deficit [28]. These patients experienced symptomatic recurrences, requiring additional surgery. The results presented below suggest that Gamma Knife may be the most attractive treatment for small-to-moderate volumes of surgical remnants, recurrencies, and arguably as the primary method of treatment.

From 1999 to 2006 eight patients were treated with Gamma Knife surgery as the primary management of trigeminal schwannomas at the Cromwell Hospital. All patients had declined open operations. Each presented with facial numbness and pain in varying proportions. Four have been followed for at least 4 years, and in all the tumor was confirmed to be considerably smaller than at the time of treatment with doses of 10 Gy, 12 Gy, 14 Gy and 14 Gy. The tumor treated with 10 Gy recurred after 2 years and was retreated with an additional 10 Gy after 28 months. It was 25% smaller than initially at the last follow-up, 3 years and 8 months after the second treatment. The other tumors have reduced to 62%, 44%, and 35% of their original volumes. The least reduction was seen in the patient who was prescribed a dose of 12 Gy. One of these patients is completely asymptomatic after treatment (Fig. 2) and two patients are much improved, complaining of only rare brief episodes of facial pain. The fourth patient, with a tumor volume reduction of 35% after a dose of 14 Gy, developed significant facial pain a few months following treatment. His pain responded to steroids, which were required for months. His pain ultimately subsided and 4 years after treatment he uses pain medication only occasionally. His facial numbness persists.

In the past 4 years many reports of Gamma Knife surgery for trigeminal schwannoma have appeared in the peer-reviewed literature (Table 2). In total the reports include 200 patients although 27 were lost to follow-up. The median follow-up of 173 patients was greater than 4 years. Tumor regression occurred in 125 of 173 patients (72%), and the tumors of another 34 remained stable, indicating tumor control in 92% patients. Even if all patients lost to follow-up are considered failures, tumor regression reaches 63%, and growth control 80%. Increased symptoms, generally numbness, occurred in 13%. Additional facial pain was reported by only 2% of the 173 patients available for follow-up. On the other hand, 93 patients (54%) reported symptomatic improvement. All four authors conclude that Gamma Knife surgery is a safe, effective primary treatment alternative for

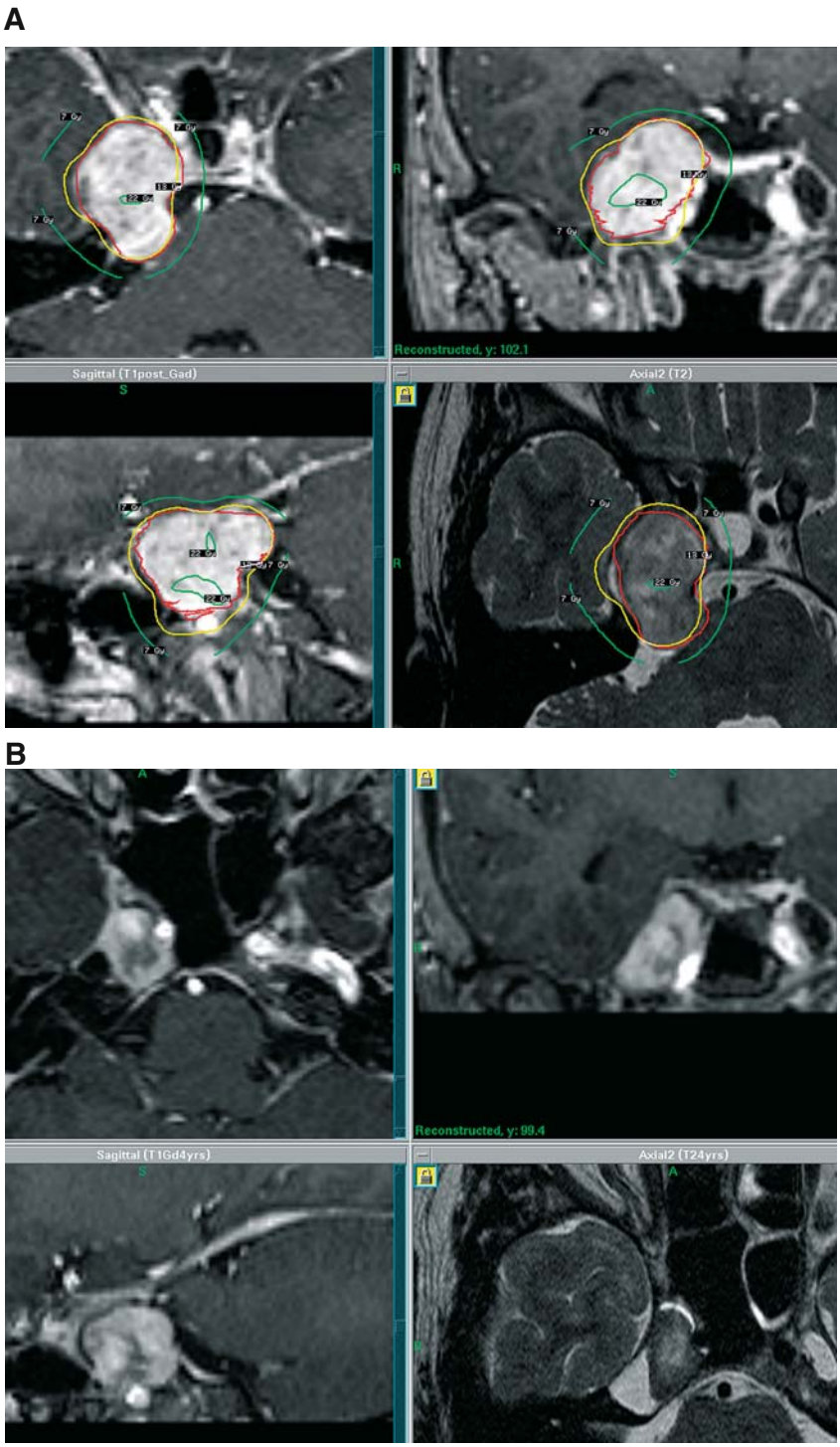

Fig. 2. Female treated by GKS for trigeminal schwannoma at age 33 in 2002. She presented with V: 1,2,3 numbness and depressed corneal reflex. **A** Tumor at time of GKS. Prescription dose of 14 Gy outlined in yellow and 7 Gy isodose line in green. Upper left: T1W Gd axial image, upper right: coronal, lower left: sagittal, lower right: T2W axial image. Tumor volume is 7.1 cc. **B** Same as A at follow up after 4 years. Tumor volume is 3.1 cc

Table 2. Results of Gamma Knife surgery for trigeminal schwannomas (literature review)

	Nettel et al. [31] Pittsburgh USA 2004	Pan et al. [35] Shanghai China 2005	Sun et al. [47] Beijing China 2006	Hasegawa et al. [16] Komaki Japan 2007
Number of Pts.	23	66	69	42
Lost to follow-up	1 unrelated death	10	11	5
Previous surgery	12	14	25	17
Prescription dose,	15 Gy	13.3 Gy	13.1 Gy	14.2 Gy
Mean (range)	(13–20)	(10–15)	(10–14.4)	(11–16)
Median	40 months	68 months	Mean 42.5 months	Mean 54 months
(range) follow-up	(12–146)	(27–114)	(9–120)	(12–140)
Clinical improvement	12	39	28	14
Stable initial symptoms	9	8	23	16
Tumor regression	15	48	38	24
Stable tumor	6	4	16	8
Tumor growth	2	4	4	5
Increased numbness	1	5	5 + 3 transient	3
Increased pain			3 Transient TN	3
Other complication	1 temporary facial paresis	1 death from growth	2 increased ICP	1 CN VI injury

trigeminal schwannomas of up to moderate size and is appropriate as secondary treatment of tumor remnants [16, 31, 35, 47].

Chordomas

Chordomas are rare extradural tumors arising from remnants of embryonic notochord. Approximately 35% occur in the skull base. Although characterized by high histologic differentiation, they exhibit locally aggressive growth patterns and are notorious for high recurrence rates. A Swedish national prognostic study revealed that patients with untreated clival chordomas may expect a mean survival of only 1 year [11]. Chordomas are generally so large at presentation that radiosurgery is not considered. Surgery may mitigate this dismal prognosis to some extent, but it remains unfavorable. In a retrospective analysis of 51 patients treated at the Mayo clinic, the estimated 5- and 10-year survival rates were 51% and 35%, respectively [14]. However, at the time of this study, 31 patients (61%) had died of their disease and only 12 (24%) were alive and free of disease. Five patients were alive with the disease and three had died of unrelated causes. Patients who had undergone resections had an improved 5-year survival (55%) compared to the group having only a biopsy.

Surgical difficulties are related to chordomas' midline skull base location, their tendency to surround important blood vessels, entangle cranial nerves, and possess indistinct tumor margins. Yet the primary mass of these tumors is usually easy to remove.

With improving microsurgical techniques more aggressive resections have been reported. Sekhar's group [50] totally removed 53 of 74 patients (71.6%). Complications were few but serious, including death (two), permanent cranial nerve palsies, hemiparesis, and cerebrospinal fluid leakage. Even more disheartening was the fact that the overall recurrence-free survival rate at 5 years was still only 41%, with an only somewhat better outcome in primary cases (47%).

The Mayo group concluded "that postoperative radiotherapy may prolong disease-free survival" [14]. Sekhar, on the other hand, expressed the opinion that "radiotherapy should be reserved for recurrencies" [50]. His 10-year recurrence-free survival rate was 42%, almost the same as his 5-year rate. This seems to justify his opinion and suggest that a cure may be achieved by surgery alone. Yet most centers include some form of postoperative radiation for chordomas. A clear dose–response relationship is apparent, with improved outcomes with doses greater than 60 Gy [39]. Conventional radiotherapy is limited since eloquent structures, such as the brain-

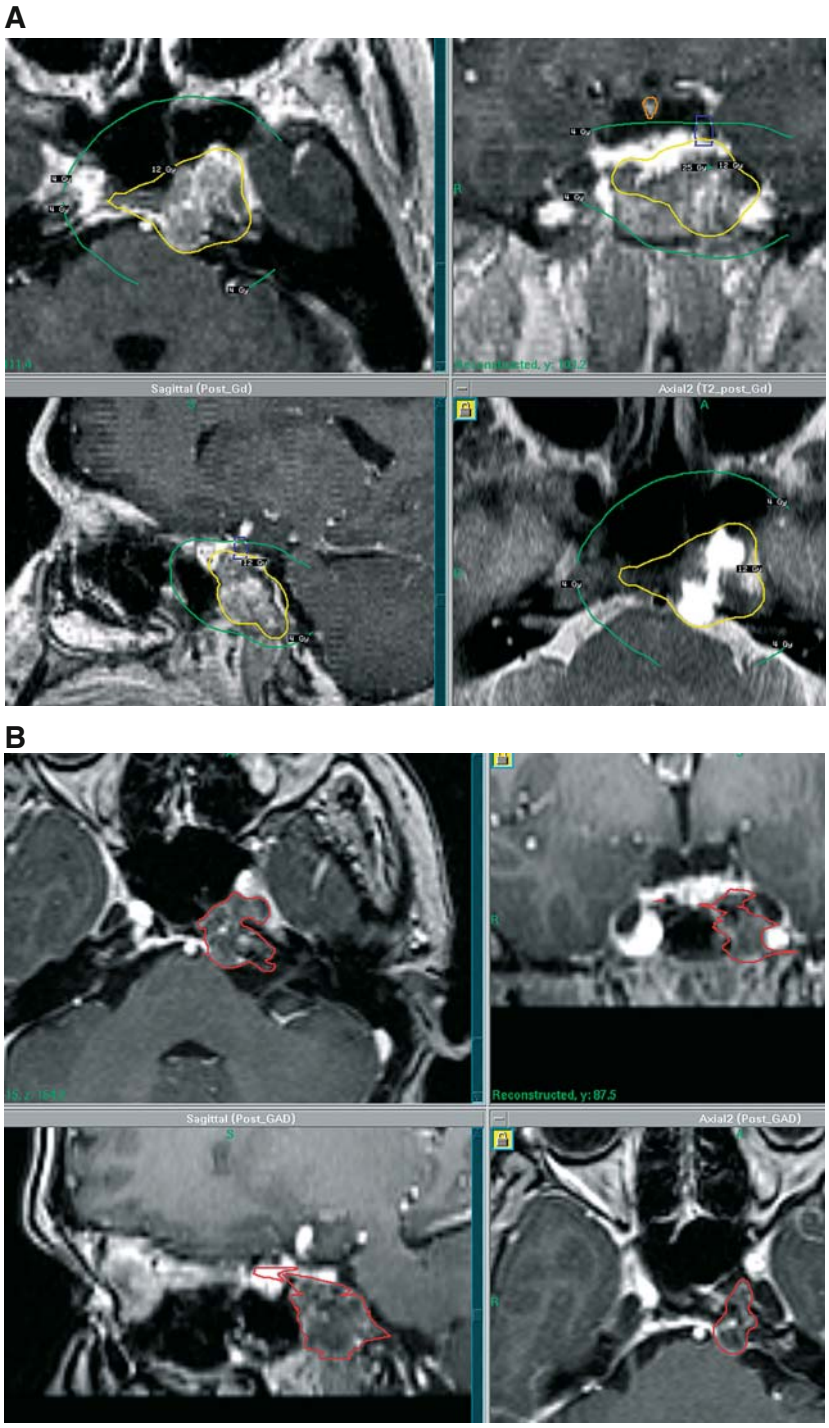

Fig. 3. Thirty-nine-year-old female. Transsphenoidal biopsy 7 years prior to admission: chondrosarcoma. Presented with facial pain, numbness, and left oculomotor nerve impairment. **A** Intracavernous chondrosarcoma with prescription dose of 12 Gy outlined (yellow) at the tumor margin. Upper left: T1W Gd axial image, upper right: coronal, lower left: sagittal, lower right: T2W axial image. Tumor volume 7 cc. **B** Tumor volume outlined (red) at 20 months after Gamma Knife surgery. Imaging sequences same as **A**. Tumor volume 4 cc

stem and cranial nerves, would be exposed to toxic doses.

Proton beam radiotherapy has shown promise and is currently used extensively in centers where the expensive equipment required is available [2, 3, 17, 46]. The Loma Linda facility reported an estimated 5-year "local control rate" of 59% for chordomas, and a 5-year overall survival rate of 79% [17]. Proton therapy was administered in daily fractions of 1.8 CGE (cobal Gy equivalents) to a total dose of 64.8–79.2 CGE. Early data on the effect of fractionated radiation with carbon ions, heavier particles with a higher RBE (relative biological effectiveness), carry hope for improved results in the future. The 2-year progression-free survival in 24 patients was 90% with this technique [39]. However, a dose delivered in one session is biologically more effective for a given target volume than the same dose delivered in fractions. This is a principle of radiosurgery. Steiner and the author have applied this principle to chordomas by using the Gamma Knife following surgical debulking in a small number of patients over the past 20 years [45]. Decreasing tumor volumes not seen after conventional radiotherapy were noted. Our experience remains small, however, and not yet sufficient for detailed analysis.

Figure 3 illustrates the result of a case treated with Gamma Knife surgery at the Cromwell Hospital. Tumor volume decreased from 7 cc to 4 cc 20 months after treatment with a dose of only 12 Gy.

The Leksell Gamma Knife Society listed 1,460 chordomas treated by Gamma Knife surgery by the end of 2005, 14 of which were treated at the Cromwell Hospital. Notwithstanding this large number of treated patients, very few outcome publications have resulted. In 1998 the Pittsburgh Gamma Knife center [30] reported nine chordoma patients with a mean tumor volume of 4 cc (range 0.98–10.3 cc). The minimum tumor dose varied between 12 Gy and 20 Gy. Unfortunately, those authors do not distinguish between chordomas and six chondrosarcomas also included. It is well known that these tumors respond differently to radiation treatment, with chondrosarcomas having a much better prognosis than chordomas. Two of the Pittsburgh patients died from tumor progression, and two of unrelated causes; eight improved clinically, and three remained stable. Among 11 survivors tumor volume reduction was verified in five cases, remained unchanged in five, and growth occurred in one. The observation period was an average of 4 years (range 1–7).

A Gamma Knife report from the Mayo clinic distinguishes between chordomas and chondrosarcomas [22]. It consists of 25 patients with chordomas and four with chondrosarcomas. The median prescription volume of all tumors was 14.4 cc (range 0.6–65.1 cc) and the median margin dose was 15 Gy (range 10–20 Gy). The median clinical follow-up was 4.8 years (range 0.8–11.4 years) and the median MR imaging follow-up was 4.5 years (range 0–9.4 years). The growth of even chordomas (28%) progressed (in-field, $n = 3$; out-of-field, $n = 4$), while 18 shrunk or remained stable. Nineteen received conventional radiotherapy in addition to Gamma Knife surgery, making the assessment of the effect of Gamma Knife treatment difficult. The actuarial tumor control rates were 89% and 32% at 2 and 5 years, respectively. Ten (34%) had radiation-induced complications related to the combination of Gamma Knife surgery and radiotherapy.

A London multidisciplinary group lead by Crockard (neurosurgeon) and Plowman (radiation oncologist) describes a treatment protocol for skull base chordomas [7]. In 42 chordoma patients managed under this protocol the primary goal was maximum tumor reduction with the least collateral damage. The decision to proceed with postoperative radiation was made if postoperative MRI showed residual tumor and/or if the tumor had a mitotic index or a Ki67 LI of 6% or higher. Fractionated radiation was given to the original tumor volume in a dose of 50 Gy with a radiosurgical boost of 10–15 Gy to any residual tumor. Survival rates of 77% at 5 years and 69% at 10 years estimated by life table statistics are among the best reported results for chordoma treatment.

Currently it appears that the best management of chordomas includes surgery to attempt total removal followed by some form of radiation. It is not clear whether heavy particle radiation offers an advantage over photon radiosurgery such as that delivered by the Gamma Knife. It remains unclear whether postoperative radiation limited to any remaining tumor residual is sufficient or whether the entire former tumor volume (possibly with a margin) should be included in the target volume. It seems to be established that the smaller the residual tumor volume, the better the chances for control with radiation. In comparison to photon radiation, heavy particle ra-

diation appears to deal effectively with larger volumes without incurring additional risks of radiation toxicity.

Chondrosarcomas

Published discussions of skull base tumor management often lump chordomas and chondrosarcomas together. They are indistinguishable by imaging studies and even by conventional histopathological techniques, and the surgical challenges each presents are also similar and formidable. There are, however, distinct immunohistochemical properties which clearly distinguish between these lesions. Precise identification is important for optimum outcomes since both surgical and radiation management are quite different.

Experience treating chondrosarcomas is limited since they are less common than chordomas, making up only 0.15% of intracranial tumors. Except for the mesenchymal variety (10% of chondrosarcomas), which are more aggressive, any treatment is more effective for chondrosarcomas than chordomas.

Crockard's group reports the outcome of 17 chondrosarcomas treated with surgery for low grade lesions, with consideration of additional surgery for recurrences [6]. Two mesenchymal chondrosarcomas were treated by aggressive cytoreductive surgery followed by radiation as prescribed for chordomas. These two patients with malignant chondrosarcomas died after 20 and 36 months respectively. The mean survival for low grade chondrosarcomas was 9.3 years with a 5-year survival rate of 93% and a 10-year projected survival rate of 84%.

Proton radiation therapy for recurrent chondrosarcomas [17] after 1–3 microsurgical procedures resulted in a 100% 5-year survival rate in a group of 25 patients followed for an average of 33 months (range 7–75 months). The estimated local tumor control rate at 5 years was 75% (Kaplan–Meir statistical analysis). Tumor volumes less than 25 cc were controlled at 5 years, but only 56% of those larger than 25 cc were.

Steiner and the author first used the Gamma Knife for postoperative treatment of a chondrosarcoma in the early 1980s with dramatic volume reduction of residual tumor [44]. The report from Pittsburgh mentioned above also included six patients with chondrosarcomas but outcomes were not analysed separately [30]. The Mayo Clinic reported four chondrosarcomas treated with the Gamma Knife with an estimated 5-year tumor control of 100% [22]. One improved clinically, two remained stable, and one worsened because of "brain necrosis," a complication of treatment. The problem with these two reports is not only the very small number of patients treated but also the short periods of follow-up. Chondrosarcomas grow very slowly, appearing to be "dormant" for as long as 14 years. The average tumor volume doubling time in Crockard's series was 51 months [6].

Follow-up information on four patients we treated with low grade chondrosarcomas in the 1990s was collected at the Karolinska Gamma Knife Center plus two patients treated more recently. In three, tumor invaded the cavernous sinus, each requiring cytoreductive surgery prior to Gamma Knife procedures. In addition, there were two patients with mesenchymal chondrosarcomas. One patient with a low grade tumor was retreated for a recurrence 7 years after the original treatment, and no further growth was noted after an additional 2 years. The Karnoffsky functional score (KPS) deteriorated from 80 to 70 over the period of observation. Another patient developed a recurrence within a year and was treated twice with Gamma Knife surgery. This patient has been followed for 51 months without apparent tumor progression, but the KPS declined from 90 at the time of presentation to 80 at follow-up. Tumor progression occurred beyond the treatment volume in both patients. The other patients are alive 23, 108, 173, and 156 months following treatment with KPSs of 80, 80, 70, and 90, respectively. In the first patient the KPS represented deterioration from 90 prior to treatment, and the second patient manifested no change from the KPS at initial presentation. The third patient declined from a pretreatment KPS of 80. The fourth patient maintained a KPS of 90 before and after the combined treatment.

Surgery was the major cause of posttreatment deterioration, but Gamma Knife surgery resulted in facial weakness at 2 months in one patient and complete right VIth cranial nerve dysfunction in one patient 5 months after the second Gamma Knife procedure. The facial paresis recovered to a House-Brackman II at 1 year, but the VIth nerve deficit did not recover. The latter patient also developed numbness of the left side of the body 1 year after the second

Gamma Knife procedure (which could be treatment related).

The volumes of the low grade chondrosarcomas treated with Gamma Knife surgery in this series were 0.9–6.5 cc and the doses prescribed were14–22 Gy. To summarize, in this series tumor control after microsurgery alone was not achieved in any patient, but additional Gamma Knife therapy provided control in all six patients treated for low grade chondrosarcomas [13]. A similar treatment protocol with Gamma Knife surgery 2–10 months after microsurgery was recently suggested by another group [12]. They treated 10 chondrosarcomas (volume range 1.4–20.3 cc) and three chordomas with a mean dose of 17 Gy (range 14–18 Gy). Two of the three chordomas exhibited tumor recurrences during the observation period averaging 17 months (range 6–36 months) while none of the chondrosarcomas recurred. The volumes of nine tumors were reduced by an average of 35.4% (range 19.7–69.8), and no complications of Gamma Knife surgery were apparent.

Hemangiopericytomas

Hemangiopericytomas originate from pericytes and are most often found in the musculoskeletal system and skin. They may also originate in the meninges, but such tumors constitute fewer than 1% of intracranial tumors [41]. They may appear anywhere in the meninges but seem to have a preference for the dural sinuses and occipital region [18]. Tumors may appear synchronously in multiple intra- or extracranial locations. Intracranial lesions may metastasise to extracranial locations even many years after the intracranial presentation [48].

Management of hemangiopericytomas is very difficult. The vascularity and location of the tumor often precludes total removal. A study from the M. D. Anderson Cancer Center in Houston reported the long-term outcomes of 29 patients with non-metastatic hemangiopericytomas treated between 1979 and 1999 [43]. Gross total resection was achieved in only 15 patients (52%), and 10 received postoperative radiotherapy. The 5-, 10-, and 15-year overall survival rates were 85%, 68%, and 43%, respectively. The local control rates at 5 and 10 years were 68% and 22%. Sixteen patients (55%) developed extraneural metastases and four patients (14%) developed spinal spread. Although it was concluded that radiotherapy "appeared to represent a reasonable approach for initial management," statistically significant improvement in local control was not demonstrated. The 5-year local control rate was considerably improved in patients after gross total removal (84%) compared to subtotal removal (38%).

Today, in order to improve local control, postoperative radiosurgery seems to be the natural choice. In the early 1980s the author and Steiner treated a patient with multifocal intracranial hemangiopericytomas in whom Gamma Knife surgery was used for a lesion at the tentorial hiatus. Remarkable tumor volume reduction was achieved. Unfortunately, the patient still succumbed to the disease in a relatively short time. However, it prompted us to continue using Gamma Knife surgery as adjuvant therapy.

A retrospective analysis of Steiner's early experience from the University of Virgina has been published [36]. It includes follow-up from 3 to 56 months in 10 patients. Two new tumors occurred in one. Of the 12 tumors treated, 10 shrank but later progressed after an average of 22 months. There were no complications and quality of life was maintained.

Figure 4 shows MRI scans before and after Gamma Knife surgery for a patient with an intracavernous hemangiopericytoma at the Cromwell Hospital. This case history illustrates nicely typical management problems and the clinical course of this disease. Fifteen years ago this 44-year-old male presented to an ENT surgeon with nasal congestion. In two surgical procedures, including a craniotomy, a subtotal excision of a hemangiopericytoma was achieved, followed by conventional radiotherapy. Six years later MRI confirmed tumor progression into the cavernous sinus requiring Gamma Knife surgery (Fig. 4A). Twenty-two months later only 20% of the original tumor volume remained (Fig. 4B), yet within an additional 30 months the tumor progressed again, with an entirely new lesion appearing in the ethmoid area, demanding treatment.

Figure 5 depicts the volumes of three intracranial tumors developing over time after an initial Gamma Knife procedure. Fifty-five months following Gamma Knife surgery and 11 years after initial diagnosis, the patient developed a paraspinal metastases. At 65 months from the initial Gamma Knife procedure a left IIIrd cranial nerve palsy and visual deterioration developed which were attributed to tumor progression rather than a complication of radiation. This

A

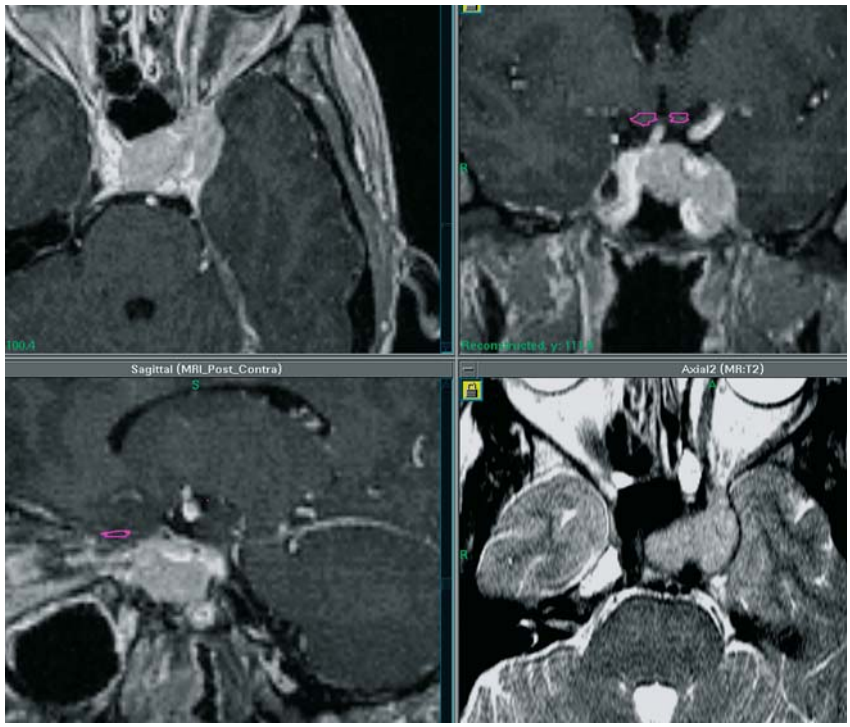
Sagittal (MRI_Post_Contra)
Axial2 (MR:T2)

B

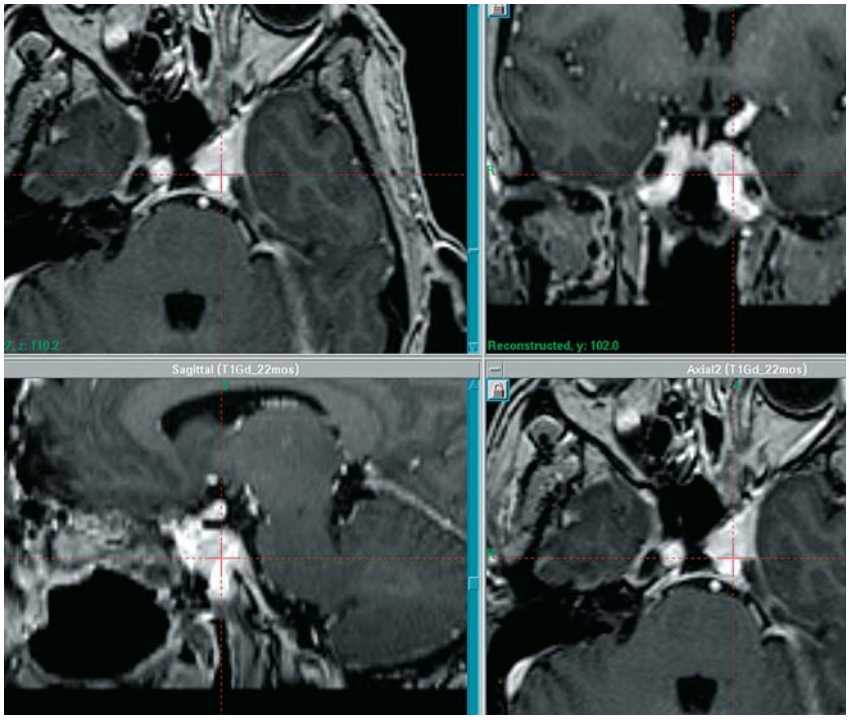
Reconstructed, y: 102.0
Sagittal (T1Gd_22mos)
Axial2 (T1Gd_22mos)

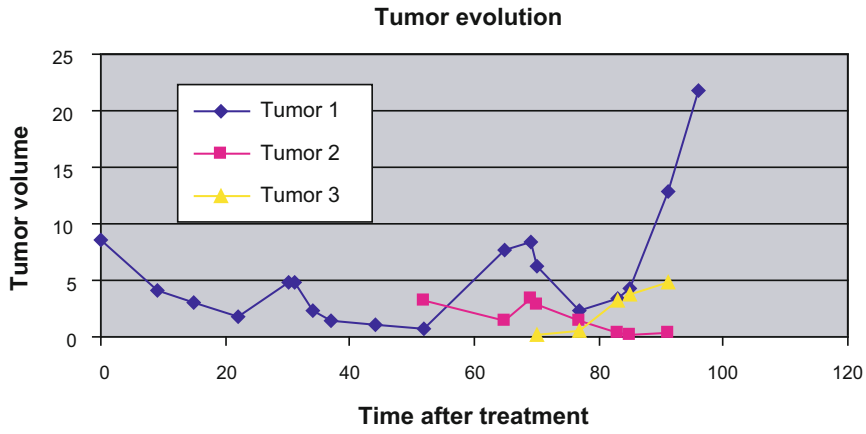

Fig. 5. Graph of volume change of hemangiopericytoma illustrated in Fig. 4 over 8 years. The cavernous sinus tumor (blue) was treated three times by Gamma Knife surgery. Each time there was a dramatic response but each recurrence begins from a higher baseline volume. A second ethmoid region tumor appears (magenta line) and it responds well to two Gamma Knife surgical treatments. A third intraorbital tumor finally appears and the three tumors merge and are only depicted by the blue line at 96 months (8 years) after the initial Gamma Knife surgery

was confirmed when vision improved after a transsphenoidal decompression operation resulted in improved vision and further improvement occurred after another Gamma Knife procedure. However, irreversible loss of vision in the left eye eventually resulted. Over the years progressive loss of pituitary function has also occurred. The patient has, however, maintained a good quality of life and he has written an acclaimed novel 14 years after the initial diagnosis was made.

Among 11 patients treated at the Mayo Clinic with Gamma Knife surgery, dramatic tumor shrinkage occurred within 6–10 months, a partial visual field defect occurring in a single patient as the only complication [5]. Long-term results are not available. The Pittsburgh group presented outcome data from 14 patients for an average follow-up of 31.3 months (range 5–76 months; median 21 months) [41]. Twelve of fifteen tumors (80%) dramatically decreased in size in response to an average tumor margin dose of 15 Gy (range 11–20 Gy). Local tumor control and survival rates at 5 years estimated by the Kaplan–Meir method were 76% and 100%, respectively. One patient experienced tumor progression at 75 months and died 99 months after Gamma Knife surgery. An additional patient exhibited worsening weakness despite radiological evidence of tumor regression. On the other hand, the neurological condition of two patients improved after treatment.

Conclusion

Non-meningeal tumors invading the cavernous sinus are among the most therapeutically challenging skull base tumors. Experienced skull base surgeons may achieve reasonable results and occasionally completely remove a cavernous sinus tumor. Such operations, however, pose considerable risk to each patient. Cytoreductive, or debulking surgery, aimed at reducing the tumor volume to a remnant amenable to local management with radiosurgery, or possibly heavy ion radiotherapy, is an attractive alternative. This author believes that Gamma Knife surgery has established itself as a treatment mod-

Fig. 4. Forty-nine-year-old male with hemangiopericytoma treated from 6 years prior to Gamma Knife surgery by endonasal surgery and craniotomy followed by radiotherapy. **A** Intracavernous tumor bulging into the sphenoid sinus and displacing the pituitary stalk. Before Gamma Knife surgery. Optic chiasm outlined in magenta color. Tumor volume 8.5 cc. Upper left: T1W Gd axial image, upper right: coronal, lower left: sagittal, lower right: T1W Gd axial image. **B** Follow up at 22 months. Note pituitary stalk in the midline. Tumor volume 1.7 cc. Imaging sequences same as **A**

ality which adds considerable benefit to patients with meningiomas and rare tumors of the cavernous sinus. Recent improvements in the technique will allow even greater precision, and open the possibility of safe-dose escalation necessary to effectively deal with the more malignant tumors of the skull base.

References

1. Al-Mefty O, Ayoubi S, Gaber E (2002) Trigeminal schwannomas: removal of dumbbell-shaped tumors through the expanded Meckel cave and outcomes of cranial nerve function. J Neurosurg 96: 453–463
2. Austin-Seymour M, Munzenrider J, Goitein M, Verhey L, Urie M, Gentry R, Bimbaum S, Ruotolo D, McManus P, Skates S, et al. (1989) Fractionated proton radiation therapy of chordoma and low-grade chondrosarcoma of the base of the skull. J Neurosurg 70: 13–17
3. Berson AM, Castro JR, Petti P, Phillips TL, Gauger GE, Gutin P, Collier JM, et al. (1988) Charged particle irradiation of chordoma and chondrosarcoma of the base of skull and cervical spine: the Lawrence Berekeley Laboratory experience. Int J Radiat Oncol Biol Phys 15: 559–565
4. Castinetti F, Taieb D, Kuhn JM, Chanson P, Tamura M, Jaquet P, Conte-Devolx B, Regis J, Dufour H, Brue T (2005) Outcome of Gamma Knife radiosurgery in 82 patients with acromegaly: correlation with initial hypersecretion. J Clin Endocrinol Metab 90: 4483–4488
5. Coffey RJ, Cascino TL, Shaw EG (1993) Radiosurgical treatment of recurrent hemangiopericytomas of the meninges: prelimary results. J Neurosurg 78: 903–908
6. Crockard HA, Cheeseman A, Steel T, Revesz T, Holton JL, Plowman N, Singh A, Crossman J (2001) A multidisciplinary team approach to skull base chondrosarcomas. J Neurosurg 95: 184–189
7. Crockard HA, Steel T, Plowman N, Singh A, Crossman J, Revesz T, Holton JL, Cheeseman A (2001) A multidisciplinary team approach to skull base chordomas. J Neurosurg 95: 175–183
8. Degerblad M, Rähn T, Bergstrand G, Thoren M (1986) Long-term results of stereotactic radiosurgery to the pituitary gland in Cushing's disease. Acta Endocrinol (Copenh) 112: 310–314
9. Dolenc VV (1994) Frontotemporal epidural approach to trigeminal neurinomas. Acta Neurochir (Wien) 130: 55–65
10. Eisenberg MB, Al-Mefty O, DeMonte F, Burson GT (1999) Benign nonmeningeal tumors of the cavernous sinus. Neurosurgery 44: 949–954
11. Eriksson B, Gunterberg B, Kindblom LG (1981) Chordoma: a clinicopathologic and prognostic study of a Swedish national series. Acta Orthop Scand 52: 49–58
12. Feigl GC, Bundschuh O, Gharabaghi A, Safavi-Abbasi S, El Shawarby A, Samii M, Horstmann GA (2005) Evaluation of a new concept for the management of skull base chordomas and chondrosarcomas. J Neurosurg 102(Suppl): 165–170
13. Förander P, Rähn T, Kihlström L, Ulfarsson E, Mathiesen T (2006) Combination of microsurgery and Gamma Knife surgery for the treatment of intracranial chondrosarcomas. J Neurosurg 105(Suppl): 18–25
14. Forsyth PA, Cascino TL, Shaw EG, Scheithauer BW, O'Fallon J, Dozier JC, Piepgras DG (1993) Intracranial chordomas: a clinicopathological and prognostic study of 51 cases. J Neurosurg 78: 741–747
15. Goel A, Muzumdar D, Raman C (2003) Trigeminal neuroma: analysis of surgical experience with 73 cases. Neurosurgery 52: 783–790
16. Hasegawa T, Kida Y, Yoshimoto M, Koike J (2007) Trigeminal schwannomas: results of Gamma Knife surgery in 37 cases. J Neurosurg 106: 18–23
17. Hug EB, Loredo LN, Slater JD, DeVries A, Grove RI, Schaefer RA, Rosenberg AE, Slater JM (1999) Proton radiation therapy for chordomas and chondrosarcomas of the skull base. J Neurosurg 91: 432–439
18. Jaaskelainen J, Servo A, Haltia M, Wahlstrom T, Valtonen S (1985) Intracranial hemangiopericytoma: radiology, surgery, radiotherapy, and outcome in 21 patients. Surg Neurol 23: 227–236
19. Jezkova J, Marek J, Hana V, Krsek M, Weiss V, Vladyka V, Lisak R, Vymazal J, Pecen L (2006) Gamma knife radiosurgery for acromegaly – long-term experience. Clin Endocrinol (Oxf) 64: 588–595
20. Kasperlik-Zaluska AA, Bonicki W, Jeske W, Janik J, Zgliczynski W, Czernicki Z (2006) Nelson's syndrome – 46 years later: clinical experience with 37 patients. Zentralbl Neurochir 67: 14–20
21. Kobayashi T, Kida Y, Mori Y (2002) Gamma knife radiosurgery in the treatment of Cushing disease: long-term results. J Neurosurg 97(Suppl 5): 422–428
22. Krishnan S, Foote RL, Brown PD, Pollock BE, Link MJ, Garces YI (2005) Radiosurgery for cranial base chordomas and chondrosarcomas. Neurosurgery 56: 777–784
23. Landolt AM, Haller D, Lomax N, Scheib S, Schubiger O, Siegfried J, Wellis G (2000) Octreotide may act as a radioprotective agent in acromegaly. J Clin Endocrinol Metab 85: 1287–1290
24. Landolt AM, Lomax N (2000) Gamma Knife surgery for prolactinomas. J Neurosurg 93(Suppl 3): 14–18
25. Lissett CA, Peacey SR, Laing I, Tetlow L, Davis JR, Shalet SM (1998) The outcome of surgery for acromegaly: the need for a specialist pituitary surgeon for all types of growth hormone (GH) secreting adenoma. Clin Endocrinol (Oxf) 49: 653–657
26. Lobato AJF, Gomez PA, Boto GR, Lagares A, Ramos A, Ricoy JR (2001) Intracranial hemangiopericytoma: a study of 12 cases. Acta Neurchir 143: 575–586
27. Mariniello G, Cappabianca P, Buonamassa S, de Divitiis E (2004) Surgical treatment of intracavernous trigeminal

schwannomas via a fronto-temporal epidural approach. Clin Neurol Neurosurg 106: 104–109
28. Moffat D, De R, Hardy D, Moumoulidis I (2006) Surgical management of trigeminal neuromas: a report of eight cases. J Laryngol Otol 120: 631–637
29. Mortini P, Losa M, Barzaghi R, Boari N, Giovanelli M (2005) Results of transsphenoidal surgery in a large series of patients with pituitary adenoma. Neurosurgery 56: 1222–1233
30. Muthukumar N, Chi M, Kondziolka D, Lunsford LD, Flickinger JC (1998) Stereotactic radiosurgery for chordoma and chondrosarcoma: further experiences. Int J Radiat Oncol Biol Phys 41: 387–392
31. Nettel B, Niranjan A, Martin JJ, Koebbe CJ, Kondziolka D, Flickinger JC, Lunsford LD (2004) Gamma knife radiosurgery for trigeminal schwannomas. Surg Neurol 62: 435–436
32. Nomikos P, Buchfelder M, Fahlbusch R (2005) The outcome of surgery in 668 patients with acromegaly using current criteria of biochemical 'cure'. Eur J Endocrinol 152: 379–387
33. Pamir MN, Kilic T, Ozek MM, Ozduman K, Ture U (2006) Non-meningeal tumours of the cavernous sinus: a surgical analysis. J Clin Neurosci 13: 626–635
34. Pamir MN, Kilic T, Ture U, Ozek MM (2004) Multimodality management of 26 skull-base chordomas with 4-year mean follow-up: experience at a single institution. Acta Neurochir (Wien) 146: 343–354
35. Pan L, Wang EM, Zhang N, Zhou LF, Wang BJ, Dong YF, Dai JZ, Cai PW (2005) Long-term results of Leksell Gamma Knife surgery for trigeminal schwannomas. J Neurosurg 102(Suppl): 220–224
36. Payne BR, Prasad D, Steiner M, Steiner L (2000) Gamma surgery for hemangiopericytomas. Acta Neurochir (Wien) 142: 527–536
37. Pollock BE, Nippoldt TB, Stafford SL, Foote RL, Abboud CF (2002) Results of stereotactic radiosurgery in patients with hormone-producing pituitary adenomas: factors associated with endocrine normalization. J Neurosurg 97: 525–530
38. Samii M, Migliori MM, Tatagiba M, Babu R (1995) Surgical treatment of trigeminal schwannomas. J Neurosurg 82: 711–718
39. Schulz-Ertner D, Haberer T, Jäkel O, Thilmann C, Krämer M, Enghardt W, Kraft G, Wannenmacher M, Debus J (2002) Radiotherapy for chordomas and low-grade chondrosarcomas of the skull base with carbon ions. Int J Radiat Oncol Biol Phys 53: 36–42
40. Sheaves R, Jenkins P, Blackburn P, Huneidi AH, Afshar F, Medbak S, Grossman AB, Besser GM, Wass JA (1996) Outcome of transsphenoidal surgery for acromegaly using strict criteria for surgical cure. Clin Endocrinol (Oxf) 45: 407–413
41. Sheehan J, Kondziolka D, Flickinger J, Lunsford LD (2002) Radiosurgery for treatment of recurrent intracranial hemangiopericytoma. Neurosurgery 51: 905–910
42. Sheehan JM, Vance ML, Sheehan JP, Ellegala DB, Laws ER Jr (2000) Radiosurgery for Cushing's disease after failed transsphenoidal surgery. Neurosurgery 93: 738–742
43. Soyuer S, Chang EL, Selek U, McCutcheon IE, Maor MH (2004) Intracranial meningeal hemangiopericytoma: the role of radiotherapy: report of 29 cases and review of the literature. Cancer 100: 1491–1497
44. Steiner L, Payne BR, Prasad D, Lindquist C, Steiner M (2000) Gamma surgery in cerebral vascular lesions, malformations, tumors, and functional disorders. In: Schmidek HH (ed) Operative neurosurgical techniques, 4th edn. Saunders, Philadelphia, pp 670–706
45. Steiner L, Sheehan J, Lindquist C, Stroila M, Steiner M (2006) Gamma surgery in cerebral vascular lesions, malformations, tumors, and functional disorders. In: Schmidek HH, Roberts DW (eds) Operative neurosurgical techniques, 5th edn. Saunders, Philadelphia, pp 530–576
46. Suit HD, Goitein M, Munzenrider J, Verhey L, Davis KR, Koehler A, Linggood R, Ojemann RG (1982) Definitive radiation therapy for chordoma and chondrosarcoma of base of skull and cervical spine. J Neurosurg 56: 377–385
47. Sun S, Liu A, Wang C, Luo B, Wang M (2006) Clinical analysis of Gamma knife surgery for trigeminal schwannomas. J Neurosurg 105: 144–148
48. Suzuki H, Haga Y, Oguro K, Shinoda S, Masuzawa T, Kanai N (2002) Intracranial hemangiopericytoma with extracranial metastasis occurring after 22 years. Neurol Med Chir (Tokyo) 42: 297–300
49. Thoren M, Rähn T, Hall K, Backlund EO (1978) Treatment of pituitary dependent Cushing's syndrome with closed stereotactic surgery by means of 60Co gamma radiation. Acta Endocrinol (Copenhagen) 88: 7–17
50. Tzortzidis F, Elahi F, Wright D, Natarajan SK, Sekhar LN (2006) Patient outcome at long-term follow-up after aggressive microsurgical resection of cranial base chordomas. Neurosurgery 59: 230–237
51. Zhang R, Zhou LF, Mao Y (2005) Microsurgical treatment of nonmeningeal tumors of the cavernous sinus. Zhonghua Yi Xue Za Zhi 85: 1373–1378

Subject index